Cytometric analysis of cell phenotype and function

Flow cytometry and laser scanning cytometry are increasingly used in clinical and research settings, following improvements in instrument design and computing power and the increased availability of fluorescent agents. This book provides a comprehensive introduction to the theory and clinical applications of these techniques in the assessment of cell phenotype and function.

With an emphasis on clinical relevance, the book presents the principles and potential of cytometry in the analysis of phenomena including cell-mediated cytotoxicity, metabolic burst, phagocytosis, cell–cell aggregation, receptor shedding and apoptosis. Guidance is given on data interpretation, quality control procedures, pitfalls and problems, together with detailed protocols from leading authorities in the field with extensive practical experience.

This is an essential handbook and reference, instructing clinicians and biomedical research scientists in the use of flow cytometry or laser scanning cytometry to assess cell phenotype and function, and in the interpretation of the results from such analyses.

D. A. McCarthy is Senior Lecturer in Virology and Immunology in the School of Biological Sciences, Queen Mary and Westfield College, London.

M. G. Macey is Senior Clinical Scientist and Honorary Senior Lecturer in the Department of Haematology, The Royal London Hospital, and author of *Flow Cytometry*, Blackwell Scientific Publications, 1994.

Cytometric analysis of cell phenotype and function

EDITED BY

Desmond A. McCarthy PhD
Senior Lecturer in Virology and Immunology
School of Biological Sciences
Queen Mary and Westfield College, London, UK

Marion G. Macey PhD, MRCPath
Senior Clinical Scientist, Department of Haematology
The Royal London Hospital, Whitechapel, London
and Honorary Senior Lecturer, Division of Haematology,
Oncology and Imaging, St Bartholomew's and
Royal London School of Medicine and Dentistry,
Queen Mary and Westfield College, London, UK

PUBLISHED BY THE PRESS SYNDICATE OF THE UNIVERSITY OF CAMBRIDGE
The Pitt Building, Trumpington Street, Cambridge, United Kingdom

CAMBRIDGE UNIVERSITY PRESS
The Edinburgh Building, Cambridge CB2 2RU, UK
40 West 20th Street, New York NY 10011-4211, USA
10 Stamford Road, Oakleigh, VIC 3166, Australia
Ruiz de Alarcón 13, 28014 Madrid, Spain
Dock House, The Waterfront, Cape Town 8001, South Africa

http://www.cambridge.org

First published 2001

Printed in the United Kingdom at the University Press, Cambridge

Typeface Utopia 8.5/12pt *System* Poltype® [VN]

A catalogue record for this book is available from the British Library

Library of Congress Cataloguing in Publication data

Cytometric analysis of cell phenotype and function / edited by Desmond A. McCarthy
and Marion G. Macey.
p. cm.
Includes bibliographical references and index.
ISBN 0 521 66029 7
1. Flow cytometry – Handbooks, manuals, etc. 2. Cytology – Handbooks, manuals, etc.
I. McCarthy, Desmond A., 1940– II. Macey, Marion G.
QH585.5.F56 C98 2001
571.6'028–dc21 00-068868

ISBN 0 521 66029 7 hardback

Contents

Contributors

Paul D. Allen PhD
Lecturer, Division of Haematology, Oncology and Imaging, St Bartholomew's and Royal London School of Medicine and Dentistry, Queen Mary and Westfield College, London E1 2AD, UK

David Barnett DipMS, PhD
Clinical Scientist and Scheme Manager/Deputy Director of UK NEQAS for Leucocyte Immunophenotyping, Department of Haematology, Royal Hallamshire Hospital, PO Box 996, Sheffield S10 2YD, UK

Mary R. Cahill MD, MRCPath
Consultant Haematologist, Department of Haematology, Regional General Hospital, Dooradoyle, Limerick, Republic of Ireland

Jamie D. Cavenagh MD, MRCPath
Consultant Haematologist, Department of Haematology, The Royal London Hospital, Whitechapel, London E1 1BB, and Honorary Senior Lecturer, Division of Haematology, Oncology and Imaging, St Bartholomew's and Royal London School of Medicine and Dentistry, Queen Mary and Westfield College, London E1 2AD, UK

Richard J. Clatch MD, PhD
Physician (Pathologist), Department of Pathology, Highland Park Hospital, 718 Glenview Avenue, Highland Park, IL 60035, USA

Charles L. Goolsby PhD
Associate Professor of Pathology, Department of Pathology, Northwestern University Medical School, Ward Building 6-204, 303 East Chicago Avenue, Chicago, IL 60611-3008, USA

David W. Hedley MD
Professor of Cellular and Molecular Biology (Ontario Cancer Institute), Princess Margaret Hospital, Departments of Medicine and Pathology, 610 University Avenue, Toronto, Ontario, MSG 2M9, Canada

Terry Hoy PhD, FRCPath
Principal Research Officer, Department of Haematology, University of Wales College of Medicine, Heath Park, Cardiff CF4 4XN, UK

James W. Jacobberger PhD
Associate Professor of Oncology, Cancer Center, School of Medicine, Case Western Reserve University, 10900 Euclid Avenue, Cleveland, Ohio 44106-4917, USA

David Lloyd DSc
Professor of Microbiology, Cardiff School of Biosciences (Microbiology), Cardiff University, PO Box 915, Cardiff CF1 3TL, UK

Mark W. Lowdell PhD
Senior Lecturer in Haematology, Department of Haematology, Royal Free Hospital School of Medicine, Rowland Hill Street, London NW3 2PF, UK

David J. Mason, PhD
Visiting Research Scientist, Department of Biological Sciences, The University of Warwick, Coventry CV4 7AL, UK

Marion G. Macey PhD, MRCPath
(Editor) Senior Clinical Scientist, Department of Haematology, The Royal London Hospital, Whitechapel, London E1 1BB, and Honorary Senior Lecturer, Division of Haematology, Oncology and Imaging, St Bartholomew's and Royal London School of Medicine and Dentistry, Queen Mary and Westfield College, London E1 2AD, UK

Desmond A. McCarthy PhD
(Editor) Senior Lecturer in Virology and Immunology, School of Biological Sciences, Queen Mary and Westfield College, Mile End Road, London E1 4NS, UK

Timothy M. Milne MSc
Senior Biomedical Scientist, Department of Haematology, The Royal London Hospital, Whitechapel, London E1 1BB, UK

Adrian C. Newland FRCP, FRCPath
Consultant Haematologist, Department of Haematology, The Royal London Hospital, Whitechapel, London E1 1BB and Clinical Professor of Haematology, Division of Haematology, Oncology and Imaging, St Bartholomew's and Royal London School of Medicine and Dentistry, Queen Mary and Westfield College, London E1 2AD, UK

John T. Reilly BSc, MD, FRCP, FRCPath
Consultant Haematologist and Director of UK NEQAS for Leucocyte Immunophenotyping, Department of Haematology, Royal Hallamshire Hospital, PO Box 996, Sheffield S10 2YD, UK

Marc T. E. Suller PhD
Research Scientist, Microbiology Research Group, Welsh School of Pharmacy, University of Cardiff, PO Box 68, Cardiff CF1 3XF, UK

Abbreviations

$\Delta\psi$m	mitochondrial membrane potential
7-AAD	7 aminoactinomycin D
ACD	acid-citrate dextrose
ACDP	Advisory Committee on Dangerous Pathogens
ADB	1,4,-diacetoxy-2,3,-dicyanobenzene
ADC	analogue to digital
ADP	adenosine bisphosphate
AIDS	acquired immunodeficiency syndrome
AIF	apoptosis-inducing factor
AIN	autoimmune neutropenia
ALCAM	activated leukocyte cell adhesion molecule
ALL	acute lymphoblastic (lymphoid) leukaemia
AM	acetoxy-methyl
AMCA	7-amino-4-methylcoumarin-3-acetic acid
AML	acute myeloid leukaemia
Apaf	apoptosis activation factor
APC	allophycocyanin
APML	acute promyelocytic leukaemia
ATCC	American Type Culture Collection
ATLL	adult T-cell lymphoma/leukaemia
ATP	adenosine trisphosphate
BAL	biphenotypic acute leukaemia
B-ALL	B lineage acute lymphoblastic leukaemia
BCECF	2',7'-bis(2-carboxyethyl)-5,6-carboxyfluorescein
BCECF-AM	2',7'-bis-(2-carboxyethyl)-5,6-carboxyfluorescein acetoxy-methyl ester
B-CLL	B-cell chronic lymphocytic leukaemia
BCSH	British Committee for Standards in Haematology
BODIPY®	4,4-difluoro-4-bora-3a,4a-diaza-s-indacene derivatives

BODIPY FL	A BODIPY substitute for fluorescein
B-PE	bacterial phycoerythrin
B-PLL	B-prolymphocytic leukaemia
BrdU	bromodeoxyuridine
BSA	bovine serum albumin
C-ALL	common acute lymphoblastic leukaemia
CALLA	common acute lymphoblastic leukaemia antigen
CAM	cell adhesion molecules
CCD	charge coupled device/detector
CD	cluster of differentiation
CDK	cyclin-dependent kinase
CDKi	cyclin-dependent kinase inhibitor
CDR	complementarity determining region
ced	cell death gene
CEA	carcinoembryonic antigen
CFU-GM	colony-forming unit, granulocyte macrophage
CHE	Chinese hamster embryo
CHO	Chinese hamster ovary cells
CLL	chronic lymphocytic leukaemia
CLP	common lymphoid progenitor
CML	chronic myeloid leukaemia
CMXRos	chloromethyl-X-rosamine
CTAD	sodium citrate, theophylline, adenosine and diapyridamole
CV	coefficient of variation
CY™3	indocarbocyanine, cyanin 3, cyan3
CY™5	indodicarbocyanine, cyanin 5, cyan5
CY™7	indotricarbocyanine, cyanin 7, cyan 7
cyt	cytoplasmic
DAPI	4',6-diamidino-2-phenylindole
DC	dendritic cell
DCFH-DA	2',7'-dichlorofluorescin diacetate
DCF	2',7'-dichlorofluorescein
DCH	2,3-dicyanohydroquinone
DI	DNA index
$DiBAC_4(3)$	bis-(1,3-dibutylbarbituric acid) trimethine oxonol
$DiIC_{18}(3)$	An octadecyl indocarbocyanine dye
$DiOC_5(3)$	3,3'-dipentyloxacarbocyanine iodide
$DiOC_6(3)$	3,3'-dihexyloxacarbocyanine iodide
$DiSC_2(5)$	A thia carbocyanine dye
$DiSC_5(3)$	dipropylthiocarbocyanine
DLBCL	diffuse large B cell lymphoma
DPH	1,6-diphenyl-1,3,5-hexatriene
dUTP	deoxyuridine trisphosphate
EB	ethidium bromide
EBV	Epstein-Barr virus
ECACC	European Collection of Cell Cultures
ECD	Energy Coupled Dye (phycoerythrin-Texas Red™. Coulter Red 613)
EDTA	ethylenediaminetetraacetic acid (used as K^+ or Na^+ salts)
EGF	epidermal growth factor
EGFR	epidermal growth factor receptor
EGIL	European Group for the Immunological Characterisation of Leukaemias
EGTA	ethyleneglycoltetraacetic acid
ELAM	endothelial leukocyte adhesion molecule
ELISA	enzyme-linked immunosorbent assays
EPICS®	Electronically Programmable Individual Cell Sorter
EQA	external quality assessment
ESACP	European Society for Cellular Analytical Pathology
ETS	A proto-oncogene-encoded transcription factor
EWGCCA	European Working Group for Clinical Cell Analysis
$F(ab')_2$	dimeric antigen binding fragment of antibody
FAB	French American British classification
Fab'	monomeric antigen binding fragment of antibody
FACS®	Fluorescent Activated Cell Sorter
FAD	flavin adenine dinucleotide
FAL	forward angle light
FALS	Forward angle light scatter
Fas-L	Fas ligand
FBS	fetal bovine serum (heat inactivated)
Fc	crystallisable/complement binding fragment of antibody
FCS	Flow Cytometry Standard
FCSC	Flow Cytometry Standards Corporation
FDA	fluorescein diacetate
FISH	fluorescence in situ hybridisation
FITC	fluorescein isothiocyanate
FL	follicular lymphoma
FLISA	fluorescence linked immunosorbence assay
FMH	fetal maternal hemorrhage
fMLP	*N*-formyl methionyl leucyl phenylalanine
FMN	riboflavin mononucleotide

FRET	fluorescence resonance energy transfer
G-CSF	granulocyte colony-stimulating factor
GlyCAM	glycosylation-dependent cell adhesion molecule
GM-CSF	granulocyte–monocyte colony-stimulating factor
GMP	granule membrane protein
GRO-α	growth-related gene product-α
GSH	reduced glutathione
h	Planck's constant (6.6×10^{27} erg s^{-1})
H_5-DCFDA	2',7'-dichlorodihydrofluorescein diacetate
HCL	hairy cell leukaemia
He–Ne	helium–neon
HEPES	*N*-(2-hydroxyethyl)piperazine-*N*'-(2-ethanesulphonic acid)
HHBSS	Hanks' balanced salts solution buffered with 10 mol l^{-1} HEPES pH 7.3
HHBSS-BSA	Hanks' balanced salts solution buffered with 10 mmol l^{-1} HEPES, pH 7.3, containing 0.5% bovine serum albumin
HIV	human immunodeficiency virus
HLA	human leukocyte antigen
HPA	human platelet antigen
HPLC	high pressure liquid chromatography
HPV	human papilloma virus
HSAC	Health Services Advisory Committee
HTLV-1	human T lymphotropic virus 1
Hz	hertz, one cycle per second
ICAD	inhibitor of the caspase activated deoxyribonuclease
ICAM	intercellular adhesion molecule (ICAM-1, CD54; ICAM-2, CD106)
ICE	interleukin 1β converting enzyme
IFN-γ	interferon γ
IgA	immunoglobulin A
IgD	immunoglobulin D
IgE	immunoglobulin E
IgG	immunoglobulin G
IgM	immunoglobulin M
IL	interleukin
IMDM	Iscoves modified Dulbecco's medium
Indo-1	ratiometric Ca^{2+} indicator, indo-1
IQC	internal quality control
ISHAGE	International Society for Hematotherapy and Graft Engineering
JC-1	5,5'6,6'-tetrachloro-1,1',3,3'-tetraethylbenzimidazol carbo-cyanide iodide
KAR	killer-activating receptors
KIR	immunoglobulin (Ig)-like killer-inhibitory receptor
LAD	leukocyte adhesion deficiency
LAM	leukocyte adhesion molecule
LASER	Light Amplification by Stimulated Emission of Radiation
LDL	low density lipoprotein
LDS-751	a styrl dye
LFA	leukocyte function antigen (LFA-1α, CD11a; LFA-2, CD2; LFA-3, CD58)
LPS	lipopolysaccharide
LTB_4	leukotriene B_4
MAdCAM	mucosal addressin cell adhesion molecule
MALT	mucosa-associated lymphoid tissue
MAPKK	mitogen-activated protein kinase kinase
MCAM	melanoma cell adhesion molecule (CD146)
MCL	mantle cell lymphoma
mClCCP	carbonylcyanide *m*-chlorophenylhydrazone
MDM	murine double minute chromosomal gene product
MGC	multiglycosylated core protein
MHC	major histocompatibility complex
MIG	monokine induced by gamma interferon
MPO	myeloperoxidase
MRD	minimal residual disease
NADH	reduced form of nicotinamide adenine dinucleotide
NADPH	reduced form of nicotinamide adenine dinucleotide phosphate
NAIg	neutrophil-associated immunoglobulin
NBD	nitro blue diazonium
NCAM-1	neuronal all adhesion molecule 1 (CD56)
NCCLS	National Committee for Clinical Laboratory Standards
NCTC	National Culture Type Collection
NEQAS	National External Quality Assessment Scheme
NFκB	nuclear factor κB
NK	natural killer cell
NO	nitric oxide
NOS	nitric oxide synthase
O_2^-	superoxide
p105	retinoblastoma protein
PADGEM	platelet activation-dependent granule external membrane protein
PAF	platelet-activating factor

PBMC	peripheral blood mononuclear cells
PBS	phosphate-buffered saline (154 mmol l^{-1} NaCl, 1.54 mmol KH_2PO_4, 2.7 mmol l^{-1} Na_2HPO_4, pH 7.4)
PBS-BSA	phosphate-buffered saline containing 1% bovine serum albumin
PBSC	peripheral blood stem cells
PBSg	phosphate-buffered saline containing 1% gelatine and 1% glucose
PCR	polymerase chain reaction
PE	phycoerythrin
PE CAM	platelet/endothelial cell adhesion molecule
PE-CY®5	phycoerythrin-indodicarbocyanine: also called Cy-chrome, Tri-color, Red670 and Quantum Red™
PerCP	peridinin–chlorophyll *a* complex
PETA	platelet endothelial tetraspan antigen
PI	propidium iodide
PIFT	platelet immunofluorescence test
PIG	phosphatidylinositol glycosyl phospholipid
PMA	phorbol myristate acetate
PMN	polymorphonuclear granulocyte
PMT	photomultiplier tube
PNH	paroxysmal nocturnal hemoglobinuria
pRb	retinoblastoma protein
PS	phosphatidylserine
PSGL	P-selectin glycoprotein ligand
PT	permeability transition
RBCs	red blood cells
RET	'rearranged during transfection'
RGD	arginine-glycine-aspartate
RhD	Rhesus D
ROI	reactive oxygen intermediates
R-PE	R-phycoerythrin (from Rhodophycae)
RPMI 1640	Roswell Park Memorial Institute 1640 (a cell culture medium)
RT-PCR	reverse transcriptase polymerase chain reaction
RYD	arginine-tyrosine-aspartate
SD	standard deviation
SDS	sodium dodecyl sulphate
SLL	small lymphocytic lymphoma
SLVL	splenic lymphoma with circulating villous lymphocytes
sm	surface membrane
SNARF-1	carboxy-seminaphthorhodafluor
SNARF-1/AM	carboxy-seminapthorhodafluor-1-acetoxy-methyl ester
SSC	side angle light scatter
S-SC	saline sodium citrate
SV40	simian virus 40
SYBR® green	DNA-specific dye
SYBR®-14	a cyanine dye for viability assays
SYTO® 16	a cell permeant nucleic acid dye
T-ALL	T lineage acute lymphoblastic leukaemia
TBS	Tris-buffered saline
TCR	T-cell receptor
TdT	terminal deoxynucleotidyl transferase
T-LGLL	T large granular lymphocyte leukaemia
T_m	melting temperature
TNF-α	tumour necrosis factor-α
TOF	time of flight
TO-PRO®-3	a monomeric cyanine dye
TOTO®-3	a dimeric cyanine dye
T-PLL	T prolymphocytic leukaemia
TR-FRET	time-resolved-fluorescence energy transfer
tris-HCl	tris(hydroxymethyl)aminomethane hydrochloride
TUNEL	terminal deoxynucleotidyl transferase dUTP nick-end labelling
VCAM	vascular cell adhesion molecule
WBC	white blood cell count
WHO	World Health Organization
YAG	yttrium aluminium garnet
YOYO®-1	A DNA dye

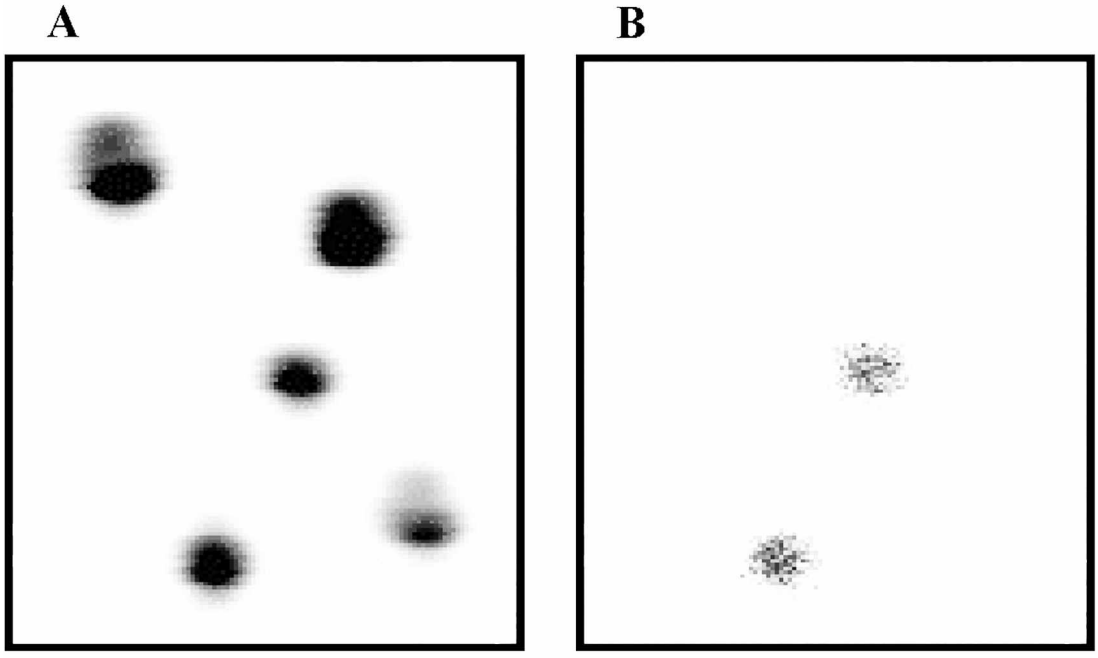

Fig. 6.2 (A) Contouring of individual cells based on light scatter. (B) Green fluorescence in two of the cells, reflecting binding of fluorescein isothiocyanate-conjugated CD3.

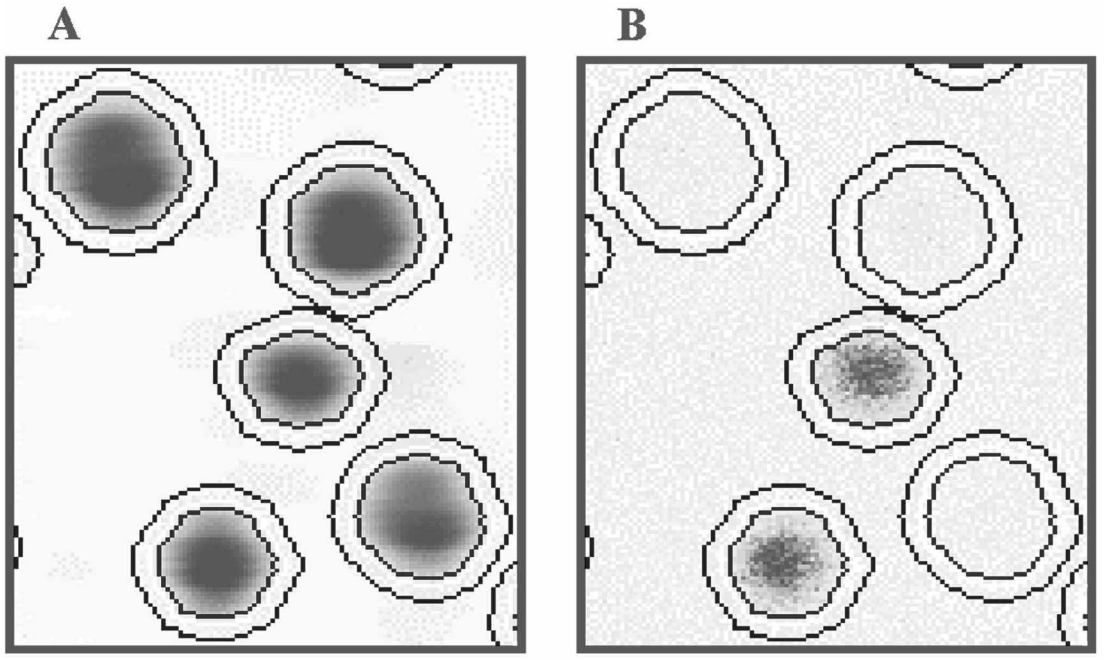
A
B

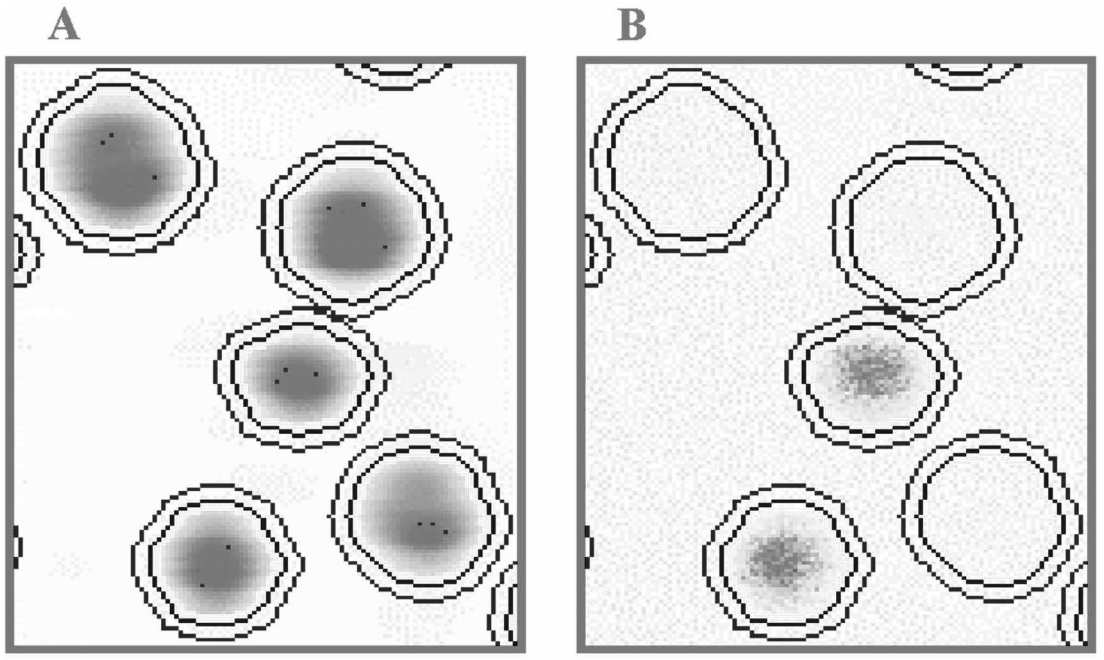
A
B

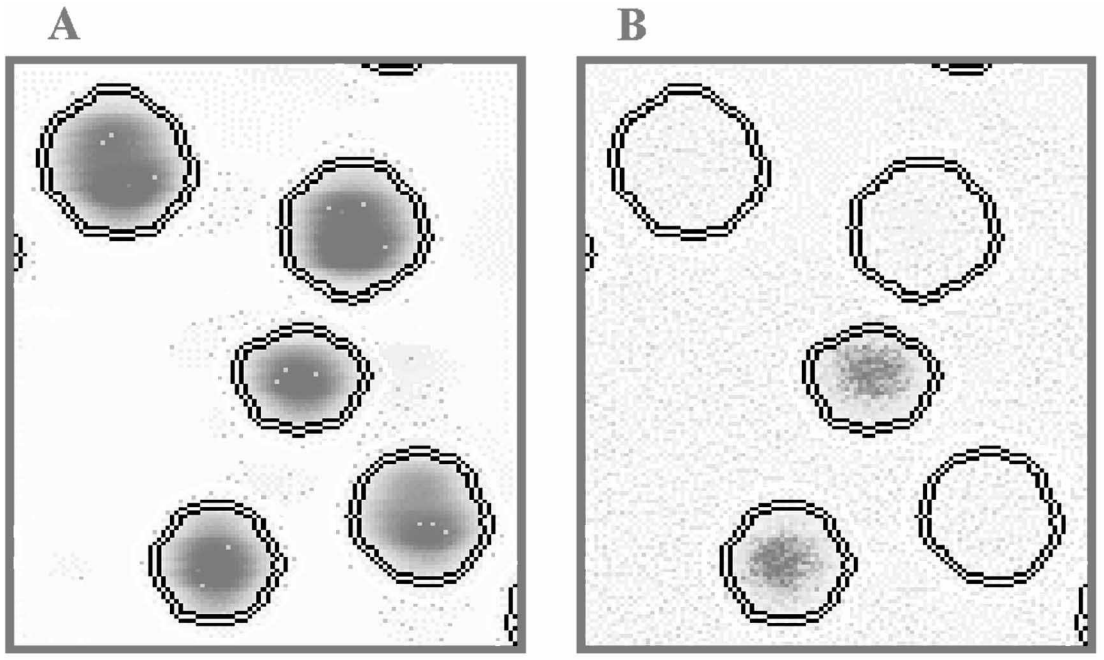
A
B

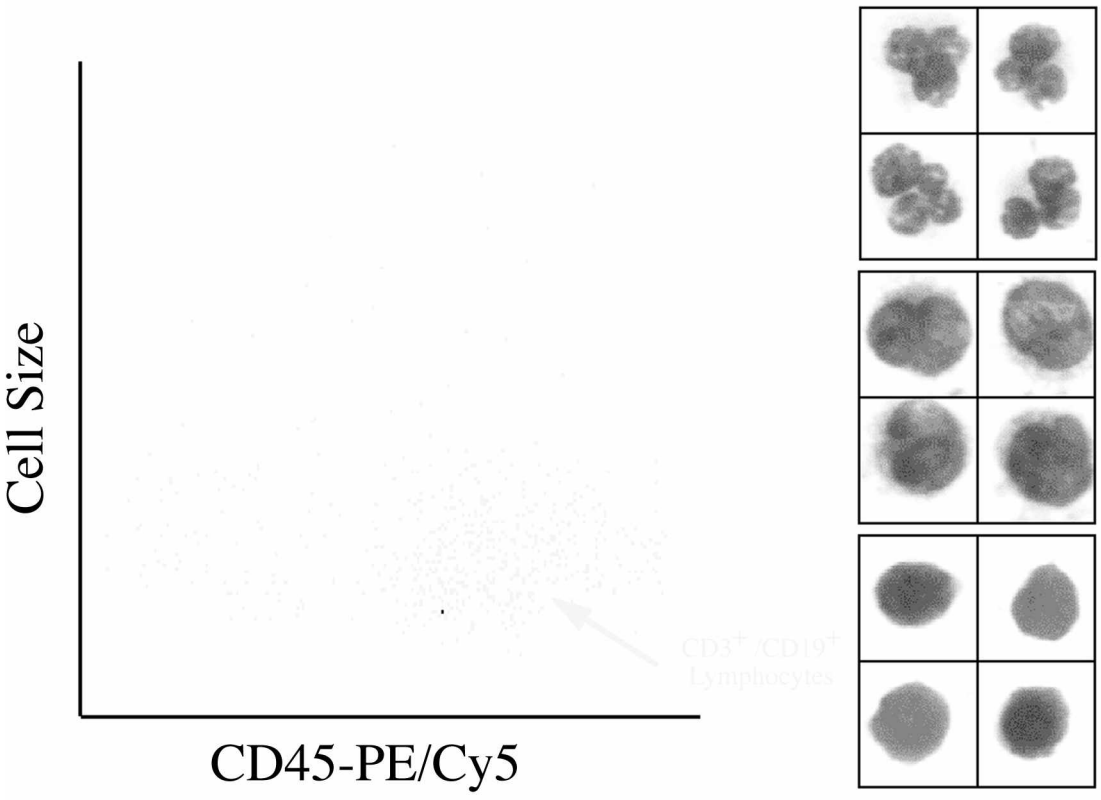

Fig. 6.4 Initial gating based on cell size and CD45 positivity.

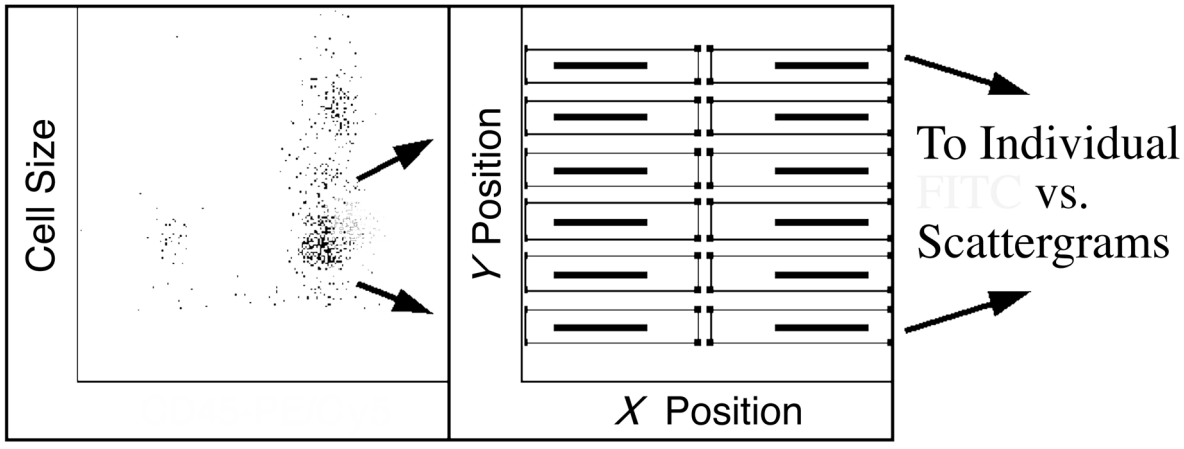

Fig. 6.5 Subsequent gating based on cell position. FITC, fluorescein isothiocyanate; PE, phycoerythrin.

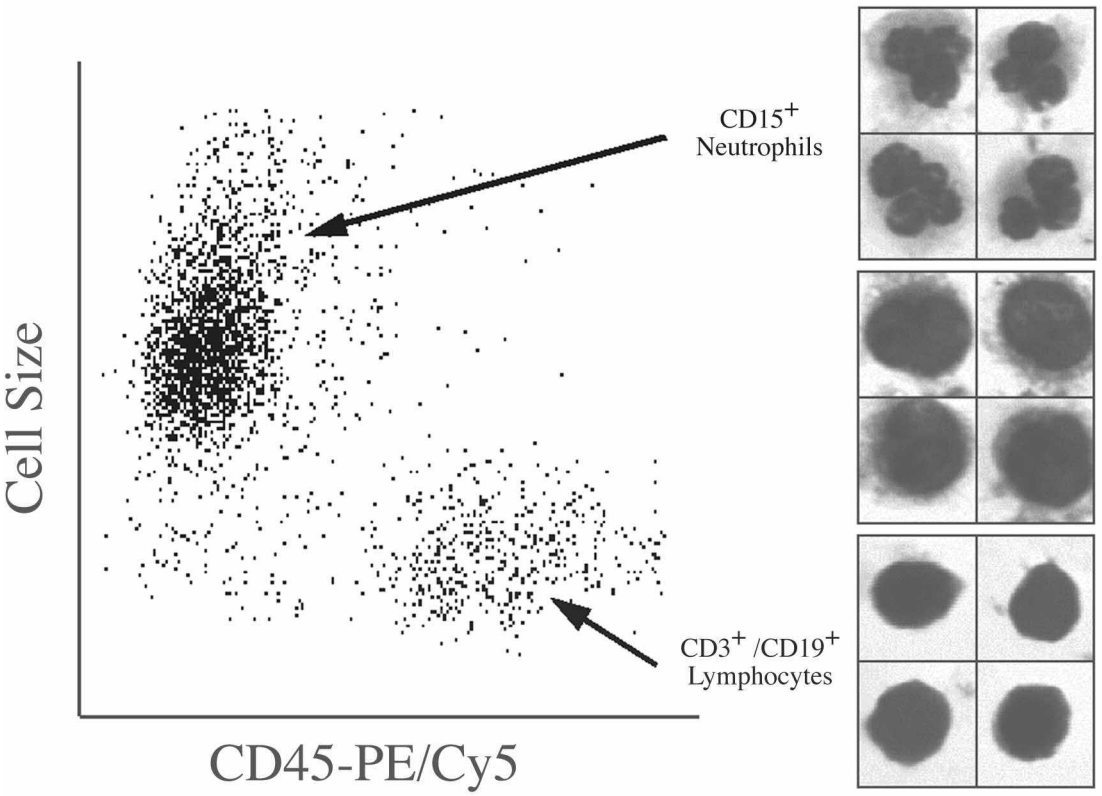
CD15+
Neutrophils
CD3+ /CD19+
Lymphocytes
Cell Size
CD45-PE/Cy5

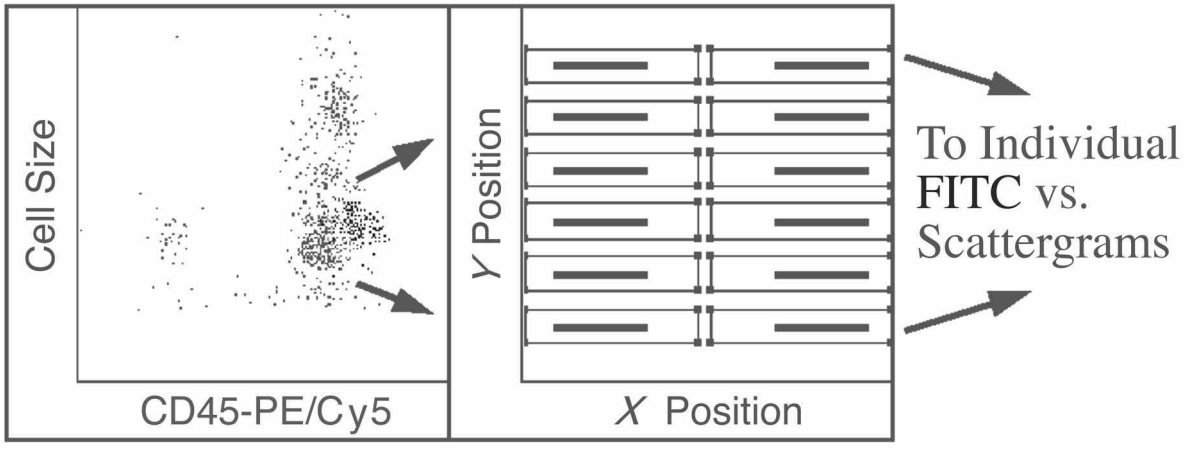
Cell Size
CD45-PE/Cy5
Y Position
X Position
To Individual
FITC vs.
Scattergrams

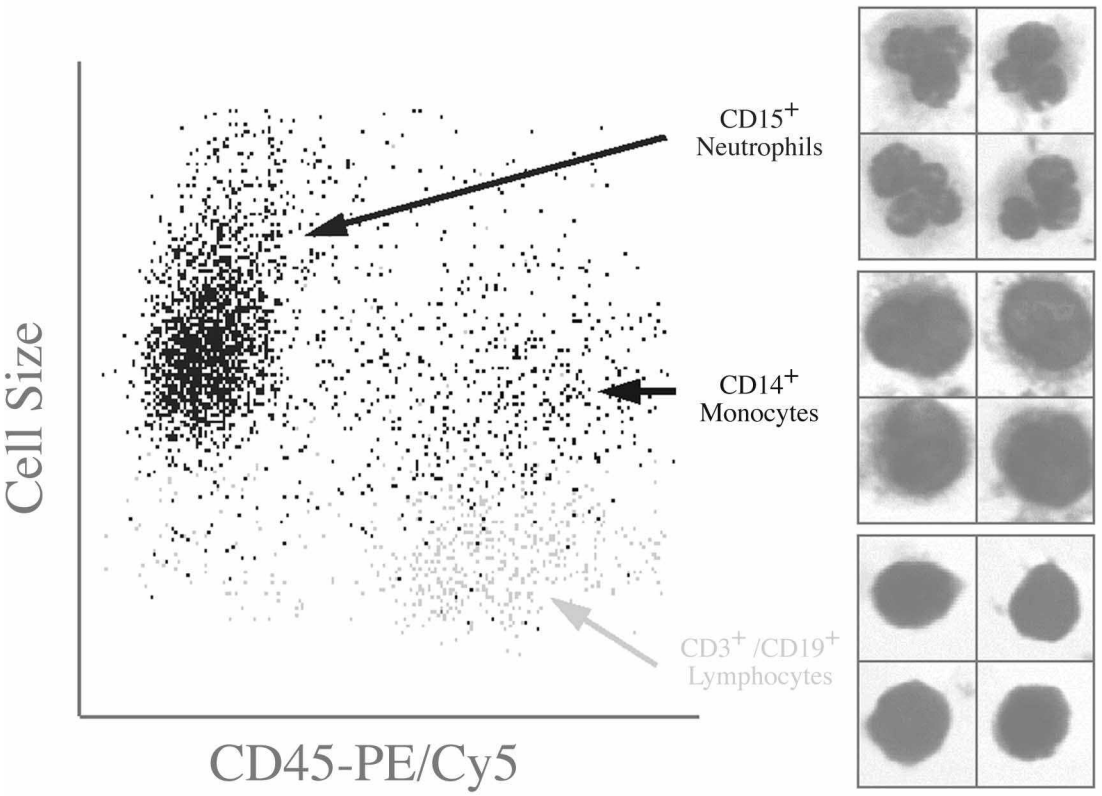
Cell Size
CD45-PE/Cy5
CD15+
Neutrophils
CD14+
Monocytes
CD3+ /CD19+
Lymphocytes

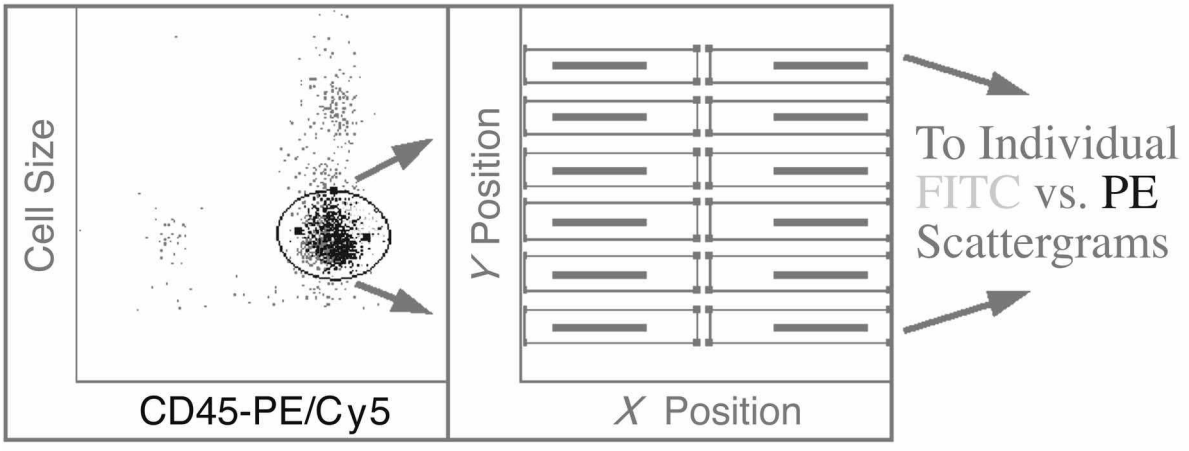
Cell Size
CD45-PE/Cy5
Y Position
X Position
To Individual
FITC vs. PE
Scattergrams

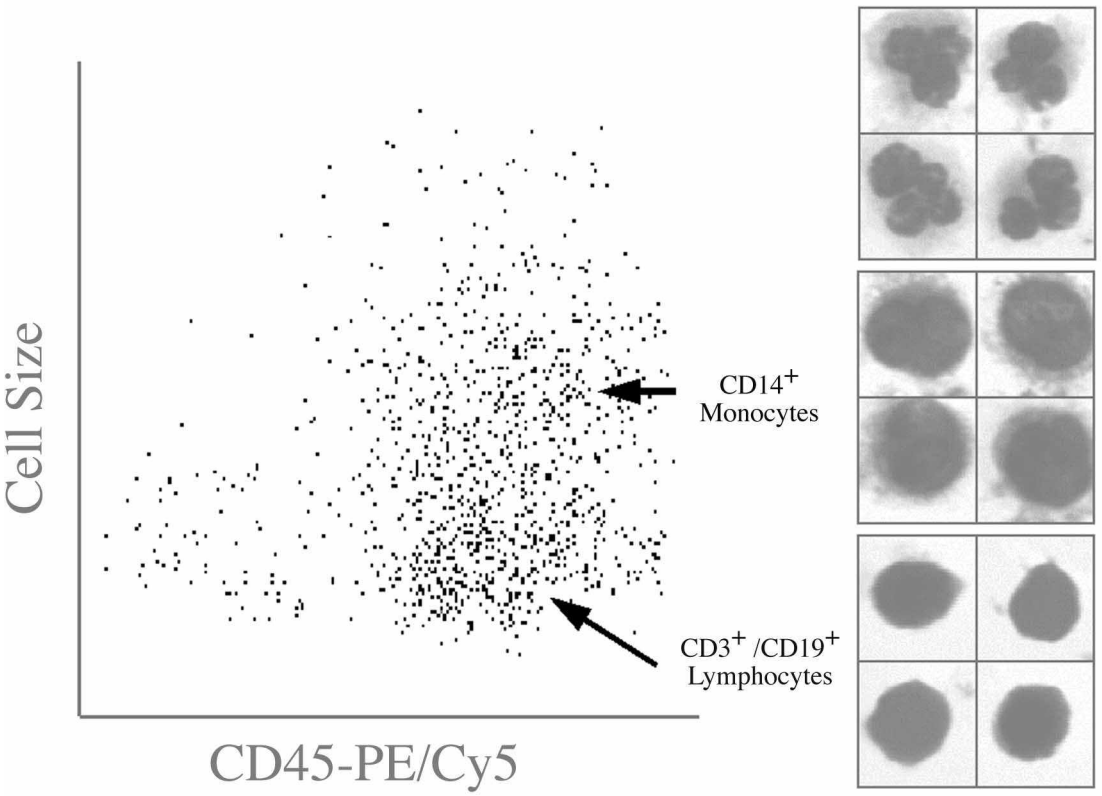
Cell Size
CD45-PE/Cy5
CD14+
Monocytes
CD3+ /CD19+
Lymphocytes

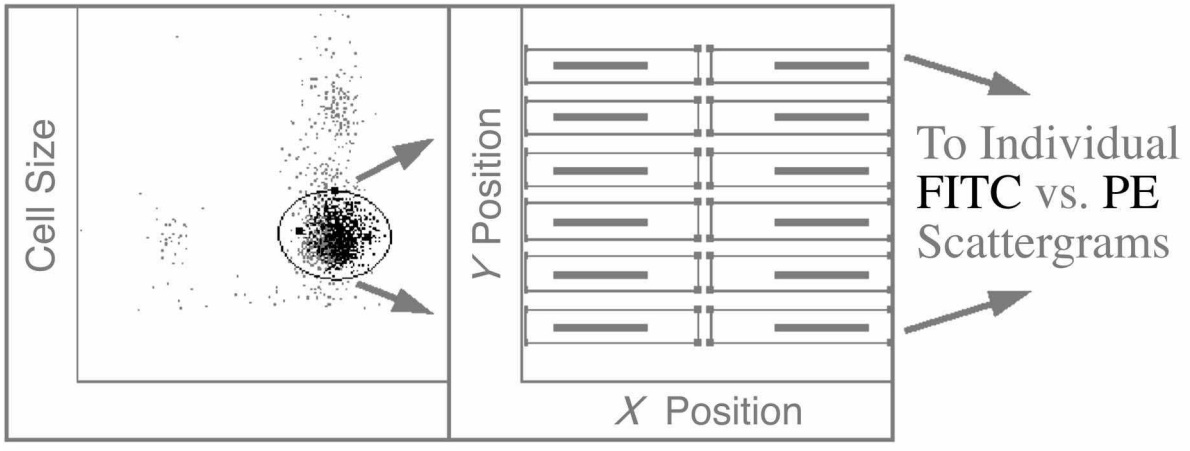
Cell Size
Y Position
X Position
To Individual
FITC vs. PE
Scattergrams

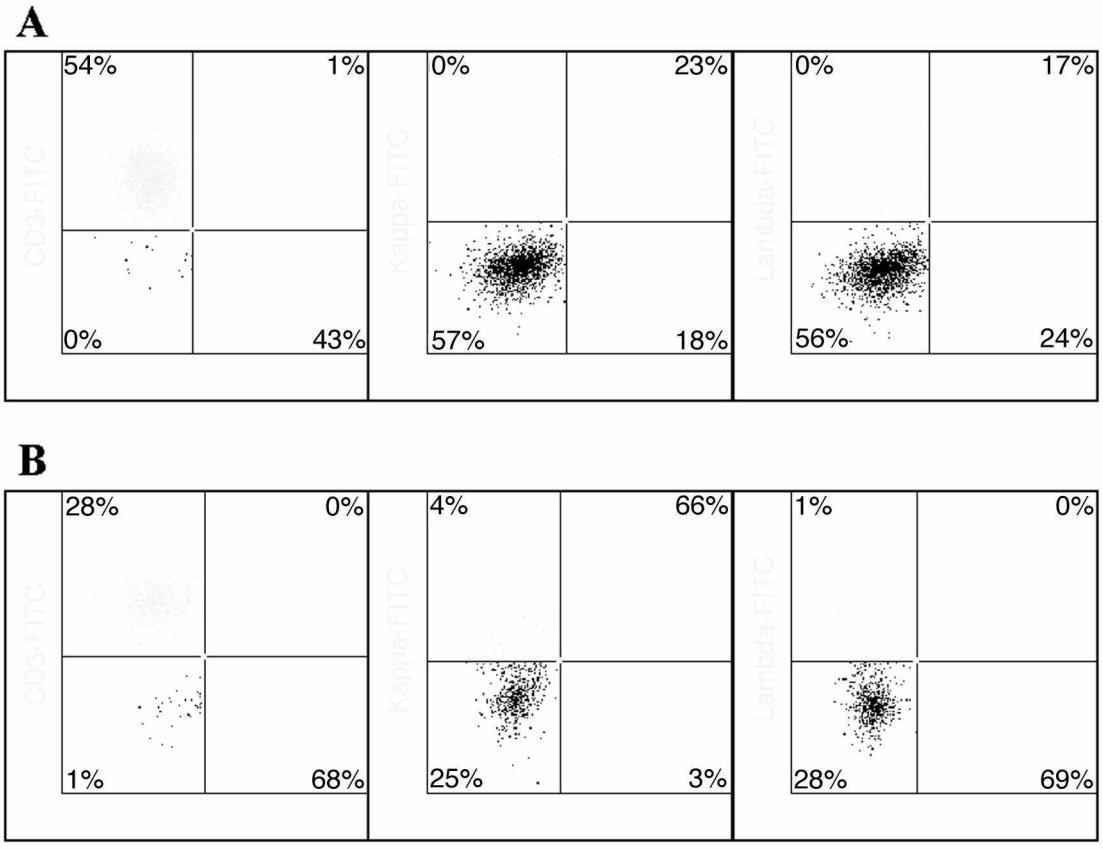

Fig. 6.6 Example of clinical results showing the binding of lymphocyte-specific and immunoglobulin light chain-specific antibodies. (A) Benign lymph node with polyclonal B-cells. (B) Malignant lymph node with monoclonal B-cells.

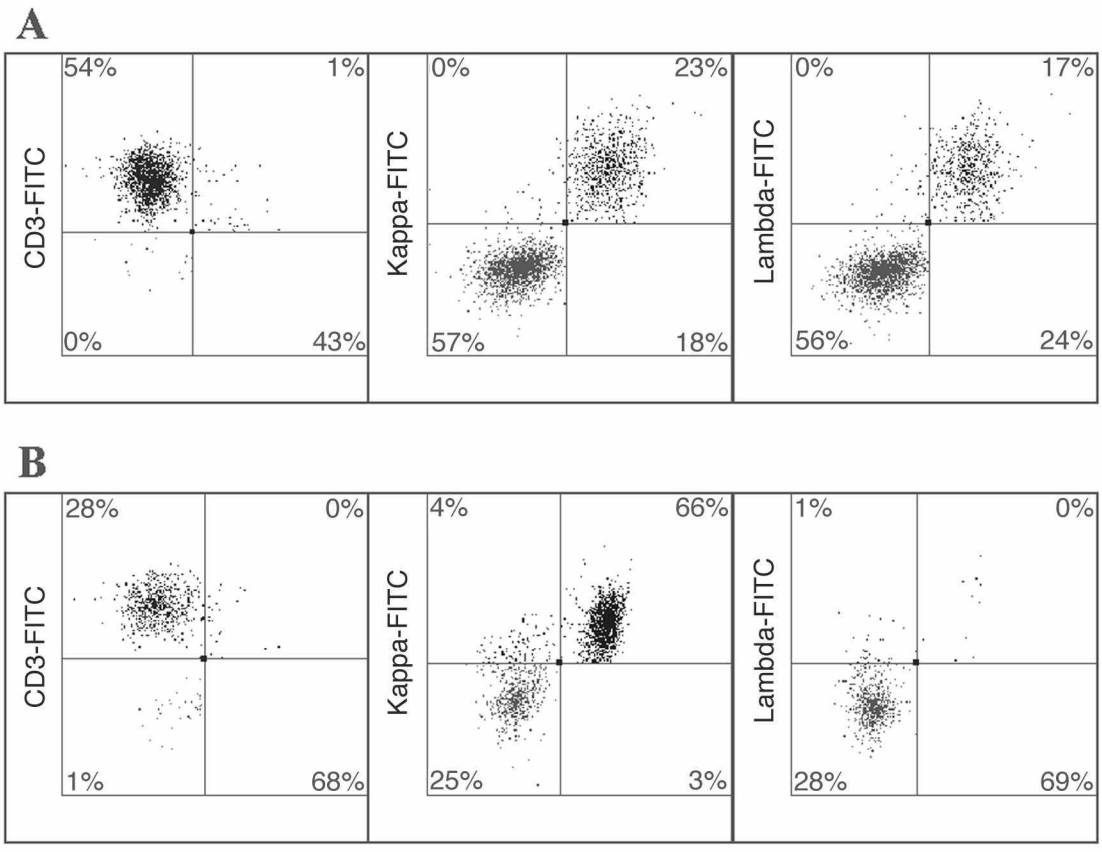
A
CD3-FITC
54%
1%
0%
43%
Kappa-FITC
0%
23%
57%
18%
Lambda-FITC
0%
17%
56%
24%
B
CD3-FITC
28%
0%
1%
68%
Kappa-FITC
4%
66%
25%
3%
Lambda-FITC
1%
0%
28%
69%

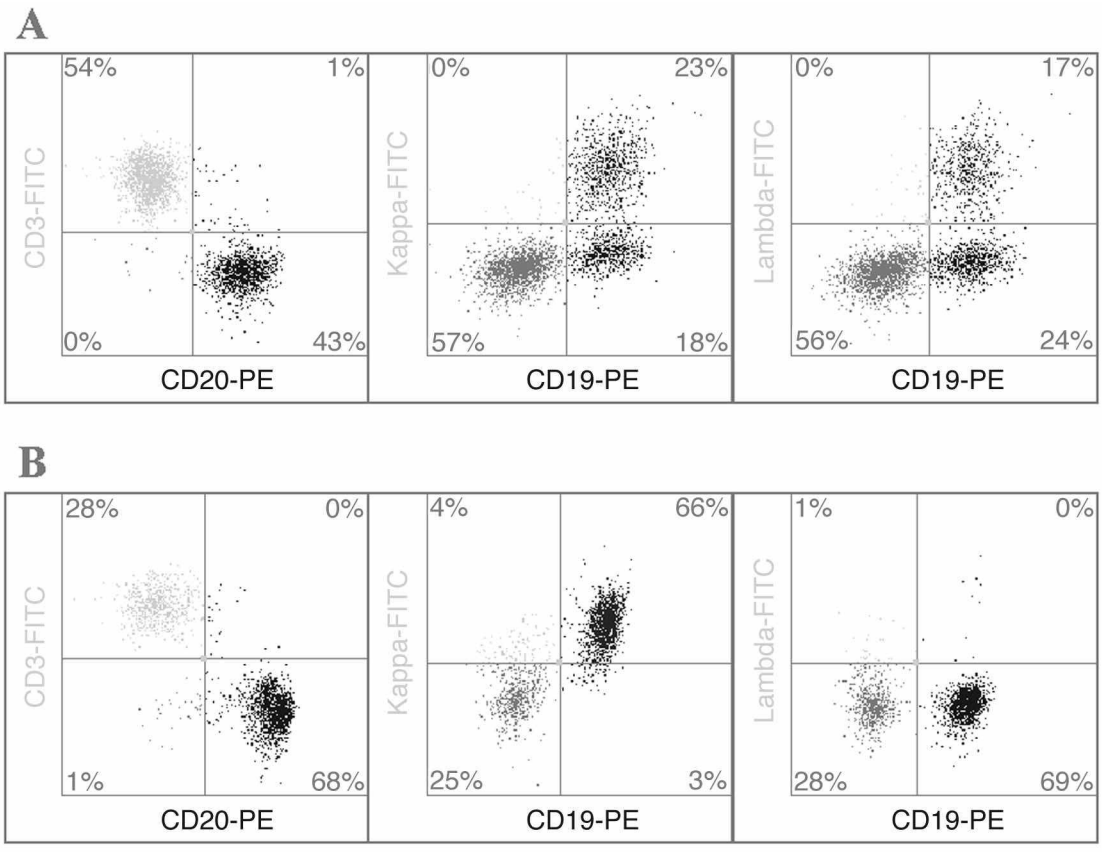
A
54%
1%
0%
43%
CD3-FITC
CD20-PE
0%
23%
57%
18%
Kappa-FITC
CD19-PE
0%
17%
56%
24%
Lambda-FITC
CD19-PE
B
28%
0%
1%
68%
CD3-FITC
CD20-PE
4%
66%
25%
3%
Kappa-FITC
CD19-PE
1%
0%
28%
69%
Lambda-FITC
CD19-PE

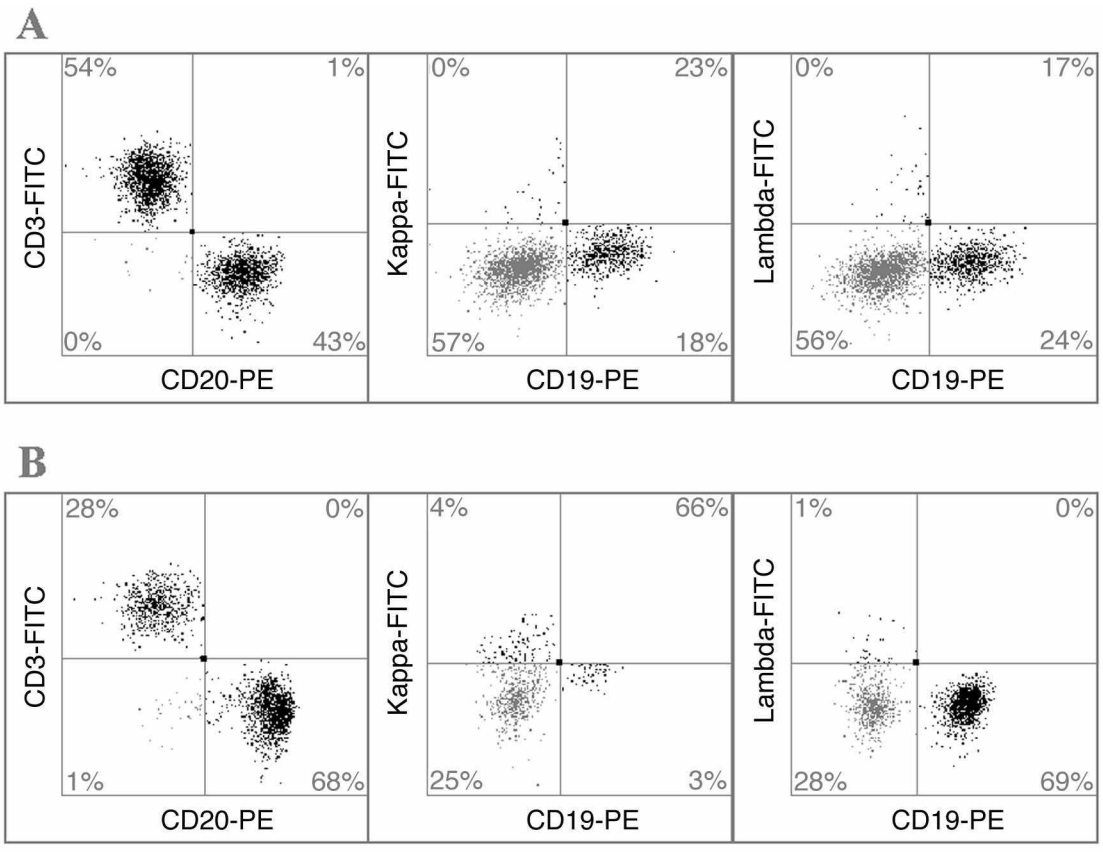
A
54%
1%
0%
43%
CD3-FITC
CD20-PE
0%
23%
57%
18%
Kappa-FITC
CD19-PE
0%
17%
56%
24%
Lambda-FITC
CD19-PE
B
28%
0%
1%
68%
CD3-FITC
CD20-PE
4%
66%
25%
3%
Kappa-FITC
CD19-PE
1%
0%
28%
69%
Lambda-FITC
CD19-PE

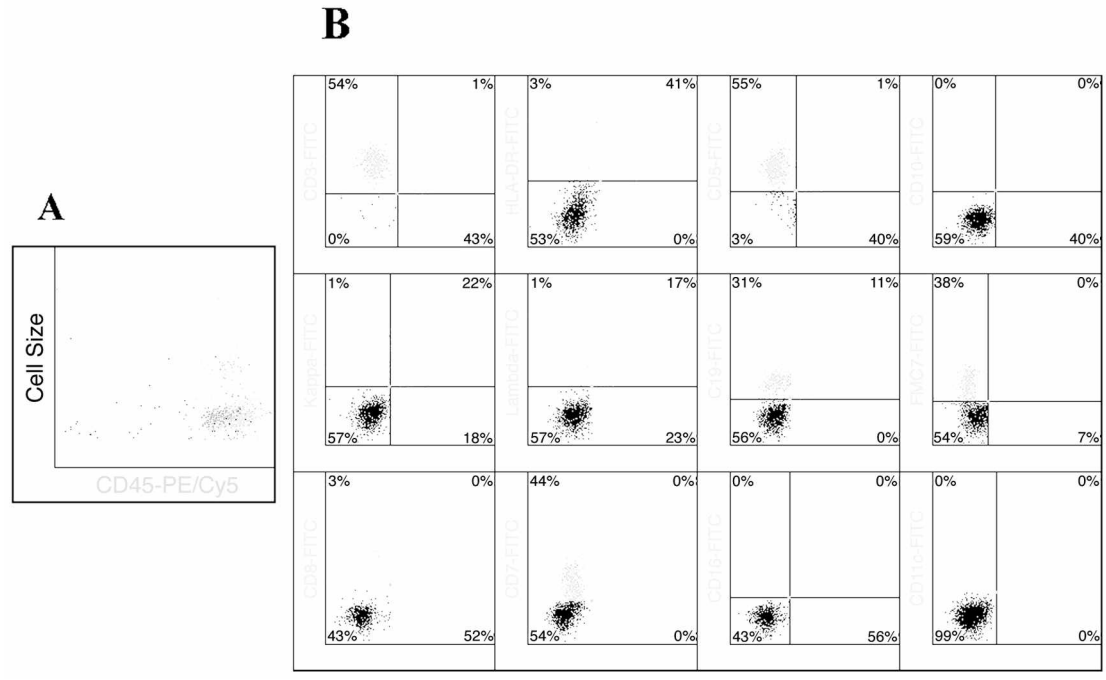

Fig. 6.7 Cells from a fine needle aspiration biopsy of a benign lymph node. $CD45^{+}$ cells were gated (A) and subsequently displayed as 12 separate fluorescein isothiocyanate (FITC) versus phycoerythrin (PE) histograms (B). See text for full details.

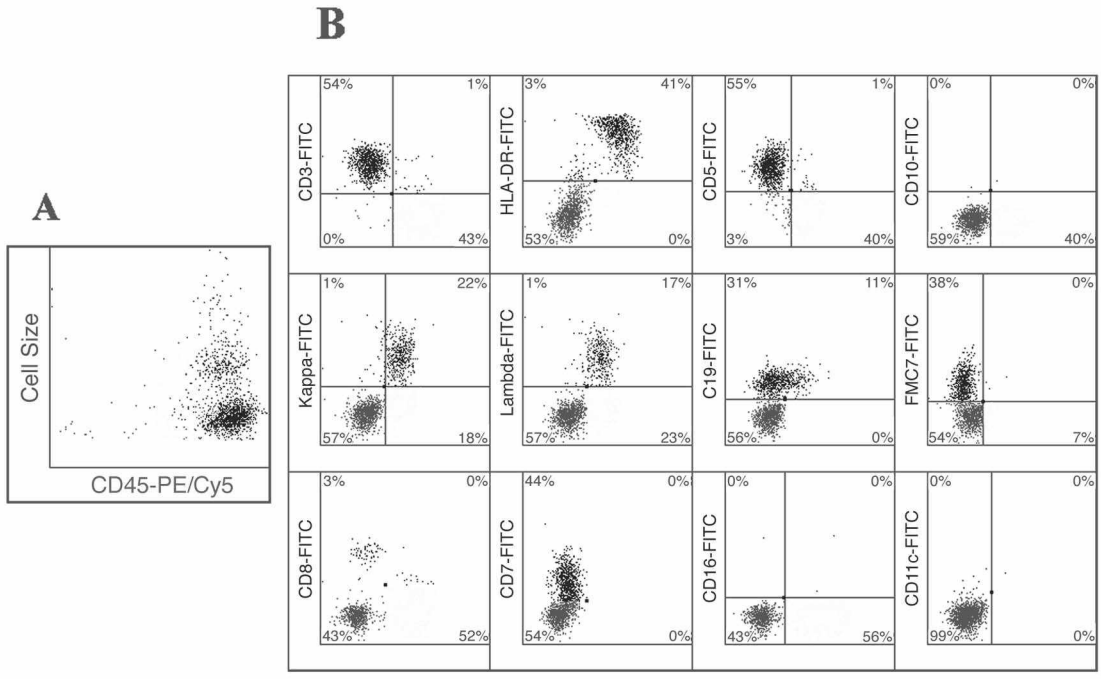
A
Cell Size
CD45-PE/Cy5
B
CD3-FITC
54%
1%
0%
43%
HLA-DR-FITC
3%
41%
53%
0%
CD5-FITC
55%
1%
3%
40%
CD10-FITC
0%
0%
59%
40%
Kappa-FITC
1%
22%
57%
18%
Lambda-FITC
1%
17%
57%
23%
C19-FITC
31%
11%
56%
0%
FMC7-FITC
38%
0%
54%
7%
CD8-FITC
3%
0%
43%
52%
CD7-FITC
44%
0%
54%
0%
CD16-FITC
0%
0%
43%
56%
CD11c-FITC
0%
0%
99%
0%

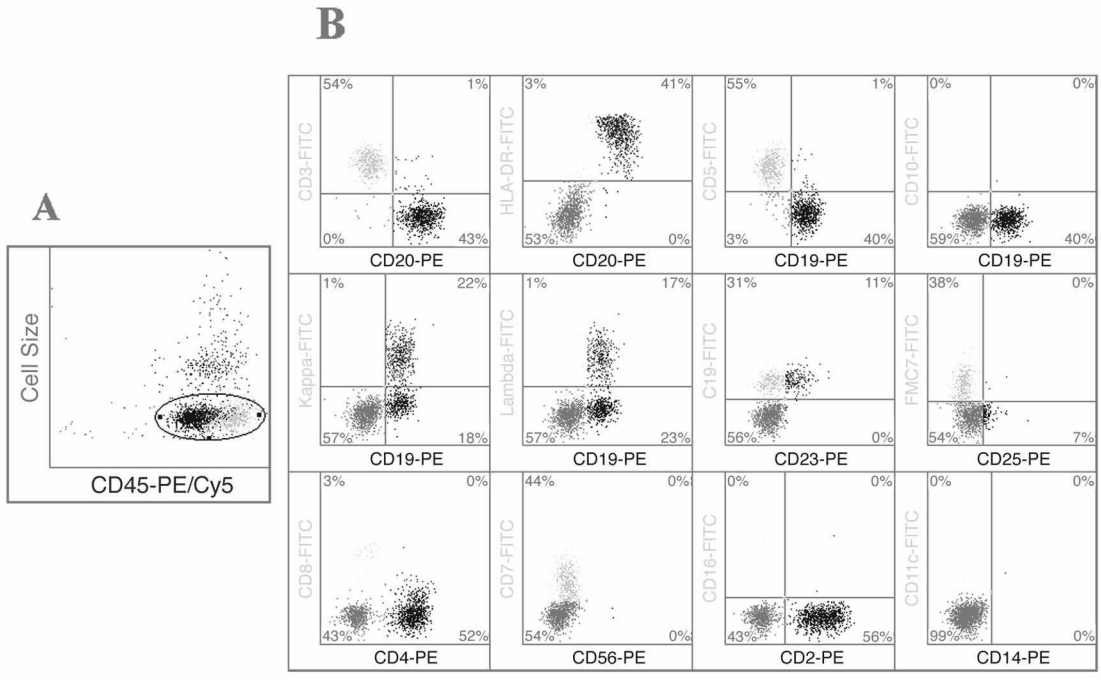
A
Cell Size
CD45-PE/Cy5
B
CD3-FITC
54%
1%
0%
43%
CD20-PE
HLA-DR-FITC
3%
41%
53%
0%
CD20-PE
CD5-FITC
55%
1%
3%
40%
CD19-PE
CD10-FITC
0%
0%
59%
40%
CD19-PE
Kappa-FITC
1%
22%
57%
18%
CD19-PE
Lambda-FITC
1%
17%
57%
23%
CD19-PE
C19-FITC
31%
11%
56%
0%
CD23-PE
FMC7-FITC
38%
0%
54%
7%
CD25-PE
CD8-FITC
3%
0%
43%
52%
CD4-PE
CD7-FITC
44%
0%
54%
0%
CD56-PE
CD16-FITC
0%
0%
43%
56%
CD2-PE
CD11c-FITC
0%
0%
99%
0%
CD14-PE

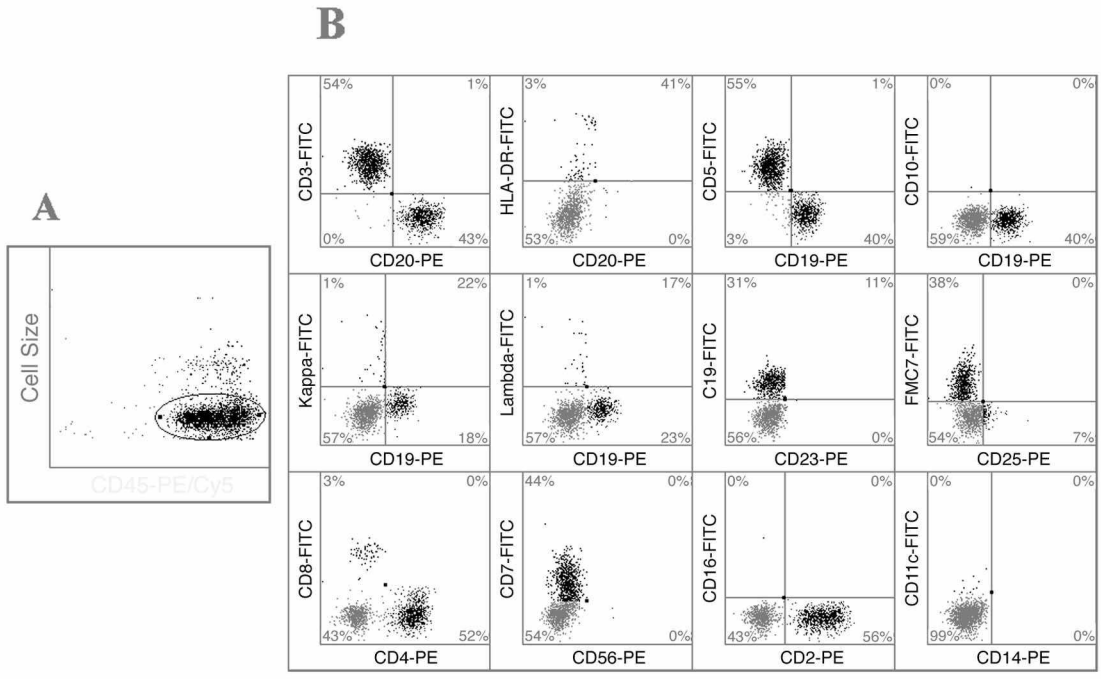
A
Cell Size
CD45-PE/Cy5
B
CD3-FITC
54%
1%
0%
43%
CD20-PE
HLA-DR-FITC
3%
41%
53%
0%
CD20-PE
CD5-FITC
55%
1%
3%
40%
CD19-PE
CD10-FITC
0%
0%
59%
40%
CD19-PE
Kappa-FITC
1%
22%
57%
18%
CD19-PE
Lambda-FITC
1%
17%
57%
23%
CD19-PE
C19-FITC
31%
11%
56%
0%
CD23-PE
FMC7-FITC
38%
0%
54%
7%
CD25-PE
CD8-FITC
3%
0%
43%
52%
CD4-PE
CD7-FITC
44%
0%
54%
0%
CD56-PE
CD16-FITC
0%
0%
43%
56%
CD2-PE
CD11c-FITC
0%
0%
99%
0%
CD14-PE

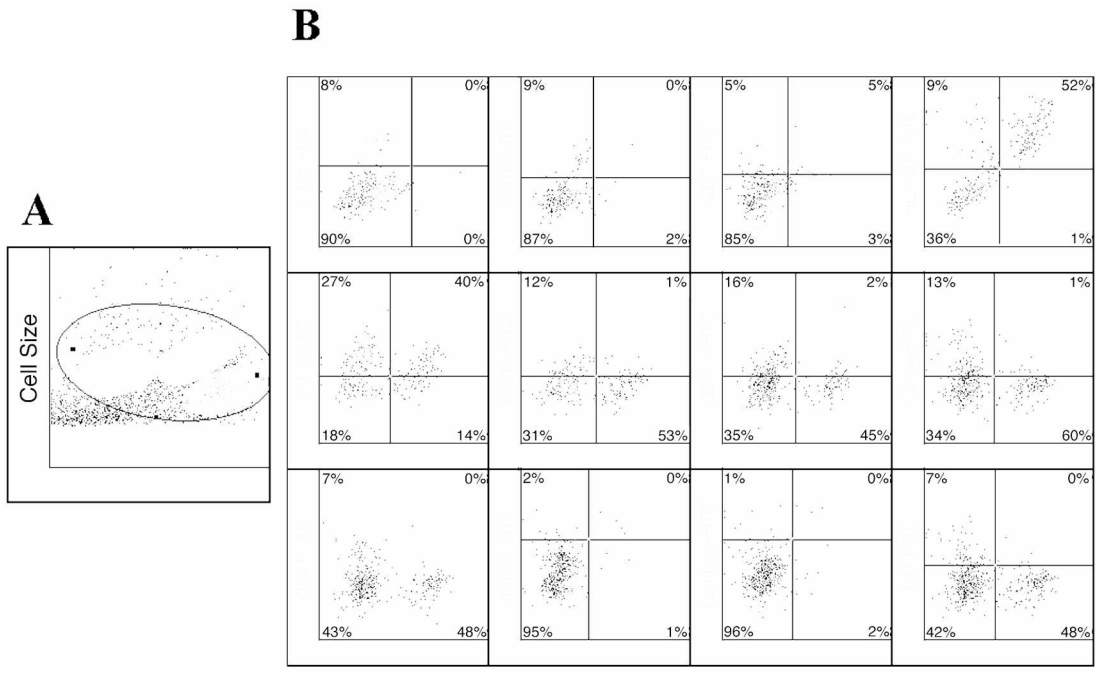

Fig. 6.8 Cells from peripheral blood of a patient with acute myeloid leukaemia. $CD45^{+}$ cells were gated (A) and subsequently displayed as 12 separate fluorescein isothiocyanate (FITC) versus phycoerythrin (PE) histograms (B). See text for full details.

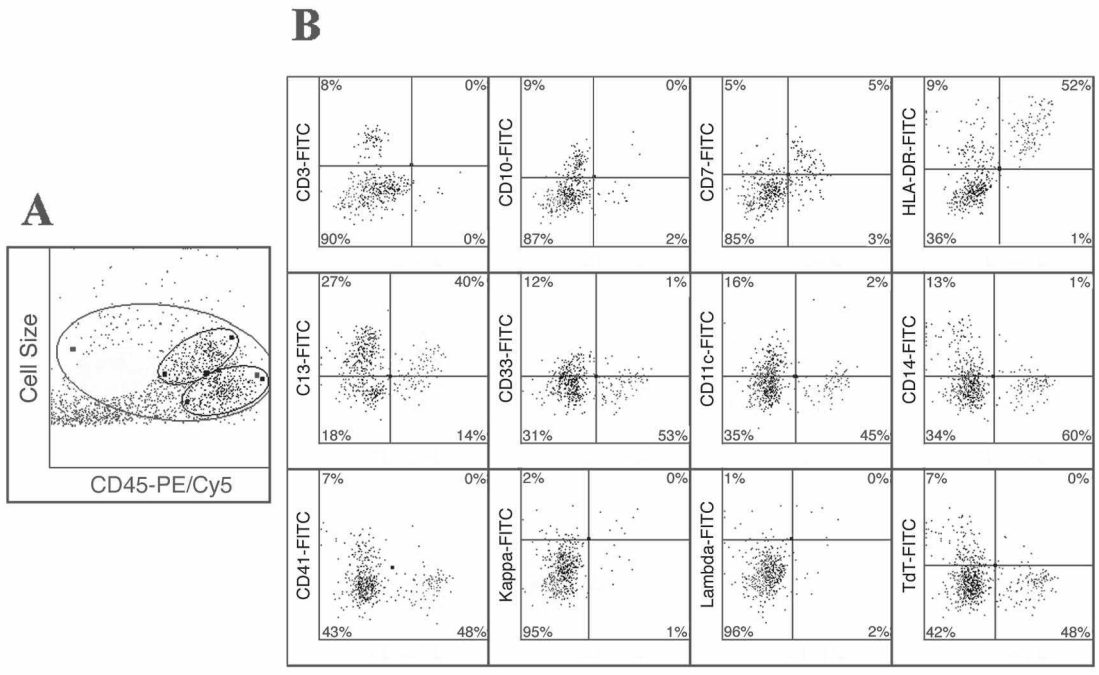
A
Cell Size
CD45-PE/Cy5
B
CD3-FITC
8%
0%
90%
0%
CD10-FITC
9%
0%
87%
2%
CD7-FITC
5%
5%
85%
3%
HLA-DR-FITC
9%
52%
36%
1%
C13-FITC
27%
40%
18%
14%
CD33-FITC
12%
1%
31%
53%
CD11c-FITC
16%
2%
35%
45%
CD14-FITC
13%
1%
34%
60%
CD41-FITC
7%
0%
43%
48%
Kappa-FITC
2%
0%
95%
1%
Lambda-FITC
1%
0%
96%
2%
TdT-FITC
7%
0%
42%
48%

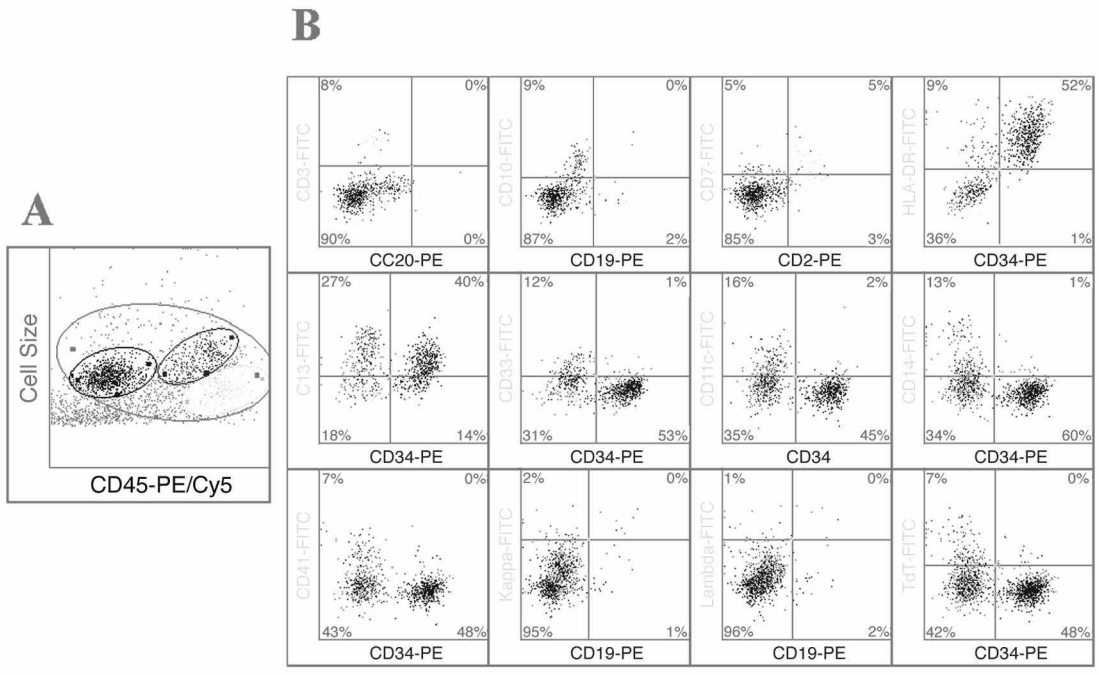
A
Cell Size
CD45-PE/Cy5
B
CD3-FITC
8%
0%
90%
0%
CC20-PE
CD10-FITC
9%
0%
87%
2%
CD19-PE
CD7-FITC
5%
5%
85%
3%
CD2-PE
HLA-DR-FITC
9%
52%
36%
1%
CD34-PE
C13-FITC
27%
40%
18%
14%
CD34-PE
CD33-FITC
12%
1%
31%
53%
CD34-PE
CD11c-FITC
16%
2%
35%
45%
CD34
CD14-FITC
13%
1%
34%
60%
CD34-PE
CD41-FITC
7%
0%
43%
48%
CD34-PE
Kappa-FITC
2%
0%
95%
1%
CD19-PE
Lambda-FITC
1%
0%
96%
2%
CD19-PE
TdT-FITC
7%
0%
42%
48%
CD34-PE

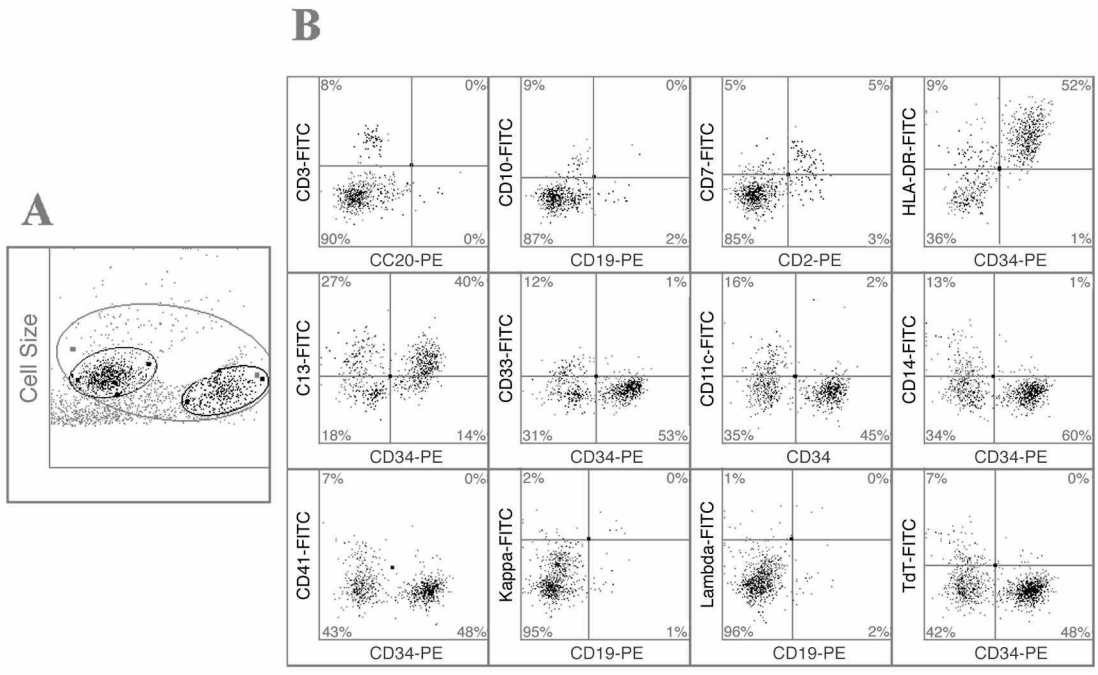
A
Cell Size
B
CD3-FITC
CC20-PE
8%
0%
90%
0%
CD10-FITC
CD19-PE
9%
0%
87%
2%
CD7-FITC
CD2-PE
5%
5%
85%
3%
HLA-DR-FITC
CD34-PE
9%
52%
36%
1%
C13-FITC
CD34-PE
27%
40%
18%
14%
CD33-FITC
CD34-PE
12%
1%
31%
53%
CD11c-FITC
CD34
16%
2%
35%
45%
CD14-FITC
CD34-PE
13%
1%
34%
60%
CD41-FITC
CD34-PE
7%
0%
43%
48%
Kappa-FITC
CD19-PE
2%
0%
95%
1%
Lambda-FITC
CD19-PE
1%
0%
96%
2%
TdT-FITC
CD34-PE
7%
0%
42%
48%

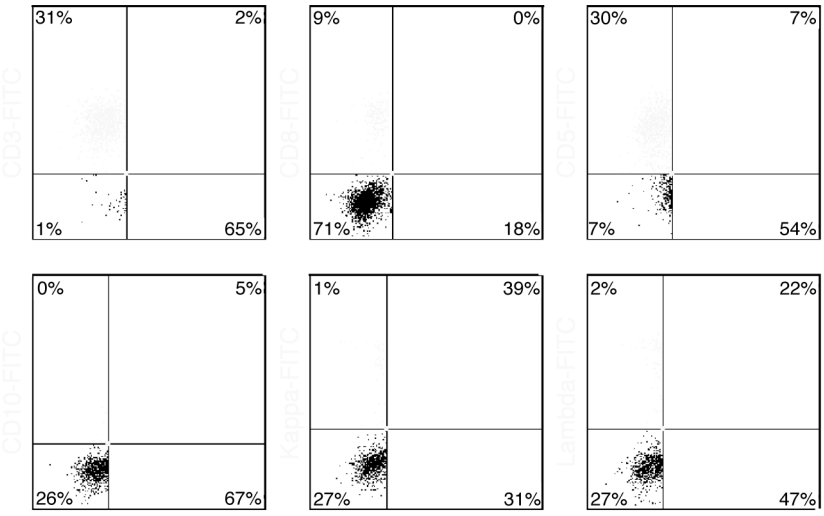

Fig. 6.9 A fine needle aspiration biopsy of a parotid mass from a 13-year-old boy with Burkitt's lymphoma. Values represent the percentage of cells found in each quadrant. See text for full details.

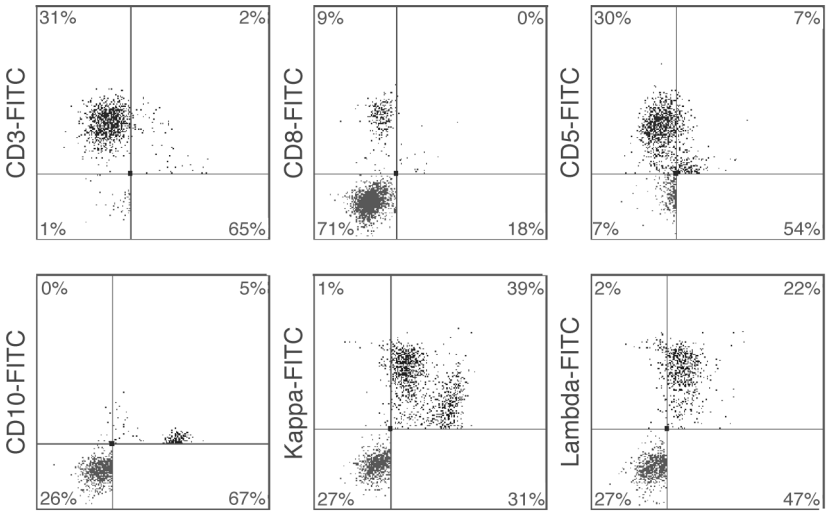
CD3-FITC
31%
2%
1%
65%
CD8-FITC
9%
0%
71%
18%
CD5-FITC
30%
7%
7%
54%
CD10-FITC
0%
5%
26%
67%
Kappa-FITC
1%
39%
27%
31%
Lambda-FITC
2%
22%
27%
47%

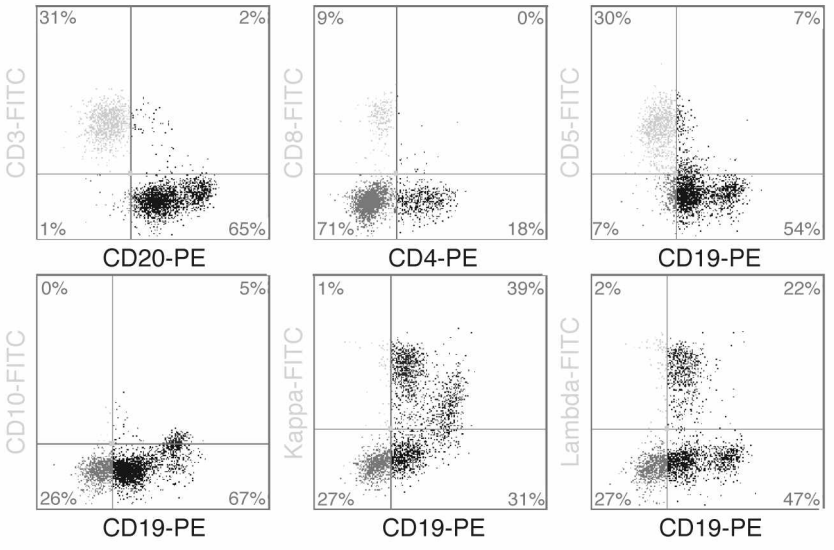
CD3-FITC
31%
2%
1%
65%
CD20-PE
CD8-FITC
9%
0%
71%
18%
CD4-PE
CD5-FITC
30%
7%
7%
54%
CD19-PE
CD10-FITC
0%
5%
26%
67%
CD19-PE
Kappa-FITC
1%
39%
27%
31%
CD19-PE
Lambda-FITC
2%
22%
27%
47%
CD19-PE

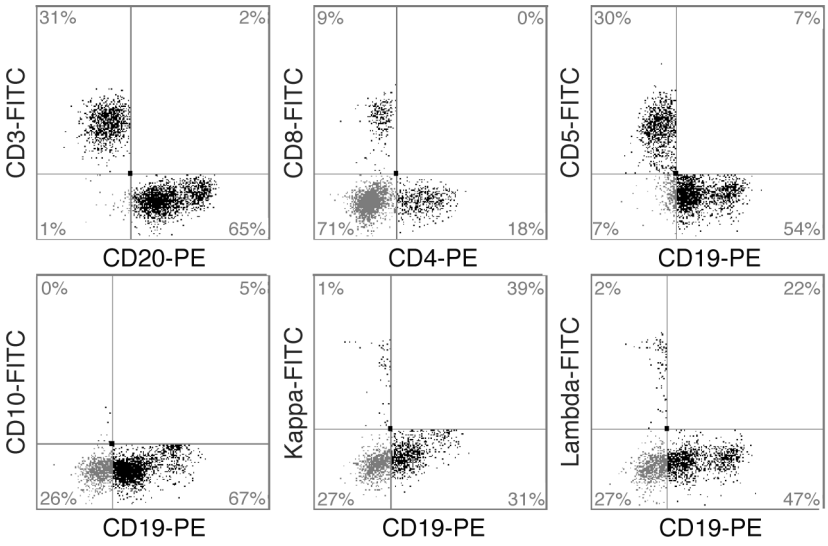
31%
2%
1%
65%
CD3-FITC
CD20-PE
9%
0%
71%
18%
CD8-FITC
CD4-PE
30%
7%
7%
54%
CD5-FITC
CD19-PE
0%
5%
26%
67%
CD10-FITC
CD19-PE
1%
39%
27%
31%
Kappa-FITC
CD19-PE
2%
22%
27%
47%
Lambda-FITC
CD19-PE

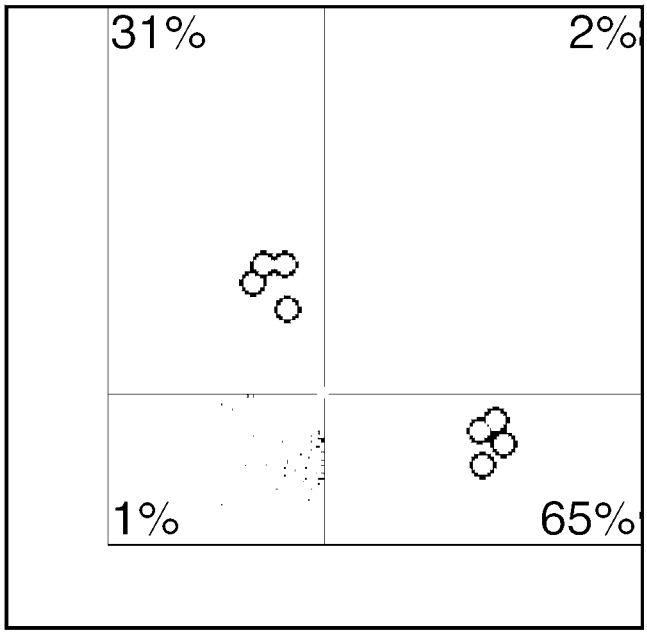

Fig. 6.10 Selection of cells for relocalisation from those used in Fig. 6.9.

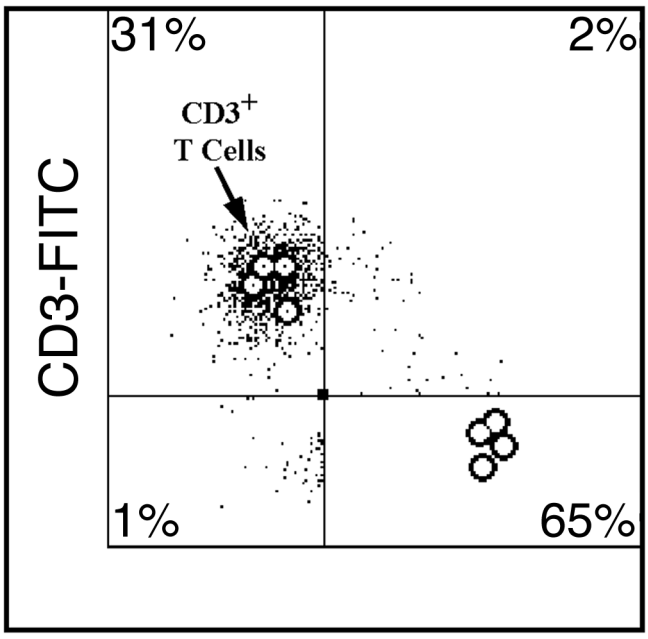
31%
2%
CD3+
T Cells
CD3-FITC
1%
65%

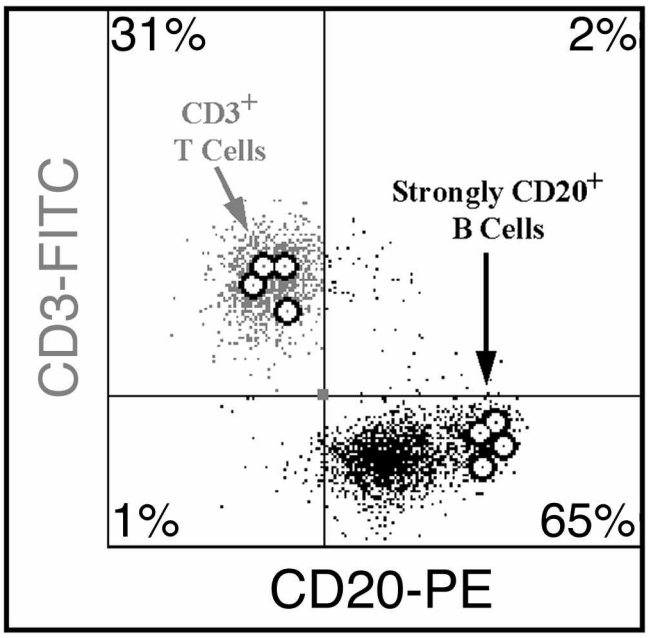
31%
2%
CD3+
T Cells
Strongly CD20+
B Cells
CD3-FITC
1%
65%
CD20-PE

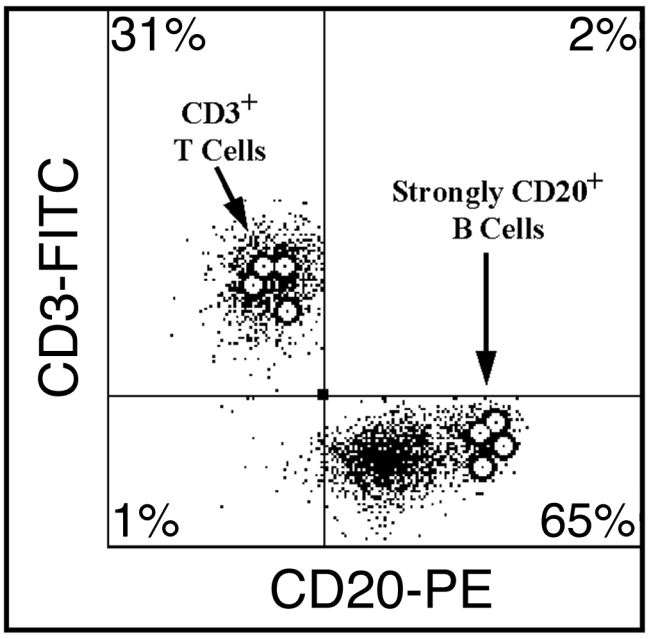
31%
2%
CD3+
T Cells
Strongly CD20+
B Cells
CD3-FITC
1%
65%
CD20-PE

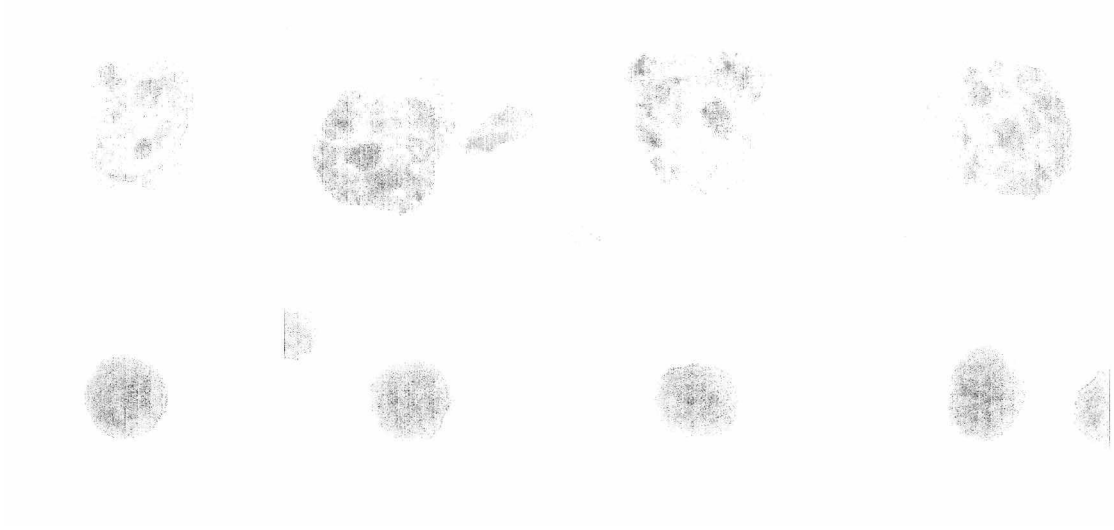

Fig. 6.11 Light microscopy of the cells relocated in Fig. 6.10. Cells are stained with Wright–Giemsa and B-cells are shown in the top row and T-cells in the bottom.

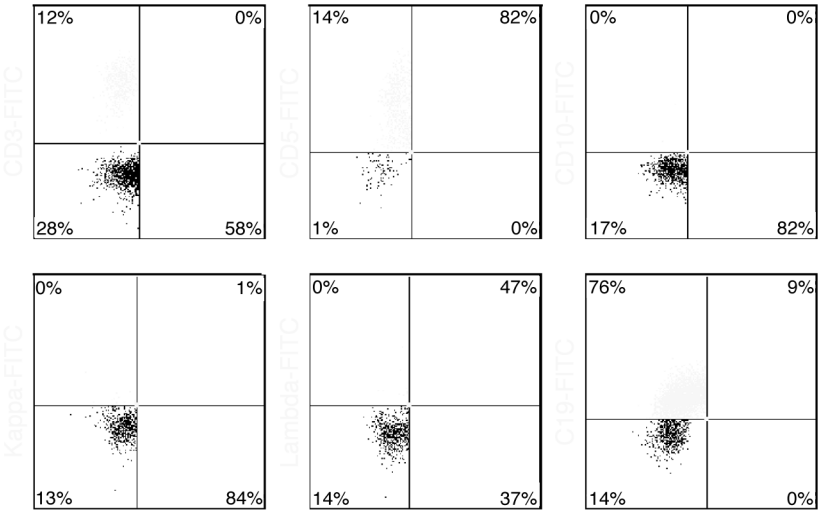

Fig. 6.12 Peripheral blood from a patient with chronic lymphocytic leukaemia.

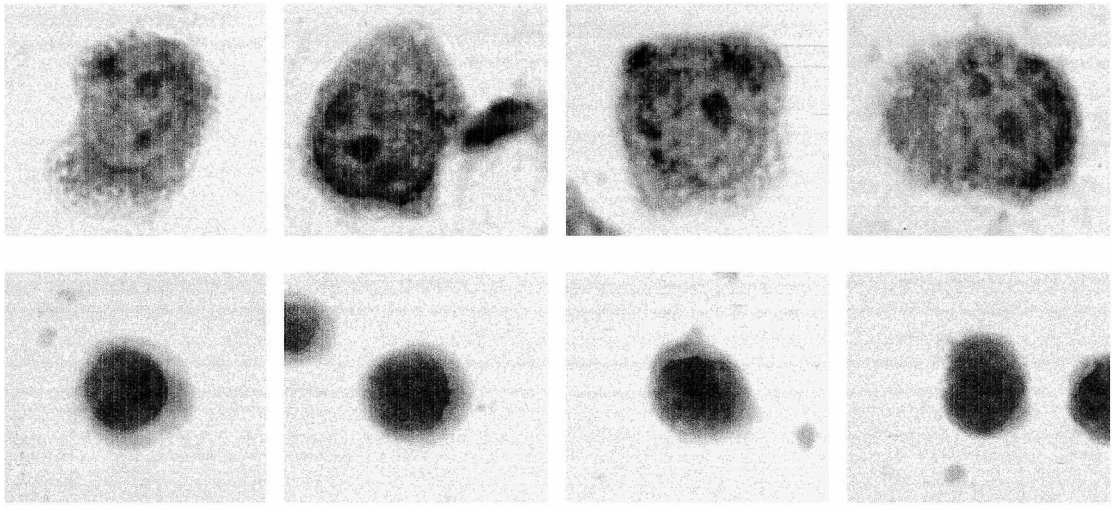

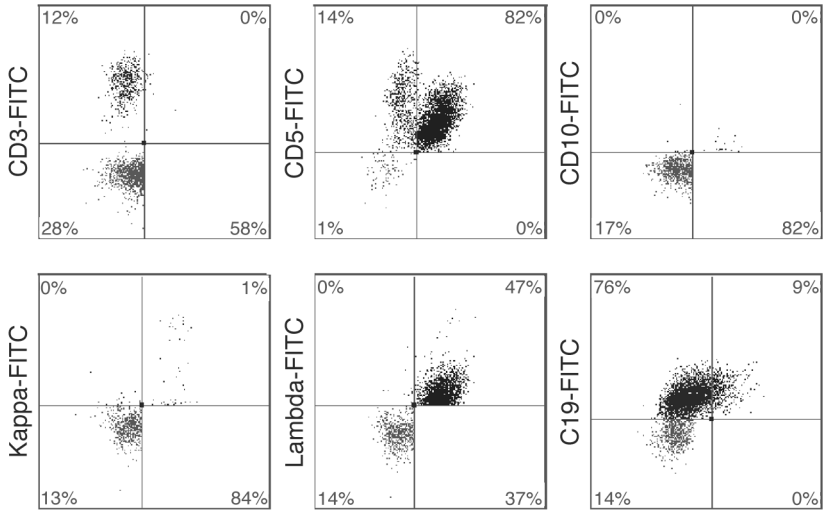
CD3-FITC
12%
0%
28%
58%
CD5-FITC
14%
82%
1%
0%
CD10-FITC
0%
0%
17%
82%
Kappa-FITC
0%
1%
13%
84%
Lambda-FITC
0%
47%
14%
37%
C19-FITC
76%
9%
14%
0%

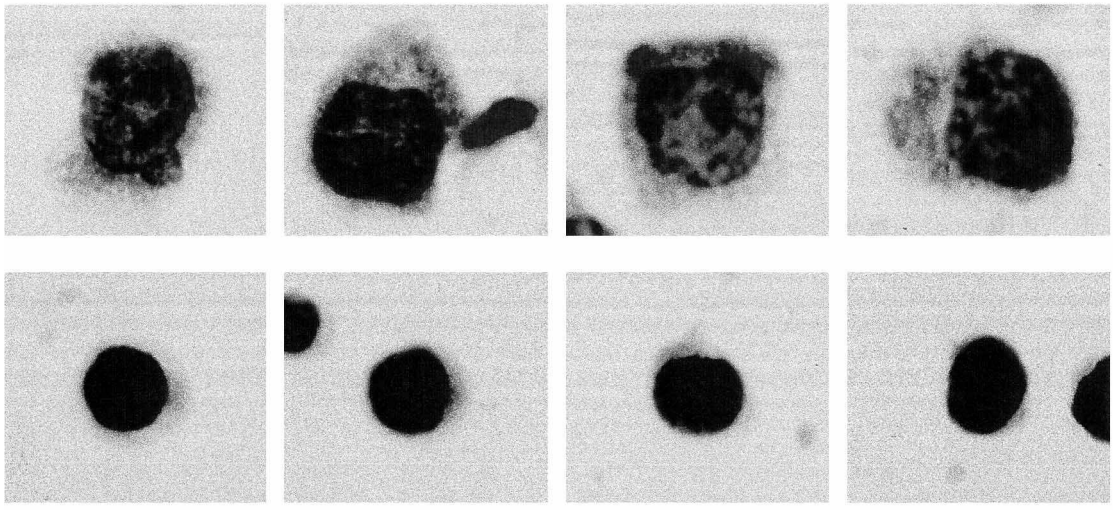

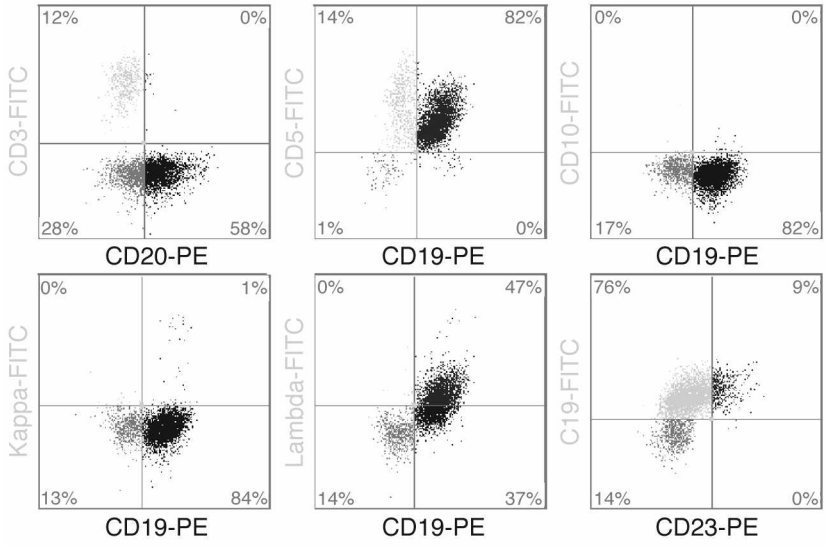
CD3-FITC
12%
0%
28%
58%
CD20-PE
CD5-FITC
14%
82%
1%
0%
CD19-PE
CD10-FITC
0%
0%
17%
82%
CD19-PE
Kappa-FITC
0%
1%
13%
84%
CD19-PE
Lambda-FITC
0%
47%
14%
37%
CD19-PE
C19-FITC
76%
9%
14%
0%
CD23-PE

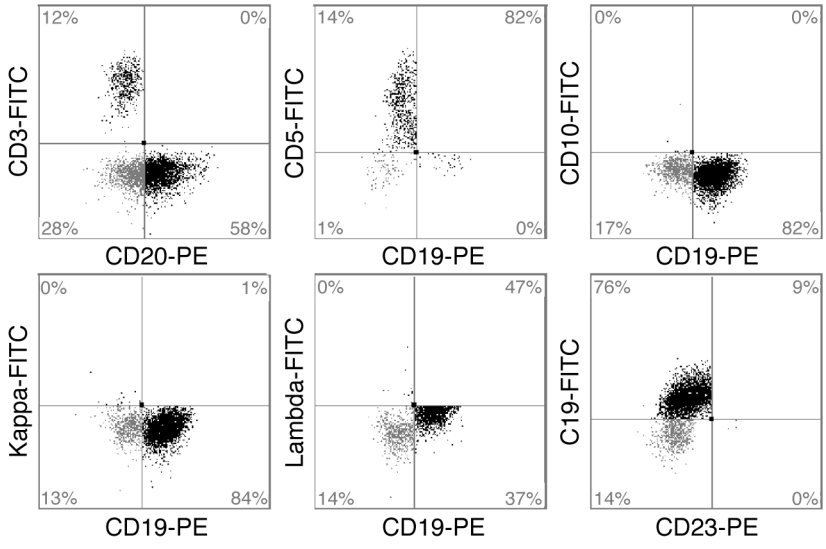
12%
0%
28%
58%
CD3-FITC
CD20-PE
14%
82%
1%
0%
CD5-FITC
CD19-PE
0%
0%
17%
82%
CD10-FITC
CD19-PE
0%
1%
13%
84%
Kappa-FITC
CD19-PE
0%
47%
14%
37%
Lambda-FITC
CD19-PE
76%
9%
14%
0%
C19-FITC
CD23-PE

Fig. 6.13 Selection of cells for relocalisation from the sample illustrated in Fig. 6.12.

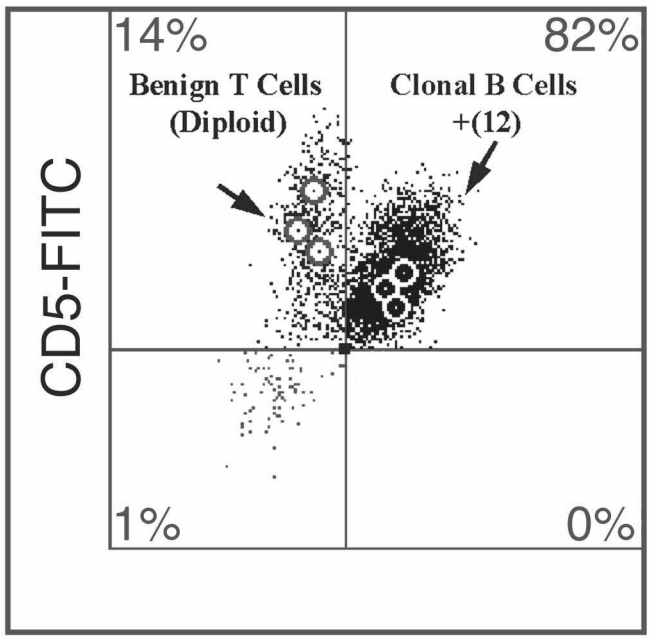
14%
82%
Benign T Cells
(Diploid)
Clonal B Cells
+(12)
CD5-FITC
1%
0%

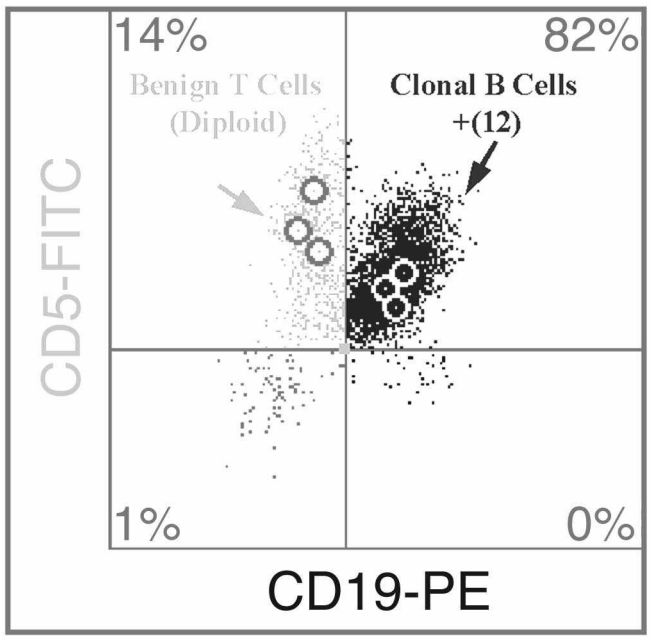
14%
82%
Benign T Cells
(Diploid)
Clonal B Cells
+(12)
CD5-FITC
1%
0%
CD19-PE

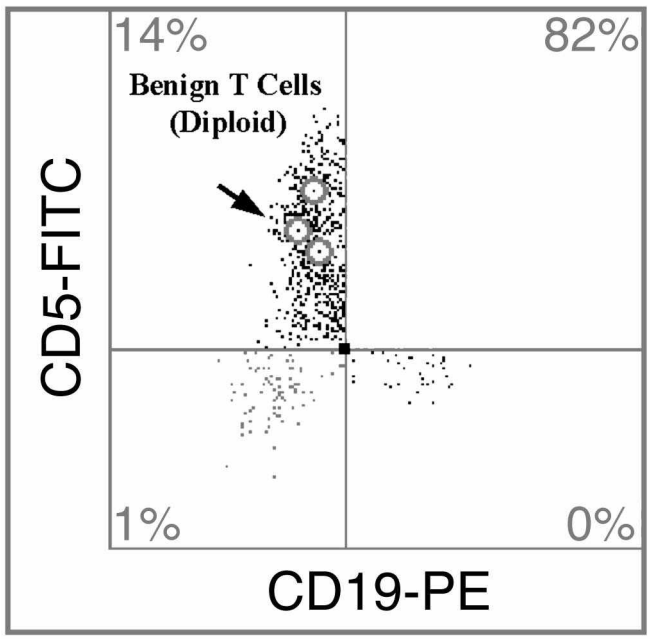
14%
82%
Benign T Cells
(Diploid)
CD5-FITC
1%
0%
CD19-PE

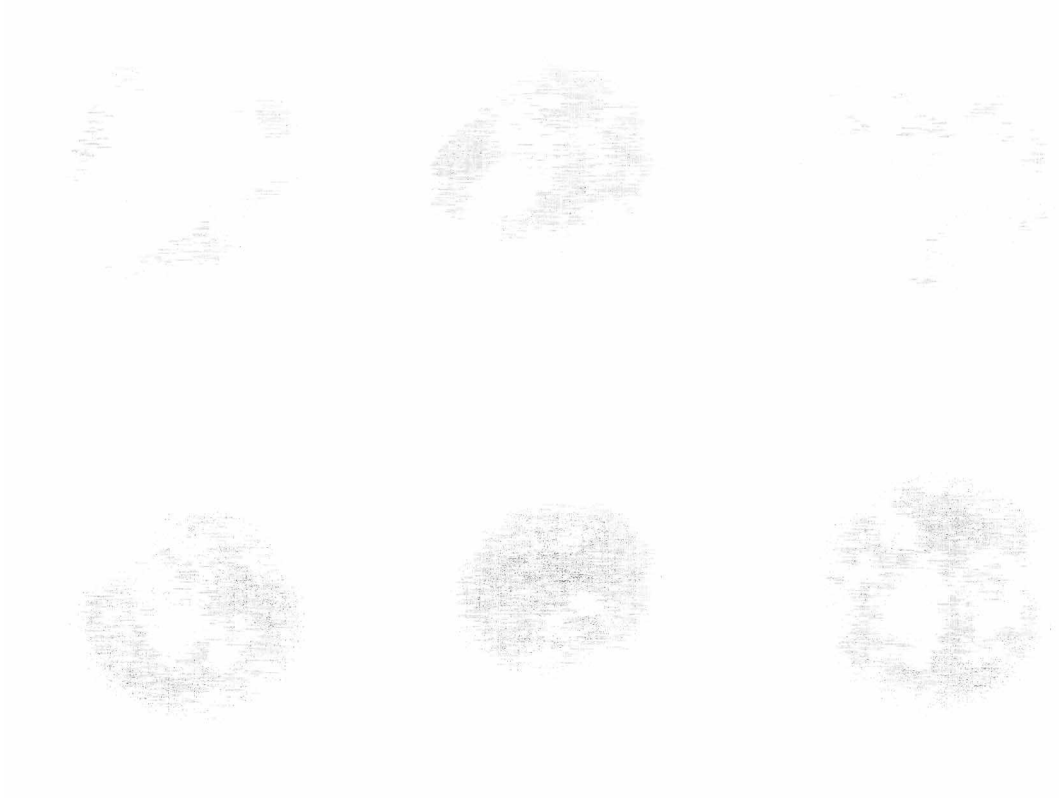

Fig. 6.14 Light microscopy of the cells relocated in Fig. 6.13. Cells are stained with Wright–Giemsa and B-cells are shown in the top row and T-cells in the bottom.

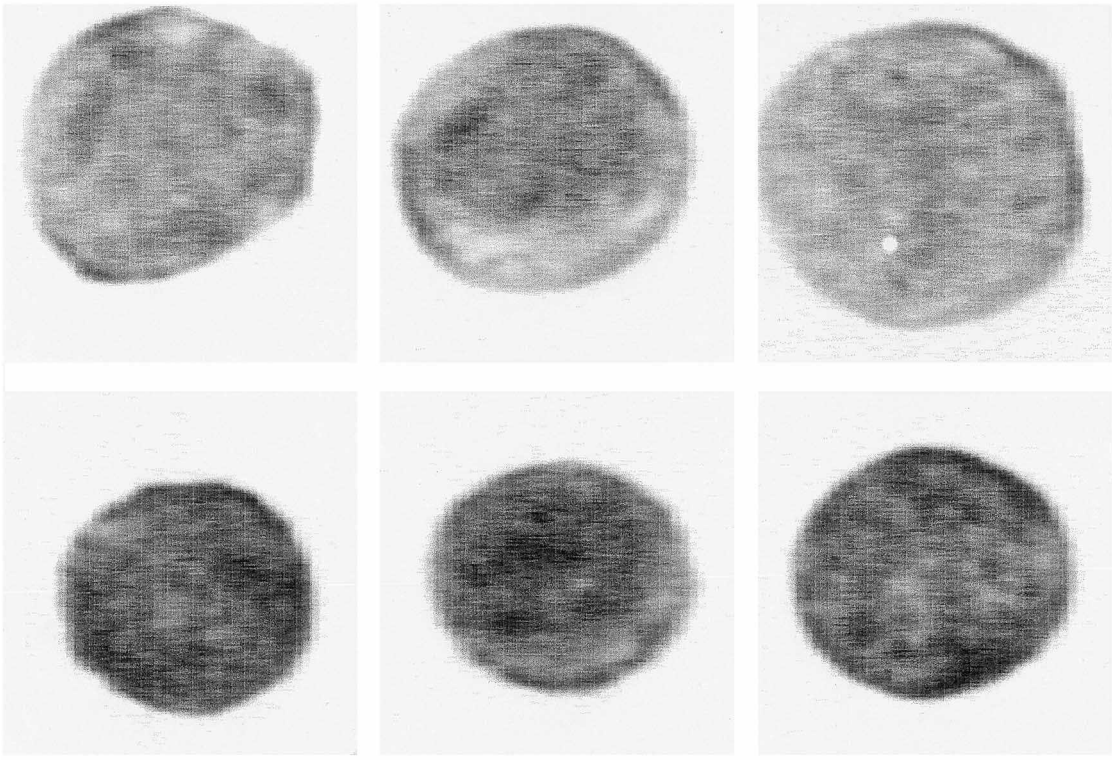

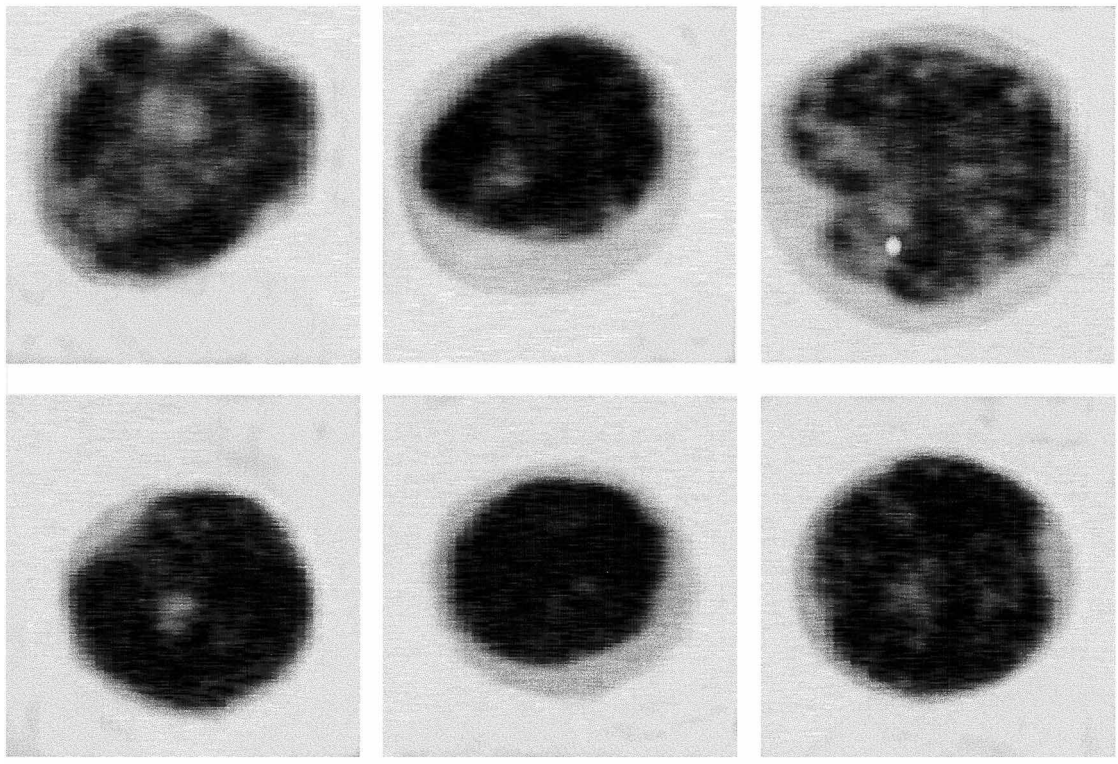

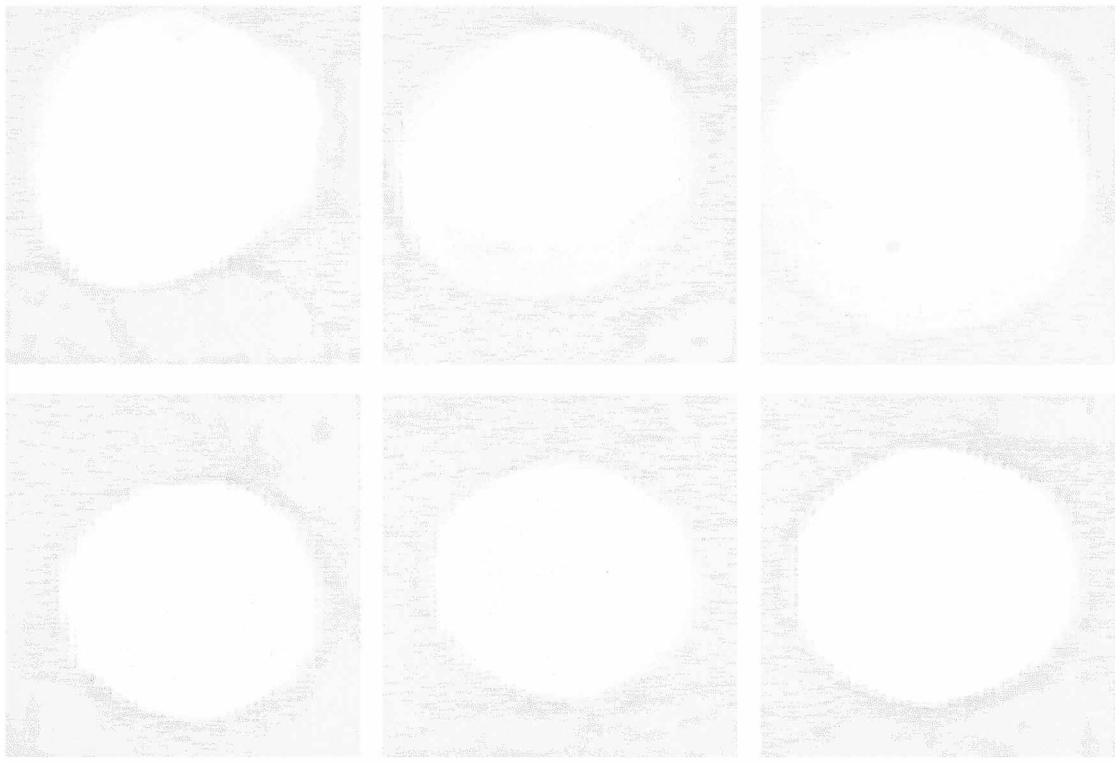

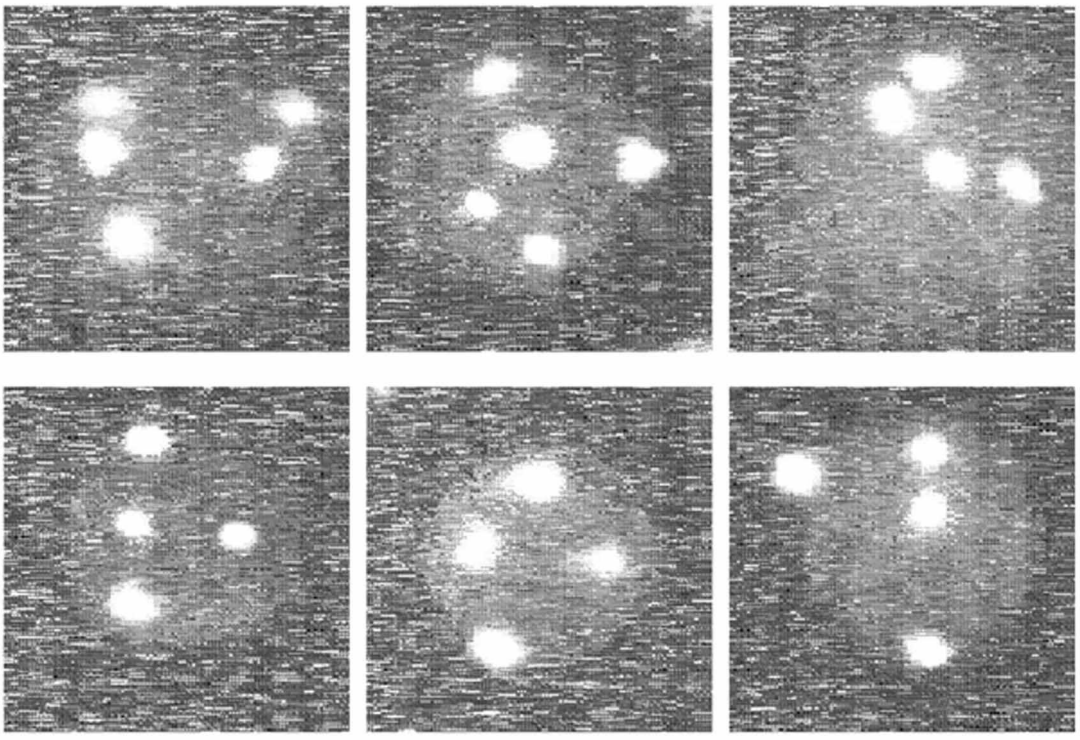

Fig. 6.15 Relocalisation of cells for in situ hybridisation by epifluorescence microscopy. The top row is the B-cells and the bottom row is the T-cells.

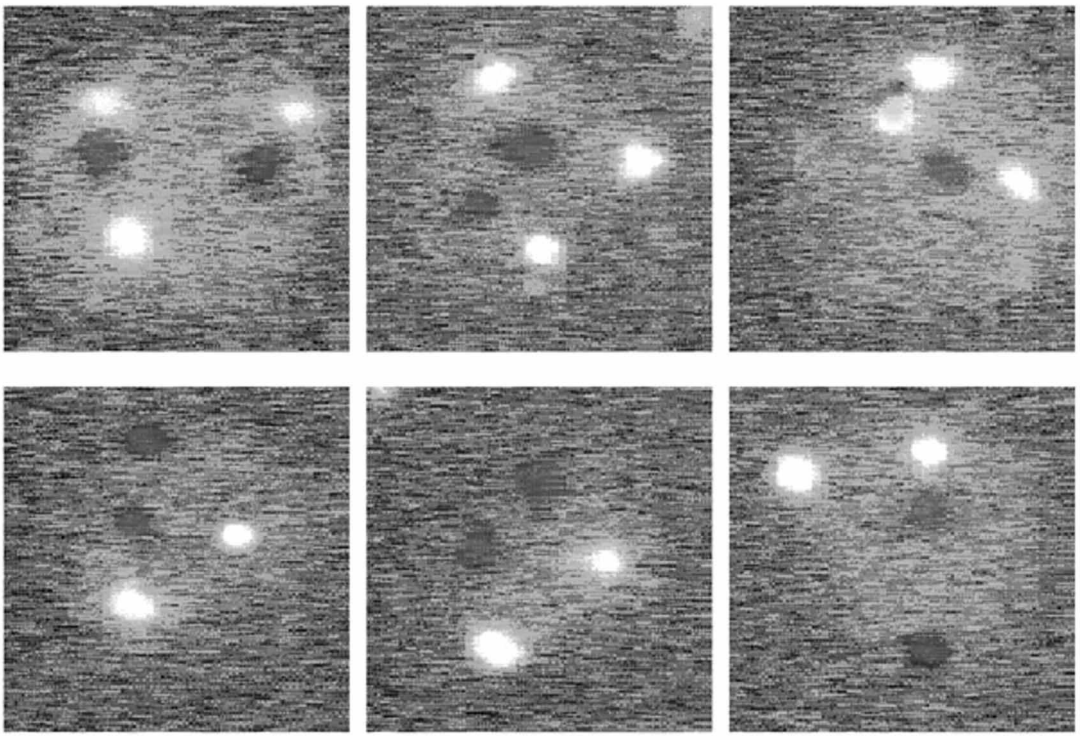

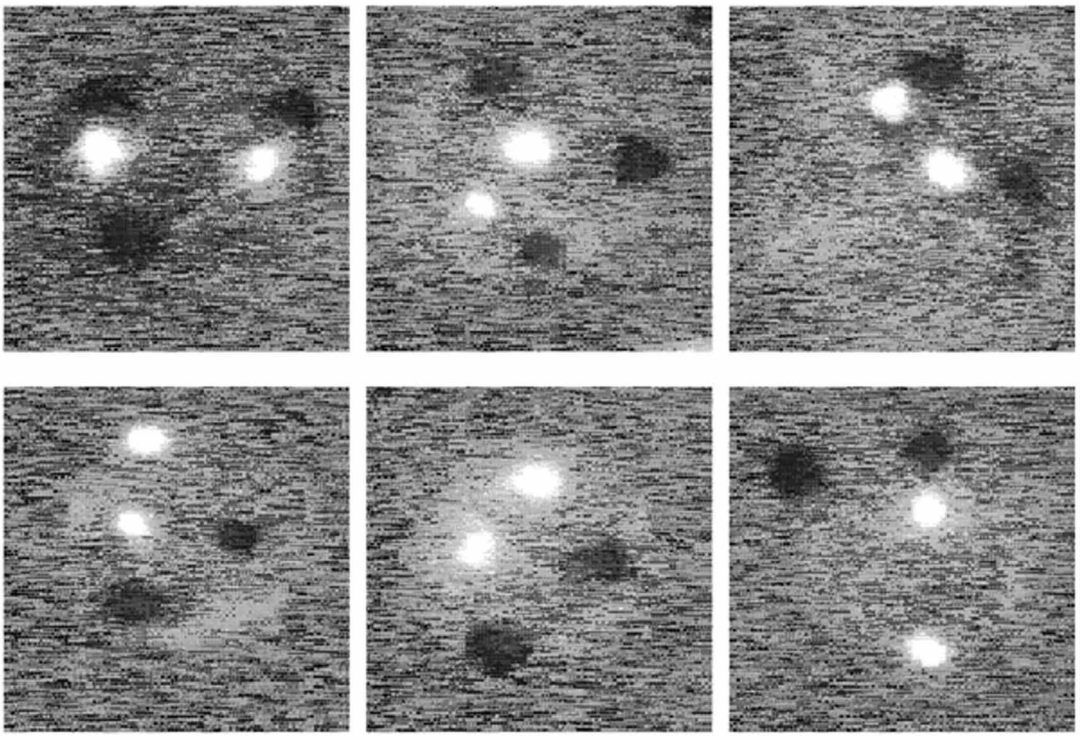

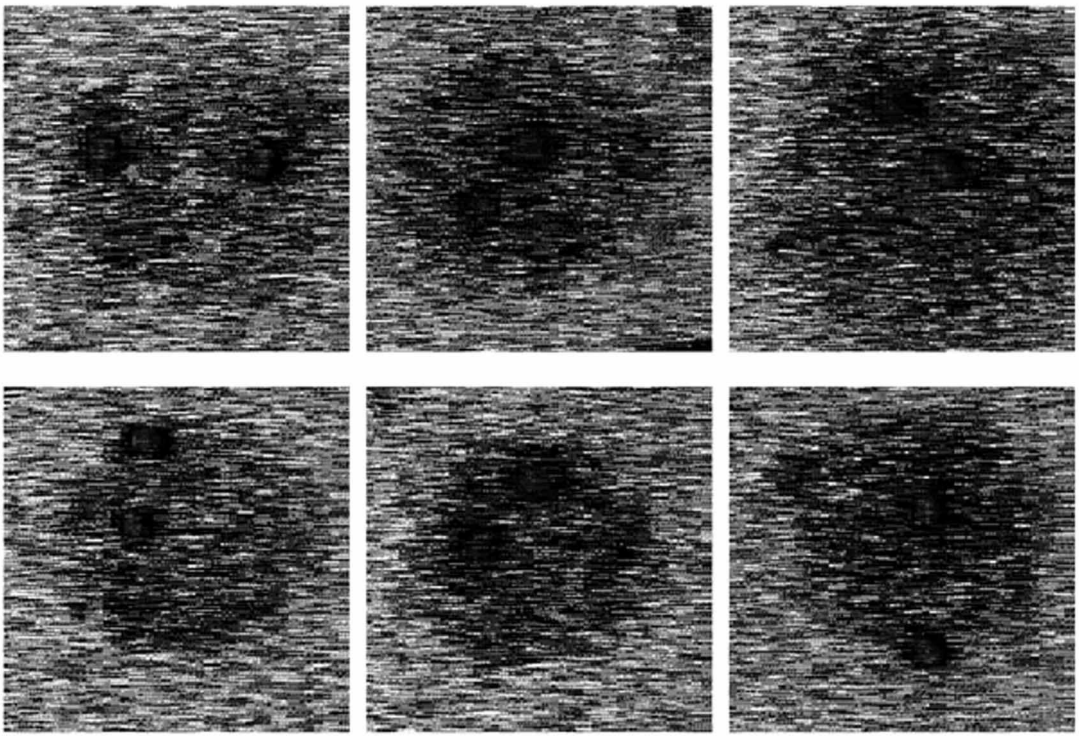

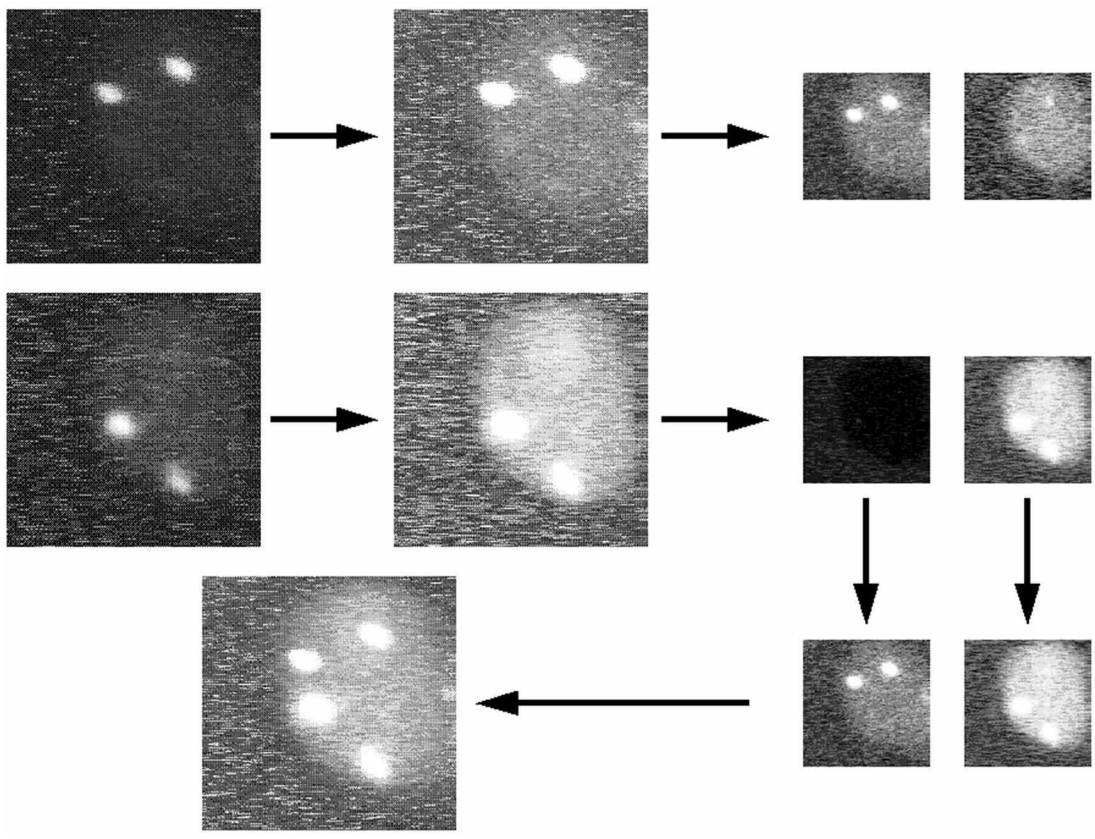

Fig. 6.16 Enhancement of the epifluorescence video images of the fluorescence in situ hybridisation probe spots in Fig. 6.15.

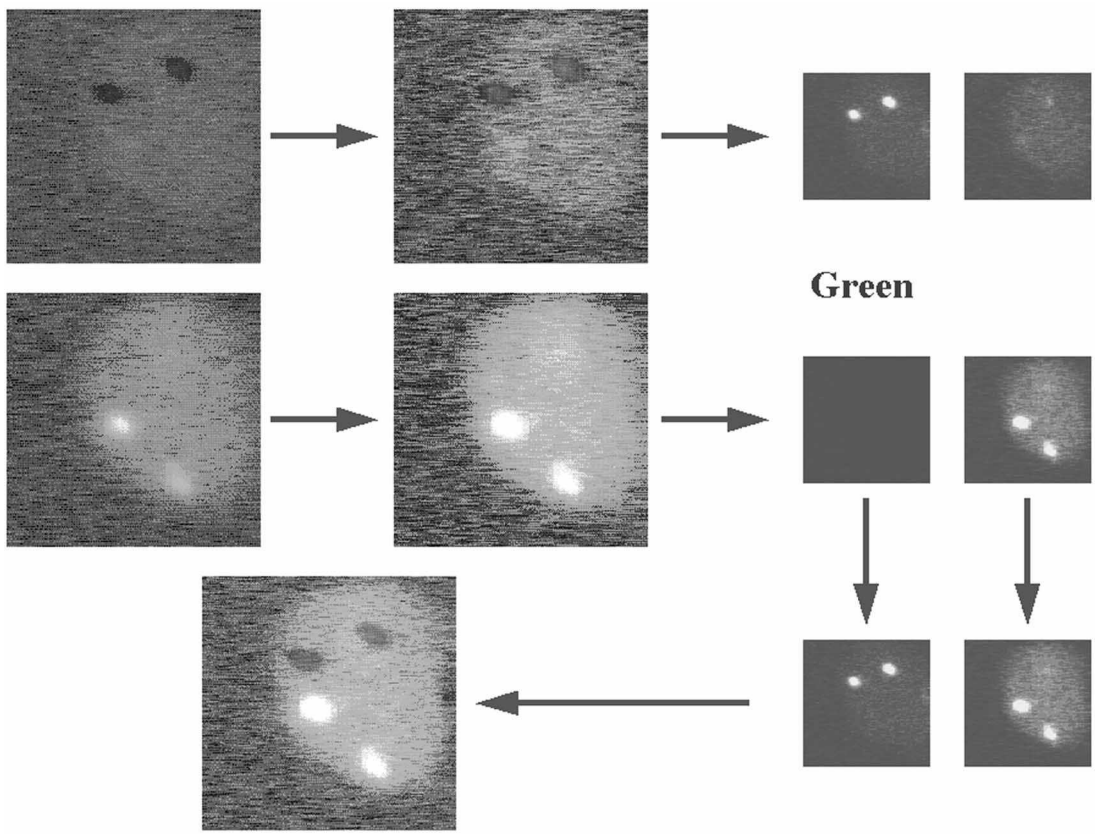
Green

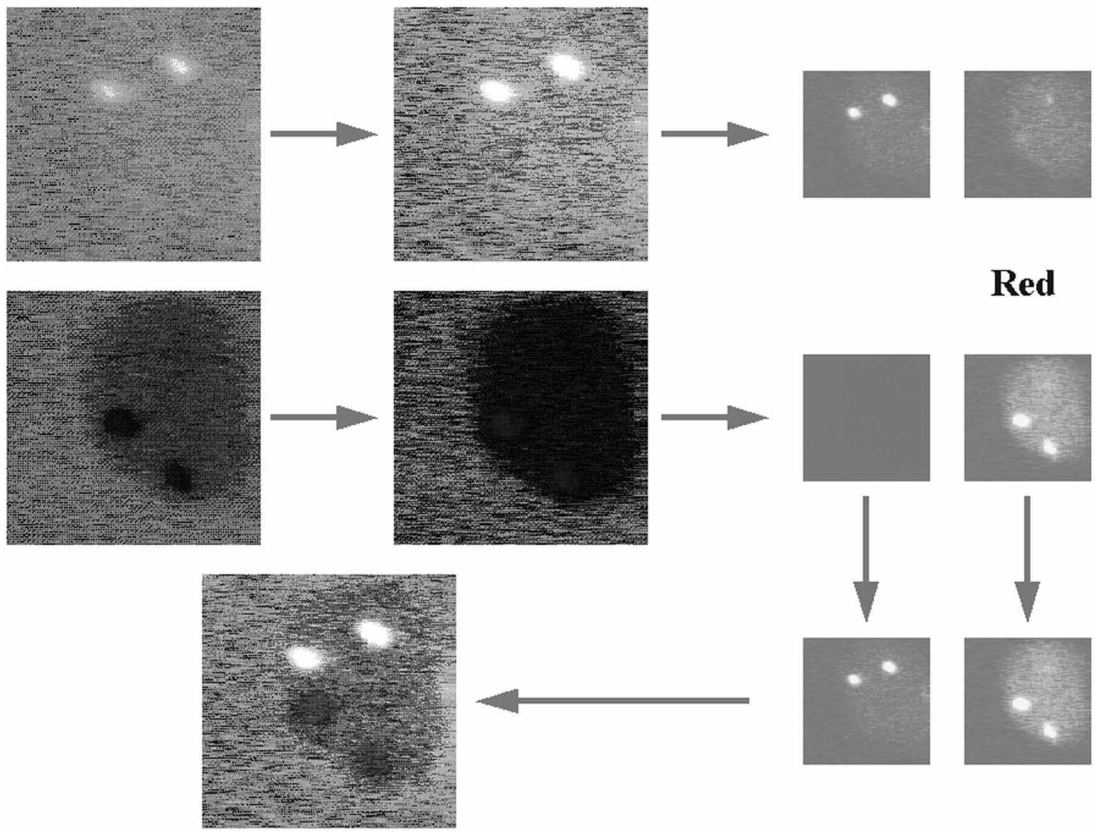
Red

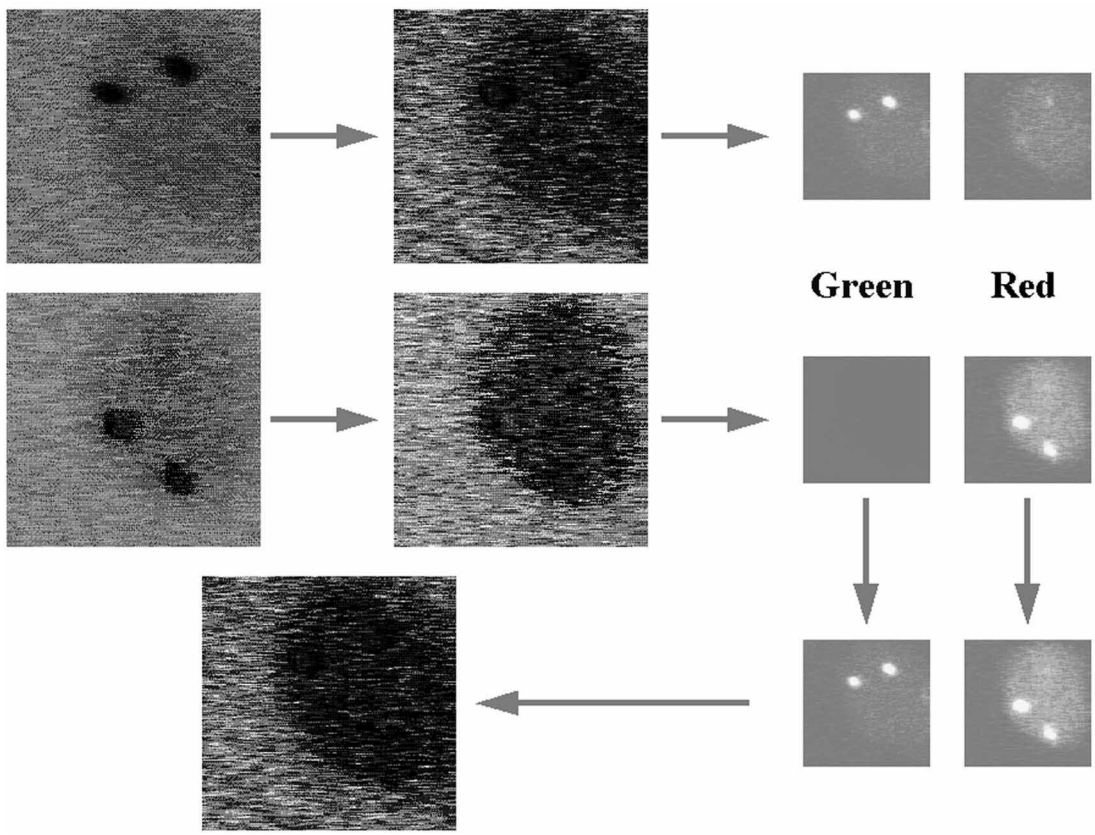
Green
Red

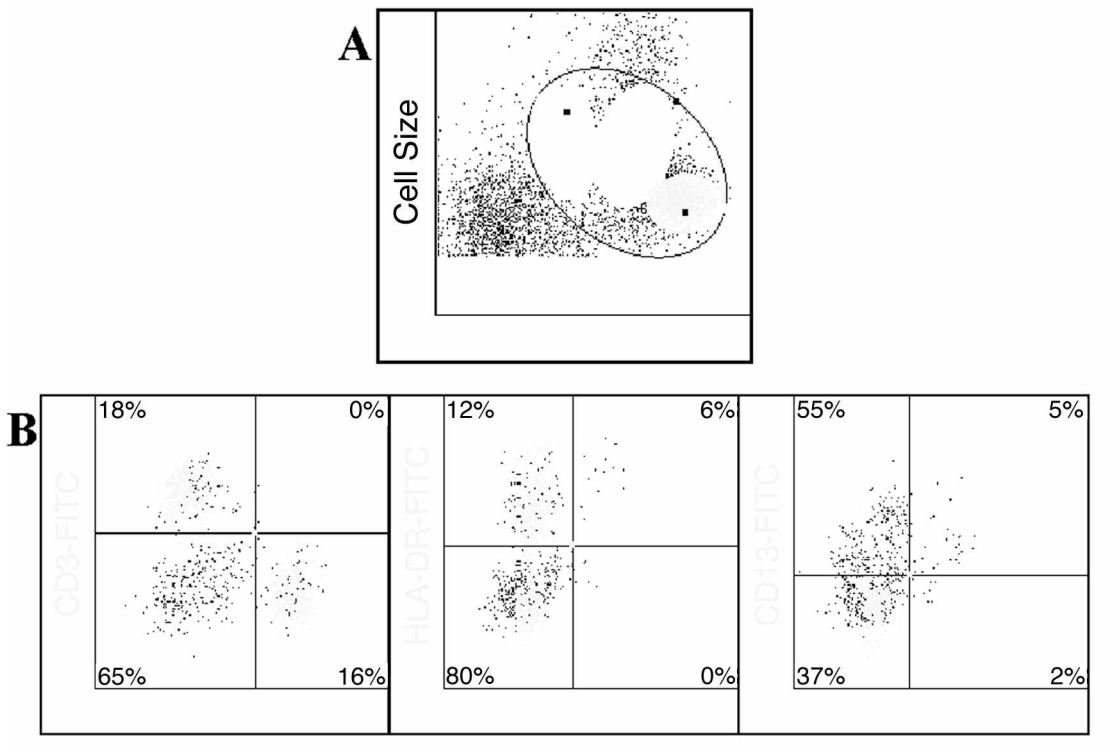

Fig. 6.17 Bone marrow aspirate from a 48-year-old woman with chronic myeloid leukaemia in blast crisis. The $CD45^{+}$ cells which were gated (A) and subsequently displayed as three separate fluorescein isothiocyanate (FITC) versus phycoerythrin (PE) histograms (B). See text for full details.

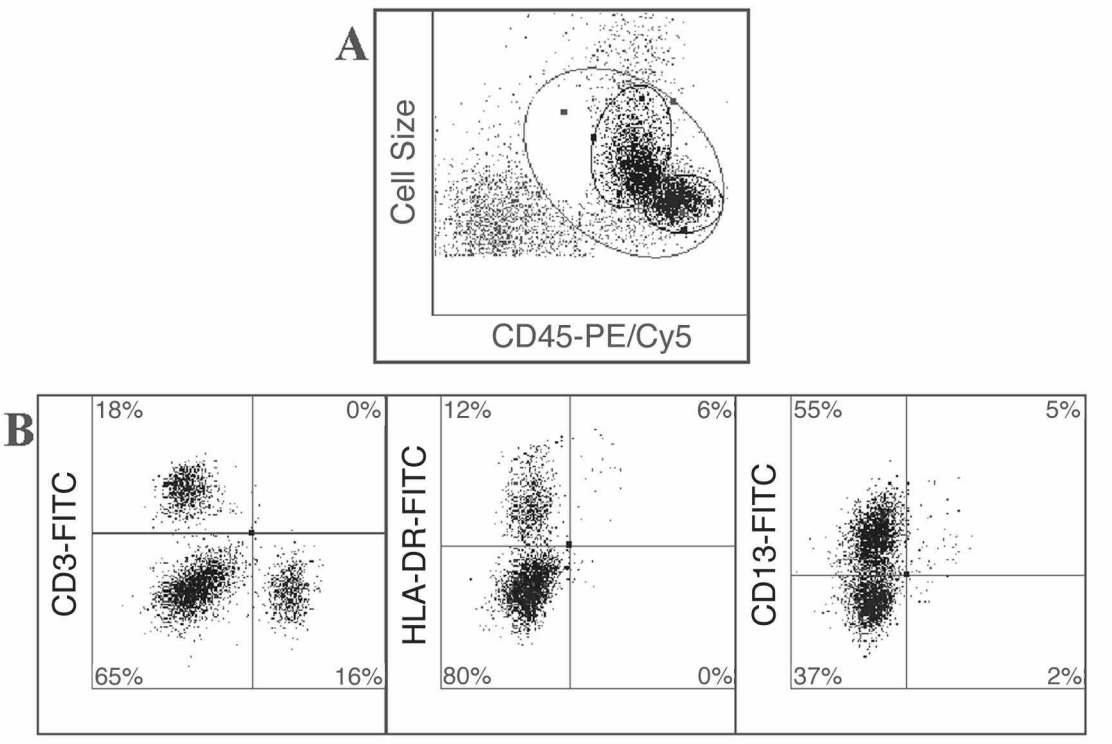
A
Cell Size
CD45-PE/Cy5
B
CD3-FITC
18%
0%
65%
16%
HLA-DR-FITC
12%
6%
80%
0%
CD13-FITC
55%
5%
37%
2%

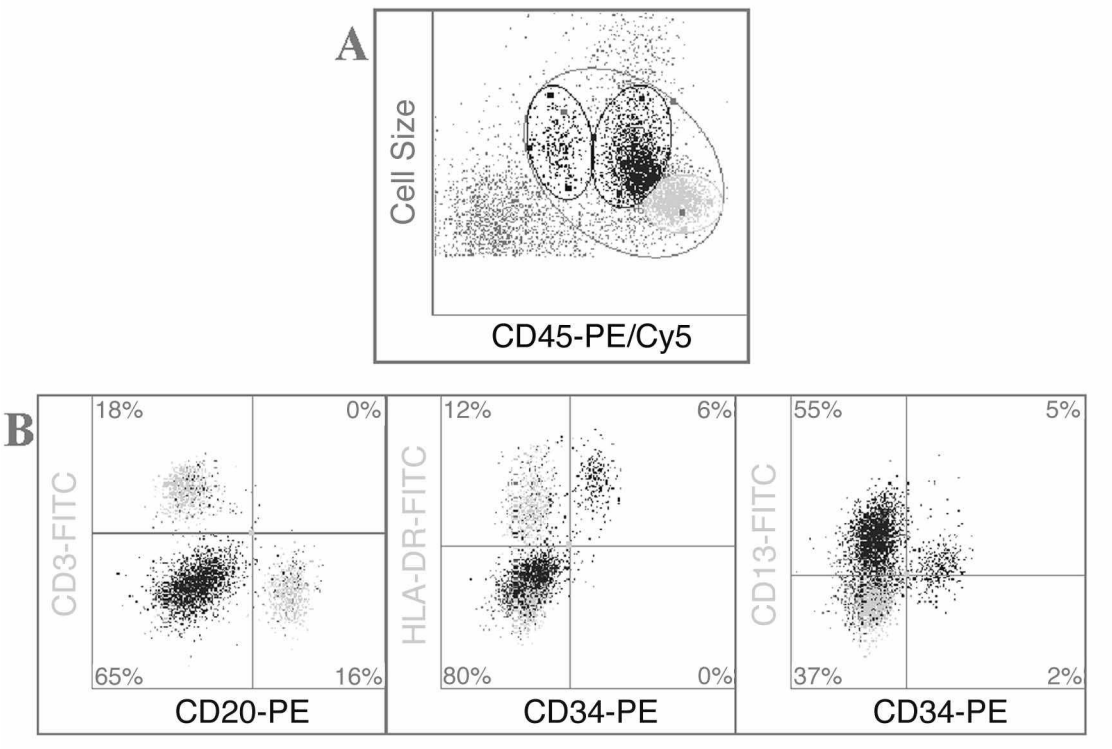
A
Cell Size
CD45-PE/Cy5
B
CD3-FITC
18%
0%
65%
16%
CD20-PE
HLA-DR-FITC
12%
6%
80%
0%
CD34-PE
CD13-FITC
55%
5%
37%
2%
CD34-PE

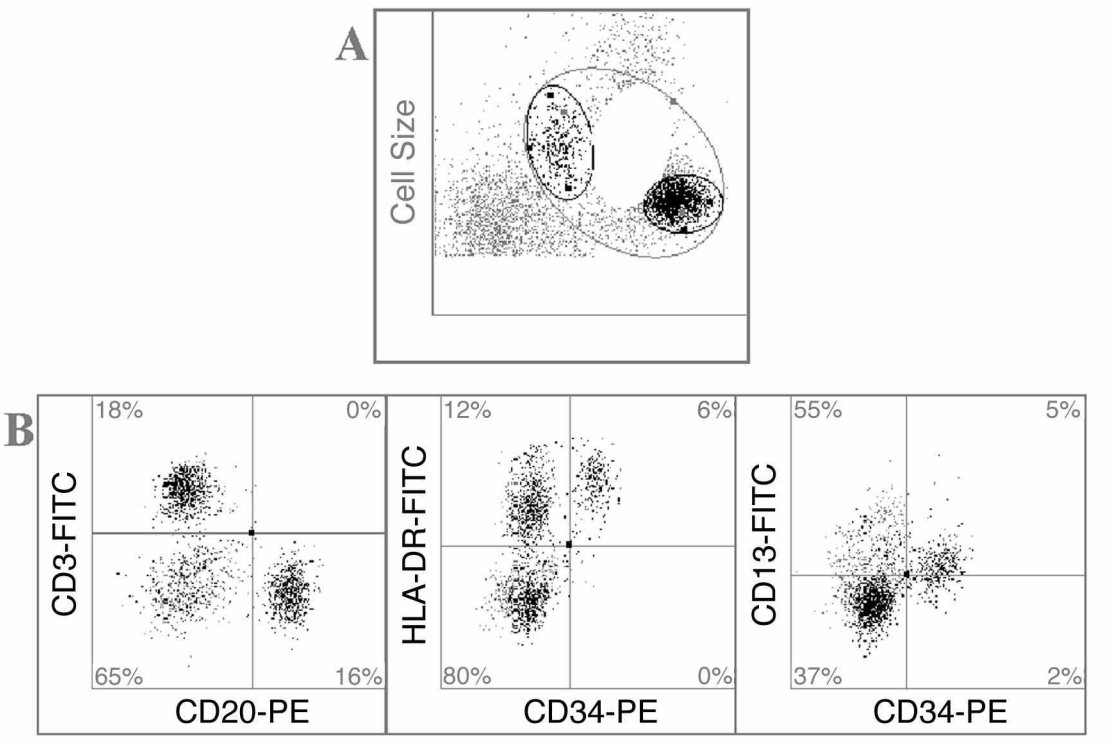
A
Cell Size
B
CD3-FITC
18%
0%
65%
16%
CD20-PE
HLA-DR-FITC
12%
6%
80%
0%
CD34-PE
CD13-FITC
55%
5%
37%
2%
CD34-PE

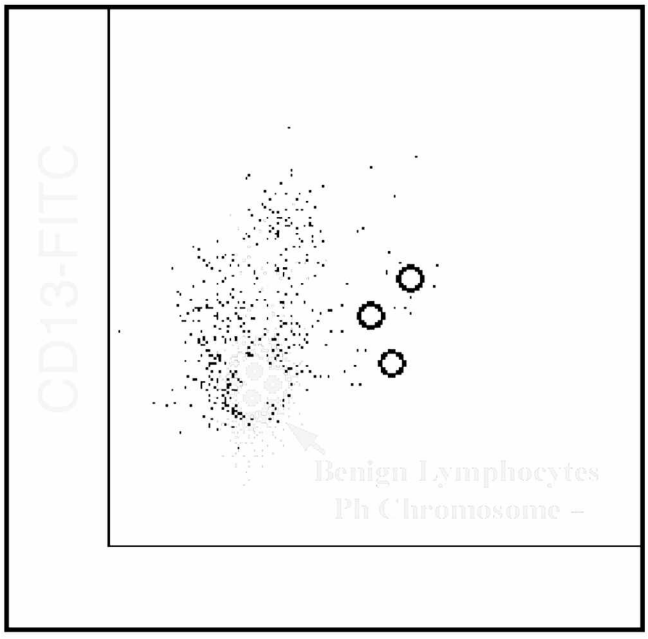

Fig. 6.18 Selection of cells for relocalisation from the $CD45^{+}$ cells that were isolated from the patient in Fig. 6.17. Ph, Philadelphia chromosome.

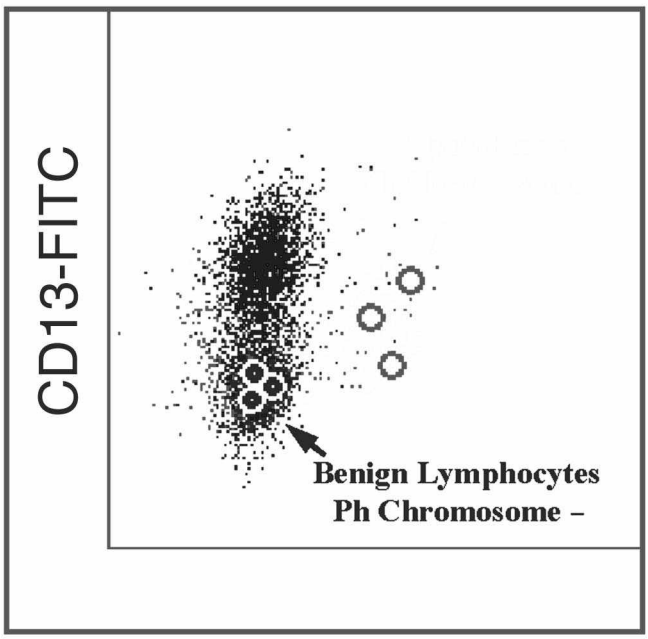
CD13-FITC
Benign Lymphocytes
Ph Chromosome –

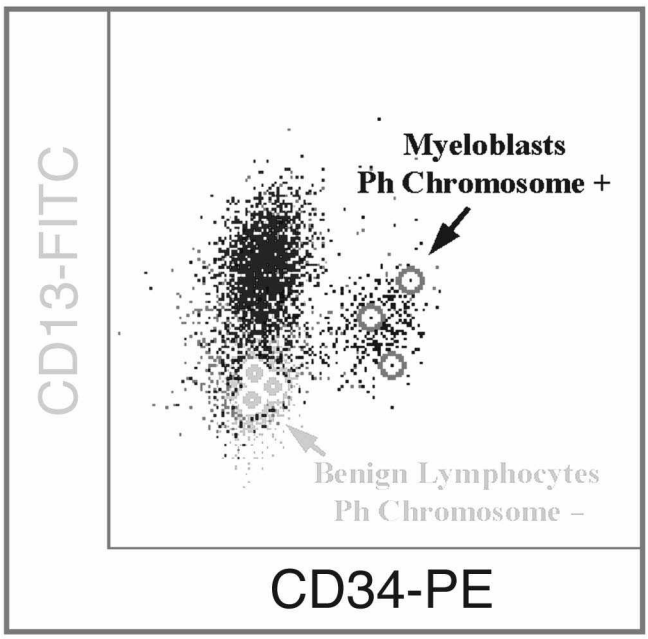
Myeloblasts
Ph Chromosome +
Benign Lymphocytes
Ph Chromosome –
CD13-FITC
CD34-PE

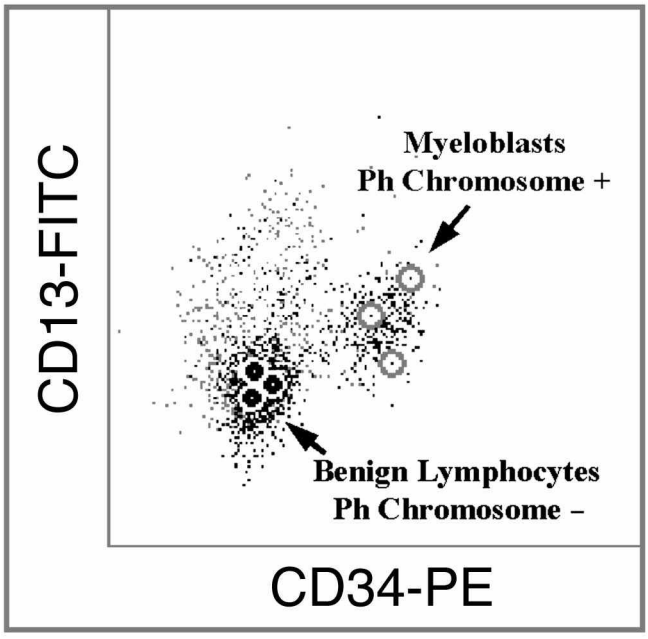
Myeloblasts
Ph Chromosome +
Benign Lymphocytes
Ph Chromosome –
CD13-FITC
CD34-PE

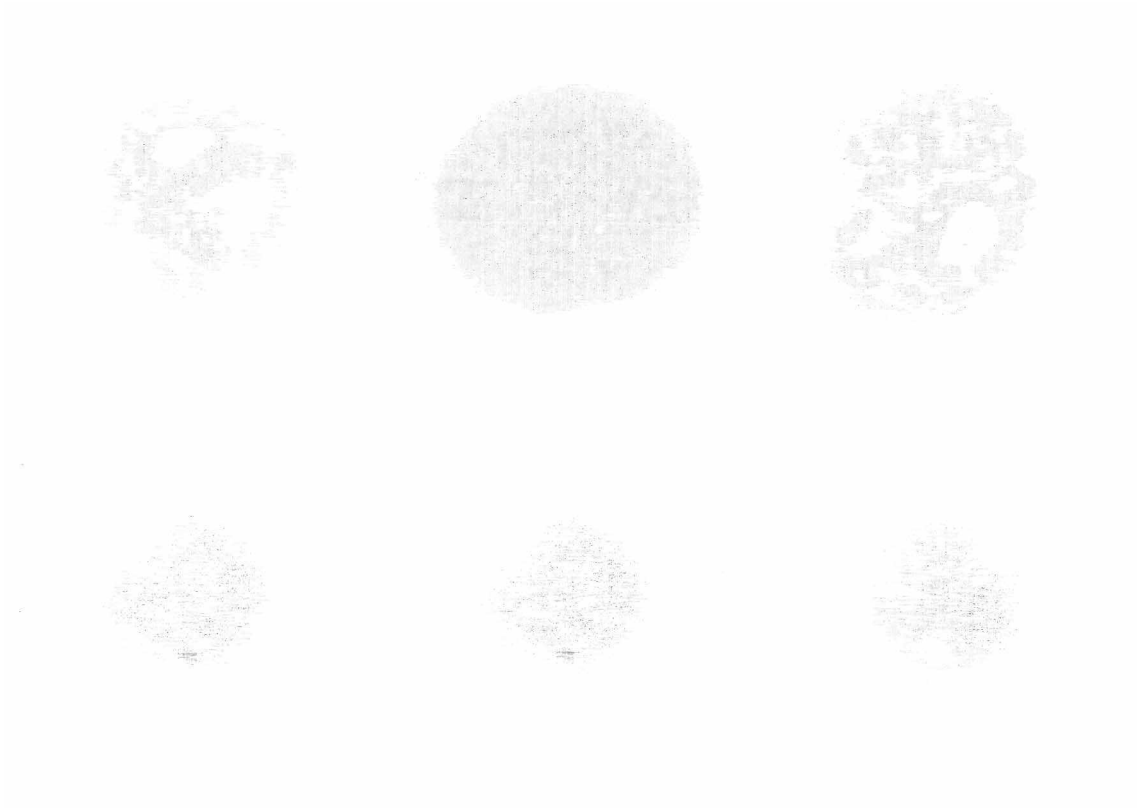

Fig. 6.19 Light microscopy of the cells relocated in Fig. 6.18 using Wright–Giemsa stain. The top row is the myeloblasts and the bottom row is lymphocytes.

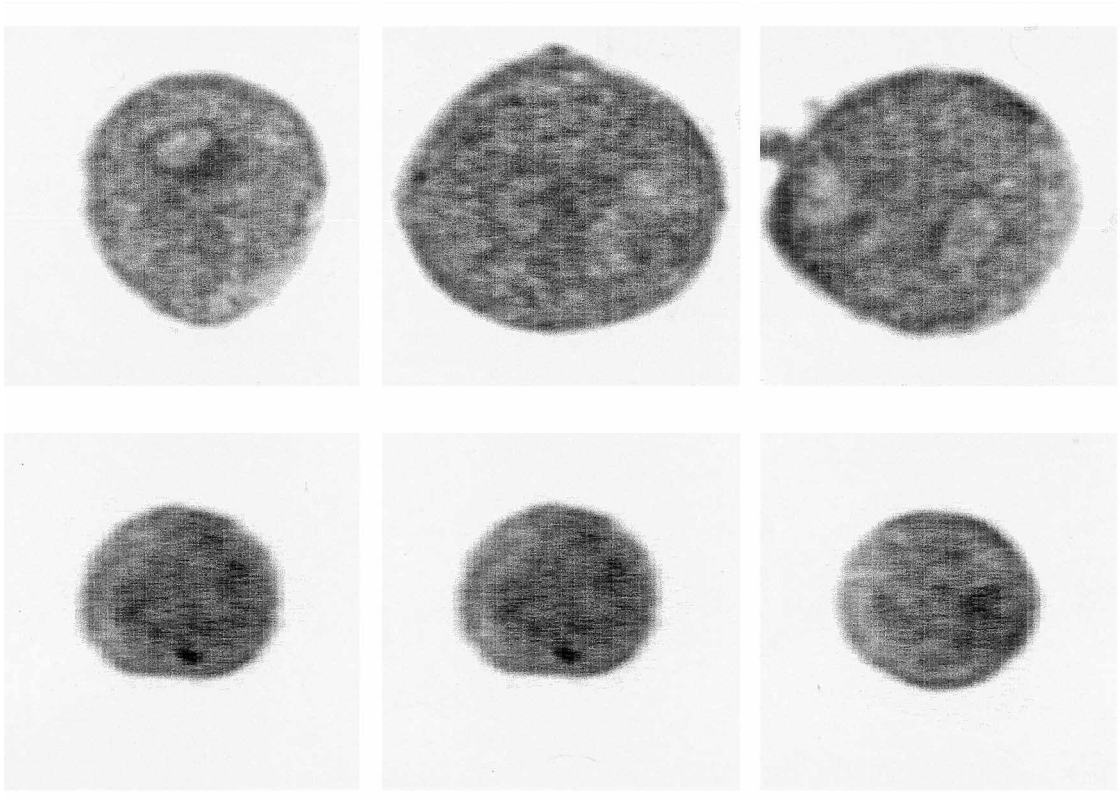

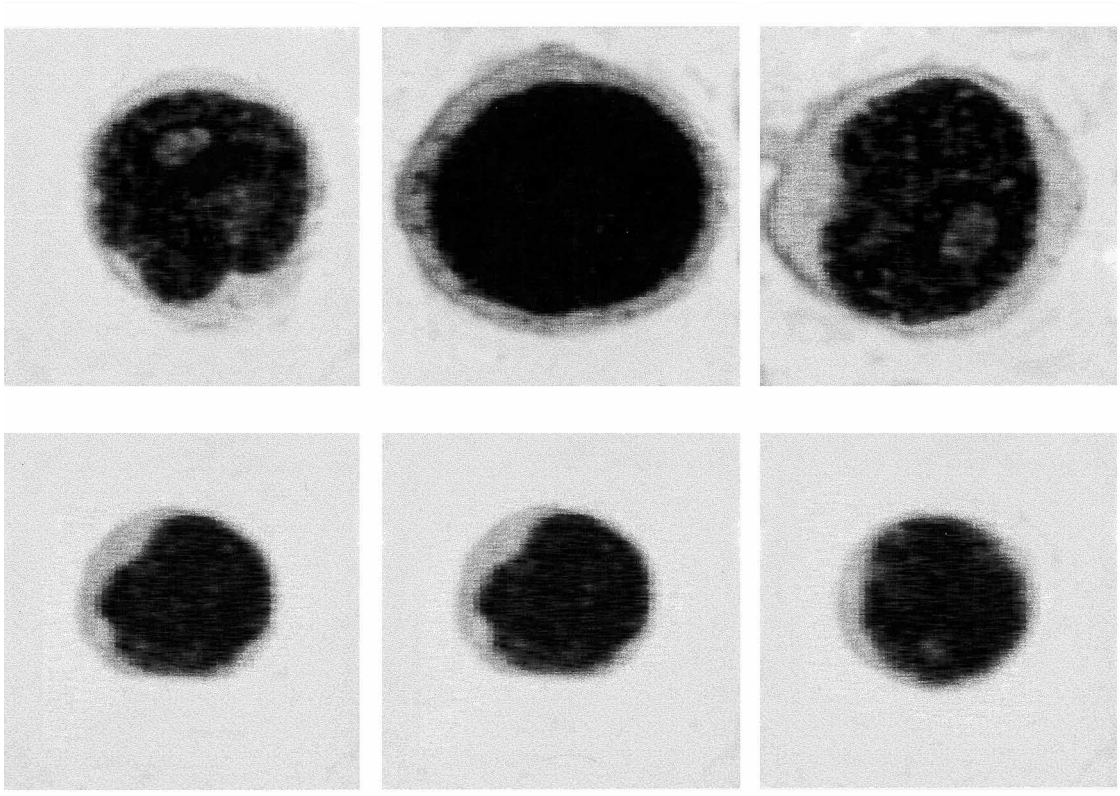

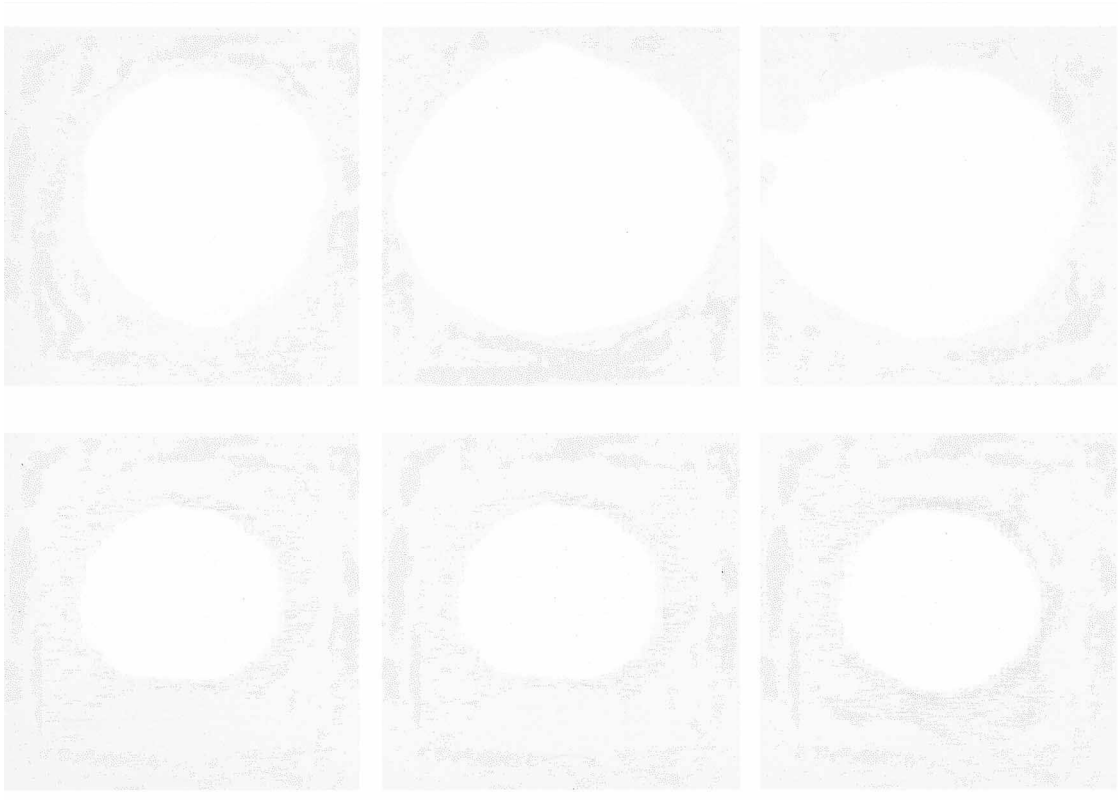

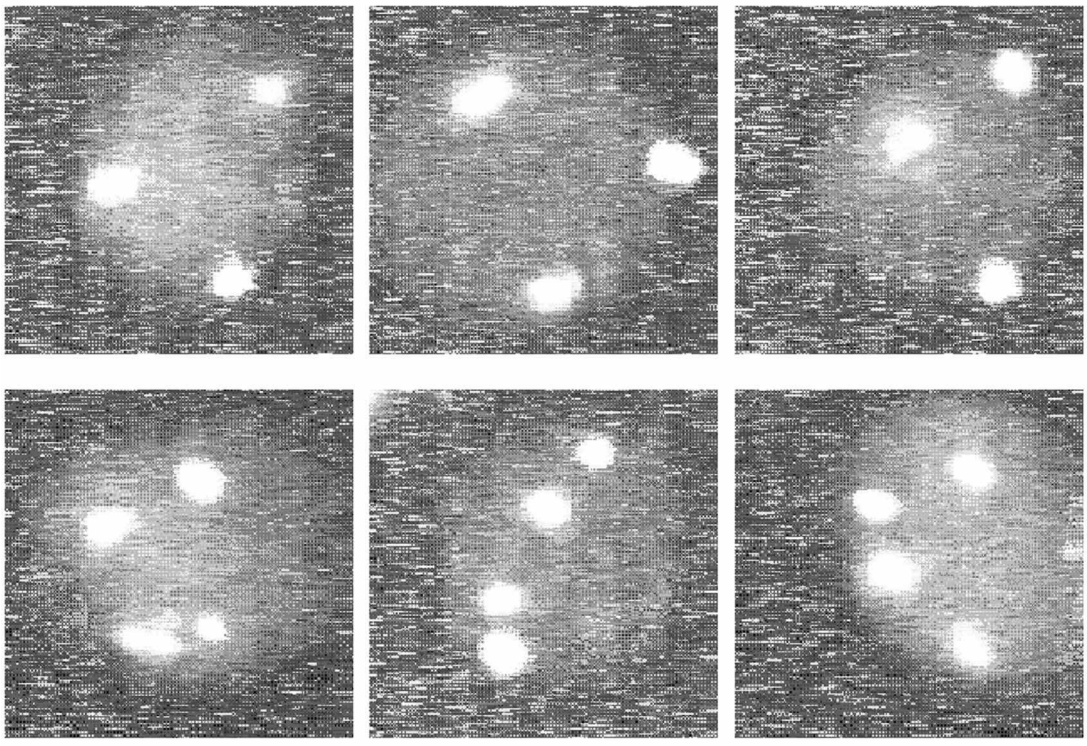

Fig. 6.20 Relocalisation of the six cells in Fig. 6.19 for in situ hybridisation by epifluorescence microscopy. The top row is the myeloblasts and the bottom row is lymphocytes.

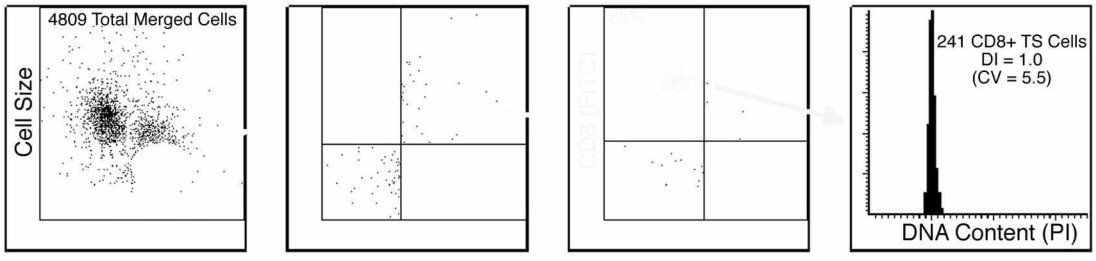

Fig. 6.21 Five-colour immunophenotyping plus DNA content analysis of peripheral blood lymphocytes. See text for details.

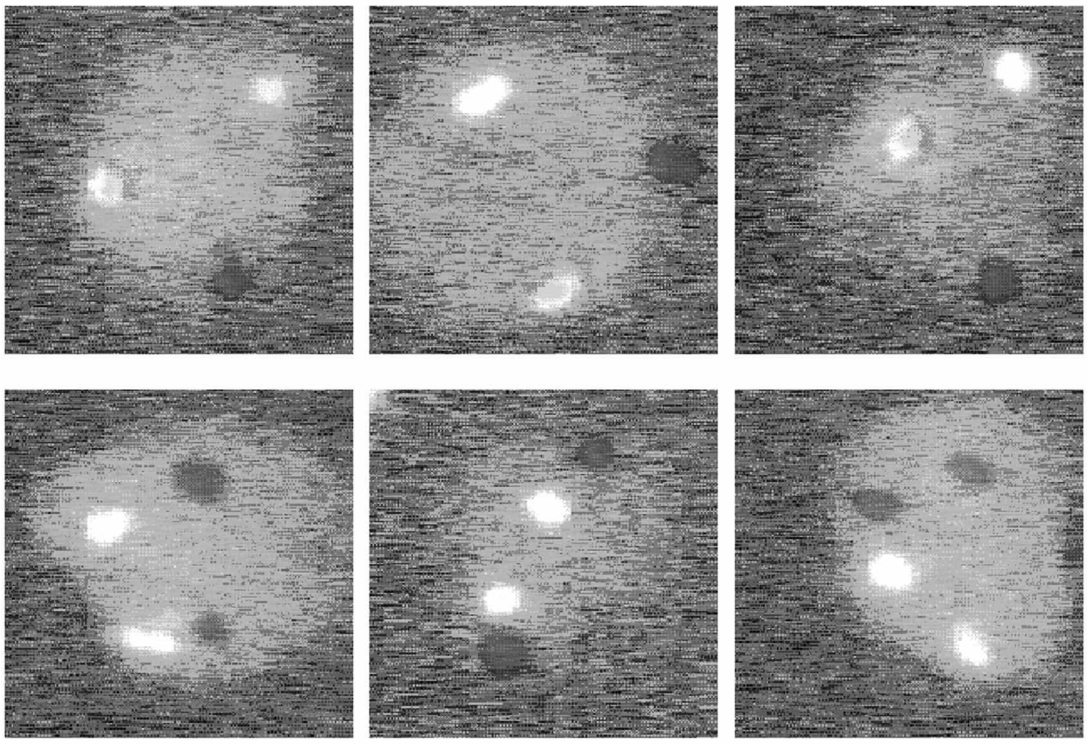

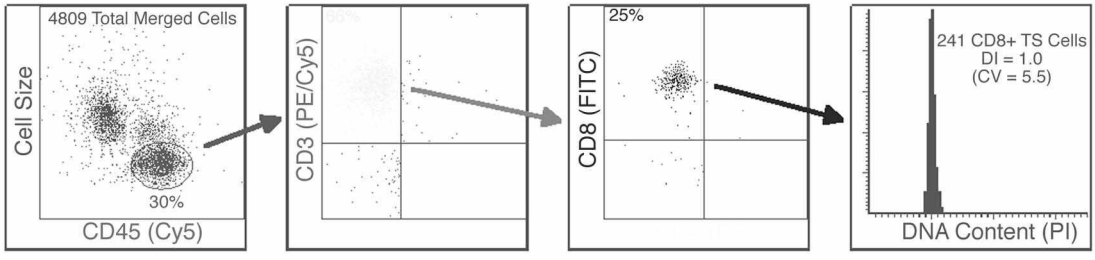
4809 Total Merged Cells
Cell Size
30%
CD45 (Cy5)
CD3 (PE/Cy5)
25%
CD8 (FITC)
241 CD8+ TS Cells
DI = 1.0
(CV = 5.5)
DNA Content (PI)

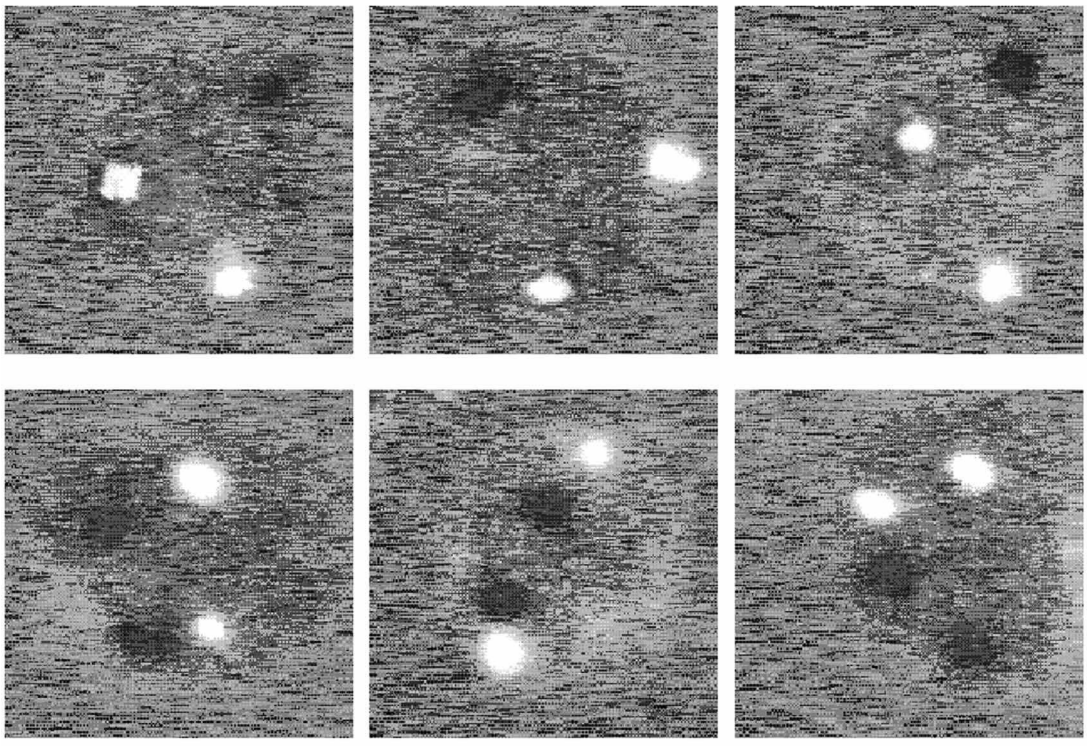

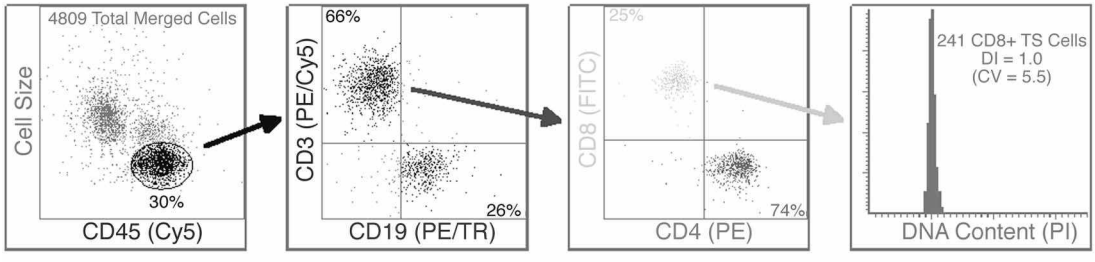
4809 Total Merged Cells
Cell Size
30%
CD45 (Cy5)
66%
CD3 (PE/Cy5)
26%
CD19 (PE/TR)
25%
CD8 (FITC)
74%
CD4 (PE)
241 CD8+ TS Cells
DI = 1.0
(CV = 5.5)
DNA Content (PI)

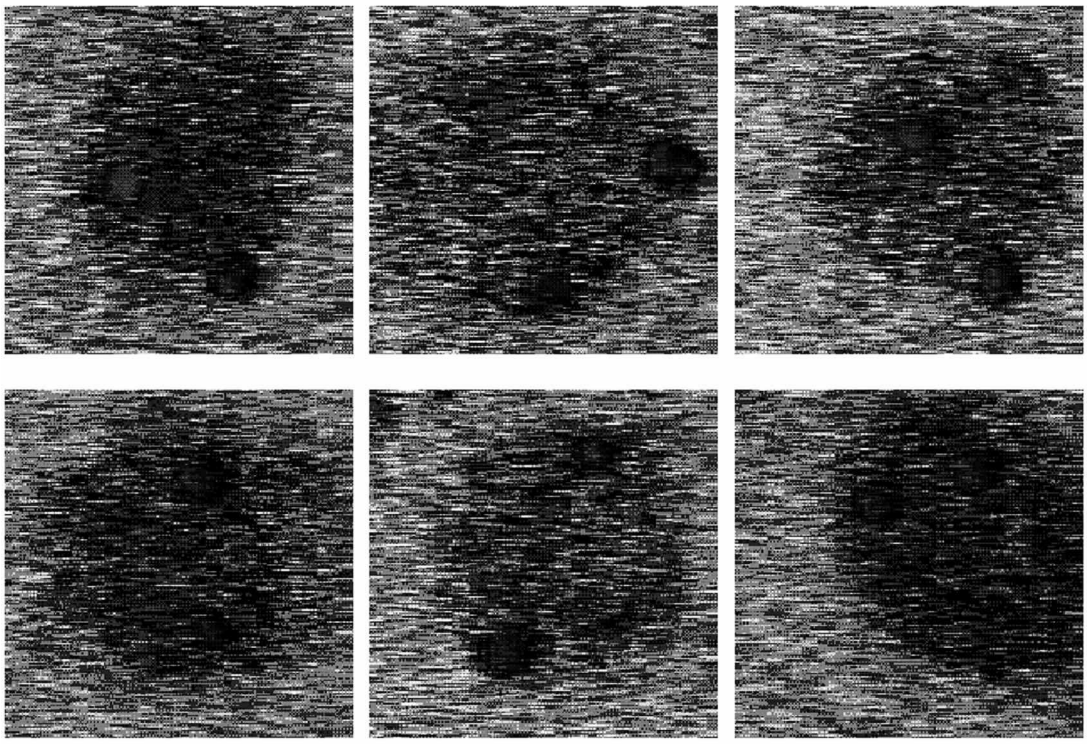

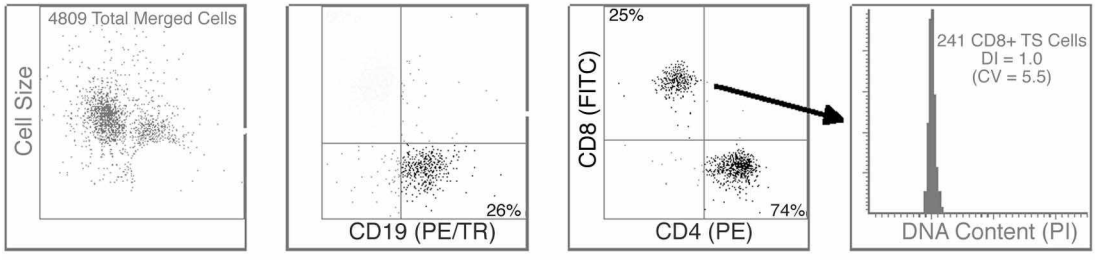
4809 Total Merged Cells
Cell Size
26%
CD19 (PE/TR)
25%
CD8 (FITC)
74%
CD4 (PE)
241 CD8+ TS Cells
DI = 1.0
(CV = 5.5)
DNA Content (PI)

1

Principles of flow cytometry

Marion G. Macey

St Bartholomew's and Royal London School of Medicine and Dentistry,
Queen Mary and Westfield College, London

1.1 History and development of flow cytometry

Wallace Coulter, in 1954, first described an instrument in which an electronic measurement for cell counting and sizing was made on cells flowing in a conductive liquid with one cell at a time passing a measuring point. This became the basis of the first viable flow analyser. Kamentsky et al. (1965) described a two-parameter flow cytometer that measured absorption and back scattered illumination of unstained cells and this was used to determine cell nucleic acid content and size. This instrument represented the first multiparameter flow cytometer; the first cell sorter was described that same year by Fulwyler (1965). Use of an electrostatic deflection ink-jet recording technique (Sweet, 1965) enabled the instrument to sort cells in volume at a rate of 1000 cells per second. By 1967, Van Dilla et al. exploited the real volume differences of cells to prepare suspensions of highly purified (>95%) human granulocytes and lymphocytes.

It is only comparatively recently that advances in technology, including availability of monoclonal antibodies and powerful but cheap computers, have brought flow cytometry into routine use. Previously, microscope-based static cytometry with cell-by-cell analysis had been the mainstay of most diagnostic work. However, with the increasing ability to measure a minimum of five parameters on 25 000 cells in 1 second, cell surface antigen analysis has become almost routine. This has not only enhanced the diagnosis and management of various disease states but also given new understanding to the pathogenesis of disease.

1.2 Principles of flow cytometry

All forms of cytometry depend on the basic laws of physics, including those of fluidics, optics and electonics (Watson, 1999). Flow cytometry is a system for sensing cells or particles as they move in a liquid stream through a laser (light amplification by stimulated emission of radiation) light beam past a sensing area. The relative light scattering and colour-discriminated fluorescence of the microscopic particles is measured. Analysis and differentiation of the cells is based on size, granularity and whether the cell is carrying fluorescent molecules in the form of either antibodies or dyes (Fig. 1.1). As the cell passes through the laser beam, light is scattered in all directions and that scattered in the forward direction at low angles (0.5–10°) from the axis is proportional to the square of the radius of a sphere (Brunsting and Mullaney, 1974) and so the size of the cell or particle. Light may enter the cell and be reflected and refracted by the nucleus and other contents of the cell; consequently, the 90° light scatter (also known as right-angled or side scatter, 90°LS) may be considered proportional to the granularity of the cell. The use of light scattering properties to distinguish cell morphology is discussed further in Ch. 8. The cells may be labelled with fluorochrome-linked antibodies or stained with fluorescent membrane, cytoplasmic or nuclear dyes. In this way, differentiation of cell types, the presence of membrane receptors and antigens, membrane potential, pH, enzyme activity and DNA content may be assessed.

Flow cytometers are multiparameter, recording

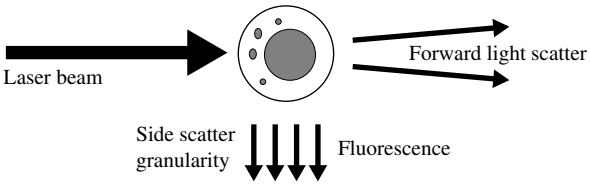

Fig. 1.1 The parameters of flow cytometric analysis: forward angle light scatter, 90° light scatter and fluorescence.

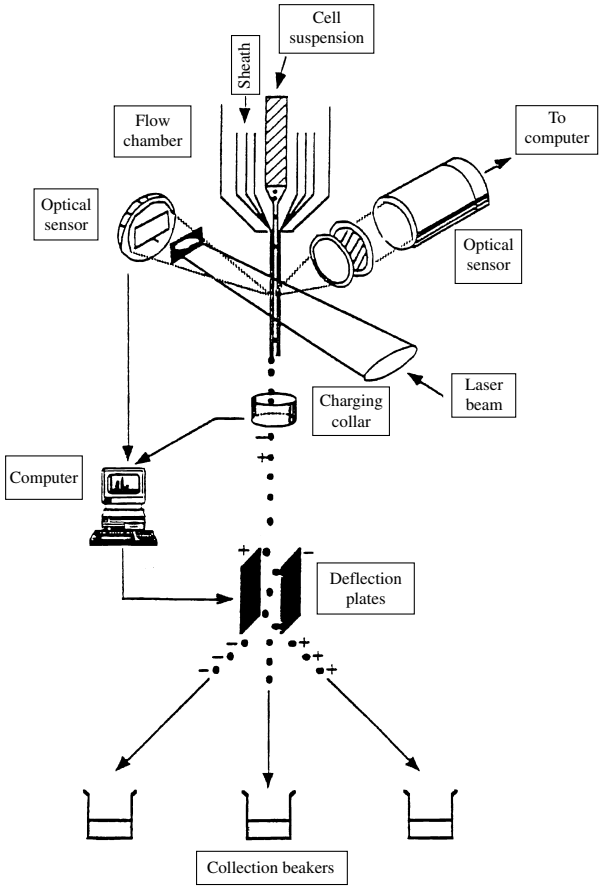

Fig. 1.2 Schematic representation of a flow cytometer showing the flow chamber, sheath stream, laser beam, sensing system, computer, deflection plates and droplet collection. (Reprinted from the EPICS® V/C Course Notes with permission from the copyright holder, Beckman Coulter.)

several measurements on each cell; therefore, it is possible to identify a homogeneous subpopulation within a heterogeneous population. This is one of the most useful features of flow cytometers and makes them preferable to other instruments such as spectrofluorimeters, in which measurements are based on analysis of the entire population.

Most commercial flow cytometers have the capacity to make five or more simultaneous measurements on every cell, but some specialised research instruments have considerably greater capacity; with three lasers it is possible to analyse up to 11 parameters (Bigos et al., 1999). A typical flow cytometer consists of three functional units: (i) a light source, or laser, and a sensing system that comprises the sample/flow chamber and optical assembly; (ii) a hydraulic system, which controls the passage of cells through the sensing system; and (iii) a computer system, which collects data and performs analytical routines on the electrical signals relayed from the sensing system (Fig. 1.2).

Flow cytometers may utilise epifluorescent microscopy or dark-ground laser illumination; in both designs, the flow chamber is instrumental in delivering the cells in suspension to the specific point that is intersected by the illuminating beam and the plane of focus of the optical assembly. Cells suspended in isotonic fluid are transported through the sensing system. Most instruments utilise a lamina/sheath flow technique (Crosland-Taylor, 1953) to confine cells to the centre of the flow stream; this also reduces blockage caused by clumping. Cells enter the chamber under pressure through a small aperture, which is surrounded by sheath fluid (Fig. 1.3A). The sheath fluid in the sample chamber creates a hydrodynamic focusing effect and draws the sample fluid into a stream (Fig. 1.3B). Accurate and precise positioning of the sample fluid within the sheath fluid is critical to efficient operation of the flow cytometer, and adjustment of the relative sheath and sample pressures ensures that cells pass one by one through the detection point. This alignment may be performed manually on some machines; in others it is fixed.

Chambers used in microscope-based flow sys-

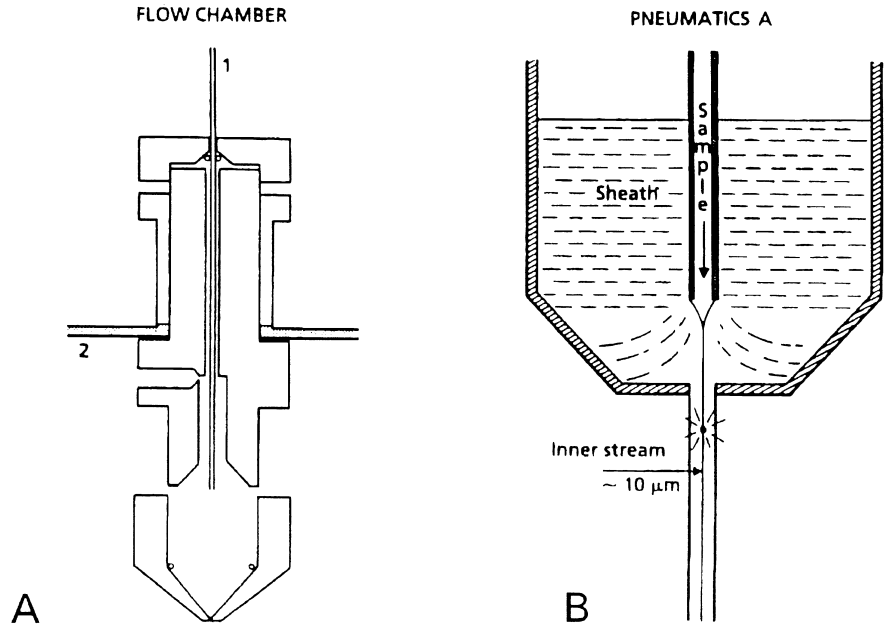

Fig. 1.3 (A) Example of a typical flow cell. 1 sample input; 2 sheath fluid input. (B) Illustration of the process of hydrodynamic focusing. (Both illustrations are reprinted from the EPICS® V/C Course Notes with permission from the copyright holder, Beckman Coulter.)

tems (where fluorescence is measured in line with the optical system) are constrained by limitations. The chamber acts as the horizontal microscope stage (Fig. 1.4) and the top of the chamber is usually a glass coverslip. Scatter measurements are restricted to within the direct optical path of the immersion objectives. Some systems do not use an enclosed channel but simply squirt the hydrodynamically focused sample at a low angle across a microscope slide, followed by vacuum aspiration to waste. Systems in which the sample remains static and where the laser scans the cell surface have been developed. These laser scanning cytometers are described further in Ch. 6.

In laser-based flow cytometers, where fluorescence is measured at right angles to the illuminating beam, chambers may comprise flat-sided cuvettes to minimise unwanted light reflections (Fig. 1.5A). Where cell sorting is required; so called stream-in-air or jet-in-air flow cells are used (Fig. 1.5B).

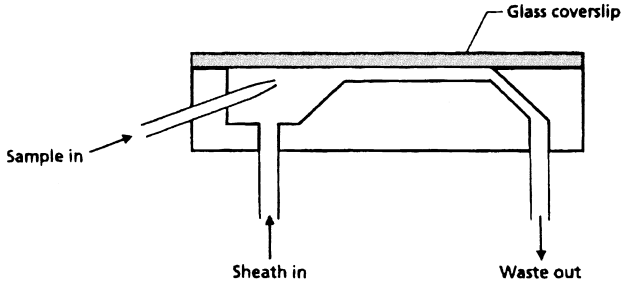

Fig. 1.4 Example of a chamber used in a microscope-based flow system.

Watecooled laser sources in the range 50 mW to 5 W output power may be used for fluorescence and light-scatter measurements. Air-cooled lasers have a maximum 100 mW output and are now more commonly used in commercial instruments. Lasers have the advantage of producing an intense beam of monochromatic light, which in some systems may be tuned to several different wavelengths. The lasers

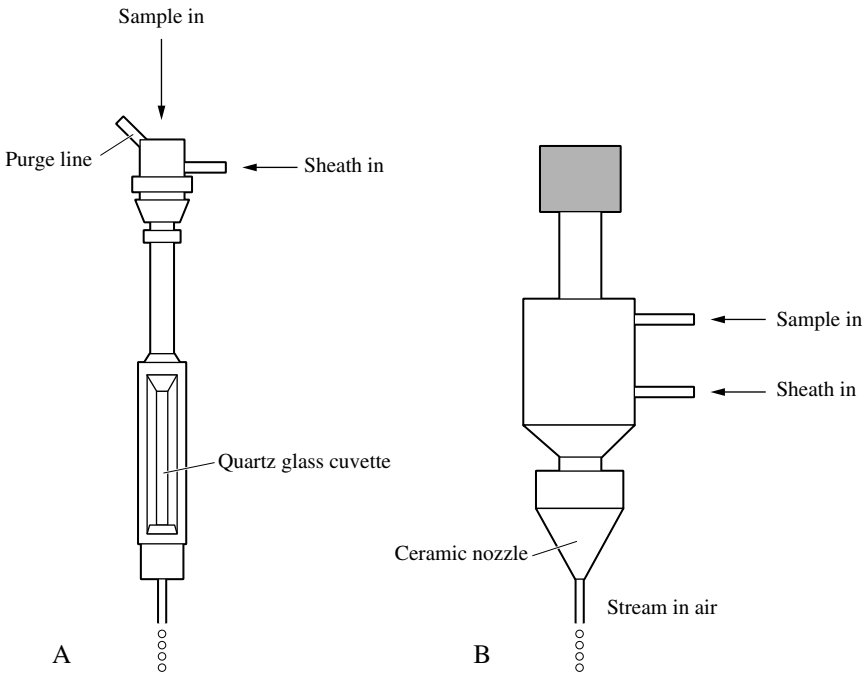

Fig. 1.5 Chambers in flow cytometers. (A) An example of a flat-sided cuvette system used to minimise unwanted light reflections and increase sensitivity. (B) An example of a stream-in-air nozzle used for sorting cells.

most commonly used in flow cytometry are argon lasers, which produce light between wavelengths 351 and 528 nm; krypton lasers, which produce light at 350–799 nm; helium–neon lasers, which produce light at 543, 594, 611 and 633 nm; and helium–cadmium lasers, which produce light at 325 and 441 nm.

1.3 Fluorescence analysis

Fluorescence is excited as cells traverse the laser excitation beam, and this fluorescence is collected by optics at 90° to the incident beam. A barrier filter blocks laser excitation illumination, while dichroic mirrors and appropriate filters (see below) are used to select the required wavelengths of fluorescence for measurement. The photons of light falling upon the detectors are converted by photomultiplier tubes (PMTs) to an electrical impulse, and this signal is processed by an analogue-to-digital converter, which changes the electrical pulse to a numerical signal. The quantity and intensity of the fluorescence are recorded by the computer system and displayed on a visual display unit as a frequency distribution, which may be single (Fig. 1.6), dual (Fig. 1.7) or multiparameter. Single-parameter histograms usually convey information regarding the intensity of fluorescence and number of cells of a given fluorescence, so that weakly fluorescent cells are distinguished from those that are strongly fluorescent.

Dual-parameter histograms of forward angle light scatter (FALS) and 90° light scatter allow identification of the different cell types within the preparation, based on size and granularity. Right angle and side scatter are alternative names used for 90° light scatter.

1.4 Light scatter and fluorescence detection

1.4.1 Filters

Light scattered by particles as they pass through a laser or light source must be efficiently detected and fluorescent light of a given wavelength requires specific identification. The amount of light scattered is generally high in comparison with the amount of fluorescent light. Photodiodes are, therefore, used as forward angle light (FAL) sensors; they may be used with neutral density filters, which proportionally reduce the amount of light received by the detector. A beam absorber (diffuser or obscuration bar) is placed across the front of the detector to stop the laser beam itself and any diffracted light from entering the detector. The scattered light is focused by a collecting lens onto the photodiode(s), which converts the photons into voltage pulses proportional to the amount of light collected (integrated pulse). These pulses may be amplified by the operator. In some systems with multiple diodes, upper and lower light may be collected, which may help to separate populations of cells or particles.

Fluorescence detectors are usually placed at right angles to the laser beam and sample stream. Stray light may be excluded by an obscuration bar in front of an aspheric (objective) lens, which collects the light and refracts it into a parallel beam. To detect the components of the beam, filters and dichroic mirrors are used to remove unwanted wavelengths of light and direct light to the correct detector(s). Table 1.1 describes some of the different types of lens and filter used.

Figure 1.8 illustrates a possible lens configuration for detecting 90° light scatter, green (either fluorescein or fluorescein isothiocyanate (FITC)), orange (phycoerythrin (PE)) and red (phycoerythrin-Texas Red® (PE-TR or Energy Coupled Dye (ECD™)) fluorescence. Typically the first filter used eliminates the 488 nm laser light that still may have passed through. The light may then be diverted to a beam splitter, or a dichroic mirror. This mirror reflects light in one band of wavelengths (usually long) while allowing another band to pass through

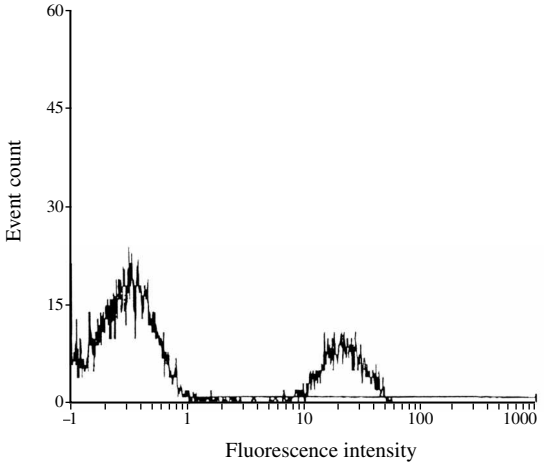

Fig. 1.6 Single-parameter histogram of fluorescence and cell count illustrating a typical distribution for weakly fluorescent and strongly fluorescent cells.

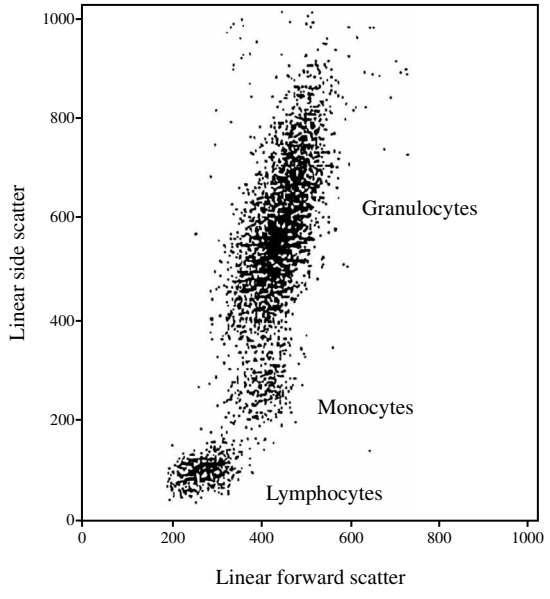

Fig. 1.7 Dual-parameter histogram of the forward scatter and side scatter analysis of leukocytes from peripheral blood showing the characteristic distribution of lymphocytes, monocytes and granulocytes.

Table 1.1 *Types of filter*

Filter type	Comments
Absorbance	The transition from absorbance to transmission occurs over a set range of wavelengths and the filters are, therefore, named at the 50% transmission point. Dye in glass band-pass filters have excellent blocking properties and very high (above 50%) pass of light. They are inexpensive but fluoresce; consequently they should not be used as primary blocking filters. They are always long-pass filters, i.e. they block short wavelengths and transmit long wavelengths
Interference	These long-pass filters are manufactured by an etching process to give a raised and cut surface with ridges at set distances; these cause interference in the wavelength of light transmitted. They are reflectance filters and the shiny side is towards the laser. They do not fluoresce but have 90% efficiency at best and poor transmittance. Also the etching process allows light of incorrect wavelength to pass. They may be termed by the centre wavelength, and band-widths are usually given (Fig. 1.8)
Dichroic mirrors	These are a combination of a mirror and an interference filter, which need to be placed at an angle of 45° to the beam. They reflect short wavelengths and let longer wavelengths pass. They are used with other filters and are normally long-pass filters
Beam splitters	These are metallic coated quartz substrates and are designed to work at 45° angle of incidence. Numbers indicate reflection/transmission values
Band-pass	These filters allow light within certain wavelengths to pass. They are interference filters with two coatings and act as a long-pass and a short-pass filter. They transmit and reflect but may suffer from attenuation
Neutral density	These attenuate all wavelengths and may be used for forward angle light scatter and 90° light scatter

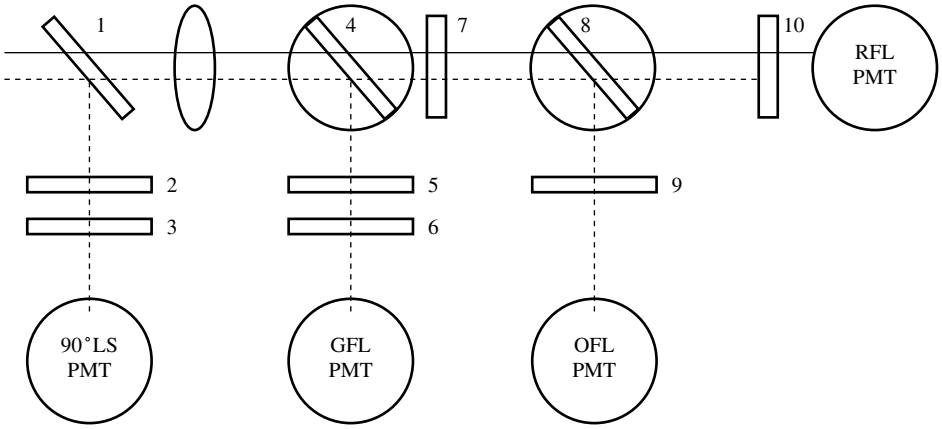

Fig. 1.8 Typical lens and mirror assembly for detection of 90° side light scatter (90° LS) and fluorescence from fluorescein isothiocyanate, phycoerythrin or Energy Coupled Dye. 1, beam splitter, normal glass; 2, laser line filter 396–496 nm band-pass: 3, diffuser; 4, dichroic mirror 570 nm long-pass; 5, laser cut filter 490 nm long-pass; 6, green filter 515–530 nm band-pass; 7, orange filter 600 nm long-pass; 8, dichroic mirror 610 nm long-pass; 9, orange filter 565–592 nm band-pass; 10, red filter 620 nm long-pass. GFL, green fluorescence; OFL, orange fluorescence; RFL, red fluorescence; PMT, photomultiplier tube.

(usually short). It should be noted that there is no direct cut-off here between reflection and transmission. There is a middle band of wavelengths that will do both. For this reason, the colour components are passed through other filters before entering the detector. These filters remove the unwanted wavelengths and allow the desired wavelengths to pass through to the detector. These filters are called

band-pass filters and are designated by whether they transmit long wavelengths (long-pass) or shorter wavelengths (short-pass).

The sensors used for side light scatter and fluorescence are PMTs. These tubes serve as detectors and also amplifiers of the weak fluorescent signals. They have their own high voltage power supplies, which provide the boost needed to amplify the signal internally within the PMT. The amount of high voltage and therefore the amplification is adjustable by the operator. A second amplification, also operator controlled, may be made on the PMT signal external to the PMT. PMTs are used only under weak light conditions; they may be damaged by high-intensity light such as normal room light.

1.4.2 Filter sets

Filters are used in sets, usually in pairs of a band-pass filter with a dichroic mirror or beam splitter. Beam splitters are metallic coated quartz substrates and are designed to work at an angle of incidence of 45°. Filters have numbers that indicate the reflection/transmission value for the centre wavelength and band-width (nm) (Fig. 1.9).

1.5 Acquisition

Light scatter signals result from a measure of a combination of parameters: (i) the size (projected surface area) of the particle, (ii) the surface topography (rough or smooth), (iii) the optical density (will be influenced by the light absorbed and the refractive index, which will determine the light refracted through the particle) and (iv) the internal structure of the particle (granular or uniform). Some of these components will contribute to all of the light scatter produced.

The purpose of analysing the light scatter or fluorescence signal is to determine the difference between particles as indicated by voltage output from detectors. There are several methods of retrieving this information. The maximum voltage (or peak) level reached as the particle passes through the laser

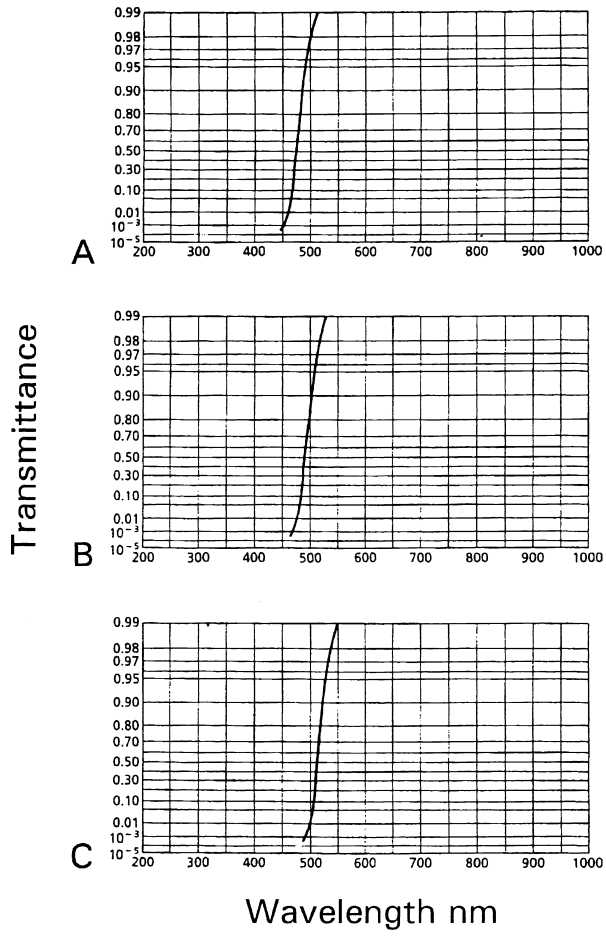

Fig. 1.9 Example of transmittance profiles of filters with 50% transmittance at 450 nm (A), 490 nm (B) and 510 nm (C). (Reprinted from the EPICS® V/C Course Notes with permission from the copyright holder, Beckman Coulter.)

beam may be measured. This pulse height may be a measure of the maximum fluorescence given off by a particle (Fig. 1.10A). Particles with different amounts of associated fluorescence have different pulse heights and so peak pulses. A particle with fluorescent molecules spread uniformly over the surface will produce a wider peak pulse than a particle with fluorescence concentrated at one point. The latter will produce a narrower and sharper peak pulse (Fig. 1.10B). However, the height of the peak

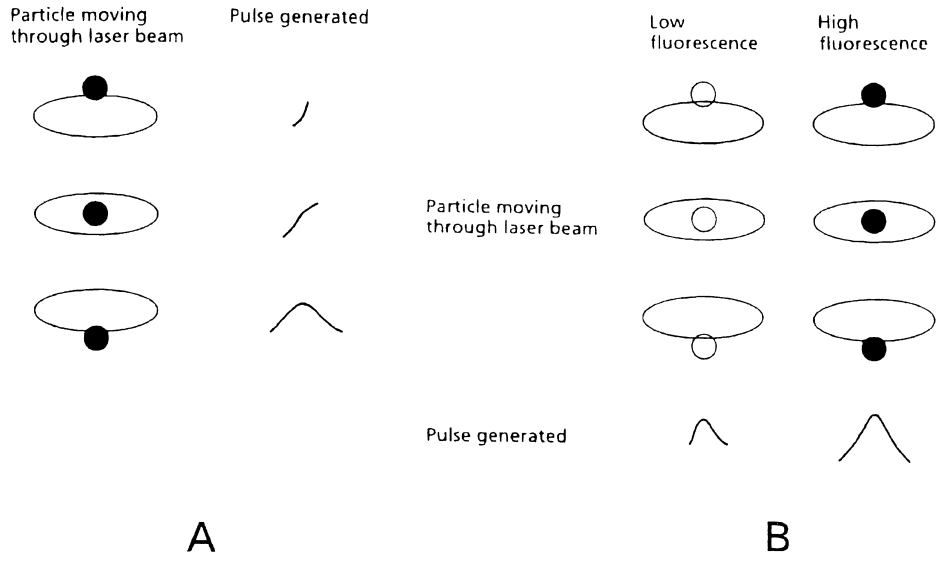

Fig. 1.10 Pulse generation. (A) The electronic pulse generated by a particle as it moves through a laser beam. (B) The pulses generated by cells with high and low fluorescence intensities.

pulse may be the same for both particles and so they become indistinguishable by this parameter. The area under the two pulses will, however, be different. The area under the pulse allows generation of a second parameter, referred to as the integrated pulse. A third parameter may also be used if the ratio of the peak to integrated pulse is measured. This is termed time of flight (TOF).

1.6 Amplification

Some particles may also be better differentiated if the original peak or integrated pulse is amplified. Normal amplification accentuates the differences between pulses, but in some cases this may not be sufficient to differentiate between small changes in pulse height. The use of logarithmic amplification makes small pulses much larger while amplifying the larger pulses by a lesser amount. The result is that the differences in the smaller pulses are accentuated.

1.7 Histograms

Particles are analysed individually but interpreted collectively. The collective picture is represented as a histogram. These may be single, two or three parameter. Single-parameter histograms are two-dimensional graphs in which the parameter to be interpreted is represented on the horizontal (x-axis) and the number of events is represented on the vertical (y-axis) axes. The parameter could be the peak pulse height, the integrated pulse height or a ratio based on the first three parameters. Light scatter or fluorescence pulses may also be used. As well as being displayed as data are accumulated, raw data acquired during 'real-time analysis' can be written in a continuous stream onto disc. This listed data or 'list mode analysis' can subsequently be re-analysed in more detail.

The production of a histogram relies on the measurement of pulses of a given value and their assignment to channels that represent different voltage levels. This type of analysis is referred to as 'pulse processing'. Each time a pulse falls into one

of these channels, a counter increments the channel. The process of counting each pulse in the appropriate channel is known as analogue-to-digital conversion. Most systems have 256 or 1024 channels for single-parameter histograms and may generate the histogram based on fluorescence, forward angle light scatter or 90° light scatter. The pulses may be amplified, in a linear or logarithmic manner. In some experiments, the peak or integral pulses may vary widely in size. With linear amplification, small pulses will be bunched up into a few channels, making it difficult to distinguish differences between them. If the amplification is increased, this helps to distinguish between the small pulses but the larger pulses are pushed off the scale of the histogram. In such cases, the operator may elect to use pulses that have gone through a logarithmic amplification before plotting. The plot may include all pulses, with the small pulses spread over more channels and the larger pulses over fewer channels. In this way all pulses are brought onto the scale of the histogram. The use of logarithmic and linear amplification is described further in Ch. 5.

1.8 Coefficients of variation

Ideally, the same particle passing repeatedly through the laser beam should produce identical light scatter or fluorescence pulses. Another particle might produce a consistent but different set of pulses. Practically, there are always some variations within the instrument that causes some variation in the pulses even though the particles are the same. Any problems with the sample flow, the laser intensity, laser alignment, beam focusing or detection may result in variation of the pulses associated with a given particle. These variations lead to variation in histograms and it is important to determine whether the variation is caused by the instrument or results from particle variation or is caused by both. The operator can assess the magnitude of the instrument variations by calculating a coefficient of variation (CV) on a good uniform test sample such as fluorescent beads (available from Beckman Coulter, BD Biosciences, Dako and Polysciences). The basic equation for CV is:

$$CV = (SD/MEAN) \times 100$$

where SD is the standard deviation and MEAN is the average value for the parameter measured for these particles (for a Gaussian distribution this would be the channel with the highest count). Most instruments calculate the CV for the operator. If the operator knows what the CV is normally, then any increase in CV will indicate that the instrument setting may be changing and is broadening the histograms. However, if the beads have a good CV and a test sample has a broad histogram then it is likely to be a genuine phenomenon. Fluorescent beads may be added to the biological sample to be tested provided they do not interfere with the sample. The use of beads to count cells within a test sample and aspects of quality control are discussed further in Ch. 4.

Once a histogram has been produced, the operator may now analyse it. The most common analysis is simply to determine what percentage of a total is a subpopulation. This is possible if the populations are nicely separated; in practice this may not be the case. However sophisticated computer programs are available to analyse overlapping populations. Computers can also be used to compare one histogram with another and determine if there are any significant differences.

All flow cytometric systems have the ability to analyse more than one signal simultaneously on particles and plot them as three-dimensional histograms. Many combinations of signals might be used. The histogram is like a chequer board of channels. Each channel, like the single-parameter histogram, has a counter but now two pulse heights for a particle must fall within a channel to increment that channel. A three-dimensional histogram is, therefore, built up as the channels are incremented for a given sample (Fig. 1.11A). The two-parameter histogram can be converted to a single-parameter histogram by viewing from the side (either axis x or y); this is called a projection (Fig. 1.11B). The two-parameter histogram may also be viewed from

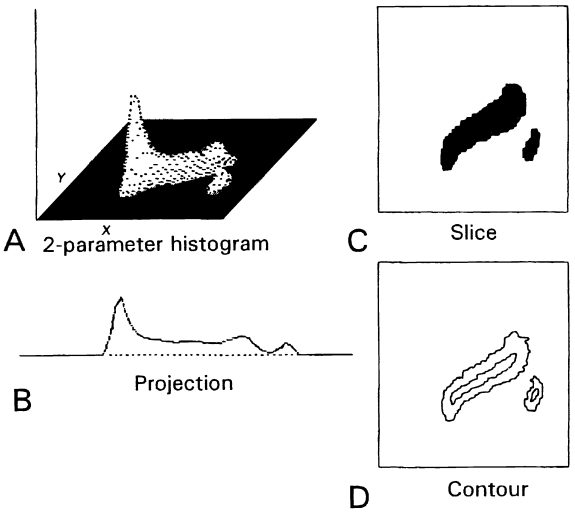

Fig. 1.11 Different ways of analysing data from flow cytometry. (A) A two-parameter three-dimensional histogram; (B) a projection histogram; (C) a slice and (D) a contour plot. (Reprinted from the EPICS® V/C Course Notes with permission from the copyright holder, Beckman Coulter.)

above and in this format it is referred to as a scattergram or dot plot. It is also possible to examine the distribution in all channels that have a certain operator-selectable minimum count. This is termed a slice (Fig. 1.11C) and an outline of a series of slices from the bottom to the top of a two-parameter histogram is termed a contour plot (Fig. 1.11D).

1.9 Spectral overlap and compensation

Each fluorochrome has a wide emission spectrum. When multiple fluorochromes are used, parts of their emission spectra will probably be at the same wavelengths. This is referred to as 'spectral overlap'. Figure 1.12 shows the emission spectra for FITC and PE. Superimposed on the spectra are the possible transmission characteristics of two band-pass filters. The FITC emission spectrum overlaps with that of PE and some of its light will be transmitted by the PE filter and so enter the PMT for PE. This spectral overlap is corrected by subtracting a fraction of the

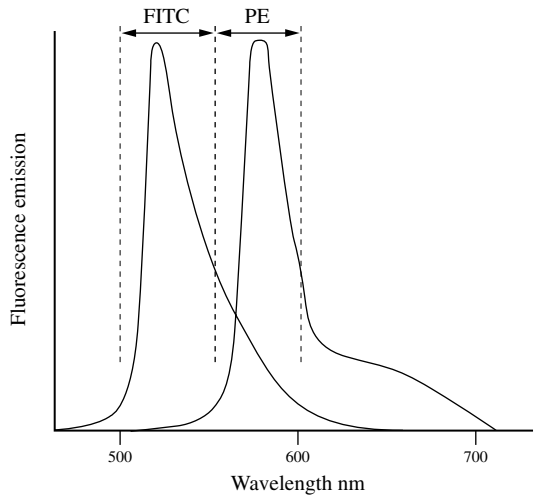

Fig. 1.12 Fluorescence emission spectra for fluorescein isothiocyanate (FITC) and phycoerythrin (PE) showing the overlap in emission for the two fluorochromes.

FITC signal from the PE signal. Similarly, a fraction of the PE signal may be subtracted from the FITC signal; this is termed compensation. Figure 1.13 shows an example of the analysis of lymphocytes labelled with PE-CD4 and FITC-CD8 without and with compensation.

1.10 Safety aspects of lasers

Hazards from lasers can be summarised as follows:

- damage to the eye: the argon–krypton laser presents a possible hazard to the eye as 'stray' diffuse blue laser radiation can be focused by the eye onto the retina; damage can occur by either thermal or photochemical effects, depending on exposure duration
- skin burns: interception of the beam by any part of the skin can possibly cause damage through thermal effects
- material combustion: any unsuitable material in the vicinity of the beam can potentially catch fire, emit toxic gases or explode if irradiated.

Under normal operation of commercially available flow cytometers, the laser requires covers to be in-

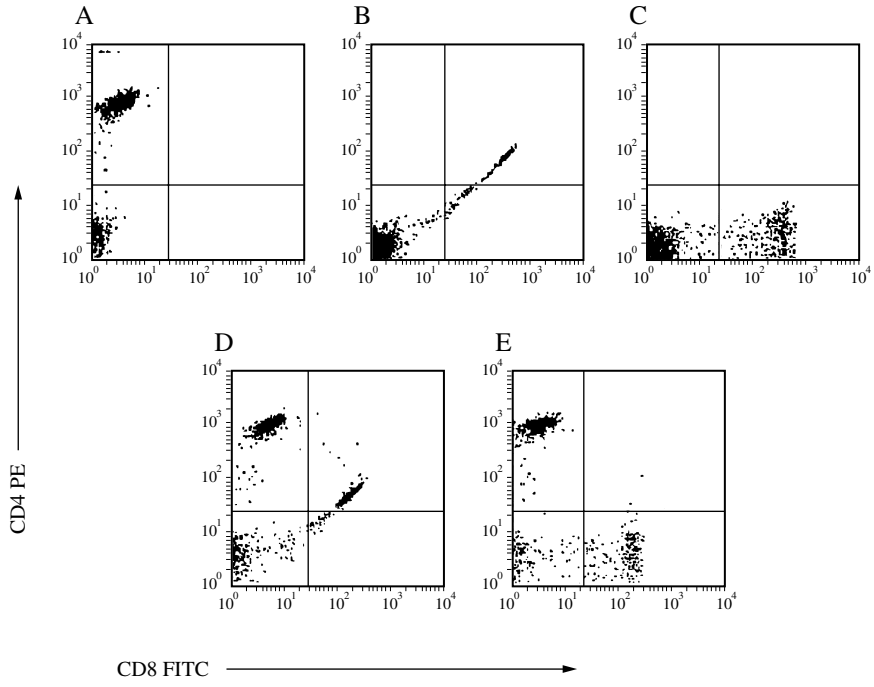

Fig. 1.13 The analysis of lymphocytes labelled with fluorochromes: (A) PE$\surd$CD4; (B) FITC$\surd$CD8 without compensation; (C) as (B) but with compensation; (D) dual labelled with PE-CD4 and FITC-CD8 without compensation and (E) as (D) but with compensation. FITC, fluorescein isothiocyanate; PE, phycoerythrin

stalled and the laser output is interrupted if the cover is removed. Under these circumstances, the laser is classified as a class 1 product and there is therefore no potential hazard. Safety standard for British Radiation Hazard number 21 in subchapter 1 applies. However, it is possible for the operator to defeat the interlock in the specimen irradiation area thus allowing the beam to be seen, although direct (intrabeam) viewing is impossible because of the layout of the equipment. A potential hazard exists from reflections. If the reflected beam is diffused in all directions, this does not present a hazard. If the beam remains focused after reflection, the maximum permissible exposure (intrabeam viewing) is 100 J m^{-2}. For an exposure of 60 seconds, it is 1.67 W m^{-2} and with a 2 W laser a safe viewing distance for such exposure would be 0.2 m. As a small source, therefore, an argon–krypton laser presents no hazard providing the operator does not view the beam reflection from any closer than 20 cm and for no longer than 60 seconds. Should prolonged viewing of the beam be necessary, the use of safety spectacles is recommended.

1.11 Cell sorting

An important function of flow cytometry is its ability to separate and collect a subpopulation of cells, identified by multiparameter analysis. Classically, this sorting of cells is accomplished as the cells exit from the sample chamber in a liquid jet. Savart (1833) showed that when a small jet of fluid was vibrated at the correct frequency the stream could be broken into a series of uniform droplets. In the flow cytometer, the sheath stream is broken into a series of uniform droplets by vibrating the sample chamber with a piezoelectric crystal at a high frequency. Cells flowing through the flow cytometer are isolated in these tiny droplets. When the

Table 1.2 *Specification of commercial flow cytometers*

Specification	FACSCalibur	FACS™ Vantage	EPICS® XL	EPICS® ALTRA	MoFlo	DAKO PAS
Light source						
Type	Air-cooled argon ion and red diode lasers	Air-cooled argon ion and red diode lasers plus the choice of a third laser	Air-cooled argon ion laser	Air-cooled argon laser plus choice of lasers	Air-cooled argon ion laser plus choice of two more lasers	Air-cooled argon ion laser with mercury arc lamp and red diode laser
Lifetime	>5000 h	Dependent on laser	>5000 h	Dependent on laser	Dependent on laser	>5000 h
Optics						
Usable spectrum (nm)	488 and 635	200–676	488	200–676	200–676	345–676
Fluorescence detectors	Green (525 nm), orange (575 nm), red (630 nm), far red (>650 nm)	Variable operator-controlled five colour detection	Green (525 nm) orange (575 nm) red (630 nm) far red (>650 nm)	Up to six colours detected	Minimum of 10 colours	Up to four colours
Light scatter	Forward angle side	Forward angle side	Forward angle side	Forward angle side	Forward angle side	Forward angle side
Alignment	Pre-aligned laminar flow	Operator controlled	Pre-aligned laminar flow	Operator controlled	Operator controlled laminar flow	Pre-aligned
Fluorescence sensitivity (number of molecules)	≥ 600 FITC, ≥ 700 PE	≥ 500 FITC, ≥700 PE	≥ 500 FITC, ≥700 PE	≥ 500 FITC, ≥700 PE	≥ 500 FITC, ≥700 PE	≥ 500 FITC, ≥700 PE
Fluorescence coefficient of variation	±2% full peak for PI-stained thymus nuclei	<2% full peak for PI-stained peripheral blood mononuclear cells	<2% full peak for PI-stained normal human lymphocytes		<2% full peak for PI-stained normal human lymphocytes	<2% full peak for PI-stained normal human lymphocytes
Light scattering sensitivity	0.1 μm	1–2 μm	0.5 μm particles over background with FALS		1–2 μm	1–2 μm
Fluidics						
Flow cell	Quartz cuvette	Jet-in-air	250 μm BioSense flow cell, quartz mounted	Quartz sort sense flow cell	Patented jet-in-air flow cell	Quartz cuvette
Sample system	Continuous	Continuous	Continuous	Continuous	Continuous	Fixed volume
Sheath flow		Operator variable	10, 30 or 60 μl min^{-1}		Operator variable	Processor controlled
Analysing rate (cells s^{-1})	Maximum 20 000, typical 2000	Typical 2000	Typical 3000	Typical 10 000	Typical 15 000	Maximum 30 000

Table 1.2 (*cont.*)

Specification	FACSCalibur	FACS™ Vantage	EPICS® XL	EPICS® ALTRA	MoFlo	DAKO PAS
Run cycle	Automated or operator controlled	Operator controlled	Automated or operator controlled	Operator controlled	Operator controlled	Automated
Additional options	Sample loader, sorter unit, cell concentrator	Integrated cell deposition system, pulse processor, 'Turbo' sort option	Autoloader	Autoclone sorting, HyPerSort system	CyCLONE sorting into 96-well plates	Sorting system
Biosafety	Enclosed flow cell assembly	Optional closed flow system	Enclosed flow cell assembly	Optional closed flow system	Optional closed flow system	Enclosed flow cell assembly

FALS, forward angle light scatter; FITC, fluorescein isothiocyanate; PE, phycoerythrin; PI, propidium iodide.

computer detects a cell that satisfies the parameters determined by the operator for sorting, an electrical charge is applied to the droplet (Thompson, 1967). The polarity of the charge, positive or negative, is determined by the sorting criteria. As the charged droplet passes an electrostatic field, it is deflected to the right or left, carrying the sorted cell. Extremely pure populations of cells may be sorted at relatively rapid rates.

More recently, an alternative technique has become available for sorting cells. The Becton Dickinson machines employ a system in which the required cell is removed from the sheath stream by a small rotating catcher tube. Up to 300 cells s^{-1} may be sorted, but only one-way sorting is available at present. The technique is not dependent on droplet formation and takes place in an enclosed environment. Therefore, no aerosols are formed, which is designed to eliminate the risk from biohazardous samples.

1.12 Commercial flow cytometers

There are four major manufacturers of flow cytometers: Coulter (now part of Beckman Coulter), Becton Dickinson (now part of BD Biosciences), Dako and Cytomation. Coulter, Becton Dickinson and Cytomation originally introduced flow cytometers capable of sorting with water-cooled lasers. Coulter produced the EPICS® (Electronically Programmable Individual Cell Sorter) series, Becton Dickinson marketed the FACS™ (Fluorescent Activated Cell Sorter) while Cytomation promoted the MoFlo. Dako, Coulter and Becton Dickinson have moved toward production of clinically orientated bench top analysers, employing air-cooled lasers and without the capacity to sort cells (Coulter EPICS® XL, Becton Dickinson FACSCalibur, Dako PAS). The Dako PAS flow cytometer is capable of determining absolute counts on cell subpopulations and Becton Dickinson have launched the FACSort and FACS™ Vantage. Table 1.2 illustrates the salient specifications of the currently available commercial flow cytometers.

1.13 REFERENCES

Coulter, W.H. (1954) High speed automatic blood cell counter and cell analyzer. *Proceedings of the National Electronics Conference* **12**, 1034–35.

Crosland-Taylor, P.J. (1953) A device for counting small particles suspended in a fluid through a tube. *Nature* **171**, 37–8.

Bigos, M., Baumgarth, N., Jager, G.C., Herman, O.C., Nozaki, T., Stovel, R.T., Parks, D.R., Herzenberg, L.A. (1999) Nine color eleven parameter immunophenotyping using three laser flow cytometry. *Cytometry* **36**, 36–45.

Brunsting, A., Mullaney, P.F. (1974) Differential light scattering from mammalian cells. *Biophysics Journal* **14**, 439–53.

Fulwyler, M.J. (1965) Electronic separation of biological cells by volume. *Science* **150**, 910–12.

Kamentsky, L.A., Melamed, M.R., Derman, H. (1965) Spectrophotometer: new instrument for ultrarapid cell analysis. *Science* **150**, 630–31.

Savart, F. (1833) Mémoire sur la constitution des veines liquides lancées par des orifices circulaires en mince paroi. *Annales de Chemie et Physiques* **53**, 337–86.

Sweet, R.G. (1965) High frequency recording with electrostatically deflected ink-jets. *Review of Science Instruments* **36**, 131–2.

Thompson, W. (1967) On a self-acting apparatus for multiplying and maintaining electric charges with applications to illustrate the voltaic theory. *Proceedings of the Royal Society of London* **16**, 67–72.

Van Dilla, M.A., Fulwyler, M.J., Boone, I.V. (1967) Volume distribution and separation of normal human leukocytes. *Proceedings of the Society for Experimental Biology and Medicine* **125**, 367–70.

Watson, J.V. (1999) The early fluidic and optical physics of cytometry. *Cytometry* **38**, 2–14.

2

Introduction to the general principles of sample preparation

Desmond A. McCarthy

Queen Mary and Westfield College, London

2.1 Introduction

When collecting and preparing samples for cytometric analysis, it is essential to use a protocol that enables the aims of the investigation to be fulfilled, because if samples are handled wrongly at the start, there is usually nothing that can be done later to remedy the situation. For many studies it may be possible to use, or to modify, an existing protocol; for others it may be necessary to devise a new one. In this chapter, the general principles relevant to collecting and preparing samples are discussed and some protocols described. Most were devised and validated using flow cytometry, but they should also be largely applicable to the newer technique of laser scanning cytometry.

2.2 Factors affecting the choice of preparation procedure

The key variables in any cytometric study are:

- the nature of the sample material and of the cells to be studied
- the cellular component(s) or molecule(s) that is(are) to be assayed
- the label(s)/probe(s) that is(are) to be used, and hence the signal(s) that is(are) to be detected.

All of these factors must be taken into account when considering how best to collect and prepare samples. A protocol that is satisfactory for one particular combination may not be suitable if applied to a different type of sample or if used to assay a different component.

2.2.1 The sample material and cells to be studied

Flow cytometers analyse the fluorescent and scattered light arising from cells illuminated in suspension, whereas laser scanning cytometers analyse the same parameters arising from cells illuminated on a microscope slide. It is possible to analyse tissue sections in the laser scanning cytometer, but in most current applications, cells are deposited onto the slide from a suspension. If the sample already comprises cells in suspension, e.g. cultured cells or peripheral blood, then it may be possible to process and analyse it directly. However, if the cells to be studied occur within a solid tissue, they must first be dissociated and dispersed, as described in Section 2.4.

Flow cytometry usually requires ~0.5 ml of a cell suspension, which ideally has a concentration in the range 10^5 to 10^6 cells ml^{-1}. Cell suspensions should be free of tissue debris and large aggregates (clumps) of cells in order to avoid clogging the flow cell and tubing; if necessary, large particulates should be removed by filtering or centrifuging prior to analysis. Laser scanning cytometry is most efficient when the cells are evenly distributed on the slide and separated by one to two cell diameters. Usually only approximately 10–20 μl of a suspension, containing approximately 2×10^5 cells ml^{-1}, is needed; however, larger volumes of less-concentrated cell suspensions can be also used, provided that a sufficient cell density can be obtained on the slide, e.g. by cytocentrifuging.

Dependent on the sample, the cells to be studied may be either homogeneous or heterogeneous with

respect to size and type. Flow cytometers can often distinguish different cell populations in heterogeneous samples solely on the basis of their forward and side light scattering characteristics. However, laser scanning cytometers, which monitor only a single (forward) light scatter component, are less able to do so. A fluorochrome-labelled antibody that is specific for a lineage or subset of cells, (e.g. CD45 antibodies for leukocytes; CD3 antibodies for T-cells), or a mixture of fluorescent antibodies, can sometimes be used to identify the cells of interest in heterogeneous samples, but this strategy decreases the number of fluorescence channels that can then be used for other purposes. Clearly, analysis is more efficient if the irrelevant cells can be removed from a sample. Therefore, it is worth considering whether samples can be enriched for the required cells, either before or after labelling, without prejudicing the aims of the study. Some methods that can be used for cell enrichment/isolation are discussed in Section 2.3.

When live cells are to be used, it needs to be decided how they should be maintained. Conversely, if fixed cells are to be used, it must be decided, how, and at what stage in the preparation procedure, they should be fixed. These issues are discussed further in Sections 2.5 and 2.6, respectively.

2.2.2 The molecules to be assayed

Where the molecule that is to be assayed occurs both inside the cell and on its surface, care needs to be taken to ensure that only molecules in the chosen location are detected. When detecting internal structures, it is often necessary to permeabilise cells in order to permit the label or probe to enter while still preserving the plasma membrane and cell ultrastructure; techniques for permeabilising cells are discussed in Section 2.7.

2.2.3 The label

Proteins and other biological molecules can be labelled (covalently conjugated) with fluorescent dyes in a way that enables them to retain their biological activity. Such conjugates can then be used to detect (both qualitatively and quantitatively) the cellular constituents to which they bind; examples of such reporter compounds include antibodies, small ligands, substrate analogues, nucleic acids and oligonucleotides. In addition, fluorescent dyes are available that bind directly to cell constituents (e.g. to nucleic acids) or for which fluorescence is sensitive to Ca^{2+} concentration, oxidoreduction state, or pH; the latter group can be used to report on the intracellular environment. Labels will have different physicochemical and biological properties, for example some will enter living cells freely while others will normally be excluded. Also, many will bind nonspecifically to structures other than the intended target and measures may need to be taken to reduce, or to account for, nonspecific binding. The principles underlying immunolabelling are introduced in Section 2.8 and the wide variety of fluorescent probes that are available and the precautions that must be taken when using them are discussed in Ch. 3.

Once these issues have been clarified, it is possible to begin to compile a protocol so that the various stages are compatible with each other and are adequate to fulfil the requirements of the investigation. At the same time, the risks from potential biological and chemical hazards need to be assessed and procedures devised to minimise them. In many instances, these matters will already be the subject of national and/or local guidelines or regulations, which will need to be implemented (see Section 2.10).

2.3 Blood and bone marrow

For some diagnostic purposes, e.g. immunophenotyping or DNA analysis, there are often reliable, well-established protocols already available, the details of which can usually be found in the guidelines produced by those organisations responsible for maintaining standards in laboratory medicine. For other purposes, there may be no consensus, with the merits of different procedures be-

ing the subject of on-going interlaboratory trials and/or vigorous debate in scientific journals. In the USA, the National Committee for Clinical Laboratory Standards (NCCLS), in the UK, the National External Quality Assurance Scheme (NEQAS), and in Europe, the European Working Group for Clinical Cell Analysis (EWGCCA) publish guidelines for immunophenotyping peripheral blood lymphocytes. In addition, a North American group (Shankey et al., 1993) and the European Society for Cellular Analytical Pathology (ESACP) (Ormerod et al., 1998) have published guidelines for the standardisation of DNA analysis.

Blood is usually collected by venepuncture directly into a tube containing an anticoagulant (e.g. Vacutainer, BD Biosciences; Monovette, Sarstedt; Venoject, Terumo). Three anticoagulants, heparin, K_3EDTA (ethylenediaminetetraacetic acid, tripotassium salt) and sodium citrate are commonly used for hematological analysis; a fourth, acid-citrate dextrose (ACD; 22.0 g l^{-1} sodium citrate ($Na_3C_6H_5O_7.H_2O$), 8.0 g l^{-1} citric acid, 24.5 g l^{-1} dextrose) is more often used for cytological analysis and cell culture but has also been used for flow cytometric studies of platelet activation. However, a recent study (Mody et al., 1999) has demonstrated that samples taken into CTAD (sodium citrate, theophylline, adenosine and diapyridamole; available as Diatube-H® tubes, BD Bioscience) showed less spontaneous platelet activation than those taken into citrate. If collecting blood for studies of platelet or leukocyte activation, it is worth discarding the first 2 ml and replacing the Vacutainer to avoid collecting blood that has been subject to stasis. Unfortunately all anticoagulants have effects in addition to preventing blood from clotting. Heparin enhances platelet activation and binds to platelets and other cells, acting as a specific blocker of inositol trisphosphate receptors and Ca^{2+} transport ATPases (see McCarthy and Macey (1996) for original references). Preservative-free heparin (10–50 U ml^{-1}) is preferred when leukocytes are to be used in functional assays. K_3EDTA and citrate-based anticoagulants decrease the free Ca^{2+} concentration of plasma and consequently may affect the antigenicity of Ca^{2+}-dependent epitopes and inhibit Ca^{2+}-dependent cell functions (Leino and Sorvajarvi, 1992; McCarthy and Macey, 1993). However, they have the advantage of decreasing platelet aggregation and reducing the loss of polymorphs and monocytes through adherence to the walls of the tube. Where it is desirable to avoid the effects of the common anticoagulants altogether, serine protease/esterase inhibitors such as leupeptin or aprotinin can be used; however, these inhibitors, in general, do not prevent clotting as effectively as do the conventional anticoagulants. Therefore, when using them, it is best to cool the sample to 4°C and to wash the cells free of plasma or to dilute samples into medium containing the inhibitor as soon as possible after collection (McCarthy and Macey, 1996).

Once collected, blood will deteriorate; heparin and ACD preserve cell morphology and light scatter characteristics better than K_3EDTA. If samples are to be immunostained, it is preferable to do so immediately and to keep the stained cells at 4°C, either with or without fixation before analysis. When this is not practicable, anticoagulated blood should be stored at 4°C for subsequent analysis of those markers that are susceptible to change, e.g. CD11b on myeloid cells (Repo et al., 1993), or at ambient temperature (20–25°C) for stable markers (Ashmore et al., 1989; Hensleigh et al., 1983). Polypropylene tubes and syringes are preferable to polystyrene or glass for collecting and handling samples because they minimise platelet and myeloid cell activation and adherence.

Bone marrow is usually aspirated from the iliac crest into medium containing heparin. It contains a mixture of different cell types including hematopoietic cells, adipocytes, endothelial cells and fibroblasts, which contribute to the extracellular support structure and microenvironment needed for hematopoiesis. Most aspirates also contain a certain amount of peripheral blood but it is impossible to distinguish the origin of the cells (i.e. blood versus marrow).

Mature non-nucleated erythrocytes constitute the major cell population in both blood and bone

marrow samples, and their high number tends to slow the analysis of leukocytes. For this reason, leukocytes are often isolated from blood (and to a lesser extent from bone marrow) samples by density gradient centrifugation (see Section 2.3.3) or by lysis of erythrocytes (see Section 2.3.5). Platelets are also present in blood in high number and, on activation, can form aggregates that are similar in size to leukocytes. If such aggregates are likely to interfere with the analysis, platelets can be removed before analysis by differential centrifugation. It is usual for leukocytes to be isolated by density gradient centrifugation before immunolabelling but for erythrocytes to be removed by lysis (and the leukocytes fixed) after immunolabelling. If the cells of interest are rare, it may also be an advantage to deplete the sample of irrelevant cells (see Section 2.3.4). Unfortunately, the techniques used for both leukocyte isolation (Romeu et al., 1992) and erythrocyte lysis (Macey et al., 1997) have the potential to cause artefacts (see below). Consequently, live whole blood procedures (Section 2.3.1) should be used whenever it is important to maintain the numbers of the different leukocyte classes, or of the lymphocyte subsets, or when it is necessary to quantify accurately those antigens that may be upregulated in vivo or are sensitive to reagents used for erythrocyte lysis and leukocyte fixation (e.g. formic acid and formaldehyde).

2.3.1 Live whole blood procedures

Mature erythrocytes and platelets can be distinguished from leukocytes in whole blood because they lack nuclei and stain only weakly with the vital nucleic acid dye LDS-751 (a styrl dye; Terstappen et al., 1988). Leukocytes, which possess a nucleus, will stain intensely with LDS-751 and also with fluorochrome-labelled CD45, a pan-leukocyte antibody (McCarthy and Macey, 1993; Repo et al., 1993; Terstappen et al., 1991). Nucleated erythrocytes, which often occur in bone marrow samples and in blood samples from newborn infants, resist lysis and have light scattering properties similar to lymphocytes. They can be distinguished from lymphocytes because they will stain positively with LDS-751 and anti-glycophorin antibodies but not with CD45 antibodies (see Protocol 2.1). The advantages of this procedure are that only small volumes of sample and antibody are required and processing is very quick (Macey et al., 1999); the disadvantage is that the analysis is slowed by the presence of erythrocytes. However, it is possible to speed the processing by using two discriminators, one to eliminate small forward scatter signals and the other to remove weak or nonfluorescent events from the analysis. Another dye with somewhat similar properties to LDS-751, and which can be used for the same purpose, is DRAQ5 (see Ch. 3) (Smith et al., 1999).

Protocol 2.1 Live whole blood procedure (LDS-751 and direct immunostaining)

Reagents

- A saturated solution of LDS-751 in methanol can be kept almost indefinitely in the dark at 4°C
- Hanks' balanced salts solution (without phenol red indicator) buffered with 10 mmol l^{-1} HEPES (*N*-[2-hydroxyethyl]piperazine-*N*'-[2-ethanesulphonic acid]), pH 7.3, containing 0.5% bovine serum albumin (HHBSS-BSA)

Protocol

1. Incubate 10 μl anticoagulated blood with 2 μl of FITC-conjugated and/or 2 μl PE-conjugated antibody at 4°C for 10 min.
2. Add 1 ml of HHBSS-BSA containing 0.1% (v/v) LDS-751 solution.
3. Keep at 4°C for 2–3 min to allow the LDS-751 to penetrate and stain the leukocytes.

Analysis

1. Analyse by flow cytometry, displaying events first in a plot of side light scatter (ordinate; linear scale) and LDS-751 fluorescence intensity (abscissa; logarithmic scale).

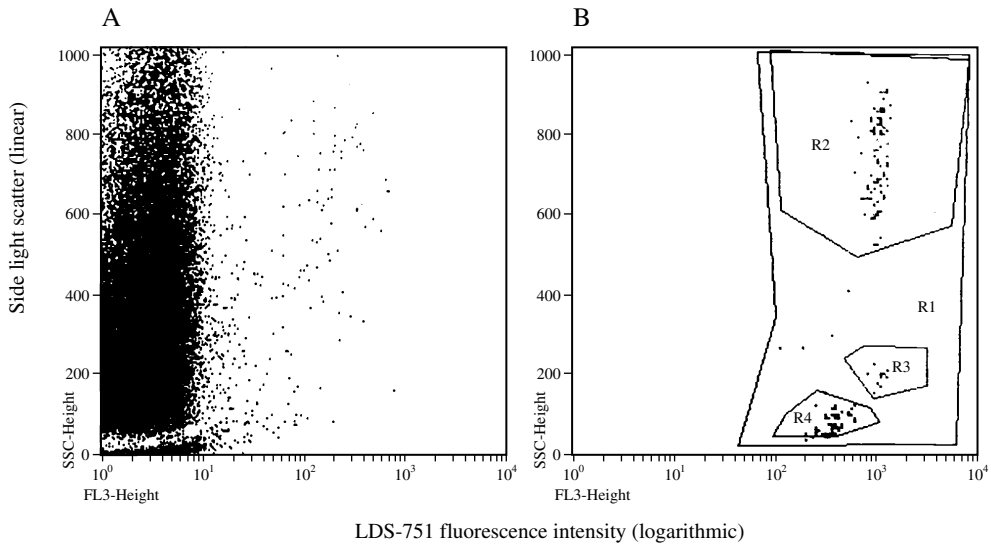

Fig. 2.1 Side scatter and fluorescence intensities of cells in whole blood stained with LDS-751. (A) The ungated bit map illustrates the high numbers of weakly fluorescent nonnucleated cells found in unlysed blood samples. A primary gate (labelled R1 in B) was set to exclude weakly staining cells (platelets and erythrocytes). (B) Secondary gates within R1, designated R2, R3 and R4, were identified as containing neutrophils, moncytes and lymphocytes respectively on the basis of their surface antigens. (Reprinted from *Journal of Immunological Methods* **163**, McCarthy, D.A., Macey, M.G., A simple flow cytometric procedure for the determination of surface antigens on unfixed leukocytes in whole blood, pages 155–60 (1993) with permission from Elsevier Science.)

2. Erythrocytes and platelets will stain only weakly and will occur in the first two fluorescence intensity decades (Fig. 2.1A); they can be eliminated from further analysis by setting a threshold on LDS-751 fluorescence intensity and/or by setting a gate to encompass all leukocytes (R1 in Fig. 2.1B).
3. Set a gate around the leukocytes of interest (e.g. R2, R3 or R4 in Fig. 2.1B) and display these events in a plot of side light scatter versus forward light scatter to confirm the light scattering characteristics of the cell population.
4. If it is satisfactory, the same events can be displayed also as a single-parameter histogram of number of events (ordinate; linear scale) versus fluorescence intensity (abscissa; logarithmic scale).
5. Alternatively, a third gate can be set around the cell population with the desired light scattering characteristics and these events displayed in the single-parameter histogram.

Note: LDS-751 (excitation/emission maxima, 543/712 nm) can be excited at 488 nm and monitored in the FL3 channel of most cytometers. The example given above used LDS-751 staining in conjunction with direct immunofluorescence but other fluorescence probes (e.g. for Ca^{2+} or O_2^-) can be used provided that their fluorescence can be monitored in the FL1 or FL2 channels (e.g. Himmelfarb et al., 1992; Macey et al., 1998).

If the leukocyte count is high, for example in pathological samples, blood should first be diluted in medium with anticoagulant so that the leukocyte numbers fall within the normal range or an increased amount of antibody should be used when immunolabelling.

When analysing those antigens that may be rapidly modulated (e.g. by capping or by internalisation) 0.1% sodium azide could be incorporated into the media used in steps 1 and 2.

2.3.2 Procedures for leukocyte enrichment and isolation

Samples can be enriched for leukocytes or the leukocytes can be isolated from them in a number of different ways. However, those procedures that involve centrifuging can lead to selective cell losses, while changes in temperature, centrifuging (Fearon and Collins, 1983; Forsyth and Levinsky, 1990), or the use of media containing trace amounts of bacterial lipopolysaccharide (Haslett et al., 1985) can result in neutrophil activation. Only endotoxin-free media should be used when studying neutrophils; endotoxin contamination can be detected using the limulus amoebocyte lysate test (Sigma) and, if necessary, removed using endotoxin removal resin; e.g. Acticlean Etox (Sterogene Bioseparations Inc.). A comprehensive account of the methods available for cell separation and isolation can be found in the treatise by Recktenwald and Radbruch (1997); Radbruch and Recktenwald (1995) discuss the detection and isolation of rare cells.

'Buffy coats' and dextran sedimentation

There are two simple procedures by which samples can be enriched for leukocytes for use subsequently in functional assays or for immunolabelling. In the first, anticoagulated blood is centrifuged for a short time at low speed and the leukocytes recovered from the interface (the buffy coat) between the erythrocytes and plasma (Protocol 2.2). In the second, anticoagulated blood is mixed with dextran and the leukocytes recovered after the erythrocytes have settled under gravity (Protocol 2.3). The advantage of these procedures is that the leukocytes are subject to the minimum of manipulation; however, the preparations are invariably contaminated by a small number of erythrocytes, which, if necessary, can be removed by lysis (see below). However, even these procedures can lead to neutrophil and monocyte activation (Macey et al., 1992, 1995).

Protocol 2.2 Preparation of 'buffy coat' leukocytes

1. Centrifuge anticoagulated blood at $200 \times g$ for 10 min at room temperature or at 4 °C.
2. Erythrocytes will settle at the bottom of the tube and leukocytes will form a band between them and the platelet-rich plasma above.
3. Carefully remove the leukocytes.
4. Depending on the study, the leukocytes can be resuspended in either the supernatant plasma or in autologous plasma from which platelets have been removed by centrifuging at $400 \times g$ for 20 min, or in medium such as RPMI 1640 (Roswell Park Memorial Institute 1640, a cell culture medium) containing 5% heat-inactivated fetal bovine serum (FBS).

Protocol 2.3 Preparation of leukocytes by dextran sedimentation

1. Mix 8 ml anticoagulated blood with 2 ml of sterile nonpyrogenic dextran (Hespan; DuPont) in a 10 ml plastic syringe that has been fitted with a wide bore (e.g. 19 gauge) needle that has its protective cover still in place.
2. Leave the syringe in a vertical position at 37 °C for 45–60 min, or until the erythrocytes have visibly settled leaving a turbid upper layer.
3. Holding the syringe in one hand and grasping the protective cover of the needle in the other, lift the cover clear of the hub of the needle and gently bend the shaft of the needle through about 90°.
4. Remove the needle cover completely, then by slightly tilting the syringe and gently pressing the plunger, deliver the leukocyte-enriched plasma into a centrifuge tube, leaving the erythrocyte layer behind in the syringe.
5. If it is necessary to remove the dextran, wash the leukocytes twice with 10 ml and resuspend in 1–2 ml of required medium. The medium chosen will depend on the particular study envisaged but

Table 2.1 *Commercial leukocyte isolation reagents*

Name	Supplier	Comments
Histopaque	Sigma	Polysucrose plus sodium diatrizoate: density 1.077 and 1.119 g ml^{-1}, for mononuclear cell or polymorph and mononuclear cell isolation
Histoprep	Sigma	Ficoll® plus metrizoic acid: density 1.077 g ml^{-1} for mononuclear cell isolation
Lymphoprep	Nycomed	Polysucrose plus sodium metrizoate: density 1.077 g ml^{-1}, for mononuclear cell isolation
Mono-Poly resolving medium	ICN	Ficoll®–Hypaque: density 1.114 g ml^{-1}, for polymorph and mononuclear cell isolation
Ficoll®–Paque PLUS	Pharmacia	Ficoll® plus sodium diatrizoate and Ca^{2+}EDTA: density 1.077 g ml^{-1} for mononuclear cell isolation
LymphoSep™	Organon-Teknika	Ficoll® plus sodium metrizoate: density 1.077 g ml^{-1}, for mononuclear cell
Lymphocyte Separation Medium	ICN	isolation
LeucoPREP™	BD Biosciences	Ready filled tubes for mononuclear cell isolation: composition not disclosed

RPMI 1640 with 5% FBS or HHBSS-BSA would be suitable for many purposes.

2.3.3 Leukocyte isolation by density gradient centrifugation

Density gradient centrifugation can be used to isolate leukocytes from blood and bone marrow samples but it can give variable/selective recovery of lymphocytes (Tamul et al., 1995) and is therefore not recommended for immunophenotyping. Two different density gradient media, iodinated aromatic compounds originally produced as X-ray contrast media and polyvinylpyrrolidone-coated silica gel particles, are commonly used to isolate blood cells (for a review, see Boyum et al., 1991).

Hypaque (Histopaque, Isopaque) and Nycodenz

Two slightly different protocols can be used. One enables only mononuclear cells (lymphocytes and monocytes) to be isolated (Protocol 2.4), whereas the other enables both polymorphs and mononuclear cells to be isolated (Protocol 2.5). A variety of reagents are commercially available (Table 2.1) under different names but they are usually mixtures of Ficoll® (a dextran polymer) and an X-ray contrast medium such as sodium diatrizoate, meglumine diatrizoate and metrizamide (supplied as Hypaque, Histopaque, or Isopaque, respectively) or Nycodenz. Ficoll® promotes erythrocyte aggregation, while the contrast media increase the osmolarity and density of the solution. The high osmolarity causes more rapid shrinkage of erythrocytes than of leukocytes, thereby increasing their density and facilitating their preferential sedimentation (Bignold and Ferrante, 1987; McCarthy et al., 1984). By adjusting the density and osmolarity of the medium, the different leukocyte classes can be sedimented to different depths in the centrifuge tube (Boyum et al., 1991; Rickwood, 1983). Protocols using a single layer of medium are routinely used for isolating lymphocytes but protocols using either a single layer or two layers of different densities can be used for isolating polymorphs (Fig. 2.2). When using these Ficoll®–Hypaque layers to isolate leukocytes from pathological samples with low mean corpuscular hemoglobin concentrations, the erythrocytes often fail to sediment. If necessary, the osmolarity and density can be adjusted in order to obtain satisfactory separations (Ferrante and Thong, 1980; McCarthy et al., 1984; Needham, 1987). Alternatively, rouleaux formation (which favours erythrocyte sedimentation) can be encouraged using an anti-erythrocyte antibody (Red-Out; Robbins Scientific).

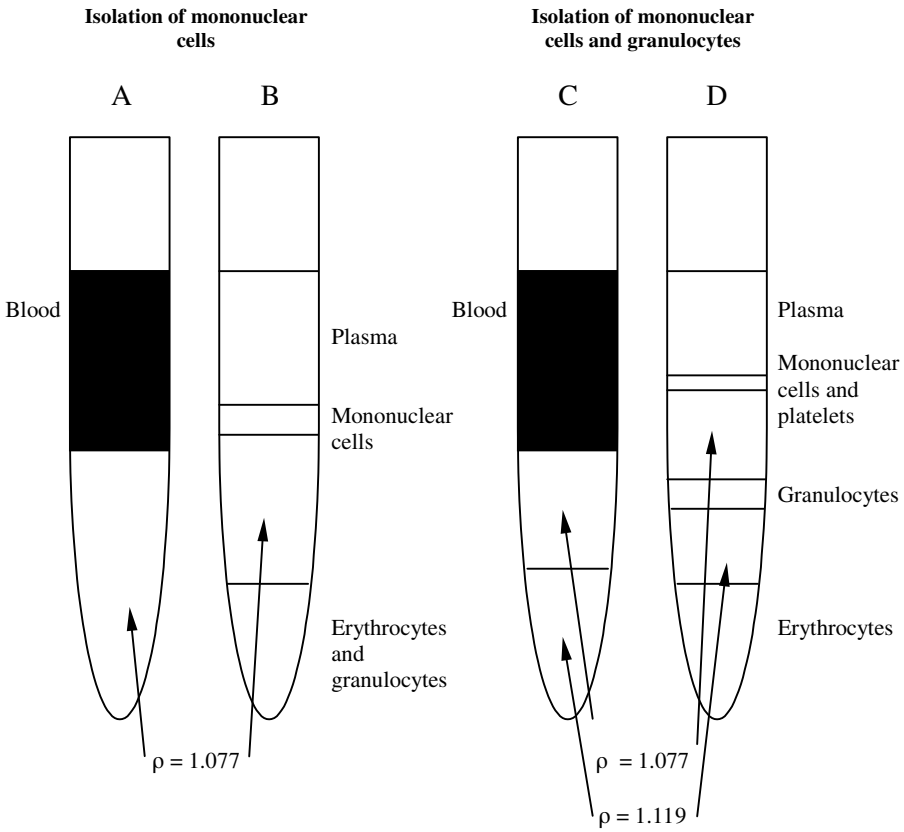

Fig. 2.2 Ficoll®–Hypaque single- and two-layer systems for the isolation of blood leukocytes. (A and B) The isolation of mononuclear cells; (C and D) the simultaneous isolation of mononuclear cells and granulocytes. (A and C) The tube contents before centrifuging; (B and D) the positions of the leukocytes and erythrocytes after centrifugation.

When isolating polymorphs, it is worth noting that the yield and purity can be improved if the height of the blood column is maximised during the first centrifugation and if the cells are centrifuged a second time over the density gradient medium (Ferrante and Thong, 1980; McFaul, 1990). It is essential to wash the cells thoroughly to reverse the shrinkage caused by the high osmolarity of the solutions.

For high-risk samples it is possible to obtain VACUTAINER® CPT™ tubes (BD Bioscience), which are evacuated tubes containing either sodium citrate or sodium heparin anticoagulant, a separation gel and a Ficoll®/density gradient liquid. Blood collected directly into the tube is centrifuged as usual and at the finish, the separation gel forms a stable barrier separating the mononuclear cells from the erythrocytes and granulocytes.

Protocol 2.4 Isolation of blood mononuclear cells on Ficoll®–Hypaque

1. Place 3 ml Histopaque 1.077 g ml^{-1} into a 10 ml plastic centrifuge tube and carefully overlay with 3 ml anticoagulated blood diluted 1 : 1 with phosphate-buffered saline (PBS; 154 mmol l^{-1} NaCl, 1.54 mmol l^{-1} KH_2PO_4, 2.7 mmol l^{-1} Na_2HPO_4, pH 7.4).

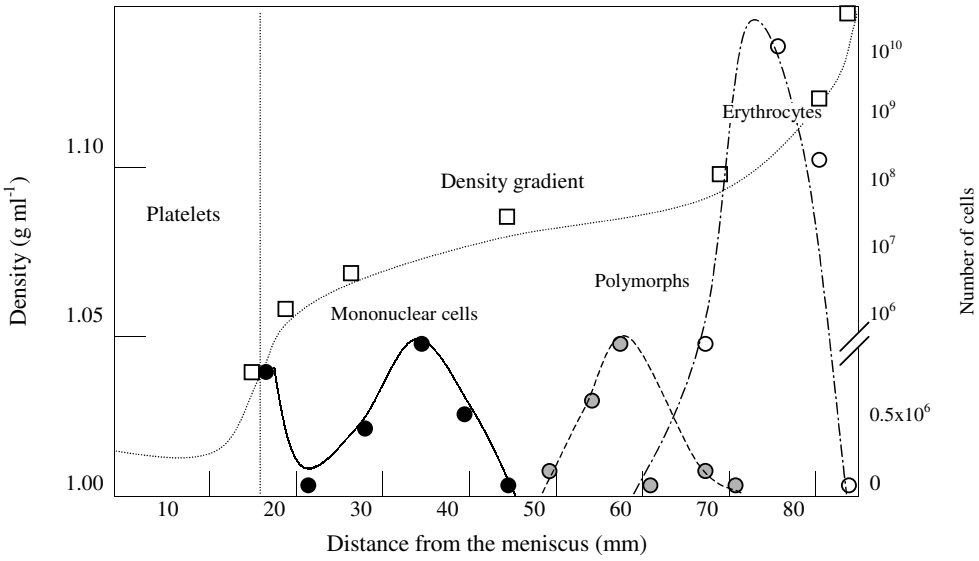

Fig. 2.3 Separation of human blood cells in a Percoll® density gradient. Blood was layered on a preformed 70% (v/v) Percoll® density gradient in 0.15 mol l^{-1} NaCl and centrifuged at 400 × *g* for 5 min. The plasma layer containing platelets was removed and centrifugation continued at 800 × *g* for 15 min resulting in isopycnic banding of the blood cells. Interpolation with a calibration curve constructed by monitoring the sedimentation of density marker beads under the same conditions indicated that erythrocytes, polymorphonuclear leukocytes and lymphocytes had densities of 1.10, 1.084 and 1.07 g ml^{-1} respectively, under iso-osmotic conditions. (Redrawn from Pertoft et al., 1979.)

2. Centrifuge at 400 × *g* for 30 min at room temperature (20–23 °C).
3. Erythrocytes aggregate and, together with the polymorphs, sediment into the Histopaque; mononuclear cells band at the interface between the plasma and the Histopaque, and platelets, for the most part, remain in the plasma layer.
4. Remove the mononuclear cells with a pipette and wash twice by centrifuging with 10 ml medium (e.g. RPMI with 5% FBS or 10 mmol l^{-1} HHBSS-BSA at 400 × *g* for 5 min.
5. Resuspend in 1 ml medium.

Protocol 2.5 Simultaneous isolation of polymorphs and mononuclear cells on Ficoll®–Hypaque

1. Place 3 ml Histopaque 1.119 g ml^{-1} into a 10 ml plastic centrifuge tube; carefully overlay with 3 ml Histopaque 1.077 g ml^{-1} and then with 3 ml anticoagulated blood diluted 1 : 1 with PBS.
2. Centrifuge at 700 × *g* for 30 min at room temperature (20–23 °C).
3. Erythrocytes aggregate and sediment into the Histopaque; polymorphs band at the interface between the two Histopaque layers, and mononuclear cells band at the interface between the plasma and the uppermost Histopaque layer. Most of the platelets remain in the upper (plasma) layer.
4. Remove the bands separately with a pipette and wash the cells twice by centrifuging with 10 ml of medium (e.g. RPMI with 5% FBS or 10 mmol l^{-1} HHBSS-BSA at 400 × *g* for 5 min.
5. Resuspend the cells from each band in 1 ml medium.

Percoll®

Percoll® is the trade name for a polyvinylpyrrolidone-coated colloidal silica preparation (with a mean particle diameter 21–22 nm) that will form a density gradient when it is centrifuged in solution. Its advantage over Ficoll®–Hypaque is that gradients of appropriate density for separating blood cells can be formed while still maintaining iso-osmotic conditions (Fig. 2.3). If diluted blood is centrifuged on preformed Percoll® density gradients, all of the different blood cells can be separated (Pertoft, 1979). However, the procedures are lengthier and more complicated than density centrifugation using X-ray contrast media and for most purposes offer little advantage. At present, the main use for Percoll® density gradient centrifugation is in isolating monocytes from mononuclear cell preparations that have been produced first by Ficoll®–Hypaque centrifugation (Denholm and Wolber, 1991).

2.3.4 Positive or negative selection of cell populations

Where the cells of interest are rare, e.g. $CD34^+$ stem cells in peripheral blood, it may be profitable to remove defined but irrelevant cells from the sample by negative immunoselection (Fig. 2.4), or to recover the required cells by positive immunoselection. There are a number of different ways in which this can be done, for example, by immunoagglutination and sedimentation, by immunoaffinity column chromatography or with immunomagnetic beads (Vettese-Dadey, 1999). For laboratories that regularly need to enrich samples, or where 90–95% purity by simple depletion alone is satisfactory for experimental purposes, an automated immunomagnetic 'pre-sorter' is available commercially (autoMACS Pre-Sorter; Miltenyi Biotec Inc.). Details of some of the commercially available reagents and kits that can be used for this purpose are given in Table 2.2.

2.3.5 Erythrocyte lysis procedures

Erythrocytes can be removed from whole blood or leukocyte preparations by hypotonic lysis with water (Protocol 2.6), by isotonic lysis with ammonium chloride (Protocol 2.7), or by damaging their membanes with saponin (Protocol 2.8). None of these procedures will remove nucleated red cells; moreover, it is rare to achieve 100% lysis of mature erythrocytes in whole blood, and the remaining leukocytes are often contaminated with erythrocyte 'ghosts'. These procedures do not seem to affect the majority of surface antigens on leukocytes and have been used on many occasions to prepare leukocytes for use in functional assays. Treatment with ammonium chloride results in acidification and then alkalinisation of the cytoplasm of the unlysed leukocytes, which may be inappropriate for some functional assays. It would be prudent, therefore, to check the effects of lysing agents on leukocytes that have been isolated by other methods. A number of reagents for lysing erythrocytes without also fixing leukocytes are available from commercial sources (Table 2.3).

Protocol 2.6 Distilled water lysis of erythrocytes

1. Mix 1 ml anticoagulated blood with 9 ml de-ionised water at room temperature for 15–30 s.
2. Add 10 ml of a twofold concentrated medium, e.g. RPMI with 10% FBS, to restore the tonicity.
3. Collect the leukocytes by centrifuging at $400 \times g$ for 5 min at room temperature.
4. Resuspend in 1 ml medium.

Protocol 2.7 Ammonium chloride lysis of erythrocytes

1. Make the lysing solution, which is 154 mmol l^{-1} NH_4Cl, 10 mmol l^{-1} $NaHCO_3$, 0.1 mmol l^{-1} EDTA, pH 7.3 by adding 0.826 g NH_4Cl, 0.1 g $NaHCO_3$, 0.0037 g Na_4EDTA to 100 ml de-ionised water and adjusting the pH to 7.3 with HCl or NaOH as necessary. The solution should be prepared daily or kept sterile because absorption of atmos-

Table 2.2 *Reagents for the negative selection of leukocyte populations*

Brand name	Manufacturer	Comments
PrepaCyte™	BioErgonomics Inc.	Rapid one-step isolation of T-cells and hematopoietic stem cells by antibody-mediated agglutination of other components
ActiCyte™	BioErgonomics Inc.	Isolation of leukocytes for in vivo culture
cellect™ and cellect™•plus	Cytovax	Isolation of T-cells or T-cell subpopulations by negative selection through a column containing a glass bead matrix
ACT-CES™	Micra	Negative selection of antibody-labelled cells by binding to nonporous beads coated with goat anti-mouse antibody or streptavidin and centrifugation
BioMag®	Polysciences	Positive or negative selection using 1 μm diameter magnetic particles coated with second antibodies, e.g. anti-fluorescein, streptavidin, etc.
StemSep	StemCell Technologies	One-step negative selection using tetrameric antibody complexes bound to colloidal magnetic dextran iron, which are retained in a magnetic column
RosetteSep	StemCell Technologies	Tetrameric antibody complexes are used to link unwanted cells to erythrocytes in the sample and the rosettes removed by centrifugation on Ficoll®–Paque
ProActive®	Bangs Laboratories	Protein (e.g. streptavidin, Protein A)-coated super-paramagnetic or nonmagnetic microspheres
SeraMag™	Serva	Streptavidin-coated super-paramagnetic 1 μm diameter microspheres
Dynabeads	Dynal	Magnetic beads of diameter 2 or 4 μm retained in a tube
MACS	BD Biosciences, Miltenyi Biotech	Magnetic activated cell sorting: using direct or indirect positive or negative immunoselection with antibody-coated 50 nm diameter magnetic microspheres

pheric CO_2 produces ammonium carbonate, which will not lyse erythrocytes.
2. Add 1 ml anticoagulated blood to 15 ml lysing solution and gently mix at room temperature for 3–5 min until the originally turbid suspension has become clear.
3. Centrifuge at 400 × *g* for 5 min.
4. Resuspend the leukocyte pellet and wash twice by centrifuging in 15 ml HHBSS-BSA at 400 × *g* for 5 min.
5. Resuspend in 1 ml HHBSS-BSA.

Protocol 2.8 Saponin lysis of erythrocytes

1. Add 1 ml of anticoagulated blood to 2 ml of a pre-cooled (4 °C) 1% solution of saponin (Sigma) in de-ionised water in a centrifuge tube and mix thoroughly and leave on ice for 5 s.
2. Add 10 ml of PBS.
3. Cap the tube and invert it intermittently over the next 30–40 s until the originally turbid suspension has cleared.
4. Collect the leukocytes by centrifuging at 400 × *g* for 5 min at room temperature.
5. Resuspend in 1 ml medium.

2.3.5 Lysed whole blood procedures (erythrocyte lysis and leukocyte fixation)

When it is important to preserve the immunostaining and distribution of leukocyte numbers present in vivo, leukocytes can be stained in whole anticoagulated blood, the erythrocytes removed by lysis and the leukocytes post-fixed; this method is known as the 'lysed whole blood' procedure (Protocol 2.9). The labelled and fixed leukocytes can be analysed immediately or up to several days later if they are kept in the dark at 4 °C. A number of manufacturers offer kits for this purpose (Table 2.4) in which different reagents are used to lyse

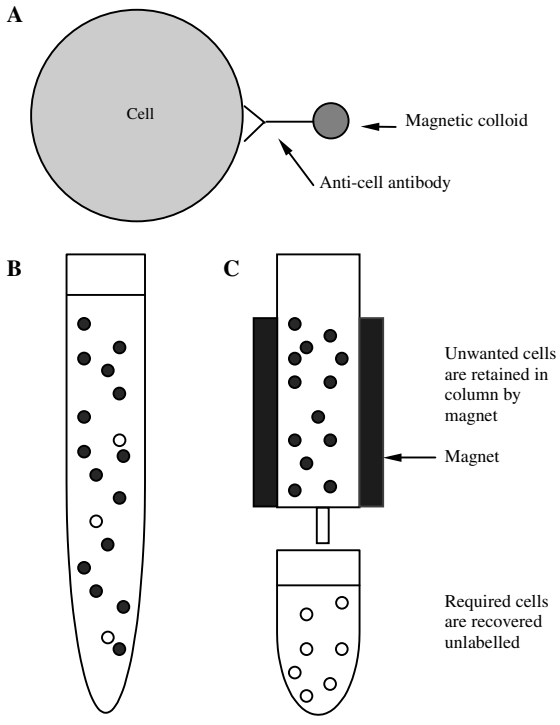

Fig. 2.4 Negative selection principle. Unwanted cells (solid) in a cell suspension are labelled with a cocktail of antibodies bound to magnetic colloid beads (A and B). Passing the cell suspension through a column surrounded by a magnet traps the unwanted cells and allows the unlabelled required cells to be collected.

erythrocytes but the leukocytes are always fixed, either simultaneously or subsequently, with formaldehyde. Those procedures that only require the reagents to be added sequentially can be automated, as is done for example in the Coulter Immunotech TQ-PREP™ system. Unfortunately, the reagents used for erythrocyte lysis and/or leukocyte fixation may alter the apparent expression of certain epitopes if they are sensitive to acid or formaldehyde (Macey et al., 1997, 1999; McCarthy et al., 1994). Furthermore, cells that are kept in formaldehyde become increasingly permeable and if the antibodies used for labelling have not been removed by washing they may subsequently bind specifically and/or nonspecifically to internal components. The particular method chosen for lysing erythrocytes can have a marked effect on immunophenotyping results and some may be more suitable for given applications than others (Bossuyt et al., 1997).

Protocol 2.9 Lysed whole blood procedure with direct immunostaining

1. Incubate 100 µl anticoagulated blood with 20 µl fluorochrome-conjugated antibody at 4°C for 10 min.
2. Process the stained blood using one of the reagent kits listed in Table 2.2, in accordance with the supplier's instructions.
3. Analyse by flow cytometry, displaying events first in a plot of side light scatter (ordinate; linear scale) and forward light scatter (abscissa; linear scale).
4. Set a gate around the leukocytes of interest and display these events as a single-parameter histogram of number of events (ordinate; linear scale) versus fluorescence intensity (abscissa; logarithmic scale) (Fig. 2.5).

2.4 Preparation of cell suspensions from solid tissues and cell cultures

Cell suspensions can readily be prepared from monolayers of cultured cells, e.g. human umbilical vein endothelial cells, by the dissociation procedures used when passaging cells (see below). They can also be prepared from solid mammalian tissues by disrupting cell–cell junctions and/or the interactions between cells and the intercellular matrix. Depending on the tissue concerned, this may be achieved by enzymic treatment and/or mechanical means. Mechanical disaggregation alone is really only suitable for those tissues in which the cells are loosely bound, e.g. bone marrow, spleen and lymph nodes. It is much less effective for tissues in which cells are tightly bound, and enzymes are normally used instead to disrupt the

Table 2.3 *Commercial erythrocyte lysis reagents without fixative*

Brand name	Manufacturer	Stated components/comments
IQ Lyse	IQ Products	Not disclosed
Lysing buffer	Immunicon	Ammonium oxalate pH 7.75, with additives
Quicklysis	Cytognos	Not disclosed
Red blood cell lysing buffer	Sigma	Ammonium chloride, tris-HCl
VitaLyse™	BioErgonomics Inc.	Not disclosed, subsequent use of fixative optional
Whole blood lyse kit	R & D Systems	Not disclosed

Table 2.4 *Commercial erythrocyte lysis and leukocyte fixation reagents*

Brand name	Manufacturer	Stated components/comments	Time (min)
FACS™ Lysing Solution	BD Biosciences	Formaldehyde, diethylene glycol, buffer	30
Immuno-Lyse	Beckman Coulter	Not disclosed	~ 10
Immunoprep	Beckman Coulter	Formic acid, buffer, formaldehyde	1.5
LF-1000 Lyse and Flow	Harlan	Formaldehyde, diethylene glycol, buffer	30
Lyse and Fix IOTest	Beckman Coulter	Lysing agent (not disclosed) and formaldehyde	~ 15
OptiLyse C	Beckman Coulter	Formaldehyde, diethylene glycol, buffer	15
Uti-Lyse	Dako	Formaldehyde, buffer	20
Q-lyse™	BioErgonomics	Separate lysing agent (not disclosed) and fixative (formaldehyde)	30
Erythro-Lyse™	ICN	Lysis at physiological pH, fixative included (use optional)	20
Cal-Lyse	Caltag	Formaldehyde	25 (no wash) or 30 (with washing)
Whole blood lyse kit	R & D Systems	Not disclosed	20

bonds that bind cells to the extracellular matrix and to each other (Protocol 2.10). Proteases, e.g. trypsin, collagenase, elastase and, more recently, dispase (a neutral metalloprotease with a mild action), and enzymes that hydrolyse the extracellular matrix, e.g. hyaluronidase and lysosyme, are commonly used to separate cells. Chelating agents (K_3EDTA or citrate) are often included in order to remove Ca^{2+} and Mg^{2+}, which are essential for matrix stability and cell–matrix interactions, but these alone will not liberate cells (Protocol 2.11). They can be used in conjunction with trypsin but not collagenase because activity of the latter is Ca^{2+} dependent. DNAase is often included to prevent cell–cell aggregation, which might otherwise be induced by the DNA released from damaged cells.

The aim is to obtain a good yield of cells, while simultaneously preserving the plasma membrane and intracellular components. If proteases are used, the possibility that they will cleave, and thereby alter the antigenicity of, cell surface glycoproteins must always be borne in mind. The viability of the dispersed cells obtained from solid tissue is generally higher following enzymic than mechanical dissociation, but the former can lead to selected losses of certain cell populations. If cell suspensions are to be used for flow cytometry, they should be filtered through nylon mesh, or single cells recovered by density gradient centrifugation (e.g. on Ficoll®–Hypaque), to avoid blocking the flow cell. As there are few comparative studies of the merits of different dissociation procedures (Visscher and

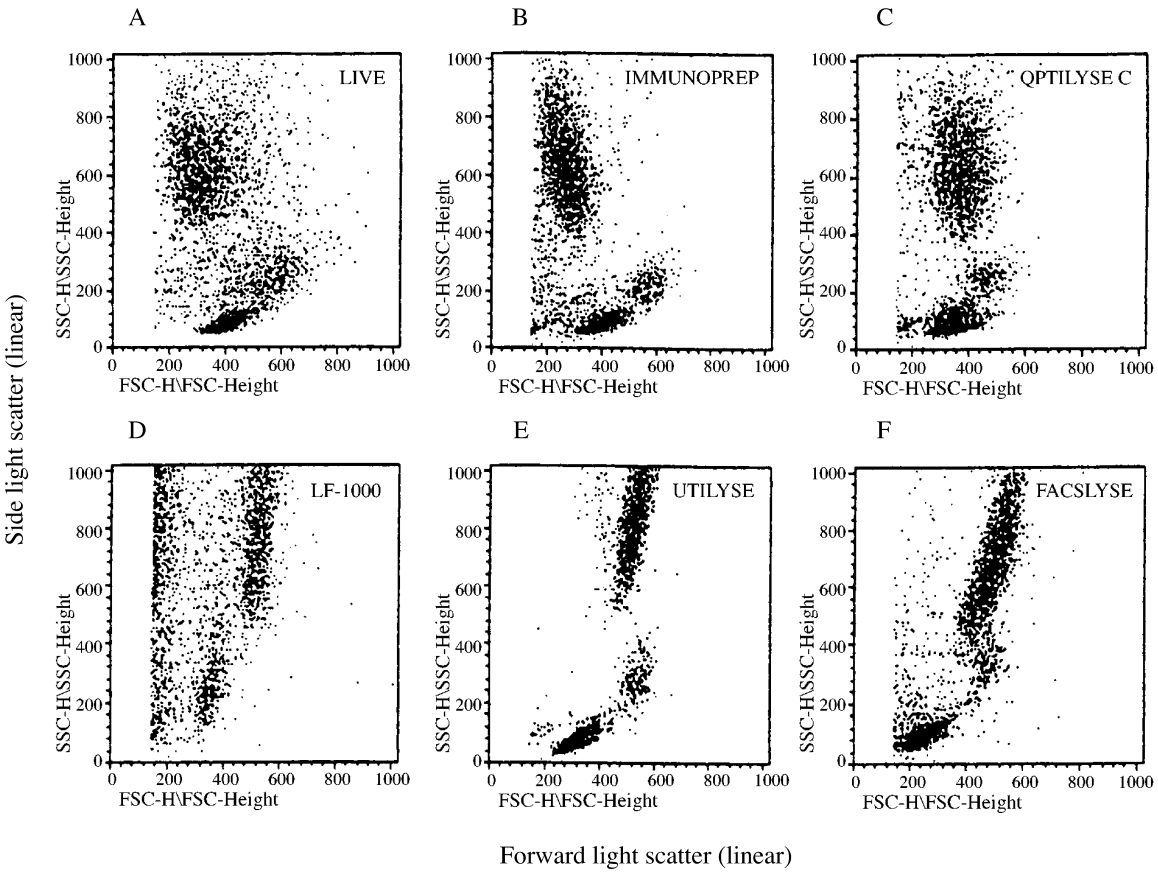

Fig. 2.5 Flow cytometric analysis of forward and side light scatter of blood from a healthy individual. (A) Leukocytes analysed by the whole live blood procedure. The histogram is produced by gating on a region similar to that denoted R1 in Fig. 2.1B. (B–F) Distributions obtained when cells were prepared using the ImmunoPrep (Beckman Coulter), OptiLyse C (Beckman Coulter), LF-1000 Lyse and Flow (Harlan Sera-Lab), Utilyse (Dako) and FACS™ Lysing Solution (BD Biosciences) reagents, respectively. (Reprinted by permission of Wiley-Liss, Inc., a subsidiary of John Wiley & Sons, Inc., from Macey, M.G., McCarthy, D.A. Newland, A.C. (1997) The Q-Prep system: effects on the apparent expression of leukocyte cell surface antigens. *Cytometry* (*Communications in Clinical Cytometry*) **30**, 67–71.)

Crissman, 1994), it is advisable to monitor the products by both cytometry and microscopy to confirm that the cells are representative of the original tissue, a factor that is of particular importance when sampling heterogeneous tumours. A mechanical tissue disaggregation system, designed specifically for preparing samples for flow cytometry, is available commercially (Medimachine System; BD Biosciences). It would be particularly useful where solid tissue samples are frequently analysed as it facilitates standardisation and removes variability in processing technique.

Protocol 2.10 Disaggregation of solid tissues

1. Collect body tissues into 10 ml RPMI 1640 medium containing penicillin/streptomycin

(0.1 ml of a 100-fold concentrate). Keep at 4°C until used; no more than 6 h later because of autolytic deterioration.
2. Place approximately 100 mg* into a Petri dish containing 5 ml of RPMI medium as above.
3. Chop into small pieces with a scalpel fitted with a number 20 blade or by using a McIlwain tissue chopper.
4. Resuspend the pieces in 5 ml medium and disrupt further by pipetting up and down using a plastic pipette, e.g. Pastette, being careful to avoid foaming.
5. As an alternative to chopping, cells can be scraped from the surfaces of the tissue using a scalpel blade; or the processing can be done in the Medimachine System (see text).
6. Collect the liberated cells and remaining tissue fragments by centrifuging, and resuspend these in 1 ml of RPMI 1640 containing collagenase type II (0.5 mg ml^{-1}), trypsin or dispase (2.5 mg ml^{-1}) and DNAase I (20 μg ml^{-1}) (protocol based on that described by Visscher and Crissman, 1994).
7. Incubate at 37°C for 1 h on a rocking platform or in a shaking water bath. Add 2 ml FBS to stop further proteolysis.
8. Allow larger fragments to settle, then remove the supernatant through a nylon mesh or micropore filter to remove any remaining cell aggregates and debris. The pore size to be used will depend on the sample, but typically would be in the range 35–100 μm; e.g. nylon mesh marketed as 'CellMicroSieve' in pore sizes ranging from 5–200 μm is available from BioDesign.
9. Wash the cells twice by centrifuging at 300 × *g* for 5–10 min in ~15 ml medium containing 10% FBS.
10. Resuspend in 1 ml medium.

*The amount of tissue may need to be varied in order to obtain a sufficient cell yield, and the constituents of the enzyme cocktail may need to be optimised for different tissues.

Protocol 2.11 Cell suspensions from anchorage-dependent cells

1. Remove culture medium.
2. Wash monolayer with PBS without Ca^{2+} and Mg^{2+}.
3. Add trypsin/EDTA (0.1% and 0.2%, respectively) in PBS.
4. Resuspend and wash the cells by centrifuging at 300 × g for 5–10 min in ~15 ml of PBS containing 10% FBS to stop further trypsin action.
5. Resuspend in 1 ml medium.

2.5 Live samples

It is clearly necessary to use living cells when assessing functional capabilities such as phagocytic ability or responses to agonists in vitro, but there are also good reasons to use live cells when attempting to assess functional characteristics such as the surface expression of adhesion molecules. In both situations, the aim is to maintain the cells in a state which matches, as closely as is possible, that found in vivo. The choice of solution environment (or medium) is, therefore, dictated by the nature of the sample, but it will usually be a buffered physiological salts solution, to which has been added some extraneous protein. Commonly used media include Hanks' balanced salts solution, Tyrode's solution and tissue culture media such as RPMI 1640. However, when using tissue culture media it is important to use only solutions that do not contain an indicator dye such as phenol red. If cells are to be maintained in media for a long time, it is probably best to use a carbonate–bicarbonate buffer in equilibrium with a 5% CO_2 atmosphere. Otherwise the pH can be maintained with one of the Good's buffers, such as HEPES, which have the advantage over the traditional inorganic and organic buffer solutions, in that the components are charged and do not enter cells. A buffer concentration of 10 mmol l^{-1} is normally adequate to maintain the pH of a solution containing cells, at the density used for

cytometric analysis, for several hours. The added protein may be essentially 'inert' and for this purpose 1–5% BSA or 5–10% human serum or FBS are frequently used. In other situations, the added protein may deliberately also contain some 'activity', e.g. when immune serum is used as a source of specific antibodies. Whatever the source, it will saturate any nonspecific protein-binding sites and act as a target for any free radicals that might be produced, e.g. by phagocytic cells. When assessing surface antigens on live leukocytes it must, of course, be remembered that some surface antigens, for example CD14, CD16, CD32, CD62L, tumour necrosis factor-α, are subject to cleavage by serum and/or endogenous enzymes, which may be activated by antibody or receptor binding (Bazil, 1995). A major advantage of using live cells in immunolabelling studies is that they bind lower levels of antibodies in a nonspecific manner than do fixed, or dead, cells.

2.6 Fixed samples

2.6.1 Fixation techniques and potential artefacts

Fixation is clearly not appropriate for functional studies but has been used extensively in conjunction with immunolabelling for phenotypic analysis. There are many potential advantages to fixing cells at some stage during the preparation procedure. Cells in samples that are fixed soon after collection, and prior to labelling, are theoretically not subject to inadvertent postcollection changes (e.g. the upregulation of adhesion molecule expression on peripheral blood neutrophils) that might otherwise occur in vitro. Moreover, they can often be processed later, at a perhaps more convenient time. However, fixation before labelling also has some drawbacks. Most important is the likelihood that antigenicity will be altered (usually diminished), leading to decreased antibody binding or even false-negative results. In addition, the 'signal to noise' ratio can be decreased because the nonspecific binding of antibodies is increased.

When contemplating the use of fixatives, it is as well to understand their mode of action. All commonly used fixatives cause chemical changes in nucleic acids and proteins that result in conformational changes which can alter, or abolish, antigenicity. In general, antigenicity is lost progressively with increasing concentration of fixative and increasing time of fixation, while ultrastructural integrity is increasingly preserved. Consequently, the conditions chosen for fixation are always a compromise between preserving ultrastructure and losing antigenicity. There are two main types of fixative: protein precipitants/coagulants and cross-linking agents. Alcohols and acetone are precipitating or coagulating fixatives. Traditional cross-linking fixatives include the aldehydes such as formaldehyde, but new bifunctional molecules initially developed for protein biochemistry studies are increasingly being used. Dialdehyde fixatives such as glutaraldehyde, which is widely used in electron microscopy, are successful because they form cross-links almost as rapidly as they form adducts. However, they cause a high background autofluorescence, which makes them unsuitable for many cytometric applications. The newer carbodiimide cross-linking reagents act by linking carboxyl to amino groups through amide (peptide) bond formation. Although not yet widely used, they have the advantage of producing only low background fluorescence.

2.6.2 Alcohols and acetone

Alcohols and acetone compete with water molecules for hydrogen bond formation and cause proteins to precipitate in situ but do not fix nucleic acids or carbohydrates, which can leach out from cells. Membrane lipids are solubilised and extracted; consequently organelles and ultrastructure are usually poorly preserved and cells are permeabilised. Their effects on proteins result in a marked increase in the refractive index of the cytoplasm, which rises from about 1.35 in living cells to about 1.5. Since the intensity of light scattering is a function of the difference in refractive index between the medium (isotonic saline has a refractive

index of ~1.355) and the cell, this enhances the signal and, in flow cytometry at least, can improve the discrimination between different cell types. Despite causing these artefacts, coagulant fixatives are useful for detecting high-molecular-weight antigens or structural proteins by light immunomicroscopy. Ethanol is a poor fixative for most cells but methanol at –20°C is a better fixative and is commonly used for blood, bone marrow and cell suspensions obtained by tissue disruption. A significant problem with these fixatives is their tendency to cause cell–cell aggregation and to cause cells to stick to the walls of plastic tubes. Acetone (but not 80% acetone in water) will also dissolve tubes made from polystyrene.

2.6.3 Formaldehyde

Formaldehyde (CH_2O, boiling point –21°C) is a water-soluble gas at room temperature and is commonly available as commercial formalin (a 37–40% aqueous solution of formaldehyde containing $<0.05\%$ formic acid and 10–15% methanol to prevent polymerisation). These additives make it unsuitable for cytometry and ultrastructural cytology. Paraformaldehyde is a polymerised form of formaldehyde that is solid at room temperature but which will dissolve slowly in aqueous solution at neutral pH. Formaldehyde solutions can be prepared from it (by heating at 60°C for ~1 h to overnight); when fresh, they are free of additives and polymers. Alternatively, an electron microscopy grade of formaldehyde can be purchased that is free of additives (and, when new, also of polymers). Formaldehyde in aqueous solutions gradually polymerises; consequently its effective concentration decreases with time. For this reason, working strength formaldehyde-containing solutions are best made fresh when required; they should be stored only for short periods (<7 days) and at room temperature.

Formaldehyde is the simplest monoaldehyde and reacts by covalent addition to most biological macromolecules (French and Edsall, 1945). There are a variety of target groups and the reactions are quite complex, but probably the most important targets are the free amino groups found on the amino acids in proteins and on the bases in nucleic acids. Adduct (hemiacetal) formation is rapid; where hemiacetal derivatives are in close proximity, methylene bridges will form slowly by condensation reactions and this will cross-link macromolecular structures. Formaldehyde is also a good fixative for lipids, especially if divalent cations (Mg^{2+} or Ca^{2+}) are present. It usually leaves the carbohydrate moieties of cell surface glycoproteins unchanged but often affects the antigenicity of surface and intracellular proteins; it also increases cell autofluorescence and adversely affects subsequent DNA staining.

For most samples, fixation is best done at room temperature, or at 37°C, because fixation is generally poorer at 4°C. Samples are usually best washed free of extraneous proteins, e.g. serum, before fixation with formaldehyde. If this is impracticable, it may be necessary to increase the formaldehyde concentration. After mild fixation with formaldehyde (e.g. 0.2% for 4 min at 37°C), cells often show increased permeability to small molecules but remain impermeable to large molecules such as antibodies (McCarthy and Macey, 1993). Stronger fixation leads to the formation of blebs in the membrane, which can detach and give rise to cell fragments in the sample and to a greater degree of membrane permeabilisation. Consequently, when immunolabelling formaldehyde-fixed cells, it must be borne in mind that both surface and internal structures may be accessible to the antibody used. Before immunolabelling, it is also essential to remove excess formaldehyde by washing and to block any free aldehyde groups by quenching with a source of amino groups such as glycine, otherwise high nonspecific binding might result.

2.6.4 Postfixation

Surface antibody binding can be preserved by washing the immunostained cells free of extraneous protein and storing them in 1% formaldehyde in PBS. Fixation under these circumstances will eventually cross-link the antibody molecules to neighbouring structures and prevents loss of the fluorescent label.

If only mild fixation, sufficient to inhibit metabolic or energy-dependent changes but insufficient to result in extensive cross-linking, is required, the cells can be washed free of formaldehyde after 10 min by centrifuging in PBS. Fixative solutions are often commercially available as separate reagents within erythrocyte lysis and leukocyte fixation kits (see Table 2.4) or may be obtained separately, e.g. Stabil-Cyte™ (BioErgonomics).

2.7 Permeabilisation techniques for immunolabelling intracellular components

In many areas of research, it is becoming increasingly important to be able to detect and/or quantify not only cell surface but also intracellular antigens including structural components (e.g. filamentous actin), enzymes (e.g. nuclear terminal deoxynucleotidyl transferase), regulatory and transcription factors (e.g. cyclins, p53) and glycoproteins destined for export or secretion (e.g. cytokines). Antibodies are quite large macromolecules and, therefore, do not enter cells readily. Consequently, if internal components are to be immunolabelled, the plasma (and perhaps organelle) membranes must be permeabilised, either prior to or simultaneously with intracellular immunostaining. At the same time, the target antigen must be prevented from diffusing out of the cells while its reactivity and the light scattering characteristics of the cells are preserved. For these reasons, it is usual to fix cells with formaldehyde to stabilise the membranes (which alone will permeabilise cells; see above) and, in addition, to treat them with permeabilising agents such as saponin, lysolecithin or a non-ionic detergent; with blocking agents such as glycine, BSA or reconstituted non-fat dried milk powder (to minimise nonspecific binding); and sometimes also with a coagulative fixative such as methanol if the cells are also to be stained for nucleic acids. High nonspecific intracellular background staining is a commonly encountered problem. Therefore, the permeabilisation process, which is highly dependent on reagent concentration, exposure time and temperature, must be optimised for each application.

Saponins are cholesterol-like sugar-containing compounds produced by several plants in which they are thought to mediate resistance against pathogens. They have a large lipophilic region that inserts into membranes and interacts with sterols, phospholipids and proteins, disrupting cholesterol–phospholipid interactions to create ring-shaped complexes with pores of 12–15 nm diameter, which permit the entry of macromolecules. Electron microscopy has shown that saponin treatment is the mildest form of permeabilisation and leaves the plasma membrane relatively intact. Pore formation is reversible and saponin-treated cells are impermeable to antibodies that have not previously bound saponin; therefore, it is essential to maintain saponin in all of the steps in which cells are incubated with antibody. Cholesterol-containing membranes, including those associated with the endoplasmic reticulum, the Golgi and lysosomes, are readily permeabilised by saponin. Those that lack cholesterol, such as the inner nuclear membrane and mitochondrial membranes, are not (Protocol 2.12).

Lysolecithins are naturally occurring lipids that insert into membranes probably by dissolving cholesterol and replacing phospholipids. At low concentrations (~50 $\mu g\,ml^{-1}$) they will permeabilise cells, forming irreversible pores of 300–400 nm diameter in erythrocyte membranes, and at higher concentrations they cause lysis. Their use has been reported only occasionally in cytometric studies, probably because they are expensive, poorly characterised and seem to offer little advantage over other permeabilising agents.

Non-ionic detergents such as Nonidet (NP40), Tween® 20 and Triton® X-100 can be used to permeabilise the membranes of unfixed or fixed cells. They act by inserting into plasma and organelle membranes, solubilising both the lipids and the transmembrane proteins. They are generally weak protein denaturants but will bind to the hydrophobic regions of proteins and may cause the loss of membrane and other hydrophobic proteins. Con-

centrations of 0.01–0.1% usually permeabilise cells while still preserving the gross structure of the membrane; higher concentrations are more likely to cause lysis and loss of cytoplasmic contents.

Cytokine production has traditionally been assessed by immunochemical methods, but it is now possible to detect cytokine production in individual cells. For instance, T-cells are divided into the T helper functional subsets, Th1 and Th2, based upon their profile of cytokine secretion. By stimulating T-cells in vivo in the presence of inhibitors of translocation, e.g. brefeldin, the cytokines that are produced remain trapped in the cell and can be detected by immunolabelling using reagents purchased separately or as a kit for the purpose (e.g. the FastImmuneCytokineSystem from BD Bioscience;, Cytodetect™ from IQ Products, or the QuantiCyte™ system from BioErgonomics). Recently, however, T-cell subsets have been distinguished by intracellular immunostaining without prior in vivo activation, using laser scanning cytometry.

There is no single permeabilisation procedure that is universally applicable, and the best technique to use for a particular purpose can usually only be determined by critical analysis of the effects of many possible variables. Reviews of the general strategies available (e.g. Bauer and Jacobberger, 1984), methods texts (listed at the end of this chapter) and previous publications (e.g. Darzynkiewicz et al., 1996; Francis and Conolly, 1996) should be consulted before attempting to design and evaluate a procedure.

A number of reagent kits that are intended primarily for permeabilising leukocytes are commercially available, some of which are listed in Table 2.5. Several of these have been the subject of comparative evaluations by external quality assurance agencies (e.g. NEQAS, UK). It is therefore worth checking the internet sites of these agencies to ascertain which might be recommended for a particular purpose.

Protocol 2.12 Detection of cell surface and intracellular antigens after fixation and permeabilization with saponin

1. Add 20 μl fluorochrome-labelled antibody to a cell surface antigen to 2×10^6 leukocytes in 100 μl PBS containing 1% FBS and 0.1% sodium azide and incubate for 10 min at 4 °C.
2. Wash with 4 ml of PBS containing 1% FBS and resuspend the cells in 200 μl PBS containing 4% formaldehyde. Incubate for 20 min at 4 °C.
3. Wash with 4 ml PBS containing 5% FBS.
4. Resupend in 100 μl PBS containing 5% FBS and 0.1% saponin. Add a second fluorochrome-labelled antibody to an intracellular component and incubate 30–60 min at 4 °C.
5. Wash the cells by centrifuging in PBS containing 5% FBS and 0.1% saponin allowing adequate time for unbound antibody to diffuse out of the cells.
6. Resuspend in PBS containing 1% FBS and analyse.

2.8 Immunolabelling

2.8.1 Antibodies

Antibodies or immunoglobulins (Ig) are heterodimeric glycoproteins comprising light (κ or λ) and heavy (α, δ, ε, γ or μ) chains. The nature of the heavy chain defines the class or isotype (IgA, IgD, IgE, IgG or IgM) and in some instances the subclass (e.g. IgG_1 to IgG_4) to which the antibody belongs. The fundamental antibody unit, as exemplified by IgG, comprises two identical light chains and two identical heavy chains linked by disulphide bonds between the heavy and light chains and between the two heavy chains (Fig. 2.6). IgG has two identical sites for combining with antigen, each of which is formed from the complementarity-determining regions (CDRs) present in the N-terminal domains of a pair of heavy and light chains. Following digestion with papain or pepsin, these antibody-combining

Table 2.5 *Commercial permeabilisation reagents*

Brand name	Manufacturer	Comments	Time (min)[a]
Cytodetect kit	IQ Products	Intended for the detection of intracellular cytokines: includes monensin for blocking export via the Golgi), fixative, permeabilising reagent	600 (including time for cell stimulation)
Cytofix/Cytoperm™	Pharmingen, Serotec	Intended for use in the detection of intracellular cytokines	60
FACS™ Lysing Solution	BD Biosciences	Although not intended for the detection of intracellular antigens it can be used for this purpose	60
FACS™ Permeabilising Solution	BD Biosciences	Contains formaldehyde and diethylene glycol	50
Fix & Perm®	Caltag	Components not disclosed but described as FIXation and PERMeabilisation media; a modification incorporating methanol is recommended for cell cycle antigens when using FITC- but not PE-labelled antibodies	40
IntraPrep™ Permeabilisation Reagent	Beckman Coulter	Formaldehyde and saponin	45
IntraStain	Dako	Reagent A (fixation) formaldehyde, Reagent B (permeabilisation) not disclosed	40
IntraStainCell	Bender MedSystems	Four reagents including monensin for blocking export via the Golgi, fixative, permeabilising reagent and resuspension buffer	70–85 (not including time for cell stimulation)
IQ Starfiqs	IQ Products	Reagent F (fixation) formaldehyde, Reagent P (permeabilisation) saponin	45
Leucoperm™	Serotec	Not disclosed	60
Permeafix	Ortho Diagnostic Systems	Not disclosed	105
PermaCyte™	BioErgonomics	Not disclosed	95

[a]Time for permeabilisation and intracellular staining, to which must be added the time taken for surface antigen staining if required.
FITC, fluorescein isothiocyanate; PE, phycoerythrin.

sites (ab') are preserved in monomeric and dimeric fragments known as F(ab') and $F(ab')_2$, respectively. A further fragment, known as Fc, produced during papain but not pepsin digestion, contains domains from only the heavy chains; it is incapable of binding antigen but contains those regions of the molecule that are responsible for binding cells and complement (Fig. 2.6). The structural feature of an antigen that is responsible for its immunologic specificity is known as an epitope (an antigen may have more than one epitope) and the complementary site on an antibody molecule to which an epitope binds is known as a paratope.

Both monoclonal antibodies and polyclonal antisera can be used for immunolabelling. Antisera contain the natural mixture of antibodies produced by those B lymphocyte clones that can react with the antigen that was used to immunise the animal. In contrast, monoclonal antibodies are the products of a single antigen-reactive B-cell clone and are consequently all chemically identical. They are obtained by fusing B-cells with plasmacytoma cells to give antibody-secreting hybridoma cells, which can be propagated indefinitely. Different monoclonal antibodies that recognise the same human leukocyte antigen are said to belong to the same cluster of

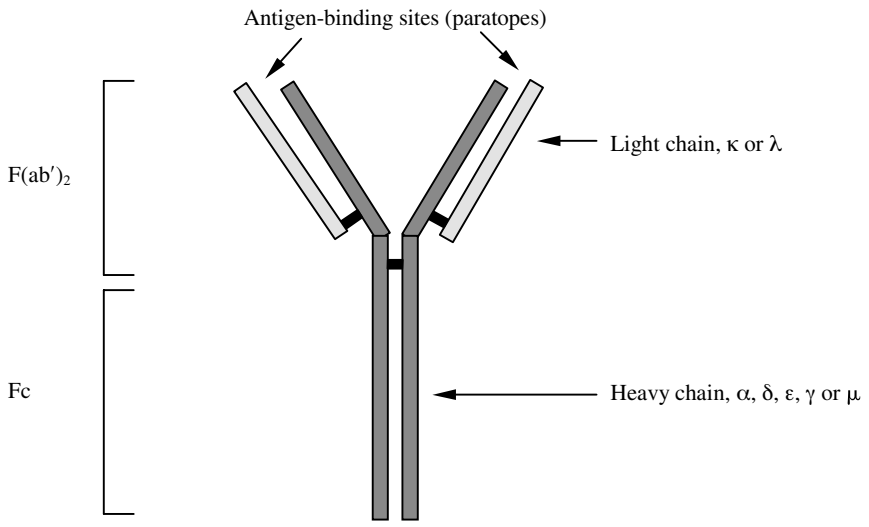

Fig. 2.6 Schematic diagram of an antibody molecule showing regions corresponding to F(ab')$_2$ and Fc fragments that would be produced by proteolytic cleavage. Interchain disulphide bonds (black) help to stabilise the structure.

differentiation (CD) and are given the same number, e.g. CD3. However, it must be remembered that monoclonal antibodies that recognise the same antigen are not necessarily identical unless they are from the same clone; in consequence, their epitope specificity, avidity, isotype and nonspecific binding may all differ. Monoclonal antibodies are generally preferable to polyclonal antisera because they are less prone to cross-reactivity, which gives rise to higher background staining.

Antibodies obtained commercially are commonly supplied as a freeze-dried (lyophilised) powder that must be reconstituted before use or as a liquid containing a preservative such as azide. Unlabelled antibodies are quite robust; their reactivity can be maintained for decades if kept at –20°C and for several years if kept with a preservative at 4°C. Repeated freezing and thawing should be avoided. Fluorochrome-labelled antibodies are considerably less stable; they should be kept at 4°C in the dark and, if obtained commercially, used before their expiry date.

2.8.2 Antibody–antigen interactions

All antibody–antigen reactions are reversible, with hydrophobic and electrostatic interactions being the major forces in the primary attraction. The equilibrium affinity constants (K_a) for monoclonal antibodies reacting with small monomeric antigens in solution are usually in the range 10^6–10^9 mol l^{-1} with reported values for the separate association (k_a) and dissociation (k_d) rate constants usually in the range 10^5–10^6 s^{-1} and 10^{-3}–10^{-5} s^{-1}, respectively. The rate of complex formation is dependent on the frequency of collision and orientation of the reactants. As an example, Karlsson and Roos (1997) demonstrate that a reaction between a soluble antigen and an antibody with moderate affinity ($K_a = 5 \times 10^8$ l mol^{-1}), which had kinetic constants of $k_a = 2 \times 10^6$ s^{-1} and $k_d = 4 \times 10^{-3}$ s^{-1}, respectively, would be 98.3% complete in 8.3 min. The lower the association rate constant the longer it will take to reach the steady state with maximum level of antibody bound; conversely, the higher the dissociation rate constant, the faster that previously bound antibody will be lost during washing. Van Regenmortel (1997) has calculated the relationship between the

Table 2.6 *The relationship between the dissociation rate constant and half-life of the antigen–antibody interaction*

Dissociation rate constant (s^{-1})	Half-life
10^{-6}	8 d
10^{-5}	19.2 h
10^{-4}	1.9 h
10^{-3}	11.5 min

From van Regenmortel (1997).

dissociation rate constant and half-life of the interaction (Table 2.6).

Consistent with theory, simple tests in which leukocytes in whole blood were stained for 1, 5, 10 and 20 min, using commercially obtainable fluorochrome-labelled monoclonal antibodies to cell surface antigens at the manufacturer's recommended dilutions, showed that near maximum staining was achieved within 5 min (unpublished observations). Therefore, for most practical purposes, an incubation time of 10 min should be sufficient for staining surface antigens, but longer times will be needed for staining intracellular antigens.

For analysis by flow cytometry, it is usually unnecessary to wash the cells free of unbound antibody, because only cell-bound antibody, as opposed to unbound antibody in solution, will contribute significantly to the fluorescence signal (Sklar and Finney, 1982). However, it is prudent to analyse washed but unfixed cells promptly because some decreases in bound antibody will occur after washing.

2.8.3 Titrating antibodies and the measurement of cell surface antigens

Antibodies obtained from commercial sources should be used in accordance with the supplier's recommendations; however, others will need to be titrated to ensure that an appropriate amount is used. The simplest way to do this for a fluorochrome-labelled antibody is to use a standard number of leukocytes, e.g. 5×10^5 cells in 100 μl of medium, and add a standard volume, e.g. 20 μl of doubling dilutions of the antibody. The mean fluorescence intensity (logarithmic scale) is determined for the positively stained and nonspecifically stained cells and these values are plotted against antibody concentration, also on a logarithmic scale. The fluorescence intensity of the positively stained cells will increase markedly with increasing antibody concentration until it reaches a plateau but near to the intial plateau value the intensity of the nonspecifically stained population will also begin to increase. The optimum antibody concentration is that which is on the plateau but which also gives the maximum difference in fluorescence intensities between the positive and negative cell populations. It will vary according to the protocol being used but in most instances it will be one or two dilution steps lower than that which just gives the plateau value (Fig. 2.7).

Often it would be useful if immunolabelling in conjunction with cytometry could be used to determine the absolute number of a cell surface component; however, the interaction of antibodies with antigens present on cell surfaces presents a far more complicated situation than the interaction in solution and one for which there are only limited data available (Pallis and Robbins, 1995; Roe et al., 1985). The majority of monoclonal antibodies used in cytometry are IgG and can therefore bind in a bivalent manner, with enhanced affinity (up to 100-fold) compared with the binding of their corresponding monovalent F(ab') fragments. A crucial assumption in the use of monoclonal antibodies for the quantification of cell surface antigen is that there will be only monovalent binding when saturating concentrations of antibody are used but the true ratio of antigen to antibody is not usually known. Bivalent antibody cannot easily be used to count cell surface antigen molecules because, for most practical purposes, the antibody concentrations required to achieve saturation are experimentally unattainable (~100 μg ml^{-1}) and would result in unacceptably high 'background' signals. The use of F(ab') fragments overcomes the problem of monovalent binding but their lower affinity is accom-

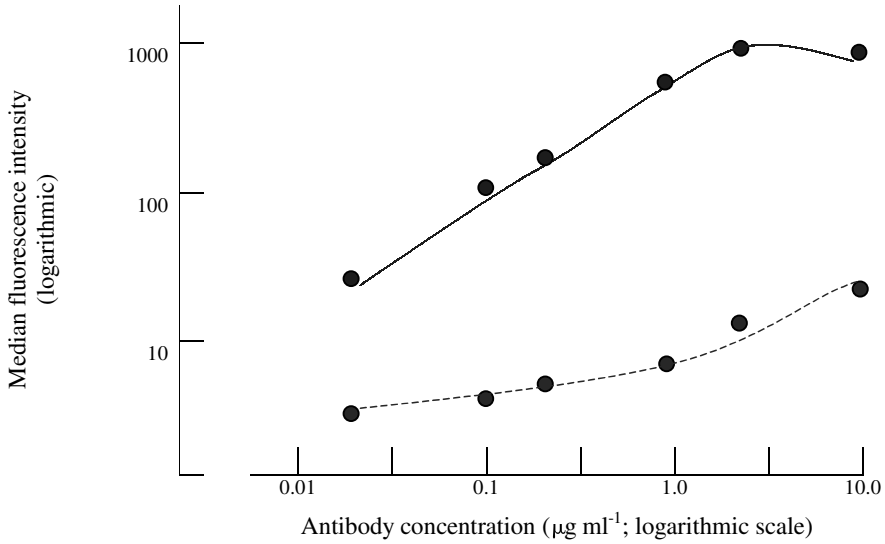

Fig. 2.7 Titration of a fluorochrome-labelled antibody. Relative fluorescence intensity of positive (solid line) and negative (dotted line) cell populations. Optimal antibody concentrations for staining are those that give the highest 'signal to noise' ratio (approximately 1–5 μg ml^{-1} here).

panied by a faster dissociation rate, which can lead to appreciable loss during washing and secondary antibody staining. Whether the antigen exists as dimers, trimers etc., as opposed to monomers, and whether it can diffuse in the plane of the membrane will also affect the interpretation (Fig. 2.8) (for a fuller discussion of the problems, see Davis et al., 1998; Junghans, 1999; Robins, 1998, 2000).

Because stoichiometric problems make it impossible in most instances to calculate antigen density, results are usually expressed instead in terms of the amount of fluorescent antibody bound. Two methods are commonly used. The first measures relative fluorescence intensity of each cell, while the second estimates the number of antibody molecules bound to each cell. In the first method, the cytometer is calibrated before use with beads containing different known amounts of fluorochrome. Results are expressed as median or mean relative fluorescence intensity levels, normally using a logarithmic scale, or as median or mean fluorescence channel number. If necessary, relative fluorescence intensity or channel numbers can be converted to an equivalent number of molecules of fluorochrome by means of a calibration curve constructed from the calibration beads. The second method uses a mixture of four microbead populations with different but defined numbers of sites for binding antibody molecules and a negative control (Quantum Simply Cellular®; Flow Cytometry Standards Corporation). The beads are incubated with antibodies under the same conditions as the sample; their fluorescence is determined and used to construct a calibration curve that relates peak channel fluorescence to their antibody-binding capacity. After the fluorescence of the cells of interest has been measured, the number of antibody molecules bound per cell can be determined by interpolation with the calibration curve.

2.8.4 Sensitivity of detection

Although some research instruments are capable of detecting individual fluorescent molecules as they pass a laser beam, the sensitivity limit of most current commercial cytometers in detecting fluorochrome-labelled cells is ~10^2–10^3 molecules of a fluorochrome or ~10^{-18} g fluorochrome per cell; a

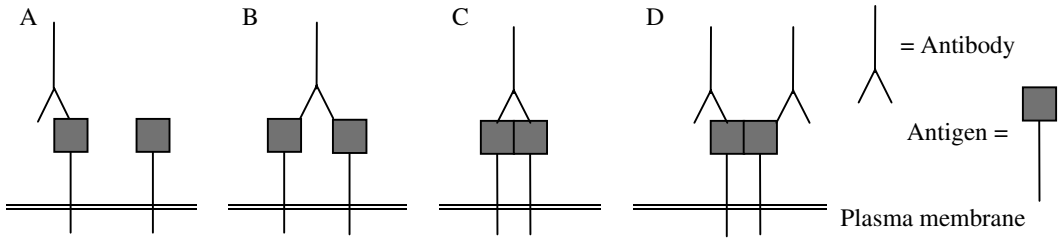

Fig. 2.8 Models for the interaction of antibodies with cell surface antigens. (A) Monovalent binding to a monomeric antigen. (B) Bivalent binding of two molecules of a monomeric antigen following diffusion of the antigen in the membrane. (C) Bivalent antibody binding to a dimeric antigen. (D) Monovalent antibody binding to a dimeric antigen. Scatchard analysis shows that the ratio of the number of antigen to antibody molecules bound versus antibody concentration varies differently in the model situations depicted in (A–D). (After Junghans, 1999.)

concentration calculated by Steen (1990) as approximately equal to that achieved if 1 g dye was dissolved and evenly distributed in the 3000 km^2 of the North Sea where it is 300 m deep. In practice, the sensitivity with which antigens can be detected by immunofluorescence is somewhat lower still, because it is affected not only by the strength of the fluorescence emitted by the labelled antibody (see Ch. 3) but also by the extent of nonspecific binding, which will increase with antibody concentration. Antibodies will attach not only through specific paratope–epitope interactions but also nonspecifically (usually with lower affinity) to other cell components by different mechanisms. Cell surface Fc receptors may bind different classes of antibody, especially aggregates formed during manufacture or storage. Antibody aggregates can be removed from solutions by brief ultracentrifugation (e.g. 10 min in a benchtop microfuge) before use but it is not recommended for IgM antibodies or phycoerythrin conjugates because both of these are large enough for appreciable quantities to be pelleted from solution. Both the Fc-mediated and nonspecific binding of antibodies can be decreased by pretreating washed or isolated cells with unlabelled normal (control) immunoglobulin or serum from the same species as used for the antibodies. This can be done by incubating 10 μg of purified control IgG with 10^6 cells for 10 min at 4 °C or by resuspending the cells in 2–5% inert serum before adding the specific antibody. Including 0.5–10% BSA or FBS in the media used for cell isolation, washing and labelling will help to minimise the number of dead cells (which show greater nonspecific antibody binding than live cells). If necessary, dead cells can be discriminated by their inability to exclude propidium iodide (PI) 5 $ng\,ml^{-1}$ or 7-amino-actinomycin D and can be omitted from the data analysis; reagents specially prepared for this purpose are commercially available (e.g. Caltag). To maximise the signal to noise ratio (specific to nonspecific binding), fluorescent antibodies are normally titrated to determine the concentration that gives a sufficient excess to ensure saturation of all of the antigen sites (maximal intensity of positives) while at the same time giving minimal nonspecific staining. Commercial antibodies to human leukocyte antigens have usually been titrated by the manufacturer in advance so that the recommended concentrations provide for a twofold to fivefold excess over saturation levels.

Care must be taken that the effective antibody concentration is not decreased by binding to a soluble form of the antigen in the sample. Antigens that are normally present on the surface of cells can also be shed (e.g. CD8, CD25, CD62L) or can be secreted (e.g. IgM on B-cells). In these instances, it may be necessary to wash the cells before immunolabelling. It may also be necessary to include 0.1% sodium azide in the medium during and after immunolabelling to inhibit metabolism and internalisation of antigens.

2.8.5 Direct and indirect immunostaining

In direct immunolabelling, cells in suspension are incubated with fluorochrome-conjugated antibody and later washed free of unbound antibody. It is quick because only a single incubation with one or a number of different labelled antibodies is required. However, it does require that all antibodies be conjugated to a fluorochrome. The correct antibody control is a fluorochrome-conjugated antibody of the same isotype (known as an isotype-matched control antibody). Multicolour analysis can usually be done using pre-mixed antibody cocktails, but the possibility exists for potential interactions between reagents. It is therefore prudent, at least on the first occasion, to include a check in which cells are labelled sequentially with the different reagents, preferably with washing in between. Pre-mixed multicolour antibody cocktails for many commonly analysed combinations of antigens are obtainable commercially. A method for the direct staining of leukocytes in live whole blood is given above (see Section 2.3.1).

In indirect immunolabelling, cells in suspension are incubated with unlabelled primary antibody, washed, then incubated with a fluorochrome-labelled secondary antibody directed against the immunoglobulins of the species from which the primary antibody was obtained and analysed (Protocol 2.13). The correct antibody control is an unconjugated isotype-matched primary antibody followed by the same fluorochrome-labelled secondary antibody. Direct immunolabelling is simpler, more convenient and less error prone than indirect immunolabelling. Although indirect labelling takes longer, it has the advantage of increased sensitivity because some signal amplification can be achieved by several fluorochrome-conjugated secondary antibodies binding to a single primary antibody. Secondary antibodies labelled with a variety of fluorochromes are readily available from commercial sources; they are stable when stored lyophilised or frozen and are relatively inexpensive. Wherever possible, it is preferable to use the $F(ab')_2$ fragment of a fluorochrome-conjugated affinity-purified secondary antibody as these fragments give less non-specific binding than the corresponding whole antibody. Where a combination of indirect and direct labelling with mouse monoclonal antibodies is applied to the same sample, it is essential that the indirect procedure is completed first and that any unoccupied anti-mouse immunoglobulin-binding sites on the secondary antibody are blocked with unlabelled normal mouse IgG before staining with the directly labelled antibody (Fig. 2.9).

A variant of the indirect labelling procedure is to use a primary antibody that is conjugated to biotin so that it can be revealed by a fluorochrome conjugated to avidin or streptavidin (see Ch. 3). When using this procedure, cells should be washed free of serum and maintained in media containing BSA instead of serum, in order to avoid adventitious binding to endogenous biotin, which may be present in serum.

Wherever possible, positive and negative cell controls should be included in the test series as a check on the effectiveness of immunolabelling. In some instances, these may occur naturally within the sample, e.g. both CD3-positive and CD3-negative (often written $CD3^+$ and $CD3^-$, respectively) cells will occur in peripheral blood. An autofluorescence control that contains no fluorochrome-labelled antibodies should also be examined. Ideally, the autofluorescence control and negative fluorochrome-labelled isotype control should give similar results. However it is common for the latter to fluoresce a little brighter than the autofluorescence control.

Protocol 2.13 Indirect immunostaining of whole blood

Reagents

- A saturated solution of LDS-751 in methanol can be kept almost indefinitely in the dark at 4°C
- HHBSS-BSA

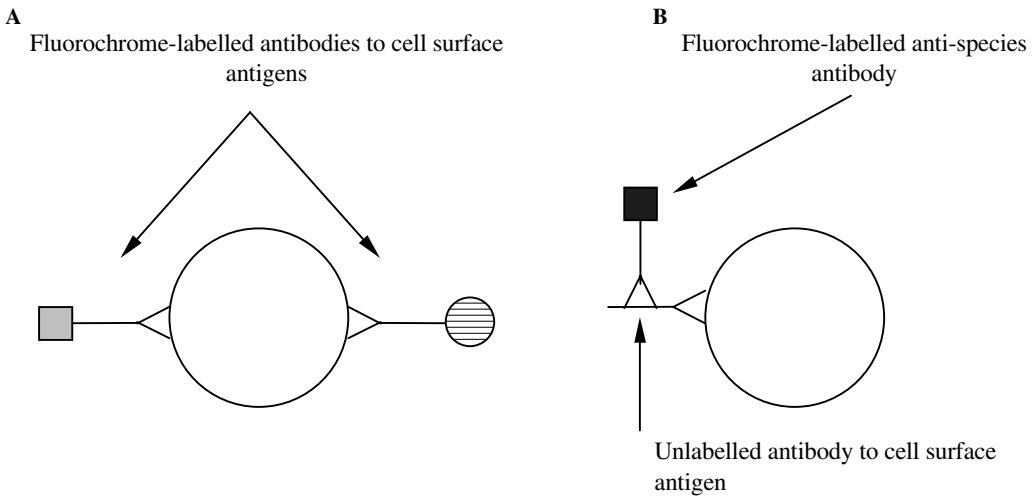

Fig. 2.9 An illustration of direct (A) and indirect (B) immunolabelling. In the direct example, the cell has bound two different antibodies each conjugated to a different fluorochrome. In the indirect example, the cell has bound an unlabelled (primary) antibody (e.g. a mouse monoclonal antibody) that has subsequently been revealed by a fluorochrome-conjugated (secondary) directed against the immunoglobulins of the species from which the primary antibody was obtained (e.g. a fluorescein isothiocyanate-conjugated goat anti-mouse immunoglobulin antibody).

Protocol

1. Pipette 100 μl anticoagulated blood carefully into the bottom of a plastic tube so that it forms a small discrete droplet at the bottom.
2. Add 20 μl unlabelled antibody* by pipetting onto the droplet of blood and mix the two by gently pipetting up and down.
3. Incubate for 10 min at 4 °C.
4. Wash the cells twice by centrifuging at 300–400 × *g* for 5–10 min in 4 ml of PBS containing 1% BSA.
5. Resuspend in 100 μl of PBS containing 1% BSA.
6. Add 30 μg normal unlabelled immunoglobulins (blocking antibody) of the same species as the secondary antibody per 10^6 cells and incubate for 10 min.
7. Add 20 μl fluorochrome-conjugated secondary antibody.*
8. Incubate for 10 min at 4 °C.
9. Wash the cells twice by centrifuging at 400 × *g* for 5 min in PBS containing 1% BSA†.
10. Either lyse the erythrocytes and fix the leukocytes as described above, or resuspend the cells in 1 ml PBS containing 1% BSA and 0.1% by volume of a saturated solution of LDS-751 in methanol.

Analysis

Analyse by flow cytometry using the gating strategy described for the live whole blood method in Protocol 2.10.

*The optimum amounts of antibody will need to be determined by titration unless specified by the manufacturer and suitable isotype negative controls will also need to be done.

† If required, the cells can also be directly immunolabelled after this stage. In which case, resuspend in 100 μl PBS containing 1% BSA, add 30 μg normal unlabelled immunoglobulins of the same species as the primary antibody per 10^6 cells and incubate for 10 min. Add 20 μl fluorochrome-conjugated antibody, incubate for 10 min at 4 °C and resuspend the cells in 1 ml of PBS containing 1% BSA and LDS-751.

Note: If there is high nonspecific binding of the primary anti-

body this may be reduced by first incubating the blood for 10 min at 4°C with 20 μl of a negative control immunoglobulin fraction from the same species as the primary antibody.

2.9 Determining absolute cell counts

On some occasions, it is necessary to determine the absolute number of different cells in a sample; this can be done in any one of the following three ways. First, all of the cells in a defined volume of a cell suspension can be counted. Second, the number of cells present in a defined volume can be calculated by counting the cells seen when the sample is flowing at a constant and known rate for a set time. Third, a defined volume of sample can be mixed with a defined volume of a suspension of microbeads of known concentration (in terms of particles per ml); both the numbers of cells and of microbeads are counted and the cell concentration calculated from the ratio of cells:microbeads recorded. A variation on the last principle is available commercially as TRUCOUNT™ Absolute Count Tubes (BD Biosciences) in which a microbead suspension has been lyophilised in tubes so that the microbeads are resuspended as the sample is added.

2.10 Safety

The hazards encountered when preparing samples for cytometric studies are twofold; infectious and chemical. The risks associated with each operation should be assessed in advance and appropriate precautions taken to minimise them. In many countries, there are guidelines or legislation covering different aspects of laboratory safety. The NCCLS in the USA and the Advisory Committee on Dangerous Pathogens (ACDP) and the Health Services Advisory Committee (HSAC) in the UK publish guidelines for this type of work (see internet sites for lists of publications). In general, these bodies specify standards of microbiological practice that aim to protect laboratory workers and others from accidental infection. Most laboratory-acquired infections result through puncture wounds, the inhalation of infectious aerosols, the accidental contamination of abraded skin or accidental ingestion. Specimens must be obtained, handled and disposed in accordance with certain minimum levels of containment and personal protection, which differ depending on the hazard that they pose. In brief, the minimum standards of personal protection require that a Dowsett and Heggie style laboratory coat and disposable gloves must be worn when handling clinical specimens; safety spectacles must be worn when there is the possibility of eye contamination through splashing. Samples must be contained in suitably robust sealed containers (e.g. capped tubes); there must be no mouth pipetting; centrifuging must be done in capped/sealed tubes within sealed safety containers that will prevent the escape of aerosols in the event of tube breakage; hazardous waste must be stored and disposed in an approved safe manner; nondisposable items should be decontaminated with a suitable disinfectant (e.g. Virkon) and, if possible, also by autoclaving. The hazards posed by chemicals vary and can be found in the 'materials safety data sheets' published by suppliers. Appropriate precautions for handling and disposal will need to be taken, which will depend on factors such as the amounts involved, the frequency and type of use. A fuller consideration of the safety aspects of specimen acquisition, handling and processing can be found in Owens and Loken (1995), Valenstein and Collinge (1997), and in the Purdue Cytometry CD-ROM (Robinson, 1997, 1998).

2.11 FURTHER READING

Al-Rubeai, M., Emery, A.N. (eds.) (1996) *Flow Cytometry Applications in Cell Culture*. Marcel Dekker, New York.

Darzynkiewicz, Z., Robinson, J.P., Crissman, H.A. (eds.) (1994) *Methods in Cell Biology,* Vol. 41, Part A, *Flow Cytometry,* 2nd edn. Academic Press, New York.

Jaroszeski, M.J., Heller, R. (eds.) (1998) *Methods in Moleular*

Biology, Vol. 92, *Flow Cytometry Protocols*. Humana Press, Totowa, NJ.

Owens, M.A., Loken, M.R. (1995) *Flow Cytometry Principles for Clinical Laboratory Practice: Quality Assurance for Quantitative Immunophenotyping*. Wiley-Liss, New York.

Preffer, F.I. (1995) *Flow cytometry*. In: Colvin, R.B. Bhan, A.K. McCluskey, R.T. (eds.) *Diagnostic Immunopathology*, 2nd edn, pp. 725–49. Raven Press, New York.

Radbruch, A. (ed.) (1999) *Flow Cytometry and Cell Sorting* 2nd edn. Springer-Verlag, Berlin.

Robinson, J.P., Darzynkiewicz, Z., Dean, P.H., Dressler, L., Tanke, H., Wheeless, L. (eds.) (1993) *Handbook of flow cytometric methods*. Wiley-Liss, New York.

Shapiro, H.M. (1994) *Practical flow cytometry* 3rd edn. Liss, New York.

Watson, J.V. (1991) *Introduction to flow cytometry*. Cambridge University Press, Cambridge, UK.

2.12 INTERNET RESOURCES

http://www.protocol-online.net/cellbio/cell—cycle/cytometry.html

Links to many sites detailing flow cytometry sample preparation and cytometry techniques.

http://www.drmr.com/abcom

Mario Roederer's site providing detailed information on the conjugation of fluorochromes and biotin to monoclonal antibodies and other proteins.

http://www.biochem.mpg.de/research-group/valet/valmeth3.html

Functional cell biochemistry by flow cytometry. G. Valet's site containing brief protocols for cell preparation, fixation, a number of functional assays and other cytometry-related information.

http://www.biochem.mpg.de/research-group/valet/eurocel2.html

European Working Group for Clinical Cell Analysis (EWGCCA): consensus document on leukaemia immunophenotyping.

http://www.ukneqas.org.uk/index.html

Home page of the UK National External Quality Assessment Scheme.

http://www.wiley.com/cp/cpc/toc.html

Table of contents of *Current Protocols in Cytometry*. A few sample chapters can be accessed directly and via other links but a subscription/purchase is necessary for full access.

http://www.hse.gov.uk/hthdir/noframes/biolhaz.html

The UK Health and Safety Executive's website for biological hazards/agents (infection risks) and for controlling the risk of infection at work.

http://www.nccls.org/homebody1.html

The USA National Committee for Clinical Laboratory Standards (NCCLS): website for the dissemination of standards and guidelines.

http://www.esacp.org/esacflow.html

Consensus report of the task force on standardisation of DNA flow cytometry in clinical pathology: European Society for Analytical Cellular Pathology.

http://www.search.lifetech.com/

Life Technologies' site which contains protocols for cell culture, cell biology and molecular biology, including many on blood cell separation and isolation.

http://www.bdfacs.com/literature/appnotes/menu.shtml

BD Immunocytometry Systems' applications notes for sample preparation and analysis.

http://www.bdfacs.com/literature/whitepapers/menu.shtml

BD Immunocytometry Systems' publications describing various immunocytometric assay systems.

2.13 REFERENCES

Ashmore L.M., Shopp, G.M., Edwards, B.E. (1989) Lymphocyte subset analysis by flow cytometry. Comparison of three different staining techniques and effects of blood storage. *Journal of Immunological Methods* **118**, 209–15.

Bauer, K.D., Jacobberger, J.W. (1984) Analysis of intracellular proteins. *Methods in Cell Biology* **41**, 352–73.

Bazil, V. (1995) Physiological enzymatic cleavage of leukocyte membrane molecules. *Immunology Today* **16**, 135–40.

Bignold, L.P., Ferrante, A. (1987) Mechanism of separation of polymorphonuclear leukocytes from whole blood by the one-step Hypaque–Ficoll method. *Journal of Immunological Methods* **96**, 29–33.

Bossuyt, X., Marti, G.E., Fleisher, T.A. (1997) Comparative analysis of whole blood lysis methods for flow cytometry. *Cytometry* **30**, 124–33.

Boyum, A., Lovhaug, D., Tresland, L., Nordlie, E.M. (1991) Separation of leucocytes: improved cell purity by fine adjustments of gradient medium density and osmolality. *Scandinavian Journal of Immunology* **34**, 697–712.

Darzynkiewicz, Z., Gong, J., Juan, G., Ardelt, B., Traganos, F. (1996) Cytometry of cyclin proteins. *Cytometry* **25**, 1–13.

Davis, K.A., Abrams, B., Iyer, S.B., Hoffman, R.A., Bishop, J.E. (1998) Determination of CD4 antigen density on cells: role of antibody valency, avidity, clones, and conjugation. *Cytometry* **33**, 197–205.

Denholm, E.M., Wolber, F.M. (1991) A simple method for the purification of human peripheral blood monocytes: a substitute for Sepracell–MN. *Journal of Immunological Methods* **144**, 247–51.

Fearon, D.T., Collins, L.A. (1983) Increased expression of C3b receptors on polymorphonuclear leukocytes induced by chemotactic factors and by purification procedures. *Journal of Immunology* **130**, 370–5.

Ferrante, A., Thong, Y.H. (1980) Optimal conditions for simultaneous purification of mononuclear and polymorphonuclear leukocytes from human blood by the Hypaque–Ficoll method. *Journal of Immunological Methods* **36**, 109–17.

Forsyth, K.D., Levinsky, R.J. (1990) Preparative procedures of cooling and re-warming increases leukocyte integrin expresssion and function on neutrophils. *Journal of Immunological Methods* **128**, 159–63.

Francis, C., Conolly, M.C. (1996) Rapid single step method for flow cytometric detection of surface and intracellular antigens using whole blood. *Cytometry* **25**, 58–70.

French, D., Edsall, J.T. (1945) The reactions of formaldehyde with amino acids and proteins. In: Anderson, M.L., Edsall, J.T. (eds.), *Advances in Protein Chemistry*, Vol. 2, pp. 277–335. Academic Press, New York.

Haslett, C., Guthrie, L.A., Kopaniak, M.M., Johnston, R.B., Henson, P.M. (1985) Modulation of neutrophil function by preparative methods or trace concentrations of bacterial lipopolysaccharide. *American Journal of Pathology* **119**, 101–10.

Hensleigh, P.A., Waters, V.B., Herzenberg, L.A. (1983) Human T lymphocyte differentiation antigens: effects of blood sample storage on LEU antibody binding. *Cytometry* **3**, 453–5.

Himmelfarb, J., Hakim, R.M., Holbrook, D.G., Leeber, D.A., Ault, K.A. (1992) Detection of granulocyte reactive oxygen species formation in whole blood using flow cytometry. *Cytometry* **13**, 83–9.

Junghans, R.P. (1999) Cruel antibody intentions: cellular antigen enumeration by 'saturation' binding. *Immunology Today* **20**, 401–6.

Karlsson, R., Roos, H. (1997) Reaction kinetics. In: Price, C.P., Newman, D.J. (eds.), *Principles and Practice of Immunoassay*, 2nd edn, pp. 101–22. Stockton Press, New York.

Leino, L., Sorvajarvi, K. (1992) CD11b is a calcium-dependent epitope in human neutrophils. *Biochemical and Biophysical Research Communications* **187**, 195–200,

Macey, M.G., Jiang, X.P., Vey, P., McCarthy, D., Newland, A.C. (1992) Expression of functional antigens on neutrophils: effects of preparation. *Journal of Immunological Methods* **149**, 37–42.

Macey, M.G., McCarthy, D.A., Vordermeier, S., Newland, A.C., Brown, K.A. (1995) Effects of cell purification methods on CD11b and L-selectin expression as well as the adherence and activation of leucocytes. *Journal of Immunological Methods* **181**, 211–19.

Macey, M.G., McCarthy, D.A., Newland, A.C. (1997) The Q-Prep system: effects on the apparent expression of leukocyte cell surface antigens. *Cytometry* (*Communications in Clinical Cytometry*) **30**, 67–71.

Macey, M.G., McCarthy, D.A., Howells, G.L., Curtis, M.A., King, G., Newland, A.C. (1998) Multiparametric flow cytometric analysis of polymorphonuclear leukocytes in whole blood from patients with adult rapidly progressive periodontitis reveals low expression of the adhesion molecule L-selectin (CD62L). *Cytometry* (*Communications in Clinical Cytometry*) **34**, 152–8.

Macey, M.G., McCarthy, D.A., Milne, T., Cavenagh, J.D., Newland, A.C. (1999) Comparative study of five commercial reagents for preparing normal and leukaemic lymphocytes for immunophenotypic analysis by flow cytometry. *Cytometry* (*Communications in Clinical Cytometry*) **38**, 153–60.

McCarthy, D.A., Macey, M.G. (1993) A simple flow cytometric procedure for the determination of surface antigens on unfixed leucocytes in whole blood. *Journal of Immunological Methods* **163**, 155–60.

McCarthy, D.A., Macey, M.G. (1996) Novel anticoagulants for flow cytometric analysis of live leukocytes in whole blood. *Cytometry* **23**, 196–204.

McCarthy, D.A., Perry, J.D., Holburn, C.M., Kirk, A.P., James, D.W., Moore, S.R., Holborow, E.J. (1984) Centrifugation of normal and rheumatoid arthritis blood on Ficoll–Hypaque and Ficoll–Nycodenz solutions. *Journal of Immunological Methods* **73**, 415–25.

McCarthy, D.A., Macey, M.G., Cahill, M.R., Newland, A.C. (1994) Effects of fixation on quantification of the expression of leukocyte function-associated surface antigens. *Cytometry* **17**, 39–49.

McFaul, S.J. (1990) A method for isolating neutrophils from moderate volumes of human blood. *Journal of Immunological Methods* **130**, 15–18.

Mody, M., Lazarus, A.H., Semple, J.W., Freedman, J. (1999) Preanalytical requirements for flow cytometric evaluation of platelet activation: choice of anticoagulant. *Transfusion Medicine* **9**, 147–54.

Needham, P. (1987) Separation of human blood using 'Mono-Poly Resolving Medium'. *Journal of Immunological Methods* **99**, 283–4.

Ormerod, M.G., Tribukait, B., Giaretti, W. (1998) Consensus report of the task force on standardisation of DNA flow cytometry in clinical pathology. DNA Flow Cytometry Task

Force of the European Society for Analytical Cellular Pathology. *Analytical Cellular Pathology* **17**, 103–10.

Owens, M.A., Loken, M.R. (1995) *Flow Cytometry: Principles for Clinical Laboratory Practice*. Wiley-Liss, New York.

Pallis, M., Robbins, R.A. (1995) What you need to know when you go with the flow: pitfalls in the use of flow cytometry. *Annals of Rheumatic Diseases* **54**, 785–6.

Pertoft, H., Hirtenstein, M., Kagedal, L. (1979) Cell separations in a new density medium, Percoll®. In: Reid, E. (ed.), *Cell Populations, Methodological Surveys (B) Biochemistry*, Vol. 9, pp. 47–80. Ellis Horwood, Chichester, UK.

Radbruch, A., Recktenwald, D. (1995) Detection and isolation of rare cells. *Current Opinion in Immunology* **7**, 270–3.

Recktenwald, D., Radbruch, A. (eds.) (1997) *Cell Separation Methods and Applications*. Marcel Dekker, New York.

Repo, H., Jansson, S.-E., Leirisalo-Repo, M. (1993) Flow cytometric determination of CD11b upregulation in vivo. *Journal of Immunological Methods* **164**, 193–202.

Rickwood, D. (1983) *Iodinated Density Gradient Media: A Practical Approach*. IRL Press, Oxford, UK.

Robins, R.A. (1998) Flow cytometric analysis of cell surface antigen density. In: Pound, J.D. (ed.), *Methods in Molecular Biology: Immunochemical Protocols,* pp. 319–36, Humana Press, Totowa, NJ.

Robins, R.A. (2000) Counting antigens using antibodies. *Immunology Today* **21**, 154–5.

Robinson J.P. (ed.) (1997) *The Purdue Cytometry CD-ROM* Vol. 3 (Guest editors Parker, J., Stewart, C.). Purdue University, West Lafayette, IN.

Robinson, J.P. (1998) *The Purdue Cytometry CD-ROM* Vol. 4 (Guest editor Watson, J.). Purdue University, West Lafayette, IN.

Roe, R., Robins, R.A., Laxton, R.R., Baldwin, R.W. (1985) Kinetics of divalent monoclonal antibody binding to tumour cell surface antigens using flow cytometry – standardization and mathematical analysis. *Molecular Immunology* **22**, 11–21.

Romeu, M.A., Mestre, M., Gonzalez, L., Valls, A., Verdaguer, J., Corominas, M., Bas, J., Massip., E, Buenida, E. (1992) Lymphocyte immunophenotyping by flow cytometry in normal adults. Comparison of fresh whole blood lysis technique, Ficoll–Paque separation and cryopreservation. *Journal of Immunological Methods* **154**, 7–10.

Shankey, T.V., Rabinovich, P.S., Bagwell, B., Bauer, K.D., Duque, R.E., Hedley, D.W., Mayall, B.H., Wheeless, L.L. (1993) Guidelines for implementation of clinical DNA cytometry. *Cytometry* **14**, 472–7.

Sklar, L.A., Finney, D.A. (1982) Analysis of ligand–receptor interactions with the fluorescence activated cell sorter. *Cytometry* **3**, 161–5.

Smith, P.J., Wiltshire, M., Davies, S., Patterson, L.H., Hoy, T. (1999) A novel cell permeant and far red-fluorescing DNA probe, DRAQ5, for blood cell discrimination by flow cytometry. *Journal of Immunological Methods* **229**, 131–9.

Steen, H.B. (1990) Characteristics of flow cytometers. In: Radbruch, A. (ed.), *Flow Cytometry and Sorting*, 2nd edn, pp. 11–25. Wiley-Liss, New York.

Tamul, K.R., Schmitz, J.L., Kane, K., Folds, J.D. (1995) Comparison of the effects of Ficoll–Hypaque separation and whole blood lysis on results of immunophenotypic analysis of blood and bone marrow samples from patients with hematologic malignancies. *Clinical and Diagnostic Laboratory Immunology* **2**, 337–42.

Terstappen, L.W.M.M., Shah, V.O., Conrad, M.P., Recktenwald, D., Loken, M.R., (1988) Discriminating between intact and damaged cells in fixed flow cytometric samples. *Cytometry* **9**, 477–84.

Terstappen, L.W.M.M., Johnson, D., Mickaels, R.A., Chen, J., Olds, G., Hawkins, J.T., Loken, M.R., Levin, J. (1991) Multidimensional flow cytometric blood cell differentiation without erythrocyte lysis. *Blood Cells* **17**, 585–602.

Valenstein, P.N., Collinge, M.L. (1997) Laboratory safety. In: Rose, N.R., de Marcio, E.C., Folds, J.D., Lane, H.C., Nakamura, R.M. (eds.), *Manual of Clinical Laboratory Immunology,* 5th edn, pp. 1213–22. ASM Press, Washington, DC.

van Regenmortel, M. H. V. (1997) The antigen–antibody reaction. In: Price, C.P., Newman, D.J. (eds.), *Principles and Practice of Immunoassay,* 2nd edn, pp. 15–32. Stockton Press, New York.

Vettese-Dadey, M. (1999) Going their separate ways. A profile of products for cell separation. *Scientist* **13**, 18–27.

Visscher, D.W, Crissman, H.A. (1994). Dissociation of intact cells from tumors and normal tissues. In: Darzynkiewicz Z., Robinson J.P., Crissman, H.A. (eds.), *Methods in Cell Biology* Vol. 41, Part A, 2nd edn, pp. 1–13. Academic Press, New York.

3

Fluorescence and fluorochromes

Desmond A. McCarthy

Queen Mary and Westfield College, London

3.1 Introduction

The great analytical power of current cytometers stems from their ability to quantify simultaneously many separate parameters on thousands of cells within a few minutes. Laser scanning cytometers and flow cytometers measure, respectively, one or two light scattering parameters, and, depending on the instrument, up to 12 fluorescence parameters. Only a few cellular components (e.g. pyridine- and flavin-containing nucleotides) are intrinsically fluorescent (autofluorescent), so cells are usually stained with compounds (known as fluorochromes, fluorophores or fluors) that fluoresce when they report the presence or activity of a particular cellular component. Three main approaches are used for staining:

- a fluorochrome-labelled antibody or other ligand is allowed to bind to complementary structures, either within or on the surface of cells
- a fluorescent dye, e.g. one that binds to nucleic acids, is allowed to accumulate within cells
- a cell-permeant precursor compound is converted by the activity, often enzymic, of some cell component into a form with distinct fluorescence.

Usually samples are stained with more than one fluorochrome and, depending on the number of fluorochromes used, the technique is known as two-colour, three-colour, etc. staining. At present, the main constraint on the number of different stains that can be measured simultaneously is the shortage of fluorochromes with distinct emission spectra and the difficulty of distinguishing those fluorochromes with emission spectra that overlap. To appreciate how fluorochromes can best be used in cytometric assays it is worth first considering how light and matter interact.

3.2 The interaction of light and matter

Light is a form of electromagnetic radiation with a wave motion defined by electric and magnetic vectors at right angles to each other and perpendicular to the direction of propagation. The waves travel at a speed close to 3×10^8 m s^{-1} (known as '*c*', the velocity of light); thus the frequency and wavelength (the distance between wave crests) of radiation are simply related by the equation:

λ (wavelength in m) $\times$ ν (frequency in cycles s^{-1}) = c (velocity of light in m s^{-1})

Visible light ranges in frequency from 0.4×10^{15} Hz to 0.75×10^{15} Hz (the hertz, Hz, being 1 cycle per second) and in wavelength from 400 nm (near ultraviolet) to 700 nm (red). Light is not emitted as a continuous long wave but as discrete short 'wave trains' called 'photons'. The production of a single wave train from most sources lasts for only about 10^{-9} s and in this time light would have travelled about $3 \times 10^8 \times 10^{-9}$ m, or 0.3 m. The electric and magnetic vectors arise from the force field that surrounds a pair of charges, the oscillating electric dipole. These can be envisaged as a positive and a negative charge that oscillate along the axis linking them, so that the distance by which they are separated is a sine function of time. An oscillating dipole, therefore, generates a moving wavelike force field radiating out in all directions from it (at the speed of

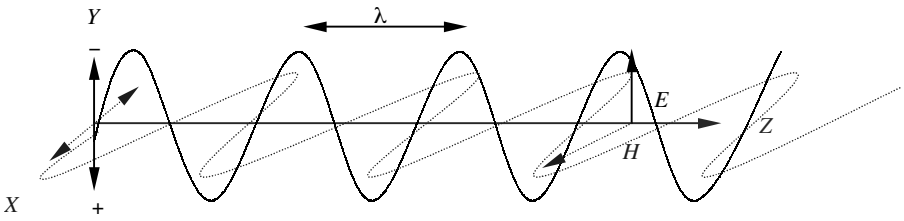

Fig. 3.1 The electromagnetic wave generated by an oscillating dipole (at the left). The magnetic vector (*H*) in the plane *YZ* is at right angles to, and in phase with, the electric vector (*E*) in the plane *XZ*. As the wave moves away from its origin in the direction *Z*, its wavelength (λ) is maintained but its amplitude decreases with distance.

light) with the electric vector in the same plane as the axis of the dipole (Fig. 3.1).

The oscillating dipole is not the only system of moving charges that can generate electromagnetic radiation but it is useful when considering the movement of electrons in atoms and molecules and their interaction with light. It corresponds to the movements of negatively charged electrons relative to the positively charged nuclei in matter. Work must be done to cause a dipole to oscillate, and a corresponding (or smaller) amount of energy can then be radiated as light. If light is absorbed by other dipoles, it can start them oscillating and, in turn, they can also radiate. The interaction of light and matter is, therefore, based on the exchange of energy between oscillating dipoles and the radiation field.

The emission of light without the high temperatures needed for incandescence is known as luminescence. It encompasses chemiluminescence, which if it occurs in vivo is usually termed bioluminescence, and two forms of photoluminescence, known as fluorescence and phosphorescence. Chemiluminescence results from a chemical reaction in which the electron in an atom or molecule is raised to a vibrationally excited state by the enthalpy (heat) of reaction. As the electron decays to its ground state, light is emitted. In photoluminescence, it is the energy acquired from the absorption of light (ultraviolet, visible or near-infrared) that results in the electron being raised to a higher energy state in an unoccupied orbital; just as in chemiluminescence, return to the ground state is accompanied by the emission of light.

Energy can only be exchanged between light and matter in discrete packets (Fig. 3.2), known as quanta or photons, the energy of which is related to the frequency by the following equation:

$$E = h\nu$$

where E is the energy (in ergs) in one quantum of radiation, which has a frequency of ν (cycles s^{-1}), and h is Planck's constant (6.6×10^{27} erg s^{-1}). For light in a vacuum, $E = hc/\lambda$ (because $\nu = c/\lambda$, from above).

Both chemiluminescence and fluorescence have been used extensively in cytometric analysis; however, there are key differences between the two processes. In chemiluminescence, the chemiluminescent substrate is irreversibly converted to a different substance during the reactions that generate light; consequently, each molecule of the chemiluminescent substrate can produce a photon only once. In fluorescence, by comparison, each molecule involved can repeat the process of photon absorption and emission many times.

3.3 Light absorption and fluorescence

In any given atom, the dipole oscillation of electrons and nuclei that accompany the absorption or emission of light occur at only certain frequencies. To raise an atom from the ground state (S_0) to the excited state to initiate these oscillations requires the absorption of a quantum with the correct energy. As the energy states of atoms can be defined almost completely by the orbits of their valence

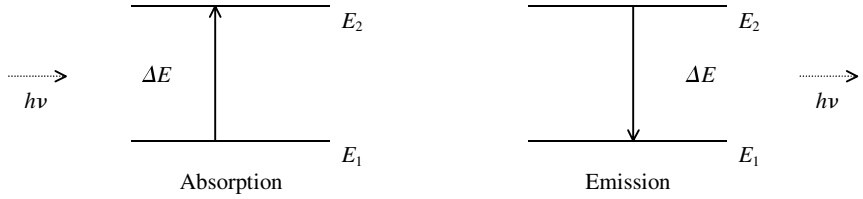

Fig. 3.2 The transition between the higher (E_2) and lower (E_1) energy states is accompanied by the absorption or emission of a quantum of light (a photon) with the energy $E = h\nu = E_2 - E_1$.

electrons, these energy differences (ΔE) are well defined and there is intense absorption of light at the wavelength that will give $\Delta E = h\nu = hc/\lambda$. Consequently the absorption spectrum of an atom is characterised by sharp lines at particular wavelengths, e.g. at 102.6, 121.6, 486.9 and 657.3 nm for the hydrogen atom. In a molecule, the electrons of many different atoms occur in close proximity and interact both with one another and with different nuclei. As a result, although there are major electronic singlet ground (S_0) and excited states (first excited singlet state, S_1; second, S_2 etc.), each is divided into a large number of possible vibrational energy levels or substates. In addition to these, there is a parallel series of triplet energy states (denoted T_1, T_2, etc.) each with a slightly lower energy level than the corresponding singlet state. In the dark at ambient temperatures, the majority of molecules are in the ground state. On irradiation, photon absorption typically excites the fluorochrome to a vibrational energy level within the first excited singlet state (S_1) but energy is lost rapidly (~10^{-12} s) by vibrational relaxation (a nonradiative process) so that it drops to the lowest vibrational substate (V_0) in the S_1 band. When photon emission occurs, all transitions begin at V_0 but can terminate in any of the vibrational substates in the electronic ground state. Overall, many different transitions are possible between the various different ground and excited substates, each of which could give rise to an absorption band. In practice, these bands are broadened by intermolecular interactions and cannot be separately resolved. They merge, instead, to form a broad band of wavelengths over which light can provide the energy required to effect all of these different transitions. Similarly, emission occurs over the wavelengths that correspond to the energy difference between the lowest vibrational substate of the excited singlet and the various vibrational substates in ground energy levels (Fig. 3.3).

The most probable transitions between the substates for absorption usually span a larger energy difference (ΔE) than those for emission. Therefore, during fluorescence, the photon emitted is always of longer wavelength (lower energy) than that which was initially absorbed because some energy is lost in other nonradiative ways, principally by vibrational relaxation. The difference between the wavelengths for maximum absorption and emission is known as the Stokes' shift (Fig. 3.4). It is this characteristic that underlies all fluorescence techniques because it allows the emitted light to be detected at wavelengths away from those of the excitation source; the greater the Stokes' shift the more easily this can be done. The absorbance spectra (identical with the excitation spectra) and emission spectra of fluorochromes often overlap and are usually mirror images of one another because the probability of an electron returning to a given energy level in the ground state is similar to the probability of the electron occurring in that position before excitation. It is important to note that the shape of the emission spectrum remains constant regardless of the excitation wavelength, but that the intensity of fluorescence will be affected by the excitation wavelength because the extinction coefficient (a measure of the amount of light absorbed) is wavelength dependent (see below).

The probability of light absorption by a substance is characterised by its extinction coefficient ε. For

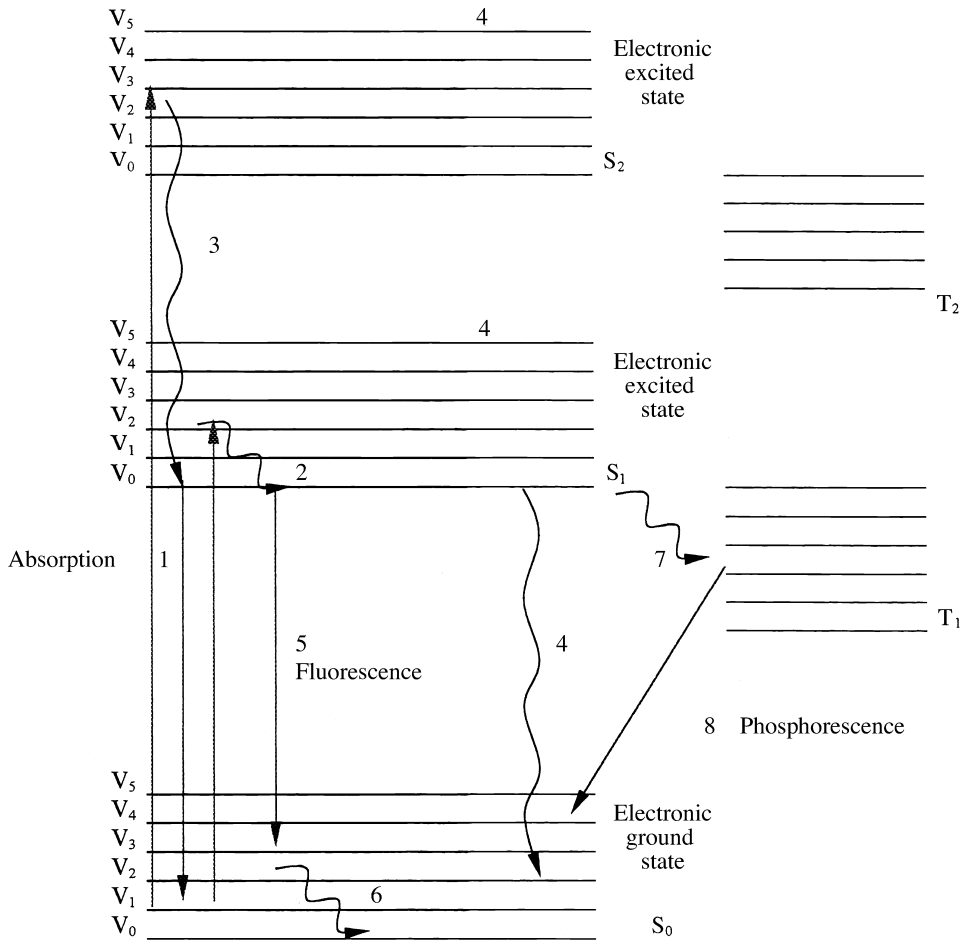

Fig. 3.3 Jablonski diagram illustrating the process of light absorption (excitation) and emission by a fluorochrome. Initial energy absorption (1) raises the molecule to an electronic excited state (S_1 or S_2). Energy can be lost in nonradiative ways by vibrational relaxation during a series of transitions (2) between substates in the electronic excited state S_1, by internal conversion in going from the S_2 to the S_1 state (3), or by external quenching (4). Those molecules in the lowest excited singlet state can then undergo the main downward transition that results in fluorescence (5). After emission, there is a further possibility for similar energy loss by vibrational relaxation as the molecule goes through the ground substates (6). Intersystem crossing from the singlet excited state S_1 to the triplet state T_1 (7) is a nonradiative process, which when followed by decay to the electronic ground state (8) results in phosphorescence. Nonradiative vibrational transitions that relax S_2 to S_1 occur faster than the de-excitation processes that return S_1 to the ground state S_0. The most probable upward energy transition will correspond to the peak of the absorption spectrum and the most probable downward transition to the peak of the emission spectrum. (After Cantor and Schimmel, 1980.)

example, fluorescein has an extinction coefficient at its wavelength of peak absorption of 75 000 cm^{-1} mol l^{-1} (molar extinction coeffficient for a 10 mm pathlength), while phycoerythrin (PE) has the exceptionally high ε value of 10^6 cm^{-1} mol l^{-1}. Light absorption by fluorochromes is extremely rapid (about 10^{-15} s); however, light emission by fluorescence is somewhat slower and is never 100% effi-

cient. In general, the stronger the absorption of light by an isolated molecule, the more rapid the subsequent emission of fluorescent radiation. The intensity of the fluorescence that is emitted is proportional to the extinction coefficient and the quantum yield (ϕ) for that particular fluorophore. The quantum yield is the ratio of photons (quanta) emitted to photons (quanta) absorbed and numerically can vary from 0 to 1.0. For a fluorophore in solution, the relationship would be:

$$F = I_o \varepsilon [C] x \phi$$

where F is the total amount of fluorescence produced (light emitted), $I_o \varepsilon [C] x$ is the total amount of light absorbed by the fluorophore, which results from Beer's law, and in which I_o is the incident light intensity, $[C]$ is the molar concentration and x is the path length in centimetres.

The other processes that compete with fluorescence to reduce the quantum yield include internal conversion, quenching of various types and intersystem crossing. All can cause the relaxation of electrons from the excited to the ground state without the emission of a photon and thereby decrease the fraction (the quantum yield) that decays through fluorescence. In internal conversion, energy is lost by collision with other molecules (e.g. solvent) or through internal vibrational and rotational modes (i.e. heat) within about 10^{-11} s. Collisions with solute molecules that are capable of quenching can also result in loss of fluorescence. Aromatic fluorochromes usually have fluorescence lifetimes (τ) of 10^{-8} to 10^{-9} s but almost every collision with a quenching molecule such as O_2 or I^- de-excites the excited singlet state. As quenching molecules are usually present in great excess, collision rates are only limited by diffusion and can approach 10^{-8} s^{-1} at millimolar concentrations of quencher. Intersystem crossing occurs when an excited electron changes its spin, resulting in the excited singlet state being converted into the excited triplet state; the latter can decay to the ground state either by phosphorescence or by internal conversion. Because the excited triplet state is at a lower energy than the excited singlet, phosphorescence is at longer wavelengths than fluorescence. However it is rarely seen in solution because the phosphorescence lifetime is measured in seconds and is outcompeted by collisions with quenchers and internal conversion. Photo-oxidation occurs when an electron is transferred from a light-excited donor molecule to an acceptor molecule, which in turn becomes reduced. This happens because the transferred electron is less tightly bound in its excited than in its ground state.

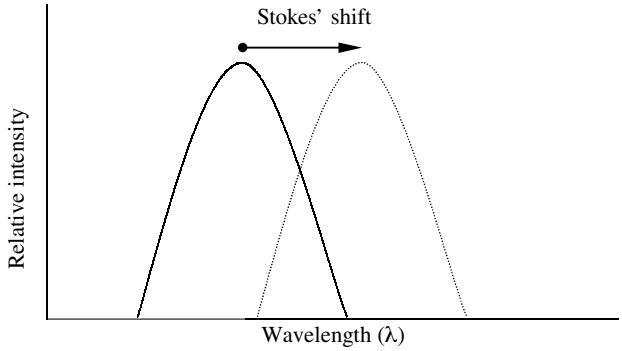

Fig. 3.4 The excitation or absorption (solid line) and emission (dotted line) spectra of a fluorochrome. The difference between the wavelengths of the absorption (excitation) and emission maxima is known as the Stokes' shift and is always in the direction of the longer wavelength (smaller energy).

Typically, fluorescein isothiocyanate (FITC) molecules go through the cycle of photon absorption and emission some 30 000–40 000 times with an average excited state (fluorescence) lifetime of 4 ns (4×10^{-9} s) before oxidative processes favoured by the excited state result in photobleaching. For comparison, a cell passes through the light beam of a flow cytometer in 5–50 μs (1 μs = 10^{-6} s), or of a laser scanning cytometer in 1–10 ms (1 ms = 10^{-3} s). The intensity of emitted fluorescence is limited by the duration of the excited state lifetime, i.e. the time that it takes for an excited molecule to return to the ground state from which further excitation cycles are possible, which is a characteristic of a particular fluorochrome and its environment. Fluorochromes differ in their susceptibilty to photobleaching by high-intensity illumination; in general, the resultant fading of the fluorescence is unimportant for flow

cytometry although it can cause problems in laser scanning cytometry. Photobleaching is dependent on the molecular oxygen reacting with either the excited singlet or triplet state to produce singlet oxygen, which is highly reactive. It can be retarded by using antioxidants/antifadants such as *p*-phenylenediamine, *n*-propyl gallate or 1,4-diazobicyclo-2,2,2-octane in the mounting medium, but it is simplest to purchase a commercial reagent that has been formulated for use with a particular fluophore (e.g. ProLong™, *SlowFade*™; Molecular Probes). These reagents should not be used with live cells.

The molecular environment, including factors such as ionic strength, pH and solvent polarity, can markedly affect the quantum yield. Therefore, to avoid artefactual changes, solution parameters such as the ionic strength and pH should be kept constant and within the physiological range unless there are specific reasons why they should be altered. Conjugation of a fluorochrome to protein ligands usually favours quenching, resulting in a decreased quantum yield. For example, coupling FITC to an antibody decreases its quantum yield from 0.85 to between 0.3 and 0.5. For most practical purposes, fluorochrome-conjugated antibodies are required that have quantum yields >0.4 when bound to cells. The fluorescence intensity of a fluorochrome-conjugated protein can be increased up to a limit by increasing the number of fluorochrome molecules attached to each molecule of the protein. However, maximum brightness with fluorescein occurs at between two and four molecules per molecule of protein, with greater fluorochrome to protein ratios resulting in decreased specific binding and increased nonspecific binding. A mechanism that was originally known as 'fluorochroming' can produce a marked increase in the quantum efficiency of some dyes when they are bound to a particular substance or occur in a particular environment. For example the intercalation of ethidium or propidium into double-stranded DNA and the binding of the Hoescht dyes to the outer groove of the DNA helix increases their fluorescence 20- to 30-fold. Comprehensive information on the spectra, structure and properties of fluorochromes used in cytometry has been compiled by Haugland (1994, 1996).

3.4 Energy transfer by resonance between fluorochromes

Fluorescence resonance energy transfer (but also known as singlet–singlet or exciton resonance energy transfer) occurs when the electronic orbitals of two different fluorochromes interact by exciton or coupled oscillator mechanisms so that energy absorbed by one (the donor) is passed to the other (the acceptor), which fluoresces. Suppose the fluorochrome with the higher energy absorption, i.e. lower excitation wavelength (the donor), is excited, it will rapidly lose energy by internal conversion until it reaches the first excited singlet state. If the energy that would be lost by the donor returning to the ground state matches that of the acceptor absorption, energy transfer will occur by resonance between the donor and acceptor; as a result, the donor is quenched and the acceptor becomes excited and subsequently fluoresces. For resonance interactions to happen, the wavelength of donor fluorescence must overlap with the wavelength of acceptor absorption. Therefore, in any system capable of resonance energy transfer, it is also possible for the additional process of photon emission by the donor and subsequent photon absorption by the acceptor to occur (Fig. 3.5). However, this does not usually happen in practice, because fluorochrome concentrations $>10^{-3}$ mol l^{-1} are needed (Forster, 1959). Resonance energy transfer occurs best over very short distances (approximately 2–10 nm), with an upper limit of 60–100 nm (i.e. less than the average thickness of a cell membrane), because the efficiency of transfer is proportional to the inverse of the sixth power of the distance separating the two fluorochromes. The technique can be used to measure the distance separating two fluorochromes and in these applications has been termed a 'molecular ruler'. Practical instructions for measuring separation distances by flow cytometry and software for perform-

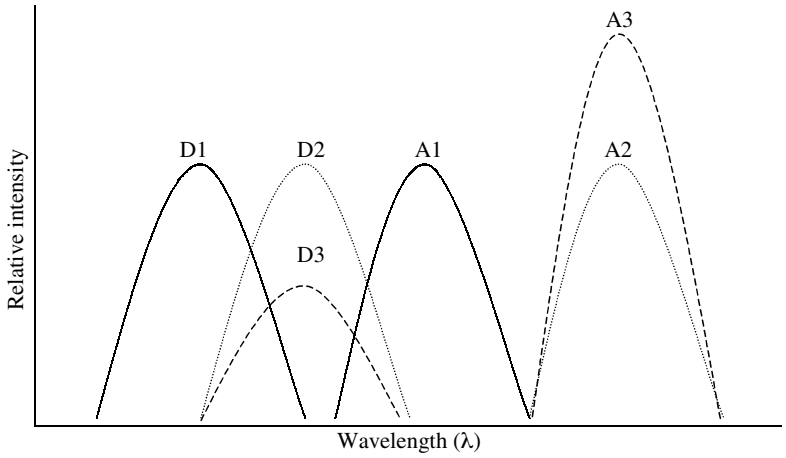

Fig. 3.5 Hypothetical spectra for a pair of donor–acceptor fluorochromes suitable for resonance energy transfer.The absorption (solid lines D1 and A1) and normal emission spectra (dotted lines D2 and A2) of the donor (D) and acceptor (A) are shown and the decreased donor emission intensity (D3) and increased acceptor emission intensity (A3) when resonance energy transfer occurs. Note the region of spectral overlap between the emission of the donor and absorption of the acceptor.

ing the essential calculations are available from SoftFlow Inc.

The principle of fluorescent resonance energy transfer has several applications in cytometry. First, it can be used to investigate whether different antigens are closely associated on the cell surface. In these procedures one antigen is targeted with an antibody conjugated to a potential donor fluorochrome and the other is targeted by an antibody conjugated to a potential acceptor fluorochrome. If, by comparison with singly labelled cells, the doubly labelled cells have decreased donor fluorescence and increased acceptor fluorescence, it can be deduced that the two antibodies, and hence the two cell surface antigens to which they are bound, must be sufficiently close for energy to be transferred by resonance. Such transfer would not occur between randomly distributed surface antigens present in similar densities on the cell surface. Second, novel fluorochromes have been synthesised by coupling a dye that can be excited at a convenient wavelength, e.g. 488 nm, to another to which energy can be passed by resonance transfer and which in consequence fluoresces at a longer wavelength than the first (so-called tandem dyes or fluorochromes). For instance, R-phycoerythrin (from Rhodophycae; R-PE), which normally emits at 578 nm, has been coupled to a number of small organic dyes (Table 3.1); see also Section 3.6.4. Although energy transfer from the acceptor to the donor is high, typically ~90%, it is never total, so there is always some donor fluorescence, which can give rise to high backgrounds. Third, substrate analogues for proteases have been synthesised in which a donor and an acceptor dye are covalently bound to different sides of a cleavage site in the peptide. Upon cleavage, the separate fragments are released, leading to a decrease in acceptor and an increase in donor fluorescence (Fig. 3.6). Fourth, rare earth ions, europium, terbium or lanthanides, which have unusually long fluorescence (phosphorescence) lifetimes (milliseconds rather than nanoseconds), have been coupled (as the energy donor) to phycobiliproteins or phycobiliprotein-based tandem dyes (as the acceptor). By incorporating a time delay into the measurement of the acceptor fluorescence, the fluorescence resulting from resonance energy transfer can be distinguished from background autofluorescence and acceptor fluorescence. These assays, which are called 'time-

Table 3.1 *The characteristics of some phycoerythrin-based tandem dyes*

Dye conjugated to phycoerythrin		Tandem dye	
Name	Synonyms/acronyms	Emission maximum (nm)	Synonyms/acronyms
Sulphonylchloride rhodamine	Texas Red® (TR)	613	Phycoerythrin–Texas Red® (PE–TR), Energy Coupled Dye (ECD™), Red613
Indodicarbocyanine	Cyanin5 (Cy™5)	670	Phycoerythrin–Cyanin5 (PE–Cy™5), Cy™-Chrome, Tri-Color®, Red670 and Quantum Red™
Indotricarbocyanine	Cyanin7 (Cy™7)	780	Phycoerythrin–Cyanin7 (PE–Cy™7)

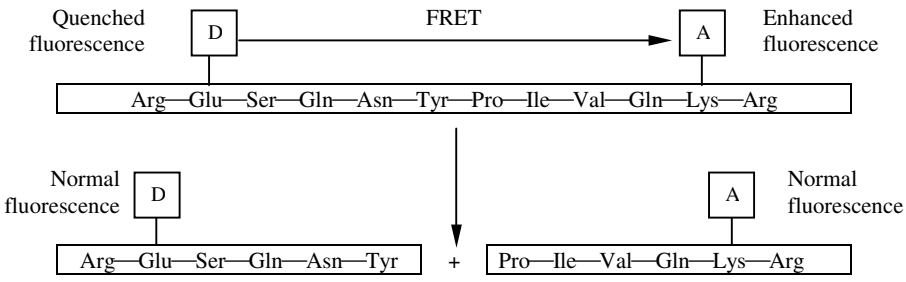

Fig. 3.6 The principle of abrogating fluorescence resonance energy transfer (FRET) in the assay of intracellular proteases. In the uncleaved peptide, the donor (D) fluorescence intensity is quenched and the acceptor (A) fluorescence intensity is enhanced; on cleavage the fragments are no longer held in close proximity and the normal fluorescence intensity of both donor and acceptor fluorochrome is restored.

resolved-fluorescence energy transfer', have not yet been widely used (see also Ch. 17).

3.5 Fluorochrome options for cytometric applications

3.5.1 Options when using instruments powered by a single 488 nm laser

In many flow cytometers and in the laser scanning cytometer, the light source is an air-cooled argon laser providing 15 mW at 488 nm. Optical filters are used to select the wavelengths of emitted (fluorescent) light that reach the various photomultipliers and the fluorescence detectors are usually numbered sequentially starting from the lowest wavelength. Instruments with a single 488 nm laser, such as the FACScan™, Research FACScan™ and FACStar™ (BD Biosciences) or EPICS® XL (Beckman Coulter), usually have three or four fluorescence detectors. For instance, the FACScan™ with three/four detection channels collects light at 530 ± 30 nm (FL1), 585 ± 42 nm (FL2), 616 ± 60 nm (FL4) and >670 nm (FL3), using band-pass (FL1, FL2 and FL4) and long-pass (FL3) filters. By comparison, the EPICS® XL with four fluorescence detectors collects light at 525 ± 25 nm (FL1), 575 ± 25 nm (FL2), 620 ± 25 nm (FL3) and 675 ± 25 nm (FL4). Where instruments are powered by a single 488 nm argon laser, it would be desirable to have fluorochromes that could be excited at the same (488 nm) wavelength but which fluoresced at different wavelengths. Unfortunately, it is not easy to find many dyes with these characteristics. Furthermore, the fluorescence intensity obtainable from a

fluorochrome under these circumstances is very often limited because it has to be excited at a wavelength (488 nm) away from its absorption (excitation) maximum.

Interference filters are very efficient in selecting the wavelengths of emitted light to be collected by a particular detector, but most fluorochromes emit over a wavelength range that is much wider than that selected by the filter. For instance, although most of the light emitted from FITC will be collected in the FL1 channel, some of it will also be of sufficiently long wavelength to pass through the filter (FL2) intended to collect PE emissions. Similarly, some of the light emitted by PE will be detected in the FL3 channel and a lesser amount in the FL1 channel. If more than one fluorochrome is being analysed, some correction for the 'spillover' of the fluorescence from one fluorochrome into the channel intended to detect another has to be made by electronically subtracting a proportion of one fluorescence signal from the other, a procedure called 'compensation'. This may be done either during or after (Bagwell and Adams, 1990) data acquisition (see also Section 1.8; Roederer, 1999; and the internet references given at the end of this chapter). Compensation during acquisition is set most easily by using a mixture comprising beads that are unlabelled and that have been singly labelled with each of the different fluorochromes, e.g. Quantibrite or Calibrite (BD Biosciences), Quantum Series (Flow Cytometry Standard Corporation), CompenFlow Flow Cytometry Compensation Kit (Molecular Probes), or QIFI kit (Dako), but final adjustments should done using cells (e.g. lymphocytes) with antigens (e.g. CD3, CD4 and CD8) labelled in the relevant colours.

FITC and PE are a good combination for two-colour immunolabelling provided that the spectral overlap of FITC is subtracted from the PE channel and vice versa. Those fluorochromes with narrow bandwidths, such as the BODIPY® dyes (see Section 3.6.1), are particularly useful for multicolour immunolabelling. For immunolabelling using three colours, FITC (FL1), PE (FL2) and peridinin–chlorophyll *a* complex (PerCP) or a tandem conjugate such as PE–indodicarbocyanine (PE–Cy™5) (FL3) can be used. Many pre-mixed reagents comprising three antibody conjugates of different colour are commercially available, e.g. TriTest™ comprising FITC–CD3/PE–CD8/PerCP–CD45 (BD Biosciences). Four-colour immunolabelling is normally achieved using FITC (FL1), PE (FL2), PE–Texas Red® (PE–TR) (FL3) and either PE–Cy™5, PerCP, or PE–indotricarbocyanine (PE–Cy™7) (FL4), although of the last three, PE–Cy™7 is most easily discriminated because its emission goes further into the long red region. In order that PerCP, Cy™7 or any of the tandem conjugates of Cy™7 can be detected effectively, it is necessary that the cytometer be equipped with one of the more recent photomultipliers (e.g. R3696; Hamamatsu Photonics K.K), which have good performance in the long red region of the spectrum. It is also necessary that the instrument software allows compensation to be set for four-colour analysis.

When both fluorescence intensities and signal to noise ratios are taken into account, PE antibody conjugates are about five- to tenfold more sensitive than comparable FITC antibody conjugates, which are in turn more sensitive than tandem dye antibody conjugates (PE–Cy™3, PE–Cy™5) and PerCP. In general, in multicolour combinations, the more weakly expressed antigens are best stained with PE and the more highly expressed antigens are best stained with tandem dyes or PerCP.

Tables 3.2 and 3.3 list those fluorochromes useful for immunolabelling and functional analysis, respectively, which can be excited at 488 nm and detected in basic instruments with three or four fluorescence detection channels.

3.5.2 Options when using instruments with excitation at multiple wavelengths

Four is the maximum number of different fluorochromes that can satisfactorily be detected at present on a single cell by instruments powered by a single laser emitting at 488 nm. As it would be an advantage in many situations to be able to measure additional parameters, some flow cytometers have an

Table 3.2 *Fluorochromes used for conjugation, for example to antibodies, that can be excited at 488 nm and are detectable in basic instruments with three or four fluorescence detection channels*[a]

Channel	Filter peak transmission (typical wavelengths; nm)	Fluorochrome	Wavelength (nm)	
			Excitation	Emission
FL1 (green)	530 BP	FITC	492	516–525
		Cy™3	512, 552	565, 615
		BODIPY® FL	503	512
		Alexa™ 488	494	519
FL2 (orange)	575–585 BP	R-PE	480, 545	575
		B-PE	480, 565	578
FL3 (red)[a]	620 BP or > 650 LP	PE–TR	480, 565	613
FL4 (long red)	675 BP or > 675 LP	PE–Cy™5	480, 565, 650	667
		PerCP	490	675
		PE–Cy™7	480, 565, 743	767

BP, band-pass; LP, long-pass; FITC, fluorescein isothiocyanate; B-PE, bacterial phycoerythrin; PE–Cy™5, phycoerythrin–indodicarbocyanine (also called CyChrome™, Tri-Color®, Red670 and Quantum Red™); PE–Cy™7, phycoerythrin–indotricarbocyanine; PE–TR, phycoerythrin–Texas Red® (also called ECD™, Coulter Red613); PerCP, peridinin–chlorophyll *a* complex; R-PE, Rhodophycae phycoerythrin.

[a]Where there are only three fluorescence detectors, FL3 will normally detect fluorochromes emitting in the red and the long red wavelengths, using, for example, a 650 nm long-pass filter.

additional laser(s) that can be used to excite other dyes at different wavelengths. For example, the EPICS® XL and EPICS® XL-MCL (Beckman Coulter), the FACScan™, FACS Calibur™ I and II, FACStar™ PLUS and FACS Vantage™ SE I and II and LSR* (BD Immunocytometry Systems) can have a second and, in some instances, a third laser, while the MoFlo® high speed cell sorter (Cytomation Inc., CO, USA) has four lasers. The most common additional lasers are a helium–neon providing excitation at 633 nm and a helium–cadmium providing excitation at 325 nm, although the FACSVantage™ with TurboSort® has a 560–640 nm dye-tunable laser. In instruments with multiple lasers, the beams may be focused at the same point in the flow stream, or parallel beams may be focused at different levels with an electronic time delay (typically 10–15 μs) used to correlate emissions from a single cell. Just a few cytometers (e.g. older Becton Dickinson and Ortho Diagnostics instruments and the BioRad BRYTE HS) use mercury or xenon arc lamps, which provide illumination across a wide range of wavelengths, the former with additional peaks at 366, 405, 436, 546 and 578 nm. Instruments in which fluorochromes can be excited at additional wavelengths are considerably more versatile but they require stringent alignment. Usually two fluorescence detectors are associated with each additional laser, and different filter combinations can be used to divide the emitted wavelengths as required. It is, for various reasons (e.g. electronic limitations, energy transfer between fluorochromes), often not feasible to use all of the possible combinations at once. At present, four-colour analysis is routine and five- or six-colour analysis can be readily achieved. This may require somewhat narrower filter bandwidths and, depending on the configuration, inter-laser compensation may be needed to ensure adequate discrimination when using tandem dyes that can be excited by both lasers. Fluorescent stains that can be excited at these additional wavelengths are listed in Table 3.4.

Possible fluorochromes that might be detected in the different channels of a FACScan™ or FACS Calibur™ equipped with 488 nm argon and 633 nm helium–neon lasers, four colour detectors and inter-

Table 3.3 *Functional stains that can be excited at 488 nm and are detectable in basic instruments with three or four fluorescence channels*[a]

Channel	Fluorochrome	Use	Excitation (nm)	Emission (nm)
FL1 (green)	Acridine orange	DNA	500	526
		RNA	460	650
	BCECF	Membrane integrity; pH (load as AM ester)	~505	525 : 640
	Calcein	Membrane integrity (load as AM ester)	494	517
	Carboxyfluorescein diacetate	Membrane integrity (load as AM ester)	511	534
	2',7'-Dichlorofluorescein diacetate	Metabolic burst, oxidative metabolism	510	532
	$DiBAC_4(3)$	Transmembrane potential	493	516
	$DiOC_6(3)$	Transmembrane potential	484	501
	Fluorescein diacetate	Membrane integrity (load as AM ester)	475	530
	JC-1	Mitochondrial trans-membrane potential	485–585	590[b]
	PicoGreen®[c]	Highly selective for DNA	502	523
	Rhodamine 123	Mitochondrial trans-membrane potential	507	529
	SYBR® Green I[c]	High sensitivity DNA stain	494	521
	SYTOX® Green	Cell-impermeant nucleic acid stain	504	523
	Thiazole orange	Nucleic acid stain	453, 515	530
	TOTO®-1	High-affinity DNA stain	514	533
	YOYO®-1	High-affinity DNA stain	491	509
FL2 (orange)	Dihydroethidium (Hydroethidine™)[d]	Metabolic burst, oxidative metabolism	518	605
	Ethidium bromide	Cell-impermeant nucleic acid stain; apoptosis	518	610
	Ethidium monoazide	Fluorescent photoaffinity nucleic acid label compatible with fixation	464	625
	Fluo-3, Fluo-4, Fluo-5	Calcium (load as AM ester)	464	526
	Propidium iodide	Cell-impermeant nucleic acid stain; viability	520	610
	SNARF®-1	Intracellular pH (load as AM ester)	488–530	580 : 640
FL3 (red)	7-AAD	Generally cell-impermeant nucleic acid stain	546	647
	Fura Red™	Calcium (load as AM ester; fluorescence decreases on binding)	450–500	~660
FL4 (long red)	LDS-751	Nuclear DNA	543	712
	DRAQ5[e]	Nuclear DNA	488, 514	665–780

7-AAD, 7-aminoactinomycin D; AM, acetoxy-methyl; BCECF, 2',7'-bis(2-carboxyethyl)-5,6-carboxyfluorescein; $DiBAC_4(3)$, bis-(1,3-dibutylbarbituric acid) trimethine oxonol; $DiOC_6(3)$, 3,3'-dihexyloxacarbocyanine iodide; SNARF®-1, a seminaphthorhodafluor dye.

[a]Where there are only three fluorescence detectors, FL3 will normally detect fluorochromes emitting in the red and the long red wavelengths.

[b]As aggregates.

[c]Originally intended for use in solution assays but has been successfully used in flow cytometric assays.

[d]After oxidation to ethidium.

[e]DRAQ5 can be excited in the ultraviolet, and at 488, 514, 568, 633 or 647 nm with increasing efficiency as the wavelengths increase.

Table 3.4 *Fluorescent dyes that can be used in instruments with lasers providing excitation at wavelengths other than 488 nm*

Excitation/emission wavelengths (nm)	Stain	Use
340/660–670	Europium–APC chelate	Conjugation to proteins
340/750–790	Europium–APC–Cy™7 chelate	Conjugation to proteins
340/570–590	Terbium–PE chelate	Conjugation to proteins
346/442	Alexa™ 350	Conjugation to proteins
346/401 : 475	Indo-1 AM	Calcium concentrations
350/461	Hoechst 33342	Vital DNA stain; AT selective
352/461	Hoechst 33258	Vital DNA stain; AT selective
353/442	AMCA	Conjugation to proteins and nucleic acids
358/461	DAPI	Vital DNA stain; AT selective
365/420–440, 500–580	DCH loaded as ADB	pH measurement (ratiometric procedure)
365, 518/605	Dihydroethidium (Hydroethidine™)	Metabolic burst, oxidative metabolism
365, 535/617	Propidium iodide	Impermeant DNA stain; viability
400/420	Cascade Blue®	Conjugation to proteins but high nonspecific binding
431/541	Alexa™ 430	Conjugation to proteins
431/480	SYTOX® Blue	DNA stain
445/575	Chromomycin A3	DNA stain; GC selective
445/575	Mithramycin	DNA stain; GC selective
480, 565, 650/670	PE–Cy™5	Conjugation to proteins
480, 565, 743/767	PE–Cy™7	Conjugation to proteins
490/675	PerCP	Conjugation to proteins
491/515	Alexa™ 488	Conjugation to proteins
491/660	Alexa™ 488 APC	Conjugation to proteins
500–570, 625, 650/682	Cy™5	Conjugation to proteins
512, 532/565, 615	Cy™3	Conjugation to proteins
531/554	Alexa™ 532	Conjugation to proteins
543/712	LDS-751	As a vital DNA stain
543/571	Texas Red®-X	Conjugation to proteins
556/573	Alexa™ 546	Conjugation to proteins
546/647	7-AAD	Impermeant DNA stain; GC selective
547/570	SYTOX® Orange	DNA stain
548/579	SNARF®-1	pH measurement
578/603	Alexa™ 568	Conjugation to proteins
587/602	Texas Red®	Conjugation to proteins
590/607	LDS-751	As a vital RNA stain
590/617	Alexa™ 594	Conjugation to proteins
610/639	Oxonol-V	Transmembrane potential
621/634	SYTO® 17	DNA stain
642/661	TO-PRO™-3	Moderately high-affinity DNA stain
490, 675/695	PerCP–Cy™5.5 (TruRed)	Conjugation to proteins
642/660	TOTO®-3	High affinity DNA stain
649/671	$DiSC_2(5)$	Transmembrane potential
650/660	APC	Conjugation to proteins
650, 755/767	APC–Cy™7 (PharRed)	Conjugation to proteins
743/767	Cy™7	Conjugation to proteins

7-AAD, 7-aminoactinomycin D; ADB, 1,4,-diacetoxy-2,3,-dicyanobenzene; AMCA, 7-amino-4-methylcoumarin-3-acetic acid; APC, allophycocyanin; Cy™3, cyanin3; Cy™5, cyanin5; Cy™7, cyanin7; DAPI, 4',6-diamidino-2-phenylindole; DCH, 2,3-dicyanohydroquinone; $DiSC_2(5)$, a thia carbocyanine dye; PE, phycoerythrin; PerCP, peridinin–chlorophyll *a* complex protein; SNARF®-1, a seminaphthorhodafluor dye; SYTO® 17, a cell-permeant cyanine dye; SYTOX® Blue, a cell-impermeant cyanine dye; TO-PRO™-3, a monomeric cyanine dye; TOTO®-3, a dimeric cyanine dye.

Table 3.5 *Fluorochromes which might be used for four-colour fluorescence in a FACScan™ or FACS Calibur™ equipped with 488 and 633 nm excitation*[a]

Channel	Wavelengths (nm)	Fluorochrome
FL1	530 ± 30	Alexa™ 488, BODIPY® FL, calcein, DTAF, FITC, Fluo-3, rhodamine 123, TOTO®-1, TO-PRO™-1,
FL2	585 ± 42	Cy™3, PE, PI
FL3	> 670	PerCP, PerCP–Cy™5, PE–Cy™5, PE–Cy™7, PE–TR, APC[a], APC–Cy™7[a]
FL4	660 ± 30	APC[a], Cy™5[a], TOTO®-3[a], TO-PRO™-3[a]

BODIPY® FL, 4,4-difluor-4-bora-3a,4a-diaza-s-indacene-3-propionic acid; Cy™3, cyanin3 (indocarbocyanine); DTAF, fluorescein dichlorotriazine; FITC, fluorescein isothiocyanate; PE, phycoerythrin; PE–TR, phycoerythrin-Texas Red®; PI, propidium iodide; TO-PRO™-1 and TO-PRO™-3, are monomeric cyanine dyes with different spectral properties; TOTO®-1 and TOTO®-3, dimeric cyanine dyes with different spectral properties; other abbreviations as in Table 3.2.
[a]Excited by 633 nm laser, others excited at 488 nm.

laser compensation are listed in Table 3.5. Some common combinations would be, FITC /PE/Quantum Red™/allophycocyanin (APC), FITC/PE/PerCP/Cy™5 or FITC/PE/PI/APC.

3.6 The characteristics of fluorochromes used for conjugating to antibodies and other proteins

FITC and PE have been very widely used to label antibodies to provide a first and second colour, while tandem dyes based on PE and PerCP have been used somewhat less widely to provide a third or fourth colour that can be excited by an argon laser at 488 nm. Tetramethylrhodamine and Texas Red®, which are commonly used in conventional immunofluorescence microscopy, have not been widely used because they are excited poorly at 488 nm. However, Cy™5, APC, APC–Cy™7 and, to a lesser extent, Texas Red® have been used to provide an extra colour for immunofluorescence analysis in those instruments equipped with an additional laser(s) emitting in the 550–650 nm range. The only fluorochromes currently available for labelling proteins that can be excited in the ultraviolet are Alexa™ 350 (see below), derivatives of 7-amino-coumarin, (e.g. 7-amino-4-methylcoumarin-3-acetic acid; AMCA) and Cascade Blue®. However there have been reports of high nonspecific binding with Cascade Blue®-labelled proteins and it is currently not recommended for flow cytometry. Most commercially available antibodies can be obtained as FITC or PE conjugates and a good proportion can be obtained conjugated to APC, PerCP or to one of the tandem dyes. Few however can be obtained conjugated to Texas Red® (Fig. 3.7C), the Alexa™ dyes, AMCA or Cascade Blue®, but these fluorochromes can usually be purchased already conjugated to anti-species immunoglobulins or to avidin or streptavidin for use in indirect labelling procedures. The structures of some small fluorochromes are illustrated in Fig. 3.7.

3.6.1 Fluorescein, fluorescein derivatives and substitutes

FITC, molecular weight 389 (excitation/emission maxima ~495/520 nm) is one of the most widely used labelling reagents (Fig. 3.7A). It can readily be conjugated to proteins, giving derivatives that are reasonably stable with a high quantum yield (~0.5) and an absorption peak that is close to the 488 nm line of argon lasers. It has generally been the fluorochrome of choice for single-colour staining but its rather broad emission is a disadvantage for multicolour applications. Other drawbacks include its high rate of photobleaching and its pH-sensitive fluorescence, which is maximal at pH 8–9. A number of fluorescein derivatives that have the same

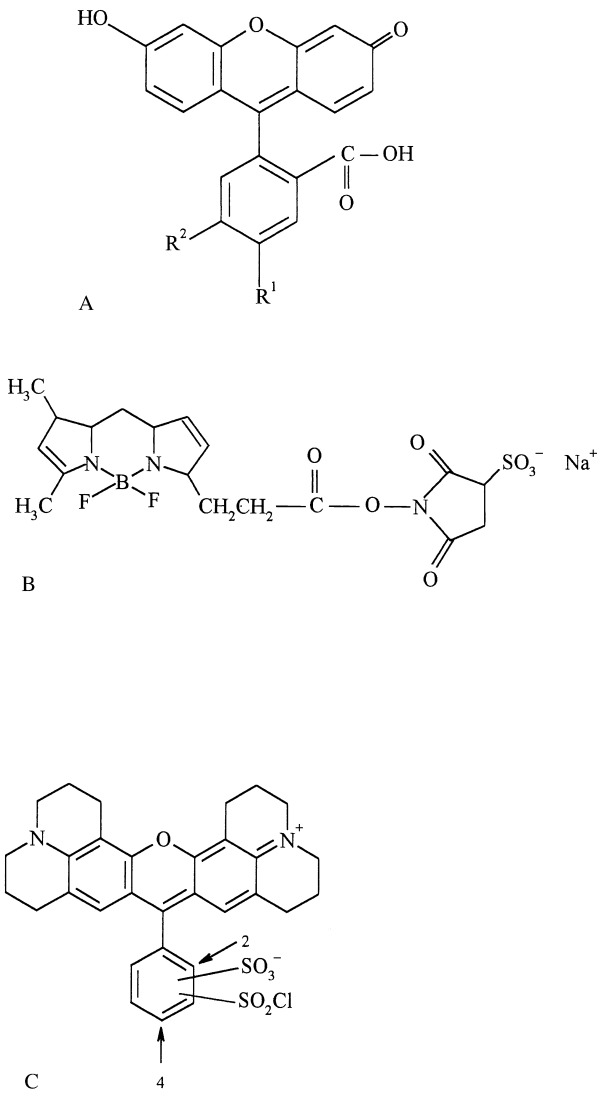

Fig. 3.7 Structure of some small flurochromes used for labelling proteins. (A) Fluorescein: R^1 = – N=C=S and R^2 = H in fluorescein 5-isothiocyanate (FITC isomer I, the more commonly used isomer) and R^1 = H and R^2 = – N=C=S in fluorescein 6-isothiocyanate (FITC isomer II). (B) 4,4-Difluoro-5,7-dimethyl-4-bora-3a,4a-diaza-s-indacene-3-propionic acid sulphosuccimidyl ester (BODIPY® FL, SSE). (C) Texas Red® sulphonyl chloride (mixed 2- and 4- isomers). See Fig. 3.8 for the details of conjugation reactions.

spectral characteristics as fluorescein yield more stable antibody and protein conjugates with higher fluorescence intensities, e.g. dichlorotriazinylamino fluorescein (DTAF), carboxyfluorescein and 2',7'-difluorofluorescein (Oregon Green™ 488). The BODIPY® series of fluorochromes (4,4-difluoro-4-bora-3a,4a-diaza-s-indacene derivatives) have largely similar spectral properties to more commonly known dyes (Fig. 3.7B). BODIPY® FL (BODIPY-3-propionic acid) is a 'fluorescein substitute' (excitation/emission maxima ~503/512 nm) that differs structurally from fluorescein and has a smaller Stokes' shift. It is, however, less pH sensitive and has a higher fluorescence intensity than FITC (Fig. 3.7B). Alexa™ 488 (excitation/emission maxima 494/519 nm) is another more photostable and brighter alternative to FITC. Again, it is only one of a range of new dyes, which also includes, Alexa™ 350, Alexa™ 430, Alexa™ 532, Alexa™ 546, Alexa™ 568 and Alexa™ 594; these are named for the laser spectral lines by which they are optimally excited (approximate peak absorptions) and have peak emissions at 442, 541, 554, 573, 603 and 617 nm, respectively.

3.6.2 Phycobiliproteins (phycoerythrin, allophycocyanin and CryptoFluor™ dyes)

Phycobiliproteins are components of photosynthetic systems comprising multiple tetrapyrole groups covalently attached to a protein; these are responsible for trapping light and passing the energy to chlorophyll by resonance energy transfer. They absorb light maximally between 470 and 650 nm and transmit the energy to chlorophyll at 670 nm. Their high extinction coefficients (e.g. bacterial PE (B–PE), 2.4×10^6 cm^{-1} mol l^{-1}) and high quantum yields (e.g. B-PE, 0.98) result in high fluorescence intensities, with the result that their conjugates are often the most sensitive probes available. It has even proved possible to detect single molecules of PE in a specialised flow cytometer using exceptionally slow flow rates and photon counting detection (Nguyen et al., 1987). The detection limit in a con-

ventional instrument under normal operating conditions is probably between 500 and 1000 fluorochrome molecules per cell. On a molar basis, the fluorescence of phycobiliproteins is about 30-fold stronger than fluorescein, but in practical applications such as cytometry, phycobiliprotein-labelled antibodies give fluorescence intensities that are between five- and tenfold greater than that of the corresponding fluorescein-labelled antibody. The fact that they absorb light over a broad range of wavelengths and can be excited at a number of different wavelengths has proved useful for both single (488 nm) and multiple laser applications. Phycobiliproteins have only a small Stokes' shift but their fluorescence can be readily distinguished from that of FITC. The most commonly encountered phycobiliproteins are B-PE, a 241 kDa water-soluble protein from cyanobacteria (excitation/emission maxima 546, 565/575 nm); R-PE, a 196 kDa (~19 nm by ~6 nm) protein from eukaryotic red algae (excitation/emission maxima 480, 546, 565/578 nm); and APC a 104 kDa protein (excitation/emission maxima 650/660 nm). R-PE has four phycoerythrobulin (absorption maximum ~565 nm) chromophores and a phycourobilin (absorption maximum ~498 nm) chromophore, which contribute to the main absorbance peak at 565 nm. APC is obtained from a cyanobacterium and has phycocyanobulin (absorption maximum ~650 nm) chromophores (six copies per molecule) and can be excited with the 633 nm line from helium–neon lasers in flow cytometers or by the 647 nm line from argon–krypton lasers in scanning microscopes. PEs and APC are quite large molecules and their size can sterically hinder binding when conjugated to proteins. This can also lead to high background staining if fixed and/or permeabilised cells are not adequately washed free of excess PE or APC antibody conjugates. Commercial PE antibody conjugates usually have about one molecule of PE per molecule of antibody and should not be frozen but stored at 4 °C with 0.1% sodium azide. The CryptoFluor™ dyes, ~30–43 kDa, (absorption/emission maxima 545–645/576–658 nm) (Martek Biosciences), which are phycobiliproteins isolated from cryptomonads, may provide a useful alternative to PE where its large size is a problem.

3.6.3 Peridinin–chlorophyll *a* complex

PerCP (excitation/emission maxima 488/677 nm) is a water-soluble, 35 kDa, photosynthetic pigment obtained from dinoflagellates. It has a high quantum yield (~1) and can be conjugated to antibodies to provide third colour or fourth colour. Its main advantage over tandem dyes is the constancy of its emission spectrum and its limited spectral overlap with PE. However, it is light sensitive and must be kept dark to minimise photodecomposition and is not recommended for use with stream-in-air flow cytometers.

3.6.4 Tandem dyes

Tandem dyes are conjugates of two fluorochromes (e.g. PE–APC, PE–TR, APC–Cy™7, PE–TR (ECD™). Coulter Red613 (emission maximum 613 nm) was one of the earliest tandem dyes, but production problems have lead to it being largely replaced by PE–Cy™5 (CyChrome™, Tri-Color™, Red670 or Quantum Red™; emission maximum 667 nm). All PE-based tandem dyes have significant spectral overlap with PE. They require larger compensation settings than other dyes and the amount of correction needed varies from lot to lot depending on the efficiency of resonance transfer in that particular tandem conjugate. Hence considerable more care is needed when setting the compensation for multicolour work. It is also important that they are not exposed to light or other conditions that would break the coupling between the two dyes because, if so, the PE component will emit in its usual wavelength range instead of at the longer wavelengths expected for the tandem.

PE–Cy™5 is one of the brightest tandem dyes currently available, because Cy™5 has a high extinction coefficient ($\sim 2 \times 10^5$ cm^{-1} mol l^{-1}) and its absorption maximum at 652 nm is optimal for resonance transfer from PE. Optimum labelling efficiency occurs when between five and eight Cy™5

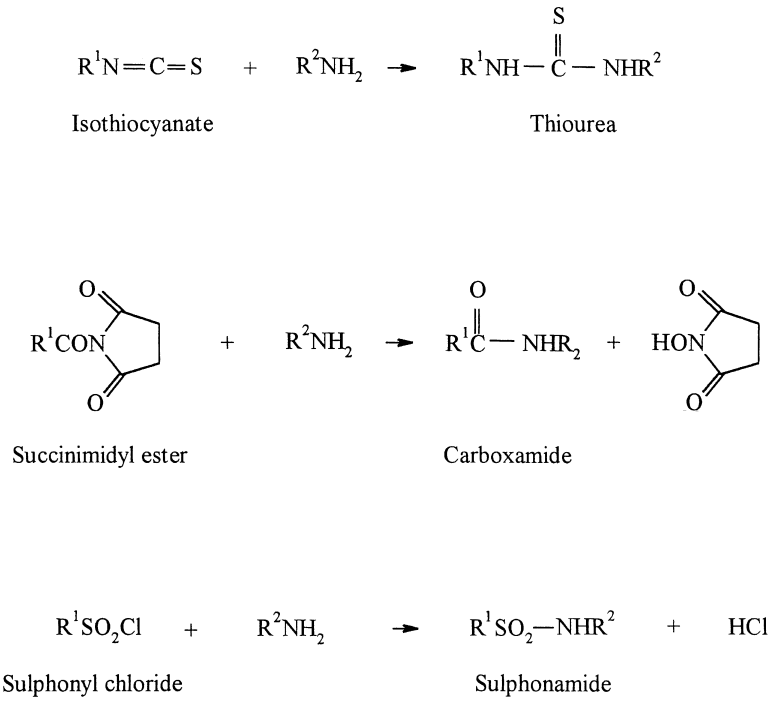

Fig. 3.8 The reactions of a primary amine with an isothiocyanate, a succimidyl ester and a sulphonyl chloride.

molecules are coupled to each PE molecule. PE–Cy™5 requires less compensation from PE than does PE–TR because of its greater Stokes' shift; in commercially available antibody conjugates it is normally present in a fluorochrome-to-antibody molar ratio of 1 : 1. For these reasons, it is generally claimed to be the best third colour for immunolabelling. However, its conjugates must be used with care because PE–Cy™5 is irreversibly degraded by ambient light in <1 h and shows high nonspecific binding to monocytes. PE– Cy™5 is not recommended for dual laser work where excitation by both lasers is possible unless there is an inter-laser compensating circuit. The recently produced Alexa™ 488–APC (green fluorescent Alexa™ cross-linked to APC, Molecular Probes) can be excited at 488 nm leading to emission at ~660 nm, thus providing a third colour for use in cytometers powered by a single 488 nm laser.

Taking this concept to the extreme, Martek Biosciences have produced supramolecular complexes, denoted PBXL™ fluors, containing many crosslinked phycobiliprotein subunits. For example, PBXL™-1 comprises B-PE, R-phycocyanin and APC; it can be excited at 488 nm and emits at 660 nm. The fluorochromes that can be conjugated to antibodies, streptavidin, biotin, etc. are the brightest labels currently available; they should have potential in the study of weakly expressed cell surface antigens where their large size would not be an impediment to binding.

3.7 Coupling fluorochromes to antibodies or other proteins

When a fluorochrome-labelled antibody (or other protein) is needed but cannot be obtained commer-

cially, it is possible to produce one by directly coupling a fluorochrome to the unlabelled antibody (or protein) in the laboratory (Haugland, 1995). Only purified antibodies (or proteins) should be conjugated with fluorochromes, because higher nonspecific binding will be given by other components present in antiserum or fractionated protein mixtures. If purified antibodies are unavailable, they can be isolated fairly easily from immune serum, culture supernatants or ascites fluids using commercially obtainable reagents and/or kits (e.g. ImmunoPure® Plus; Pierce). A reactive form of the fluorochrome, usually the isothiocyanate, the succinimidyl ester or, less frequently, the sulphonyl chloride (Fig. 3.8) is used in the coupling reactions. All of these derivatives react with the amine groups on the N-terminus or with ε-amino group of lysine residues in proteins; reactions with the isothiocyanates usually require a pH > 9 but those with the succinimidyl ester can be usually done at a pH of ~8.5.

PE is most easily conjugated to antibodies (and other proteins) by using its reactive pyridyldisulphide derivative or by crosslinking (e.g. Protein–Protein Crosslinking Kit; Molecular Probes). For each fluorochrome–protein combination, there is an optimum range of substitution; overconjugation may lead to decreased affinity and higher nonspecific binding, while underconjugation may lead to insufficient sensitivity. Substitution levels can easily be determined by absorbance spectroscopy.

Reactive derivatives of fluorochromes are also available with aliphatic spacers between the fluorochrome and the reactive group, which reduces steric hindrance and allows adduct formation with recessed amine groups as well as with those that are more accessible on the surface. Various reactive derivatives of fluorochromes as well as complete reagent kits for conjugating to antibodies are available commercially, e.g. QuickTag Conjugation Kit (Boehringer Mannheim); Calbiochem; ProZyme Inc.; Alexa™ protein labelling kits (Molecular Probes). Some of the reagent kits enable conjugations to be completed in 1 h at room temperature without the need for gel filtration or dialysis.

3.8 Linking antibodies to fluorochromes through protein A or G, avidin– or streptavidin–biotin links

An alternative to directly conjugating antibodies with fluorochromes is to link the two indirectly through protein A or protein G, or through an avidin– or streptavidin–biotin bridge. FITC-labelled protein A can be used instead of a fluorochrome-labelled secondary antibody in indirect labelling procedures, or biotin-labelled protein G can be used as a bridge between the unlabelled primary antibody and any of the wide range of fluorochrome–avidin or fluorochrome–streptavidin conjugates that are available. Avidin–biotin and streptavidin–biotin interactions are very useful in immunolabelling because they can occur with high specificity and affinity. Avidin is a 66 kDa glycoprotein with an isoelectric point (p*I*) ~10.5; it is, therefore, basic (i.e. positively charged) and can interact nonspecifically with negatively charged cell components (e.g. nucleic acids and polysaccharides), which sometimes causes a high background. Streptavidin is the bacterial counterpart; it is a 60 kDa nonglycosylated protein with an isoelectric point near pH 7.0, which generally results in less nonspecific binding than avidin. However, it does contain a homologue, Arg-Tyr-Asp, of the recognition sequence Arg-Gly-Asp that binds integrins and this may give rise to high backgrounds under certain circumstances. Both avidin and streptavidin bind four molecules of biotin per molecule with an affinity constant (K_a) of ~10^{14} mol l^{-1}. Labelling antibodies with biotin is simple and can be done with several different reactive derivatives that will attach to amine, sulphydryl, carboxyl or carbohydrate groups (Haugland and You, 1995). As with fluorochromes, some derivatives can be obtained with an aliphatic spacer between biotin and the reactive group, which can enhance coupling to less accessible sites.

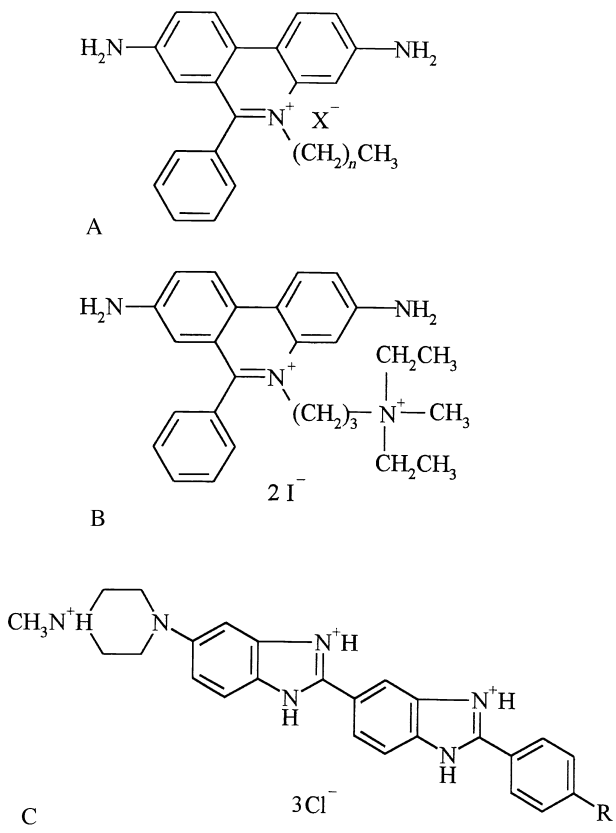

Fig. 3.9 Structures of some nucleic acid-binding dyes. (A) Ethidium bromide ($n = 1$ and X = Br) and the cell-permeant dye hexidium iodide ($n = 5$ and X = I). (B) Propidium iodide. (C) Hoechst dyes, R = OH in Hoechst 33258 and R = OCH_2CH_3 in Hoechst 33342.

3.9 Fluorescent dyes for labelling nucleic acids

Currently there is no dye available that will specifically label RNA as opposed to DNA. The most useful RNA stains are pyronin-Y and thiazole orange, which have absorption maxima, respectively, at 540 and 510 nm; therefore both can be excited by argon lasers with outputs at 488 nm and 514 nm. Pyronin-Y also binds to DNA and glycosaminoglycans but about 75% of the fluorescence from stained cells can be abolished by treatment with RNAase. Thiazole orange has a higher quantum yield when bound to RNA than DNA but shows a marked preference for AT-rich regions when binding to DNA. There are a number of dyes available for staining DNA (for reviews, see Latt and Langlois, 1990; Waggoner, 1990). The dyes commonly used to stain DNA will also bind to RNA; therefore when quantifying DNA, e.g. for cell cycle analysis, it is usual to treat fixed samples with RNAase (50–100 μg ml^{-1}) to avoid fluorescence from the dyes binding to RNA. The structures of some dyes binding to nucleic acid are given in Fig. 3.9.

3.9.1 7-Aminoactinomycin D

7-Aminoactinomycin D (7-ADD; molecular weight 1270; excitation/emission maxima ~500, ~580/~660 nm) is excluded from live cells and like PI can be used to label the DNA of dead cells in which it preferentially binds to GC-rich regions. Its quantum efficiency is low (0.035) but because it can be excited by a 488 nm laser it is used in conjunction with FITC and PE when a measurement of DNA content is required in the context of two-colour immunofluorescence. However, DNA distributions are broader than with the Hoechst dyes.

3.9.2 4',6-Diamidino-2-phenylindole

4',6-Diamidino-2-phenylindole (DAPI) has similar properties to the Hoechst dyes and is also AT specific (see below).

3.9.3 DRAQ5

DRAQ5 is synthetic anthroquinone (1,5-bis{[2-(methylamino)ethyl]amino}-4,8-dihydroxyanthracene-9,10-dione) that enters living or dead cells and binds strongly by intercalation to DNA. It is optimally excited by red light (excitation maximum ~650 nm) and emits in the far-red to short infrared (from ~665 to beyond 780 nm); it can also be excited suboptimally by the 488 nm line of an argon laser and in the ultraviolet. DRAQ5 fluorescence has been demonstrated to reflect DNA content during the cell

cycle and, importantly, it can be used in conjunction with FITC- and PE-conjugated antibodies without the need for compensation (Smith et al., 1999). It has several advantages over LDS-751 but is not yet available commercially.

3.9.4 Ethidium bromide and propidium iodide

Ethidium bromide (EB) (excitation/emission maxima 518/605 nm) (Fig. 3.9A) and propidium iodide (PI) (excitation/emission maxima 535/617 nm) (Fig. 3.9B) are structurally similar but cannot be used interchangeably. EB enters intact cells slowly but PI, which has a higher water solubility and one more positive charge, is excluded from cells with an intact membrane. Consequently, PI rather than EB is used to test membrane integrity, although EB has been used to probe the slight increases in membrane permeability that occur during the early stages of apoptosis. Both dyes intercalate into double-stranded nucleic acids with little sequence preference. On binding, their fluorescence increases 20- to 30-fold (hyperchrome) and is accompanied by changes in their absorption and emission maxima. PI was initially introduced as an alternative to EB for staining DNA when fluorescein/FITC was required for staining other components because its emission is 10–15 nm further into the red than that of EB. It also gives lower coefficients of variation in ploidy studies than EB. To ensure binding only to DNA, cells need to be fixed and RNA digested with RNAase before staining, to avoid binding to double-stranded regions of RNA. Staining kits containing PI and stable RNAase can be obtained commercially (e.g. DNA stain; Beckman Coulter).

3.9.5 Hoechst 33258 and Hoechst 33342

Hoechst 33258 and Hoechst 33342 (excitation/emission maxima ~350/460 nm) (Fig. 3.9C) are cell-permeant dyes that bind preferentially to AT-rich regions of DNA. They can be used for DNA quantification but stoichiometric vital staining by Hoechst 33342 requires a concentration of 5–10 (μmol l^{-1} for at least 30 min, whereas concentrations of ≤ 3 (μmol l^{-1} are sufficient for fixed or permeabilised cells. Apopotic cells have membrane damage and show an increased rate of dye uptake by comparison with live cells. The dyes are best excited with the 325 nm line of a 1–10 mW helium–cadmium laser.

3.9.6 LDS-751

LDS-751 is a cell-permeant stain that binds to both RNA (excitation/emission maxima ~590/607 nm) and DNA (excitation/emission maxima ~543/~712 nm) and undergoes an approximate 20-fold increase in fluorescence on binding to double-stranded DNA (Lanier and Recktenwald, 1991). It can be used to discriminate intact nucleated cells from non-nucleated and damaged cells, and to identify leukocytes in whole blood. Its long emission wavelength makes it particularly useful for multicolour analysis in instruments equipped with a single 488 nm laser.

3.9.7 Mithramycin

Ethanol-treated cells are permeable to the antitumour antibiotic mithramycin, which forms fluorescent complexes with GC-rich regions of DNA but does not bind to RNA. Optimum staining requires 50–100 μg ml^{-1} of dye and Mg^{2+} concentrations of 15–200 mmol l^{-1}. Mithramycin (excitation/emission maxima 440/575 nm) has a relatively low quantum efficiency but can be excited by the 441 nm line from a helium–cadmium laser or the 457 nm line from an argon laser. If cells are stained with a combination of EB and mithramycin and excited by blue–violet light, energy absorbed by the mithramcin can be transferred to EB by resonance. The fluorescence coming from EB under these circumstances is then DNA specific because mithramycin (unlike EB) does not bind to RNA.

3.9.8 SYTO® dyes

The members of the SYTO® dye series have different spectral characteristics, some of which overlap with FITC. A number of the SYTO® dyes are cell

permeant and will stain nucleic acids. However they cannot be used for DNA quantification because they also stain other components.

3.10 Probes for cell viability and death: necrosis and apoptosis

Cells die either by necrosis or by apoptosis and as they do so they undergo many changes that ultimately result in a total loss of biological activity. Some of the earliest changes may be damaging but reversible and it is often difficult to determine the point beyond which recovery is no longer possible. These two distinct modes of cell death were initially characterised by light microscopy but can now also be studied by multiparameter flow cytometry. A wide range of different criteria have been used to distinguish 'live' from 'dead' cells and to determine whether cells are undergoing changes typical of apoptosis. Criteria for viability that can be monitored by fluorescence-based cytometry include loss of membrane integrity, esterase activity, transmembrane potential (which requires good membrane integrity) and ATP generation. Criteria for apoptosis include impaired membrane integrity, exposure of phosphatidylserine on the cell surface, loss of mitochondrial transmembrane potential, exposure of neoantigens on cytokeratins following caspase action and DNA strand breakage. When immunophenotyping cells, it is important to exclude dead cells from the analysis because they bind antibodies nonspecifically and may appear as a distinct subset of cells; this can cause the data to be wrongly interpreted. For this purpose, membrane integrity revealed by DNA staining is a reliable single-parameter method. However, if the main object of the study is to characterise cell death, it would be prudent to use multiple criteria. Several reagents and kits for monitoring viability and apoptosis are available commercially (Tables 3.6 and 3.7) (for reviews, see Defrancesco, 1997, 1999). The structures of some probes used for monitoring viability, oxidative metabolism and intracellular ion concentrations are given in Fig. 3.10.

3.10.1 Membrane integrity

Membrane integrity can be probed using dyes or fluorochrome-labelled antibodies that will react with internal cell components but are normally excluded from cells that have an intact membrane. DNA-binding dyes such as 7-AAD and PI were initially used to identify cells with damaged membranes but the newer DNA stains such as SYBR®-14, YOYO®-1 and YO-PRO™-1 (Molecular Probes) can also be used. An alternative strategy is to use dyes that enter but do not diffuse out of live cells. These are often supplied in the form of acetoxy-methyl (AM) esters; these can be hydrolysed by ubiquitous nonspecific esterases to yield the fluorescent dye, which remains trapped within the cell. The AM esters are poorly soluble in water, so they are normally dissolved in dimethylsulphoxide as a 1–10 mmol l^{-1} stock solution and added to the medium at concentrations in the range 1–25 μmol l^{-1}. At 37°C, uptake and hydrolysis of the AM ester is fairly rapid, resulting in intracellular dye concentrations of >25 μmol l^{-1} within 10 to 60 min (Haugland, 1994). Examples detectable in the channel routinely used for detecting fluorescein include, fluorescein diacetate, 2',7'-bis(2-carboxyethyl)-5,6-carboxyfluorescein AM ester (BCECF-AM) (Fig. 3.10A), carboxyfluorescein diacetate and calcein-AM, which is probably the best because it is rapidly taken into cells and is better retained than the others. A similar dye, which can be monitored in the channel used routinely for PE, is Fura-Red. These dyes can also be used to load target cells for lymphocyte cytotoxicity assays.

Whenever it is necessary to label cells so that viability can be determined after fixation, cells can be incubated with ethidium monoazide, which does not cross intact membranes but will covalently link to any nucleic acid when photoactivated. Consequently, after photoactivation, only damaged cells will be labelled and fluoresce. An alternative is to treat samples with Tri-Color®-labelled streptavidin (streptavidin coupled to the tandem dye PE–Cy™5), which specifically and irreversibly enters dead cells and is not removed by washing, permeabilisation or fixation (Levelt and Eichman, 1994).

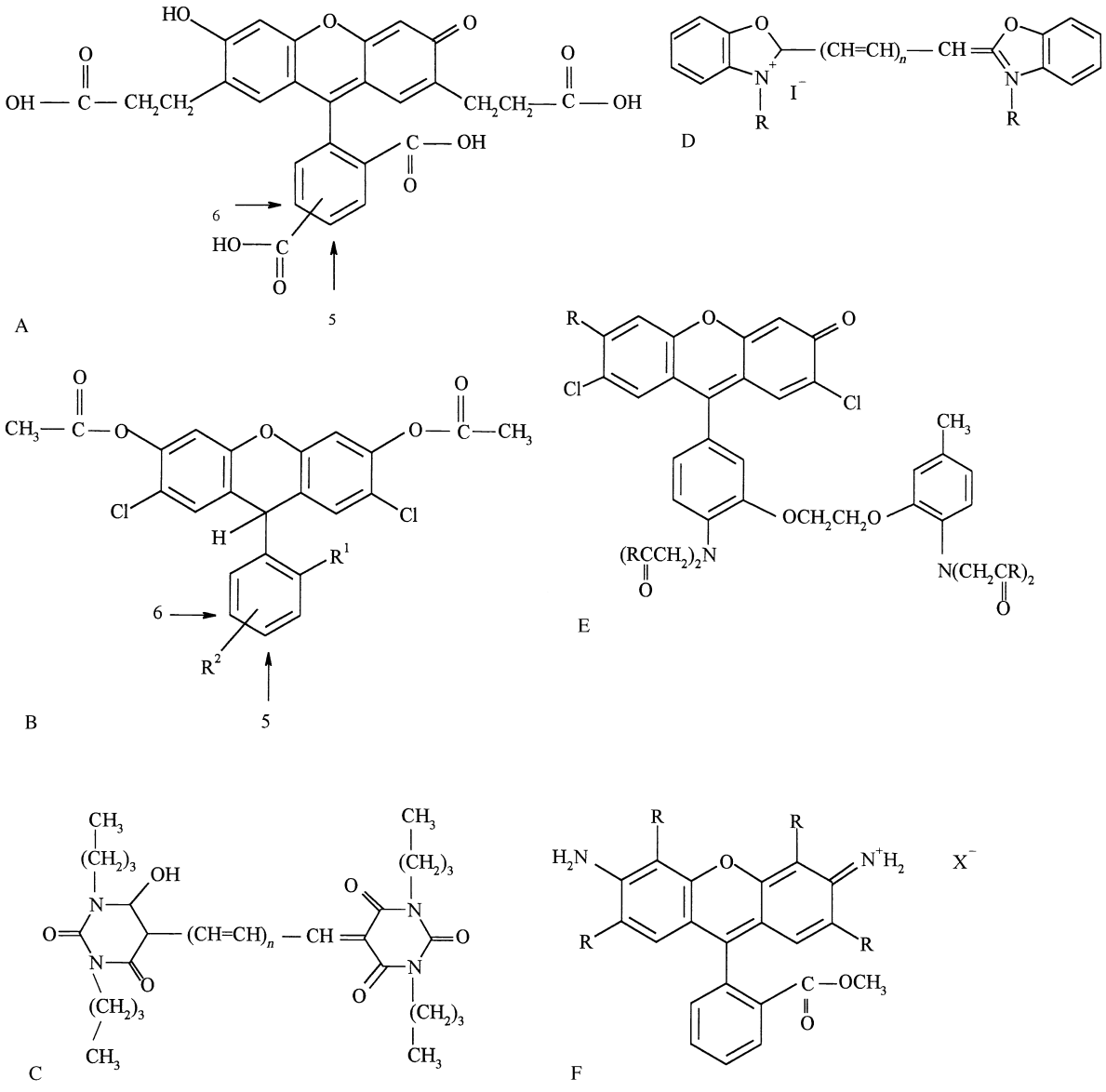

Fig. 3.10 Structures of some fluorescent functional probes. (A) 2',7'-Bis(carboxyethyl)-5-(and -6-)-carboxyfluorescein (mixed 5- and 6-isomers of BCECF), a pH-sensitive probe. (B) 5- (and 6-)-Carboxy-2',7'-dichlorodihydrofluorescein diacetate (mixed 5- and 6-isomers of carboxy-H_2DCFDA), a probe for intracellular oxidation that exhibits less leakage than DCFDA. (C) Bis-barbituric acid oxonols (DiBAC) are slow response membrane potential dyes: $n = 1$ in bis(1,3-dibutylbarbituric acid)trimethine oxonol ($DiBAC_4(3)$) and $n = 2$ in in bis(1,3-dibutylbarbituric acid)pentamethine oxonol $DiBAC_4(5)$. (D) Oxa carbocyanines (DiOC) are slow response membrane potential dyes: R = $-(CH_2)_4CH_3$ and $n = 1$ in 3,3'-dipentyloxacarbocyanine iodide ($DiOC_5(3)$); R = $((CH_2)_5CH_3$ and $n = 1$ in 3,3'-dihexyloxacarbocyanine iodide ($DiOC_6(3)$). (E) Fluo-3 is a cell-permeant Ca^{2+} indicator; R = O^- in Fluo-3, or (OCH_2COOCH_3 in Fluo-3 AM (Fluo-3 acetoxy-methyl ester). (F) rhodamine 123 is a mitochondrial transmembrane probe.

Table 3.6 *Viability reagents*

Supplier	Reagent	Assay principle
Molecular Probes	LIVE/DEAD Viability/Cytotoxicity Kit	Esterase action on calcein acetoxy-methyl ester and exclusion of ethidium homodimer I
Molecular Probes	LIVE/DEAD *Bac*Light Bacterial Viability Kit	SYBR® 9 and propidium iodide label live and dead bacteria, respectively

Table 3.7 *Apoptosis reagents*

Supplier	Reagent	Assay principle
Molecular Probes	YO-PRO™-1	Selective uptake by apoptotic cells
OncoImmunin	PhiPhiLux, CaspaLux	Profluorescent caspase substrates
Oncor	ApopTag® Plus In Situ Apoptosis Detection Kit	TUNEL assay
PharMingen	APO-BRDU™ and APO-DIRECT™ kits	TUNEL assay
R & D	Apoptosis detection kit	Annexin V binding
R & D	FlowTACS™	TUNEL assay
R & D/Trevigen	DePsipher™	Mitochondrial transmembrane potential
Roche/Boehringer-Mannheim	In Situ Cell Death Detection Kit	TUNEL assay
Roche/Boehringer-Mannheim	Annexin-V FLUOS Staining Kit	Annexin V binding and/or exclusion of propidium iodide

TUNEL, terminal deoxynucleotidyl transferase dUTP nick-end labelling.

3.10.2 Transmembrane potential

The interior of cells is electronegative relative to the exterior and because the two are separated by a membrane a measurable potential difference (usually around 0.07 V) exists. This transmembrane potential is created by concentration gradients of K^+, Na^+ and Cl^- across the cell membrane, which arise partly from the impermeability of the plasma membrane to ions and partly from the action of energy-dependent ion pumps located in the membrane. It is, therefore, a useful indicator of cell status and can be probed using dyes that redistribute across membranes. Cationic carbocyanine dyes, such as 3,3'-dihexyloxacarbocyanine iodide ($DiOC_6(3)$), are positively charged probes that bind readily to negatively charged cells. $DiOC_6(3)$ can be excited at 488 nm and its mean channel fluorescence, detectable in FL1, provides an indication of the transmembrane potential. The main disadvantage of $DiOC_6(3)$ is that it binds also to negatively charged mitochondria, which can affect the interpretation of results. Bis(1,3-diethyl barbituric acid trimethine oxonol ($DiBAC_4(3)$) is a anionic lipophilic dye that can be used similarly to $DiOC_6(3)$ but, because of its positive charge, does not bind to mitochondria and is, therefore, the better dye for measuring plasma membrane potential. Both rhodamine 123 and $DiBAC_4(3)$ have been widely used for measuring transmembrane potential in bacteria but $DiBAC_4(3)$ is probably preferable to $DiOC_6(3)$ for mammalian cells (Shapiro, 1994). Cells must be in protein-free media. Hyperpolarising and depolarising controls need to be incorporated and the optimum conditions for dye equilibration determined. A calibration curve constructed by establishing different membrane potentials using valincomycin (a potassium ionophore) and buffers of varying K^+ concentrations can be used to relate fluorescence intensity in an approximate way to the transmembrane potential (Tanner and Welhausen, 1998).

3.10.3 Apoptosis

Phosphatidylserine

The lipids in plasma membranes are distributed asymmetrically; consequently, in live cells phosphatidylserine occurs almost exclusively on the inner leaflet. An early event in apoptosis (which occurs after onset of chromatin condensation but before the loss of membrane integrity) is the loss of asymmetry and exposure of phosphatidylserine, to which annexin V, a Ca^{2+}-dependent phospholipid-binding protein will bind. Phosphatidylserine exposure also occurs during necrosis but two-colour staining, e.g. with PI for viability and FITC-conjugated annexin V, will distinguish between the two states.

Mitochondrial transmembrane potential and plasma membrane integrity

Rhodamine 123 is a cationic dye taken up by mitochondria and live cells that produces a strong green fluorescence. As cells enter the apoptotic pathway, they lose their mitochondrial transmembrane potential but their plasma membrane is still intact; therefore, they show diminished rhodamine 123 fluorescence but still exclude PI. Later on, they have no rhodamine 123 fluorescence and are unable to exclude PI. A variant of this strategy, which appears to be a more sensitive indicator of apoptosis, employs rhodamine 123 and EB (Ferlini et al., 1996).

DNA strand breakage

A characteristic feature of most apoptotic cells is cleavage of chromosomal DNA by an endonuclease at linker regions between nucleosomes. These strand breaks can be detected in several ways. If cells are fixed in alcohol or acetone, low-molecular-weight DNA fragments will be lost when the cells are washed, resulting in less DNA and hence DNA staining in apoptotic cells. Cells should not be fixed with formaldehyde because the resultant crosslinking prevents extraction of low-molecular-weight DNA. Strand breaks can also be detected by using the enzyme terminal deoxynucleotidyl transferase to label the 3'-OH ends of broken DNA strands directly by the addition of dUTP nucleotides that have been conjugated either to a fluorochrome or to another molecule (e.g. biotin or digoxigenin) that can act as a bridge to a fluorochrome (so-called, terminal deoxynucleotidyl transferase dUTP nick-end labelling, or TUNEL assay).

Caspase activation

The activity of certain caspases and other enzymes associated with the apoptotic pathway can be measured with substrate analogues that produce a fluorescent signal after enzymic conversion, e.g. CellProbe™ (Beckman Coulter) and PhiPhiLux (OncoImmunin) reagents.

3.11 Fluorescent dyes for the detection of intracellular ions

Fluorochromes are available for the intracellular estimation of pH and detection of several biologically important ions including Ca^{2+}, Mg^{2+}, Na^{+}, K^{+} and Cl^{-}. A requirement for these dyes is that they must bind the target ion stoichiometrically with a dissociation constant that is close to the expected intracellular ion concentration and, on binding, undergo a change in spectral properties that can be detected. Typically this can be an increase or decrease in quantum yield or a shift in the absorbance spectrum, with a concomitant shift in the emission spectrum. Only the smallest possible amount of dye must be used so as not to buffer the ion or sway normal cell function, yet it must be detectable by its fluorescence. Most ion-selective dyes are impermeant because they contain one or more carboxyl groups that are charged at pH 7.3, so they are most often introduced as cell-permeant lipophilic esters (which masks the charge), particularly AM esters. These are normally dissolved in dimethyl sulphoxide and added to the medium at concentrations in the range 1–10 μmol l^{-1}. Hydrolysis within the cell releases the ion-sensitive dye (Haugland, 1994).

3.11.1 Calcium concentrations

Calcium ions play a key regulatory role in eukaryotic

cells and very low cytoplasmic Ca^{2+} concentrations (100–150 nmol l^{-1} or ~10^{-7} mol l^{-1}) are maintained despite much higher external concentrations (1.3 mmol l^{-1} or ~10^{-3} mol l^{-1}). A rapid influx of Ca^{2+} into the cytosol from the exterior, or from internal stores (e.g. calciosomes or the sarcoplasmic reticulum), in response to external stimuli is an important means of transmitting signals across cell membranes. In this, Ca^{2+} can act as a second messenger, often aided in this role by binding to calmodulin, a ubiquitous eukaryotic Ca^{2+}-binding protein that undergoes a conformational change on binding Ca^{2+}; this enables it to participate in many different regulatory processes. Increases in cytoplasmic Ca^{2+} concentration are, therefore, one of the earliest indicators of cellular activation following signal transduction.

Two types of Ca^{2+} indicator dye are useful for cytometric studies; one undergoes a wavelength shift on binding Ca^{2+}, e.g. Indo-1 (excitation/emission maxima: in low Ca^{2+} 346/495 nm and in high Ca^{2+} 330/408 nm), and the other undergoes an increase in fluorescence intensity on binding Ca^{2+}, e.g. Fluo-3 (excitation/emission maxima 506/526 nm) and its analogues. Indo-1 fluorescence is best monitored using a ratio procedure: measurements are made on the same cell at the two different emission wavelengths. However, the fluorescence of Fluo-3, Fluo-4 and Fluo-5 can be monitored in a single channel. Fluo-4 has an increased excitation at 488 nm compared with Fluo-3, resulting in a stronger fluorescence signal. Fluo-5 is an analogue of Fluo-4 that has a lower binding affinity, making it more suitable for detecting Ca^{2+} concentrations in the 1 μmol l^{-1} to 1 mmol l^{-1} range, which would saturate Fluo-3 and Fluo-4. All are loaded into cells as their AM ester. The Ca^{2+} chelator ethyleneglycoltetraacetic acid (EGTA), which does not cross the plasma membrane, can be used to determine whether external Ca^{2+} is involved in a response. A calibration curve should be constructed in situ at the end of the experiment using a Ca^{2+} ionophore with Ca^{2+} concentrations set by a Ca^{2+} EGTA solution.

3.11.2 Intracellular pH values

Eukaryotic cells have a large negative potential (the transmembrane potential, see above) across their plasma membrane, which leads to the passive inward diffusion of H^+ and which, if uncontrolled, would result in conditions that were too acidic for the cell to function. Consequently the intracellular cytoplasmic pH (pH_i) of most cells is usually regulated to near neutral (~pH 7.2) by one or more types of Na^+-driven antiporters (Na^+–H^+ exchangers). These proteins located in the membrane use energy stored in the Na^+ gradient to export H^+, which has entered by diffusion or has been produced during metabolism. Flow cytometry has shown that there is a strong correlation between pH_i and cell proliferation, with pH_i being related to stages in the cell cycle in cells as diverse as yeasts and lymphocytes. In cultured mammalian cells, alkalinisation to pH_i values of 7.4–7.5 is linked to cell proliferation. Acidification to pH values of 7.1–7.2 is linked to quiescence or to pH 6.8 to decline. An approximately linear relationship has been observed between pH_i and growth rate, at least over the pH range 7.4–7.6 in both batch and continuous cultures.

All pH indicator probes are weak acids; therefore, their pK_a must be matched to the expected range of pH values to be measured. Three main pH indicator dyes are available: 2,3-dicyanohydroquinone (DCH), BCECF and carboxy-seminaphthorhodafluor (SNARF®-1). DCH has a pK_a of 8, an absorption maximum in the ultraviolet and a high leakage rate; for these reasons, it is not much used. BCECF, which permeates in its AM ester form, has a pK_a of 7, which makes it useful for measurements in the physiological range. Moreover, it is confined mostly to cytosol and is well retained, enabling measurements to be made over 1–2 h, if necessary. It has a relatively low quantum yield but its pH-dependent absorption maximum at 500 nm makes it easily excitable by a 488 nm argon laser. The intensity of its emission at 520 nm increases with pH and it is normally used by measuring the ratio of its fluorescence intensity at ~525 and >610 nm (FL1 and FL3 in a basic instrument), which circumvents potential variability ow-

ing to differences in dye loading or cell size. SNARF®-1 offers a number of avantages over BCECF and, loaded in its AM form, is now probably the most frequently used pH probe. Like BCECF, it can be excited at 488 nm, but it has greater pH-dependent changes in fluorescence intensity, which occur at two wavelengths. Increases in pH cause a decrease in emission intensity at ~575 nm and a concomitant increase at ~625 nm; therefore, ratio measurements at the two wavelengths give better sensitivity in the pH range 7.0 to 8.0 than can be obtained with BCECF. When using these probes, it is essential to establish the optimum conditions for dye loading and to construct a pH calibration curve using cells where the pH_i has been set using buffers of different pH values containing high K^+ concentrations and the ionophore nigericin, which exchanges K^+ for H^+ across membranes.

3.12 Probes for phagocytosis and oxidative metabolism

3.12.1 Phagocytosis

The phagocytic ability of cells, e.g. neutrophils, can be assessed in vivo using fluorochrome-labelled latex microspheres, bacteria, zymosan or yeasts, either alone or in conjunction with measurements of the oxidative burst. A number of different strategies have been used. Generally, fluorescent particles that have been opsonised with serum or specific IgG are mixed with blood, or with isolated leukocytes, in particle : cell ratios from 5 : 1 to 100 : 1 at 37°C. Samples are taken at a defined time(s), washed to remove unattached particles, resuspended and the fluorescence from internalised and adherent particles determined. If FITC-labelled bacteria have been used, then after the cells have been washed, EB (50 μg ml^{-1}), which binds to DNA, can be added. This will stain only the external (attached but not yet internalised) bacteria, because it cannot penetrate the phagocyte cell membrane. Phagocytic cells that have internalised bacteria have the fluorescence of the FITC-labelled bacteria and those to which bacteria are adhering fluoresce red, partly from fluorescence energy transfer from the FITC to the EB and partly from the fluorescence of the EB itself binding to the bacterial DNA. Other ways to discriminate adherent from internalised particles at the end of the assay include adding a dye such as trypan blue or crystal violet to the medium, which will quench fluorescence from the external but not the internal particles, or lowering the pH. In the dye-quenching procedure, duplicate samples with and without the quenching dye are analysed; in the absence of the dye, fluorescence results from internalised and adherent particles but in its presence it results only from internalised particles. However, neither procedure seems to give reproducible results. If it is necessary only to distinguish phagocytic from nonphagocytic cells, the size of the ingested particle is of little importance. If it is necessary to score the number of particles ingested, it is better to use small particles such as fluorescent microspheres. If large particles such as yeasts are used, it is not usually possible to determine how many particles each cell has ingested, but microspheres give sharper peaks in histograms of fluorescence intensity, corresponding to cells that have ingested one, two, three etc. particles. Microspheres (0.5–2.0 μm), bacteria, such as *Escherichia coli* and *Staphylococcus aureus*, and zymosan can be obtained ready labelled with a number of different fluorochromes from commercial sources (e.g. Molecular Probes). A complete diagnostic reagent kit based on FITC-labelled *E. coli* can be obtained commercially (e.g. Phagotest® from Orpegen Pharma; Vibrant™ from Molecular Probes).

3.12.2 Oxidative metabolism

The intracellular production of oxidants can be detected using several different dyes including, 2',7'-dichlorodihydrofluorescin diacetate (H_2DCFH-DA), carboxy-H_2DFCDA, dihydroethidium (Hydroethidine™; Prescott Labs) and dihydrorhodamine 123, all of which are nonfluorescent cell-permeant precursors that are converted to a fluorescent form on oxidation. H_2DCFH-DA is converted by esterases

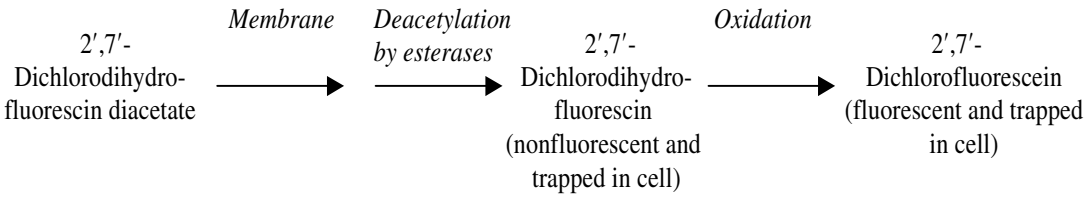

Fig. 3.11 Uptake and conversion of 2',7'-dichlorodihydrofluorescin diacetate to 2',7'-dichlorodihydrofluoresin (nonfluorescent) and its subsequent oxidation within the cell to 2',7'-dichlorofluorescein (fluorescent).

to 2',7'-dichlorofluorescin (DCFH) which is nonfluorescent but retained in the cell. This is then further converted by H_2O_2 together with peroxidases and superoxide (O_2^-) produced during the respiratory burst to 2',7'-dichlorofluorescein (DCF), which is fluorescent and also well retained in cells (Fig. 3.11). DCFH can also be oxidised by nitric oxide as well as by H_2O^2 and O_2^-; this is not usually a problem when measuring the oxidative burst in neutrophils because they have little L-arginine. If used in conjunction with inhibitors of the oxidative burst (e.g. diphenylene iodinium), H_2DCFH-DA can be used to study nitric oxide production in monocytes. A new dye, 1,2-diaminoanthroquinone (Molecular Probes), is nonfluorescent until it reacts with nitric oxide, when it produces a red fluorescent precipitate that may be used to detect nitric oxide production directly in vivo (see Ch. 7).

Hydroethidine is produced from EB by reduction with sodium borohydride; it enters cells freely and, on oxidation, gives EB, which intercalates into DNA and fluoresces in the red. Cells are normally labelled with hydroethidine for 10 min at 37°C and then exposed to a stimulus that will provoke a respiratory burst while the fluorescence of EB is being monitored. If required, the H_2DCFH-DA and hydroethidine assays can be run simultaneously.

Currently the oxidation of nonfluorescent dihydrorhodamine 123 to rhodamine 123 by H_2O_2 and peroxidases is probably the most sensitive technique for detecting the respiratory burst because the product is positively charged and accumulates in mitochondria. A diagnostic reagent kit based on unlabelled *E. coli* and dihydrorhodamine 123 as the fluorogenic substrate (Phagoburst®) is obtainable from Orpegen Pharma.

An interesting development is the Fc OxyBURST® reagents (Molecular Probes) which comprise complexes of bovine serum albumin (BSA) and anti-BSA covalently coupled to H_2DCFH-DA. After binding to cellular Fc receptors, the immune complexes are internalised and the nonfluorescent DCFH is oxidised by the respiratory burst to fluorescent DCF. As, unlike H_2DCFH-DA, the dye does not need to be first processed by intracellular esterases, it is useful for monitoring phagocytosis by monocytes or other cells that have only low esterase activity.

3.13 Fluorochrome-labelled substrate analogues for measuring enzyme activity

Enzymes are key cellular components; the presence or absence of an enzyme and the level of its activity are frequently dependent on cell type, differentiation stage and/or the functional status of a cell. Esterase and/or peroxidase activity has long been monitored by absorbance in conventional hematology analysis as a means of distinguishing leukocyte classes. This principle has been extended by using substrate analogues that enter live cells freely and are converted enzymically into a fluorescent form that is retained in the cell. In this way, enzyme activity can be monitored by flow cytometry, a technique named 'cytoenzymology' by Beckman Coulter. By using these probes in conjunction with immunolabelling of cell surface markers, various cell types and subsets can be more fully characterised.

Enzyme activities for which suitable probes are available include microsomal dealkylases, β-galactosidase, β-glucuronidase, glycosidases, peptidases, peroxidases and several caspases. The techniques are applicable to isolated cells, cells in whole blood and microorganisms, but it is essential that cells are live before analysis. Commercially available reagents include the CellProbe™ range (Beckman Coulter, Inc.), the PhiPhiLux resonance energy transfer-based peptide analogues for caspases (OncoImmunin, Inc.), and the diverse range of substrates produced by Molecular Probes.

3.14 Fluorescent ligands

Ligands other than antibodies can be fluorochrome labelled and used to detect or sort cells, or to probe aspects of cell function (McGrath et al., 1996). Some fluorochrome-labelled ligands of surface receptors, e.g. *N*-formylmethionyl leucyl phenylalanine (Molecular Probes) and many cytokines are obtainable commercially. The use of fluorescent ligands should allow the time course of binding (see Section 18.7.1) and the relative affinity and number of receptors per cell to be determined under different conditions. For instance, the occurrence of cytokine receptors has been detected with biotin- or PE-labelled cytokines. Ligand-based staining of cytokine receptors can be compatible with simultaneous immunofluorescence staining of surface antigens such as CD4 or CD8, enabling receptor expression on lymphocyte subsets to be determined. Reagent kits for staining cytokine receptors are available commercially, e.g. Fluorokine™ (R & D Systems).

Several fluorescent ligands able to bind to components of the cytoskeleton can also be obtained commercially. Phalloidin and phallacidin are available conjugated to coumarin, fluorescein, BODIPY® FL, Oregon Green™ 488, and rhodamine, as well as to biotin (Molecular Probes). Fluorescent phallotoxins can be used to detect filamentous actin (F-actin); they bind well to large and small F-actin polymers but not to monomeric G-actin. Fluorescence intensity is proportional to the F-actin content of cells. Other examples include recombinant chitin-binding proteins conjugated to fluorescein *N*-hydroxysuccinimide for the detection of bacteria, *Candida albicans* and other fungi, including yeasts and spores (e.g. Bacterase™, Candidase™ and Fungalase™ from Anomeric™ Inc.). Many of these ligands were developed for use originally in fluorescence microscopy but could also be useful for flow and laser scanning cytometry studies.

3.15 Fluorescent dyes for measuring total protein

Total protein content can be estimated using a number of acidic dyes that bind ionically or can attach covalently to positively charged groups on proteins. These dyes react mainly with amino groups and consequently can bind to materials other than proteins. When used in conjunction with DNA stains, they can be useful for measuring growth and metabolism in heterogeneous populations. For example, FITC will bind covalently to proteins and remains attached after washing and sulphorhodamine 101, available as FluoReporter® Fluorometric Cell Protein Assay Kit (Molecular Probes), forms electrostatically stable complexes at low pH values, which can be assayed flow cytometrically.

3.16 Autofluorescence

Although it has long been known that the bright autofluorescence of eosinophils (resulting from their cytoplasmic granules) allows them to be distinguished from other leukocytes, there have been relatively few studies of natural fluorescence of blood cells. A notable exception being the measurement of reduced nicotinamide adenine dinucleotide phosphate (NADPH) fluorescence to monitor the respiratory burst in neutrophils. The excitation and emission spectra of the various blood leukocytes is largely similar but there are marked differences in relative fluorescence intensities

(Monici et al., 1995). In mammalian cells, intrinsic fluorescence in the visible range arises mainly from the pyridine and flavin nucleotides, flavin adenine dinucleotide (FAD) and riboflavin mononucleotide (FMN) (excitation/emission maxima 455/515 nm) and reduced nicotinamide adenine dinucleotide (NADH) (excitation/emission maxima 340/455 nm), although some cells will also contain porphyrins, including hemoglobin, which absorb in the ultraviolet to blue region ($<$ 430 nm) and fluoresce in the orange to red 570–660 nm. When excited by light at 488 nm, the autofluorescent emission at ~530 nm from unstained lymphocytes is equivalent in intensity to that of cells which have bound ~10 000 molecules of a fluoresceinated antibody; it is autofluorescence that ultimately limits the sensitivity of detection by fluorescein. If problems of autofluorescence are encountered, they are probably best avoided by using probes that can be excited at wavelengths $>$600 nm.

3.17 FURTHER READING

Brand, L., Johnson, M.L. (eds.) (1997) *Methods in Enzymology,* Vol. 278: *Fluorescence Spectroscopy*. Academic Press, New York.

Dewey, T.G. (1991) *Biophysical and Biochemical Aspects of Fluorescence*, Plenum Press, New York.

Mason, W.T. (ed.) (1999) *Fluorescent and Luminescent Probes for Biological Activity*, 2nd edn. Academic Press, New York.

Robinson, J.P. (ed.) (1997) *Current Protocols in Cytometry*, Wiley, New York.

3.18 INTERNET SITES

http://www.drmr.com/abcon.html

Protocols for the conjugation of antibodies with the more frequently used fluorochromes (by M. Roederer).

http://www.drmr.com/compensation.html

Procedures for setting compensation for three- and four-colour flow cytometric analysis (by M. Roederer).

http://www.cyto.purdue.edu/flowcyt/research/cytotech/amfc/data/page9.html

A multiparameter approach to immunophenotyping: a discussion of the choice of fluorochromes and of procedures for setting compensation for two-, three- and four-colour flow cytometric analysis (by C. Ortolani).

http://www.probes.com

The Molecular Probes website containing the latest electronic version of their *Handbook of Fluorescent Probes and Research Chemicals* together with product information sheets, technical bulletins, materials safety data sheets, bibliographies and search facilities.

http://fluorescence.bio-rad.com

The Bio-Rad fluorescence database, where you can obtain plots of excitation and emmision spectra and overlay these with filter data curves and laser lines.

3.19 REFERENCES

Bagwell, C.B., Adams, E.G. (1990) Fluorescence spectral overlap compensation for any number of flow cytometry parameters. *Annals of the New York Academy of Sciences* **677**, 167–84.

Cantor, C.R., Schimmel, P.R. (1980) *Biophysical Chemistry* Part 2, pp. 433–465. Freeman, London.

Defrancesco, L. (1997) The death of a cell: a profile of apoptosis kits and reagents. *Scientist* **11**, 22–6.

Defrancesco, L. (1999) Dead again: adventures in apoptosis. *Scientist* **13**, 17–21.

Ferlini, C., Di Cesare, S., Rainaldi, G., Malorni, W., Samoggia, P., Biselli, R., Fattorossi A. (1996) Flow cytometric analysis of the early phases of apoptosis by cellular and nuclear techniques. *Cytometry* **24**, 106–15.

Forster, T. (1959) Transfer mechanisms of electronic excitation. *Discussions of the Faraday Society* **27**, 7–17.

Haugland, R.P. (1994) Spectra of fluorescent dyes used in flow cytometry. In: *Methods in Cell Biology,* Vol. 42, Part B, 2nd edn, pp. 641–63. Academic Press, New York.

Haugland, R.P. (1995) Coupling of monoclonal antibodies with fluophores. In: Davis, W.C. (ed.), *Methods in Molecular Biology*, Vol. 45, *Monoclonal Antibody Protocols,* pp. 205–11. Humana Press, Totowa, NJ.

Haugland, R.P. (1996) Handbook of fluorescent probes and research chemicals 6th edn. Molecular Probes, Eugene, OR.

Haugland, R.P., You, W.W. (1995) Coupling of monoclonal antibodies with biotin. In: Davis, W.C. (ed.), *Methods in Molecular Biology,* Vol. 45, *Monoclonal Antibody Protocols,* pp. 223–33. Humana Press, Totowa, NJ.

Lanier, L.L., Recktenwald, D.J. (1991) Multicolor immunofluorescence and flow cytometry methods. *Companion to Methods in Enzymology*, **2**, 192–9.

Latt, S.A., Langlois, R.G. (1990) Fluorescent probes of DNA

microstructure and DNA synthesis In: Melamed, M.R., Lindmo, T., Mendelsohn, M.I. (eds.), *Flow Cytometry and Sorting,* 2nd edn, pp. 249–290, Wiley-Liss, New York.

Levelt, C.N., Eichmann, K. (1994) Streptavidin–Tri-Color is a reliable marker for nonviable cells subjected to permeabilization or fixation. *Cytometry* **15**, 84–6.

Mason, W.T. (ed.) (1999) *Fluorescent and Luminescent Probes for Biological Activity,* 2nd edn, Academic Press, New York.

McGrath, J.C., Arribas, S., Daly, C.J. (1996) Fluorescent ligands for the study of receptors. *Trends in Pharmacological Sciences* **17**, 393–9.

Monici, M., Pratesi, R., Bernabei, P.A., Caporale, R., Ferrini, P.R., Croce, A.C., Balzarini, P., Bottiroli, G. (1995) Natural fluorescence of white blood cells: spectroscopic and imaging study. *Journal of Photochemistry and Photobiology B: Biology* **30**, 29–37.

Nguyen, D.C., Keller, R.A., Jett, J.H., Martin, J.C. (1987) Detection of single molecules of phycoerythrin in hydrodynamically focused flows by laser induced fluorescence. *Analytical Chemistry* **59**, 2158–2202.

Roederer, M. (1999) Compensation: the gruesome details (online). Available: http://www.drmr.com/compensation.html [Accessed 2000 February 3].

Shapiro, H.M. (1994) *Practical Flow Cytometry,* 3rd edn, pp. 307–8, Wiley-Liss, New York.

Smith, P.J., Wiltshire, M., Davies, S., Patterson, L.H., Hoy, T. (1999) A novel cell permeant and far red-fluorescing DNA probe, DRAQ5, for blood cell discrimination by flow cytometry. *Journal of Immunological Methods* **229**, 131–9.

Tanner, M.K., Wellhausen, S.R. (1998) Flow cytometric detection of fluorescent redistributional dyes for measurement of cell transmembrane potential. In: Jaroszeski, M.J., Heller, R. (eds.), *Methods in Molecular Biology,* Vol. 91 pp. 85–95, Humana Press, Totowa, NJ.

Waggoner, A.S. (1990) Fluorescent probes for cytometry. In: Melamed, M.R., Lindmo, T., Mendelsohn, M.L. (eds.), *Flow Cytometry and Sorting,* 2nd edn, pp. 209–15. Wiley-Liss, New York.

4

Quality control in flow cytometry

David Barnett and John T. Reilly

Royal Hallamshire Hospital, Sheffield

4.1 Introduction

Flow cytometry, during the 1990s has become an integral part of diagnostic pathology. Indeed, many pathology laboratories currently use flow cytometry routinely to provide diagnostic and therapeutic support for clinicians treating a wide variety of malignant and nonmalignant disorders. Leukaemia immunophenotyping and the monitoring of lymphocyte subset counts are two of the most common uses, while flow cytometry is being increasingly used to determine the optimum time for peripheral blood stem cell (PBSC) harvesting, as well as for leukocyte and reticulocyte counting, platelet analysis (e.g. Bernard–Soulier and Glanzmann's syndrome) and red cell analysis (e.g. paroxysmal nocturnal hemoglobinuria and feto–maternal hemorrhage). In the twenty-first century, the flow cytometer is poised to revolutionise DNA and RNA molecular analysis through technologies such as multiplexing. The need to have instrument and methodological quality control procedures in place has become paramount as the use of the flow cytometer increases in the clinical setting. These procedures must be used in such a manner that they underpin the quality of results generated and should be performed frequently enough to identify problem areas. Consequently, it is essential to have both internal quality control (IQC) and external quality assessment (EQA) procedures in place. This chapter will focus on the current issues of IQC and EQA and highlight problems that may manifest during flow cytometric procedures.

4.2 Internal quality control

IQC can be defined as a set of procedures that monitor the instrument, analytical method and operator performance, as well as validating the reports generated. Such procedures are generally performed on a frequent enough basis to ensure that drift, or bias, can be detected and they should be supported by fully documented standard operating procedures. IQC should be one of the first areas to be investigated once problems arise and may provide vital clues as to the underlying error. All staff should be made familiar with the procedures involved for IQC. The following section highlights key areas.

4.3 Instrument quality control

Flow cytometry in the past generally required highly trained individuals. However, the introduction of bench-top flow cytometers into clinical laboratories has resulted in the involvement of more junior staff, while many hospitals rotate laboratory staff on a regular basis. Therefore, the use of a properly controlled flow cytometer will provide additional confidence to individuals undergoing training. Instrument control procedures should involve daily calibration or, at the very least, every time the instrument is switched on. Simple protocols are available to assist the monitoring of the laser, fluidics and optics.

Daily calibration is usually performed using commercially available latex beads and biological controls that will allow the operator to monitor: (i) light

Table 4.1 *Physical characteristics of various bead standards for instrument set up, calibration and antibody binding*

Characteristic and use	Type 0	Type I (alignment)		Type II (reference)			Type III (calibration)		
	Certified blank	Ia	Ib	IIa	IIb	IIc	IIIa	IIIb	IIIc
Size relative to lymphocytes	Equal	Smaller	Equal	Equal	Equal	Equal	Equal	Equal	Equal
Population coefficient of variation $< 2\%$	No	Yes	Yes	No	No	No	No	No	No
Instrument alignment	No	Good	Good	Poor	No	No	Poor	No	No
Instrument compensation	No	No	No	No	Poor	Good	No	Poor	Good
Instrument linearity	No	No	No	No	No	Yes	No	No	No
Antibody binding capacity	No	No	No	No	No	Yes	No	No	Yes
Fluorescence intensity	Very low	Very bright	Very bright	Bright	Bright	Bright (after antibody labelling)	Dim-bright	Dim-bright	Dim-bright
Number of fluorescence intensity levels	One	One	One	One	One	One	Multiple	Multiple	Multiple

See text for the basis of the categorisation.
From Schwartz et al., 1998.

scatter and fluorescence peak channel coefficients of variation (CVs), (ii) light and fluorescence peak channel drift, and (iii) instrument sensitivity and the facilitation of compensation set-up to adjust for spectral overlap. Furthermore, biological controls, particularly those that are 'full process' controls, will assist both in the training of staff and the monitoring of the staining process. For instrument control, several types of bead standard are available: (i) blank beads (type 0), (ii) alignment (type I) beads, (iii) reference beads (type II), (iv) compensation beads (type II/III) and (v) calibration and antibody-binding beads (type III) (see Table 4.1, which is based on work by Schwartz et al. (1998)). The three major categories established by Schwartz et al. (1998) (type I, alignment; type II, reference; and type III, calibration) are further subdivided according to whether the beads are the same size or smaller than cells (types Ib and Ia, respectively), whether their excitation and emission spectra does (types IIa and IIIa), or does not (types IIb and IIIb), match those of the sample, and whether they have antibody-binding capacity (types IIc and IIIc). These authors also provide a convenient list of the various types of standard that are available from the major suppliers for instrument set-up and calibration.

4.3.1 Type 0 beads

Type 0 beads are certified blank and have a size similar to that of lymphocytes but with a broad CV ($> 2\%$). The fluorescence intensity is lower than the

autofluorescence of labelled cells and so is used to establish the 'noise level' in conjunction with antibody-binding or calibration standards.

4.3.2 Alignment standards (type Ia and Ib)

Type Ia and Ib beads are either the same size or smaller than cells and facilitate the verification of fluidic and optical alignment. They are a single uniform population and generate CV values of $< 2\%$. The fluorescent intensity is usually very bright and generally it does not match that of the tested samples. Type I beads have limited value for the bench top flow cytometer, since the manufacturer will have set the alignment of such instruments, but have an important role in the manual alignment of the larger cell sorters. When used on a daily basis to monitor the peak channel of detection, as well as the CV of light scatter and fluorescence parameters, specific information can be obtained that will alert the operator to potential problems in these areas.

4.3.3 Reference standards (type IIa–c)

Type II beads are usually used to establish photomultiplier tube (PMT) settings and can also be used to establish compensation. Daily monitoring of the bead target channel value facilitates a consistency check. However, type II beads have recently been used to establish unified instrument set-up across different platforms and, in theory, to facilitate direct data comparison. Reference beads are homogeneous, with a fluorescence intensity similar to cells. However, they have broad CV ranges, a fact that precludes their use for alignment purposes. It should be noted that, as with alignment beads, the emission spectrum does not usually match that of the samples.

4.3.4 Calibration standards (type IIIa–c)

Type III beads are required to check the linearity, sensitivity and detection levels of each PMT and generally have a size and fluorescence intensity similar to stained cells. However, the emission spectra may not necessarily match that of samples and may not respond to microenvironmental changes. In addition, type III beads can be used to determine antigen density, by using either beads with predefined amounts of fluorochrome, enabling the fluorescence scale to be appropriately calibrated, or beads that specifically bind monoclonal antibody, which can then be used to calculate the amount of antibody bound to cells.

4.3.5 Biological controls

The final optimisation of the flow cytometer is best achieved using biological procedural controls. The use of assay calibration provides an important component of IQC and facilitates the monitoring of the relationship between measurement response and the 'known' value. Unfortunately, however, no universally accepted reference material exists. Nevertheless, several commercial products are available that provide the operator with target values to validate the operating system and methodology. It is important that such products are stable over time, are transportable and have matrix properties that resemble, as closely as possible, the samples under test. An important factor in quantitative assays is that procedural controls should reflect levels of the cell population under study. For example, if the laboratory routinely counts $CD34^+$ cells then the procedural control should have $CD34^+$ counts that reflect those usually encountered in clinical practice. In qualitative assays, the use of procedural controls should reflect the level of cellular antigen expression normally encountered. Most biological controls have an antigen density similar to that found on fresh specimens, although no procedural controls exist for leukaemia/lymphoma immunophenotyping as the diversity of such disorders makes the selection and preparation of controls difficult. However, within a given pathological specimen, several normal cell phenotypes may exist that could act as internal controls for the staining technique (Keeney et al., 1998b). Finally, the increasing importance of monitoring minimal residual disease in hematological malignancies has presented a new

challenge for IQC. It has been suggested that this may be overcome by spiking malignant cells with a unique phenotype (either antigen expression or antigen density) into a normal blood sample (San Miguel et al., 1997), although the concentration should reflect the detection limit, e.g. 1 malignant cell per 10^4 leukocytes.

Since the development of the first stable whole blood preparation in the mid-1990s (Barnett et al., 1996; Fay et al., 1994), a number of preparations are now commercially available that can be used as full process controls, permitting the use of lysing reagents and multiple colour staining, e.g. Absolute-Control (Ortho), CD-Chex and CD-Chex Plus™ (BD Biosciences), Fluoro-Trol™ (BioErgonomics), Immuno-Trol™ and Cyto-Trol™. (Beckman Coulter) and Status Flow (R&D). Fresh normal specimens, or cryopreserved cells, are not ideal as process controls because of individual variability, but they may be used for instrument set-up and for optimising compensation. However, even if stable biological controls are used, the final optimisation of the flow cytometer is best achieved using freshly stained biological material. A review of some of those currently available can be found in Bergeron et al. (1998).

4.3.6 Logging control data

It is essential that maximal use is made of the data generated by the above quality control materials. Data from beads and biological controls should be logged daily, together with instrument settings. It is important that all settings are re-established following a change in bead or biological control batch, or after an instrument service. The use of Levy–Jennings type plots will help highlight any potential instrument or methodological problem.

Time versus count and time versus fluorescence plots provide useful information when acquiring bead data, and it is important to compare histograms on successive days. Such data can assist in identifying errors that result from fluidic and/or optical problems, although, since these generate individual histograms, no Levy–Jennings type plots can be generated. Examples of using time as a parameter are shown in Fig. 4.1.

It is important, when performing IQC, to have procedures in place that facilitate the interpretation and troubleshooting of collected data. Unacceptability criteria should be established and remedial action taken if values lie outside established ranges. The use of Levy–Jennings type plots facilitates the visual identification of trends on a daily basis. Furthermore, it is important that there are procedures in place that allow the constant review of patient data (e.g. comparison of the previous CD4 counts) and that, within any immunophenotyping procedure, allow consistency checks (e.g. comparison of replicate CD3 values).

4.4 Quality control issues and pitfalls

Three areas in which problems occur in immunophenotyping are (i) specimen processing, (ii) data acquisition and (iii) data analysis/reporting.

4.4.1 Specimen processing

It is important that specimens are as fresh as possible (Ekong et al., 1993b), especially when undertaking antigen density quantification or cytoplasmic staining. Several guidelines have been published that address the issues of specimen integrity (Barnett et al., 1997; Borowitz et al., 1997; Nicholson, 1994; Sutherland et al., 1996). Correct handling and transportation procedures need to be established, while the choice of anticoagulant is important. K_3EDTA (ethylenediaminetetraacetic acid, tripotassium salt), for example, is preferred since it maintains the morphology and the flow cytometric profile of the cellular components (Barnett et al., 1997; Nicholson, 1994). Red cell lysis and cell separation procedures are frequent causes of analytical variation (Romeu et al., 1992). Unless exposure to lytic reagents is carefully controlled, changes in forward angle light scatter (FALS) and side angle light scatter (90°; SSC) patterns, quenching of fluorochromes (particularly if aldehyde-based lysis reagents are used) and selective cell loss may result. In contrast, poorly lysed specimens retain red cells, which may impair the identification of specific cell populations

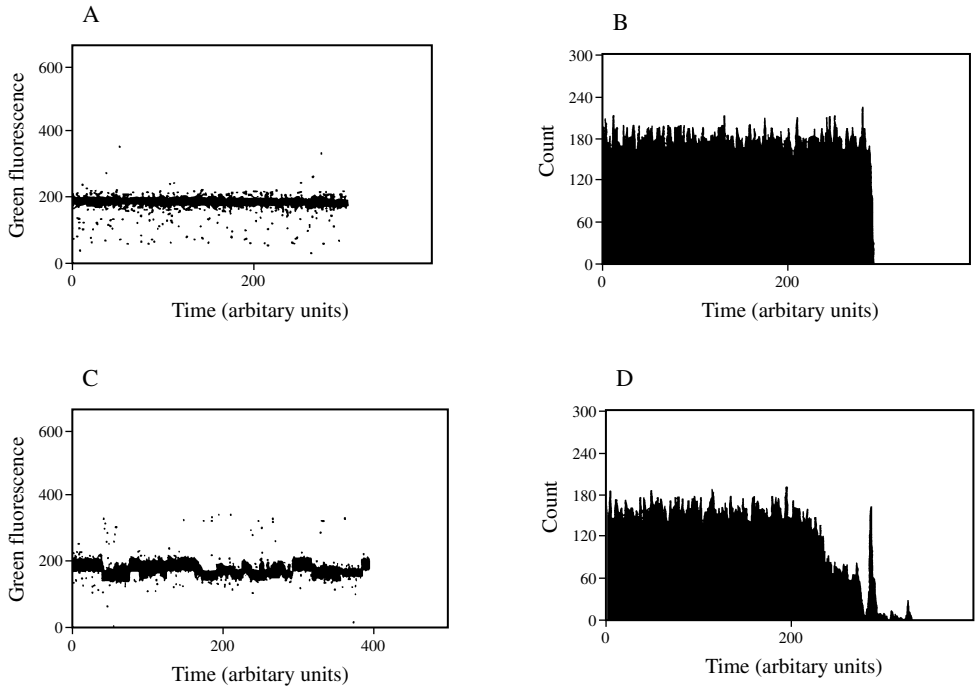

Fig. 4.1 Using time (in seconds) as a quality control parameter on a FACSCalibur™. The data were acquired using CellQuest and monitoring (A) Coulter Flow Check Fluorospheres normal laser pattern when bead fluorescence was plotted against time. Note the low coefficient of variation. (B) Normal fluidic pattern observed for beads acquired in (A) over the same time period. (C) Abnormal laser pattern seen using fluorescent beads. (D) Abnormal fluidic pattern observed when the flow cell is blocked.

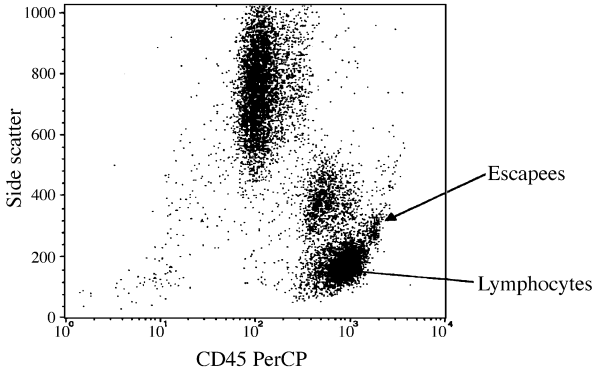

Fig. 4.2 Cells labelled with peridinin–chlorophyll *a* protein (PerCP)-conjugated CD45 displayed in a histogram of PerCP fluorescence versus side angle light scatter (SSC) showing lymphocyte escapees.

and produce tube-to-tube variation in forward and side scatter patterns, making consistent gate placement difficult. Inappropriate vortexing conditions may similarly lead to tube-to-tube variation. For example, samples treated too vigorously exhibit excessive cell debris or develop separation of granulocyte populations. Furthermore, under-vortexing may result in cell doublets, termed 'escapees', that will be excluded from routine gating strategies (Fig. 4.2) (Gratama et al., 1997a).

Centrifugation can be a major cause of cell loss and poor final sample preparation. Excessive centrifugation causes cell damage and alters the FALS and SSC characteristics, as well as increasing the level of cell debris, while cell loss may occur during the washing step if centrifugation is too gentle (J. Peel and D. Barnett, unpublished observation).

4.4.2 Data acquisition

The number of events acquired and the configuration of the instrument are two important variables influencing the reproducibility of results. The configuration and optimisation of the instrument has already been discussed, although final optimisation of the light scatter histograms may be required on an individual sample basis. The FALS versus SSC histogram should adjusted to facilitate the visualisation of all cell populations, with the lymphocyte population placed approximately midway along the *x*-axis. In addition, the negative cell population should be located within the first log decade when analysed on the fluorescence channel.

It is important that sufficient events are acquired to facilitate accurate identification of individual cell populations; for example, if a lymphoproliferative disorder is being analysed, at least 5000 lymphocyte events should be acquired, while $CD34^+$ stem cell enumeration requires a minimum of 100 $CD34^+$ events to ensure robust statistical analysis (Sutherland et al., 1996). In addition, recent $CD4^+$ T lymphocyte enumeration guidelines recommend the collection of at least 2500 lymphocyte events (Barnett et al., 1997), while 100 000 events should be analysed when detecting minimal residual disease.

4.4.3 Data analysis

A number of variables may affect data analysis: (i) the gating strategy and gate placement/analysis region used (Kromer and Grossmuller, 1994), (ii) the establishment of acceptability criteria, (iii) the use of automated gating, (iv) the use of quality control checks (within-assay replicates), (v) the cursor placement for isotype controls and (vi) the development of artefactual staining patterns.

In the late 1980s, the improvement in software, coupled with the discovery of additional fluorochromes, enabled $CD4^+$ T lymphocyte identification and characterisation by either light scatter gating procedures or differential staining with CD45 and CD14 (Loken et al., 1990). These approaches are now recognised to have several disadvantages. First, a FALS/SSC gate approach does not identify gate contaminants and may result in falsely low percentage values, while the need for larger panels (i.e. up to six tubes) increases analysis time, specimen handling and ultimately cost. Second, it is not possible to detect tube-to-tube variation when a light scatter gate is derived from CD45/CD14 'back-gating' and, in addition, the isotype control fails to control for CD45/CD14 staining. Therefore, it is recommended that $CD4^+$ T lymphocyte enumeration is performed using three-colour immunophenotyping using one of the three gating strategies highlighted below. A summary of the evolution of current gating techniques has been published (Mandy et al., 1997), while the advantages and disadvantages of each technique are detailed in the recently published British Committee for Standards in Hematology (BCSH) guidelines (Barnett et al., 1997).

The results issued from a laboratory will depend on the gating strategy employed. For example, when using the T-gating approach (Mandy et al., 1992), it is important that values for $CD4^+$ and $CD8^+$ T lymphocytes are expressed as a percentage of the total T lymphocyte population and not of the total lymphocyte population. The placement of the analysis region is a further factor for consideration. If the gate is too tight there is a possibility of excluding relevant cells, while an overgenerous gate will include contaminating cells and result in falsely low results (Kromer and Grossmuller, 1994). Failure to establish acceptability criteria can lead to the release of erroneous results. Recent guidelines for $CD4^+$ T lymphocyte enumeration have suggested that tube-to-tube variation for replicate antigens should be less than 3%, with monocyte contamination within a CD45/SSC gate being less than 5% and a 'lymphosum' (i.e. the sum of the percentages of the $CD3^+ + CD19^+ + NK$ cells (natural killer: $CD16^+$ and/or $CD56^+$ cells) being equal to $100 \pm 3\%$ (Barnett et al., 1997; Nicholson, 1994).

A similar evolution of gating strategies has occurred for $CD34^+$ stem cell enumeration, the most important being the Milan (Siena et al., 1991), Mulhouse (Bender et al., 1994), the Dutch Cooperative Study Group on Immunophenotyping of Hema-

tological Malignancies (SIHON) (Gratama et al., 1997b) and the International Society of Hematotherapy and Graft Engineering (ISHAGE) strategies (Sutherland et al., 1996).

The Milan protocol is the simplest, and involves the use of FALS and SSC to gate out red cells, debris and cell aggregates. The gated, nucleated cell population is then plotted on a histogram of CD34 fluorescence intensity versus SSC. Only $CD34^+$ events with low SSC are used to calculate the number of PBSC. The Mulhouse protocol is a logical development of the Milan protocol and uses $CD45^+$ events to identify the leukocytes. The latter are then plotted as CD34 versus SSC. Only $CD34^+$ events with low SSC are used to calculate the number of PBSCs, expressed as a percentage of $CD45^+$ cells. The SIHON approach incorporates a DNA/RNA laser-excited dye (LDS-751) to identify nucleated cells during data collection. In addition, by incorporating antibodies directed against CD14 and CD66e, monocytoid ($CD14^+$) and mature myeloid ($CD66e^+$) cells are excluded during list-mode data analysis since false-positive staining owing to F_c receptor-mediated monoclonal antibody binding will be eliminated. Finally, the ISHAGE approach takes advantage of the dim CD45 expression of $CD34^+$ stem cells with low SSC and incorporates a sequential gating strategy. Such a strategy has been adopted by the Stem Cell Enumeration Committee of ISHAGE (Sutherland et al., 1996) and is currently the most popular gating strategy in the UK (Barnett et al., 1998a).

A single-platform version of the ISHAGE protocol has been developed, termed 'Stem-Kit' (Coulter-Immunotech), in which a known concentration of micro-beads is added to a known amount of stained, lysed whole blood (Keeney et al., 1998a). The absolute $CD34^+$ cell count is calculated from the observed ratio between the number of counted beads and $CD34^+$ cells. Finally, a single-platform, software-driven method using a proprietary DNA/RNA stain to threshold on nucleated cells (ProCount kit, BD Biosciences) has been developed (Verwer and Ward, 1997).

In contrast to $CD4^+$ T lymphocyte enumeration, where it is accepted that CD45/SSC is the best gating strategy, it is unlikely that standardisation of $CD34^+$ PBSC enumeration will be achieved in the foreseeable future. As a result it has been suggested that 'the most effective approach to reducing inter-laboratory variation in CD34 enumeration consists of the adherence to consensus protocols formulated in general terms' (Gratama et al., 1998). These protocols, combined with real-time evaluation of performance by the organisations for EQA, will assist in ensuring that site-to-site interlaboratory variation is reduced. Indeed, an Australian study reported the results of a multicentre study to address these issues (Chang and Ma, 1996). The major methodological variations were the parameters used for gating $CD34^+$ cells and the denominator used for calculating the percentage of $CD34^+$ cells (i.e. of $CD45^+$ events or percentage of total nucleated cells). It was concluded that less than half of participating centres obtained reproducible results without standardisation and that, of the standardised protocols, the ISHAGE gating strategy was the most reproducible. Additional demands on quality control will occur in the future if quantification of $CD34^+$ cell subsets becomes routine because neutrophil and platelet recovery after transplantation appears to correlate best with $CD34^+/CD38^+$ and $CD34^+/CD41^+$ subsets, respectively (Feng et al., 1998; Novelli et al., 1998; Perey et al., 1998). The enumeration of $CD34^+$ subsets will require the incorporation of a third fluorochrome, increasing further the potential for interlaboratory variation. The findings from a study involving 24 European sites, currently being undertaken by the European Working Group for Clinical Cell Analysis, are awaited.

An additional factor that may influence data analysis is the isotype control. The value of isotype controls, however, has been questioned (Keeney et al., 1998b; O'Gorman and Thomas, 1999) and recent guidelines state that $CD4^+$ T lymphocyte and $CD34^+$ cell enumeration may be undertaken without isotype controls (Barnett et al., 1997; Sutherland et al., 1997). The situation with respect to leukaemia/lymphoma typing is unclear. However, it is important that isotype controls, if they are used, are matched

to the test antibody with respect to both fluorochrome and antibody concentration, and that the cursor is correctly placed during data analysis.

Finally, operators should be aware of the nature of false-positive staining reactions. These may occur through the nonspecific binding of antibody by F_c receptors, often observed with acute monoblastic leukaemias and from technical errors, for example the use of inappropriate antibody or the inclusion of dead cells in the analysis. Blocking the binding site, with a preincubation step using rabbit serum, can reduce nonspecific antibody binding via the F_c receptor. In addition, the identification of clonal B lymphocyte populations, by the demonstration of light chain restriction, may be masked by cytophilic antibody binding. This problem can be overcome if the immunoglobulin is removed by suspending and subsequently washing the cells in phosphate-buffered saline (PBS) at 37°C for 30 min. More recently, this approach has been applied to whole blood techniques with good effect. Briefly, 0.5 ml of whole blood is suspended in 9.5 ml of PBS at 37°C for 30 min, with gentle inversion of the tube every 10 min, followed by washing three times in PBS. Care is needed when removing the supernatant so as not to disturb the cell pellet, which is then resuspended in 0.5 ml PBS before analysis as for whole blood. In addition, artefactual double staining of T lymphocytes (i.e. $CD4^+CD8^+$) can occur in 17% of human immunodeficiency virus (HIV)-positive and 6% of normal individuals (Ekong et al., 1993a) and may be related to a plasma/serum factor that precipitates with ammonium sulphate.

Finally, inappropriate instrument set-up can be a source of erroneous results; this is usually attributed to inappropriate flow cytometric compensation (for further details see Owens and Loken, 1995).

4.5 External quality assessment

Despite the general acceptance and routine use of immunophenotypic analysis, EQA has only recently begun to address the important issues of quality control and standardisation in flow cytometry. Local, regional, national and international EQA schemes have now been established (Barnett et al., 1996, 1998a; Gratama et al., 1997b,c; Johnsen and Knudsen, 1996; Lowdell and Bainbridge, 1996; Lumley et al., 1996; Paxton et al., 1989). In principle, EQA is designed to test the whole analytical and reporting procedure and should be used by the laboratory to complement their IQC activities. The nature of EQA means that sample distribution, in most instances, is restricted to four to six times per year and, therefore, only provides a 'snapshot' of laboratory performance. Nevertheless, because EQA involves many laboratories, significant information can be obtained about the performance of specific instrumentation as well as about the effectiveness of specific reagents and methodological approaches. In addition, an individual laboratory performance can be compared over a period of time with a group using the same technique; this, in conjunction with IQC procedures, can be used to help to identify specific problem areas.

Participation in an EQA scheme is currently compulsory in some countries (e.g. USA and Canada) although it remains voluntary in most European countries. In the UK, the implementation of an accreditation process for clinical pathology laboratories (operated by Clinical Pathology Accreditation (UK) Ltd) has made the participation in an EQA scheme desirable. Such accreditation processes are also being applied to EQA schemes within the UK by Clinical Pathology Accreditation (UK) Ltd following the establishment of a clinical pathology accreditation EQA committee.

One of the prerequisites for an EQA scheme is that it should reflect, as closely as possible, the procedures and tests employed in the clinical laboratory. The materials issued should meet the same exacting standards encountered in IQC. Furthermore, while an EQA scheme should have the ability to identify specific problem areas it should also provide a strong educational element.

The following sections highlight three key problem areas supported by data from UK National External Quality Assessment Scheme (NEQAS) for leukocyte immunophenotyping (Barnett et al.,

1996, 1998a; Forrest and Barnett, 1989), namely (i) reagent selection, (ii) definition of the 'positive' value and, more recently, (iii) absolute count enumeration.

4.6 Reagent selection

The commercial availability of a large number of different specific monoclonal antibody reagents has made interlaboratory reproducibility, and hence EQA, difficult. A survey of routine UK laboratories in 1989 revealed a total of 86 antibodies being used as front-line reagents for leukaemia diagnosis. Furthermore, the use of monoclonal anti-myeloperoxidase antibody, one of the most informative reagents (Storr et al., 1990), was frequently omitted. The publication of the BCSH guidelines, which include recommended minimum antibody panels for acute and chronic leukaemia immunophenotyping (BCSH, 1994a,b), has resulted in a greater degree of standardisation within the UK. Similarly, a recent European consensus protocol has suggested practical two-colour reagent panels in an attempt to define a basis for cross-evaluation against the currently established laboratory protocols (Rothe and Schmitz, 1996). Many problems still remain, however, including the lack of standardisation of analysis techniques, and the use of different antibody sources, antibody dilutions, fluorochrome conjugates and lysing and fixation reagents.

4.6.1 Monoclonal antibody clones

Different clones of monoclonal antibodies, directed against the same cluster of differentiation, may vary in their ability to detect the corresponding antigen on leukaemic cells. For example, detection of the expression of CD34, a membrane-associated glycoprotein found on pluripotential stem cells, lineage-committed hematopoietic progenitors and some mature populations of both endothelial and stromal lineage (Civin et al., 1989; Simmons and Torok-Storb, 1991; Terstappen et al., 1993), may be dependent on the choice of reagent. It has been found that CD34 monoclonal antibodies react with different sites on the CD34 antigen (at least three as defined by their sensitivity to neurominidase) and, as a result, have different binding properties (Civin et al., 1989; Sutherland and Keating, 1992; Sutherland et al., 1992). The epitope recognised by B13C5 is sialic acid dependent, in contrast to that recognised by ICH3. Therefore, it is not surprising that different antibodies vary in their estimation of CD34 estimation and in their sensitivity in identifying circulating hematopoietic progenitors (Siena et al., 1991; Titley et al., 1997). Indeed, such differences in epitope sensitivity could partly explain the conflicting data on the prognostic significance of $CD34^+$ cells in acute myeloid leukaemia (AML). For example, several reports have correlated $CD34^+$ in patients with AML with the failure to achieve complete remission and a shorter overall survival (Campos et al., 1989; Geller et al., 1990), whereas others, using a different clone, have not (Selleri et al., 1991). The UK NEQAS for leukocyte immunophenotyping has supportive data for an epitope effect; in a patient with AML (AML M1) 70% of laboratories using TüK3 obtained $> 20\%$ positive blast cells whereas only 10% of laboratories using alternative clones returned a value of $> 20\%$.

The use of different panels and even clones of monoclonal antibodies may account for the wide variation in incidence reported for myeloid antigen expression in acute and chronic lymphoproliferative disorders. The coexpression of myeloid- and lymphoid-associated antigens in childhood acute lymphoblastic leukaemia is well described, although the incidence of aberrant expression ranges from less than 5% to over 30% (Basso et al., 1992; Cantú-Rajnoldi et al., 1991). This discrepancy can be partly explained by the use of different panels of monoclonal antibodies, but significant differences still occur when comparing antibodies to the same CD antigen. For example, in two studies, the incidence of patients expressing CD13 and/or CD33 was 4% and 16%, respectively (Fink et al., 1993; Piu et al., 1991). In addition, the expression of myeloid antigens has been reported to be of prognostic importance by some (Basso et al.,

1992) but not all groups (Piu et al., 1990). Interestingly, a further study (Howard et al., 1994) noted that the detection of myeloid antigens in childhood acute lymphoblastic leukaemia was dependent, in part, on the commercial source of antibody. Similar conflicting data have been reported for CD13 and CD33 expression in B-cell chronic lymphocytic leukaemia (Molica et al., 1991; Polliack et al., 1993). Furthermore, CD14 was not detected by Polliack and colleagues (1993) while others have described between 29 and 84% of patients who were positive (Molica et al., 1991; Morabito et al., 1987). Interestingly, Pinto and colleagues (1992) demonstrated that the CD14 epitope is only detected with the My-4 antibody and not by other CD14 antibodies. We have reported similar findings in chronic lymphatic leukaemia, where CD13 and CD33 were only detected using a particular reagent (Reilly et al., 1995).

4.6.2 Fluorochrome conjugates

It is important that the correct choice of fluorochrome-conjugated antibody is made. For example, it has been reported that cells directly labelled with fluorescein isothiocyanate (FITC)-conjugated antibodies will not be as bright as those stained using indirect FITC methods and that this decreased sensitivity may be in the order of five- to sixfold (Shapiro, 1994). This is of practical importance when antigen expression is low. Phycoerythrin (PE) and the newer fluorochromes (e.g. tandem colour fluorochromes) have a much higher quantum yield than FITC, thus increasing sensitivity. As a result, statistically significant differences have been documented between samples analysed with FITC- and PE-conjugated antibodies for the following antigens: CD3, CD5, CD13, CD14, CD33 (Reilly et al., 1995; Reilly, 1996). In a UK NEQAS survey investigating CD13 detection for example, 8 of 24 laboratories that used FITC-conjugated antibodies obtained values of less than 50% (overall 58%); three of these eight recorded negative results. In contrast, all 12 laboratories using PE-conjugated reagents obtained values greater than 50% (mean 77%). Therefore, PE conjugates, or tandem colour fluorochromes (e.g. PE–Cyanin™ 5), should be used for single-colour analysis. In multicolour analysis, the more sensitive fluorochrome-conjugated antibody should be used for detecting the weaker antigen, typically CD13, CD19 and CD33, while strongly expressed antigens (e.g. CD45 or HLA-DR) can be detected using FITC or peridinin–chlorophyll *a* complex protein (PerCP). In addition, steric hindrance, resulting from the simultaneous binding of different monoclonal antibodies, should always be considered when selecting reagent combinations (e.g. CD3 and the T-cell receptor complex). We have recently shown that, when performing antigen density measurements, the use of single-colour staining will give markedly different results from those derived using multicolour staining (Barnett et al., 1998b).

Finally, the development of additional fluorochromes that can be detected with a single laser, and the availability of computer software capable of rapid data analysis, has enabled the incorporation of triple-colour analysis in the routine diagnostic laboratory (Campana, 1994). This will lead to further technical problems, including more complicated spectral compensation, as well as the need for added expertise in instrument set-up, data collection and analysis.

4.7 Definition of positive values

Data from UK NEQAS, together with a review of the literature, have demonstrated considerable differences in the definition of antigen positivity. The development of newer and more sensitive fluorochromes, coupled with multiparametric technology, will further increase this dilemma. The simplistic approach using an arbitrary cut-off point (for example $> 10\%$ for immunocytochemistry, $> 20\%$ for immunofluorescence analyses), as suggested in the BCSH Guidelines (BCSH, 1994a), will probably not be applicable in the future. Data analysis procedures that currently employ the placement of a cursor at the boundary of the negative population

are likely to be inappropriate. More biologically relevant procedures, such as antigen density quantification, may yield more meaningful information. Such evaluations would require the production of reference materials that express the antigens of clinical importance. Developments in this area are underway (Barnett et al., 1996, 1998b), although the technical difficulties should not be underestimated, especially for pathological preparations.

4.8 Absolute count enumeration

The enumeration of absolute $CD4^+$ T lymphocyte and $CD34^+$ hematopoietic stem cells is important for the clinical management of HIV-infected individuals and for cancer patients undergoing peripheral blood stem cell transplantation, respectively. The need for an accurate and reproducible method for absolute cell counting may take on even more importance following the National Blood Authority strategy to issue blood products with an absolute white cell count of less than 5×10^6 leukocytes per blood product unit (BCSH, 1994c).

Currently, PBSC and lymphocyte subset analysis is routinely undertaken by flow cytometry, employing either a dual- or, less frequently, a single-platform approach. The dual-platform technique utilises immunophenotypic data derived from the flow cytometer together with the total white blood cell count, or the total absolute lymphocyte count, obtained from a hematology analyser. It is recognised, however, that a major factor contributing to the high interlaboratory CV values reported for absolute $CD4^+$ lymphocyte counts is the white blood cell count generated by different machines (Robinson et al., 1992). In addition, the intermachine variance for white blood cell counts increases significantly for values below $0.1 \times 10^9\ l^{-1}$, precluding this approach for the quality control of leukocyte-depleted blood products. In contrast, single-platform technology derives the absolute cell count directly from the flow cytometer, using either precision fluidics or microbead technology (Keeney et al., 1998a; Mercolino et al., 1995; Verwer and Ward, 1997).

Data from UK NEQAS for leukocyte immunophenotyping showed that interlaboratory CV values for $CD4^+$ T lymphocyte counts were consistently lower for single-platform (mean 13.7%; range 10–18.3%) than for dual-platform methodology (mean 23.4%; range 14.5–43.7%). Subgroup analysis of single-platform users demonstrated mean overall interlaboratory CV values of 17.2, 13 and 7.1% for the Flow-Count (Beckman Coulter), TruCOUNT™ (BD Biosciences) and volumetric approach, respectively. The lowest interlaboratory CV values obtained for a single sample according to each single-platform approach were 4% (TruCount), 4.4% (volumetric), 4.6% (FACSCount™; BD Biosciences) and 12.7% (FlowCOUNT™). Similarly, the mean interlaboratory CV for $CD34^+$ stem cell enumeration using nonstandardised single-platform approaches was 18.6% (range 3.1–36.9%) compared with 28.6% (range 19–44.2%) for the dual-platform technology. Our results suggest absolute cell subset enumeration should be performed by single-platform technology and that such an approach should improve the quality control of multicentre clinical trial data for $CD4^+$ T lymphocyte and $CD34^+$ stem cells (Barnett et al., 1999).

4.9 Conclusion

The implementation of quality control procedures, both internal and external, should be considered as good laboratory practice. Several measures have been outlined within this chapter that can provide the laboratory with the basics for such procedures. Further measures of good practice also extend to the logging of reagent use, monitoring refrigerator and freezer temperatures and ensuring that staff have an excellent career development programme. However, the most important factor when performing any flow cytometric procedure is *if in doubt repeat!*

4.10 REFERENCES

Barnett, D., Granger, V., Mayr, P., Storie, I., Wilson, G.A., Reilly, J.T. (1996) Evaluation of a novel stable whole blood quality control material for lymphocyte subset analysis: results from the UK NEQAS Immune Monitoring Scheme. *Cytometry* **26**, 216–22.

Barnett, D., Bird, G., Hodges, E., Linch, D.C., Matutes, E., Newland, A.C., Reilly, J.T. (1997) Guidelines for the enumeration of $CD4^+$ T lymphocytes in immunosuppressed individuals. *Clinical and Laboratory Haematology* **19**, 231–41.

Barnett, D., Granger, V., Storie, I., Peel, J., Pollitt, R., Smart, T., Reilly, J.T. (1998a) Quality assessment of CD34+ stem cell enumeration: experience of the United Kingdom National External Quality Assessment Scheme (UK NEQAS) using a unique stable whole blood preparation. *British Journal of Haematology* **102**, 553–65.

Barnett, D., Storie, I., Wilson, G.A., Granger, V., Reilly, J.T. (1998b) Determination of leucocyte antibody binding capacity (ABC): the need for standardization. *Clinical and Laboratory Haematology* **20** 155–64.

Barnett, D., Granger, V., Whitby, L., Storie, I., Reilly, J.T. (1999) Absolute $CD4^+$ T-lymphocyte and CD34+ stem cell counts by single platform flow cytometry: the way forward. *British Journal of Haematology* **106**, 1059–62.

Basso, G., Putti, M.C., Cantú-Rajnoldi, A., Saitta, M., Santostasis, T., Santoro, N., Lippi, A., Comelli, A., Felici, L., Favre, C., Mancuso, G.R., Guglielmo, C., Paolucci, P., Biondi, A., Rondelli, R., Pession, A. (1992) The immunophenotype in infant acute lymphoblastic leukaemia: correlation with clinical outcome. An Italian Multicentre Study (AIEOP). *British Journal of Haematology* **81**, 184–91.

BCSH (British Committee for Standards in Hematology) (1994a) Immunophenotyping in the diagnosis of acute leukemias. *Journal of Clinical Pathology* **47**, 777–81.

BCSH (British Committee for Standards in Hematology) (1994b) Immunophenotyping of chronic (mature) lymphoproliferative diseases. *Journal of Clinical Pathology* **47**, 871–5.

BCSH (British Committee for Standards in Hematology) (1994c) Guidelines on the clinical use of leukocyte-depleted blood components. *Transfusion Medicine* **8**, 59–71.

Bender, J.G., Unverzagt, K., Walker, D. (1994) Guidelines for determination of $CD34^+$ cells by flow cytometry: application to the harvesting and transplantation of peripheral blood stem cells. In: Wunder, E., Sovalat, H., Henon, P., Serke, S. (eds.) *Hematopoietic Stem Cells – The Mulhouse Manual*, pp. 31–43. AlphaMed Press, Dayton, OH.

Bergeron, M., Faucher, S., Minkus, T., Lacroix, F., Ding, T., Phaneuf, S., Somorjai, R., Summers, R., Mandy, F. and Participating Flow Cytometry Laboratories Canada (1998) Impact of unified procedures as implemented in the Canadian quality assurance program for T lymphocyte subset enumeration. *Cytometry* **33**, 146–55.

Borowitz, M.J., Bray, R., Gascoyne, R., Melnick, S., Parker, J.W., Picker, L., Statler-Stevenson, M. (1997) US–Canadian consensus recommendations on the immunophenotypic analysis of hematologic neoplasia by flow cytometry: data analysis and interpretation. *Cytometry* **30**, 236–44.

Campana, D. (1994) Applications of cytometry to study acute leukemia: in vitro determination of drug sensitivity and detection of minimal residual disease. *Cytometry* **18**, 68–74.

Campos, L., Guyotat, D., Archimbaud, E., Devaux,Y., Treille, D., Larese, A., Maupas, J., Gentilhome, O., Ehrsam, A., Fiere, D. (1989) Surface marker expression in adult myeloid leukaemia: correlations with initial characteristics, morphology and response to therapy. *British Journal of Haematology* **72**, 161–6.

Cantú-Rajnoldi, A., Putti, C., Siatta, M., Granchi, D., Foà, R., Schiro, R., Castagni, M., Valeggio, C., Jankovic, M., Miniero, R., Paolucci, P., Basso, G. (1991) Co-expression of myeloid antigens in childhood acute lymphoblastic leukaemia: relationship with stage of differentiation and clinical significance. *British Journal of Haematology* **79**, 40–3.

Chang, A., Ma, D. (1996) The influence of flow cytometric gating strategy on the standardisation of $CD34^+$ cell quantitation: an Australian multi-centre study. *Journal of Hematotherapy* **5**, 605–16.

Civin, C.I., Trischmann, T.M., Fackler, M.J., Bernstein, I.D., Buhring, H.J., Campos, L., Greaves, M.F., Kamoun, M., Katz, D.R., Lansdorp, P.M., Look, A.T., Seed, B., Sutherland, D.R., Tindle, R.W., Uchanska-Ziegler, B. (1989) Report on the CD34 Cluster Workshop. In: Knapp, W., Dorken, B., Gilks, W.R., Rieber, E.P., Schmidt, R.E., Stein, H., von dem Borne, A.E.G.Kr. (eds.), *Leucocyte Typing IV: White Cell Differentiation Antigens*, pp. 818–25. Oxford University Press, Oxford, UK.

Ekong, T., Gompels, M., Clark, C., Parkin, J., Pinching, A. (1993a) Double-staining artefact observed in certain individuals during dual-colour immunophenotyping of lymphocytes by flow cytometry. *Cytometry* **14**, 679–84.

Ekong, T., Kupek, E., Hill, A., Clark, C., Davies, A., Pinching, A. (1993b) Technical influences on immunophenotyping by flow cytometry. The effect of time and temperature of storage on the viability of lymphocyte subsets. [Published erratum appears in *Journal of Immunological Methods* **166**, 301] *Journal of Immunological Methods* **164**, 263–73.

Fay, S.P., Barnett, D., Granger, V., Mercolino, T. (1994) Absolute control – a novel stabilized whole blood preparation for leukocyte immunophenotyping full process control. *Cytometry* **18**, 177.

Feng, R., Shimazaki, C., Inaba, T., Takahashi, R., Hirai, H., Kikuta, T., Sumikuma, T., Yamagata, N., Ashihara, E., Fujita, N., Nakagawa, M. (1998) $CD34^+/CD41^+$ cells best predict platelet recovery after autologous peripheral blood stem cell transplantation. *Bone Marrow Transplantation* **21**, 1217–22.

Fink, F.M., Koller, U., Mayer, H., Haas, O.A., Grumayer-Panzer, R., Urban, C.E., Dengg, K., Mutz, I., Tuchler, H., Gatterer-Menz, I. (1993) Prognostic significance of myeloid associated antigen expression on blast cells with acute lymphoblastic leukaemia. *Medical and Pediatric Oncology* **21**, 340–6.

Forrest, M.J., Barnett, D. (1989) Laboratory control of immunocytochemistry. *European Journal of Haematology* **42**, 67–71.

Geller, R.B., Zahurak, M., Hurwitz, C.A., Burke, P.J., Karp, J.E., Piantadosi, S., Civin, C.I. (1990) Prognostic importance of immunophenotyping in adults with acute myelocytic leukaemia: the significance of the stem-cell glycoprotein CD34 (My10). *British Journal of Haematology* **76**, 340–7.

Gratama, J.W., van der Linden, R., van der Holt, B., Bolhuis, R.L., van de Winkel, J.G. (1997a) Analysis of factors contributing to the formation of mononuclear cell aggregates ('escapees') in flow cytometric immunophenotyping. *Cytometry* **29**, 250–60.

Gratama, J.W., Kraan, J., Levering, W., van Bockstaele, D.R., Rijkers, G.T., van der Schoot, C.E. (1997b) Analysis of variation in results of $CD34^+$ hematopoietic progenitor cell enumeration in a multicenter study. *Cytometry* **30**, 109–17.

Gratama, J.W., Kraan, J., van den Beemd, R., Hooibrink, B., van Bockstaele, D.R., Hooijkaas, H. (1997c) Analysis of variation in results of flow cytometric lymphocyte immunophenotyping in a multicenter study. *Cytometry* **30**, 166–77.

Gratama, J.W., Orfao, A., Barnett, D., Brando, B., Huber, A., Janossy, G., Johnsen, H.E., Keeney, M., Marti, G.E., Preijers, F., Rothe, G., Serke, S., Sutherland, D.R., van der Schoot, C.E., Schmitz, G., Papa, S. for the European Working Group on Clinical Cell Analysis (1998) Flow cytometric enumeration of $CD34^+$ hematopoietic stem and progenitor cells. *Cytometry* **34**, 128–42.

Howard, M.R., Thomas, L., Reid, M.M. (1994) Variable detection of myeloid antigens in childhood acute lymphoblastic leukaemia. *Journal of Clinical Pathology* **47**, 1006–9.

Johnsen, H.E., Knudsen, L.M. (1996) Nordic flow cytometry standards for $CD34^+$ cell enumeration in blood and leukapheresis products: report from the second Nordic workshop. *Journal of Hematotherapy* **5**, 237–45.

Keeney, M., Chin-Yee, I., Weir, K., Popma, J., Nayar, R., Sutherland, D.R. (1998a) Single platform flow cytometric absolute CD34+ cell counts based on the ISHAGE guidelines. *Cytometry* **34**, 61–70.

Keeney, M., Gratama, J.W., Chin-Yee, I.H., Sutherland, D.R. (1998b) Isotype controls in the analysis of lymphocytes and $CD34^+$ stem and progenitor cells by flow cytometry – time to let go! *Cytometry* **34**, 280–3.

Kromer, E., Grossmuller, F. (1994) Light scatter based lymphocyte gate – helpful tool or source of error? *Cytometry* **15**, 87–9.

Loken, M.R., Brosnan, J.M., Bach, B.A., Ault, K.A. (1990) Quality control in flow cytometry: 1. Establishing optimal lymphocyte gates for immunophenotyping by flow cytometry. *Cytometry* **11**, 453–9.

Lowdell, M.A., Bainbridge, D.R. (1996) External quality assurance for CD34 cell enumeration – results of a preliminary national trial. *Bone Marrow Transplantation* **17**, 849–53.

Lumley, M.A., McDonald, D.F., Czarnecka, H.M., Billingham, L.J., Milligan, D.W. (1996) Quality assurance of $CD34^+$ cell estimation in leucapheresis products. *Bone Marrow Transplantation* **18**, 791–6.

Mandy, F.F., Bergeron, M., Recktenwald, D., Izaguirre, C.A. (1992) A simultaneous three-color T cell subsets analysis with single laser flow cytometers using T cell gating protocol. Comparison with conventional two-color immunophenotyping method. *Journal of Immunological Methods* **156**, 151–62.

Mandy, F.F., Bergeron, M., Minkus, T. (1997) Evolution of leukocyte immunophenotyping as influenced by the HIV/AIDS pandemic: a short history of the development of gating strategies for $CD4^+$ T-cell enumeration. *Cytometry* **30**, 157–65.

Mercolino, T.J., Connelly, M.C., Meyer, E.J., Knight, M.D., Parker, J.W., Stelzer, G.T., DeChirico, G. (1995) Immunologic differentiation of absolute count with an integrated flow cytometric system: a new concept for absolute T cell subset determinations. *Cytometry* (*Communications in Clinical Cytometry*) **22**, 48–59.

Molica, S., Dattilo, A., Albert, A. (1991) Myelomonocytic antigens in B-chronic lymphocytic leukaemia: analysis of clinical significance. *Leukemia and Lymphoma* **5**, 139–44.

Morabito, F., Prasthofer, E.F., Dunlap, N.E., Grossi, C.E., Tielden, A.B. (1987) Expression of myelomonocytic antigens on chronic lymphatic leukaemia B cells correlates with their ability to produce interleukin-1. *Blood* **70**, 1750–7.

Nicholson, J.K.A. (1994) Immunophenotyping specimens from HIV-infected persons: laboratory guidelines from the Centers for Disease Control and Prevention. *Cytometry* **18**, 55–9.

Novelli, E.M., Ramirez, M., Civin, C.I. (1998) Biology of $CD34^{+}CD38^{-}$ cells in lymphohematopoiesis. *Leukemia and Lymphoma* **31**, 285–93.

O'Gorman, M.R., Thomas, J. (1999) Isotype controls – time to let go? *Cytometry* (*Communications in Clinical Cytometry*) **38**, 78–80.

Owens, M.A., Loken, M.R. (1995) *Flow Cytometry Principles for Clinical Laboratory Practice: Quality Assurance for Quantitative Immunophenotyping*, pp. 129–54. Wiley-Liss, New York.

Paxton, H., Kidd, P., Landay, A., Giorgi, J., Flomenberg, N., Walker, E., Valentine, F., Fahey, J., Gelman, R. (1989) Results of the flow cytometry ACTG quality control program: analysis and findings. *Clinical Immunology and Immunopathology* **52**, 68–84.

Perey, L., Peters, R., Pampallona, S., Schneider, P., Gross, N., Leyvraz, S. (1998) Extensive phenotypic analysis of CD34 subsets in successive collections of mobilized peripheral blood progenitors. *British Journal of Haematology* **103**, 618–29.

Pinto, A., Zagonel, V., Carbone, A., Serraino, D., Marotta, G., Volpe, R., Colombatti, A., Del Vecchio, L. (1992) CD13 Expresson in B-cell chronic lymphocytic leukaemia is associated with the pattern of bone marow infiltration. *Leukemia and Lymphoma* **6**, 209–18.

Piu, C-H., Behm, F.G., Singh, B., Gaston, K., Schell, M.J., Roberts, W.M., Crist, W.M., Mirro, J. (1990) Myeloid-associated antigen expression lacks prognostic value in childhood acute lymphoblastic leukaemia treated with intensive multiagent chemotherapy. *Blood* **75**, 198–202.

Piu, C-H., Raimondi, S.C., Head, D.R., Schell, M.J., Rivero, G.K., Mirro, J., Crist, W.M., Behm, F.G. (1991) Characterisation of childhood acute leukaemia with multiple myeloid and lymphoid markers at diagnosis and relapse. *Blood* **78**, 1327–37.

Polliack, A., Rabinowitz, R., Leizerowitz, R., Keren-zur, Y., Schlesinger, M. (1993) Myelomonocytic antigens are rarely expressed on B-lymphocytic leukaemia cells. *Leukemia and Lymphoma* **9**, 125–31.

Reilly, J.T. (1996) Use and evaluation of leukocyte monoclonal antibodies in the diagnostic laboratory: a review. *Clinical and Laboratory Haematology* **18**, 1–6.

Reilly, J.T., Granger, V., Temperton, P.F., Barnett, D. (1995) Leukaemia immunophenotyping: effect of antibody source and fluorochrome on antigen detection. *Journal of Clinical Pathology* **48**, 186.

Robinson, G., Morgan, L., Evans, M., McDermott, S., Pereira, S., Wansbrough-Jones, M., Griffin, G. (1992) Effect of type of hematology analyser on CD4 count. *Lancet* **340**, 485–6.

Romeu, M.A., Mestre, M., Gonzalez, L., Valls, A., Verdaguer, J., Corominas, M., Bas, J., Massip, E., Buendia, E. (1992) Lymphocyte immunophenotyping by flow cytometry in normal adults. Comparison of fresh whole blood lysis technique, Ficoll–Paque separation and cryopreservation. *Journal of Immunological Methods* **154**, 7–10.

Rothe G., Schmitz G. (1996) Consensus protocol for the flow cytometric immunophenotyping of hematopoietic malignancies. Working Group on Flow Cytometry and Image Analysis. *Leukemia* **10**, 877–95.

San Miguel, J.F., Martínez, A., Macedo, A., Vidriales, M.B., López-Berges, C., González, M., Cabaliero, D., García-Marcos, M.A., Ramos, F., Fernández-Calvo, J., Calmuntia, M.J., Diaz-Mediavilla, J., Orfao, A. (1997) Immunophenotyping investigation of minimal residual disease is a useful approach for predicting relapse in acute myeloid leukemia patients. *Blood* **90**, 2465–70.

Schwartz, A., Marti, G.E., Poon, R., Gratama, J.W., Fernández-Repollet, E. (1998) Standardizing flow cytometry: a classification system of fluorescence standards used for flow cytometry. *Cytometry* **33**, 106–14.

Selleri, C., Notaro, R., Catalano, L., Fontana, R., del Vechio, L., Rotoli, B. (1991) Prognostic irrelevance of CD34 in acute myeloid leukaemia. *British Journal of Haematology* **82**, 479–82.

Shapiro, H.M. (1994) *Practical Flow Cytometry*, 3rd edn. Wiley-Liss, New York.

Siena, S., Bregni, M., Brando, B., Belli, N., Ravagnani, F., Gandola, L., Stern, A.C., Lansdorp, P.M., Bonadonna, G., Gianni, A.M. (1991) Flow cytometry for the clinical estimation of circulating hematopoietic progenitors for autologous transplantation in cancer patients. *Blood* **77**, 400–9.

Simmons, P.J., Torok-Storb, B. (1991) CD34 expression by stromal precursors in normal human adult bone marrow. *Blood* **78**, 2848–53.

Storr, J., Dolan, G., Coustan-Smith, E., Barnett, D., Reilly, J.T. (1990) Value of monoclonal anti-myeloperoxidase (MPO7) for diagnosing acute leukaemia. *Journal of Clinical Pathology* **43**, 847–9.

Sutherland, D.R., Marsh, J.C.W., Davidson, J. (1992) Differential sensitivity of CD34 epitopes to cleavage by *Pasteurella haemolytica* glycoprotease: implications for purification of CD34-positive progenitor cells. *Experimental Hematology* **20**, 590–9.

Sutherland, D.R., Anderson, L., Keeney, M., Nayar, R., Chin-Yee, I. (1996) The ISHAGE guidelines for $CD34^{+}$ cell determination by flow cytometry. *Journal of Hematotherapy* **5**, 213–26.

Sutherland, D.R., Anderson, L., Keeney, M., Nayar, R., Chin-Yee, I. (1997) Re: toward a worldwide standard for CD34+

enumeration (response to letter to the editor). *Journal of Hematotherapy* **6**, 85–9.

Sutherland, D.R., Keating, A. (1992) The CD34 antigen: structure, biology and potential clinical applications. *Journal of Hematotherapy* **1**, 115–29.

Terstappen, L.W., Gandour, D., Huang, S., Lund-Johansen, F., Manion, K., Nguyen, M., Mickaels, R., Olweus, J., Topker, S. (1993) Assessment of hematopoietic cell differentiation by multidimensional flow cytometry. *Journal of Hematotherapy* **2**, 431–47.

Titley, I., Healy, L.E., Gordon, M.Y. (1997) CD34 epitope expression on hemopoietic tissues. *British Journal of Haematology* **98**, 779–80.

Verwer, B.J.H., Ward, D.M. (1997) An automated classification algorithm for ProCount flow cytometric acquisition and analysis. *Journal of Hematotherapy* **6**, 169.

5

Data analysis in flow cytometry

Mark W. Lowdell

Royal Free Hospital School of Medicine, London

5.1 Introduction

Errors in flow cytometry can only arise from two discrete processes: data acquisition and data analysis. In general, data acquisition errors can be avoided by good sample preparation and accurate instrument set-up. Quality assurance reagents are available to confirm most aspects of sample preparation in routine applications and internal experimental controls should be designed to provide the same level of assurance in experimental applications. Instrument standards, such as fluorescent beads or fixed nuclei, can be used to confirm instrument performance in both settings. The only aspect of data acquisition for which controls are unavailable is the ability of the operator to design the correct experiment. This is obviously common to any analytical procedure but is particularly relevant to applications such as flow cytometry where the only output is a digitised signal presented on a computer screen.

5.2 Experiment design

The most common acquisition error made by users of flow cytometers is insufficient data points. Often huge files of list mode data are collected, sometimes with tens of thousands of data points, which, upon analysis, contain mostly debris or irrelevant cells. This is an easily avoided error. The traditional way to guarantee the acquisition of a specific number of cells of interest is to apply an acquisition gate or region based upon one or more characteristics of the cells of interest. This is effective but limits the data analysis solely to the cells that were thought to be of interest at the time of analysis and necessarily excludes any other cell populations that may be of interest subsequently. A more flexible approach requires setting an acquisition region or gate that is used solely for counting. Thus all events above a set threshold will be stored but the analysis will continue until a predetermined number of one cell subset has been acquired. A good example of the use of such a technique is the enumeration of rare events such as $CD34^+$ hematopoietic stem cells. Here it is important that enough positive events are collected to guarantee a given level of accuracy determined as the coefficient of variation (CV) of the assay. Rare events within a population are distributed according to a Poisson distribution and the CV will be described by the formula $100/\sqrt{n}$, where n is the number of positive events acquired. Therefore, 100 cells of interest must be acquired to give a CV of 10%. Plainly, the more cells acquired the better the CV and the greater the reliance that can be accorded to the data. The disadvantage to using an acquisition strategy such as this is that the data files may become very large indeed, and this has restricted the use of this approach in the past. Modern computer processors and inexpensive data storage systems such as Zip drives makes this technique much more feasible.

5.3 Analysis of flow cytometric cell phenotyping data

Analysis of phenotype is certainly the most common application of the majority of flow

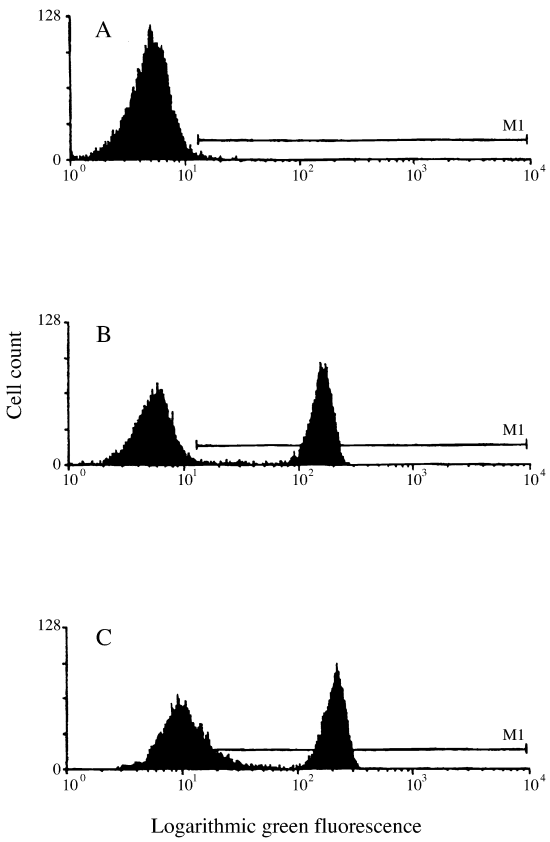

Fig. 5.1 The fluorescence associated with an isotype control antibody from manufacturer 1 (histogram A) together with the fluorescence associated with binding of a fluorescein isothiocyanate (FITC)- conjugated CD3 antibody from the same manufacturer (histogram B) and that obtained when FITC–CD3 from a second manufacturer was used (histogram C). In histogram C, the background binding of the antibody is higher than that in histograms A and B and could lead to spurious results. For this reason, it is always preferable to use control and test antibodies from the same manufacturer.

cytometers but nonetheless it is an area in which controversies exist. Until the early 1990s, the standard practice for analysis of phenotyping data was to run an isotype-matched control monoclonal antibody conjugated with the same fluorochrome as the antibody of interest and to set a cursor (or analysis marker) on the negative sample such that less than 5% of the cells were classed as positive. Subsequently, the test sample was acquired and the proportion of cells falling to the right of the marker was calculated. While this may work in many situations, it is fallible and relies upon several assumptions that the operator is often not in a position to make. First, the isotype control antibody must have the same fluorochrome to protein ratio as the test antibody. That is, the average number of fluorochrome molecules must be the same on both antibodies. High-quality manufacturers endeavour to achieve this across their range of reagents but an isotype control antibody from one manufacturer is unlikely to be an appropriate control for antibodies supplied by other manufacturers. A second assumption is that the two clones have the same proportion of monovalent and divalent binding antibody molecules and that the kinetics of nonspecific binding are similar. Figure 5.1 shows an example of fluorescence histograms where an isotype-matched control antibody is used to delineate the nonspecific binding of fluorescein isothiocyanate-conjugated CD3 (FITC–CD3) antibodies from the same manufacturer and an alternative manufacturer. This is plainly an extreme example but it does demonstrate the potential pitfalls of relying upon a single analysis strategy.

5.4 Cluster analysis

During the 1980s the term ‘cluster’ or ‘cloud’ analysis was coined to describe the use of the internal negative cell population for discrimination of ‘positive’ versus ‘negative’ events. It was argued that, in a heterogeneous cell population such as peripheral blood lymphocytes, some cells were likely to express an antigen (positive) while others would lack the molecule (negative). Given a sufficiently high signal to noise ratio between the two populations, it should be possible to identify the positive cells without an isotype-matched control. Current guidelines for CD4 and CD34 cell subset enumeration do not require isotype-matched controls to be run (Keeney et al., 1998) and at least one commercial manufacturer has produced semi-automated analysis soft-

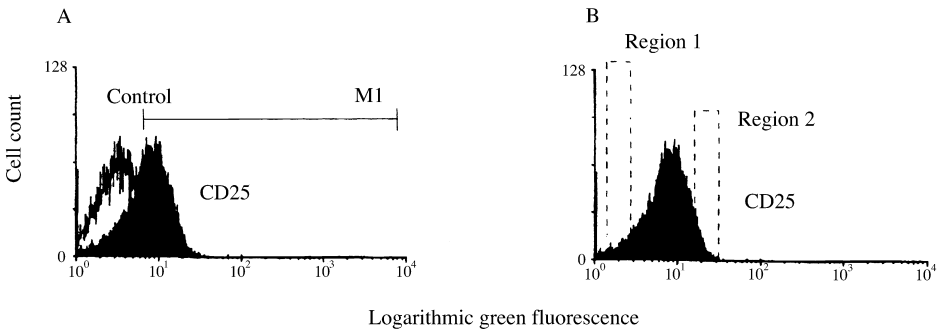

Fig. 5.2 Histogram A shows the overlapping distribution of control (unfilled histogram) and fluoroscein isothiocyanate-conjugated CD25 antibody (FITC–CD25; solid histogram). If a cursor is defined with the isotype control antibody then a proportion of the cells labelled with CD25 would be deemed negative for this antigen. However, in reality, all cells are positive but those in region 2 bind 10 times as much antibody as those in region 1, as shown in histogram B, which shows only the FITC–CD25 labelled cells.

ware that only requires an isotype-matched control to check retrospectively for nonspecifically fluorescent cells in the analysis gate.

In some cases, cluster analysis is difficult to apply, for example when analysing cell lines or leukaemic clones when there may be no negative cells in the sample and an isotype control is required. Nonetheless, the data should be interpreted intelligently and with caution. When the test histogram overlaps the negative control histogram (as in Fig. 5.2A), it is tempting to describe the cells to the right of the marker as positive and those to the left as negative. This is a poor analysis of the data. Cells falling in region 1 of the test histogram (Fig. 5.2B) bind very little test antibody whereas cells in region 2 bind ten times as much test antibody; both populations of cells, however, are positive for the antigen. In an experiment, the expression of interleukin 2 receptors (CD25) on an interleukin 2-dependent cell line was studied, the results were similar to the two histograms in Fig. 5.2. For cells labelled with anti-interleukin 2 receptor, cells falling in region 1 and those in region 2 were sorted and cultured in separate flasks in the presence of interleukin 2. After 3 days in culture, the cells recovered from regions 1 and 2 showed identical distributions of fluorescence to that of the preselected sample. In other words, the distribution of interleukin 2 receptors was a normal biological phenomenon. In a case like this in which the distribution is univariate and overlapping the negative control, it is usually more valuable to describe the distribution by virtue of the degree of fluorescence rather than by the percentage that are positive. Such histograms may be compared using Kolmogorov–Smirnov statistics to determine if and how different they are; this is indicated by the assignment of a value: the D value. The D value is the maximum vertical displacement between two cumulative frequency distributions for the control and test samples, where the fluorescence intensity is measured on the *x*-axis and the relative number of events is measured on the *y*-axis (Young, 1977). This is probably the most robust analytical approach available, although it should be recognized that the choice of D value that must be exceeded in this test before the histograms are considered different is still arbitrary (Borowitz *et al.*, 1998).

The examples shown in Fig. 5.2 are presented as single-parameter histograms since only one fluorochrome was applied to the cells. While this can be economical in terms of data storage and even data presentation, it often obscures the analysis. Figure 5.3 shows the result of labelling a normal peripheral blood sample with an isotype control and with FITC–CD4 antibody and analysis of the granulocyte cluster. The control histogram (Fig. 5.3A) shows two peaks of fluorescence and a marker

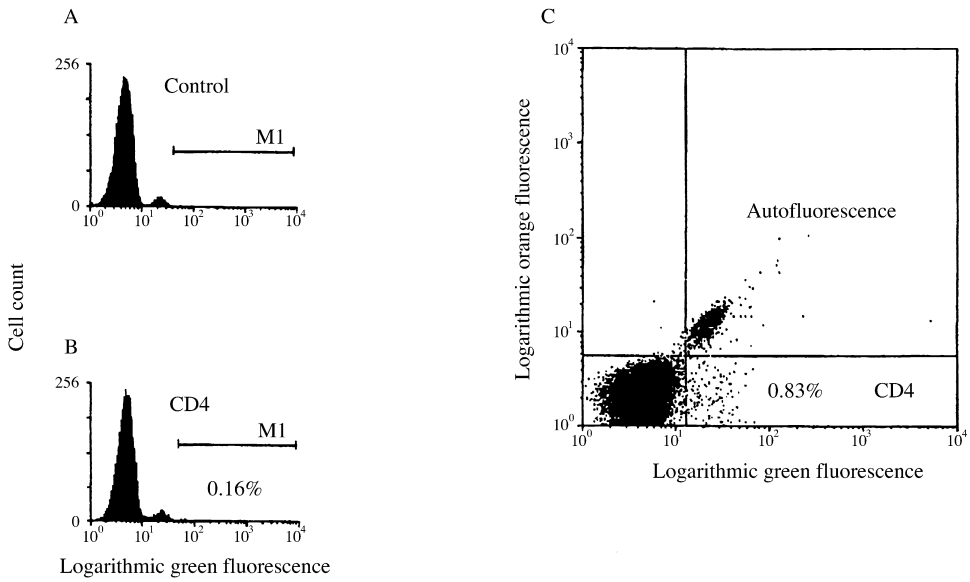

Fig. 5.3 The benefit of dual-parameter analysis of single fluorochrome-labelled samples. (A) Background nonspecific binding and autofluorescence are shown. (B) Binding of CD4; because of the high autofluorescence, the weak binding of CD4 is masked. (C) The use of dual parameter analysis allows distinction between autofluorescence and true CD4 binding and so facilitates determination of a more accurate measure of $CD4^+$ cells.

was set to the right of the smaller peak. Analysis of the CD4-labelled sample (Fig. 5.3B) using the same marker setting identifies a $CD4^+$ basophil subpopulation of 0.16%. However, by collecting the FL2 fluorescent signals from each of the cells and arraying FL1 (CD4) versus FL2 (autofluorescence) from each granulocyte we are able to resolve the weakly labelled $CD4^+$ cells from the autofluorescent cells and obtain a more accurate estimate of the population (Fig. 5.3C). This required no additional fluorochrome.

This approach is shown again in Fig. 5.4 where myeloid leukaemic cells that have been cultured in vitro for a prolonged period have been labelled with a solution of isotonic propidium iodide (PI). The histogram (A) clearly shows three cell populations: cells excluding the dye (1), cells showing low level fluorescence (2) and a small subpopulation showing higher levels of fluorescence (3). We would imagine that the first cell population contained the live cells, those in the second subset were apoptotic and those showing high-level fluorescence were dead cells. Figure 5.4B shows that the cells with low levels of PI fluorescence (2) have the same forward light scatter index as the cells that exclude the dye (1), suggesting that they are healthy cells. This is, in fact, the case and the weakly fluorescent cells are autofluorescent myeloid cells. The truly apoptotic and necrotic cells have a lower forward light scatter signal (3) and can be resolved on this basis.

5.5 Measurement of fluorescent intensity

Measurement of fluorescent intensity is one of the most common applications of flow cytometers and probably the least well understood by the majority of cytometrists (Nicholson and Stetler-Stevenson, 1998). Historically, the most common use of fluorescent intensity measurements was the analysis of cellular DNA content to determine relative proportions of cells at different stages of the cell cycle. These calculations have the advantage that the entire dataset can be resolved over 256 or 1024 data

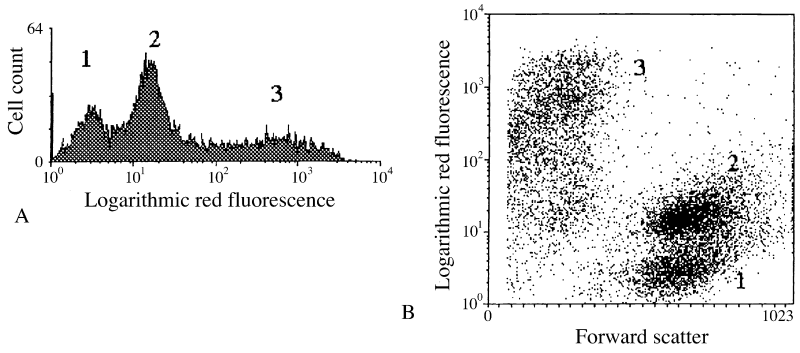

Fig. 5.4 The use of forward angle light scattering and propidium iodide labelling for the identification of apoptotic and necrotic cells (3) from live (1) and autofluorescent cells (2) (Schmid et al., 1994).

channels with linear signal amplification since the dynamic range is restricted. The difficulties associated with DNA histogram analyses are related to the overlapping nature of the individual distributions of cells in G_0–G_1, S and G_2–M phases, as well as the occurrence of aneuploid nuclei. There are almost as many algorithms for dissembling these overlapping histograms as there are cytometrists trying to do so, and it is inappropriate to discuss them here. An excellent review of DNA histogram analysis may be found in Watson et al. (1987).

Cytometrists involved in the analysis of DNA histograms are usually more aware of the mathematical constraints of their analyses than are hematologists and immunologists who study cell surface antigen expression. Furthermore, the greater dynamic range of fluorescent intensities associated with immunofluorescent labelling means that these data are generally acquired after logarithmic amplification, which adds further complexity to the mathematics.

First, it is necessary to understand how the histogram or dot-plot data are generated by the electronic digital circuits of the cytometer and its associated computer. The light signals (photons) scattered by the cell, whether incident or fluorescent light, are detected by the photodiodes and photomultiplier tubes and converted into analogue electrical signals (electrons), which are then amplified and converted to digital signals that can be processed by the microprocessor of the computer. Most modern flow cytometers use 10-bit analogue to digital converters (ADC) to resolve the analogue electrical signals to digital output for processing. A 10-bit ADC can resolve data into 1024 channels. This means that a cell in channel 1024 is just over 1000 times brighter than a cell in channel 1. Unfortunately, the fluorescence signals from cells labelled with monoclonal antibodies frequently exceed this range and the most convenient solution has been the logarithmic amplification of the analogue electronic signals prior to processing by the ADC. This gives an apparent range of 10 000-fold increases in fluorescence but the data are still only divided into 1024 channels; consequently the resolution changes across the distribution, which skews the data.

Let us consider the cells labelled with CD3 antibodies in Fig. 5.1. The expression of an antigen on the surface of a population of cells as measured by a flow cytometer usually follows a 'normal' distribution when acquired with logarithmic amplification. That is, it appears as a bell-shaped curve, as shown in Fig. 5.1. If we delineate the positive cells in this example with a histogram marker, we can determine the percentage positive as well as a variety of statistical measurements that describe the position and shape of the distribution. To gain some idea of the fluorescence intensity of the positive cells, we need to estimate the centre of the distribution. Three estimates of central tendency are generally available; a mean, a mode and a median channel. How the channel is calculated will be dealt with

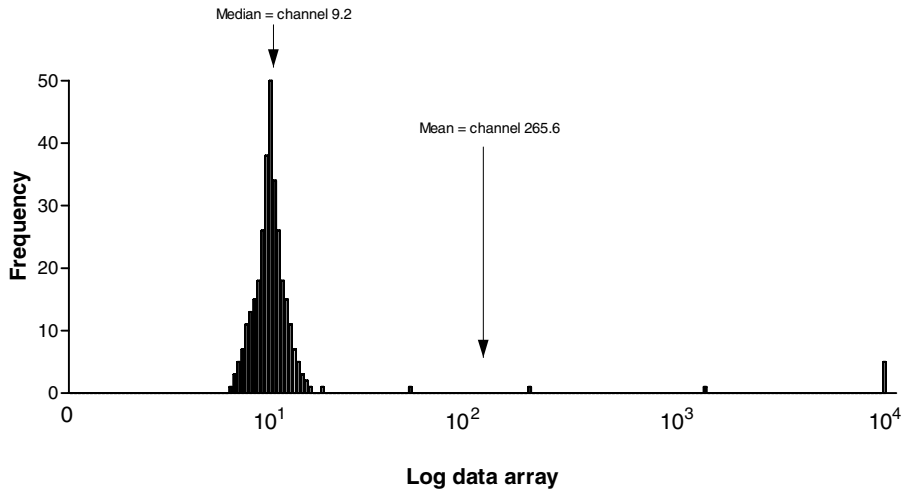

Fig. 5.5 The use of mean fluorescence may not be representative of the events analysed. Here the data are very markedly skewed and the median value should be used.

below but here it is important to decide which parameter will give the most meaningful and reliable estimate of the center of the fluorescent distribution.

Figure 5.5 shows a typical fluorescent histogram of a weakly fluorescent cell population acquired with conventional logarithmic amplification of the fluorescent signals. The centre of the distribution as determined by eye is about 10^1 on this four decade logarithmic scale. The mode, that is the channel with the most events in it, is 10^1 and it has 50 events. This gives it a total weighting to the distribution of $50 \times 10 = 500$. In contrast, five events fell in the last channel of the fluorescent histogram. These were probably rogue events owing to nonspecific antibody uptake, cell clumping or simply dead cells. However, these five events weight the distribution disproportionately $5 \times 10\,000 = 50\,000$ and skew the mean channel fluorescence alarmingly to give a value of 265.6. This over-represents the true central tendency of the fluorescent histogram by almost 30 times!

The median channel of this fluorescent distribution represents the point at which 50% of the events fall above and 50% fall below and has a value of 9.2. Plainly this is a better representation of the fluorescent characteristics of the expression of this antigen on this cell population. The use of the median channel value becomes more important when some events fall in the first or last channel, that is they are 'off-scale', since it is not possible to determine how far they are beyond the limits of the instrument and, therefore, their effect on a mean cannot be calculated. A word of caution is appropriate here; the analysis of fluorescent intensity must be restricted to univariate populations. A mean or median of data falling into two separate populations is biologically meaningless, so set analysis regions appropriately before calculating the central tendency of the distribution. If you feel justified in including 'off-scale' data in a median analysis it should be confirmed that the 'off-scale' data do not include separate distributions. Most flow cytometric analyses will produce data that are skewed and in this case the median should be used as the measure of central tendency. If, however, the data are normally distributed then the mean may be used.

Having decided the appropriate measure of central tendency as the median channel fluorescence, it is necessary to resolve how to use the data. The following discussion will be restricted to the measurement of the intensity of fluorescence de-

rived from cell antigen studies rather than DNA histograms. Let us assume that we are interested in measuring the effect of phorbol myristate acetate (PMA) on the expression of the CD3 antigen on T lymphocytes. One approach would be to label some freshly isolated peripheral blood mononuclear cells (PBMC) with FITC–CD3 and to compare the level of fluorescence with that of cells from the same donor labelled with FITC–CD3 after incubation for 1 h with a mitogenic dose of PMA. Having acquired several thousand $CD3^+$ events, one would present a histogram of FITC fluorescence and place a marker on the $CD3^+$ population from which distribution statistics can be derived. In terms of fluorescence intensity, the default setting for most commercial flow cytometers gives the median channel of the logarithmic amplified data displayed on a logarithmic scale. Figure 5.6A is the fluorescent histogram of CD3 expression on T-cells within the fresh PBMC. The median channel fluorescence on the logarithmic scale is 202 units. Figure 5.6B shows the effect of incubation for 1 h with PMA. The CD3 expression has reduced and the median channel fluorescence has fallen to 46.1 units. This is a fall of 155.9 units. However, these data are meaningless unless it is stated that they were acquired over four logarithmic decades, as shown in the figure.

If one calculates 155.9 as a percentage of the starting value, i.e. 202, we get a figure of 77.18%, which is the proportionate reduction in fluorescence. In other words, 'the level of CD3 expression on the surface of the cells has fallen by three quarters', which is much more meaningful biologically.

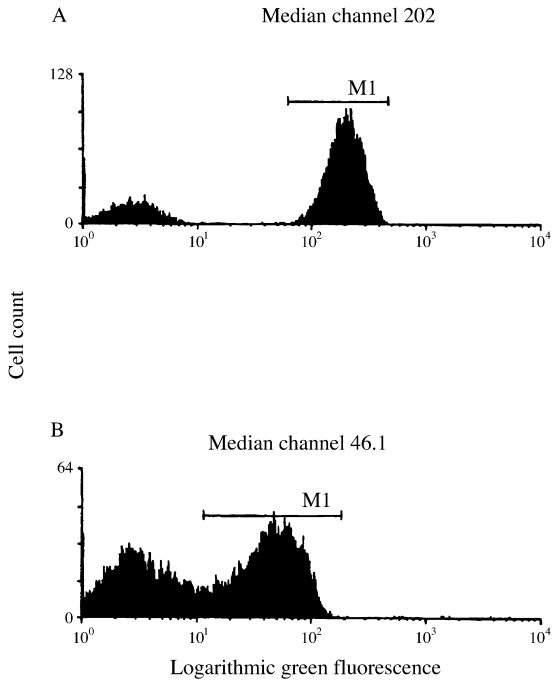

Fig. 5.6 The use of median fluorescence intensity to measure changes in antigen density on cell populations. (A) The fluorescent histogram of CD3 expression on T-cells within fresh peripheral blood mononuclear cells. The median channel fluorescence on the logarithmic scale is 202 units. (B) The effect of incubation for 1 h with phorbol myristrate acetate. The CD3 expression has reduced and the median channel fluorescence has fallen to 46.1 units. The level of CD3 expression on the surface of the cells has fallen by three quarters. The M1 cursors were set against appropriate negative controls.

5.6 Standardisation

The above approach to data analysis works well when the data are acquired on the same day on the same flow cytometer. If the study ran over several days or weeks, then other considerations have to be taken into account. First, the flow cytometer should be standardised; this can be done easily with a reliable fluorescent bead standard. The instrument settings used on the initial data can be used to set up the cytometer for subsequent analyses and the beads should be run to confirm that the same median channel fluorescence is obtained on each occasion. If necessary, the instrument settings can be modified to re-attain the same median channel fluorescence for the beads and, therefore, the results obtained from the stained cell population will be comparable with previous findings. The second important consideration is changes in innate background fluorescence of the cells during culture. In Fig. 5.6, the median channel fluorescence of the $CD3^+$ subset was used for comparison. A better ex-

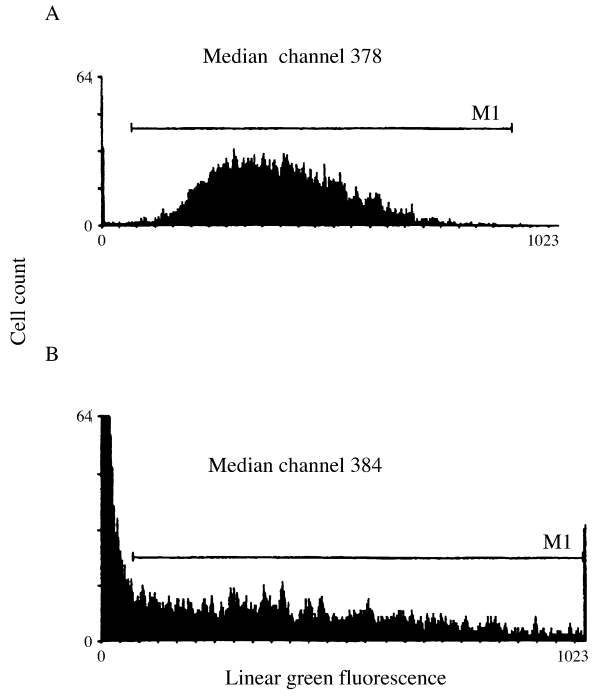

Fig. 5.7 (A) The CD3 expression on freshly isolated T-cells with linear fluorescence amplification. (B) The expression on T-cells treated with phorbol myristrate acetate with fourfold linear fluorescence amplification. For accurate comparison of the results in the two analyses, the median channel value in histogram B should be divided by 4. The M1 cursors were set against appropriate negative controls.

periment would have first analysed the background fluorescence of unlabelled cells and subtracted this from the median channel fluorescence of the CD3 population. In practice, this is only likely to be important in cells cultured for protracted periods.

5.7 Logarithmic and linear amplification

The use of logarithmically amplified data can be problematic because of inconsistencies in the performance of logarithmic amplifiers. This is particularly relevant at the lower levels of fluorescence in the first logarithmic decade. The example here has involved analysis of populations falling in the second logarithmic decade and beyond, which is more reliable (Shapiro, 1994). The most reliable estimate of fluorescence intensities comes from linearly amplified data. Figure 5.7A shows the same sample as Fig. 5.6A but after linear amplification. The negative cell population falls within the first channel and cannot be resolved on the same plot. Similarly, the level of CD3 expression after treatment with PMA also fell below the resolution at this level of amplification; consequently, the linear amplifier was increased fourfold, to give the plot shown in Fig. 5.7B. The median channel fluorescence of the treated cells is 384 but this must be divided by 4 since that was the level of linear amplification. This gives a value of 96, which can be subtracted from the original CD3 median channel fluorescence of 378 to give 282 channels. As 282 is 74.6% of 378, this confirms that incubation with PMA for 1 h led to a reduction in CD3 expression of three quarters.

5.8 Fluorescence calibration and quantification

Sometimes investigations can involve multicentre studies where many flow cytometers are used in a similar experiment and the data need to be comparable. This is made possible by using fluorescent bead standards, which comprise several bead subpopulations each carrying different known concentrations of fluorochrome. There are several suppliers of this type of reagent and each has benefits and disadvantages. None is a panacea. If a multicentre study is planned and it is likely to run beyond the shelf-life of a single batch of beads, it is important to compare multiple batches of the same bead product from a single supplier to confirm that reproducible results can be obtained from different batches. Guidelines for the procedure for flow cytometric fluorescence calibration and standardisation may be found in Stezler et al. (1997).

For these analyses, it is generally more reliable to resolve logarithmically amplified data back to the linear data array channels. This can be selected within the instrument software at the analysis stage and distributes the data within the 256 or 1024 channels into which the events were placed by the

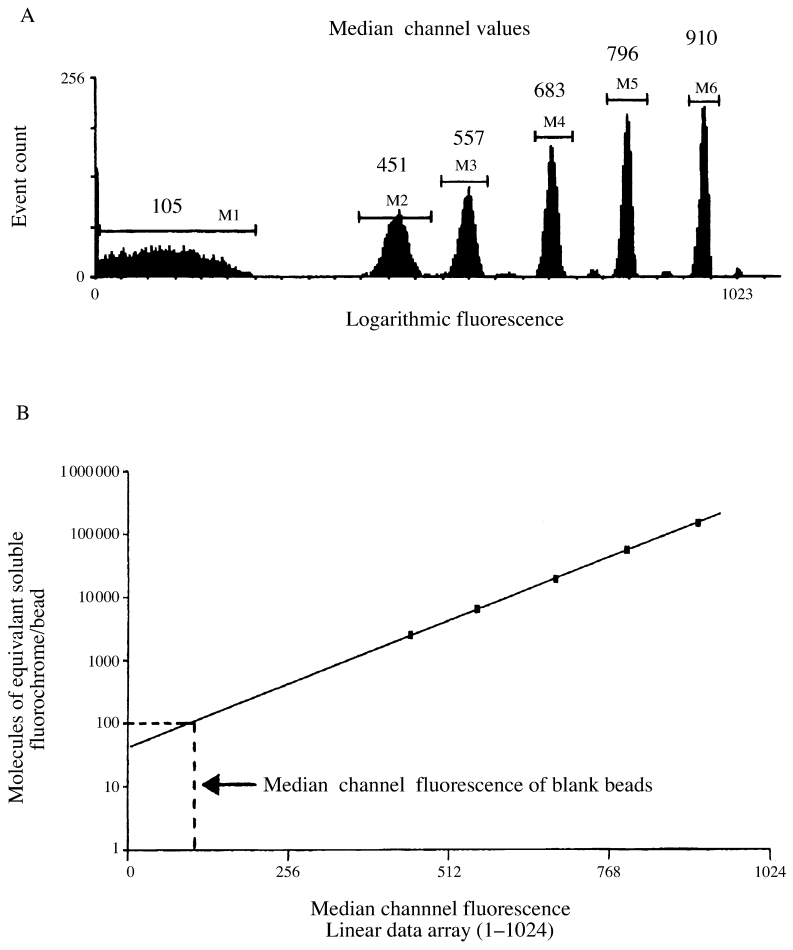

Fig. 5.8 (A) Multiparameter fluorescent beads are analysed with logarithmic acquisition and linear data array. (B) The correlation between median channel linear data array of logarithmically amplified fluorescence and molecules of soluble fluorochrome/bead as defined by the bead manufacturer.

ADC. Figure 5.8A shows the fluorescent histogram of a typical multibead reagent after logarithmic amplification but arrayed in linear fluorescence channels. The linear median channel fluorescence for each bead population is given above each peak and these can be plotted on linear–logarithmic graph paper against the quoted fluorochrome concentration for each bead, as supplied by the manufacturer. The plot of these beads is shown in Fig. 5.8B.

Using CD3 expression before and after PMA treatment as an example, Fig. 5.9A shows the initial CD3 expression histogram with the linear data array channels resolved to 1024, giving a median channel fluorescence value of 590 channels. From Fig. 5.8B, the standardised fluorescence intensity of 8000 molecules of equivalent soluble fluorochrome (MESF) can be derived by interpolation from the line. Figure 5.9B shows the same array of the sample after PMA treatment and gives a median channel fluorescence of 427 channels. Interpolation of this

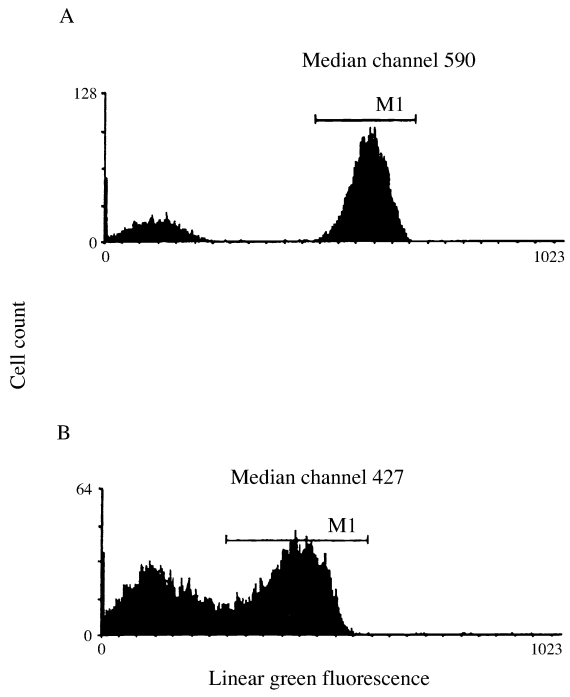

Fig. 5.9 (A) The expression of CD3 on lymphocytes prior to culture with phorbol myristrate acetate. (B) The decrease in expression of CD3 after culture. The equivalent numbers of molecules of soluble fluorochrome bound by the cells before and after treatment with phorbol myristrate acetate can be determined by interpolation with the calibration curve illustrated in Fig. 5.8. Please see text for full details.

channel value gives a standardised fluorescence of 2000 MESF, a reduction of 6000 MESF or 75% as we found before.

A final word of caution is appropriate when considering measurements of relative fluorescent intensity. One should control for changes in cell size. For example, in many publications attempts are made to compare antigen densities between resting cells and activated cells or between normal cells and leukaemic blasts of the same lineage. In both cases, the two cell populations are likely to be of different size and will, therefore, innately scatter more or less light in the 90° axis, the angle over which fluorescent emissions are collected. Figure 5.10 shows the background fluorescent signals from two bead

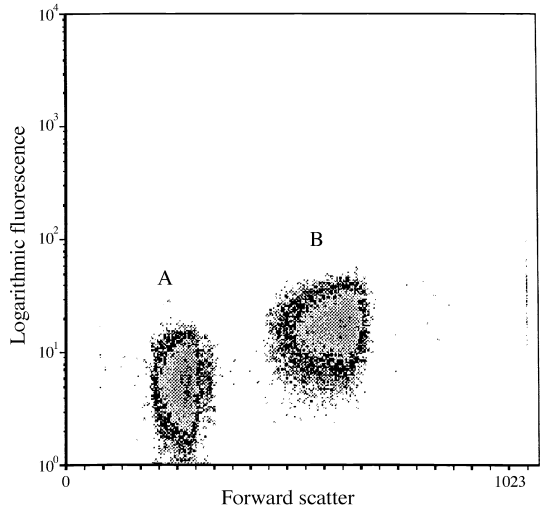

Fig. 5.10 The effect of size on fluorescent signals from otherwise identical unlabelled particles (A are 6 μm and B 9 μm in diameter).

populations. The 'A' beads are 6 μm latex particles that have not been labelled with any fluorochrome. The 'B' particles are 9 μm beads of the same latex material. Plainly the background fluorescence is higher from the larger beads. This can be taken into account by comparing the ratio of background fluorescent signals with the ratio of the antigen-specific signals of the two cell populations, but the mathematics are not straightforward. One should be pragmatic in such circumstances and realise that marginal differences in fluorescence intensities between two cell populations can be affected by several factors and be cautious of over-interpreting data in such a setting.

Relative fluorescent intensities can be measured both on a single instrument and in a standardised manner across multiple instruments and data can be derived in terms that are meaningful to fellow biologists. The 'holy grail' in this field is the calculation of absolute numbers of molecules on the cell surface, and some reagents are available that come close to allowing this. Commercial bead preparations are available that have predetermined numbers of antibody-binding sites on their surface and can be incubated with a fluorochrome-conjugated

monoclonal antibody of choice to determine specific levels of fluorescence. Using a standard curve such as that in Fig. 5.8B, the number of binding sites can be calculated for the same monoclonal antibody on cell populations and hence the number of molecules of antibody bound per cell ligand. Unfortunately, things are never this simple. The monoclonal antibody binds to the reference beads via its Fc site. It binds to its ligand via Fab and the binding coefficient is likely to be entirely different. Furthermore, some monoclonal antibodies bind in a monovalent fashion while others can bind divalently. At least one manufacturer has produced monovalent and divalent preparations from the same clone and has shown them to produce entirely different results with regard to antigen density studies. One can only conclude that the holy grail still eludes us but the CellQuest (a terrible pun that will be recognised by users of BD Biosciences instruments) continues and we await the definitive reagents.

5.9 Conclusions

Flow cytometers are powerful tools for the investigation of many aspects of cell biology and can generate extremely robust data. These data are, however, only as good as the experimental design and the analytical processes applied to them. Some of the common pitfalls in both these areas have been discussed here but there are many more; professional cytometrists, like all good scientists, should be critical of their data. A relevant paraphrase from the British politician Benjamin Disraeli would be: 'There may be three types of deceit – lies, damned lies and flow cytometry'!

5.10 REFERENCES

Borowitz, M.J., Bray, R., Gascoyne, R., Melnick, S., Parker, J.W., Picker, L., Stetler-Stevenson, M. (1998) US–Canadian consensus recommendations on the immunophenotypic analysis of hematologic neoplasia by flow cytometry: data analysis and interpretation. *Cytometry* **30**, 236–44.

Keeney, M., Gratama, J.W., Chin-Lee, L.H., Sutherland, D.R. (1998) Isotype controls in the analysis of lymphocytes and $CD34^+$ stem and progenitor cells by flow cytometry – time to let go! *Cytometry* **34**, 280–3.

Nicholson, J.K.A., Stetler-Stevenson, M. (1998) Quantitative fluorescence: to count or not to count. Is that the question? *Cytometry* **34**, 203–4.

Schmid, I., Uittenbogaart, C.H., Keld, B., Giorgi, J.V. (1994) A rapid method for measuring apoptosis and dual colour immunofluorescence by single laser flow cytometry. *Journal of Immunological Methods* **170**,145–57.

Shapiro, H.M. (1994) *Practical Flow Cytometry,* 3rd edn, pp. 307–8. Wiley-Liss, New York.

Stelzer, T.G., Marti, G., Hurley, A., McCoy, P. Jr, Lovett, E.J., Schwartz, A. (1997) US–Canadian consensus recommendations on the immunophenotypic analysis of hematologic neoplasia by flow cytometry: standardization and validation of laboratory procedures. *Cytometry* **30**, 214–30.

Watson, J.V., Chambers, S.H., Smith, P.J. (1987) A pragmatic approach to the analysis of DNA histograms with a definable G1 peak. *Cytometry* **8**, 1–8.

Young, I.T. (1977) Proof without prejudice: use of the Kolmogorov–Smirnov test for the analysis of histograms from flow systems and other sources. *Journal of Histochemistry and Cytochemistry* **25**, 935–41.

6

Laser scanning cytometry: application to the immunophenotyping of hematological malignancies

Richard J. Clatch

Highland Park Hospital, Highland Park, IL, USA

6.1 General considerations for the immunophenotyping of leukaemias and lymphomas

Immunophenotypic analysis of hematological specimens is a useful laboratory adjunct to surgical pathology and cytology to confirm or characterise further diagnoses of leukaemia or lymphoma (Duque and Braylan, 1991; Knowles et al., 1992; Sun, 1993; Willman, 1992). In a generic sense, immunophenotypic analysis can pertain to any type of tumour or tissue; but for the purposes of this chapter, discussion will be confined to hematological and lymphoreticular specimens. Methods of immunophenotyping vary most significantly in the type of detection system used to ascertain the occurrence of antigen–antibody binding, and the instrumentation used to observe or quantify that binding. The most common detection systems used for immunophenotyping are based on fluorescence and enzymatic histochemistry. Instrumentation ranges from flow cytometry to laser scanning cytometry, to epifluorescence microscopy, to immunohistochemistry and bright-field light microscopy. Before describing the techniques of laser scanning cytometric immunophenotyping, we will first examine certain technical aspects of the various existing methodologies, so that the reader may choose the method best suited to the clinical or research purpose at hand.

The optimal method should be capable of assessing multiple antigens simultaneously. Simultaneous assessment of at least two and, better yet, even three or four antigens on individual cells permits definitive identification of different populations and subpopulations of cells within a particular specimen. For example, in the quantitative analysis of helper and suppressor T-cells, it is mandatory to have first defined the population of T lymphocytes in general, apart from all other cell types. Similarly, this is true in the assessment of κ- and λ-light chains of immunoglobulins on B lymphocytes, which is currently by far the most useful means of evaluating B-cell clonality. Most immunofluorescence systems, such as immunophenotyping by flow cytometry or laser scanning cytometry, can easily assess three or four antigens simultaneously.

By comparison, immunohistochemical means of immunophenotyping hematological or lymphoreticular specimens suffer in that at most two antigens can be assayed simultaneously. Moreover, in current clinical practice, immunohistochemistry is almost always a single antigen assay, making conclusions regarding the inter-relationship of different antigens incumbent on the microscopist based on cytological and architectural morphology.

It is also important for clinical immunophenotyping that reliable antibodies are available which are specific for the antigens to be tested. Moreover, antibodies must be available for those antigens in whatever state (fresh, fixed, dried, etc.) a particular method demands. In this regard, methods designed to work on fresh unfixed and undried cells have a distinct advantage simply because of the overwhelming abundance of available antibodies. With time, as antibody development progresses, as many

antibodies may be available to formalin-fixed cluster of differentiation (CD) antigens, as there are antibodies to fresh CD antigens today.

Another important consideration in designing or choosing a method of clinical immunophenotyping is the ability to assess small specimens. In the realm of hematopathology, fine needle aspiration biopsies of lymph nodes and other masses, hypocellular body fluids, hypocellular bone marrows, biopsies of skin, and endoscopic biopsies of gastrointestinal or mucosal tissues are becoming more and more common. Methods that require millions of cells for analysis are simply not suitable for many of these specimens. Moreover, because of the interpretative limitations of cytology alone, it is precisely with such limited specimens that immunophenotypic analysis can often prove to be of greatest diagnostic value (Clatch and Walloch, 1997; Hanson, 1994; Pitts and Weiss, 1992).

One additional, and potentially very important, attribute of certain clinical immunophenotyping methods is the ability of the method to correlate antigen expression with cell and/or tissue structure. This is the realm in which immunohistochemistry truly shines; at least for correlation with cell morphology. Laser scanning cytometric immunophenotyping is also particularly advantageous. Although subtle, lymph nodes do have architecture, and this is extremely important in the assessment of potential lymphoid neoplasms. Tissue architecture is also extremely important in evaluating lymphoid infiltrates in nonlymphoid organ systems such as the skin or gastrointestinal tract. Unfortunately, apart from frozen sections, good light microscopical assessment of tissue morphology requires formalin fixation and paraffin embedding, which can often mask or destroy important hematological antigens. This limitation will only be overcome when antibodies specific for formalin-fixed antigens become available. In clinical situations where correlation of individual cell immunophenotype and architectural morphology is imperative, immunohistochemistry is the only practically viable solution. Laser scanning cytometry does offer the ability to correlate antigen expression with cell structure but, as yet, it has not been adapted to tissue applications for clinical purposes. Consequently, simultaneous multiparameter immunophenotyping on tissue sections stained for light microscopy using a broad array of antigens (as are available for flow cytometric and other laser scanning cytometric applications) remains impossible.

Another important characteristic of immunophenotyping is its sensitivity for detecting weakly expressed antigens or subtle differences in antigen density expression between different populations of cells. In this arena, immunofluorescence and automation are invaluable. Immunofluorescence systems, compared with immunohistochemical systems, are generally linear because (at least for direct systems) there is no amplification built into the detection means. That is, fluorescence intensity can be stoichiometrically related to antigen density. However, immunofluorescence requires the use of complex instrumentation to excite the fluorochromes, and the fluorescence intensity and spectral characteristics of those fluorochromes are often outside the limited detection capabilities of the naked human eye. Immunohistochemistry generally results in accumulation of an easily visible chromogen overlying the positive tissues but because enzymes are utilised as a means of amplifying the signal, the stoichiometric relationship is lost and subtle distinctions in antigen density are often not possible.

Additional considerations in evaluating clinical immunophenotyping methods include issues such as simplicity, time and cost. All three technologies – immunohistochemistry, flow cytometry and laser scanning cytometry – have evolved to become quite simple and reliable, but there are significant cost differences. Laser scanning cytometry and flow cytometry require the purchase of expensive capital equipment, whereas the capital equipment necessary for automated immunohistochemistry is significantly less expensive. Once capital equipment has been purchased, reagent costs become the driving economic factor and reagent usage for most laser scanning cytometric methods is small compared with that of either flow cytometry or immunohistochemistry.

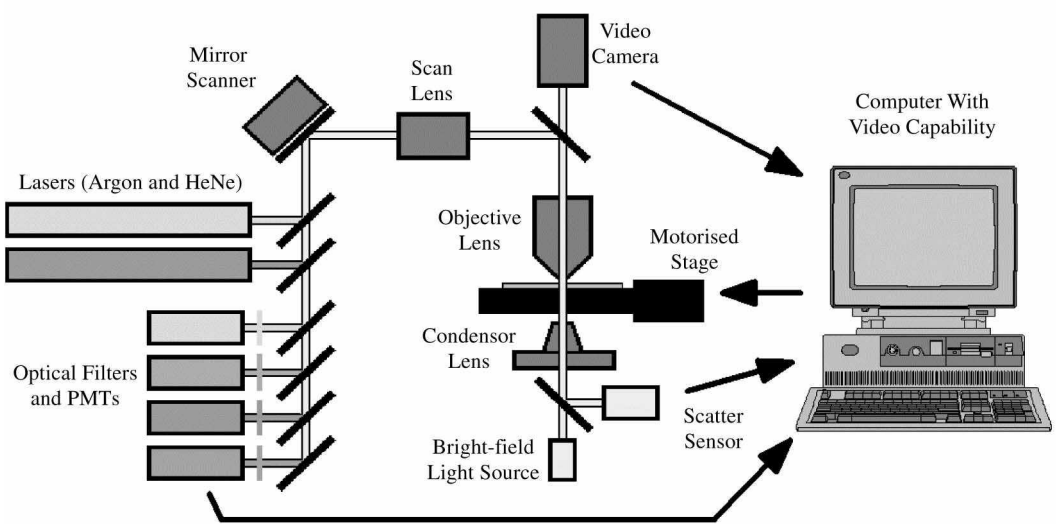

Fig. 6.1 Block diagram illustrating the components of a laser scanning cytometer. He–Ne, helium–neon; PMT, photomultiplier tubes.

The discussions in the subsequent sections of this chapter will be confined to laser scanning cytometric immunophenotyping techniques, which can vary quite markedly as the clinical or research needs demand.

6.2 The laser scanning cytometer

Laser scanning cytometry is a relatively new laboratory technology, most similar to flow cytometry. In both laser scanning cytometry and flow cytometry, cells treated with one or more fluorescent reagents are interrogated by a laser beam, with light scatter and emitted fluorescence at multiple wavelengths rapidly measured to determine multiple features of the cells. The principal difference between the two technologies is that for laser scanning cytometry the cells are located on a solid surface such as a glass slide, whereas for flow cytometry the cells are in a fluid suspension. A block diagram of the laser scanning cytometer is shown in Fig. 6.1.

For most applications including immunophenotyping, flow cytometry and laser scanning cytometry both primarily utilise an argon laser with an excitation wavelength of 488 nm. In flow cytometry, the cells flow past the laser beam in a flow cell and exit to a waste container. In laser scanning cytometry, the cells are measured and retained on a solid support such as a glass slide. The position of the slide and laser beam are simultaneously moved under computer control such that all cells within a specific area on the slide are interrogated. For both flow cytometry and laser scanning cytometry, emitted fluorescence is divided into wavelengths via filters and dichroic mirrors and collected by a set of fluorescence sensors, usually photomultiplier tubes. In the flow cytometer there are also routinely two light scatter detectors, one of which collects light scattered in the forward angle, and the other of which collects 90° (right angle) scattered light. Within the laser scanning cytometer, there is only a forward angle light scatter detector.

Laser optics for both flow cytometry and laser scanning cytometry are purposefully designed to be nonconfocal in order to illuminate entire cells uniformly and thereby obtain accurate measurements of whole cell features. However, also by design, laser scanning cytometry has significantly increased spatial resolution compared with flow cytometry.

Flow cytometry derives only a single feature value for each of the fluorescence and light scatter parameters for each cell. Laser scanning cytometry initially collects much more information, subsequently derives several feature values per parameter and does all this in a different manner. This can be advantageous, but a major consequence is that laser scanning cytometry is significantly slower than flow cytometry.

In flow cytometry, each fluorescent and light scatter parameter is initially measured as a single electronic signal, which is integrated over time to produce a single feature value for each parameter per cell. This is effectively a zero-order resolution imaging system. The simplicity of this system and the design of the flow cell make flow cytometric data collection extremely fast.

Data collection in laser scanning cytometry differs significantly. For a detailed description, the reader is referred to Kamentsky and coworkers (Kamentsky and Kamentsky, 1991; Kamentsky et al., 1997a,b) but a brief description is offered here. Within the area of the slide to be analysed, data are initially collected with a spatial resolution of approximately 0.5 μm and a dynamic range of 14 bits (0–16 383). For each parameter, 768 000 (768 × 1000) pixels of such information are temporarily collected. In real-time as data are being collected, the computer software contours individual cells by finding and segmenting clusters of adjacent pixels that are brighter than the surrounding background. This contouring operation occurs for only one of the fluorescence or scatter parameters as chosen by the user. The contouring threshold and certain other controlling aspects of the contouring operation (such as minimum cell size) are also defined by the user. The contours so defined are translated to the other noncontouring parameters so that a list of features for each cell can be determined. For the contouring parameter, the feature list includes:

- the peak pixel value within the contour (range 0–4095)
- the integrated value of the contour (range 0–16 383 multiplied by the number of pixels within the contour)
- the area of the contour (the number of pixels within the contour)
- the *x*- and *y*-positions of the contour's peak pixel value (in micrometres)
- the perimeter of the contour (in micrometres)
- the computer clock time when the measurement was taken
- a binary tag determining if the event represents more than one cell.

For the noncontouring parameters, each cell has feature values of only:

- the peak pixel value within the contour
- the integrated value of the contour.

These data are stored in a list mode data file format, and the original 768 000 pixel measurements (for each parameter) are discarded before the process begins anew for the next adjacent area on the slide. This relatively complex process of data acquisition limits laser scanning cytometry to data collection rates of approximately 1000 cells per second. For most laser scanning cytometry applications, this is actually approximately 100 cells per second. Nevertheless, this is sufficiently fast for most purposes, including immunophenotyping of hematological specimens. In addition, the fact that the cells are fixed in known locations on a solid surface creates interesting possibilities and advantages for laser scanning cytometry relative to flow cytometry.

Both data collection and analysis are accomplished through a single Windows-compatible software program (WinCyte) developed specifically for the laser scanning cytometer. Data are stored in a *.fcs list mode file format, and through the WinCyte software or other flow cytometry software the data can be displayed and manipulated. Scattergrams or histograms can be created to inter-relate any of the collected cell features, with gating, colouration and statistics provided all at the control of the analyst.

Although completely unnecessary for the integral functioning of the laser scanning cytometer, certain enhancements to the microscope within the laser scanning cytometer are standard and quite valuable. These include a colour, high-resolution charge-coupled device (CCD) camera and an

epifluorescence illumination system. Addition of a 35 mm conventional camera is also possible. The video signal from the colour CCD camera is connected to a video capture card within the laser scanning cytometer computer, making it possible to capture light microscopic or epifluorescence images of individual cells that have been relocalised based on user-defined cell features. Another possibility, because the cells remain in fixed locations, is that slides can be reanalysed at a later time with a different laser excitation wavelength, or after being stained in a different fashion. The feature values from each run can be combined for each cell on the slide using position as the merge key. Therefore, it is feasible with laser scanning cytometry to make multiple kinetic measurements of individual (potentially viable) cells, or to expand the number of cellular features beyond the initial limitation of a given number of light scatter and photomultiplier fluorescence sensors.

6.3 Immunophenotyping by laser scanning cytometry

6.3.1 Development and description of the method

In designing a method of immunophenotyping for laser scanning cytometry, certain fundamental issues must be addressed. Issues to be considered include the following:

- how to do the immunofluorescence reactions?
- how to get the specimen on the slide?
- how to contour?
- how to gate?
- how to minimise compensation requirements?
- how to stain for light microscopy and relocalisation?

Many of these issues are inter-related, but each will be discussed in turn to illustrate the features of our preferred method of immunophenotyping and to highlight other possibilities. In order to decide how the immunofluorescence reactions should be performed, one must examine the nature of the specimen to be tested. Most important, is the specimen fresh or is it dried, fixed or paraffin-embedded? Fresh specimens, or suspensions thereof, offer the tremendous advantage that antigenicity is virtually undisturbed, making the antigen–antibody reactions reliable without antigen retrieval techniques or amplification. Even so, fresh specimens might be reacted with antibodies in a number of different ways. Cell suspensions may be reacted with antibodies in test tubes, microtitre wells or reaction chambers built into slides. Of course, different physical systems will have different advantages and disadvantages.

There is a wide variety of different types of dried or fixed specimen. They may include cytospin preparations, touch and smear preparations, paraffin-embedded tissue sections or frozen sections. Depending on the exact preparation, specific antigens will remain intact to a greater or lesser degree, and the investigator must take this variability into account. In most cases, some type of antigen retrieval technique and/or amplification of the signal will be required. Additionally, particularly for hematological specimens, there are far fewer antibodies available for dried or fixed antigens than for fresh antigens. However, dried or fixed specimens do potentially offer advantages because, at least for tissue sections, architectural tissue relationships are not necessarily lost. Nevertheless, for a clinical method of immunophenotyping hematological specimens, we decided to assay specimens fresh prior to any fixation steps (Clatch et al., 1998). That is, suspensions of fresh unfixed cells in saline were reacted with antibodies in a fashion closely analogous to conventional flow cytometry techniques.

Clinical specimens may include peripheral blood, bone marrow aspirates, body fluids, solid tissue biopsies and fine needle aspiration biopsies; they are treated initially using methods similar to those used for flow cytometric immunophenotyping. The goal for all specimens is to obtain a suspension of dissociated leukocytes with relatively few contaminating red blood cells. Red blood cells can be removed from bloody specimens using either Ficoll®–Hypaque density centrifugation or ammonium chloride lysis techniques (see Ch. 2). Solid tissue biopsies

can be mechanically disaggregated by pressing the specimen through a 200 μm stainless steel mesh with the plunger of a syringe. Unless they are particularly bloody, body fluid and fine needle aspiration biopsy specimens often require virtually no preparation apart from counting the leukocytes present and making an appropriate dilution.

Because of the nature of laser scanning cytometry, the specimen must eventually be placed on a solid surface, such as a glass slide, for analysis. Even if the immunofluorescence reactions are performed on suspensions of fresh unfixed cells in test tubes, the cells must eventually be placed on a slide. This might be accomplished in several ways, some of which result in subsequent drying of the cells, potentially compromising pH or chemically sensitive fluorochromes as well as the integrity of the antigen–antibody complexes themselves. Cytospin, touch or smear preparations offer some advantages in that individual cells are fixed in location on the slide to be analysed, and methods for subsequent light microscopic staining are well established. However, drying and/or fixing cells, even after the immunofluorescence reactions have already occurred, significantly compromises the fluorescence signals from many fluorochromes particularly the large and complex molecules such as phycoerythrin (PE) that are widely utilised in flow cytometric applications (R. J. Clatch, unpublished observations). Therefore, methods were developed wherein the specimen was always maintained in an aqueous environment, not only for the immunofluorescence reaction, but also afterwards during specimen analysis (Clatch et al., 1998).

Once a specimen has been reacted with antibodies and is located on a slide or other solid surface, the means of cell contouring needs to be defined. As described above, cell contouring is a critical step in any form of laser scanning cytometry. Contouring must be based on one of the fluorescence parameters or on the scatter parameter. Fluorescence might reflect binding of a fluorochrome-conjugated antibody (i.e. immunofluorescence) or it might reflect binding of a fluorochrome that, by its chemical nature, binds to some cellular constituent. A great many laser scanning cytometric applications use red fluorescence from the dye propidium iodide (PI), which binds nucleic acids, as the contouring parameter (Clatch and Walloch, 1997; Clatch et al., 1997a,b; Darzynkiewicz et al., 1998; Furuya et al., 1997; Gorczyca et al., 1997a,b; Hanson, 1994; Juan and Darzynkiewicz., 1998; Kamentsky et al., 1997b; Li and Darzynkiewicz, 1995; Li et al., 1995, 1996; Martin-Reay et al., 1994; Numa et al., 1996; Reeve and Rew, 1997; Sasaki et al., 1996). For most applications, PI fluorescence is an excellent choice because all nucleated cells can be intensely stained, making the contouring operation very robust and simple. Also, when used in combination with RNAase, PI stoichiometrically binds DNA, making analysis of cell ploidy and proliferation possible. Working with tissue culture and cytospin preparations, other investigators have shown that it is possible to differentiate leukocyte subsets one from another, and to differentiate cells in different phases of the cell cycle, using only PI staining and laser scanning cytometric analysis with PI-based contouring (Bedner et al., 1997; Gorczyca et al., 1996; Kakino et al., 1996; Kawasaki et al., 1997; Luther and Kamentsky, 1996).

However, for the purposes of immunophenotyping hematological specimens, PI-based contouring has a great many drawbacks. First and foremost, PI is a very bright and broadly fluorescent fluorochrome, dominating the orange, red and even the long red wavelengths. It is quite simple to perform one-colour immunophenotyping using a single fluorescein isothiocyanate (FITC)-conjugated antibody in combination with PI fluorescence as the contouring parameter. However, additional antibodies conjugated to fluorochromes such as PE, PE–Cyanin5 (PE–Cy™5) and others would be totally useless in such a system. Therefore, if the goal is to perform multiparameter (two- or three-colour) immunophenotyping of hematological specimens, PI fluorescence cannot be used as the contouring parameter. Furthermore, PI requires permeabilisation of the cells, and in some cases this may also affect antigenicity.

Immunofluorescence might also be used as the

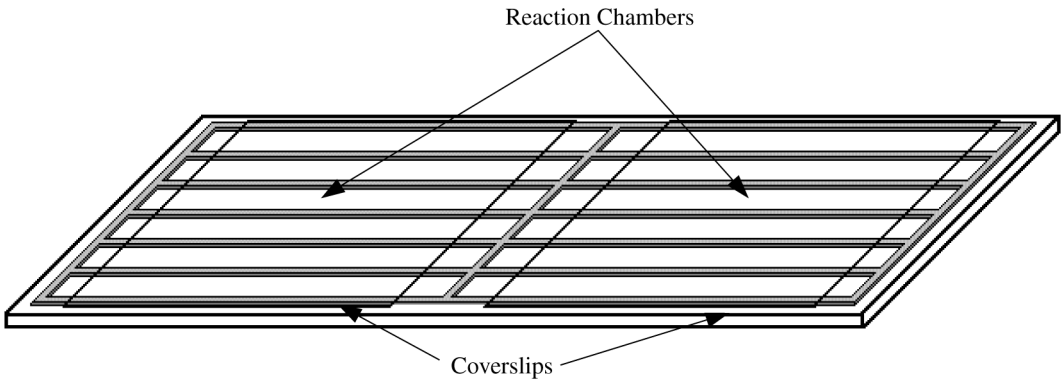

Fig. 6.3 A chamber slide used for immunophenotyping. Coverslips that are a little shorter than the length of the chambers are used so that liquids can be added and removed at the ends of the chambers.

contouring parameter provided that the antibody chosen for contouring reliably binds all leukocyte subsets of interest. CD45 antibodies seem the most likely candidates for most applications, although pan-T-cell, pan-B-cell, and other antibodies might also be used in specific circumstances. Indeed, we have used CD3, CD14, CD15, CD20 and CD45 antibodies conjugated to FITC, PE or PE–Cy™5 in several experimental circumstances with excellent results. However, for routine purposes in a clinical immunophenotyping laboratory, what seems most desirable is a parameter that reliably contours all cells regardless of their type without obstructing any fluorescence wavelength. Although there are certain limitations, as described below, light scatter provides such a contouring parameter (Fig. 6.2 (colour plate)).

Using light scatter, all cells within a specimen regardless of their type can be reliably contoured and good cell size determinations made. The limitations and difficulties of using light scatter as the contouring parameter, which are manageable (R. J. Clatch, unpublished observations), are described below. First, the use of light scatter requires that the specimen be located on a transparent solid surface such as glass slide because the light scatter detector measures laser light scattered in the forward direction through the slide itself. For strictly fluorescence applications, it would be possible to use opaque solid surfaces although these would also prohibit bright-field microscopy. Second, the use of forward scatter dictates that the specimen be overlaid by a coverglass to control the refractive interface as the laser strikes the specimen. Third, unlike the fluorescence signals, which have been purposefully designed to be focus insensitive, good light scatter-based contouring is quite sensitive to focus, making it imperative that the stage and slide are level (orthogonal to the laser beam). Fourth, because scatter is a simple physical property of all cells and many particles, undesired events such as red blood cells and platelets may also be contoured. Under most circumstances, these undesired events can be effectively gated out during data analysis, but if the number of these events is overwhelming relative to the number of leukocytes, data acquisition may be compromised or impossible without additional specimen purification to remove the undesired constituents.

At this juncture, it is most useful to describe the first method that was developed for immunophenotyping hematological specimens and the subsequent refinements that led to the method which is now in use. Suspensions of lymphoreticular or other hematological cells were divided into portions and reacted with FITC-, PE- and PE–Cy™5- conjugated monoclonal antibodies, washed by centrifugation, resuspended in an appropriate volume of phosphate-buffered saline (PBS), pipetted onto glass slides, and covered with a slip. Such

'drop preparations' of immunostained lymphoreticular cells were analysed using the laser scanning cytometer, contouring on light scatter, to generate immunofluorescence scattergrams directly comparable to those of flow cytometry. This enabled a systematic comparison to be made of this laser scanning cytometric 'drop preparation' method with conventional flow cytometry on 71 consecutive clinical hematological specimens (Clatch et al., 1997a). While successful, the first method did not take full advantage of the capabilities of the laser scanning cytometer, mostly because the cells were not fixed in specific locations on the slide and were simply 'floating' under the coverglass. Attempts to remove the coverglass and stain the cells for light microscopic examination were completely unsuccessful because the cells washed away or changed location. Clearly what was necessary was an entirely different means of affixing the cells to the slide, without the complications of drying or fixation. Therefore, a specialised chamber slide, as shown in Fig. 6.3, is now used.

These chamber slides are integral to our current and preferred method of immunophenotyping, as well as to several extensions of the method to be described later in this chapter. Each slide has 12 individual chambers measuring 27 mm × 2 mm × 260 μm, with each chamber thereby defining a volume of 14 μl. In order to use these chamber slides optimally, it is necessary that (after disaggregation and red blood cell removal as may be necessary) specimens are optimally diluted in PBS without serum or protein additives to an approximate concentration of 4000 cells μl^{-1} or less. Depending on the specimen's original cellularity, dilutions may be made as low as 400 cells μl^{-1} without compromising the number of antibodies to be tested. If desired, viability can be assessed using trypan blue dye exclusion. All of the 12 chambers are individually filled with 16 μl (slightly overfilling each chamber to allow for some drying) of the diluted and purified cell suspension (equating to 6400–64 000 cells per chamber). The dry chambers fill very easily through capillary action. The slide is then stored for 15 min at room temperature in a humidified chamber. During this time, the leukocytes settle by gravity and adhere firmly by an electrostatic interaction with the bottom glass surface of the chambers. Thereafter, various monoclonal antibody combinations can be pipetted into each of the chambers, displacing the original fluid by slightly inclining the slide and absorbing the effluent with a paper towel or other absorbent material. To allow for some dead space and intrachamber mixing, we routinely use 18 μl prediluted antibody combinations for each chamber. The antibodies used are triple combinations of FITC, PE and PE–Cy™5 conjugates diluted 1 : 10 in PBS. In this way it is possible to react a single specimen with 36 different antibodies on a single slide. However, for gating and other comparative purposes, there is usually some redundancy of the antibodies tested in typical lymphoma or leukaemia panels, as shown in Table 6.1.

The cells adherent within the chambers of the slide are allowed to react with the antibody combinations for 30 min at 4 °C in a humidified chamber. Then, the chambers of the slide are all washed simultaneously by passing 200 μl PBS through each end of the chamber slide twice, 1 min apart.

The slide is then placed onto the stage of the laser scanning cytometer, which has been programmed to scan automatically a rectangular area within the centre of each of the chambers. Individual cells are contoured based on light scatter. Green, orange and long-red fluorescence are subsequently assessed for each cell with all results stored in a single list mode data file. Currently only approximately 10% of the entire area of each chamber is scanned. Data acquisition for all 12 chambers takes a total of approximately 25 min, with the data for each chamber covering between approximately 600 and 6000 cells depending on cellularity. For extremely hypocellular specimens, enlarging the scan area within each chamber provides a means of easily increasing the number of cells assayed. The current method of clinical immunophenotyping recommended for laser scanning cytometry by the author (Clatch et al., 1998) is given in outline form in Protocol 6.1.

Table 6.1 *Antibody panels used for clinical immunophenotyping*

Lymphoma/CLL panel			Acute leukaemia panel		
FITC	PE	PE–Cy™5	FITC	PE	PE–Cy™5
CD3	CD20	CD45	CD3	CD20	CD45
HLA-DR	CD20	CD45	CD10	CD19	CD45
CD5	CD19	CD45	κ-Light chain	CD19	CD45
CD10	CD19	CD45	λ-Light chain	CD19	CD45
κ-Light chain	CD19	CD45	CD7	CD20	CD45
λ-Light chain	CD19	CD45	HLA-DR	CD34	CD45
CD19	CD23	CD45	CD13	CD34	CD45
FMC7	CD25	CD45	CD13	CD34	CD45
CD8	CD4	CD45	CD11c	CD34	CD45
CD7	CD56	CD45	CD14	CD34	CD45
CD16	CD2	CD45	CD41	CD34	CD45
CD11c	CD14	CD45	TdT	CD34	CD45

CLL, chronic lymphocytic leukaemia; FITC, fluorescein isothiocyanate; HLA-DR, human leukocyte antigen DR; PE, phycoerythrin; Cy™5, Cyanin™5; TdT, terminal deoxynucleotidyl transferase.

Protocol 6.1 Immunophenotyping by laser scanning cytometry

Samples

- Blood and bone marrow: lyse red cells first.
- Solid tissues: disaggregate by pressing through a 200 μm stainless steel mesh; also filter through a 80 μm nylon mesh if necessary.

Method

1. Load specimens into slide; use 6400 to 64 000 cells in 16 μl per chamber.
2. Add chosen combinations of pre-diluted FITC-, PE- and PE–Cy™5-conjugated antibodies.
3. Incubate at 4 °C for 30 min.
4. Wash twice with 200 μl PBS.

Analysis

Analyse on laser scanning cytometer contouring on forward light scatter.

Data analysis, gating, and compensation are accomplished within the WinCyte software in a fashion directly analogous to flow cytometry. For gating purposes, it is most practical to include PE–Cy™5–conjugated CD45 as one component of all the antibody combinations (R. J. Clatch, unpublished observations). A routine method of analysing clinical cases includes first displaying all cells from all 12 chambers in a single scattergram inter-relating cell size and CD45 expression. Lymphocytes, neutrophils, monocytes, maturing myeloid cells and blasts are normally well separated in this scattergram, allowing only cells of interest to be gated and passed to other scattergrams (Fig. 6.4 (colour plate)).

The gated cells are next displayed in a scattergram showing their locations on the slide (possible because the *x*- and *y*-positions are part of the list mode data file). This effectively provides a map of the chamber slide itself (Fig. 6.5 (colour plate)).

The 12 rectilinear regions created in this cell location scattergram allow data from each of the chambers to be passed to one of 12 individual scattergrams reflecting binding of the FITC- and PE-conjugated antibodies that are unique for each chamber. Figure 6.6 (colour plate) shows, for two patients, three scattergrams representing binding of

basic lymphocyte-specific antibodies. At the top, cells from a patient with a benign condition are benign T and B lymphocytes obtained from a reactive lymph node. The bottom three scattergrams also show a lymph node with mixture of T and B lymphocytes but here the B-cells monotypically express κ-light chains rather than the λ-light chain of surface membrane immunoglobulin, indicative of a clonal B-lineage lymphoproliferative disorder such as non-Hodgkin's lymphoma.

6.3.2 Examples of immunophenotyping results

Example immunophenotyping results from two additional clinical cases are shown in Figs. 6.7 and 6.8.

Figure 6.7 (colour plate) shows the results from a fine needle aspiration biopsy of a left cervical lymph node from a 41-year-old woman who presented to medical attention complaining of lymphadenopathy of several weeks' duration. The lymph node was easily palpable and tender, and a fine needle aspiration biopsy was performed using a 25 gauge hypodermic needle and no anaesthesia. Approximately 350 000 total lymphoid cells were obtained and processed routinely for the possibility of lymphoma using the antibody panel shown in Table 6.1. As shown in Fig. 6.7, there was a single well-defined population of small to medium-sized moderately to strongly $CD45^+$ cells, which were gated (as shown on the left) and subsequently displayed within the 12 separate FITC versus PE scattergrams (shown to the right). In this example, the colouration of each of the FITC versus PE scattergrams is based solely on the quadrants drawn for the individual scattergrams, with negative cells coloured black, FITC-positive cells coloured green, PE-positive cells coloured red and dual FITC-positive and PE-positive cells coloured blue. The colouration within the cell size versus PE–Cy™5–CD45 scattergram is a reflection of that within the FITC–CD3 versus PE–CD20 scattergram, effectively showing T-cells in green and B-cells in red. The minor population of larger $CD45^+$ cells seen in the cell size versus CD45 scattergram is composed of doublets. The immunophenotyping results in this case are clearly benign. There is a mixed population of T and B lymphocytes with a cell ratio of approximately 1.25 : 1. The T-cells correctly express all pan-T-cell antigens and are appropriately divided into $CD4^+$ and $CD8^+$ subpopulations with an increased ratio of approximately 17 : 1. The B-cells are also antigenically normal without aberrant expression of CD5 or CD10 and there is good polyclonal expression of both κ- and λ-light chains in surface membrane immunoglobulin. Combined with the cytological assessment of the smears stained with Wright–Giemsa and Papanicolou stains, these immunophenotypic findings strongly supported a benign reactive cause for the patient's lymphadenopathy, which, in fact, spontaneously resolved several weeks after the biopsy.

The second example shown in Fig. 6.8 (colour plate) is a peripheral blood specimen from a patient with acute myeloid leukaemia. The specimen was obtained from a 37-year-old woman presenting with purpura. A complete blood count showed a marked leukocytosis with a white blood cell count of 35 000 μl^{-1} ($35 \times 10^9\ l^{-1}$) with a manual differential showing approximately 50% morphologically undifferentiated blasts. The specimen was treated with ammonium chloride to remove red blood cells and processed for immunophenotyping using the acute leukaemia panel shown in Table 6.1. The gating in this case is slightly more complex. The cell size versus CD45 scattergram shows at least three well-defined populations of cells. By experience, one can surmise that the smaller more brightly $CD45^+$ cells (coloured green) are benign lymphocytes. The larger moderately $CD45^+$ cells (coloured blue) are most likely mature and maturing myeloid and/or monocytoid cells. The relatively large population of medium-sized weakly $CD45^+$ cells (coloured red) are most likely the blasts. In this example, the colouration is more conventional in that the colours are defined by the bitmaps drawn within the cell size versus CD45 gating scattergram and transposed into the various FITC versus PE scattergrams. The immunophenotyping data clearly show that the suggested origins of the three cell populations are indeed correct. There is a relatively minor popula-

Table 6.2 *Comparative merits of immunophenotyping by flow and laser scanning cytometry*

Flow cytometry
Allows more precise gating of cell populations by employing both forward and side light scatter
Counts more cells and the analysis is quicker
Laser scanning cytometry
A complete analysis can be obtained using only 64 000 cells
The methodology is simpler
Consumable costs are lower as antibody usage is reduced by $> 80\%$

Relocalisation enables the direct correlation of immunophenotyping results with cytology and fluorescence in situ hybridization

tion of lymphocytes, which are mostly T-cells ($CD2^+$, $CD3^+$, and $CD7^+$) and also a significant population of mature and maturing myelomonocytoid cells, which variably and weakly express CD10 and HLA-DR and moderately to strongly express CD11c and CD13. The blasts in this case strongly express HLA-DR and the human progenitor cell antigen CD34. They are moderately positive for the myeloid antigen CD13 but are negative for other myeloid, monocytoid, megakaryocytoid and lymphoid antigens. The diagnosis of acute myeloblastic leukaemia, subtype M2 in the French–American–British (FAB) staging was substantiated by cytochemical special stains showing myeloperoxidase and Sudan black positivity in some of the blast cells. Appropriate chemotherapy was begun. In several laser scanning cytometry laboratories, clinical immunophenotyping of this type has been performed with considerable success, for thousands of patients.

6.3.3 What are the advantages and disadvantages of laser scanning cytometry?

A brief comparison of the merits of flow cytometry and laser scanning cytometry for the purpose of clinical immunophenotyping is shown in Table 6.2.

Flow cytometry clearly has the advantage of speed and is the method of choice in situations where hundreds of thousand of cells need to be counted. Also, because of the addition of a side angle light scatter detector, gating of complex cell populations is more precise by flow cytometry.

Laser scanning cytometry is highly suited to the analysis of very small specimens such as fine needle aspiration biopsies and hypocellular body fluids. The method is remarkably simple to perform, and antibody usage is reduced by $>80\%$ compared with flow cytometric methods. As discussed in detail below, with laser scanning cytometry it is possible to relocalise individual cells after immunophenotyping, enabling direct correlation of antigenic characteristics, cytology and other cell features that may be apparent after special staining procedures such as fluorescence in situ hybridisation (FISH).

6.4 Extensions to the basic method

6.4.1 Relocalisation for light microscopy and fluorescence in situ hybridisation

Relocalisation is a relatively simple process that can be done at any time following the immunophenotyping procedure from minutes to months after analysis. Following data acquisition, the slide can be dismantled and the specimen fixed as desired with the rows of cells remaining adherent to the slide.

In certain clinical cases, we have found it very useful to fix and stain the slides for light microscopic examination, and then to relocalise individual cells based on their immunofluorescence (antigenic) characteristics. This relocalisation is accomplished automatically by the laser scanning cytometer upon placement of the stained slide onto the microscope stage.

Results from an interesting clinical case in which relocalisation proved to be useful are shown in Figs.

6.9 to 6.11. The specimen is a fine needle aspiration biopsy of a right parotid mass from a 13-year-old boy . The most significant immunophenotyping results are shown in Fig. 6.9 (colour plate).

There are three distinct populations of lymphoid cells within the specimen. The first is one of T lymphocytes and constitutes approximately 30% of all lymphoid cells in the specimen. The T-cells correctly express the pan-T-cell antigens CD3 and CD5 and are appropriately divided into $CD4^+$ and $CD8^+$ subpopulations with a ratio of approximately 2:1. There is also a population of benign B lymphocytes constituting approximately 50% of the specimen. These B-cells moderately express the pan B-cell antigens CD19 and CD20, do not aberrantly express CD5 or CD10 and show good polyclonal expression of both κ- and λ-light chains of their surface membrane immunoglobulin. Last, there is a relatively minor population of clonal B-cells that more strongly express CD19 and CD20, weakly and aberrantly express CD10 and monotypically express κ- rather than λ-light chains in surface membrane immunoglobulin. After immuno-phenotyping, the slide was dismantled and stained with a Wright–Giemsa stain. Four of the strongly $CD20^+$ clonal B-cells and four of the $CD3^+$ T-cells were chosen for relocalisation as shown in Fig. 6.10 (colour plate).

The light microscopic images of these eight cells captured through the CCD camera of the laser scanning cytometer are shown in Fig. 6.11 (colour plate).

The pathological diagnosis based on the morphology of the fine needle aspirate biopsy smears and the immunophenotyping results was Burkitt's lymphoma, and appropriate chemotherapy was begun.

After taking photographs or capturing video images, the slides can be destained and processed for FISH to demonstrate known or suspected chromosomal abnormalities. A brief account of the entire method that was developed, including immunophenotyping and relocalisation for light and epifluorescence microscopy, is given in Protocol 6.2.

Protocol 6.2 Immunophenotyping with relocalisation for light microscopy and fluorescence in situ hybridisation

Samples

Lysed red cells or disaggregated solid tissues

Method

1. Load specimens into slide; use 6400 to 64 000 cells in 16 μl per chamber.
2. Add chosen combinations of pre-diluted FITC-, PE- and PE–Cy™5-conjugated antibodies.
3. Incubate at 4 °C for 30 min.
4. Wash twice with 200 μl PBS.

Analysis

1. Analyse on laser scanning cytometer contouring on forward light scatter.
2. Stain slide for light microscopy; using Wright–Giemsa, hematoxylin and eosin, peroxidase–anti-peroxidase, etc.
3. Relocalise individual cells for light microscopy based on immunophenotype.
4. Destain and fix with methanol then with Carnoy's fixative.
5. Perform FISH.
6. Relocalise the same individual cells for epifluorescence microscopy.

Two interesting cases with known chromosomal abnormalities were chosen for relocalisation for light microscopy and FISH with the results shown in Figs. 6.12–6.15 and 6.17–6.20 (all colour plates). Samples from both patients were first subjected to full panel immunophenotyping and secondarily stained for light microscopy. Based on their antigenic characteristics, individual cells were relocalised and photographed under light microscopy. The slides were then hybridized in situ with fluorescent probes for the cytogenetic abnormalities in question, and the same cells again relocalised and photographed under epifluorescence microscopy. Figure 6.16

(colour plate) shows the use of computer-guided enhancement of this fluorescence.

The first of these two patients is a 67-year-old man with a marked lymphocytosis. Immunophenotypic analysis of peripheral blood showed a clonal population of B lymphocytes with a pattern of antigenicity highly characteristic of chronic lymphocytic leukaemia (Fig. 6.12 (colour plate)). The B-cells had diminished expression of CD20, strong and aberrant expression of CD5, weak but monotypic expression of λ- rather than κ-light chains in surface membrane immunoglobulin and preserved expression of CD23. Based on the FITC–CD5 versus PE–CD19 scattergram, three T lymphocytes and three B lymphocytes were selected for relocalisation. (Fig. 6.13).

The Wright–Giemsa staining of B-cells and T-cells are shown in the top and bottom rows, respectively, of Fig. 6.14 (colour plate). As might be expected, the morphological differences between the clonal malignant B-cells and the benign T-cells are relatively subtle.

The slide was subsequently destained and hybridised with a spectrum green-labelled probe specific for chromosome 3 and a spectrum orange-labelled probe specific for chromosome 12. The same six cells were again relocalised, in this case using epifluorescence microscopy, with the results shown in Fig. 6.15 (colour plate). The T-cells in the bottom row all have two green probe spots and two red probe spots, indicating that they are normal diploid cells. The three B-cells in the top row all have two green probe spots and three red probe spots, indicating that they are positive for the trisomy (12) chromosomal abnormality that is relatively common in B-lineage chronic lymphocytic leukaemia.

The epifluorescence images shown in Fig. 6.15 (colour plate) have been artificially enhanced by a simple computerised method (Fig. 6.16 (colour plate)). The individual green and red fluorescence images from a single cell are first amplified and then each is broken into its individual green and red components. The red component of the red epifluorescence image is combined with the green component of the green epifluorescence image to yield a single image in which both the red and green probe spots are clearly visible, without the expense of complex optical systems.

The second example from a patient is shown in Figs. 6.17 to 6.21 (colour plates). The specimen is a bone marrow aspiration biopsy from a 48-year-old woman with a known history of chronic myeloid leukaemia who was complaining of increasing fatigue. Peripheral blood was initially drawn and shown to contain rare blast cells. A bone marrow aspiration and biopsy was then performed. The most relevant scattergrams of the immunophenotypic analysis performed on the bone marrow aspirate are shown in Fig. 6.17 (colour plate). The cell size versus PE–Cy™5–CD45 scattergram clearly shows four populations of cells. The large population of ungated relatively small $CD45^{-}$ cells are mostly nucleated erythroid cells that have escaped the ammonium chloride lysis procedure. The three other populations of coloured cells are gated to be included in the FITC versus PE immunophenotyping scattergrams shown at the bottom of Fig. 6.17 (colour plate). The small strongly $CD45^{+}$ cells (coloured green) are a nearly even mixture of T and B lymphocytes. The larger moderately $CD45^{+}$ cells (coloured blue) are mature and/or maturing myeloid cells, as evidenced by the variable but strong CD13 positivity. Lastly, the population of relative large but only weakly $CD45^{+}$ cells (coloured red) consists of myeloblasts. The blasts constitute between 6–8% of all non-erythroid cells based on this analysis and moderately express the human progenitor cell antigen CD34, strongly express HLA-DR and weakly to moderately express the myeloid antigen CD13.

The patient had a known t(9;22) translocation (Philadelphia chromosome), which provided an opportunity to demonstrate the ability of the laser scanning cytometer to relocalise individual cells for light and epifluorescence microscopy. Based on the CD13 versus CD34 scattergram (Fig. 6.18 (colour plate)), three myeloblasts and three benign lymphocytes were chosen for relocalisation after staining for light microscopy. The cells stained with Wright–Giemsa are shown in Fig. 6.19 (colour plate)

with the myeloblasts in the top row and the lymphocytes in the bottom row.

After destaining and further fixation, the slide was reacted with a spectrum green probe for chromosome 9 and a spectrum orange probe for chromosome 22, and the same six cells relocalised under epifluorescence (Fig. 6.20 (colour plate)). The blasts in the top row clearly have colocalised green and red probe spots indicative of the t(9;22) translocation, whereas the lymphocytes in the bottom row do not. Interestingly, the acid fixation necessary for FISH has resulted in the apparent enlargement of the lymphocyte images in the bottom row.

These capabilities of laser scanning cytometry are of interest not only because of their novelty, but also for their potential usefulness in medical research and clinical diagnosis. Because individual cells can be automatically relocalised, it is simple to correlate subtle variabilities in antigen expression within a population of tumour cells with any potentially corresponding cytogenetic or morphological variability. A knowledge of tumour heterogeneity is now considered essential for understanding tumour evolution and evaluating potential therapies and both of these should benefit from this technology. For clinical purposes, the method may be most applicable to the detection of residual disease after chemotherapy or radiation therapy. Without complex sorting techniques, it is relatively simple to determine, for example, whether the small percentage of $CD34^+$ blasts that may be present in a patient's bone marrow following induction chemotherapy represents normal regenerating marrow precursors or residual acute leukaemia. To enhance sensitivity while retaining the capabilities of full-panel immunophenotyping and relocalisation for light and epifluorescence microscopy, it would also be relatively simple to substitute an in situ polymerase chain reaction (PCR) in place of the FISH procedure. Such work is now in progress.

6.4.2 Multipass and multiplex systems

As described above, three-colour immunophenotypic analysis of hematological specimens is easily performed using the laser scanning cytometer. It can be accomplished in a single scan pass using the argon laser and a combination of antibodies bound to three fluorochromes such as FITC, PE and PE–Cy™5. An alternate fluorochrome combination such as PE, PE–Texas Red® conjugate (PE–TR), and PE–Cy™5 works equally well, but with somewhat greater compensation requirements. Regardless of the fluorochrome combination chosen, in order to achieve simultaneous three-colour immunophenotypic analysis with a single laser and a single scan pass, it is necessary to rely on light scatter-based contouring of the cells in the specimen. This is true because of the wide fluorescence emission spectral characteristics of PI and the many other DNA-binding dyes that are often used for contouring purposes in laser scanning cytometry applications.

Because, for most laser scanning cytometry applications, the locations of individual cells within a specimen remain fixed, it is a simple matter to scan the same specimen more than once using the same laser and different experimental conditions, or even using a different laser. Algorithms built into the software of the laser scanning cytometer enable merging of individual computer data files created using different experimental conditions or lasers, such that all the separate fluorescence and physical measurements obtained can be simultaneously inter-related during data analysis. This process of merging separate data files collected for a single specimen at different times is designated as a multipass system. The laser scanning cytometer also has a built-in 'multiplex' capability that enables different lasers to be used in the collection of a single data file. For multiplex systems, corresponding fields of raw uncontoured data (768 000 pixels) are sequentially collected with each of the two lasers, one at a time, and then merged in real-time. As a result, a laser scanning cytometer equipped with both helium–neon (He–Ne) and argon lasers and the WinCyte software enables more than three colours to be used when performing immunophenotypic analysis.

The He–Ne laser is optimally suited to excite the

Table 6.3 *Multipass system of five-colour immunophenotyping plus DNA content analysis by laser scanning cytometry*

Laser	Pass 1 helium–neon	Pass 2 argon	Pass 3 argon
PMT 1	Orange	Orange	Green
	–	PE, Ab 2 (CD4)	FITC, Ab 5 (CD8)
PMT 2	Red	Red	Red[a]
	–	PE–TR, Ab 3 (CD19)	PI, DNA content
PMT 3	Far-red	Far-red	–
	Cy™5, Ab 1 (CD45)	PE–Cy™5, Ab 4 (CD3)	–
PMT 4	Scatter[a]	Scatter[a]	–

Ab, antibody; Cy™5, Cyanin™5; FITC, fluorescein isothiocyanate; PE, phycoerythrin; PI, propidium iodide; PMT, photomultiplier tube; TR, Texas Red®.
[a] Contouring parameter.

fluorochrome Cy™5. This fluorochrome is available conjugated to anti-mouse immunoglobulin antibodies and, therefore, is an optimal secondary immunofluorescent reagent to use with the He–Ne laser. Unfortunately, few if any other fluorochromes appropriate for use with the He–Ne laser (most desirably with longer Stokes' shifts) are commercially available. Nevertheless, because Cy™5 alone does not excite with the argon laser, multiplexing or a simple two scan-pass system (one pass with the He–Ne laser and another with the argon laser) makes four-colour immunophenotypic analysis possible. Cellular contouring for both scan passes would be based on light scatter.

The current laser scanning cytometer has four fluorescence photomultiplier tubes and one light scatter detector. However, because of the design of the laser scanning cytometer's electronics, data collection can simultaneously occur from only four of the total of these five input sources. Since one of these must be utilised for the light scatter-based contouring parameter, in any individual scan pass it is only possible to collect three fluorescence parameters simultaneously. However, as described above, there are at least four fluorochromes (commercially available bound to antibodies) with sufficiently distinct emission spectral characteristics to work very well with the argon laser: specifically FITC, PE, PE–TR, and PE–Cy™5. Because of the limitation in the number of available input channels, in order to collect fluorescent data for all four of these fluorochromes, it is necessary at present to make two separate passes with the argon laser, each scan pass with a different optical configuration defining the photomultiplier tubes.

Although at first glance cumbersome, the necessity of this second scan pass with the argon laser can be put to further advantage by using the second pass to also collect fluorescence data defining cellular DNA content. This can be simply accomplished by reacting PI with the specimen between the two argon laser scan passes. The PI fluorescence is so bright that any residual fluorescence of PE, PE–TR, or PE–Cy™5 that may remain is inconsequential. Thus, a three scan-pass system as shown in Table 6.3 accomplishes five-colour immunophenotyping plus DNA content analysis using only a single sample.

The results from an actual experiment using this three scan-pass system are shown in Fig. 6.21 (colour plate) (Clatch and Foreman, 1998). Peripheral blood leukocytes were purified by lysing the red blood cells with ammonium chloride. The leukocytes were then placed into a single chamber of an immunophenotyping chamber slide and simultaneously reacted with a combination of five different fluorochrome-conjugated antibodies: Cy™5–CD45, PE–Cy™5–CD3, PE–TR–CD19, PE–CD4 and FITC–CD8. After washing unbound antibody from the chamber, the slide was scanned

twice, first with the He–Ne laser and second with the argon laser. Then the cells in the chamber were permeabilised with 70% ethanol and subsequently reacted with PI (50 μg ml^{-1}) with RNAase in PBS. After again washing unbound reagents from the chamber, and after changing the optical filters defining the photomultiplier tubes, the slide was scanned again with the argon laser. The individual data files from these three scan passes were merged in the WinCyte software, and the data were analysed and displayed as shown in Fig. 6.21 (colour plate). Beginning with a total of 4809 merged peripheral blood leukocytes, 1448 (30%) lymphocytes were gated based on CD45 positivity. Of the lymphocytes, 957 (66%) were $CD3^+$ T-cells, and 241 (25%) were $CD8^+$ T-cells. As to be expected, the gated $CD8^+$ T-cells were shown to be diploid with a DNA index of 1.0.

One advantage of laser scanning cytometry relative to flow cytometry, which was at first unrecognised and discovered during the course of these experiments, is the ability to minimise the unwanted artifacts of spectral crossover between fluorescence channels that are typically addressed through mathematical or instrument compensation. Because the optical design of the laser scanning cytometer is similar to that of modern flow cytometers, compensation requirements and methods are similar to those used for flow cytometric applications and single laser scan-pass laser scanning cytometric applications. In the three scan-pass system that has just been described for five-colour immunophenotyping plus DNA content analysis by laser scanning cytometry (Clatch and Foreman, 1998), spectral crossover is particularly problematic for orange light from the bright PE fluorochrome contaminating (crossing over into) the red photomultiplier channel used for the relatively dim PE–TR fluorochrome. In flow cytometers, such problems can only be addressed through mathematical or instrument compensation or by using multiple lasers and different fluorochromes. In laser scanning cytometry, because the same cells within an individual specimen can be scanned over and over again at will, a problem of this kind can be solved simply by resorting to an additional scan pass, the data from which can be merged with that from former and subsequent passes.

For example, since there is no compensation problem relative to the Cy™5 and PE–TR fluorochromes (because different lasers are used to excite them), the antibodies bound to these two fluorochromes can be added simultaneously to the specimen to begin the experiment. A first scan pass with the He–Ne laser collects immunofluorescence data relative to the Cy™5-conjugated antibody. A second scan pass with the argon laser collects immunofluorescence data relative to the PE–TR-conjugated antibody regardless of PE-induced spectral crossover because PE is not present in the specimen at this time. After a subsequent reaction with FITC-, PE- and PE–Cy™5-conjugated antibodies (for which compensation requirements are significant but easy to manage), a third scan pass with the argon laser is made. Because the PE–TR fluorochrome is relatively dim compared with PE and PE–Cy™5, there is little if any problem with spectral crossover in this direction. After this third scan pass, the specimen is reacted with PI and RNAase. A fourth scan pass with the argon laser effects DNA content analysis. This four-scan pass system also eliminates any requirement to compensate FITC and PI, as is necessary with the three-scan pass system described above.

Although these experimental techniques are somewhat tedious and time consuming, they are not technically demanding and serve well to highlight the potential capabilities of the laser scanning cytometry technology for any number of scientific applications requiring the analysis of multiple cellular constituents on a single population of cells. Of course, after analysis, the specimen can be stained for light or epifluorescence microscopy as desired, and individual cells meeting user-defined fluorescent or physical parameters can be individually relocalised for cytological examination.

6.5 Conclusions

Modern diagnostic categorisation of hematological

neoplasms is increasingly dependent on special laboratory methods to characterise the antigenicity or phenotype of the cells in question. Currently, this is most often accomplished by one of two methods: flow cytometry or immunohistochemistry. Immunohistochemistry is invaluable when it is necessary to correlate tissue architecture with antigenic features. Flow cytometry precludes this correlation but allows innumerable antigens to be tested because the antigen–antibody reactions occur prior to fixation or drying and because so many antibodies are commercially available. Laser scanning cytometry is a practical alternative method of immunophenotyping hematological specimens, with some advantages relative to flow cytometry and immunohistochemistry. Most important of these are the adaptability of the technology to very small clinical specimens and the capability to relocalise individual cells for microscopic examination after immunophenotyping. Immunophenotyping by laser scanning cytometry has been extended to include sequential light microscopy and epifluorescence microscopy for FISH. The technology has also been adapted to multipass systems, greatly increasing the potential number of antigens that can be sequentially assayed and simultaneously reducing compensation problems. Laser scanning cytometry provides many new research opportunities in hematology and molecular and cell biology, and it has immediate practical relevance for clinical immunophenotyping of small specimens.

6.6 INTERNET SITES

http://www.compucyte.com/

Home page of CompuCyte, manufacturers of the laser scanning cytometer. Contains information on recent developments, applications and protocols.

6.7 REFERENCES

Bedner, E., Burfeind, P., Gorczyca, W., Melamed, M.R., Darzynkiewicz, Z. (1997) Laser scanning cytometry distinguishes lymphocytes, monocytes, and granulocytes by differences in their chromatin structure. *Cytometry* **29**, 191–6.

Clatch, R.J., Foreman, J.R. (1998) Five-colour immunophenotyping plus DNA content analysis by laser scanning cytometry. *Communications in Clinical Cytometry* **34**, 36–8.

Clatch, R.J., Walloch, J.L. (1997) Multiparameter immunophenotypic analysis of fine needle aspiration biopsies and other hematologic specimens by laser scanning cytometry. *Acta Cytologica* **41**, 109–22.

Clatch, R.J., Walloch, J.L., Zutter, M.M., Kamentsky, L.A. (1997a) Immunophenotypic analysis of hematologic malignancy by laser scanning cytometry. *American Journal of Clinical Pathology* **105**, 744–55.

Clatch, R.J., Walloch, J.L., Foreman, J.R., Kamentsky, L.A. (1997b) Multiparameter analysis of DNA content and cytokeratin expression in breast carcinoma by laser scanning cytometry. *Archives of Pathology and Laboratory Medicine* **121**, 585–92.

Clatch, R.J., Foreman, J.R., Walloch, J.L. (1998) Simplified immunophenotyping by laser scanning cytometry. *Communications in Clinical Cytometry* **34**, 3–16.

Darzynkiewicz, Z., Bedner, E., Traganos, F., Murakami, T. (1998) Critical aspects in the analysis of apoptosis and necrosis. *Human Cell* **11**, 3–12.

Duque, R.E., Braylan, R.C. (1991) Applications of flow cytometry to diagnostic hematopathology. In: Coon, J.S., Weinstein, R.S. (eds.), *Diagnostic Flow Cytometry*, pp. 89–102. Williams & Wilkins, Baltimore, MD.

Furuya, T., Kamada, T., Murakami, T., Kurose, A., Sasaki, K. (1997) Laser scanning cytometry allows detection of cell death with morphologic features of apoptosis in cells stained with PI. *Cytometry* **29**, 173–7.

Gorczyca, W., Melamed, M.R., Darzynkiewicz, Z. (1996) Laser scanning cytometer (LSC) analysis of fraction of labelled mitoses (FLM). *Cell Proliferation* **29** 539–47.

Gorczyca, W., Darzynkiewicz, Z., Melamed, M. (1997a) Laser scanning cytometry in pathology of solid tumors. A review. *Acta Cytologica* **4**, 98–108.

Gorczyca, W., Sarode, V., Juan, G., Melamed, M., Darzynkiewicz, Z. (1997b) Laser scanning cytometric analysis of Cyclin B1 in primary human malignancies. *Human Pathology* **10**, 457–62.

Hanson, C.A. (1994) Fine-needle aspiration and immunophenotyping: a role in diagnostic hematopathology? *American Journal of Clinical Pathology* **101**, 555–6.

Juan, G., Darzynkiewicz, Z. (1998) Detection of cyclins in individual cells by flow and laser scanning cytometry. *Methods in Molecular Biology* **91**, 67–75.

Kakino, S., Sasaki, K., Kurose, A., Ito, H. (1996) Intracellular localization of cyclin B_1 during the cell cycle in glioma cells. *Cytometry* **24**, 49–54.

Kamentsky, L.A., Kamentsky, L.D. (1991) Microscope-based multiparameter laser scanning cytometer yielding data comparable to flow cytometry data. *Cytometry* **12**, 381–7.

Kamentsky, L.A., Burger, D.E., Gershman, R.J., Kamentsky, L.D., Luther, E. (1997a) Slide-based laser scanning cytometry. *Acta Cytologica* **41**, 123–43.

Kamentsky, L.A., Kamentsky, L.D., Fletcher, J.A., Kurose, A., Sasaki, K. (1997b) Methods for automated multiparameter analysis of fluorescence in situ hybridized specimens with a laser scanning cytometer. *Cytometry* **27**, 117–25.

Kawasaki, M., Sasaki, K., Satoh, T., Kurose, A., Kamada, T., Furuya, T., Murakami, T., Todoroki, T. (1997) Laser scanning cytometry (LSC) allows detailed analysis of the cell cycle in PI stained human fibroblasts (TIG-7). *Cell Proliferation* **30**, 139–47.

Knowles, D.M., Chadburn, A., Inghirami, G. (1992) Immunophenotypic markers useful in the diagnosis and classification of hematopoietic neoplasms. In: Knowles, D.M. (ed.), *Neoplastic Hematopathology*, pp. 73–167. Williams & Wilkins, Baltimore, MD.

Li, X., Darzynkiewicz, Z. (1995) Labelling DNA strand breaks with BrdUTP. Detection of apoptosis and cell proliferation. *Cell Proliferation* **28**, 571–9.

Li, X., Traganos, F., Melamed, M.R., Darzynkiewicz, Z. (1995) Single-step procedure for labeling DNA strand breaks with fluorescein- or BODIPY-conjugated deoxynucleotides: detection of apoptosis and bromodeoxyuridine incorporation. *Cytometry* **20**, 172–80.

Li, X., Melamed, M.R., Darzynkiewicz, Z. (1996) Detection of apoptosis and DNA replication by differential labeling of DNA strand breaks with fluorochromes of different colour. *Experimental Cell Research* **222**, 28–37.

Luther, E., Kamentsky, L.A. (1996) Resolution of mitotic cells using laser scanning cytometry. *Cytometry* **23**, 272–8.

Martin-Reay, D.G., Kamentsky, L.A., Weinberg, D.S., Hollister, K.A., Cibas, E.S. (1994) Evaluation of a new slide-based laser scanning cytometer for DNA analysis of tumors: comparison with flow cytometry and image analysis. *American Journal of Clinical Pathology* **102**, 432–8.

Numa, Y., Matsudaira, K., Tsukazaki, H., Kawamoto, K., Sato, T., Kiyomatsu, Y. (1996) Analysis of cell nuclei and the quantity of chromosomal DNA by laser scanning cytometer (LSC). *Human Cell* **9**, 237–43.

Pitts, W.C., Weiss, L.M. (1992) The role of fine needle aspiration biopsy in diagnosis and management of hematopoietic neoplasms. In: Knowles, D.M. (ed.), *Neoplastic Hematopathology*, pp. 385–405. Williams & Wilkins, Baltimore, MD.

Reeve, L., Rew, D.A. (1997) New technology in the analytical cell sciences: the laser scanning cytometer. *European Journal of Surgical Oncology* **23**, 445–50.

Sasaki, K., Kurose, A., Miura, Y., Sato, T., Ikeda, E. (1996) DNA ploidy analysis by laser scanning cytometry (LSC) in colorectal cancers and comparison with flow cytometry. *Cytometry* **23**, 106–9.

Sun, T. (1993) *Colour Atlas-Text of Flow Cytometric Analysis of Hematologic Neoplasms*, pp. 3–8 (Instrumentation), pp. 18–25 (Classification of Hematologic Neoplasms) and pp. 206–11 (Sample Preparation). Igaku Shoin, New York.

Willman, C.L. (1992) Flow cytometric analysis of hematologic specimens. In: Knowles, D.M. (ed.), *Neoplastic Hematopathology*, pp. 169–95. Williams & Wilkins, Baltimore, MD.

7

Leukocyte immunobiology

Marion G. Macey

St Bartholomew's and Royal London School of Medicine and Dentistry, Queen Mary and Westfield College, London

7.1 Introduction to human leukocytes and leukocyte antigens

The most widely used application for flow cytometry must be the identification and enumeration of human leukocyte subpopulations. This has been facilitated by the measurement of cell surface antigens by immunofluorescence labelling using monoclonal antibodies. The leukocyte lineages express specific antigens on their cell surface that allow the different subpopulations to be identified. In some cases, a single antigen may be used to identify a specific cell type; in other cases, the presence of two or more antigens may be required to characterise a particular cell. Numerous monoclonal antibodies that bind to these specific antigens have been generated and grouped together based upon their specificity.

7.2 Monoclonal antibodies and clusters of differentiation

Since 1975 when Kohler and Milstein introduced a method for generating clones of hybrid cells capable of producing monospecific immunoglobulins in high titres, a multitude of different monoclonal antibodies have been generated recognising cell surface antigens. To organise these antibodies into a classification there have been, to date, seven international workshops, the aim of which has been to group antibodies into clusters based on their cellular reactivity. These clusters have been termed clusters of differentiation or CDs. After the seventh workshop, 247 CDs were defined (see Ch. 17) and these are shown in Table 17.2. The structure and function of the antigens for many of the CDs are now known.

7.3 Surface antigen changes during hematopoiesis

Multidimensional flow cytometric analysis has been used for the characterisation of hematopoietic cell differentiation and maturational pathways (Lansdorp, 1990; Loken et al., 1987a,b; Robinson et al., 1981; Terstappen et al., 1993). By the detection of gradual, coordinated changes in the expression of lineage-specific or lineage-associated cell surface and cytoplasmic antigens, it is possible to reconstruct the maturational pathways of hemopoietic cells. In addition, gradual changes in cell morphology may be assessed by forward light scatter, related to cell size (Brunsting and Mullany, 1974), and side light scatter, related to cell granularity (de Grooth et al., 1987; Salzman et al., 1975).

In a dual-parameter histogram of both light scatter parameters, peripheral blood neutrophils, eosinophils, basophils, monocytes, granular lymphocytes and nongranular lymphocytes each are located in typical positions (de Grooth et al., 1987; Macey et al., 1999; Terstappen et al., 1986). In normal bone marrow aspirates, the positions of each of these cell populations are similar to those in blood but are less distinct because of the presence of precursor cells of each of the cell lineages, with distinct light scattering properties. Figure 7.1A shows a typical example of forward and logarithmic side light scatter of normal human bone marrow cells. The

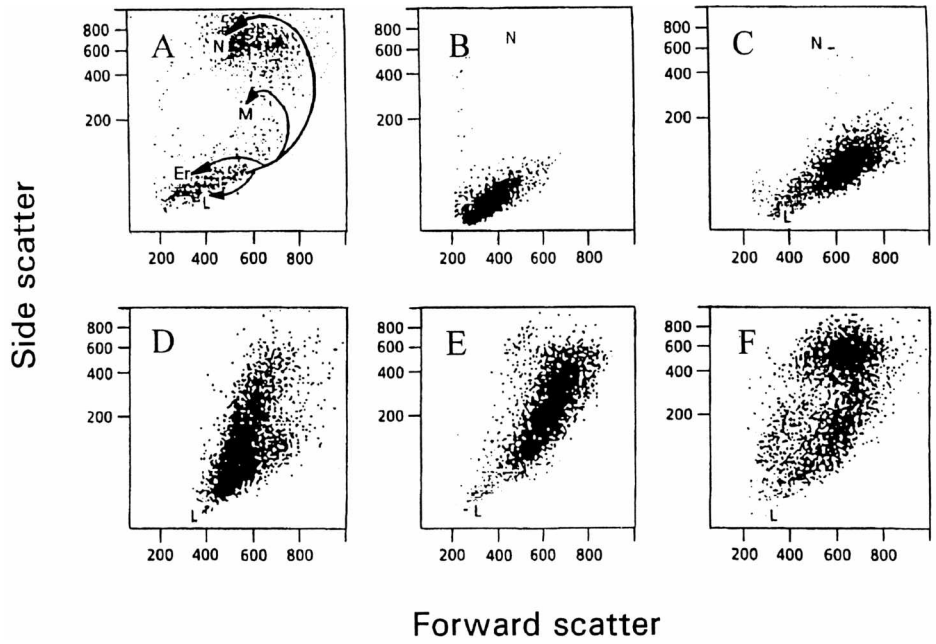

Fig. 7.1 Forward and side light scatter profiles of bone marrow aspirates from donors with (A) normal cells; (B) B-cell acute lymphoblastic leukaemia ; (C) acute myeloid leukaemia (AML FAB (French–American–British staging) M1); (D) AML (FAB M2); (E) AML (FAB M3); and (F) AML (FAB M4). The position of the neutrophils (N), monocytes (M), lymphocytes (L) and the erythrocytes (E) are indicated in the figures. The arrows indicate the pathway followed during the maturation of neutrophils, monocytes, B lymphocytes and erythrocytes in normal bone marrow.

arrows in the figure start at the position of the progenitor cells and follow the pathways ending at positions for the end maturational stages of neutrophils, monocytes, lymphocytes and erythrocytes. In contrast with normal bone marrow, the majority of cells from a patient with acute leukaemia are located in one specific light scatter region. The position of the predominant cell cluster in the scatter display varies considerably with the type of leukaemia, as illustrated for five patients in Fig. 7.1B–F (Terstappen et al., 1991a,b).

7.4 Progenitor cell differentiation

Normal bone marrow cells expressing the CD34 antigen represent a heterogeneous progenitor cell population of which most of the cells are committed to erythroid, lymphoid or monomyeloid cell lineages (Terstappen et al., 1991a). Lineage commitment of the $CD34^+$ bone marrow cells has been demonstrated by cell morphology, presence of lineage-specific or lineage-associated antigens and formation of colonies with lymphoid, myeloid or erythroid features. Cells with the phenotype $CD34^+CD38^{-/low}$HLA-DR^+ have been shown to contain the most immature hematopoietic progenitors (bright/high and dim/low are used synonymously). Upon maturation the cell surface expression of the CD34 antigen decreases and the expression of CD38 and of the lineage-associated antigens CD7, CD19, CD64 and CD71 increases on T lymphocytes, B lymphocytes, myeloid cells and erythroid cells, respectively (Olweus et al., 1994, 1995) (Fig. 7.2). The identification of $CD34^+$ progenitor cells by flow cytometry has become important in all stages of hematopoietic cell transplantation (Law et al., 1999) and several different sets of guidelines for their

Table 7.1 *Antigens associated with monocytoid maturation*

Myeloid stem cell	Myelomonocytic stem cell	Monocyte precursor	Monoblast	Promonocyte	Monocyte			Macrophage	
CD33	CD13	CD13	CD13	CD13	CD4	CD49f	CD121	CD11c	CD23
CD34	CD33	CD15	CD14	CD14	CD9	CD63	CD123	CD14	CD25
CD117	CD34	CD33	CD15	CD15	CD11b	CD64	CD127	CD16	CD69
CD123	CD115	CD115	CD33	CD33	CD11c	CD65	CD128	CD26	CD105
CD131	CD116	CD116	CD115	CD115	CD12	CD68	CD132	CD31	CD153
CD135	CD123	CD123	CD116	CD116	CD13	CD74	CD137	CD32	
CD151	CD131	HLA-DR	CD123	CD123	CD14	CD84	CD139	CD36	
HLA-DR	CD135				CD17	CD85	CD141	CD45RO	
	HLA-DR				CD31	CD86	CD148	CD45RB	
					CD32	CD87	CD149	CD63	
					CD33	CD89	CD155	CD68	
					CD35	CD91	CD156	CD71	
					CD36	CD92	CD162	CD74	
					CD38	CD93	CD164	CD87	
					CD40	CD98	CD165	CD88	
					CD43	CD101	HLA-DR	CD101	
					CD45	CD102	CD142[a]	CD119	
					CD49b	CD115	CD163[a]	CD121b	
					CD49e	CD119		CD163	

[a]Expressed on activation

quantification have been established (Gratama et al., 1998; see also Ch. 4). Maturation of the monomyeloid and lymphoid cells may be completed in the tissues and organs. T lymphoid development, in particular, occurs in the thymus. Because the phenotypes of the stem cells and the most primitive thymic precursors are different, it is assumed that the stem cell progeny traverse a number of cellular stages before they arrive in the thymus. The nature of these stages and the anatomical sites at which they develop are unknown. One potential transitional cell type has the phenotype $CD34^+CD10^+CD45RA^+$ and lacks antigens associated with mature lymphoid cells. These cells have common lymphoid progenitor (CLP) activity ($CD34^+CD10^+CD45RA^+$) as they possess the capacity to develop into all lymphoid lineages – T-, B-, natural killer (NK) and dendritic cell (DC) – but are unable to develop into myeloid and erythroid cells.

7.5 Myeloid maturation

One of the earliest antigens to appear on the cell surface of progenitor cells that differentiate into the myeloid lineage is sialoadhesion molecule CD33. Cells coexpressing CD33 and CD34 can give rise to burst-forming unit erythroid and colony-forming unit granulocyte–macrophage (Andrews et al., 1989, 1990). More recently, CD64 has been shown to be a granulocyte–monocyte lineage-specific antigen on $CD34^+$ hematopoietic progenitor cells (Olweus et al., 1995). Commitment to the erythroid lineage is accompanied by a loss of CD33 and the expression of the transferrin receptor (CD71) (Loken et al., 1987a). Differentiation of the myeloid cells into the monocyte and neutrophil lineages can be assessed by the differential expression of cell surface antigens, as shown in Tables 7.1 and 7.2. Early neutrophils (myeloblasts, promyelocytes) can be distinguished from cells differentiating along the monocyte lineage by their expression of CD15. In-

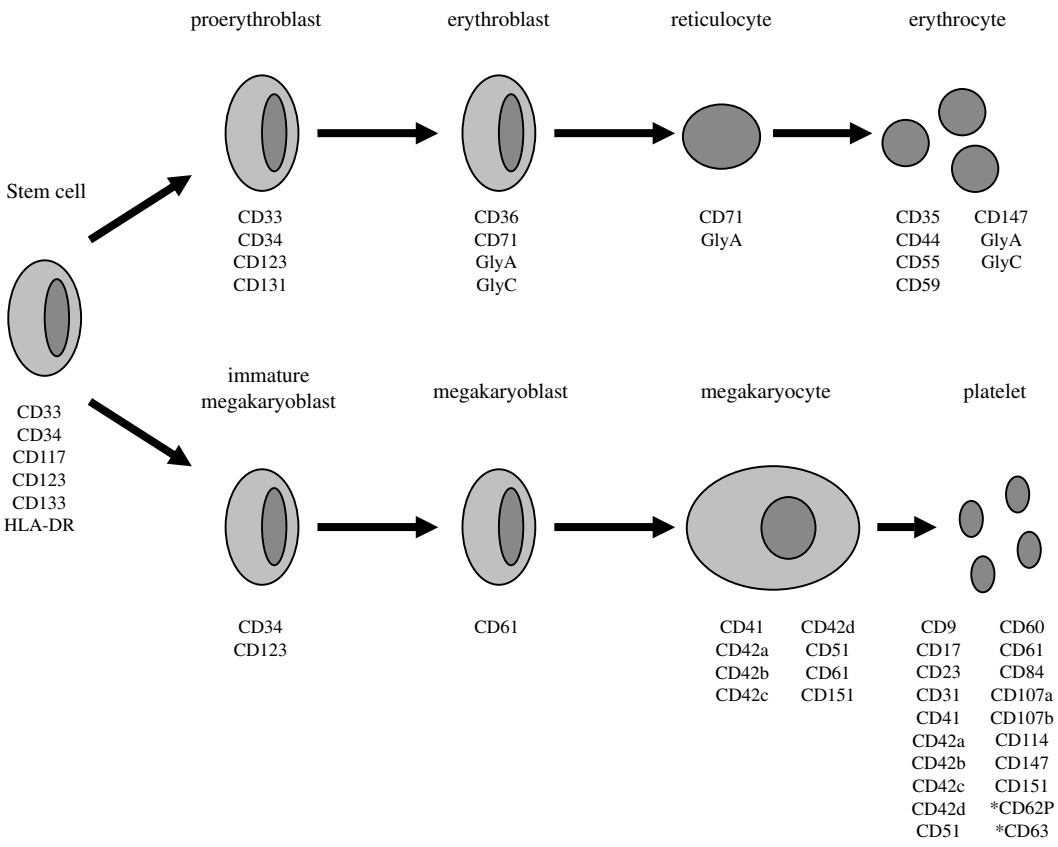

Fig. 7.2 Schematic illustration of erythroid and thrombocytoid maturation showing the antigens associated with differentiation.

creasing densities of the CD11b antigen occur during both neutrophil and monocyte maturation. Expression of both CD14 and CD16 occurs late during neutrophil maturation (bands, segmented neutrophils). The CD10 antigen present on early T and B lymphocytes appears on the neutrophils concurrently with the CD14 and CD16 antigens. To date, no cell surface antigens are found that specifically identify only the monocyte or neutrophil maturational pathways. Assessment of maturation of these lineages can, therefore, only be achieved by analysis combining various cell surface antigens with light scattering properties (Terstappen et al., 1990a,b).

7.6 B lymphocyte maturation

The signal transduction molecule CD19 is the earliest antigen to appear on the cell surface of progenitor cells that differentiate into the B lymphoid lineage and remains present throughout B lymphocyte maturation up to the final maturation into the plasma cells, at which stage it is lost (Terstappen et al., 1990c). CD10 in contrast to CD19 is not B lineage specific and appears on T-cell precursors and is expressed late in neutrophil development. The sequential expression of cell surface antigens and intranuclear terminal deoxynucleotidyl transferase expression during B lymphocyte maturation is schematically represented in Fig. 7.3. and the full

Table 7.2 *Antigens associated with myeloid maturation*

Myeloid stem cell	Myelomonocytic stem cell	Myeloid precursor	Myeloblast	Promyelocyte	Neutrophil		
CD33	CD13	CD13	CD13	CD13	CD10	CD52	CD132
CD34	CD33	CD15	CD15	CD15	CD11b	CD66a	CD139
CD117	CD34	CD33	CD33	CD33	CD11c	CD66c	CD141
CD123	CD115	CD116	CD38	CD116	CD12	CD66d	CD147
CD131	CD116	CD123	CD116	CD123	CD13	CD87	CD148
CD135	CD123	CD131	CD123	CD131	CD15	CD89	CD149
CD151	CD131	CD131			CD16b	CD92	CD151
HLA-DR	CD135	HLA-DR			CD17	CD93	CD153
	HLA-DR				CD24	CD101	CD156
					CD31	CD116	CD162
					CD32	CD123	CD14[a]
					CD35	CD128	CD63[a]
					CD43	CD131	CD64[a]

[a]Expressed on activation.

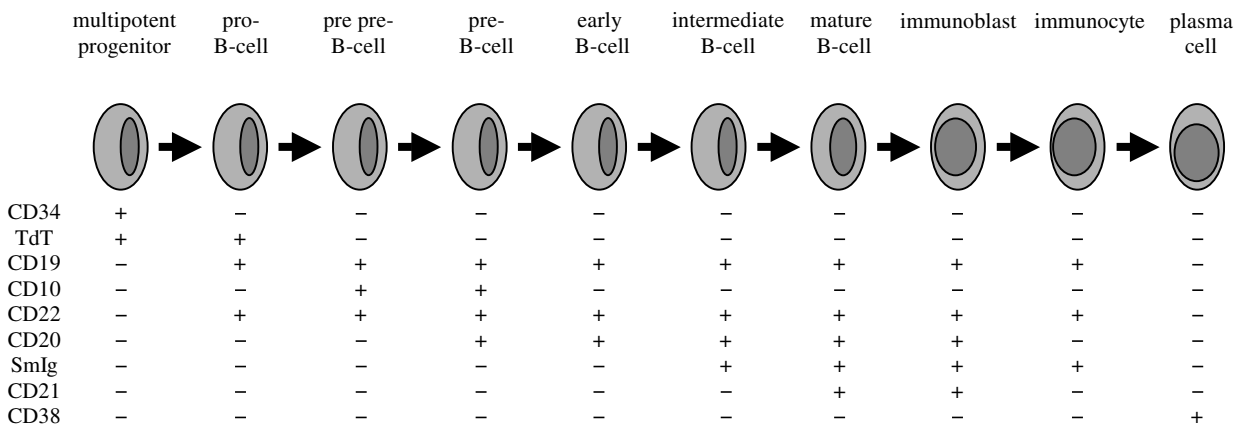

Fig. 7.3 Schematic representation of antigens associated with B-cell differentiation. Antigen-independent early stages leading to the formation of mature B-cells occurs in the human bone marrow. Antigen-dependent clonal proliferation and maturation to plasma cells occurs principally in the secondary lymphoid tissues and organs, lymph nodes, spleen and lymphoid follicles. Some plasma cells, particularly those involved in long-term antibody production to infectious disease, are found in bone marrow. Thus bone marrow can function as both a primary and a secondary lymphoid organ. smIg, surface membrane immunoglobulin; TdT, terminal deoxynucleotidyl transferase.

list of CDs associated with the B-cell lineage is given in Table 7.3.

7.7 T lymphocyte maturation

T-cells are derived from pluripotent stem cells that migrate from the primary lymphoid organs, the fetal liver and bone marrow to the thymus, where they develop into functional T-cells. While differentiating into T-cells, the progenitors traverse distinct cellular stages that can be discriminated on the basis of the expression of cell surface and cytoplasmic antigens. Within the thymus, multipotential progenitor cells rapidly restrict their developmental

Table 7.3 *Antigens associated with B-cell development*

Stem cell	Pro-B-cell	Pre-B-cell	Intermediate B-cell	Mature B-cell	
CD10	CD19	CD9	CD19	CD5C	CD85
CD34	cytCD22	CD10	CD20	CDw17	CD98
CD38	CD24	CD20	CD22	CD19	CD99
CD90	CD38	cytCD22	CD24	CD20	CD102
CD117	CD72	CD24	CD32	CD21	CD119
CD124	cytCD79a	CD38	CD35	CD22	CDw121b
CD127	cytCD79b	CD40	CD37	CD24	CD124
HLA-DR	CD81	CD72	CD40	CD32	CD138
TdT	CD124	CD74	CD48	CD35	smIgM
	CD135	cytCD79a	CD52	CD37	FMC-7
	CD139	cytCD79b	CD72	CD39	
	TdT	CD81	CD74	CD40	CD23[a]
		CD124	CDw76	CD48	CD25[a]
		CD135	CDw78	CD49b	CD30[a]
		CD139	cytCD79a	CD49c	CD69[a]
			cytCD79b	CD49c	CD70[a]
			CD80	CD52	CD80[a]
			CD85	CD72	CD83[a]
			CD99	CD74	CD124[a]
			CD124	CD78	CDw125[a]
			smIgM	cytCD79a	CD126[a]
				cytCD79b	CD139[a]
				CD80	CDw150[a]
				CD84	

cyt, cytoplasmic; smIgM, surface membrane IgM; TdT, terminal deoxynucleotidyl transferase.
[a]Expressed upon cell activation.

potential to become committed to the T-cell lineage by the initiation of rearrangements of the T-cell receptor (TCR) genes (Fig. 7.2). Recent studies with human thymocytes have provided some insight into the developmental stages of thymic T-cells.

In normal adult bone marrow the majority, if not all, of the T lymphocytes are mature T-cells expressing the T-cell receptor CD3 on the cell surface (Terstappen et al., 1992). In contrast, T-cell precursors can be readily identified in fetal bone marrow and are characterised by coexpression of CD34 with the T-cell-associated antigen CD7 (Res et al., 1996). The immunoglobulin superfamily member CD7 is the earliest antigen to appear on the cell surface of progenitor cells that differentiate into the T lymphoid lineage. These T-cell precursors are believed to seed the thymus, the environment of which then promotes T-cell maturation. The sequential expression of cell surface antigens during T lymphocyte maturation is shown in Fig. 7.4 and the full list of CDs associated with the T-cell lineage is given in Table 7.4.

During maturation, the CD10 antigen is lost before cell surface expression of the TCR complex. The majority of T-cells in the thymus are referred to as 'double positive' because they coexpress both CD4 and CD8. The expression of L-selectin (CD62L) is reciprocal to CD1 expression during T-cell maturation in the thymus (Picker et al., 1993). CD4 and CD8 are expressed on T-helper and T-cytotoxic

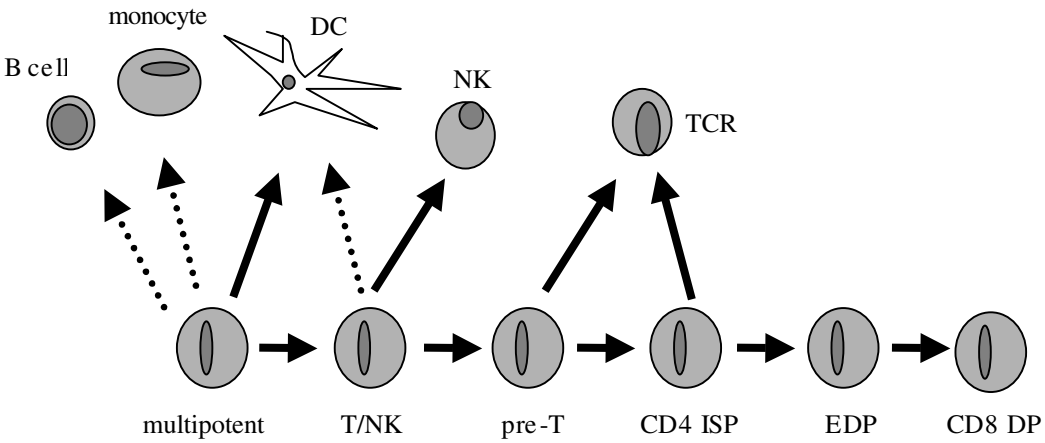

	multipotent	T/NK	pre-T	CD4 ISP	EDP	CD8 DP
CD34	++	++	+	+/–	–	–
CD1a	–	–	+	+	+	+
CD2	–	+	+	+	+	+
CD4	–	–	–	+	+	+
CD5	–	+	+	+	+	+
CD7	++	++	+	+	+	+
CD8α	–	–	–	–	+	+
CD8β	–	–	–	–	–	+
CD33	+	+/–	–	–	–	–
CD38	+/–	+	++	++	++	+
CD44	++	++	+	+/–	–	–
CD45RA	++	++	+/–	–	–	–

Fig. 7.4 Schematic hypothetical model of the antigens associated with T-cell differentiation in the human thymus. DC, dendritic cells; DP, double positive; EDP, early double positive for $CD4^+CD8^+$; ISP, immature single positive for either CD4 or CD8; NK, natural killer cells; TCR, T-cell receptor.

(plus T-cytotoxic subgroups), respectively, and those cells that express CD56 and/or CD57 are characterised as either large granular lymphocytes or NK cells.

7.8 Natural killer cell maturation

T- and NK cells share a substantial number of cell surface antigens and functional activities. Indeed there are no known cell surface antigens that are exclusively expressed on either one of the two lineages except for the products of the TCR genes. Antigens such as CD16, CD56, CD94, NKRP-1 and the immunoglobulin (Ig)-like killer-inhibitory receptors (KIRs) and killer activating receptors (KARs) are abundantly expressed on NK cells but are also present on (subsets) of T-cells. Additionally T-cell antigens such as CD2, CD7 and CD28 are also expressed on (subsets of) mature NK cells or their precursors. Most notably, NK cells were shown to express CD3 proteins, previously considered to be present exclusively on T-cells. These observations have led to the proposal that T- and NK cells share a common precursor that is distinct from the common lymphoid stem cell.

The issue of which is the major site for NK cell development is as yet unresolved. $CD34^+$ bone marrow cells have the capacity to develop into NK cells under appropriate conditions, but this does not necessarily mean that NK cells develop in the bone marrow, and other sites such as the thymus and

Table 7.4 *Antigens associated with T-cell development*

Stem cell	Cortical thymocyte	Medullary thymocyte	Mature T-cell	
CD10	CD1a	CD2	CD2	CD121a
CD34	CD1a	CD3	CD3	CD122
CD38	CD1c	CD4	CD4/CD8	CD124
CD90	CD2	CD5	CD5	CD127
CD117	cytCD3	CD7	CD6	CDw128
CD124	CD4	CD8	CD7	CD137
CD127	CD5	CD27	CD11c	CD150
HLA-DR	CD7	CD28	CD27	CD162
TdT	CD8	CD38	CD28	
CD38	CD48	CD31	CD25[a]	
	CD52	CD49d	CD35	CD26[a]
	CD165	CD49f	CD37	CD30[a]
	TdT	CD52	CD43	CD38[a]
		CD69	CD45RB	CD49b[a]
		CD99	CD48	CD49f[a]
		CD121a	CD49d	CD69[a]
		CD127	CD49f	CD70[a]
		CD165	CD57	CD83[a]
			CDw60	CD87[a]
			CD73	CD96[a]
			CDw75	CDw108[a]
			CDw76	CD109[a]
			CD94	CD122[a]
			CD99	CD124[a]
			CD101	CD132[a]
			CD102	CD134[a]
			CD103	CD137[a]

cyt, cytoplasmic; TdT, terminal deoxynucleotidyl transferase.
[a]Expressed upon cell activation.

fetal liver have been suggested (Spits et al., 1998). The major obstacle for assessing NK cell maturation is the lack of antigens specific for NK progenitors in the $CD34^+$ compartment. NK cell antigens such as CD56 and CD94 have not been found on $CD34^+$ bone marrow cells. However CLP cells, which are able to develop into NK cells in vitro, are resident in the bone marrow and these cells might develop into NK cells at this site in vivo. The observation that $CD34^+CD38^+$ fetal liver cells develop into NK cells but not T-cells indicates that this population contains committed NK progenitor cells and suggests that the liver is a site for NK cell development (Jaleco et al., 1997). In vitro kinetic studies of NK development from $CD34^+CD38^+$ fetal liver cells have led to a model of the early stages of NK cell maturation that is shown in Fig. 7.5. NK cells that develop from cytokine-stimulated $CD34^+$ cells in vitro do not progress to KIR^+ NK cells. The conditions required for regulation of expression of KIRs have yet to be defined. The relationship between $CD56^+CD16^+$ and $CD56^+$ $CD16^-$ cells is also not resolved. In the peripheral blood of most adults, $CD56^+CD16^{high}$ cells form the majority (95%) of $CD56^+$ NK cells. It is possible that the $CD16^{high}$ NK cells are the only endpoint cells. It is also conceivable that the mature NK cell pool consists of two subsets, one expressing high levels of CD16 and the other lacking or expressing low levels of CD16. No in vitro conditions have been described that induce high levels of CD16 on purified peripheral blood $CD16^-CD56^+$ NK cells, arguing against a simple precursor/progeny relationship between mature $CD56^+CD16^-$ and the $CD56^+CD16^{high}$ NK cell subset.

7.9 Dendritic cell maturation

DCs are antigen-presenting cells distributed widely in lymphoid and nonlymphoid tissues. Several subsets of DCs have been demonstrated in peripheral blood, skin, lymphoid organs and thymus. DCs developing in the thymus appear to be biologically distinct from extrathymic DCs. Bone marrow, peripheral blood and umbilical cord blood hemopoietic progenitor cells cultured with growth factors and cytokines generate mixed colonies containing monocytes and DCs that typically express myeloid cell antigens. In contrast, thymic DCs express molecules normally associated with lymphoid cells (Miralles et al., 1998). There is increasing evidence to suggest that cells of the $CD34^+CD38^{dim}$ lineage in the thymus contain tripotential cells able to develop into T, NK and DCs (Miralles et al., 1998; Res et al., 1996; Sanchez et al., 1994). Whether T- and NK cells branch from the DC through a common progenitor,

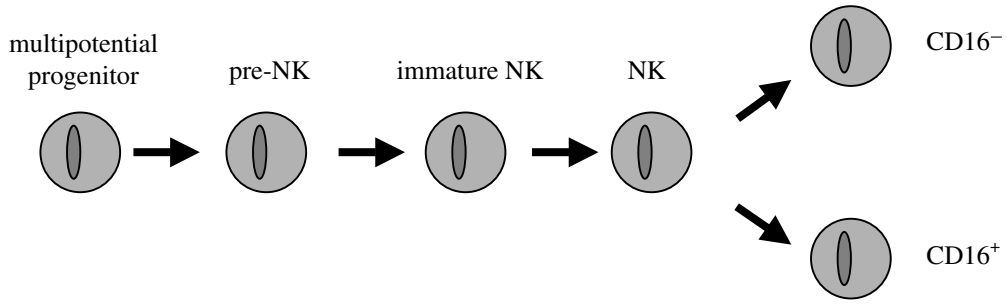

CD34	+	–	–	–	–
CD38	+	+	+	+	+
CD7	+/–	+	+	+	+
CD161	–	–	+	+	+
CD56	–	–	+	+	+
CD94	–	–	–	+	+
CD16	–	–	–	–	+

Fig. 7.5 A hypothetical model of the early stages of human natural killer cell development.

as suggested in the model depicted in Fig. 7.4, or NK and DC share a common progenitor that lacks T-cell precursor activity remains to be established. There are no antigens that are specific for DCs, but these cells have a distinct morphology, express high levels of MHC class I and II and do not express CD2, CD14, CD16, CD19, CD56 or CD64, the antigens associated with other hematopoietic cells. In peripheral blood they may be identified as HLA^+-lineage cells (Macey et al., 1998).

7.10 Peripheral blood lymphocyte subpopulations: normal ranges

The reference distribution and absolute count of peripheral blood lymphocyte subsets has been established for normal Caucasian adults (Tables 7.5 and 7.6). Age and sex differences exist for some antigens (D'Arena et al., 1998; Shahabuddin et al., 1998). Age-related trends have been found to be similar for both sexes (range 0–80 years). NK cells and $CD4^+$ cells increase significantly with age as a percentage of lymphocytes (Lighart et al., 1986; Utsayama et al., 1992). The $CD4^+$ cell percentage does not change significantly in adulthood. However, because the $CD8^+$ percentage does change, the CD4 : CD8 cell ratio decreases with age in adults. Definite differences between sexes have been found for T-cells and NK cells (Levi et al., 1988). The lymphocytes and NK cells of normal individuals also exhibit circadian and diurnal rhythms (Levi et al., 1988); for this reason, in sequential studies of blood samples from normal controls and patients, venesection should be at the same time on each occasion.

Despite changes in lymphocyte subpopulations the sum of the percentage T-, B- and NK cells approximates 100% throughout life. The total may be greater than 100% when dual $CD8^+CD4^+$ or $CD2^+CD56^+$ cells are present or when $CD16^+CD56^+$ NK cells have been excluded from the flow-cytometric gate (Lagaay et al., 1990). Dual-positive $CD4^+CD8^+$ lymphocytes are considered to be immature thymocytes (Fujii et al., 1992; Sancho et al., 1992) but increased numbers have also been found in adult T-cell leukaemia (Kamihira et al., 1992), in Hashimoto's disease and thyroiditis (Iwatani et al.,

Table 7.5 *Reference range for lymphocyte numbers in normal Caucasians*

	Lymphocyte numbers (% positive) as median (25–75 percentile)						
Cells	Cord blood	1 day–11 months	1–6 years	7–17 years	18–70 years	Age variation (% decrease per decade)	Sex difference (male : female)
Lymphocyte	41 (35–47)	47 (39–59)	46 (38–53)	40 (36–43)	32 (28–39)	0.2	NS
T-cells[a]	55 (49–62)	64 (58–67)	64 (62–69)	70 (66–76)	72 (67–76)	NS	1 : 2.5
B-cells[b]	20 (14–23)	23 (19–31)	24 (21–28)	16 (12–22)	13 (11–18)	NS	NS
NK cells[c]	20 (14–30)	11 (8–17)	11 (1–15)	12 (9–16)	14 (10–19)	1.2	3.7 : 1
$CD4^+$ T-cells	35 (28–42)	41 (38–50)	37 (30–40)	37 (33–41)	42 (38–46)	NS	NS
$CD8^+$ T-cells	29 (26–33)	21 (18–25)	29 (25–32)	30 (27–35)	35 (31–40)	0.9	1.6 : 1
$CD4^+$: $CD8^+$ ratio	1.2 (0.8–1.8)	1.9 (1.5–2.9)	1.3 (1.0–1.6)	1.3 (1.1–1.4)	1.2 (1.0–1.5)	0.07	0.19 : 1

NS, no significant difference.
[a]Derived from CD3 analysis.
[b]Derived from CD19 or CD20 analysis.
[c]Derived from $CD3^-CD16^+CD56^+$ analysis.

Table 7.6 *Reference range for lymphocyte numbers in normal Caucasians*

	Lymphocyte numbers (absolute $\times 10^9\ l^{-1}$) as median (25–75 percentile)				
Cells	Cord blood	1 day–11 months	1–6 years	7–17 years	18–70 years
Lymphocytes	5.4 (4.2–6.9)	4.1 (2.7–5.4)	3.6 (2.9–5.1)	2.4 (2.0–2.7)	2.1 (1.6–2.4)
T-cells	3.1 (2.4–3.7)	2.5 (1.7–3.6)	2.5 (1.8–3.0)	1.8 (1.4–2.0)	1.4 (1.1–1.7)
B-cells	1.0 (0.7–1.2)	0.9 (0.6–1.5)	0.9 (0.7–1.2)	0.4 (0.3–0.8)	0.3 (0.2–0.4)
NK cells	0.9 (0.8–1.8)	0.5 (0.3–0.7)	0.4 (0.2–0.6)	0.3 (0.2–0.3)	0.3 (0.2–0.4)
$CD4^+$ T-cells	1.9 (1.5–2.4)	2.2 (1.7–2.8)	1.6 (1.0–1.8)	0.8 (0.7–1.1)	0.8 (0.7–1.1)
$CD8^+$ T-cells	1.5 (1.2–2.0)	0.9 (0.8–1.2)	0.9 (0.8–1.5)	0.8 (0.6–0.9)	0.7 (0.5–0.9)

[a]Derived from CD3 analysis.
[b]Derived from CD19 or CD20 analysis.
[c]Derived from $CD3^-CD16^+CD56^+$ analysis.

1992), in myesthenia gravis and thymoma (Ichikawa et al., 1992), in lymphomas positive for human T-cell lymphotropic virus 1 (HTLV-1) (Shih et al., 1992) and in normal peripheral blood of infants (Calado et al., 1999). Most studies have been performed on Caucasian individuals, but there is evidence for ethnic variation. For example, oriental individuals have relatively more NK cells (Prince et al., 1985) and significant sex differences for lymphocyte subset counts (Kam et al., 1996). Similarly, adult Thai males have been found to have lower numbers of $CD4^+$ T-cells and greater numbers of NK cells compared with Caucasians (Webster et al., 1996). Therefore studies with such populations will require appropriate reference ranges to be determined.

Immunophenotyping results can be expressed as the absolute number of cells of each lymphocyte subgroup in a unit volume (microlitre or litre) as a percentage of the total lymphocyte population. If a sample of the patient's blood is analysed by a hematology counter at the same time as it is analysed by flow cytometry, the white blood cell (WBC) count and the lymphocyte differential can be determined.

The absolute count for the lymphocyte subsets is the WBC count multiplied by the percentage of WBC that is lymphocytes and the percentage of lymphoctes as the subset. For example, if flow cytometry shows T-cells to comprise 85% of the lymphocytes and the hematology counter shows that lymphocytes comprise 35% of the cells in a WBC count of 7×10^9 cells l^{-1}, the absolute number of T-cells is $7 \times 0.85 \times 0.35$ 10^9 cells l^{-1} (or 2.08 cells l^{-1}).

However, studies have shown that the median values obtained for WBC varied greatly from site to site and for samples within the adult normal range (Comprehensive Hematology Limited Coagulation Module Survey, 1988). This variation is caused by the intrinsic differences among hematology instruments produced by different manufacturers. Until the problem of comparability in absolute counts for the WBC is resolved, both percentage and local absolute values should be considered in making interpretations of lymphocyte subset population parameters. The use of a single platform for the enumeration of lymphocyte subpopulations has resulted in better interlaboratory coefficients of variation. In these systems, the subpopulations are identified and enumerated directly with the flow cytometer. Commercial kits have been developed to facilitate the enumeration of $CD4^+$, $CD8^+$ and $CD34^+$ lymphocytes. These strategies rely on the addition of a known concentration of microbeads to a known volume of stained lysed whole blood. The absolute cell count is calculated from the observed ratio between the number of beads and the number of cells counted. The enumeration of cells is discussed further in Chs. 4 and 9.

7.11 The identification of leukocyte subclasses by flow cytometry

7.11.1 Single- and dual-colour immunofluorescence

One-colour immunofluorescence is widely used to characterise functional cell types within a heterogeneous population but, since the expression of one surface antigen is rarely specific for a functional subset, this technique may often be inappropriate. This limitation may be reduced through the use of two different antibody labels. In this context, two-colour immunolabelling has been practised to detect double staining of cells using the combination of two fluorochromes, among which fluorescein isothiocyanate (FITC) and phycoerythrin (PE) together allow good sensitivity (Protocol 7.1). Both fluorochromes are excited by the 488 nm line of argon lasers. However, there is some overlap between the spectral emission of the two fluorochromes but electronic compensation may be used to correct for this overlap when necessary.

Protocol 7.1 Identification of leukocyte subclasses

1. Cells are prepared using Ficoll®–Hypaque separation; tissue dispersal or whole blood methods may be used.
2. It is preferable to use directly conjugated monoclonal antibodies. However, if these are not available the first-stage antisera should have different isotypes and the FITC\PE-conjugated second-stage antisera should then be specific for the two isotypes. Alternatively, one of the first-stage antisera may be biotin conjugated and identified by an avidin-linked fluorochrome.
3. Samples of cells are incubated with the antisera, appropriate controls include:
   (a) unlabelled cells for background fluorescence
   (b) dual stained mouse FITC–Ig and mouse PE–Ig isotype control for nonspecific binding
   (c) single-stained test FITC-conjugated monoclonal antibody with low and high level fluorescence for adjusting the green photomultiplier (PMT) gains or voltage and to apply any adjustment to compensate for green spectral overlap into the PE PMT

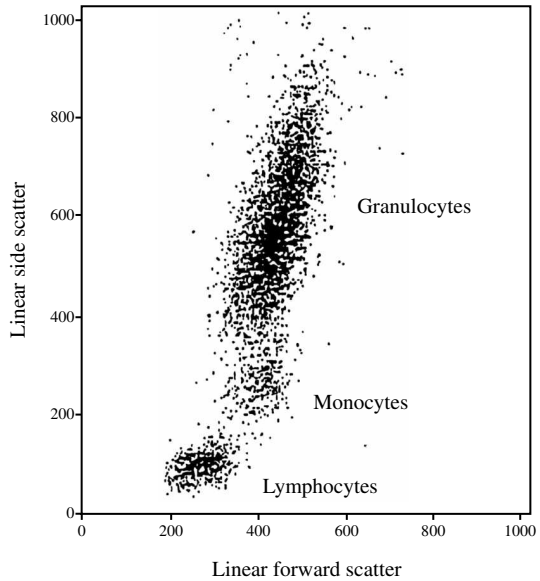

Fig. 7.6 A standard two-parameter dot plot of linear forward and linear side scatter for leukocytes in normal blood. Clusters of cells may be identified as lymphocytes, monocytes and granulocytes.

(d) single-stained test PE-conjugated monoclonal antibody with low and high fluorescences for adjusting the PE PMT gains and spectral overlap as in (c)
(e) dual-stained FITC- plus PE-conjugated antibodies on control normal cells and test cells.

4. The negative controls and single-stained test sample are analysed prior to analysis of the dual-labelled cells.
5. The use of compensation may result in loss of sensitivity. To check for this, the total number of $FITC^+$ or PE^+ cells in the dual-labelled sample should be the same as the single-stained samples without compensation.
6. Loss of sensitivity may also be caused by quenching and or steric hindrance (see text).

Normal leukocytes, either isolated or in whole blood, have characteristic forward and side (90°) light scattering properties (Fig. 7.6). In most instances, lymphocytes, monocytes and neutrophils may be identified based upon their light scattering properties. However, preparation procedures may alter these light scattering characteristics (Macey et al., 1999) and abnormal samples may have atypical light scatter properties. Dual fluorescence combined with forward and side light scatter has been used to provide an unambiguous identification of monocytes within normal blood (Terstappen et al., 1992). In this procedure, monocytes within the lymphocyte gate are identified by their expression of PE–CD14 and FITC–CD45. The CD45 antigen is expressed on all normal leukocytes but not on non-hemopoietic cells or mature erythrocytes (Shah et al., 1988). CD14 antibodies stain monocytes very brightly and have low reactivity with cells of other lineages (Griffin et al., 1981). The clear discrimination of monocytes from other cells may be made based on the surface expression of $CD14^{bright}CD45^{bright}$ whereas lymphocytes are $CD14^-CD45^{bright}$ and neutrophils are $CD14^-CD45^{dim}$. Similarly, T-cells and B-cells could be identified by their expression of $CD3^{bright}CD45^{bright}$ and $CD19^{bright}CD45^{bright}$, respectively (Fig. 7.7).

7.11.2 Three-colour immunofluorescence

Antibodies coupled to fluorochromes with emission spectra above 600 nm have become readily available (Red 613, Gibco; CyChrome, AMS; Quantum Red, Sigma). These are based on energy transfer between two fluorochromes, PE and Cyanin^{TM} 5 ($Cy^{TM}5$) and have made three-colour immunofluorescence more amenable than the previous procedures (Lansdorp et al., 1991). It is preferable to use directly conjugated antibodies and appropriate controls should be included. Reagents are available commercially that allow the simultaneous determination in a single test of the major lymphocyte subpopulations, including the total number of T and B lymphocytes and NK cells, as well as $CD4^+$ and $CD8^+$ T-cell subsets in peripheral blood and other body fluids by means of a three-colour direct

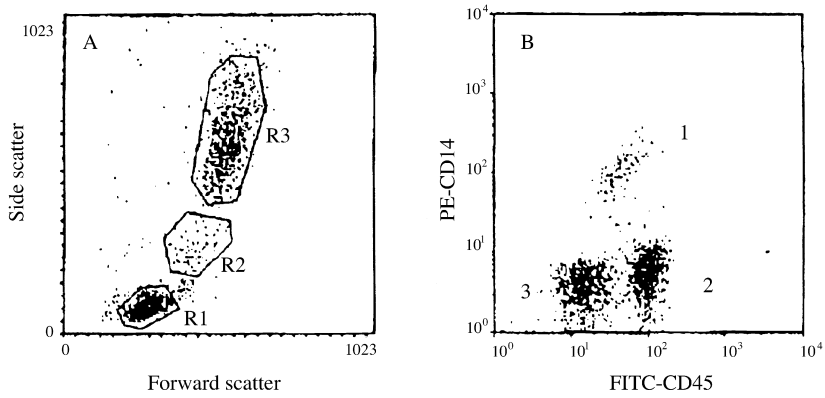

Fig. 7.7 Identification of monocytes. (A) Monocytes within the lymphocyte gate (R1) may be identified by their expression of PE–CD14 and FITC–CD45. The CD45 antigen is expressed on all normal leukocytes. CD14 antibodies stain monocytes very brightly and have low reactivity with cells of other lineages. (B) Monocytes may be clearly discriminated from other cells based on the surface expression of $CD14^{bright}CD45^{bright}$. Lymphocytes are $CD14^{-}CD45^{bright}$ and neutrophils are $CD14^{-}$ $CD45^{dim}$.

immunofluorescence technique. One such reagent LYMPHOGRAM™ (Exalpha Biologicals) may be used for the analysis of lymphocyte subpopulations in patients with human immunodeficiency virus (HIV) infection, immunodeficiencies or autoimmune diseases.

7.11.3 Immunofluorescence with four or more colours

Fluorochromes that emit in the far-red spectrum of light (>650 nm) have been developed. PE–Cy™5 and PE–Cy™7 (Cyanin™ 7) are energy-transfer conjugates and have maximum emission at 685 and 750 nm, respectively, when excited at 488 nm. The use of these fluorochromes, therefore, facilitates four-colour analysis with a single 488 nm laser. Four-colour compensation, however, becomes more complicated and it is necessary to analyse dual- and triple-labelled cells of known pattern to verify compensation (Stewart and Stewart, 1999). If more lasers are incorporated into the instrument, then more fluorochromes may be used. A procedure for nine-colour 11-parameter immunophenotyping, using three lasers, has been described (Bigos et al., 1999).

7.11.4 Quenching

High concentrations of PE can completely quench the fluorescein or FITC signal in dual-fluorescent analysis of lymphocytes when some combinations of antibodies are used. Reduction in the fluorescein or FITC signal has been shown to correlate with the intensity of PE staining (Chapple et al., 1990). This may seriously compromise interpretation of dual fluorescence studies. It can be avoided by (i) careful analysis of single colour control, (ii) the use of fluorescein or FITC–antibody conjugates with the same or greater protein to fluorochrome ratio than the PE–antibody conjugate, (iii) always labelling the antigen with a higher density distribution with fluorescein or FITC if the distributions differ, and (iv) enhancing the fluorescein or FITC signal by indirect labelling.

7.11.5 Steric hinderance

In dual-fluorescence studies, steric hindrance of antibody binding may occur because of the close proximity of antigens or, in the case of a single antigen, because of adjacent epitopes on the same antigen. In addition, the higher fluorochrome to protein ratio of FITC-conjugated antibodies results in a higher net negative charge, which diminishes

the ability to bind to the epitope. There is no obvious solution to this problem except to try antibodies to different epitopes on the antigens.

7.12 Analysis of surface and intracellular molecules

Dual immunofluorescence has been used extensively to examine the expression of surface molecules in relation to cytoplasmic IgM (Loftin et al., 1985; Zipf et al., 1984), viral antigens (Jacobberger et al., 1986), nuclear Ki-67 antigen (Drach et al., 1989), tumour necrosis factor α (Andersson et al., 1989), CD3, CD16 and CD22 (Jacob et al., 1991), intracellular K^+ (Balkay et al., 1997), hemoglobin variants (Campbell et al., 1999), intracellular Ca^{2+} (Greimers et al., 1996) and cholesterol (Hassell and Graham, 1995). A variety of agents have been used to permeabilise cells including ethanol (Braylan et al., 1982), lysolecithin (Schroff et al., 1984), paraformaldeyde (Clevenger et al., 1985), saponin (Andersson et al., 1989; Jacob et al., 1991) and Nonidet p40 (Holm et al., 1998). Saponin has also been used for the simultaneous analysis of DNA content and cell surface molecules (Rigg et al., 1989). Schmenti and Jacobberger (1992) comprehensively evaluated techniques for the analysis of DNA content and this is also discussed further in Ch. 10.

7.13 Characteristic changes in lymphocyte subsets in disease

The changes in lymphocyte subsets have been investigated in a variety of disorders including glomerulonephritis (van Alderwegen et al., 1997), uveitis (Ohta et al., 1997), juvenile dermatomyositis (Eisenstein et al., 1997), colorectal cancer (McMillan et al., 1997), Graves' disease (Gonzalez et al., 1998), rheumatoid arthritis (Kadioglu and Sheldon, 1998) and coeliac disease (Kerttula et al., 1998). Most studies have attempted to correlate peripheral blood lymphocyte subsets with the disease progression and/or treatment regimen. However, perhaps the most intensive analysis of lymphocyte subsets has been in patients with HIV infections, where plasma viraemia correlates strongly with the number of peripheral blood $CD4^+$ lymphocytes (Burgisser et al., 1999; Landay et al., 1998; Zanussi et al., 1999). HIV-1 utilises CD4 and certain β-chemokine receptors, mainly CCR-5 and CXCR4, for attachment and virus entry into the T lymphocytes and monocyte/macrophages. There has, therefore, been much investigation of the role of chemokines on different leukocytes in the pathogenesis of HIV-related disorders (Celilia et al., 1998, Guntermann et al., 1999; Lee et al., 1999; Kewal et al., 1998)

7.14 The identification and quantification of lymphocyte functional subsets

In addition to identifying the major subpopulations of leukocytes within samples by using multiple immunofluorescence analysis, it is also possible to identify functional subgroups. Some examples of these subgroups are given in Table 7.7.

7.15 Measurement of leukocyte activation

Leukocyte activation may be determined by flow cytometry in several ways. First, the expression of neo antigens that only occur on the surface of activated cells may be identified. These antigens are often associated with molecules stored in granules or the cytoplasm and only expressed on the cell surface after an appropriate stimulus, for examples the expression of CD14, the receptor for lipopolysaccharide, on neutrophils after stimulation with interferon-γ or CD69 on lymphocytes after culture with phorbol esters. Second, there may be an increase in the expression of an antigen as a result of degranulation and/or changes in the ruffling of the cell surface membrane. This may be observed with monocytes, where there is an increase in expression of CD11c after incubation with bacteria. Third, while no change in the level of expression of an antigen may occur, there can be a change

Table 7.7 *Functional subgroups identified by immunophenotyping*

Subpopulation	Functional subgroup	Function	Reference
$CD3^+$ T lymphocyte	T-cells bearing T-cell receptor α, β, γ, δ, ν and ζ chains	Antigen recognition	Lazarus et al. (1998)
$CD3^+$ T lymphocyte	$CD25^+CD69^+$ cells	Activated T lymphocytes	Rutella et al. (1999)
$CD4^+$ T lymphocyte	$CD45RA/RO^+$ cells	Associated with naive and memory T-cells	
$CD4^+$ T lymphocyte	Intracellular cytokines Th1 to Th2 ratio	Associated with Th1 and Th2 cell-mediated immune responses	Kerttula et al. (1999)
$CD16^+$ monocytes	$ILT4^+$ cells	HLA-G modulation of myelomonocytic behaviour	Allan et al. (1999)
$CD16^+$ lymphocyte	$CD56^+$ and $CD57^+$ cells	Natural killer cells associated with cell-mediated cellular cytotoxicity	Lowdell et al. (1997)
$CD19^+$ B lymphocyte	$CD5^+$ B-cells	Autoimmunity and B-cell receptor function	Lydyard et al. (1999)
$CD56^+$ cells	$CD94/NKG2^+$ cells	HLA-E control of natural killer cell function	Braud et al. (1999)

Th1 and Th2, T-cell helper type 1 and 2, respectively.

Table 7.8 *Hemopoietic cell lines*

Cell line	Cell type	Reference
CCRF-CEM	T-cell acute lymphoblastic leukaemia	Uzman et al. (1966)
HUT-78	$CD4^+$ mature T-cells	Gootenberg et al. (1981)
HL60 M2	Lymphoblast with capacity for neutrophil differentiation	Bunce et al. (1988)
K562	Undifferentiated multipotential myeloid	Lozzio and Lozzio (1979)
KG1a	Undifferentiated bone marrow cell	Koeffler (1983)
MEG-01	Megakaryoblast	Takeuchi et al. (1991)
MOLT-4	T-cell leukaemia	Ziegler and Milstein (1979)
RAJI	Burkitt's lymphoma	Pulvertaft (1964)
RPMI 8226	Plasma cell	Matsuoka et al. (1967)
TAK3	B-cell	Lefranc et al. (1982)
U937	Monocytic cells of histiocytic origin	Koren et al. (1979)

in epitope expression on the antigen after activation. Molecules with activation-dependent epitopes include CD11b, the receptor for the complement component C3bi, protease-activated receptor 1, the receptor for thrombin, and glycoprotein IIbIIIa (CD41a), the receptor for fibrinogen, fibronectin and von Willebrand factor. Antibodies have been generated that react with only the activation-dependent epitope and these allow identification of activated cells. Finally, there may be loss of molecules from the cell surface through shedding or internalisation. The adhesion molecule L-selectin (CD62L) is rapidly shed from the surface of neutrophils and monocytes upon activation; similarly P-selectin (CD62P) is transiently expressed on the surface of endothelial cells upon activation before it is internalised.

7.16 Human hemopoietic cell lines

A variety of hematopoietic cell types have been immortalised and are available as cell lines from culture collections such as the European Collection of Cell Cultures (ECACC) and the American Type Culture Collection (ATCC). A few of the more useful cell lines are given in Table 7.8.

7.17 REFERENCES

Allan, D.S., Colonna, M., Lanier, L.L., Churalova, T.D., Abrams, J.S., Ellis, S.A., McMichael, A.J., Braud, V.M. (1999) Tetrameric complexes of human histocompatibility leukocyte antigen (HLA)-G binding to peripheral blood myelomonocytic cells. *Journal of Experimental Medicine* **189**, 1149–56.

Andersson, U., Gunther, A., Dohlsten, M., Moller, G. (1989) Characterisation of individual tumor necrosis factor alpha and beta producing cells after polyclonal T cell activation. *Journal of Immunological Methods* **123**, 233–40.

Andrews, R.G., Singer, J.W., Bernstein, I.D. (1989) Precursors of colony-forming cells in humans can be distinguished from colony forming cells by expression of the CD33 and CD34 antigens and light scattering properties. *Journal of Experimental Medicine* **169**, 1721–31.

Andrews, R.G., Singer, J.W., Bernstein, I.D. (1990) Human hematopoietic precursors in long term culture: single $CD34^+$ cells that lack detectable T cell, B cell, and myeloid cell antigens produce multiple colony forming cells when cultured with marrow stromal cells. *Journal of Experimental Medicine* **172**, 155–8.

Balkay, L., Marian, T., Emri, M., Krasnai, Z., Tron, L. (1997) Flow cytometric determination of intracellular free potassium concentration. *Cytometry* **28**, 42–9.

Bigos, M., Baumgarth, N., Jagger, G.C., Herman, O.C., Nozaki, T., Stovel, R.T., Parks, D.R., Herzenberg, L.A. (1999) Nine colour eleven parameter immunophenotyping using three laser flow cytometry. *Cytometry* **36**, 36–45.

Brunsting, A., Mullany, P.F. (1974) Differential light scattering from spherical mammalian cells. *Biophysics Journal* **14**, 439–53.

Braud, V.M., Allan, D.S., McMichael, A.J. (1999) Functions of nonclassical MHC and non MHC-encoded class I molecules. *Current Opinions in Immunology* **11**, 100–8.

Braylan, R.C., Benson, N.A., Nourse, V., Kruth, H.S. (1982) Correlation analysis of cellular DNA membrane antigens and light scatter of human lymphoid cells. *Cytometry* **2**, 337–43.

Bunce, C.M., Lord, J.M., Wong, A.K.Y., Brown, G. (1988) Near neighbour analysis of variant cell lines derived from the promyeloid cell line HL60. *British Journal of Cancer* **57**, 559–63.

Burgisser, P., Hammann, C., Kaufman, D., Battegay, M., Rutschmann, O.T. (1999) Expression of CD28 and CD38 by $CD38^+$ T lymphocytes in HIV-1 infection correlates with markers of disease severity and changes towards normalisation under treatment. The Swiss HIV Cohort Study. *Clinical and Experimental Immunology* **115**, 458–63.

Calado, R.T., Garcia, A.B., Facao, R.P. (1999) Age related changes of immunophenotypically immature lymphocytes in normal peripheral blood. *Cytometry* **38**, 133–7.

Campbell, T.A., Ware, R.E., Mason, M. (1999) Detection of hemoglobin variants in erythrocytes by flow cytometry. *Cytometry* **35**, 242–63.

Celilia, D., Kewal, C.D., Ramani, V.N., O'Leary, J., Volsky, B., Nyambi, P., Xu, S., Littman, D.R., Zolla-Pazner, S. (1998) Neutralisation profiles of human immunodeficiency virus type 1 isolates in the context of coreceptor usage. *Journal of General Virology* **72**, 6988–96.

Chapple, M.R., Johnson, G.D., Davidson, R.S. (1990) Fluorescence quenching, a practical problem in flow cytometry. *Journal of Microscopy* **159**, 245–53.

Clevenger, C.V., Bauer, K.D., Epstein, A.L. (1985) A method for simultaneous nuclear immunofluorescence and DNA quantification using monoclonal antibodies and flow cytometry. *Cytometry* **6**, 280–6.

Comprehensive Hematology Limited Coagulation Module Survey (1988) *CAP Surveys Set H1-A*. College of American Pathologists, Washington, DC.

D'Arena, G., Musto, P., Casavilla, N., Di Giorgio, G., Fusilli, S., Zendoli, F., Carotenuto, M. (1998) Flow cytometric characterisation of human umbilical cord blood lymphocytes: immunophenotypic features. *Hematologica* **83**, 197–203.

de Grooth, B.G., Terstappen, L.W.M.M., Puppels, G.J., Greve, J. (1987) Light scattering polarization measurements as a new parameter in flow cytometry. *Cytometry* **8**, 539–44.

Drach, J., Gattringer, C., Glassi, H., Schwarting, R., Stein, H., Huber, H. (1989) Simultaneous flow cytometric analysis of surface markers and nuclear Ki-67 antigen in leukaemia and lymphoma. *Cytometry* **10**, 743–9.

Eisenstein, D.M., O'Gorman, M.R., Pachman, LM. (1997) Correlation between change in disease activity and changes in peripheral blood lymphocyte subsets in patients with juvenile dermatomyositis. *Journal of Rheumatology* **24**, 1830–2.

Fujii, Y., Okamura, M., Inada, K., Nakahara, K., Matsuda, H.

(1992) CD45 isoform expression during T cell development in the thymus. *European Journal of Immunology* **22**, 1843–50.

Gonzalez, A., Calleja, A., Santago, E., de Miguel, C., Lopez-Zabalza, M.J., Lopez-Moratella, N. (1998) Correlation of activated monocytes or B cells with T lymphocyte subsets in patients with Grave's disease. *Biorganic and Medical Chemistry Letters* **1**, 95–103.

Gootenberg, J.E., Ruscetti, F.W., Mier, J.E., Gadzar, A., Gallo, R.C. (1981) Human cutaneous T cell lymphoma and leukaemia cell lines produce and respond to T cell growth factor. *Journal of Experimental Medicine* **154**, 1403–18.

Gratama, J.W., Orfao, A., Barnett, D., Brando, B., Huber, A., Janossy, G., Johnsen, H.E., Keeney, M., Marti, G.E., Preijers, F., Rothe, G., Serke, S., Sutherland, D.R., van der Schoot, C.E., Schmitz, G., Papa, S. (1998) Flow cytometric enumeration of $CD34^+$ hematopoietic stem and progenitor cells. *Cytometry* **34**, 128–42.

Greimers, R., Trebak, M., Moutscen, M., Jacobs, N., Boniver, J. (1996) Improved four colour flow cytometry using Fluo-3 and triple immunofluorescence for analysis of intracellular calcium ion fluxes among mouse lymph node B- and T-lymphocyte subsets. *Cytometry* **23**, 205–17.

Griffin, J.D., Ritz, J., Nadler, L.M., Schlossman, S.F. (1981) Expression of myeloid differentiation antigens on normal and malignant myeloid cells. *Journal of Clinical Investigation* **68**, 932–41.

Guntermann, C., Murphy, B.J., Zheng, R., Qureshi, A., Eagles, P.A., Nye, K.E. (1999) Human immunodeficiency virus-1 infection requires pertussis toxin sensitive G-protein coupled signalling and mediates cAMP down regulation. *Biochemical and Biophysical Research Communications* **256**, 429–35.

Hassell, D.G., Graham, A. (1995) Changes in free cholesterol content, measured by filipin fluorescence and flow cytometry, correlates with changes in the cholesterol biosynthesis in THP-1 macrophages. *Cytometry* **21**, 352–62.

Holm, M., Thompson, M., Hoyer, M., Hokland, P. (1998) Optimization of a flow cytometric method for the simultaneous measurement of cell surface antigen, DNA content, and *in vitro* BrdUrd incorporation into normal and malignant hematopoietic cells. *Cytometry* **32**, 28–36.

Ichikawa, Y., Shimizu, H., Yoshida, M., Arimori, S. (1992) Two-color flow cytometric analysis of thymic lymphocytes from patients with myesthenia gravis and/or thymoma. *Clinical Immunology and Immunopathology* **62**, 91–6.

Iwatani, Y., Amino, N., Hidaka, Y., Kaneda, T., Ichihara, K., Tamaki, H., Matsuzuka, F., Fukata, S., Kuma, K., Miyai, K. (1992) Decreases in alpha beta T cell receptor negative T cells and CD8 cells, an increase in $CD4^+CD8^+$ cells in active Hashimoto's disease and subacute thyroiditis. *Clinical and Experimental Immunology* **87**, 444–9.

Jacob, M.C., Favre, M., Bensa, J.C. (1991) Membrane permeabilisation with saponin and multiparametric analysis by flow cytometry. *Cytometry* **12**, 550–8.

Jacobberger, J.W., Fogleman, D., Lehman, J.M. (1986) Analysis of intracellular antigens by flow cytometry. *Cytometry* **7**, 356–64.

Jaleco, A.C., Blom, B., Res, P., Weijer, K., Lanier, L.L., Phillips, J.H., Spits, H. (1997) Fetal liver contains committed NK progenitors, but is not a site for development of CD34+ cells into T cells. *Journal of Immunology* **159**, 694–702.

Kadioglu, A., Sheldon, P. (1998) Steriod pulse therapy for rheumatoid arthritis: effects on lymphocyte subsets and mononuclear cell adhesion. *British Journal of Rheumatology* **37**, 282–6.

Kam, K.M., Leung, W.L., Kwok, M.Y., Hung, M.Y., Lee, S.S., Mak, W.P. (1996) Lymphocyte subpopulation reference ranges for monitoring human immunodeficiency virus-related Chinese adults. *Clinical and Diagnostic Laboratory Immunology* **3**, 326–30.

Kamihira, S., Sohda, H., Atogami, S., Toriya, K., Yamada, T., Tsukazaki, K., Momita, S., Ikeda, S., Kusano, M., Amagasaki, T. (1992) Phenotypic diversity and prognosis of adult T-cell leukaemia. *Leukaemia Research* **16**, 435–41.

Kerttula, T.O., Holm, K., Partanen, J., Polvi, A., Maki, M. (1998) Circulating T lymphocyte subsets in coeliac disease (CoD) patients and healthy family members. *Clinical and Experimental Medicine* **111**, 536–40.

Kerttula, T.O., Collin, P., Maki, M., Hurme, M. (1999) Normal T-helper 1/T-helper 2 'balance' in peripheral blood of coeliac disease patients. *Scandinavian Journal of Immunology* **49**, 197–202.

Kewal, C.D., Ramani, V.N., O'Leary, J., Volsky, B., Nyambi, P., Burda, S., Xu, S., Littman, D.R., Zolla-Pazner, S. (1998) Neutralisation profiles of primary human immunodeficiency virus type-1 isolates in the context of coreceptor usage. *Journal of Virology* **72**, 6988–96.

Koeffler, H.P. (1983) Induction of differentiation of human acute myelogeneous leukaemia cells. Therapeutic implications. *Blood* **62**, 709–21.

Koren, H.S., Anderson, S.J., Larrick, J.W. (1979) *In vitro* activation of a human macrophage-like cell line. *Nature* **279**, 328–30.

Lagaay, A.M., Bosman, C.B., van der Keur, M., Lighart, G.T., Schuit, H.R.E., Tanke, H.J., Hijmans, W. (1990) Gating of so-called 'lymphocytic' cell population for the natural killer cells ($CD16^+$) by flow cytometry causes loss of CD16 positive

cells. *Journal of Immunological Methods* **133**, 235–44.

Landay, A.L., Bethel, J., Schnittman, S. (1998) Phenotypic variability of lymphocyte populations in peripheral blood and lymph nodes from HIV-infected individuals and the impact of antiretroviral therapy. *AIDS Research on Human Retroviruses* **14**, 445–51.

Lansdorp, P.M., Sutherland, H.J., Eaves, C.J. (1990) Selective expression of CD45 isoforms on functional subpopulations of CD34 positive hemopoietic cells from human bone marrow. *Journal of Experimental Medicine* **172**, 363–6.

Lansdorp, P.M., Smith, C., Safford, M., Terstappen, L.W.M.M., Thomas, T.E. (1991) Single laser three colour immunofluorescence staining procedures based on energy transfer between phycoerythrin and cyanine 5. *Cytometry* **12**, 723–30.

Law, P., Traylor, L., Recktenwald, D.J. (1999) Cell analysis for hematopoietic stem/progenitor cell transplantation. *Cytometry* **38**, 47–52.

Lazarus, A.H., Ellis, J., Blanchette, V., Freedman, J., Sheng-Tanner, X. (1998) Permeabilisation and fixation conditions for intracellular flow cytometric detection of the T-cell receptor zeta chain and other intracellular proteins in lymphocyte subpopulations. *Cytometry* **32**, 206–13.

Lee, B., Ratajchak, J., Doms, R.W., Gewirtz, A.M., Ratajchek, M.Z. (1999) Coreceptor/chemokine receptor expression on human hematopoietic cells: biological implications for human immunodeficiency virus type-1 infection. *Blood* **93**, 1145–56.

Lefranc, M.P., Lefranc, G., Rabbitts, T.H. (1982) Inherited deletion of immunoglobulin heavy chain constant region genes in normal human individuals. *Nature* **300**, 760–2.

Levi, F.A., Canon, C., Touitou, Y., Sulon, J., Mechkouri, M., Ponsart, E.D., Touboul, J.P., Vannetzel, J.M., Mowzowicz, I., Reinberg, A., Mathe, G. (1988) Circadian rhythms in circulating T lymphocyte subsets and plasma testosterone, total and free cortisol in five healthy men. *Clinical and Experimental Immunology* **71**, 329–35.

Lighart, G.J., van Vlokhoven, P.C., Schuit, H.R.E., Hijmans, W. (1986) The expanded null cell compartment in ageing: increase in the number of natural killer cells and changes in T cell and NK cell subsets in human blood. *Immunology* **59**, 353–60.

Loftin, K.C., Reuben, J.M., Hersh, E.M., Sujansky, D. (1985) Cytoplasmic IgM in leukaemic B cells by flow cytometry. *Leukaemia Research* **9**, 1379–87.

Loken, M.R., Shuh, V.O., Datilio, K.L., Civin, C.I. (1987a) Flow cytometric analysis of human bone marrow: Normal erythroid development. *Blood* **69**, 255–63.

Loken, M.R., Shuh, V.O., Datilio, K.L., Civin, C.I. (1987b) Flow cytometric analysis of human bone marrow: Normal B lymphoid development. *Blood* **70**, 1316–24.

Lowdell, M.W., Ray, N., Crastin, R., Corbett, T., Deane, M., Prentice, H.G. (1997) The *in vitro* detection of anti-leukaemic specific cytotoxicity after autologous bone marrow transplantation for acute leukaemia. *Bone Marow Tranplantation* **19**, 891–7.

Lozzio, B.B., Lozzio, C.B. (1979) Properties and usefulness of the original K-562 human myelogeneous leukaemia cell line. *Leukaemia Research* **3**, 363–70.

Lydyard, P.M., Jewell, A.P., Jamin, C., Youinou, P.Y. (1999) CD5 B cells and B-cell malignancies. *Current Opinions in Hematology* **6**, 30–6.

Macey, M.G., McCarthy, D.A., Vogaitzi, D., Brown, K.A., Newland, A.C. (1998) Rapid flow cytometric identification of putative CD14- and CD64- dendritic cells in whole blood. *Cytometry* **31**, 199–207.

Macey, M.G., McCarthy, D.A., Milne, T., Cavenagh, J.D., Newland, A.C. (1999) Comparative study of five commercial reagents for preparing normal and leukaemic lymphocytes for immunophenotypic analysis by flow cytometry. *Cytometry* **38**, 153–60.

Matsuoka, Y., Moore, G.E., Yagi, Y., Pressman, D. (1967) Production of free light chains of immunoglobulin by a hematopoietic cell line derived from a patient with multiple myeloma. *Proceedings of the Society of Experimental Biology and Medicine* **125**, 1246–50.

McMillan, D.C., Fyffe, G.D., Wotherspoon, R.A., Cooke, T.G., McArdle, C.S. (1997) Prospective study of circulating T-lymphocyte subpopulations and disease progression in colorectal cancer. *Diseases of the Colon and Rectum* **40**, 1068–71.

Miralles, G.D., Smith, C.A., Whichard, L.P., Morse, M. A., Haynes, B.F., Patel, D.D. (1998) $CD34^+CD38^-lin^-$ cord blood cells develop into dendritic cells in human thymic stromal monolayers and thymic nodules. *Journal of Immunology* **160**, 3290–8.

Ohta, K., Norose, K., Wang, X.C., Ito, S., Yoshimura, N. (1997) Abnormal naive and memory T lymphocyte subsets in the peripheral blood of patients with uveitis. *Current Eye Research* **16**, 650–5.

Olweus, J., Lund-Johansen, F., Terstappen, L.W.M.M. (1994) Expression of cell surface markers during differentiation of $CD34^+$, CD38-/lo fetal and adult bone marrow cells. *Immunomethods* **5**, 179–88.

Olweus, J., Lund-Johansen, F., Terstappen, L.W.M.M. (1995) CD64/Fc gamma RI is a granulo-monocytic lineage marker on $CD34^+$ hematopoietic progenitor cells. *Blood* **85**, 2402–13.

Picker, L.J., Treer, J.R., Ferguson-Darnell, B., Collins, P.A., Buck,

D., Terstappen, L.W.M.M. (1993) Control of lymphocyte recirculation in man, I. Differential regulation of the peripheral lymph node homing receptor L-selectin on T cells during the virgin to memory transition. *Journal of Immunology* **150**, 1105–21.

Prince, H.K., Hirji, K., Waldbeser, S., Paeger-Marshall, S., Kleinman, S., Lanier, L. (1985) Influence of racial background on the distribution of T cell subsets and Leu 11 positive lymphocytes in healthy blood donors. *Digestive Immunology* 3, 33–9.

Pulvertaft, R.J.V. (1964) Cytology of Burkitts tumour (African lymphoma). *Lancet* **i**, 238–240.

Res, P., Maryinez, C.E., Jaleco, A.C., Noteboom, E., Weijer, K., Spits, H. (1996) $CD34^{+}CD38^{dim}$ cells in the thymus can differentiate into T, natural killer and dendritic cells but are distinct from stem cells. *Blood* **87**, 5196–206.

Rigg, K.M., Shenton, B.K., Murray, I.A., Givan, A.L., Taylor, R.M.R., Lennard, T.W.J. (1989) A flow cytometric technique for simultaneous analysis of human monoclonal cell surface antigens and DNA. *Journal of Immunological Methods* **123**, 177–84.

Robinson, F.J., Sieff, C., Deilia, D., Edwards, P.A.W., Greaves, M. (1981) Expression of cell surface HLA-DR and glycophorin during erythroid differentiation. *Nature* **289**, 68–71.

Rutella, S., Rumi, C., Lucia, M.B., Barberi, T., Puggioni, P.L., Lai, M., Romano, A., Cauda, R., Leone, G. (1999) Induction of CD69 antigen on normal $CD4^{+}$ and $CD8^{+}$ lymphocyte subsets and its relationship with the responding T-cells. *Cytometry* **38**, 95–101.

Salzman, G.C., Crowell, J.M., Martin, J.C. (1975) Cell classification by laser light scattering: Identification and separation of unstained leukocytes. *Acta Cytology* **19**, 374–7.

Sanchez, M.J., Muench, M.O., Roncarolo, M.G., Lanier, L., Philips, J.H. (1994) Identification of a common T/NK progenitor in human fetal thymus. *Journal of Experimental Medicine* **180**, 569–76.

Sancho, J., Silverman, L.B., Castigli, E., Ahern, D., Laudano, A.P., Terhorst, C., Geha, R.S., Chatila, T.A. (1992) Developmental regulation of transmembrane signaling via the T cell antigen receptor/CD3 complex in human T lymphocytes. *Journal of Immunology* **148**, 1315–21.

Schmenti, K.J., Jacobberger, J.W. (1992) Fixation of mammalian cells for flow cytometric evaluation of DNA content and nuclear immunofluorescence. *Cytometry* **13**, 48–59.

Schroff, R.W., Bucana, C., Klein, R.A., Farrell, M.M., Morgan, A.C. (1984) Detection of intracytoplasmic antigens by flow cytometry. *Journal of Immunological Methods* **70**, 167–77.

Shah, V.O., Civin, C.I., Loken, M.R. (1988) Flow cytometric analysis of human bone marrow: IV. differential quantitative expression of T200 common leukocyte antigen during normal hematopoiesis. *Journal of Immunology* **140**, 1861–7.

Shahabuddin, S., Al-Ayed, I., Gad El-Rab, M.O., Qureahi, M.I. (1998) Age-related changes in blood lymphocyte subsets of Saudi Arabian healthy children. *Clinical and Diagnostic Laboratory Immunology* **5**, 632–5.

Shih, L.Y., Kuo, T.T., Dunn, P., Liaw, S.J. (1992) HTLV-1 positive and HTLV-1 negative peripheral T-cell lymphoma in Taiwan Chinese. *International Journal of Cancer* **21**, 186–91.

Spits, H., Blom, B., Jaleco, A., Weijer, K., Verschuren, H.C.M., van Dongen, J.J.M., Heemskerk, M.H.M., Res, P.C.M. (1998) Early stages in the development of human T, natural killer and thymic dendritic cells. *Immunological Reviews* **165**, 75–86.

Stewart, C.C., Stewart, S.J. (1999) Four color compensation. *Cytometry* **38**, 161–75.

Takeuchi, K., Ogura, M., Saito, H., Satoh, M., Takeuchi, M. (1991) Production of platelet like particles by a human megakaryoblastic leukaemia cell line (MEG-01). *Experimental Cell Research* **193**, 223–6.

Terstappen, L.W.M.M., de Grooth, B.G., ten Napel, C.H.H., van Berkel, W., Greve, J. (1986) Discrimination of human cytotoxic lymphocytes from regulatory and B lymphocytes by orthogonal light scattering. *Journal of Immunological Methods* **95**, 211–16.

Terstappen, L.W.M.M., Hollander, Z., Meiners, H., Loken, M.R. (1990a) Quantitative comparison of myeloid antigens on five lineages of mature peripheral blood cells. *Journal of Leukocyte Biology* **48**, 138–48.

Terstappen, L.W.M.M., Mickaels, R., Dost, R., Loken, M.R. (1990b) Increased light scattering resolution facilitates multidimensional flow cytometric analysis. *Cytometry* **11**, 506–12.

Terstappen, L.W.M.M., Safford, M., Loken, M.R. (1990c) Flow cytometric analysis of human bone marrow III. Neutrophil development. *Leukaemia* **4**, 657–63.

Terstappen, L.W.M.M., Huang, S., Safford, M., Lansdorp, P.M., Loken, M.R. (1991a) Sequential generation of hematopoietic colonies derived from single non lineage committed progenitor cells. *Blood* **77**, 1218–27.

Terstappen, L.W.M.M., Konemann, S., Safford, M., Loken, M.R., Zurlutter, K., Bucher, T., Hiddemann, W., Wormann, B. (1991b) Flow cytometric characterisation of acute myeloid leukaemias. I. Significance of light scattering properties. *Leukaemia* **5**, 315–21.

Terstappen, L.W.M.M., Huang, S., Picker, L.J. (1992) Flow cytometric assessment of human T-cell differentiation in thymus and bone marrow. *Blood* **79**, 666–77.

Terstappen, L.W.M.M., Gandour, D., Huang, S., Lund-Johan-

sen, F., Manion, K., Nguyen, M., Mickaels, R., Olweus, J., Topker, S. (1993) Assessment of hematopoietic cell differentiation by multidimensional flow cytometry. *Journal of Hematotherapy* **2**, 431–47.

Utsayama, M., Hirokawa, K., Kurashima, C., Fukayama, M., Inamatsu, T., Suzuki, K., Hashimoto, W., Sato, K. (1992) Differential age-change in the numbers of $CD4^+CD45RA^+$ and $CD4^+CD29^+$ T cell subsets in human peripheral blood. *Mechanisms of Ageing* **63**, 57–68.

Uzman, B.G., Foley, G.E., Farber, S., Lazarus, H. (1966) Morphologic variations in human leukaemic lymphoblasts (CCRF-CEM cells) after long term culture and exposure to chemotherapeutic agents. *Caner* **19**, 1725–42.

van Alderwegen, I.E., Bruijn, J.A., de Heer, E. (1997) T cell subsets in immunologically-mediated glomerulonephritis. *Histology and Histopathology* **12**, 241–50.

Webster, H.K., Pattanapanyasat, K., Phanupak, P., Wasi, C., Chuenchitra, C., Ybarra, L., Buchner, L. (1996) Lymphocyte immunophenotype reference ranges in healthy Thai adults: implications for the management of HIV/AIDS in Thailand. Southeast Asian *Journal of Tropical Medicine and Public Health* **27**, 418–29.

Zanussi, S., Simonelli, C., Bortolin, M.T., D'Andrea, M., Comar, M., Tirelli, U., Giacca, M., De Paoli. P. (1999) Dynamics of provirus load and lymphocyte subsets after interleukin 2 treatment in HIV- infected patients. *AIDS Research in Human Retroviruses* **15**, 97–103.

Zeigler, A., Milstein, C. (1979) A small polypeptide different from β_2-microglobulin associated with a human cell surface antigen. *Nature* **279**, 243–4.

Zipf, T.F., Bryant, L.D., Koskowich, G.N., MacGregor, S.E., Chin, L., Johnson, H. (1984) Enumeration of cytoplasmic μ immunoglobulin positive acute lymphoblastic leukaemia cells by flow cytometry: Comparison with fluorescence microscopy. *Cytometry* **5**, 610–13.

8

Immunophenotypic analysis of leukocytes in disease

Jamie D. Cavenagh[1], Marion G. Macey[1] and Timothy M. Milne[2]

[1] St Bartholomew's and Royal London School of Medicine and Dentistry, Queen Mary and Westfield College, London

[2] The Royal London Hospital, London

8.1 Introduction

Hemopoietic cells express a wide range of antigens on the cell membrane as well as within the cytoplasm and nucleus. Some of these antigens are widely distributed whereas others are restricted to specific cell types. The overall spectrum of antigen expression by a particular cell is defined as its immunophenotype and the technique of immunophenotyping can be applied to many areas of hematology, immunology and other clinical fields. Immunophenotyping is of paramount importance in the diagnosis of hematological malignancies but it can be used in any situation where cellular antigen expression needs to be analysed; consequently it has widespread applications within clinical and research medicine (Table 8.1). The focus of this chapter will be the application of immunophenotyping to the diagnosis of hematological malignancies.

The existence of the pluripotential stem cell is a fundamental concept in hematology. These cells possess the dual capabilities of self-renewal and multilineage differentiation (Botnick et al., 1976). Thus, a single pluripotential stem cell has the capability of producing all classes of terminally differentiated hemopoietic cell. The first step in lineage commitment occurs when this cell divides into progeny committed to either myeloid or lymphoid development. These multipotential cells can give rise, respectively, to all classes of myeloid cell (granulocytic, monocytic, erythroid and megakaryocytic) and lymphoid cell (B-, T- and natural killer (NK) cells). During this process of lineage commitment and subsequent differentiation, cells express a number of molecules such that the antigen expression profile of an individual cell is highly characteristic of a particular stage of hemopoietic differentiation. Since it is generally accepted that hematological malignancies represent the clonal proliferation of a single cell that has been 'arrested' at a specific stage of differentiation, the immunophenotype of a particular leukaemia or lymphoma can be used to identify the malignant cell of origin (Harris et al., 1994; Kuppers et al., 1999).

Immunophenotyping is used to discriminate between myeloid and lymphoid malignancies and to determine the level of differentiation of a particular neoplasm. An important concept in lymphoid malignancy is the distinction between 'central' or 'precursor' as opposed to 'peripheral' or 'mature' neoplasms. A mature B- or T-cell is defined by its expression of a functional antigen receptor molecule on its cell membrane. Thus, a mature B-cell expresses surface membrane immunoglobulin (smIg) and a mature T-cell expresses the T-cell receptor (TCR) on its surface membrane. Immature cells that are still undergoing the process of antigen receptor gene rearrangement are defined as precursor cells, and these cells are situated in the 'central' lymphoid organs (the bone marrow and thymus gland for B- and T-cell precursors, respectively). During antigen receptor gene rearrangement, the enzyme terminal deoxynucleotidyl transferase (TdT) is active in the cell nucleus and its presence is, therefore, characteristic of precursor cell neoplasms. Generally speaking, precursor or central lymphoid malignancies are defined by the expression of TdT whereas mature or peripheral lymphoid malig-

Table 8.1 *Examples of the application of immunophenotyping in disease*

Application	Examples
Diagnosis of hematological malignancies	Leukaemia and lymphoma
Red cell disorders	Paroxysmal nocturnal hemoglobinuria (deficiency of PIG-linked membrane proteins)
White cell disorders	Leukocyte adhesion deficiency (CD18 deficiency)
Platelet disorders	Bernard–Soulier syndrome (GPIb/IX deficiency) Glanzmann's thrombasthenia (GPIIb/IIIa deficiency)
Monitoring levels of leukaemia/lymphoma following chemotherapy	'Minimal residual disease'
Prognostic information in leukaemia/lymphoma	Drug resistance (e.g. multidrug resistance) Cellular proliferation (e.g. Ki-67) Childhood acute lymphoblastic leukaemia (ALL, e.g. DNA ploidy)
Enumerating stem cell numbers	Stem cell harvests (e.g. $CD34^+$ numbers)
Monitoring post-transplant immune recovery	Naive T cell production ($CD45RA^+$)
Diagnosis of immunodeficiency states	Severe combined immunodeficiency (SCID)
Monitoring response to treatment in immunodeficiency states	$CD4^+$ count in HIV infection

PIG, phosphatidylinositol glycosyl phospholipid.

nancies are characterised by membrane expression of smIg or TCR.

8.2 Classification of leukaemias

The classification of hematological malignancies is a complex subject in its own right and is constantly under revision. Early classification systems were based predominantly on morphology and cytochemistry alone (Table 8.2). These often failed to identify specific disease entities, which were subsequently defined as detailed cytogenetic and molecular information became available. More contemporary classification systems have attempted to recognise these entities by the analysis of their combined clinical, morphological, immunophenotypic, cytogenetic and molecular features (Harris et al., 1994, 1999). Although this chapter focuses on the role of immunophenotyping in the diagnosis of hematological malignancies, it is most important to bear in mind that rarely does the immunophenotype by itself identify a specific disease entity and it must always be interpreted along with all other available information.

8.2.1 The acute leukaemias

The acute leukaemias are characterised by the accumulation of immature blast cells in the bone marrow and peripheral blood, resulting in bone marrow failure. In most cases, acute leukaemia is diagnosed when at least 20–30% of the bone marrow cells are blasts and the first step is to distinguish acute myeloid leukaemia (AML) from acute lymphoblastic leukaemia (ALL; also called acute lymphoid leukaemia). The most widely used classification of acute leukaemias is the French–American–British (FAB) system, which was first published in 1976 (Table 8.3) (Bennett et al., 1976, 1985a,b). The FAB system relies predominantly on morphology and cytochemistry since at its inception immunophenotyping was not generally available. Therefore, a diagnosis of AML was made when a minimum of 3% of the blasts stained positively for myeloperoxidase (MPO) or Sudan black B in cytochemical reactions. Those cases of acute leukaemia with less than 3% positivity were classified as ALL. Subsequently, with the advent of routine immunophenotyping, it was confirmed that the vast majority of such leukaemias were indeed lymphoid in origin. However, a minority were found to express typical myeloid antigens and these were subsequently classified as 'AML with minimal evidence of

Table 8.2 *Differentiation of leukaemic blast cells*

Characteristic	Lymphoblast	Myeloblast
Nucleoli	Usually one	More than two
Cytoplasm	Scanty; high nuclear/cytoplasmic ratio	Abundant; low nuclear/cytoplasmic ratio
Auer rods	Absent	Present
Sudan black B stain	Negative	Positive
Periodic acid–Schiff base stain	Strong block positive	Negative/weak positive
Acid phosphatase	Negative except in T lymphoblasts	Positive
Naphthol AS-D acetate esterase	Negative	Positive; myeloid resistant to fluoride; monocytic abolished by fluoride
Chloracetate esterase	Negative	Positive

AS-D, β-hydroxynaphthol acid anilide.

Table 8.3 *The FAB classification of acute leukaemia*

FAB type	Description
Acute myeloid leukaemia (AML)	
M0	AML with minimal evidence of myeloid differentiation
M1	AML without differentiation
M2	AML with differentiation
M3	Acute promyelocytic leukaemia (APML)
M4	Acute myelomonocytic leukaemia
M5a	Acute monoblastic leukaemia
M5b	Acute monocytic leukaemia
M6	AML with predominant erythroid differentiation
M7	Acute megakaryoblastic leukaemia
Acute lymphoblastic leukaemia (ALL)	
L1	Small monomorphic ALL
L2	Large convoluted and heterogeneous ALL
L3	Burkitt-cell type ALL with basophilia and granules

FAB, French–American–British staging.

differentiation' (AML M0) (Bennett et al., 1991).

Since the publication of the FAB classification, a number of groups have made additional proposals for the immunological classification of the acute leukaemias (Bene et al., 1995; First and Second MIC Cooperative Study Group, 1986, 1988). The European Group for the Immunological Characterisation of Leukaemias (EGIL) (Bene et al., 1995) suggested that a primary panel of antigens are used initially to characterise the leukaemia as AML, B-lineage ALL or T-lineage ALL (Table 8.4). The primary panel includes the most specific antigens for myeloid and lymphoid lineages that are expressed at early stages of differentiation in addition to other antigens that are expressed by 'stem cells', albeit in a nonlineage-restricted fashion. The aim of the secondary panel is to divide the leukaemias into subgroups (Table 8.4). A number of guidelines for the use of these panels in the immunophenotypic classification of leukaemias by flow cytometry have been proposed (Scott et al., 1995; Steltzer et al., 1997).

8.3 Acute myeloid leukaemia

The overwhelming majority of patients with AML will be positive for at least one of the 'pan-myeloid' antigens in the primary panel such as MPO, CD13, CD33, CD65 and CD117 (c-kit; the receptor for stem-cell growth factor) (Table 8.4). However, expression of these antigens is by no means uniform in all FAB types. For instance, CD33 is often negative in patients with AML M0 and CD13 is negative in AML M7. It will be evident that detection of MPO forms part of the cytochemical FAB system as well as part of all immunological classifications. In the former, MPO is detected by demonstrating its enzymatic activity in a conventional cytochemical reaction whereas in the latter it is detected by antibodies

Table 8.4 *Immunophenotypic panels for leukaemia diagnosis*

	Panel of antisera for acute leukaemias		Panel of antisera for chronic lymphoid disorders	
Cell type	Primary	Secondary	Primary	Secondary
B-cell	CD10	cyt μ-chain	CD5	CD11c
	CD19	smIg μ-chain	CD10	CD25
	CD22[a]	κ-, λ-Light chains	CD19	CD38
	CD79a	CD20	CD22	CD45
		CD24	CD23	CD56
			FMC7	CD103
			smIg heavy and light chains	CD22[a]
T-cell	CD2	CD1a	CD3	CD2
	CD3	CD4		CD4
	CD3[a]	CD5		CD5
	CD7	CD8		CD7
		TCR α/β- and γ/δ-subunits		CD8
				CD10
				CD11c
				CD16
				CD25
				CD56
				CD57
Myeloid/monocytic cell	CD13	CD14	Myeloid transformation analyse as	
	CD33	CD15	for acute leukaemia	
	CD65	CD64		
	CD117	Glycophorin A		
	MPO	Lysozyme		
Megakaryocyte		CD41		
		CD61		
Nonspecific	CD34	Cytokeratin	HLA-DR	TdT
	CD45	TdT		
	HLA-DR			

MPO, myeloperoxidase; smIg, surface membrane immunoglobulin; TdT, terminal deoxyribonucleotidyl transferase.
[a]Cytoplasmic staining.

that recognise both the active form and the inactive proenzyme form of MPO. Hence, the immunological assay for MPO is more sensitive than the cytochemical assay, as is seen in those with AML M0 (Bennett et al., 1991).

AML antigen expression is summarised in Table 8.5. Only a subset of AML FAB types can reliably be identified purely by immunological methods (e.g. most AML M0, M6 and M7). This highlights the fact that any morphological or immunological classification of AML is 'biologically' inexact. The recent World Health Organization (WHO) classification of hematological malignancies recognises this fact and defines, as far as is possible, distinct clinicopathological entities (Harris et al., 1999). For example, it defines a group of AMLs with recurrent cytogenetic translocations such as acute promyelocytic leukaemia (APML) with t(15;17), AML with t(8;21) and AML with inv(16). As it happens, virtually all patients with FAB AML M3 will

Table 8.5 *Immunophenotypes of the FAB types of acute myeloid leukaemia (AML)*

FAB AML type	'Pan-myeloid antigens' (CD13, CD33 CD65, CD117, MPO)	Comments
M0	+	Negative for MPO/SBB by cytochemistry
M1	+	
M2	+	t(8;21) typically $CD19^+$ (Reading et al., 1993)
		$CD56^+$ poor prognosis (Baer et al., 1997)
M3	+	Usually $CD2^+CD34^-HLA\text{-}DR^-$ (Claxton et al., 1992; Reading et al., 1993)
		$CD13^+$ associated with all-*trans*-retinoic acid syndrome (Vahdat et al., 1994)
		$CD56^+$ poor prognosis (Murray et al., 1999)
M4	+	Often $CD4^+CD11b^+CD14^+CD64^+$
		M4 (Eo) often $CD2^+$ (Adriaanson et al., 1993)
M5	+	Often $CD4^+CD11b^+CD14^+CD64^+$
M6	+	No reliable marker for primitive cases
		Glycophorin A expressed in more mature disease (Cuneo et al., 1990)
M7	+	Usually $CD41^+CD42^+CD61^+$
		Usually $CD13^-$

FAB, French–American–British staging; MPO, myeloperoxidase; SBB, Sudan black B.

possess the t(15;17) translocation whereas only a minority with AML M2 and AML M4 will have the t(8;21) and inv(16) abnormalities, respectively. Therefore, it is important to recognise the limitations of immunological classifications of AML since they will fail to identify certain specific disease entities. Nevertheless, in conjunction with light microscopy, immunophenotypic analysis is a rapid and convenient way to identify the lineage of an acute leukaemia and to direct the attending physician towards appropriate therapy.

CD34 is an antigen of 'immature' stem cells and CD34 positivity is found in patients with AML M0, M1 and M5a as well as with the primitive ALLs (Cuneo et al., 1990). As explained above, TdT expression typically is seen in lymphoid precursors but is also found in 15–20% of the most primitive classes of AML (M0 and M1) and thus may represent an aspect of 'lineage promiscuity' found in acute leukaemia (Farahat et al.,1995). Other typically lymphoid antigens are also sometimes expressed in AML such as CD7, which is found in 10–25% of AML M0, M1 and M5 (del Poeta et al., 1995). CD7 expression in AML indicates a poor prognosis. HLA-DR is generally expressed by all AML subtypes with the important exception of AML M3, so giving rise to the characteristic immunophenotype of AML M3, which is $CD13^+CD33^+CD34^-HLA\text{-}DR^-$.

8.4 The classification of B-cell acute lymphoblastic leukaemia

Most B-lineage ALLs are derived from B-cell precursors. It will be recalled that these cells are defined by the absence of smIg and that once smIg is expressed the cell is designated a 'mature' B-cell. B-lineage ALL is defined by the presence of the early expressed pan-B-cell anitgens CD19, CD79a and CD22. It is best to test for the presence of cytoplasmic CD22 (cytCD22) since this antigen is expressed earlier in the cytoplasm than on the cell membrane (Table 8.4) (Janossy et al., 1989).

B-cell precursors are undergoing immunoglobulin gene rearrangement and, therefore, also express TdT in the nucleus, since this enzyme is required for the generation of additional diversity at the junctional regions of antigen receptor molecules. Only mature B-ALL is TdT negative and so should not strictly be defined as derived from a

Table 8.6 *The EGIL classification of B-lineage acute lymphoblastic leukaemia (B-ALL)*

B-ALL subtype	Description	Immunophenotype	Comments
	All subtypes	$CD19^+CD22^+CD79^+$	
B-I	Pro-B	$CD10^-cytIgM^-smIg^-TdT^+$	Infant pro-B-ALL has a poor prognosis and is often associated with MLL gene rearrangements at 11q23 (Chen et al., 1993)
B-II	Common ALL (C-ALL)	$CD10^+cytIgM^-smIg^-TdT^+$	Childhood C-ALL often associated with t(12;21) (*TEL–AML1* fusion) and a good prognosis (Raimondi et al., 1997)
B-III	Pre-B-ALL	$CD10^+cytIgM^+smIg^-TdT^{+/-}$	Subset with t(1;19) (*E2A–PBX* fusion) (Chessels et al., 1997)
B-IV	Mature B-ALL	$CD10^{+/-}cytIgM^+smIg^+TdT^-$	Characteristic morphology (ALL L3) with basophilic cytoplasm and vacuolation Associated with t(8;14), t(2;8) and t(8;22) (Copelan and McGuire, 1995)

EGIL, European Group for Immunological Classification of Leukaemias; cyt, cytoplasmic; sm, surface membrane.

B-cell precursor, and indeed the cell of origin is now known to be peripheral (postfollicular) (Jennings and Foon, 1997). Pro-B-ALL is the most primitive B-lineage ALL and is characterised by the expression of certain pan-B-lineage antigens without any evidence of further differentiation. Developing B-cell precursors then express the antigen CD10. The type of ALL corresponding to this stage of development is termed common ALL (C-ALL) because it expresses the 'common ALL antigen' or 'CALLA' (CD10), which was first discovered when mice were immunised with human childhood ALL cells and the resulting antibody reactivity analysed. C-ALL is the commonest form of childhood ALL and has a favourable prognosis in children between the ages of 2 and 6 years, particularly when associated with t(12;21), which occurs in approximately 25% (Raimondi et al., 1997). As B-cell precursors develop, they go on to produce a successful IgH gene rearrangement and this is found first in the cytoplasm, at which stage the B-cell precursor is designated a 'pre-B-cell'. Subsequently, the immunoglobulin molecule is expressed on the cell surface such that the cell is termed a 'B-cell'. The EGIL classification of B-lineage ALL is shown in Table 8.6. B-lineage ALL is always associated with recurrent chromosomal translocations that juxtapose the c-*myc* oncogene on chromosome 8 with the immunoglobulin heavy or light chain genes (on chromosomes 14 and 2 or 22, respectively) (Copelan and McGuire, 1995). This translocation brings c-*myc* under the control of one of the immunoglobulin gene promoters such that it is greatly overexpressed, resulting in excessive cellular proliferation. Exactly the same chromosomal translocation is found in Burkitt's lymphoma, which can be considered as the peripheral lymphoid tissue equivalent of the FAB ALL L3. Indeed, the new WHO classification of the acute lymphoblastic leukaemias has clarified this issue by defining mature B-ALL as 'Burkitt cell leukaemia' (Harris et al., 1999). This point highlights the fact that certain specific biological entities can present as either leukaemia or lymphoma.

8.5 T-lineage acute lymphoblastic leukaemia

T-lineage ALL is derived from early, precursor T-cells found in the thymus, which is the 'central' T-cell organ (Zuniga-Pflucker and Lenardo, 1996). This is entirely analagous to B-lineage ALL, which arises from 'central', bone marrow-derived B-cell precursors. During the process of T-cell precursor differentiation, the cells rearrange their TCR genes during which time the enzyme TdT is expressed and active. Once a functional TCR molecule has been

Table 8.7 *The EGIL classification of T lineage acute lymphoblastic leukaemia (T-ALL)*

T-ALL type	Description	Immunophenotype
T-I	Pro-T	$CD1a^{-}CD2^{-}cytCD3^{+}smCD3^{-}CD5^{-}CD7^{+}$
T-II	Pre-T	$CD1a^{-}CD2^{+}cytCD3^{+}smCD3^{-}CD5^{+}CD7^{+}$
T-III	Cortical T	$CD1a^{+}CD2^{+}cytCD3^{+}smCD3^{+/-}CD5^{+}CD7^{+}$
T-IVa	Mature T (TCR $\alpha\beta^{+}$)	$CD1a^{-}CD2^{+}cytCD3^{+}smCD3^{+}CD5^{+}CD7^{+}$ and usually $CD4^{+}$ or $CD8^{+}$
T-IVb	Mature T (TCR $\gamma\delta^{+}$)	$CD1a^{-}CD2^{+}cytCD3^{+}smCD3^{+}CD5^{+}CD7^{+}$ and usually $CD4^{-}CD8^{-}$

EGIL, European Group for Immunological Classification of Leukaemias; TCR, T-cell receptor.
All patients are positive for cytoplasmic (cyt) or surface membrane (sm) CD3 and terminal deoxyribonucleotidyl transferase (TdT); some are $CD10^{+}$.

produced, the processes of positive and negative selection take place. During 'positive selection', the ability of the nascent TCR to bind to self class I or class II antigens of the major histocompatibility complex (MHC) is tested, and cells that fail to do so are clonally deleted since they will be unable to perform their required function of recognising foreign peptide when associated with self MHC (Chan et al., 1994). Conversely, cells that bind with too great an avidity to self peptide presented by MHC are also deleted since they are likely to be autoreactive (negative selection) (Clayton et al., 1997). Prior to this period of positive and negative selection, T-cell precursors do not express either CD4 or CD8 ('double negative' cells). During the selection process, they express both CD4 and CD8 ('double positive') before becoming committed to either single $CD4^{+}$ or $CD8^{+}$ T-cells (Zuniga-Pflucker and Lenardo, 1996). In terms of the immunological classification of T-lineage ALL, CD4 positivity is not sufficient to assign lineage specificity since a significant percentage of patients with AML (especially those with a monocytic component) are also $CD4^{+}$. Similarly, the T-cell antigens CD2 and CD7 are expressed by a proportion of those with AML (Bene et al., 1995).

As T-cell precursors differentiate along these pathways, they move physically from the thymic cortex towards the medulla. Cortical thymocytes express CD1a. The defining feature of T-lineage ALL is the presence of cytoplasmic or membrane CD3 (Bene et al., 1995). CD3 forms an integral part of the TCR antigen complex and once the TCR–CD3 complex is expressed on the cell membrane, then the cell is defined as a 'T-cell'. Prior to this stage, T-cell precursors express CD3 in the cytoplasm (cytCD3) in an analogous manner to pre-B-cells, which express cytoplasmic IgM (μ) heavy chains.

Patients with T-lineage ALL are classified according to their place within this sequence of differentiation. The early MIC classification simply divided T-lineage ALL into 'early precursor T-ALL' ($CD2^{-}$) and 'T-ALL' ($CD2^{+}$) (First MIC Cooperative Study Group, 1986). Both groups are predominantly TdT^{+} and $CD7^{+}$. Subsequent classifications have tried to mirror thymic T-cell precursor differentiation in more detail and have highlighted the paramount importance of cytoplasmic $CD3^{+}$ ($cytCD3^{+}$) or surface membrane $CD3^{+}$ ($smCD3^{+}$) in assigning T lineage (Table 8.7) (Bene et al., 1995). In T-lineage ALL, HLA-DR and TdT positivity is the rule especially in the less mature cases. In contrast to B-lineage ALL, immunologically defined subtypes of T-lineage ALL are not specifically associated with certain cytogenetic abnormalities or prognostic categories. However, generally speaking, the more immature subtypes have a worse prognosis (Theil et al., 1989) while $CD10^{+}$ is a favourable prognostic indicator (Pui et al., 1993). A number of recurring chromosomal translocations are found in T-lineage ALL and many of these involve the TCR α/δ locus (14q11-13), the TCR β locus (7q32-36) or the TCR γ locus (7p13) (Thandla and Aplan, 1997).

8.6 Biphenotypic and undifferentiated acute leukaemia

Rarely, cases of acute leukaemia cannot be assigned

to a myeloid or lymphoid lineage since the leukaemic cells coexpress antigens belonging to two lineages. It has already been noted that aberrant expression of nonlineage antigens occurs relatively frequently in acute leukaemia (e.g. CD7 and TdT in AML) but the criteria for the diagnosis of biphenotypic acute leukaemia (BAL) are highly stringent. Various scoring systems have been devised that assign a high score to lineage-specific antigens and lower scores to lineage-associated antigens (Table 8.8) (Bene et al., 1995; Matutes et al., 1997). Ideally, dual immunofluorescence techniques should be used in these analyses, although when the percentage expressions are high, this is not always strictly necessary. The correct identification of BAL has considerable practical importance since such patients are often difficult to treat and may require both AML- and ALL-directed therapies. In addition, the t(9;22) chromosomal translocation is relatively frequently associated with BAL and is associated with a particularly poor prognosis (Saikevych et al., 1991). For such patients, aggressive treatment is indicated, including the early consideration of bone marrow transplantation.

It has already been noted that the expression of a single inappropriate marker is not sufficient for a diagnosis of BAL. AML with expression of one or more lymphoid antigens is termed 'AML with lymphoid antigen expression' (Ly^+AML) or, conversely, 'ALL with myeloid antigen expression' (My^+ALL) when the criteria for a diagnosis of BAL are not met.

Table 8.8 *The EGIL scoring system for the definition of biphenotypic acute leukaemia (BAL)*

Points[a]	B-lineage	T-lineage	Myeloid lineage
2	$CD79a^+$ $cytIgM^+$ $cytCD22^+$	$cytCD3^+/smCD3^+$ TCR (α/β or γ/δ)$^+$	MPO^+
1	$CD10^+$ $CD19^+$ $CD20^+$	$CD2^+$ $CD5^+$ $CD8^+$ $CD10^+$	$CD13^+$ $CD33^+$ $CD65^+$
0.5	$CD24^+$ TdT^+	$CD1a^+$ $CD7^+$ TdT^+	$CD14^+$ $CD15^+$ $CD64^+$ $CD117^+$

EGIL, European Group for Immunological Classification of Leukaemias; MPO, myeloperoxidase (demonstrated by any method); cyt, cytoplasmic; sm, surface membrane; TdT, terminal deoxyribonucleotidyl transferase.

[a]To qualify as biphenotypic, the score of two separate lineages should be > 2.

8.6.1 Undifferentiated acute leukaemia

Very rarely, it is impossible to assign a lineage to a case of acute leukaemia. These leukaemias express no lineage-specific antigens and are characterised by the expression of nonlineage-specific antigens alone. Such patients are typically $CD34^+$ and $HLA\text{-}DR^+$ and may be TdT^+ or $CD7^+$ (Brito-Babapulle et al., 1987, 1990). Often, the patients have cytogenetic abnormalities usually associated with AML (such as $5q^-$) and it is, therefore, likely that they are 'biologically' closer to AML than ALL (Cuneo et al., 1996). Unfortunately, such forms have a poor prognosis.

8.7 B-cell lymphomas and chronic leukaemias

Historically, the diagnosis of B-cell lymphoproliferative disorders has centred on lymph node histology for 'lymphoma' and blood and marrow cytology for the 'leukaemias'. This divergence has led to somewhat distinct diagnostic approaches towards lymphoma and leukaemia. In 1989, the FAB group published guidelines for the diagnosis of the chronic lymphoid leukaemias without reference to many other B-cell lymphomas that did not commonly involve the blood or marrow (Bennett et al., 1989). This distinction between lymphomas and leukaemias is entirely artefactual and has led to several confusions. For instance, the same biological entity was termed 'chronic lymphocytic leukaemia' (CLL) when blood involvement predominated and 'small lymphocytic lymphoma' (SLL) when lymph node involvement predominated. Fortunately, these artificial distinctions are no longer made in contemporary classifications. Therefore, in the WHO classification of lymphoid neoplasms, there is a single entity termed 'B-cell CLL/SLL' (Harris et al., 1999).

This section will concentrate on lymphoid neoplasms that tend to involve the blood and marrow for the simple reason that these are most amenable to diagnostic immunophenotyping utilising flow cytometry. Lymphoid neoplasms that are predominantly lymph node based are usually diagnosed by nodal histology, coupled with immunocytochemistry performed on paraffin sections. However, a significant number of lymphoproliferative disorders that are traditionally considered to be lymph node centred can involve blood and marrow and so are amenable to immunophenotyping using flow cytometry. Furthermore, flow cytometry can also be performed on cell suspensions made from freshly biopsied lymph nodes, although this methodology has not yet found widespread application. Immunophenotyping is particularly useful for determining whether a lymphoid population is clonal or not. Monoclonal B-cell populations are defined by their expression of a single light chain ('light chain restriction') whereas polyclonal, reactive B-cells express both κ- and λ-light chains, normally in the approximate ratio of 2 : 1.

In order to understand the cellular origin of B-cell lymphomas, one must recall the normal sequence of events in B-cell biology (Kuppers et al., 1999). B-cell precursors undergo IgH gene rearrangements in the marrow and if a functional antigen receptor is produced these cells exit the marrow as naive B-cells. The majority of these cells are $CD5^{-}IgM^{+}IgD^{+}CD27^{-}$ although a subset are $CD5^{+}$. When naive B-cells recognise antigen they collect in the germinal centres of secondary lymphoid organs (lymph nodes, spleen and the mucosa-associated lymphoid tissue (MALT). Under the influence of the follicular environment, of which activated T-cells are an important component, the B-cells' genes for immunoglobulin undergo various modifications including somatic hypermutation of the variable region and class switching. As a result of somatic hypermutation, immunoglobulin molecules produced by most cells lose their affinity for cognate antigen and the cells undergo apoptosis. However, in a minority of cells, the resulting immunoglobulin molecule has a higher affinity for antigen than previously and these cells are positively selected. This process results in 'affinity maturation', which is typically observed during secondary immune responses. Simultaneously, germinal centre B-cells switch from expressing IgM and IgD to expressing IgG, IgA or IgE. Class switching is brought about by a recombination event that deletes the DNA between the relevant gene segments of the immunoglobulin constant regions of the heavy chain genes.

Following such an interaction between a naive B-cell and its cognate antigen in the lymphoid follicle, memory B-cells and plasma cells are produced that are typically class-switched (IgG or IgA expressing) and possess a somatically mutated immunoglobulin variable region. One can analyse the mutation status of B-cell lymphoma cells and thus identify them as the clonally expanded products of cells that have or have not been exposed to the environment of the lymphoid follicle. In this manner, it has been demonstrated that mantle cell lymphoma and some cases of B-cell chronic lymphocytic leukaemia (B-CLL) have unmutated immunoglobulin genes and so represent malignancies of naive B-cells. In contrast, most examples of B-cell lymphoma possess mutated immunoglobulin genes and thus represent tumours of B-cells that have passed through the follicle. Examples include follicular lymphoma (FL), lymphoplasmacytic lymphoma, Burkitt's lymphoma, diffuse large B-cell lymphoma (DLBCL), marginal zone lymphomas, hairy cell leukaemia (HCL), prolymphocytic leukaemia (B-PLL), multiple myeloma and some cases of CLL. Furthermore, some lymphomas demonstrate ongoing variable region somatic mutation, indicating that they remain under the influence of the lymph node follicle. The most important examples of this are FL and lymphoplasmacytic lymphoma (Kuppers et al., 1999).

Lymphomas derived from B-cells that have passed through the follicular environment tend to share a common immunophenotype. Such cells express the pan-B antigens CD19, CD20, CD24, CD79a and CD79b, as well as high levels of smIg, FMC7 and CD22. They are also typically negative for CD5 and CD23 (Harris et al., 1994). The most important dis-

ease entities will now be described in turn, emphasising the utility of immunophenotyping in aiding diagnosis.

8.7.1 Chronic lymphocytic leukaemia

B-CLL is the most common adult leukaemia and its incidence increases with age. Most cases of B-CLL display a typical morphology with numerous 'smear cells' and small lymphocytes with clumped chromatin. (CLL cells often become broken and disrupted when smeared onto slides for microscopic examination, hence the term smear cells.) The FAB group also recognises cases with more heterogeneous cytology or with 10–55% 'prolymphocytes' (CLL with increased prolymphocytes or CLL/PL) and together these are termed 'CLL, mixed cell type' (Bennett et al., 1989). Both these subsets probably have a worse prognosis.

B-CLL cells express the pan-B-cell markers CD19, CD20 (although weakly), CD24 and CD79a. smIg (IgM and IgD) is weakly expressed with clonally restricted light chain expression. Characteristically, CD22 expression is absent or very weak and FMC7 is not expressed, features that are otherwise unusual for peripheral B-cell neoplasms. Highly specific immunological features are the expression of CD23 and CD5 (Table 8.9) (Matutes et al., 1994a). CD5 is usually considered as a T-cell-restricted antigen but is also expressed by a subset of B-cells that represents approximately 15% of normal naive B-cells and is found in particularly large numbers in fetal and neonatal blood. Typically, these cells express 'germline' IgH molecules without somatic mutation and, certainly in mice, do not participate in T-cell-dependent reactions (Fischer et al., 1997; Stall et al., 1996). It is a contested point whether B-CLL represents a clonal expansion of the human equivalent of these cells.

Whatever the case, the characteristic spectrum of antigen expression in CLL has encouraged the development of a highly predictive scoring system for the positive identification of this leukaemia (Table 8.10) (Matutes et al., 1994a). Weak smIg expression is highly characteristic of B-CLL whereas all other chronic B-cell leukaemias and lymphomas express smIg strongly. It is likely that this low level expression is consequent on defective CD79b expression, since CD79a and CD79b are integral and necessary parts of the B-cell antigen receptor complex. Consequently, CD79b negativity is also a specific marker for B-CLL (Moreau et al., 1997).

It has recently become apparent that there are, in fact, two distinct biological subsets of B-CLL. Using IgH gene rearrangement analysis, B-CLL can be roughly equally divided between those with unmutated and those with mutated immunoglobulin V_H genes, corresponding to 'naive' and 'memory' B-cells, respectively. These two subtypes of CLL have a number of important differences in laboratory and clinical features (Table 8.11) (Damle et al., 1999; Hamblin et al., 1999). Most importantly, survival was three times longer for stage A patients with the mutated, 'memory' phenotype. CD38 expression was strongly correlated with the unmutated class and this may well become a simple and widely applicable prognostic indicator, although larger numbers of patients need to be analysed.

8.7.2 B-prolymphocytic leukaemia

B-PLL is a disorder characterised by a high white count, splenomegaly and a male preponderance. Cytology is also typical with relatively abundant cytoplasm and the presence of a prominent, often central, nucleolus. The B-PLL phenotype is that of a B-cell that has passed through the lymphoid follicle and, therefore, has the 'consensus' phenotype shared by most B-cell lymphomas and leukaemias (Table 8.9). The CLL score tends to be 0/5 or 1/5, which helps to distinguish B-PLL from B-CLL and its variants, including CLL/PL (Rozman and Montserrat, 1995).

8.7.3 Mantle cell lymphoma

Mantle cell lymphoma (MCL) generally presents with lymph node enlargement, although marrow and blood involvement are also common and

Table 8.9 *Immunophenotype of the chronic B-cell leukaemias and lymphomas*

B-cell neoplasm	B-cell antigens	Surface immunoglobulin (smIg)		Cytoplasmic immunoglobulin (cytIg) expression	Characteristic antigens	Overall immunophenotype
		Expression	Class			
CLL	$CD19^+CD20^+CD22^-$ $CD79a^+CD79b^-FMC7^-$	Weak	M^+D^+	–	$CD5^+CD23^+$	$CD5^+CD19^+CD20^+CD22^-CD23^+CD79a^+$ $CD79b^-$ $FMC7^-$smIg Weak (IgM/D)
PLL	$CD19^+CD20^+CD22^+CD79$ $a^+CD79b^+FMC7^+$	+	M^+ or M^+D^+	–		$CD5^-CD19^+CD20^+CD22^+CD23^-$ $CD79a^+CD79b^+FMC7^+smIg^+$ (IgM or IgM/D)
MCL	$CD19^+CD20^+CD22^+CD79$ $a^+CD79b^+FMC7^+$	+	M^+ or M^+D^+	–	$CD5^+CD23^-$	$CD5^+CD19^+CD20^+CD22^+CD23^-$ $CD79a^+CD79b^+FMC7^+smIg^+$(IgM or IgM/D)
FL	$CD19^+CD20^+CD22^+CD79$ $a^+CD79b^+FMC7^+$	+	M^+, M^+D^+, G^+ or A^+	–	$CD10^+$	$CD5^-CD10^+CD19^+CD20^+CD79a^+CD22^+$ $CD23^-$ $CD79b^+FMC7^+smIg^+$ (IgM, IgM/D, IgG or IgA)
LPC	$CD19^+CD20^+CD22^+CD79$ $a^+CD79b^+FMC7^+$	+	M^+	+		$CD5^-CD19^+CD20^+CD22^+CD23^-$ $CD79a^+CD79b^+FMC7^+smIg^+(IgM)cytIg^+$
DLBCL	$CD19^+CD20^+CD22^+CD79$ $a^+CD79b^+FMC7^+$	+	M^+, G^+ or A^+	+ / –		$CD5^-CD19^+CD20^+CD22^+$ $CD23^-$ $CD79a^+CD79b^+FMC7^+smIg^+$ (IgM, IgG or IgA)$cytIg^{+/-}$
MZL	$CD19^+CD20^+CD22^+CD79$ $a^+CD79b^+FMC7^+$	+	M^+, G^+ or A^+	+ /–		$CD3^-CD5^-CD19^+CD20^+$ $CD22^+$ $CD79a^+CD79b^+FMC7^+smIg^+$(IgM, IgG or IgA)$cytIg^{+/-}$

CLL, chronic lymphocytic leukaemia; DLBCL, diffuse large B cell lymphoma; FL, follicular lymphoma; LPC, lymphoplasmacytic lymphoma; MCL, mantle cell lymphoma; MZL, mantle zone lymphoma; PLL, prolymphocytic leukaemia.

Table 8.10 *A scoring system for the immunophenotypic diagnosis of chronic lymphocytic leukaemia (B-CLL)*

Antigen	Score[a]
Surface membrane immunoglobulin weak	+1
CD5 positive	+1
CD22 weak or negative[b]	+1
CD23 positive	+1
FMC7 negative	+1

[a]A score of 4/4 or 4/5 confirms B-CLL (Matutes et al., 1994a).
[b]An alternative for CD22 is CD79b (see text).

Table 8.11 *Features of B-cell chronic lymphocytic leukaemia (B-CLL) associated with unmutated and mutated* V_H *genes*

Feature	Unmutated V_H gene	Mutated V_H gene
Cytology	Atypical	Typical
Sex ratio	Male > female	Male = female
CD38 expression	$CD38^+$	$CD38^-$
Frequent karyotype	Trisomy 12	
Prognosis	Poor	Good
Median survival (stage A patients) (months)	95	293

patients frequently present as a B-cell leukaemia. Often, there is gastrointestinal involvement and the prognosis is generally poor. MCL results from a specific chromosomal translocation, t(11;14), that juxtaposes the gene *BCL-1* with the gene for IgH and brings the former under the control of the IgH enhancer, resulting in overexpression of the *BCL-1* gene product cyclin D_1 (Banks et al., 1992). This protein is involved in the control of the cell cycle and its overexpression drives cellular proliferation. MCL expresses the consensus B-cell nonHodgkin lymphoma phenotype but is also $CD5^+$ (Table 8.9). MCL should be considered in any B-cell malignancy that has the $CD5^+CD23^-$ phenotype. MCL is unusual among the B-cell neoplasms in that its V_H genes are in germline configuration and so, akin to many B-CLL cases, it represents a tumour of naive, pregerminal centre B-cells (Kuppers et al., 1999). Developing techniques for analysing cytoplasmic antigens (e.g. cyclin D_1) by flow cytometry may well prove to be important for improving the diagnosis of MCL.

8.7.4 Other B-cell lymphomas

Several other B-cell lymphomas have a propensity for involving the blood and bone marrow to a greater or lesser extent, including FL, lymphoplasmacytic lymphoma, nodal and extranodal marginal zone lymphomas, Burkitt lymphoma and DLBCL. Burkitt lymphoma, although biologically a tumour of postfollicular B-cells, is discussed with the ALLs because of its historical (FAB) classification as such. The WHO classification has abolished the L1–L3 morphological designations entirely, such that ALL L3 is now designated 'Burkitt lymphoma in leukaemic phase' (Harris et al., 1999).

FL is the commonest type of lymphoma and characteristically has a relatively indolent course, although transformation to a more high-grade, aggressive form is not uncommon. A fundamental feature of FL is the t(14;18) translocation, which juxtaposes the *BCL-2* gene with the IgH enhancer region (Weiss et al., 1987). The consequent overexpression of Bcl-2, a potent antiapoptotic protein, results in deficient programmed cell death and the accumulation of neoplastic FL cells. FL cells express the consensus B lymphoma antigen phenotype but also generally express CD10, which is therefore useful in distinguishing FL in leukaemic phase from other B-cell neoplasms (Jennings and Foon, 1997). High levels of cytoplasmic Bcl-2 expression are found consistently in FL but are also seen in other B-cell malignancies such as B-CLL.

Lymphoplasmacytic lymphoma is a neoplasm resulting from the clonal expansion of a B-cell that has been exposed to the follicular environment and thus has a mutated V_H region (Kuppers et al., 1999). However, class switching has usually not occurred so these tumours are generally $smIgM^+$ and also are likely to be $cytIgM^+$ and to secrete an IgM paraprotein (although IgG^+ cases do occur) (Harris et al.,

1994). The term 'Waldenstrom's macroglobulinaemia' refers to a particular clinical presentation of lymphoplasmacytic lymphoma dominated by bone marrow and splenic involvement along with a high level of IgM paraprotein, resulting in symptoms of hyperviscosity. The lymphoplasmacytic immunophenotype tends to conform to the consensus B-cell immunophenotype (Table 8.9). Some patients will express cytIg, usually of IgM isotype (Harris et al., 1994). DLBCL rarely becomes leukaemic and usually there is no diagnostic difficulty since a positive diagnosis has already been established by lymph node biopsy. Patients with DLBCL express normal B-cell associated antigens without any specific or unique features.

Lymphomas arising from the marginal zone can involve lymph nodes, spleen or MALT (Harris et al., 1999). These tumours rarely involve blood or marrow and their immunophenotype is largely the consensus B lineage phenotype without positive distinguishing features. However, a subset of splenic marginal zone lymphomas are characteristically accompanied by peripheral blood lymphocytosis, and this entity is often referred to as 'splenic lymphoma with circulating villous lymphocytes' or (SLVL) (Matutes et al., 1994b; Melo et al., 1987). This last entity shares cytological features with HCL and is discussed below.

8.7.5 Hairy cell leukaemia, hairy cell leukaemia variant and splenic lymphoma with circulating villous lymphocytes

HCL, HLC variant (HCL-V) and SLVL are discussed together because they share certain cytological and clinical characteristics. In all three, the malignant cells have cytoplasmic projections ('hairs' or villi) and splenomegaly is a cardinal feature. Immunophenotyping is an extremely important adjunct to detailed morphological examination in the differential diagnosis of these three conditions.

HCL typically presents with significant splenomegaly, pancytopenia with striking monocytopenia and relatively few circulating hairy cells. These have a rather 'bland' oval or indented nucleus with abundant cytoplasm and 'hairy' projections. HCL expresses the 'consensus' B-cell immunophenotype and is typically $CD5^{-}CD23^{-}smIg^{+}$ and sometimes $cytIg^{+}$ (of IgM, IgM/D, IgG or IgA isotype) (Jennings and Foon, 1997). In addition, HCL has a highly characteristic marker profile which has been adapted for use as a HCL scoring system (Table 8.12) (Matutes and Catovsky, 1994).

HCL-V is often confused with HCL because of its shared features, namely splenomegaly and 'hairy cell' cytology. However, the nucleus is dissimilar and shares features with B-PLL cells rather than HCL. In addition, the white count is usually significantly elevated and monocyte numbers are normal (Sainati et al., 1990). The HCL-V immunophenotype is analogous to that of B-PLL, and the HCL 'score' is less than 3/4 (Matutes and Catovsky, 1994). CD11c is occasionally positive.

SLVL is a marginal zone lymphoma of the spleen with circulating lymphoma cells. These cells also have cytoplasmic projections but these tend to be at either end of the cell ('polar') rather than circumferential. Otherwise, the cells bear more resemblance to atypical B-CLL cells, while a minority show plasmacytic differentiation. Indeed, SLVL is quite commonly $CD38^{+}cytIg^{+}$ and associated with a paraprotein. The 'hairy cell score' is again helpful in differentiating SLVL from HCL, although up to 50% of patients are $CD11c^{+}$ (Matutes et al., 1994b).

8.7.6 Plasma cell leukaemia

Multiple myeloma is usually restricted to the bone marrow but more aggressive forms of the disease are accompanied by circulating plasma cells and when these number greater than 2×10^{9} cells l^{-1} the term 'plasma cell leukaemia' is applied. Plasma cells are terminally differentiated B-cells with the function of secreting immunoglobulin. Therefore, they no longer require an extensive range of membrane molecules with which to communicate with other cells since their functional role is already irrevocably determined. Consequently, plasma cells are characterised by negativity for B-cell antigens including smIg. Obviously, since they are actively

Table 8.12 *A scoring system for the immunophenotypic diagnosis of hairy cell leukaemia (HCL)*

Antigen	Score
$CD11c^+$	+1
$CD25^+$	+1
CD103+	+1
$HC2^+$	+1

Scores of 0–2 indicate HCL variant or 'splenic lymphoma with circulating villous lymphocytes' (SLVL); scores ≥ 3 indicate HCL.

secreting Ig, they are strongly $cytIg^+$. Potentially useful markers are CD38 and CD138 (syndecan-1), which are typically expressed by both normal and malignant plasma cells (San Miguel et al., 1995).

8.8 Chronic T-cell leukaemias

The chronic T-cell leukaemias are all derived from 'mature', 'peripheral' or post-thymic T-cells and are, therefore, $CD3^+$, TCR^+ and TdT^-. Mature T-cells are in most patients either $CD4^+$ or $CD8^+$, although rare exceptions are seen. A characteristic feature of the more common $CD4^+$ T-cell leukaemias is a propensity for skin infiltration.

8.8.1 $CD4^+$ T-cell leukaemias

The important $CD4^+$ T-cell malignancies with predominant blood involvement are T prolymphocytic leukaemia (T-PLL), Sezary syndrome and adult T-cell lymphoma/leukaemia (ATLL).

T-PLL was so designated because of its cytological similarity to B-PLL. Characteristically, there is a high white count and splenomegaly and there may be lymphadenopathy, skin infiltration and serous effusions (Matutes et al., 1991). Recurrent chromosomal abnormalities involve the TCR $\alpha\delta$ locus at 14q11 and the *TCL1* oncogene at 14q32. These translocations are analagous to those associated with B-cell malignancies involving the immunoglobulin genes. T-PLL expresses the pan-T markers CD2, CD3 and CD5 (Table 8.13) as do all other T-cell leukaemias. However, CD7 is virtually always expressed at high levels and this feature is particularly helpful for distinguishing T-PLL from other $CD4^+$ T-cell leukaemias (Matutes et al., 1991).

Sezary syndrome is a term that refers to the coexistence of a T-cell leukaemia with an erythrodermic lymphomatous skin infiltration. In reality, it is closely related to the better known T-cell skin lymphoma mycosis fungoides. The malignant cell is the same in both conditions although in the latter the tumour is largely restricted to the skin whereas in Sezary syndrome there is skin and blood involvement. Cells in the blood can be either large or small and typically the nucleus has a 'cerebriform' appearance. The immunophenotype is $CD2^+CD3^+CD5^+$ but mostly $CD7^-$. This distinguishes Sezary syndrome from T-PLL and the $CD4^+CD7^-CD25^-$ phenotype is characteristic of Sezary syndrome (Bogen et al., 1996).

ATLL is of particular interest because it is one of the few lymphomas that is known to result from a viral infection, in this case human T-cell lymphotropic virus-1 (HTLV-1) (Manns et al., 1993). It occurs predominantly in people of Japanese or West African origin and consequently is found in the Caribbean and to a lesser extent in the USA and Europe. Typically, ATLL involves the skin, nodes, bone marrow and blood. The nuclei of circulating lymphoma cells have a characteristic 'flower' appearance (Shimoya et al., 1991). The presence of antibody to HTLV-1 confirms the diagnosis in patients with other typical features of ATLL. The immunophenotype is also highly specific: $CD2^+CD3^+CD5^+CD7^{+/-}CD25^+$. The expression of CD25, the interleukin 2 receptor, is characteristic of ATLL and is also important pathophysiologically since interleukin 2 production helps to drive proliferation of the malignant cells.

8.8.2 $CD8^+$ T-cell leukaemias

The only commonly occurring $CD8^+$ T-cell leukaemia is T large granular lymphocyte leukaemia (T-LGLL) (Loughran, 1993). This represents a clonal expansion of $CD8^+$ cytotoxic T-cells and is often

Table 8.13 *Immunophenotypes of chronic T-cell leukaemias*

Disorder	CD2	CD3	CD5	CD7	CD4	CD8	CD25
T-PLL	+	+	+	+	+	–	+/–
SS	+	+	+	+/–	+	–	–
ATLL	+	+	+	+/–	+	–	+
T-LGLL	+	+	+/–	+/–	–	+	–

ATLL, adult T-cell lymphoma/leukaemia; T-LGLL, T large granular lymphocyte leukaemia; SS, Sezary syndrome; T-PLL, T prolymphocytic leukaemia.

found in association with rheumatoid arthritis and presents with splenomegaly, modest lymphocytosis and neutropenia. The immunophenotype of T-LGLL is highly characteristic: $CD2^{+}CD3^{+}CD5^{+/-}CD7^{+/-}CD8^{+}CD16^{-}CD56^{-}CD57^{+}$. This phenotype is very helpful in distinguishing this disorder from natural killer large granular lymphocyte leukaemia, which is indistinguishable morphologically. This disorder occurs most commonly in the Far East and is exceptionally rare in the West (Loughran, 1993). Its phenotype is $CD2^{+}CD3^{-}CD5^{-}CD4^{-}CD8^{-}CD16^{+}CD56^{+}CD57^{-}$, which is easily distinguishable from T-LGLL.

T-LGLL expansions are often considered malignant because of the associated finding of clonal TCR gene rearrangements. However, clonal TCR rearrangements are also found in nonmalignant, 'reactive' conditions such as human immunodeficiency virus (HIV) infection and so the 'neoplastic' nature of these clonal T-cell expansions remains uncertain (Smith et al., 2000). Indeed, a significant proportion occur in the setting of chronic inflammatory conditions such as rheumatoid arthritis.

8.9 Myeloproliferative disorders

Classification of the myeloproliferative disorders is difficult because there is a spectrum of disease without clearly defined parameters and because one disorder is capable of transforming into another. The most prevalent disorder is chronic granulocytic leukaemia also known as chronic myeloid leukaemia (CML). The Philadelphia chromosome (Ph') is an acquired translocation between chromosomes 22 and 9 and is highly characteristic of chronic granulocytic leukaemia, being present in 96% of patients. It is clear that AML is a disorder of stem cells common to granulocytopoiesis, erythropoiesis and thrombocytopoiesis. Most descendents from the diseased stem cell fail to differentiate and remain as blast cells. In CML, the progeny of the leukaemic stem cells have differentiated to some extent and may give rise to functionally useful cells. The mechanism by which useful hemopoiesis is apparently suppressed in the presence of leukaemic cells remains enigmatic. However, of those patients with this disorder, 80% transform to acute leukaemia, usually myeloid.

8.10 Flow cytometric analysis of leukaemic samples

The different types of leukaemia clearly have distinguishing immunophenotypes; however, one of the problems associated with the flow cytometric analysis of leukaemias is the identification of the disease population of cells in the blood or bone marrow (Borowitz et al., 1997). If the blood or bone marrow sample from the patient contains predominantly disease cells then these may be identified by atypical light scattering properties. Some examples of the light scattering properties of different leukaemias are illustrated in Fig. 8.1. However, if this is not the case, then dual- and triple-fluorescence analysis may be necessary in which, for example, the phenotype of $CD34^{+}$ cells is assessed (Chen et al., 1996). An example of this type of backgating is illustrated in Fig. 8.2.

8.11 Therapeutic monitoring

8.11.1 Recovery after chemotherapy and transplantation

The assessment of immune status following immunotherapy, and correlation between immu-

nological status and clinical course, are important in a variety of situations. After bone marrow transplantation, the patient is severely immune deficient. It is, therefore, necessary to monitor lymphocyte subpopulations to ensure that (i) a normal hemopoietic system develops, (ii) any onset of graft-versus-host disease is identified so that chemotherapy may be modified, (iii) graft versus leukaemia in CML is followed, and (iv) development of residual disease is detected (see below).

The recovery of lymphocyte subpopulations after bone marrow transplantation may take up to a year, with the $CD8^+$ T-cell population recovering first. These $CD8^+$ cells are large granular lymphocytes that exhibit NK cell activity (Jacobs et al., 1992; Lowdell et al., 1997). The $CD4^+$ T lymphocytes may not reach normal levels for at least 6 months after transplantation.

During the 1990s peripheral blood stem cells have been used as an alternative to bone marrow for use in autologous transplantation (Gale et al., 1992; Law et al., 1999; Zimmerman et al., 1995). The levels of peripheral blood stem cells are increased after standard chemotherapy and after high-dose chemotherapy such as cyclophosphamide. The myeloid growth factors granulocyte colony-stimulating factor (G-CSF) and granulocyte–macrophage colony-stimulating factor (GM-CSF) have also been used to enhance stem cell production (Ho et al., 1996). The generation of stem cells may be monitored by determining the percentage of $CD34^+$ cells in peripheral blood by flow cytometry and there are many publications on the standardisation of this process (Keeney et al., 1998; Law et al., 1999; Sutherland et al., 1997).

8.11.2 Monitoring response to treatment in immunodeficiency states

$CD4^+$ and $CD8^+$ T lymphocytes have been used to correlate immune equilibrium with disease course. Although ratios significantly different from the normal range (0.6–2.8) have been found in many diseases, functional studies have all too often not correlated with immune imbalance, perhaps because there is also normal circadian variation, as described above, and factors such as exercise that influence cell numbers (Fry et al., 1992). One exception is the imbalance in the acquired immunodeficiency syndrome (AIDS). Early in the course of this disorder, affected individuals have a reversed ratio because of the profound depletion of $CD4^+$ T-cells, and this is highly predicative of clinical disease progression (Macey, 2000; Moses et al., 1998; Schmid et al., 1999).

8.11.3 Rare event analysis

Although one of the major advantages of flow cytometry is the ability to analyse large numbers of cells on a discrete basis, some implications of this have not been fully appreciated until recently. Flow cytometry offers a means of quantifying minor subpopulations of cells (rare events) to a degree that was impossible by manual techniques. This rare event analysis is limited to a frequency of 1 in 100 000, beyond which only rough estimates can be obtainable even after collecting 10^7 events. However this form of analysis has been used to detect reticulocytes, malarial parasites, transfused blood survival, the presence and/or genotypic and phenotypic characteristics of fetal cells in maternal blood and, of much interest recently, the detection of $CD34^+$ cells in peripheral blood from patients undergoing stem cell transplantation regimens. Rare event analysis has also been used for the detection of minimal residual disease (MRD).

8.11.4 Detection of minimal residual disease

Leukaemia relapse is still the major cause of failure in the treatment of acute leukaemia. Relapse rates vary from 60 to 80% after chemotherapy and from 20 to 50% after allogeneic or autologous bone marrow transplantation, respectively. MRD is defined as those relatively few leukaemic cells that have survived initial remission-inducting chemotherapy. The number of cells in the entire bone marrow compartment is in the order of 10^{12}. The conventional detection level of MRD of less than 5% blast

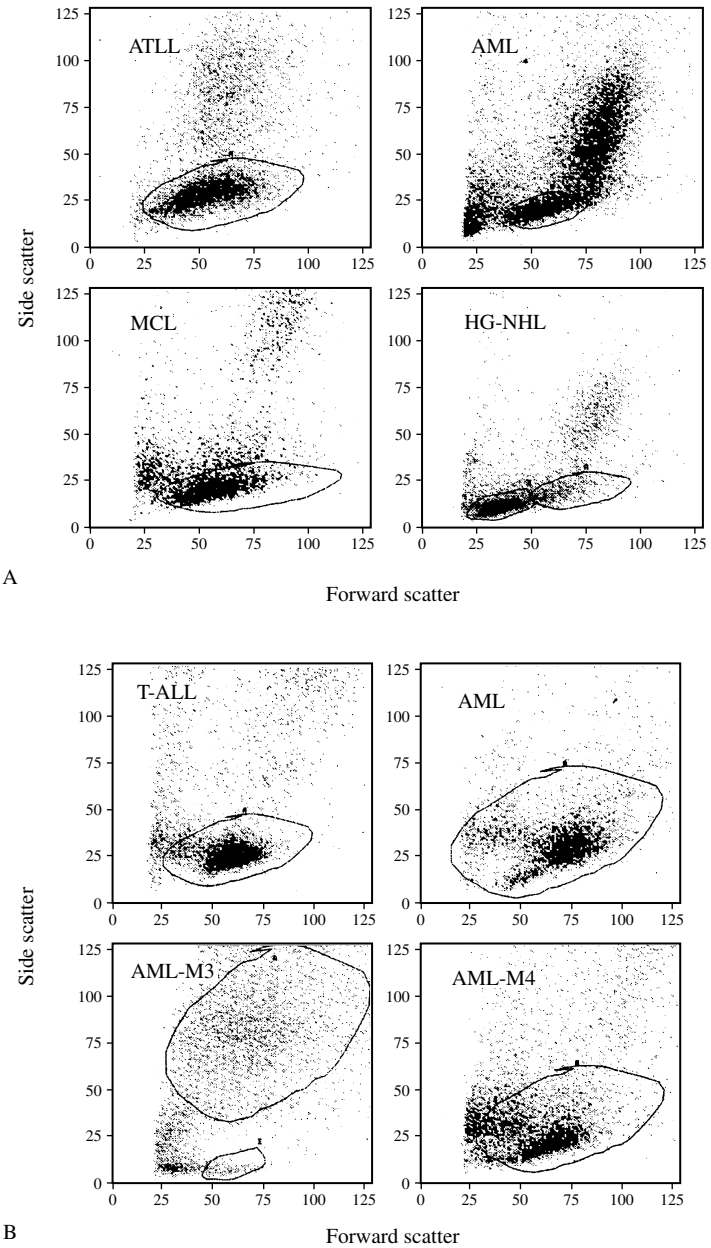

Fig. 8.1 The forward and side light scattering properties of different disease populations are illustrated in peripheral blood (upper panel) and bone marrow (lower panel) samples. ATLL, acute T lymphocytic leukaemia; AML, acute myeloid leukaemia; MCL, mantle cell leukaemia; HG-NHL, high-grade nonHodgkin lymphoma; T-ALL, T acute lymphoblastic leukaemia.

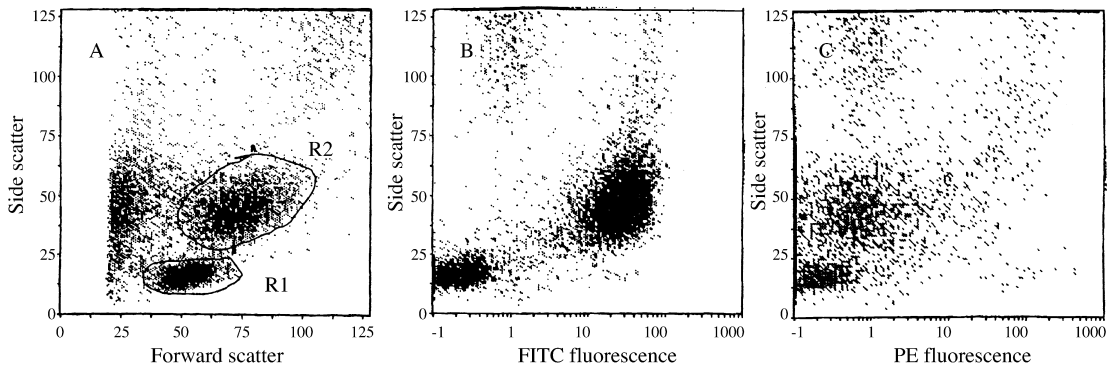

Fig. 8.2 Analysis of blood from a patient with hairy cell leukaemia. (A) Two populations of cells can be identified, which appear to be lymphocytes (R1) and monocytes (R2). The leukaemic B-cells might be expected to lie in the lymphoid region; however the analysis of kappa (histogram B) and lambda (histogram C) light chains on the cells show that the monoclonal disease population is to be found in the monocyte region.

cells would require 10^{10} leukaemic cells to be present in the bone marrow. In bone marrow, the distribution of MRD is extremely heterogeneous. Analysis of marrow samples from different bones yields differences in leukaemic cell frequencies; consequently, the measured leukaemic frequency in one specific marrow sample may not reflect the concentration in other compartments. Furthermore, in humans, one bone marrow aspiration contains only 0.0001% of the entire marrow compartment. Therefore, quantification of MRD in a given patient based on a simple bone marrow aspiration is likely to be unsuccessful. However, monoclonal antibodies and flow cytometry may be used for the immunological detection of MRD.

Current strategies for detecting residual disease rely on combinations of leukocyte antigens normally not seen in peripheral blood and bone marrow. Such leukaemia-associated phenotypes can be identified by double-, triple- or quadruple-colour staining techniques performed with antibodies conjugated to different fluorochromes (Campana and Coustan-Smith, 1999). Additional capabilities of flow cytometry such as cell sorting followed by fluorescent in situ hybridisation (FISH; Engel et al., 1997), or simultaneous analysis of phenotype and DNA content (Nowak et al., 1997) may also contribute to MRD studies.

Differences in the antigenic expression of ALLs and normal progenitor cells may be qualitative or quantitative (Table 8.14). Qualitative differences are seen in immunophenotypic combinations expressed by leukaemic cells but extremely rarely by normal bone marrow cells. Quantitative differences in antigen expression can also be used to distinguish leukaemic blasts from subsets of normal cells with similar phenotypes. The phenotypic differences between leukaemic myeloblasts and normal bone marrow cells are mostly quantitative (Table 8.15).

Campana and Coustan-Smith (1999) used these combinations to detect 1 leukaemic cell per 10 000 normal cells in marrow samples that morphologically appeared to be in complete remission, and the detection of MRD correlated with the occurrence of subsequent leukaemia relapse. To monitor residual disease it is essential to have detailed information about the immunophenotypic features of the patient's leukaemic cells at the time of diagnosis. These dictate the selection of appropriate antigen combinations. Figure 8.3 summarises the flow cytometric protocol for MRD detection. The light scattering and immunophenotype of 2000-10 000 cells are first recorded. These data are then used to define two gates, one enclosing events reflecting light scattering of the leukaemic blasts (gate 1) and

Table 8.14 *Immunophenotypic combinations used to study minimal residual disease in acute lymphoblastic leukaemia (ALL)*

ALL lineage	Leukaemia-associated differences[a]	Phenotype	Frequency (%)[b]
B	Mostly quantitative	$CD10^+CD19^+CD34^+TdT^+$	30–50
		$CD10^+CD19^+CD22^+CD34^+$	20–30
		$CD10^+CD19^+CD38^+CD34^+$	30–50
		$CD10^+CD19^+CD34^+CD45^+$	30–50
	Mostly qualitative	$CD10^+CD13^+CD19^+CD34^+$	10–20
		$CD10^+CD15^+CD19^+CD34^+$	5–10
		$CD10^+CD19^+CD33^+CD34^+$	5–10
		$CD10^+CD19^+CD34^+CD65^+$	5–10
		$CD10^+CD19^+CD21^+CD34^+$	5–10
		$CD10^+CD19^+CD34^+CD56^+$	5–10
		$CD10^+CD19^+CD34^+KORSA3544^+$	10–20
		$CD19^+CD34^+TdT^+cyt\mu^+$	10–20
		$CD19^+7.1^+$	3–5
		$CD19^+p53^+$	3–5
T	Qualitative	TdT^+CD3^+	90–95
		$CD34^+CD45^+$	30–50

cytμ, cytoplasmic IgM μ-chain; TdT, terminal deoxyribonucleotidyl transferase.

[a]Differences between leukaemic and normal cells in immunophenotypic expression may reflect differences in intensity of expression of one or more antigen (quantitative) or the expression of the antigen may not be found on normal lymphoid progenitors (qualitative).

[b]The percentage frequency represents the proportion of childhood ALL cases in which 1 leukaemic cell in 10 000 normal bone marrow cells can be detected using the listed immunophenotypic combination. Most cases express more than one suitable combination.

one around events expressing specific antigens (gate 2). Boolean instructions are used to identify events that fulfil the criteria delineated by both gates. This method allows screening of 1×10^6 or more bone marrow cells and the retention of data from only the relevant cells. The antigen-associated captured data is back-gated to a light scatter plot to ensure that they form a tight cluster, which is indicative of a homogeneous cell population. At least 10 to 20 events should be captured. The light scatter profile and intensity of antigen expression should reproduce those of malignant cells characterised at the time of diagnosis.

False-negative results in the immunological detection of MRD may result from (i) the presence of very few leukaemic cells in the sample under study, (ii) sampling error owing to heterogeneous distribution of cells within the marrow and (iii) phenotypic switch. A limited number of cases have been reported in which a phenotypic switch occurs between analysis at presentation and relapse.

8.11.5 Analysis of cell function

The use of flow cytometry to measure cell function, including neutrophil and monocyte phagocytosis and metabolism, cell-mediated cytotoxicity, actin polymerisation and calcium flux is now widely appreciated. Many of these assays may be carried out in whole blood without the need to isolate the leukocytes. Much interest has focused on the measurement of molecules associated with adhesion on monocytes and neutrophils, particularly during treatment with growth factors G-CSF and GM-CSF during stem cell transplant programmes (Williams et al., 1995) and in sepsis (Williams et al.,

Table 8.15 *Immunophenotypic combinations used to study minimal residual disease in acute myeloid leukaemia (AML)*

Leukaemia-associated differences	Phenotype	Frequency (%)[a]
Mostly quantitative	$CD11b^+CD13^+CD33^+CD34^+$	10–15
	$CD13^+CD33^+CD34^+CD65^+$	10–20
	$CD15^+CD13^+CD33^+CD34^+$	10–20
	$CD13^+CD33^+CD34^+CD56^+$	10–15
	$CD13^+CD33^+CD34^+CD38^+$	10–15
	$CD13^+CD33^+CD34^+CD117^+$	20–40
	$CD15^+CD33^+CD34^+CD117^+$	20–40
	$CD33^+CD34^+CD117^+HLA\text{-}DR^+$	10–15
	$CD11b^+CD33^+CD34^+CD117^+$	10–20
	$CD13^+ CD19^+CD33^+CD34^+$	5–10
	$CD2^+CD13^+CD33^+CD34^+$	5–10
	$CD7^+CD13^+CD33^+CD34^+$	20–30

[a]The percentage frequency represents the proportion of childhood AML cases in which 1 leukaemic cell in 10 000 normal bone marrow cells can be detected using the listed immunophenotypic combination. Most patients express more than one suitable combination.

1998). Similarly, the identification of the degree of expression of an antigen on the cell surface of leukocytes is becoming increasingly important in the understanding of cellular function and disease process. In these studies, cellular activation has been correlated with disease severity. Examples are the upregulation of CD69 expression following cell activation and its relation to immune function (Craston et al., 1997; Maino et al., 1996; Waldrop et al., 1997), elevation of CD38 on $CD8^+$ T-cells as a prognosticator late in AIDS (Liu et al., 1996), decrease in HLA-DR expression on monocytes as an indicator of deactivation in advanced sepsis (Docke et al., 1997) and elevation of CD64 on neutrophils as a early indicator of sepsis (Davis, 1996). Flow cytometric analysis of whole blood without cell isolation procedures offers the best method for the detection and quantification of molecules associated with adhesion and activation.

8.12 Diagnosis of other hematological disorders

The phenotypic analysis of lymphocytes and leukaemias is well established; however, the analysis of monocytes and neutrophils may also be used in the diagnosis of a number of hematological conditions.

8.12.1 Paroxysmal nocturnal hemoglobinuria

There are more than 40 surface protein molecules that have a phosphatidylinositol glycosyl phospholipid (PIG) linkage in the membrane of different cells. These include the FcRIII receptor for human IgG (CD16) on neutrophils, decay accelerating factor (CD55) on erythrocytes and the receptor for lipopolysaccharide (CD14) on monocytes. Deficiency in these molecules will, therefore, affect the function of a variety of cells. Paroxysmal nocturnal hemoglobinuria is an acquired hematopoietic stem cell disorder in which a somatic mutation of the X-linked *PIG-A* gene results in a partial or absolute lack of synthesis of the PIG linkage that anchors proteins to the cell membrane. Most if not all patients with paroxysmal nocturnal hemoglobinuria have evidence of underlying bone marrow failure. The hemolytic anaemia associated with this disorder is caused by an intrinsic defect resulting from a lack of CD55 in the red cell membrane, which renders the cells susceptible to complement-mediated lysis.

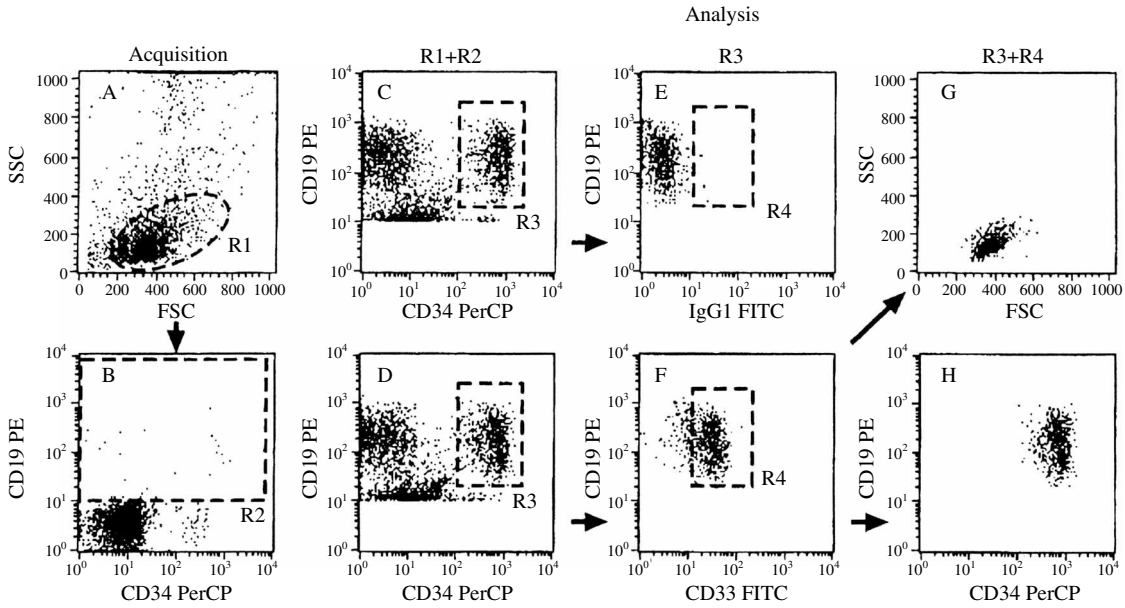

Fig. 8.3 Protocol for flow cytometric detection of minimal residual disease. Dot plots illustrate the study of a bone marrow sample from a patient with acute lymphoblastic leukaemia during clinical remission. Leukaemic cells at diagnosis expressed CD19, CD34 and CD33. Mononuclear cells from the remission bone marrow sample were labelled with PE–CD19, PerCP–CD34 and FITC–CD33. In a parallel tube, CD33 was replaced by control FITC–IgG_1. After analysing 10 000 mononuclear cells, two gates were drawn: one to include cells with lymphoid morphology (R1) (A) and one to include cells expressing CD19 (B). The protocol then accumulated 450 000 events from which only those events that fulfilled the criteria of R1 and R2 were retained (B, C). The immunophenotype of $CD19^+CD34^+$ cells (R3) was analysed for the expression of CD33 (D, E): most cells were $CD33^+$ (F) and negative for the isotype-matched control antibody (E). The light scatter and the immunophenotypic features of $CD19^+CD34^+CD33^+$ cells (R3 + R4) corresponded to those determined at diagnosis (G, H). Residual leukaemic cells formed 0.14% of the total bone marrow mononuclear cells. FITC, fluorescein isothiocyanate; PE, phycoerythrin; PerCP, peridinin–chlorophyll *a* complex. (Reprinted by permission of Wiley-Liss, Inc., a subsidiary of John Wiley & Sons, Inc., from Campana, D., Coustan-Smith, E. (1999) Detection of minimal residual disease in acute leukaemia by flow cytometry. *Cytometry* **38**, 139–52.

8.12.2 Autoimmune neutropenia

Patients with autoimmune neutropenia are diagnosed by having a neutropenia in isolation and may have neutrophil-associated immunoglobulin. Neutropenia may occur associated with an expansion of large granular lymphocytes. Often this occurs without an obvious lymphocytosis in the patient's blood. This expansion is readily detectable by flow cytometry.

8.12.3 Primary immunodeficiency

Primary immunodeficiency disorders that are caused by a single gene defect often have a family history that points to either an X-linked or an autosomal recessive or dominant mode of inheritance. Infants with T-cell abnormalities often present with *Pneumocystis carinii* and fungal infection in addition to bacterial infections, often before the age of 3 months. In contrast, patients with a predominant B-cell abnormality do not develop symptoms until maternal antibodies have disappeared, and they are mostly troubled by infections of the lower and upper respiratory system. Patients with

neutrophil defects may present at any age with skin infections, abscesses and lymphadenopathy caused by staphylococci, *Serratia, Klebsiella* or *Aspergillus* spp. Older patients with primary immunodeficiency diseases may present with chronic lung disease, including bronchitis, or with chronic sinusitis and mastoiditis, gastrointestinal complaints or arthritis (Chapel and Webster, 1999). Severe combined immune deficiencies are rare disorders affecting both the T and B-cells. Affected patients typically present during the first few months of life with failure to survive, skin rashes, sparse hair, diarrhoea, weight loss, and bacterial, fungal and viral infections. Flow cytometry may be used to quantify the numbers of T-cell subsets, B-cells, NK cells and metabolic burst activity in neutrophils in these patient and so can aid in the diagnosis of the underlying immune dysfunction.

8.13 Analysis of genetic variation in polymorphic markers

8.13.1 NA1/NA2 and SH

The granulocyte antigens NA1 and NA2 are two allelic gene products of the gene for FcγRIIIB (CD16 antigen). These antigens are frequently targets of the granulocyte-specific allo- and autoantibodies that cause neutropenia. Different distributions of these antigens have been found in population studies. Recently, a third alloantigen, SH, on the FcγRIIIB was identified (Bux et al., 1997). Some individuals have been found to lack one or more of these antigens and this appears to influence a number of immune functions. FcγRIIIB is the low-affinity receptor for the Fc region of complexed IgG antibodies and preferentially removes immune complexes from the circulation. It is released from the neutrophil membrane during apoptosis, and soluble FcγRIIIB can inhibit proliferation and production of stimulated B-cells. Antibodies are available that are specific for the different antigens: monoclonal antibodies GRM1 and PEN1 are specific for NA2 but the reactivity of PEN1 is sixfold higher on cells that are SH^+. The use of these antibodies allows the flow cytometric detection of the different antigens in individuals within the population (Koene et al., 1998). Studies have provided evidence for the relevance of FcγRIIIB polymorphisms as risk factors for a number of infectious and autoimmune diseases (van der Pol and van de Winkel, 1998).

8.13.2 HLA-B27 typing

HLA-B27 (B27) is a disease-associated genetic antigen important in the diagnosis of ankylosing spondylitis, Reiter's disease, anterior uveitis and psoriatic arthritis. The classic B27 determination is through tissue typing, which involves time-consuming steps of mononulcear cell isolation and subjective visual reading of microcytotoxicity plates. Flow cytometry is now the method of choice in B27 typing because of the rapidity, sensitivity, objectivity, low cost and amenability to automation. Numerous studies examining flow cytometric analysis of B27 have been undertaken. These have suggested the need to (i) identify $CD3^+$ T lymphocytes rather than gating on all the mononuclear cells, (ii) use more than one antibody to HLA-B27 (i.e. a cocktail of antibodies) and (iii) use only antibodies that do not cross-react with HLA-B7 (Coates and Darke, 1998; Hoffman and Janssen, 1997)

8.14 Transplantation crossmatching

A crossmatch is an indirect antiglobulin technique to detect lymphocyte-reactive antibodies in the sera of blood donors. These antibodies are primarily anti-HLA class I and class II antibodies, and they may be further characterised as IgG, IgM or IgA isotypes. The target cells are usually T lymphocytes although B lymphocytes and cells transformed by Epstein–Barr virus have also been used. The cells are incubated with the test serum and reactivity assessed by immunofluorescent flow cytometry. Recently, beads that are coated with a panel of HLA antigens have become available commercially (FlowPRA™; One Lambda) and have been found to

be highly sensitive for detecting antibodies. The European Federation of Immunogenetics has suggested a number of guidelines for crossmatching by flow cytometry including the following.

1. The cell to serum ratio should be optimised by titration to ensure that low concentrations of antibody are detected; and cell to serum ratios used (expressed as cells in 10 μl serum) may range from 0.2×10^6 to 5.0×10^6.
2. Controls should include a negative control of AB serum from a pool of several donors and a positive control serum from a pool of highly sensitised patients whose antibodies cover a wide range of HLA specificities.
3. The binding of human immunoglobulin should be assessed by incubation with fluorescein isothiocyanate-labelled F(ab') anti-human IgG at 22°C.
4. The antihuman antibody should be titred to determine the dilution with optimal activity.
5. The number of washes and wash volume should be adequate to ensure that all excess antibody is removed prior to the addition of the second-stage fluorochrome-conjugated antihuman antibody.
6. The binding of human immunoglobulin to different cell populations should be assessed by two- or three-colour immunofluorescence by incubation at 4°C with fluorochrome-conjugated monoclonal antibodies such as phycoerythrin–CD3 for T-cells or Quantum Red™–CD19 or CD20 for B-cells.
7. Two- or three-colour staining of other immunoglobulin classes may also be justified (i.e. IgM and IgA).
8. Labelled cells should be analysed rapidly to avoid significant loss of bound human immunoglobulin or loss of any cell subpoulation.
9. Whether reporting mean, median, mode or mean channel shifts, relative mean fluorescence or number of molecules of fluorescence, a threshold for a positive crossmatch should be established and consistently maintained.

The flow cytometric crossmatch has been used extensively in renal transplantation and is recommended for patients with previously failed transplants, potential recipients of related transplants and highly sensitive primary transplants. Sera collected at the time of previous transplant(s) failure, at the time of highest panel reactivity and within a month of the proposed transplant should be crossmatched at the same time. In addition, a serum sample must be taken and crossmatched immediately prior to the transplant, if there have been any potentially sensitising events since the date of the previous sample. Regular screening of sera before transplantation is an important factor in the interpretation of crossmatch results, and identification of HLA-specific antibodies has been shown to be associated with an increased risk of graft rejection. In addition, the use of the flow cytometric crossmatch both pre and post-transplantation may help to indicate patients for whom the immunosuppressive protocol may be desirable (Harmer, 1998).

8.15 REFERENCES

Adriaanson, H.J., te Boekhorst, P.A.W., Hagemeijer, A.M., van der Schoot, C.E., Delwel, H.R., van Dongen, J.J.M. (1993) Acute myeloid leukemia M4 with bone marow eosinophilia (M4Eo) and inv(16) (p13q22) exhibits a specific immunophenotype with CD2 expression. *Blood* **81**, 3043–50.

Baer, M.R., Stewart, C.C., Lawrence, D. (1997) Expression of the neural cell adhesion molecule CD56 is associated with short remission duration and survival in acute myeloid leukemia with t(8;21)(q22;q22). *Blood* **90**, 1643–8.

Banks, P.M., Chan, J., Cleary, M.L., Delsol, G., de Wolf-Peeters, C., Gatter, K., Grogan, T.M., Harris, N.L., Isaacson, P.J., Jaffe, E.S., Mason, D., Pileri, S., Ralfkiaer, E., Stein, H., Warnke, R.A. (1992) Mantle cell lymphoma: a proposal for unification of morphologic, immunologic and molecular data. *American Journal of Surgical Pathology* **16**, 637–75.

Bene, M.C., Castoldi, G., Knapp, W., Ludwig, W.D., Matutes, E., Orfao, A,. van't Veer, M.B. (1995) European Group for the Immunological Characterisation of Leukemias (EGIL): proposals for the immunological classification of acute leukemias. *Leukemia* **9**, 1783–6.

Bennett, J.M., Catovsky, D., Daniel, M.T., Flandrin, G., Galton, D.A.G., Gralnick, H.R., Sultan, C. (1976) Proposals for the classification of the acute leukaemias (FAB Cooperative

Group). *British Journal of Haematology* **33**, 451–8.

Bennett, J.M., Catovsky, D., Daniel, M.T. (1985a) Criteria for the diagnosis of acute leukemia of megakaryocytic lineage (M7): a report of the French–American–British Cooperative Group. *Annals of Internal Medicine* **103**, 460–2.

Bennett, J.M., Catovsky, D., Daniel, M.T., Flandrin, G., Galton, D.A.G., Gralnick, H.R., Sultan, C. (1985b) Proposed revised criteria for the classification of acute myeloid leukemia. *Annals of Internal Medicine* **103**, 620–9.

Bennett, J.M., Catovsky, D., Daniel, M.T., Flandrin, G., Galton, D.A.G., Gralnick, H.R., Sultan, C. (1989) Proposals for the classification of chronic (mature) B and T lymphoid leukaemias. *Journal of Clinical Pathology* **42**, 567–84.

Bennett, J.M., Catovsky, D., Daniel, M.T., Flandrin, G., Galton, D.A.G., Gralnick, H.R., Sultan, C. (1991) Proposal for the recognition of minimally differentiated acute myeloid leukaemia (AML M0) *British Journal of Haematology* **78**, 325–9.

Bogen, S.A., Pelley, D., Charif, M., McCusker, M., Koh, H., Foss, F., Garifallou, M., Arkin, C., Zucker-Franklin, D. (1996) Immunophenotypic identification of Sezary cells in the peripheral blood. *American Journal of Clinical Pathology* **106**, 739–48.

Borowitz, M.J., Bray, R., Gascoyne, R., Melnick, S., Parker, J.W., Picker, L., Stetler-Stevenson, M. (1997) US–Canadian consensus recommendations on immunophenotypic analysis of hematologic neoplasia by flow cytometry: data analysis and interpretation. *Cytometry* **30**, 236–44.

Botnick, L.E., Hannon, E.C., Hellman, S. (1976) Nature of the hematopoietic stem cell compartment and its proliferative potential. *Blood Cells* **5**, 5–7.

Brito-Bapapulle, V., Pomfret, M., Matutes, E., Catovsky, D. (1987) Cytogenetic studies on prolymphocytic leukemia. II. T cell prolymphocytic leukemia. *Blood* **70**, 926–31.

Brito-Bapapulle, F., Pullon, H., Layton, D.M., Etches, A., Huxtable, A., Mangi, M., Bellingham, A.J., Mufti, G.J. (1990) Clinicopathological features of acute undifferentiated leukaemia with a stem cell phenotype. *British Journal of Haematology* **76**, 147–55.

Bux, J., Stein E.L., Bierling, P., Fromont, P., Clay, M., Stoncek, D., Santoso, S. (1997) Characterisation of a new alloantigen (SH) on the human neutrophil Fcγ receptor IIIb. *Blood* **89**, 1027–34.

Campana, D., Coustan-Smith, E. (1999) Detection of minimal residual disease in acute leukaemia by flow cytometry. *Cytometry* **38**, 139–52.

Chan, S.H., Waltzinger, C., Baron, A. (1994) Role of coreceptors in positive selection and lineage commitment. *European Molecular Biology Journal* **13**, 4482.

Chapel H.M., Webster D.B. (1999) Assessment of the immune system. In: Ochs, H.D., Smith, C.I.E., Puck, J.M. (eds.), *Primary Immunodeficiency Diseases*, pp. 419–31. Oxford University Press, New York.

Chen, C.S., Sorensen, P.H.B., Domer, P.H., Reaman, G.H., Korsmeyer, S.J., Heerema, N.A., Hammond, G.D., Kersey, J.H. (1993) Molecular rearrangements on chromosome 11q23 predominate in infant acute lymphoblastic leukemia and are associated with specific biologic variables and poor outcome. *Blood* **81**, 2386–90.

Chen, J.C., Davis, B.H., Bigelow, N.C., Ceckowski, C., Robinson, J., Sounart-Miscovich, C., Steel K.A. (1996) Flow cytometric HLA-B27 typing using CD3 gating and molecules of equivalent soluble fluorochrome (MESF) quantitation. *Cytometry* **26**, 286–92.

Chessels, J.M., Swansbury, G.J., Reeves, B., Bailey, C.C., Richards, M. (1997) Cytogenetics and prognosis in childhood lymphoblastic leukaemia: results in MRC UKALL X. *British Journal of Haematology* **99**, 93–100.

Claxton, D.F., Reading, C.L., Nagarajan, L., Tsujimoto, Y., Anderson, B.S., Estey, E., Cork, A., Huh, Y.O., Trujillo, J., Deisseroth, A.B. (1992) Correlation of CD2 expression with PML gene breakpoints in patients with acute promyelocytic leukemia. *Blood* **80**, 582–6.

Clayton, L.K., Ghendler, Y., Mizoguchi, E. (1997) T-cell receptor ligation by peptide/MHC induces activation of a caspase in immature thymocytes: the molcular basis of negative selection. *European Molecular Biology Journal* **16**, 2282–6.

Coates, E., Darke, C. (1998) Routine HLA-B27 typing by flow cytometry: differentiation of the products of HLA-B*2702, B*2705, B*2708. *European Journal of Immunogenetics* **25**, 29–37.

Copelan, E.A., McGuire, E.A. (1995) The biology and treatment of acute lymphoblastic leukemia in adults. *Blood* **85**, 1151–6.

Craston, R., Koh, M., Mc Dermott, A., Ray, N., Prentice, H.G., Lowdell, M.W. (1997) Temporal dynamics of CD69 expression on lymphoid cells. *Journal of Immunological Methods* **209**, 37–45.

Cuneo, A., van Orshoven, A., Michaux, J.L., Boogaerts, M., Louwagie, A., Doyen, C., Dal Cin, P., Fagioli, F., Castoldi, G., van den Berghe, H. (1990) Morphologic, immunologic and cytogenetic studies in erythroleukemia: evidence for multilineage involvement and identification of two distinct cytogenetic-clinicopathological types. *British Journal of Haematology* **75**, 346–50.

Cuneo, A., Ferrant, A., Michaux, J.L., Bosly, A., Chatelain, B., Stul, M., Dal Cin, P., Dierlamm, J., Cassiman, J.J., Hossfeld, D.K., Castoldi, G., van den Berghe, H. (1996) Cytogenetic and clinicobiological features of acute leukemia with stem cell phenotype. *Cancer Genetics and Cytogenetics* **93**, 31–6.

Damle, R.N., Wasil, T., Fais, F., Ghiotto, F., Valetto, A., Allen, S.L., Buchbinder, A., Budman, D., Dittmar, K., Kolitz, J., Lichtman, S.M., Schulman, P., Vinciguerra, V.P., Rai, K.R., Ferrarini, M., Chiorazzi, N. (1999) Ig V gene mutation status and CD38 expression as novel prognostic indicators in chronic lymphocytic leukemia. *Blood* **94**, 1840–7.

Davis, B.H. (1996) Quantitative neutrophil CD64 expression: promising diagnostic indicator of infection or systemic acute inflammatory response. *Clinical Immunology Newsletter* **16**, 121–9.

del Poeta, G., Stasi, R., Venditti, A., Cox, C., Aronica, G., Masi, M., Bruno, A., Simone, M.D., Buccisano, F., Papa, G. (1995) CD7 expression in acute myeloid leukemia. *Leukemia and Lymphoma* **17**, 111–19.

Docke, W.D., Randow, F., Syrbe, U., Krausch, D., Asadulla, K., Reinke, P., Volk, H.D., Kox, W. (1997) Monocyte deactivation in septic patients: Restoration by IFN-gamma treatment. *Nature Medicine* **3**, 678–81.

Engel, H., Goodacre, A., Keyhani, A, Jiang, S., Van, N.T., Kimmel, M., Sanchez-Williams, G., Andreeff, M. (1997) Minimal residual disease in acute myelogeneous leukaemia and myelodysplastic syndromes: a follow-up of patients in clinical remission. *British Journal of Haematology* **99**, 64–75.

Farahat, N., Lens, D., Morilla, R., Matutes, E., Catovsky, D. (1995) Differential TdT expression in acute leukemia by flow cytometry: a quantitative study. *Leukemia* **9**, 583–7.

First MIC Cooperative Study Group (1986) Morphologic, immunologic and cytogenetic (MIC) working classification of acute lymphoblastic leukaemias. *Cancer Genetics and Cytogenetics* **23**, 189–97.

Fischer, M., Klein, U., Kuppers, R. (1997) Molecular single-cell analysis reveals that CD5-positive peripheral blood B cells in healthy humans are characterized by rearranged V kappa genes lacking somatic mutation. *Journal of Clinical Investigation* **100**, 1667–76.

Fry, R.W., Morton, A.R., Crawford, G.P., Keast, D. (1992) Cell numbers and in vitro responses of leukocytes and lymphocyte subpopulations following maximal exercise and interval training sessions of different intensities. *European Journal of Applied Physiology* **64**, 218–27.

Gale, R.P., Heron, P., Juttner, C. (1992) Blood stem cell transplants come of age. *Bone Marrow Transplantation* **9**, 151–55.

Hamblin, T.J., Davis, Z., Gardiner, A., Oscier, D.G., Stevenson, F.K. (1999) Unmutated Ig VH genes are associated with a more aggressive form of chronic lymphocytic leukemia. *Blood* **94**, 1848–54.

Harmer, A.W. (1998) Utilization of cross match techniques for renal transplantation. *Current Opinion in Nephrology and Hypertension* **7**, 687–90.

Harris, N.L., Jaffe, E.S., Stein, H., Banks, P.M., Chan, J.K.C., Cleary, M.L., Delsol, G., de Woolf-Peeters, C., Falini, B., Gatter, K.C., Grogan, T.M., Isaacson, P.G., Knowles, D.M., Muller-Hermelink, H., Pileri, S.A., Piris, M.A., Ralfkiaer, E., Warnke, R.A. (1994) A revised European–American classification of lymphoid neoplasms: a proposal from the International Lymphoma Study Group. *Blood* **84**, 1361–92.

Harris, N.L., Jaffe, E.S., Diebold, J., Flandrin, G., Muller-Hermelink, H., Vardiman, J., Lister, T.A., Bloomfield, C.D. (1999) World Health Organization classification of neoplastic diseases of the hematopoietic and lymphoid tissues: report of the clinical advisory committee meeting – Airlie House, Virginia, November 1997. *Journal of Clinical Oncology* **17**, 3835–49.

Ho, A.D., Young, D., Marauyama, M., Corringham, R.E., Mason, J.R., Thompson, P., Grenier, K., Law, P., Terstappen, L.W., Lane, T. (1996) Pluripotent and lineage committed $CD34^+$ subsets in leukapheresis products mobilized by G-CSF and GM-CSF vs. a combination of both. *Experimental Hematology* **24**, 1460–8.

Hoffmann, J.J., Janssen, W.C. (1997) HLA-B27 phenotyping with flow cytometry: further improvement by multiple monoclonal antibodies. *Clinical Chemistry* **43**, 1975–81.

Jacobs, R., Stoll, M., Stratmann, G., Leo, R., Link, H., Schmidt, R.E. (1992) CD16, $CD56^+$ natural killer cells after bone marrow transplantation. *Blood* **79**, 3239–44.

Janossy, G., Coustan-Smith, E., Campana, D. (1989) The reliability of cytoplasmic CD3 and CD22 antigen expression in the immuno-diagnosis of acute leukemia: a study of 500 cases. *Leukemia* **3**, 170–81.

Jennings, C.D., Foon, K.A. (1997) Recent advances in flow cytometry: application to the diagnosis of hematologic malignancy. *Blood* **90**, 2863–92.

Keeney, M., Chin-Yee, I., Weir, K., Popma, J., Nayar, R., Sutherland, R. (1998) Single platform flow cytometric absolute $CD34^+$ cell counts based on the ISAGE Guidelines. *Cytometry* **34**, 61–70.

Koene, H.R., Kleijer, M., Roos, D., de Haas, M., von dem Borne, A.E.G.Kr. (1998) FrγRIIIB gene duplication: evidence for presence and expression of three distinct FrγRIIIB genes in NA(1+,2+)SH+ individuals. *Blood* **91**, 673–9.

Kuppers, R., Klein, U., Hansmann, M., Rajewsky, K. (1999) Cellular origin of human B-cell lymphomas. *New England Journal of Medicine* **341**, 1520–9.

Law, P., Traylor, L., Recktenwald, D.J. (1999) Cell analysis for hematopoietic stem/progenitor cell transplantation. *Cytometry* **38**, 47–52.

Liu, Z., Hultin, L.E., Cumberland, W.G., Hultin, P., Schmidt, I., Matud, J.L., Detels, R., Giorgi, J.V. (1996) Elevated relative fluorescence intensity of CD38 antigen expression on $CD8^+$ T cells is a marker of poor prognosis in HIV infection: results of

6 years of follow-up. *Cytometry* **26**, 1–7.

Loughran, J.P. (1993) Clonal disease of large granular lymphocytes. *Blood* **82**, 1–14.

Lowdell, M.W., Ray, N., Craston, R., Corbett, T., Deane, M., Prentice, H.G. (1997) The in vitro detection of anti-leukaemic-specific cytotoxicity after autologous bone marrow transplantation for acute leukaemia. *Bone Marrow Transplantation* **19**, 891–7.

Macey, M.G. (2000) Leukocyte immunophenotyping. *Biomedical Scientist* **44**, 29–35.

Maino, V.C., Ruittenberg, J.J., Suni, M.A. (1996) Flow cytometric method for analysis of cytokine expression in clinical samples. *Clinical Immunology Newsletter* **16**, 95–8.

Manns, A., Cleghorn, F.R., Falk, R.T., Hanchard, B., Jaffe, E.S., Bartholomew, C., Hartge, P., Benichou, J., Blattner, W.A. (1993) The HTLV Lymphoma Study Group: role of HTLV-1 in the development of non-Hodgkin lymphoma in Jamaica and Trinidad and Tobago. *Lancet* **342**, 1447–50.

Matutes, E., Catovsky, D. (1994) The value of scoring systems for the diagnosis of biphenotypic leukemia and mature B-cell disorders. *Leukemia and Lymphoma* **3**(Suppl. 1), 11–14.

Matutes, E., Garcia, R., Talavera, J., O'Brien, M., Catovsky, D. (1991) Clinical and laboratory features of 78 cases of T-prolymphocytic leukemia. *Blood* **78**, 3269–74.

Matutes, E., Owusu-Ankomah, K., Morilla, R., Garcia-Marco, J., Houlihan, A., Que, T.H., Catovsky, D. (1994a) The immunological profile of B-cell disorders and proposal for a scoring system for the diagnosis of CLL. *Leukemia* **8**, 1640–5.

Matutes, E., Morilla, R., Owusu-Ankomah, K., Houlihan, A., Catovsky, D. (1994b) The immunophenotype of splenic lymphoma with villous lymphocytes and its relevance to the differential diagnosis with other B-cell disorders. *Blood* **83**, 1558–62.

Matutes, E., Morilla, R., Farahat, N., Carbonell, F., Swansbury, J., Dyer, M. (1997) Definition of biphenotypic leukemia. *Haematologica* **82**, 64–6.

Melo, J.V., Hegde, U., Parreira, A., Thompson, I., Lampert, I.A., Catovsky, D. (1987) Splenic B lymphoma with circulating villous lymphocytes: differential diagnosis of B cell leukaemias with large spleens. *Journal of Clinical Pathology* **40**, 329–42.

Moreau, E.J., Matutes, E., A'Hern, R.P., Morilla, A.M., Morilla, R., Owusu-Ankomah, K.A., Seon, B.K., Catovsky, D. (1997) Improvement of the chronic lymphocytic leukemia scoring system with the monoclonal antibody SN8 (CD79b). *American Journal of Clinical Pathology* **108**, 278–82.

Moses, A., Nelson, J., Bagby, G.C. (1998) The influence of the immunodeficiency virus-1 on hematopoiesis. *Blood* **91**, 1479–84.

Murray, C.K., Estey, E., Paietta, E., Howard, R.S., Edenfield, W.J., Pierce, S., Mann, K.P., Bolan, C., Byrd, J.C. (1999) CD56 expression in acute promyelocytic leukemia: a possible indicator of poor treatment outcome? *Journal of Clinical Oncology* **17**, 293–7.

Nowak, R., Oelschlaegel, U., Schuler, U., Zengler, H., Hofmann, R., Ehninger, G., Andreeff, M. (1997) Sensitivity of combined DNA/immunophenotype flow cytometry for the detection of low levels of aneuploid lymphoblastic leukaemia cells in bone marrow. *Cytometry* **30**, 47–53.

Pui, C.H., Rivera, G.K., Hancock, M.L., Raimondi, S.C., Sandlund, J.T., Mahmoud, H.H., Ribeiro, R.C., Furman, W.L., Hurwitz, C.A., Crist, W.M., Behm, F.G. (1993) Clinical significance of CD10 expression in childhood acute lymphoblastic leukemia. *Leukemia* **7**, 35–9.

Raimondi, S.C., Shurtleff, S.A., Downing, J.R., Rubnitz, J., Mathew, S., Hancock, M., Pui, C.H., Rivera, G.K., Grosveld, G.C., Behm, F.G. (1997) 12p abnormalities and the TEL gene (ETV6) in childhood acute lymphoblastic leukemia. *Blood* **90**, 4559–66.

Reading, C.L., Estey, E.H., Huh, Y.O., Claxton, D.F., Sanchez, G., Terstappen, L.W.M.M., O'Brien, M.C., Baron, S., Deisseroth, A.B. (1993) Expression of unusual immunophenotype combinations in acute myelogenous leukemia. *Blood* **81**, 3083–7.

Rozman, C., Montserrat, E. (1995) Chronic lymphocytic leukemia. *New England Journal of Medicine* **333**, 1052–5.

Saikevych, I.A., Kerrigan, D.P., McConnell, T.S., Head, D.R., Appelbaum, F.R., Willman, C.L. (1991) Multiparameter analysis of acute mixed lineage leukemia: correlation of a B/myeloid immunophenotype and immunoglobulin and T-cell receptor gene rearrangements with the presence of the Philadelphia chromosome translocation in acute leukemias with myeloid morphology. *Leukemia* **5**, 373–8.

Sainati, L., Matutes, E., Mulligan, S., de Oliveira, M.P., Rani, S., Lampert, I.A., Catovsky, D. (1990) A variant form of hairy cell leukemia resistant to α interferon: clinical and phenotypic characteristics in 17 patients. *Blood* **76**, 157–62.

San Miguel, J.F., Garcia-Sanz, R., Gonzales, M., Orfao, R. (1995) Immunophenotype and DNA content in multiple myeloma. *Baillière's Clinical Haematology* **8**, 735–59.

Schmid, I., Kunki, A., Nicholson, J.K.A. (1999) Biosafety considerations for flow cytometric analysis of human immunodeficiency virus-infected samples. *Cytometry* **38**, 195–200.

Scott, C.S., den Ottolander, G.J., Swirsky, D., Pangalis, G., Vives Carrons, L., De Pasquale, A., van Hove, L., Bennett, J.M., Namba, K., Flandrin, G., Lewis, S.M., Polliack, A. (1995) Recommended procedures for the classification of acute leukaemias. *Leukaemia and Lymphoma* **18**, 1–12.

Second MIC Cooperative Study Group (1988) Morphologic, immunologic and cytogenetic (MIC) working classification

of acute myeloid leukaemias. *British Journal of Haematology* **68**, 487–94.

Shimoya, M. and members of the Lymphoma Study Group (1984–1987) (1991) Diagnostic criteria and classification of adult T-cell leukaemia–lymphoma: a report from the Lymphoma Study Group. *British Journal of Haematology* **79**, 428–37.

Smith, P.R., Cavenagh, J.D., Milne, T., Howe, D., Wilkes, S.J., Sinnott, P., Forster, G.E., Helbert, M. (2000) Benign monoclonal expansion of $CD8^+$ lymphocytes in HIV infection. *Journal of Clinical Pathology* **53**, 177–81.

Stall, A.M., Wells, S.M., Lam, K.P. (1996) B-1 cells: unique origin and functions. *Seminars in Immunology* **8**, 45–59.

Steltzer, G.T., Marti, G., Hurley, A., McCoy, P., Lovett, E.J., Schwartz, A. (1997) US–Canadian consensus recommendations on immunophenotypic analysis of hematologic neoplasia by flow cytometry: standardization and validation of laboratory procedures. *Cytometry* **30**, 214–30.

Sutherland, R., Anderson, L., Keeney, M., Nayar, R., Chin-Yee, I. (1997) Re: towards a worldwide standard for $CD34^+$ enumeration. *Journal of Hematotherapy* **6**, 86–9.

Thandla, S., Aplan, P.D. (1997) Molecular biology of acute lymphocytic leukemia. *Seminars in Oncology* **24**, 4–56.

Thiel, E., Kranz, B.R., Raghavachar, A., Bartram, C.R., Loffler, H., Messerer, D., Ganser, A., Ludwig, W.D., Buchner, T., Hoelzer, D. (1989) Prethymic phenotype and genotype of pre-T ($CD7^+$/ER-) cell leukemia and its clinical significance within adult lymphoblastic leukemia. *Blood* **73**, 1247–53.

Vahdat, L., Maslak, P., Miller, W.H., Eardley, A., Heller, G., Scheinberg, D.A., Warrell, R.P. (1994) Early mortality and the retinoic acid syndrome in acute promyelocytic leukemia: impact of leukocytosis, low-dose chemotherapy, PML/RAR-α isoform and CD13 expression in patients treated with all-*trans*-retinoic acid. *Blood* **84**, 3843–8.

van der Pol, W., van de Winkel, J.G. (1998) IgG receptor polymorphisms: risk factors for disease. *Immunogenetics* **48**, 222–32.

Waldrop, S.L., Pitcher, C.J., Peterson, D.M., Maino, V.C., Picker I.J. (1997) Determination of antigen specific memory/effector $CD4^+$ T cell frequencies by flow cytometry: evidence for a novel, antigen specific homeostatic mechanism in HIV-associated immunodeficiency. *Journal of Clinical Investigation* **99**, 1739–50.

Weiss, L.M., Warnke, R.A., Sklar, J., Cleary, M.L. (1987) Molecular analysis of the t(14;18) chromosome translocation in malignant lymphomas. *New England Journal of Medicine* **371**, 1185–8.

Williams, M.A., Kelsey, S.M., Collins, W.P. (1995) Administration of rHuGM-CSF activates monocyte reactive oxygen species secretion and adhesion molecule expression in vivo in patients following high-dose chemotherapy. *British Journal of Haematology* **90**, 31–40.

Williams, M.A., White, S.A., Miller, J.J., Toner, C., Withington, S., Newland, A.C., Kelsey, S.M. (1998) Granulocyte-macrophage colony stimulating factor induces activation and restores respiratory burst activity in monocytes from septic patients. *Journal of Infectious Diseases* **177**, 107–15.

Zimmerman, T.M., Lee, J.G., Bender, R., Williams, S.F. (1995) Quantitative CD34 analysis may be used to guide peripheral-blood stem-cell harvests. *Bone Marrow Transplantation* **15** 439–49.

Zuniga-Pflucker, J.C., Lenardo, M.J. (1996) Regulation of thymocyte development from immature progenitors. *Current Opinion in Immunology* **8**, 215–9.

9

Analysis and isolation of minor cell populations

Terry Hoy
University of Wales College of Medicine, Cardiff

9.1 Introduction

The application of statistics to experimental data is usually a prerequisite for publication and obviously applies to the discipline of flow cytometry. However, in this field, the application of statistics to individual data files, which can often be informative and becomes essential when examining small populations, has often been overlooked. The probable reason for this oversight is the inherent 'reliability' of individual datasets when considering significant subpopulations and acquiring information on at least 5000 events, which is often the case in flow cytometry.

The statistics pertaining to these 'reliable' situations will be outlined and developed into the realm of rare event analysis. During this process, the additional requirements placed on datasets to produce statistics of a predetermined quality will become apparent.

Flow cytometers, by definition, operate on a suspension of cells or other particles that are hydrodynamically focused in a stream of fluid. Assuming that the sample has been suitably agitated, the particles will arrive at a point for analysis in a random order. The time interval between these events is, therefore, also random and this has important consequences if the cytometer is being used for sorting. Analysis is performed either online, in real-time, or offline from a dataset stored electronically. Data from flow cytometers collected in list mode to the Flow Cytometry Standard (FCS) will contain a sequential list of all the parameters collected for each of these randomly ordered events and real-time can, on some instruments, be one of these measurements. Whether the analysis is online or offline, decisions are usually being made as to whether events fall within certain regions that can be defined by the user or by some particular software. These regions can be combined using Boolean logic to form gates. No matter how many regions are defined or how complex the gating logic, any event either meets a criteria or does not, i.e. it is a simple binary decision true or false. The statistics of populations governed by these rules are determined by the binomial distribution (a discontinuous probability distribution).

$$F_{(r)} = [P^r][(1-P)^{n-r}]\ n!/r!(n-r)! \tag{9.1}$$

where n is the total number of events observed, r is the number of events meeting a required criterion, P is the probability of a particular event meeting the required criterion, and $F_{(r)}$ is the frequency with which events meeting the criterion will occur.

A useful introduction to the different distribution functions can be found in Altman (1991) and Watson (1992), the latter containing examples pertinent to flow cytometry. Detailed discussions can, of course, be found in more advanced textbooks on statistics (Armitage and Berry, 1987). For the purposes of this chapter, the important consequences of these distributions will be presented in a usable format with the mathematics simplified as far as possible. For example, if from a total of n events, the number of events meeting a criterion is r, then the proportion of events meeting this criterion (positives) is r/n, which is also the probability (P) of any particular event being positive ($0.0 \geq P \leq 1.0$).

The variance of the number of positive events,

var(r), observed for a binomial distribution, is given by:

$$\text{var}(r) = nP(1-P) \text{ or } r(1-r/n) \quad (9.2)$$

From the variance, the standard deviation (SD) and coefficient of variation (CV) can be derived from the usual formulae:

$$\text{SD} = \sqrt{(\text{var})}$$
$$(\text{CV})\% = 100 \times \text{SD/r}$$

Providing $r > 100$, confidence limits can be calculated for 90, 95 and 99% levels at ±1.64, ±1.96 and ±2.58 SD, respectively. If fewer than 100 positive events are observed, these figures give progressively poorer approximations and the limits also become asymmetric. It is then prudent to refer to statistical tables or a software package.

Finally, it should be noted that errors could also be calculated after correcting for background levels providing the variances are handled correctly:

$$\text{var(test – background)} = \text{var(test)} + \text{var(background)}$$

9.2 Application of statistical equations to conventional situations

The implications of applying these equations to a typical flow cytometric application such as the analysis of lymphocyte subsets is now considered. If the starting material is a preparation of mononuclear cells taken from normal peripheral blood and a marker for B-cells is included, this would be present on about 15% of the total cells. If 5000 events are listed, the number of B-cells to be expected is 5000×0.15 or 750. The probability of any one cell being a B-cell is 0.15 and the variance (Equation 9.2) associated with the 750 events is $750(1 - 0.15)$ or 750×0.85, which is 635.5. The square root of this, 25.25, gives the SD and the CV calculates as 25.25/750 or 3.4%. This is a measure of the variation expected if a large number of datasets of 5000 events were repeated on the same sample. If the whole experimental process was repeated, errors could arise from sources such as diurnal variations, pipetting errors, differential cell losses during separation on gradients and centrifugation, stability of antibodies and subjective processes such as how to place regions to identify lymphocytes on the acquired data. The statistics on these errors would be derived from the normal (Gaussian) distribution as for any experimental data. We might well expect the errors to compound to a figure larger than 3.4%, explaining why it is unnecessary to collect more than one dataset per sample; in these situations, the individual datasets are very reliable.

In the early years of immunophenotyping by flow cytometry, comparisons were being made with the existing technology of fluorescence microscopy, where low levels of fluorescence were notoriously difficult to detect and counting 100 cells required considerable dedication. The same sample examined by fluorescence microscopy would now reveal only 15 cells, with a variance of 15×0.85 or 12.75 and an SD of 3.57 with a CV of 23.8%. It should now be obvious why flow cytometry was quickly recognised as a powerful alternative! Using fluorescence microscopy, the limit of detection was then considered to be around 5%, typical of levels found in control samples and for some strange reason this dogmatic figure was adopted in the early years of flow cytometry. It was quite common to set markers to define 5% of cells as positive with a control sample and to subtract 5% from any subsequent tests.

Fortunately it was soon realised that flow cytometric measurements of immunofluorescence were capable of detecting much lower levels of immunofluorescence without the problem of photobleaching that plagued conventional microscopic methods.

9.3 Application of statistical equations to small subpopulations (rare events)

As progressively smaller populations are encountered, r/n tends to zero and the term $(1 - r/n)$ in Equation 9.2 approaches 1.0. This then simplifies to

Table 9.1 *Calculation of the total number of events required for a given precision*

Frequency of positive events		Total number of events that must be collected to achieve a recorded number of positive events with a given coefficient of variation (CV)				
(%)	1 : *n*	10 000 at CV 1.0%	1600 at CV 2.5%	400 at CV 5.0%	100 at CV 10%	25 at CV 20%
10	10	100 000	16 000	4000	1000	250
1	100	10^6	160 000	40 000	10 000	2500
0.1	1000	10^7	1.6×10^6	400 000	100 000	25 000
0.01	10 000	10^8	1.6×10^7	4×10^6	10^6	250 000
0.001	100 000	10^9	1.6×10^8	4×10^7	10^7	2.5×10^6

The number of events to be collected, which are shown as exponents, would require considerable acquisition times. For example, at a flow rate of 5000 s^{-1}, it would take approximately 3.5 min to observe 10^6 events.

$\text{var}(r) = r$
$\text{SD} = \sqrt{r}$
$\text{CV} = 100/\sqrt{r}$

This approximation can be safely applied to subpopulations below 5% of the total and gives very small errors when used below the level of 1%.

A simple calculation, $r = (100/\text{CV})^2$ derived by transforming Equation 9.3 can be used to determine the size of dataset that will provide a given precision. For example, a CV of 5% requires 400 positive events to be recorded; if they are a subpopulation of 1%, a total of 40 000 events must be collected. This calculation has been used to construct Table 9.1, which can be used as a guide in all cases of rare event analysis.

9.4 Practical examples illustrating different features of rare event analysis

9.4.1 The enumeration of reticulocytes in peripheral blood

The power of flow cytometry over manual counting methods was rapidly appreciated and as an example we can use the enumeration of reticulocytes in peripheral blood. In normal individuals, these form 0.6–2.7% of the red blood cell count. Obviously the errors encountered by counting a traditional field of 1000 cells were considerable, falling to a CV of 40% at the lower end of normal range. This led to the acceptance that reticulocyte counts were a somewhat crude measure of erythroid activity within the bone marrow and were, therefore, a parameter that detected only major changes such as those seen following acute blood loss. Fluorescent stains specific for nucleic acids were rapidly utilised for detecting reticulocytes by flow cytometry (Lee et al., 1986; Schmitz and Werner, 1986; Tanke et al., 1980) but by then it had become somewhat dogmatic to collect data on 5000 or 10 000 events. Taking the first figure with a true reticulocyte count of 0.6%, 30 positives would be expected with an associated CV of 18%, which was much better than could be obtained by the traditional manual method. Some early software packages for analysing reticulocytes actually fixed the number of events at these levels under the mistaken belief that a 'good' estimate was being provided.

It was postulated by some hematologists that, if it could be measured accurately, the reticulocyte count might well be a sensitive measure of effective erythroid activity. The answer was simple: use a flow-based assay and collect more data. Considering the example above and acquiring 100 000 events, 600 positives would be expected with an associated CV of 4.1%, i.e. improved precision was obtainable by spending a few more seconds at the data collection stage. Flow cytometric examination of reticulocytes also had the advantage of being able to quantify the RNA present, an extremely difficult task by conventional microscopic methods. When

developing erythrocytes expel their nuclei and become immature reticulocytes, they have a relatively high RNA content, which diminishes as they mature. The initial response to erythroid stress can, therefore, be monitored by changes in the reticulocytes of high RNA content and maturity indices have been developed to follow their development (Davis and Bigelow, 1989).

Proprietary kits are available for enumerating reticulocytes but Protocol 9.1 is easy to establish.

Protocol 9.1 The enumeration of reticulocytes

Specimen requirements and reagents

A 1 mg ml^{-1} stock solution of thiazole orange in methanol (this is stable at 5 °C for long periods)

- Diluent, phosphate-buffered saline (PBS) with 2 mmol l^{-1} EDTA (ethylenediaminetetraacetic acid) and 0.02% sodium azide
- A working solution is prepared by diluting the stock 1 in 10 000 and is stable for up to 1 week at room temperature if kept in the dark
- Whole blood, anticoagulated with K_3EDTA or heparin.

Method

1. Add 5 μl blood to 1 ml working solution and 5 μl blood to 1 ml diluent as a control.
2. Incubate at 20 °C for 1 h.

Acquiring data on the cytometer

1. Analyse on a flow cytometer within 40 min of finishing the incubation.
2. Use logarithmic amplification on forward and side scatter to assist discrimination of red cells and reticulocytes from white cells and platelets.
3. Collect sufficient data for the precision you require, as discussed in the text.

Analysing the data

1. Display forward versus side light scatter as shown in Fig. 9.1A and place a region around the red cells; this population has a characteristic shape after logarithmic amplification. Using this region as a gate, overlay histograms of the fluorescence from stained (test) and unstained (control) samples (Fig. 9.1B).
2. The histogram for the majority of events in the stained sample may be slightly displaced; this is caused by background staining of the mature red cells, which may be enhanced if overstained.
3. Display the red cell events in a plot of thiazole orange fluorescence versus forward light scatter (both on logarithmic scales; Fig. 9.2A). Determine the percentage reticulocytes within an appropriate marker region placed above the mature red cells and below any nucleated cells.
4. Examine the high fluorescence region and eliminate any very bright events; these can be caused by nucleated red cells in the sample (Fig. 9.2).
5. A maturity index may be derived if required by classifying the RNA distribution of the reticulocytes as shown in Fig. 9.2B and counting those in each marker region (Davis and Bigelow, 1989).

The gating strategy for identifying reticulocytes is relatively straightforward using logarithmic amplification of the light scatter signals; this usually resolves platelets from red cells but can be difficult if giant platelets are present. Nucleated cells, erythroid and leukocytes stain very brightly with thiazole orange, which is a nucleic acid stain not specific to the RNA detected in reticulocytes. However, the correct population of cells is not always so easy to delineate, as will be apparent in other examples.

9.4.2 The quantification of fetal–maternal hemorrhage

Assessment of fetal–maternal hemorrhage (FMH) is a further example where traditional microscopic methods are prone to large counting errors. The Kleihaur test is based on acid elution of hemoglobin F from any fetal cells present in the maternal circulation; counts are often estimated from the number

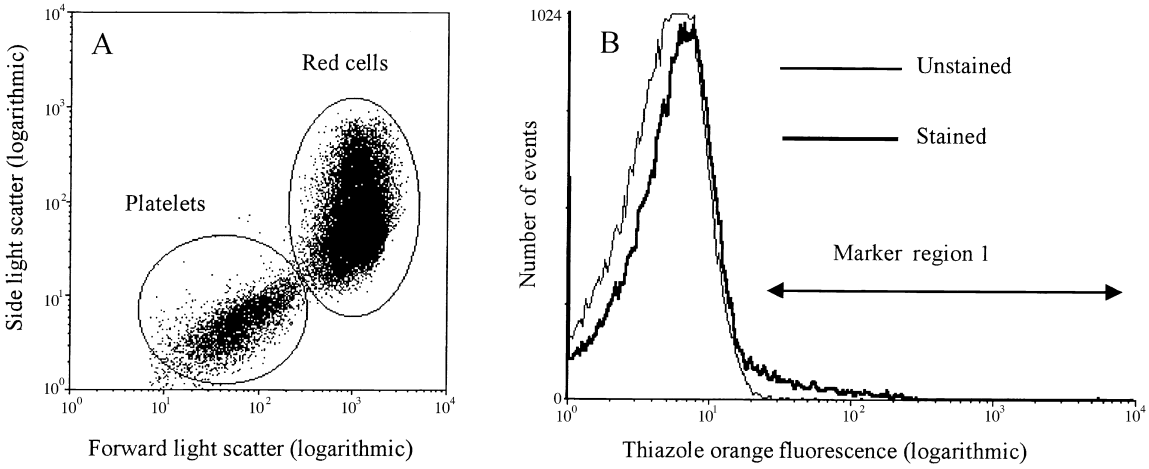

Fig. 9.1 (A) Light scatter profile of red cells and platelets from a peripheral blood sample after logarithmic amplification of forward and side light scatter signals. (B) Overlaid histograms of thiazole orange fluorescence from a stained sample and background fluorescence from an unstained sample of the same blood. Marker region 1 was set on the unstained sample at the 0.5% level and 2.5% positives were recorded for the stained sample.

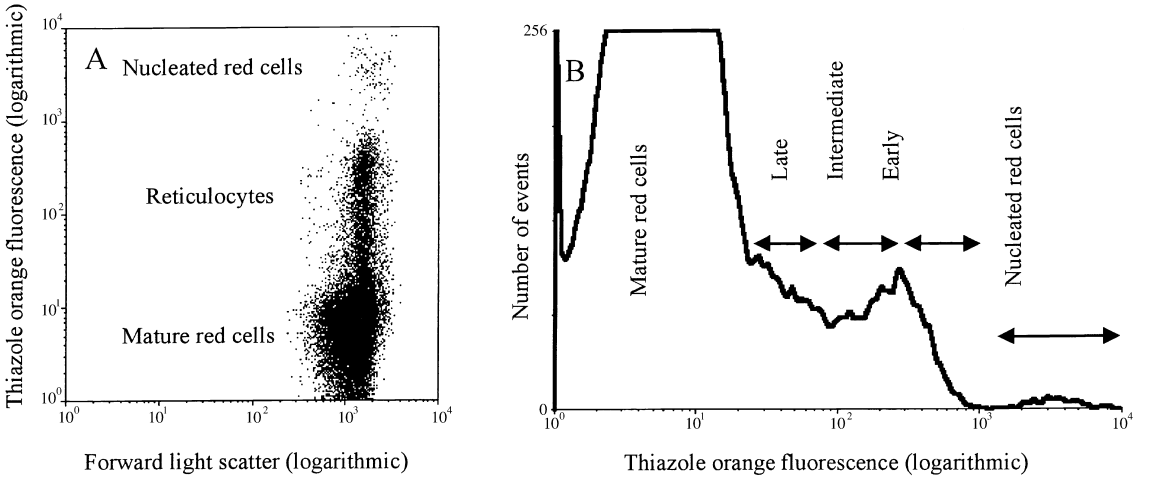

Fig. 9.2 (A) Forward light scatter versus thiazole orange fluorescence from a peripheral blood sample containing a high percentage of reticulocytes and some nucleated red cells. (B) Fluorescence histogram of the same sample indicating three regions for counting reticulocytes of different maturity: 2.3% early, 4.7% intermediate and 4.9% late. The nucleated red cells form 0.5% of the total.

of positive cells observed per low-power field. This is frequently as low as 0, 1, 2, resulting in very unreliable statistics. The number of 'positive' cells per field of view is used with a mean figure for the volume of the maternal circulation to estimate the size of any FMH and the technique needs to provide results down to 0.2% positive, almost an order of magnitude lower than the example of reticulocyte measurement. The flow cytometric measurement is based on the detection of Rhesus D (RhD)-positive cells in a RhD-negative mother (Protocol 9.2). Improvements in the suitability of anti-D antibodies

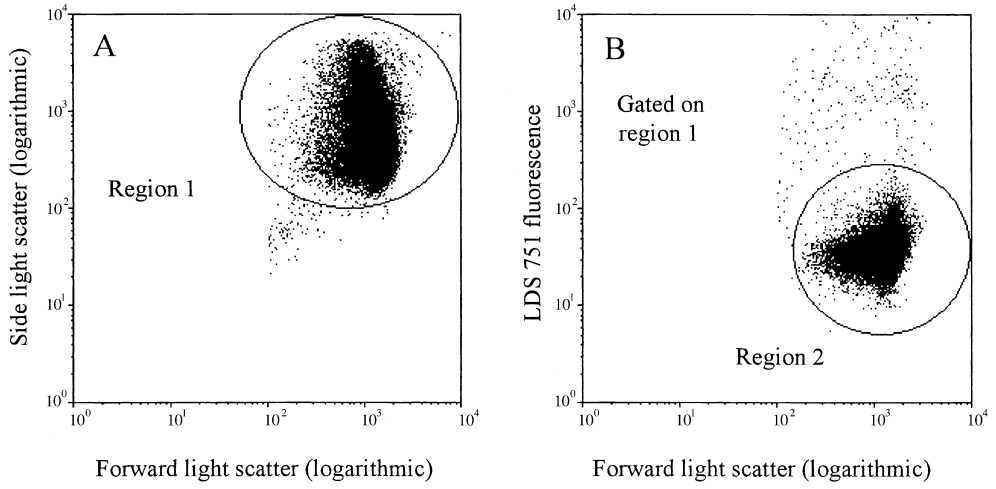

Fig. 9.3 Maternal peripheral blood sample after delivery of a RhD-positive infant. (A) Light scatter profile of red cells after logarithmic amplification of forward and side light scatter signals. Region 1 defines the red cells; platelets in this sample are mostly below the scatter threshold. (B) Forward light scatter versus LDS-751 fluorescence of the cells falling within region 1; region 2 is placed around the weakly staining red cells.

for use with flow-based assays and the inclusion of other markers for assisting in the correct gating of both maternal and fetal red cells have resulted in reliable assays (Lloyd-Evans et al., 1999). Guidelines indicating the role and relevance of flow-based assays to other methodologies for the determination of FMH have also been published (Chapman et al., 1999).

Protocol 9.2 for determining foetal–maternal hemorrhage

Samples

Ideally the maternal blood sample should be taken prior to anti-D administration. In a post-anti-D sample all the D-binding sites would not theoretically be saturated and, therefore, the bleed could be detected but some fetal red cells may have been cleared from the maternal circulation, as shown below in Fig. 9.5B. It is also advisable to include some control samples. The correct control to use for subtraction of background staining is 100% rr RhD-negative cells from a male. A positive control comprising a 1% dilution of ABO compatible R_1r or R_2r RhD-positive cells in rr RhD-negative cells is important. This takes into account the different epitope densities found between genotypes, the r component representing that found on the fetal cells and R that of the mother.

Method

1. Prepare duplicates of all samples.
2. Dilute 2 μl blood (20×10^6 red cells) from a well-mixed sample to 2 ml with PBS.
3. Wash cells three times with PBS by centrifuging at $350 \times g$ for 4 min.
4. Add recommended amounts of directly conjugated antibody or unlabelled human anti-D to all test and positive control samples.
5. Incubate samples as appropriate for the antibodies used, mixing at least once during this incubation.
6. Wash cells twice with PBS and resuspend directly labelled cells in 0.5 ml PBS for analysis.
7. Incubate cells labelled with human anti-D with appropriate amount of fluorescein isothiocyanate (FITC)-labelled anti-human IgG for 30 min on roller mixer.

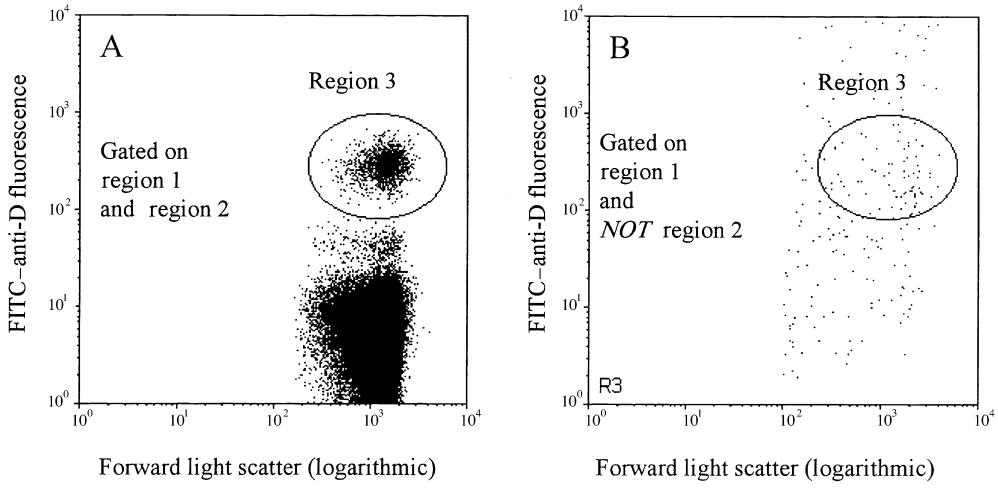

Fig. 9.4 Further analysis of the forward light scatter versus fluorescein isothiocyanate (FITC) anti-D fluorescence for the sample in Fig. 9.3. (A) Gating on region 1 and region 2 produces region 3, which defines the RhD-positive cells (1.96%). (B) Gating on region 1 and not region 2 shows that no clustering is apparent in region 3, indicating that few nucleated red cells are present.

8. Wash cells twice with PBS and resuspend cells in about 0.5 ml PBS for analysis.
9. (Optional) Add 50 μl LDS-751 (of a freshly prepared 1 : 100 dilution in PBS made from a 0.2 mg ml^{-1} stock solution of LDS-751 in methanol, which is stored in the dark) to samples in order to stain any nucleated cells.

Acquisition of data

1. Samples can be stored at 4°C for up to 6 h before analysis.
2. For small positive populations it is important to minimise any carryover. Wipe the probe between tubes with a damp tissue and flush with sheath fluid. To minimise carryover, acquire data on samples in the following order: 1% positive control, test sample and background samples.
3. Acquiring data on 200 000 cells per sample will provide a reliable result down to 0.1% positive. More data will be required for lower levels, refer to Table 9.1. Use logarithmic amplification for forward and side scatter measurements to aid discrimination of red cells from other events.

Analysis

1. Display a scatter plot of forward versus side light scatter and define a region round the red cells (Fig. 9.3A). Fetal red cells are slightly larger than adult red cells, take care not to exclude these.
2. LDS-751 fluorescence can be used to eliminate any nucleated cells by setting a second region around the weakly stained red cells (Fig. 9.3B).
3. The anti-D fluorescence of events falling in logic region 1 (and region 2, if used) are displayed versus forward light scatter in Fig. 9.4A, which should show a distinct group of positive cells well separated from the negatives (1.96% in this sample). These are defined within region 3.
4. Figure 9.4B shows the events in logic region 1 and *not* region 2. These are nucleated cells, check for any evidence of clustering in region 3; if any clustering is present it would involve nucleated fetal red cells and a correction needs to be applied to include these.
5. Figure 9.5A shows a control sample with RhD-negative cells (0.04%) and Fig. 9.5B a sample from the same mother after administration of

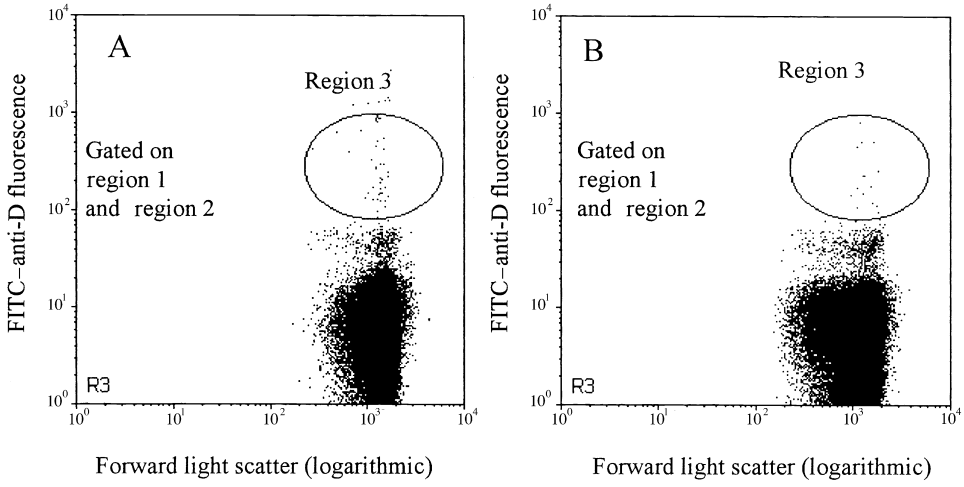

Fig. 9.5 (A) Rhesus-negative control for the sample illustrated in Fig. 9.4A. (B) Sample from the same mother after administration of anti-D demonstrating clearance of the RhD-positive cells. Region 3 contains 0.04% and 0.02% of the total red cells in (A) and (B), respectively.

anti-D (0.02%), demonstrating the effective clearance of the RhD positive cells.

6. The FMH can be calculated as a volume of fetal red cells by converting the percentage of RhD-positive cells. This assumes that the red cell mass of the mother is 1800 ml and that fetal red cells are 22% greater in volume than adult red cells (Chapman et al., 1999).

   FMH (ml) of red cells (uncorrected for fetal red blood cell (RBC) volume)

   F = (percentage of cells Rh D positive × 1800) / 100

   FMH ml of red cells (corrected for fetal RBC volume) = 1.22 F
7. The calculation of dose of anti-D for administration is determined knowing that 100–125 IU of anti-D is recommended to destroy 1 ml of fetal RhD-positive cells.

9.4.3 The enumeration of CD34$^+$ cells in peripheral blood stem cell harvests and bone marrow harvests

The previous two examples were concerned with identifying subpopulations in the range 0.6–2.7% and down to 0.2%, respectively, within parent populations that were easy to identify. However, this is not always the case; the enumeration of CD34$^+$ cells in peripheral blood stem cell harvests requires the use of sequential gating and back-gating in order to identify subpopulations that not only express CD34 but also have the scatter characteristics of 'blast' cells. Peripheral blood stem cell harvests are now used for the treatment of several malignancies (Holyoake and Alcorn, 1994) and for a successful engraftment to take place, the number of stem cells reinfused should be above a certain threshold. Accurate enumeration of a subpopulation containing these cells can be achieved using a combination of CD34 and CD45 antibodies (Sutherland et al., 1994).

The light scatter profile of cells from a peripheral blood stem cell harvest (Fig. 9.6A) is unlike those observed for cells from lysed whole blood or separated by density gradient centrifugation, and the position of blast cells cannot be identified directly with any confidence. Several strategies have been published for seeking these cells. The following is a variation of the International Society for Hematotherapy and Graft Engineering (ISHAGE) guidelines, which employs a combination of CD34 and

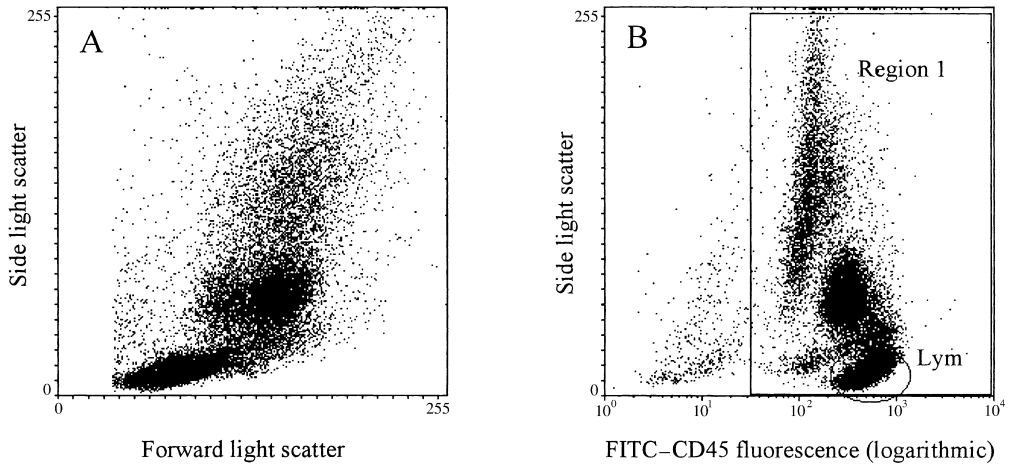

Fig. 9.6 Sample from a peripheral blood stem cell harvest. (A) Light scatter profile. (B) (FITC)–CD45 fluorescence versus side light scatter; region 1 defines the leukocytes and Lym the lymphocytes ($CD45^{bright}$, low side scatter). FITC, fluorescein isothiocyanate.

CD45 antibodies to identify leukocytes correctly (Sutherland et al., 1996).

Protocol 9.3 The detection of blast cells in stem cell harvests

Samples

Peripheral blood or bone marrow harvests are usually taken and supplied in acid-citrate dextrose (ACD).

Method

1. A portion of the blood or bone marrrow sample is diluted with PBS containing 0.5% bovine serum albumin (PBS-BSA) to give a leukocyte count of about $20 \times 10^9\,l^{-1}$.
2. Using appropriate amounts of antibody, as recommended or determined by titration, add FITC-labelled CD45 (use an antibody that detects all isoforms and glycoforms) and phycoerythrin (PE)-labelled CD34 (avoid all class I antibodies and class II FITC conjugates) to one tube and (optional) FITC-labelled CD45 and a PE-labelled isotype control to a second tube.
3. Add 50 μl of the diluted cell suspension to each of the tubes. Mix gently and incubate at 4°C for 20 min, mixing again after 10 min.
4. Lyse the red cells as appropriate.
5. Centrifuge at $300 \times g$ for 5 min.
6. Remove the supernatant, resuspend the cells, add 3 ml PBS-BSA and centrifuge at $300 \times g$ for 5 min. Repeat this stage.
7. Resuspend the cells and add 300 μl 2% paraformaldehyde solution.
8. Samples are best left at 4°C for 10 min before analysing on a cytometer.

Acquisition of data on the cytometer

Small populations are under investigation; therefore, it is important to minimise contamination. Wipe the probe with a damp tissue and flush with sheath fluid between samples.

1. Check cytometer for performance and compensation.
2. Dilute the stained samples with PBS to approximately 0.5–1 ml.
3. Collect 50 000 events for the CD45/CD34 tube followed by the (optional) CD45/control tube.
4. Display CD45 fluorescence versus side light

scatter and define a region around the $CD45^+$ cells as a large rectangle (region 1 in Fig. 9.6B). This region identifies leukocytes (any red cells and debris should be excluded); it is used to determine the white cell count.

5. Display an ungated plot of CD45 versus CD34 fluorescence and define a second region that includes all the $CD34^+$ cells and somewhat fainter events (region 2 in Fig. 9.7A). Leaving this plot ungated, check that region 1 is not excluding any CD34 cells expressing low levels of the CD45 antigen; adjust region 1 if necessary.
6. When you are satisfied with regions 1 and 2, acquisition of the final data files can begin. This will depend on the cytometer; you must count all events in region 1 although it is not essential to list them all. If there is sufficient sample, acquire cells to list 3000 events in logical region (region 1 and region 2). This will provide CV values better than 3% on all but very low samples.
7. After acquisition of each sample, record the number of cells you have acquired in order to get the 3000 events, i.e. the total cells in region 1.

Analysing data

1. The datasets from the 3000 collected events can be used for the analysis, but it is prudent to display the dot plots from the 50 000 events to visualise the light scatter profile of the cells in the whole sample (Fig. 9.6A). Display side light scatter versus PE fluorescence plots for the 3000 events (Fig. 9.7B). Place a region (region 3) around the population of $CD34^+$ cells, which is usually clearly seen as a cluster of cells with low side scatter.
2. Check the light scattering profile of the $CD34^+$ events that were gated in region 3 (Fig. 9.8A). This procedure is known as back-gating. These cells should fall in a region of low to medium forward light scatter and low side light scatter, which is characteristic of blast cells. Experience is essential at this stage; however, the light scattering profile of lymphocytes (Fig. 9.8B) can be used as a guide, having previously defined the lymphocytes on Fig. 9.6B in region Lym ($CD45^{bright}$, low side scatter). Adjust the final regions if the cells have inappropriate scatter characteristics. If it is not possible to collect data on 3000 events, as suggested above, at least 100 events should be recorded for the final 'blast' region. This will result in CV values of approximately 10%.
3. If you are using the optional control, repeat the measurement for this tube and subtract any background counts. These should be very low compared with the sample counts, explaining why this is now considered an optional control. However, if the method is used to count very low frequencies, the effect of subtracting control counts will eventually become significant. If calculating errors, it must be remembered that statistically $\mathrm{var}(a-b) = \mathrm{var}(a) + \mathrm{var}(b)$.

There are several variations on this method some of which employ a nucleic acid stain such as LDS-751 to discriminate nucleated cells from red cells and debris, as used in the FMH example.

There have been reports of 'single-platform' methods (Keeney et al., 1998) in which a known concentration of beads is included with each sample to obtain an absolute count independent of the traditional method of using a count from another machine ('dual-platform' methods). Indeed, a recent study organised by the UK National External Quality Assurance Scheme (UK NEQAS) has shown that interlaboratory CV values for $CD34^+$ stem cell (and $CD4^+$ T lymphocyte) enumeration were higher using dual-platform than using single-platform methods and consequently recommended using the latter (Barnett et al., 1999; Ch. 5). Cytometers employing volumetric methods to derive an absolute count are also now appearing.

9.5 The statistics of sorting using a flow cytometer

The binomial distribution of events obviously applies to all flow cytometric data, but when sorting some additional aspects have to be considered.

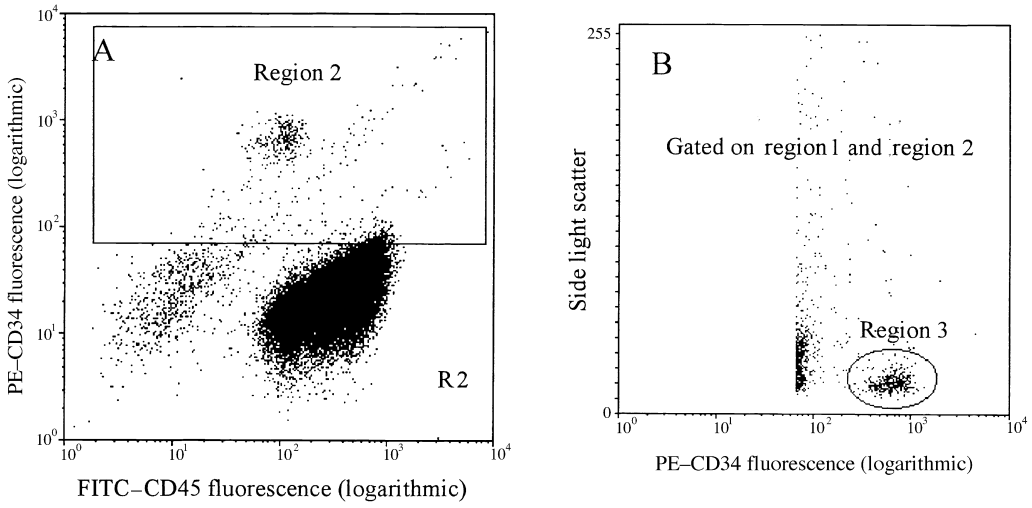

Fig. 9.7 Analysis of the same sample as in Fig. 9.6. (A) FITC–CD45 versus PE–CD34 fluorescence. Region 2 includes all $CD34^+$ events and some negatives. This is ungated. Comparison with Fig. 9.6B indicates that all positive events would be included in region 1. (B) PE–CD34 fluorescence versus side light scatter of the 3000 events collected in region 1 and region 2. Region 3 defines the proposed $CD34^+$ stem cells (low side scatter). FITC, fluorescein isothiocyanate; PE, phycoerythrin.

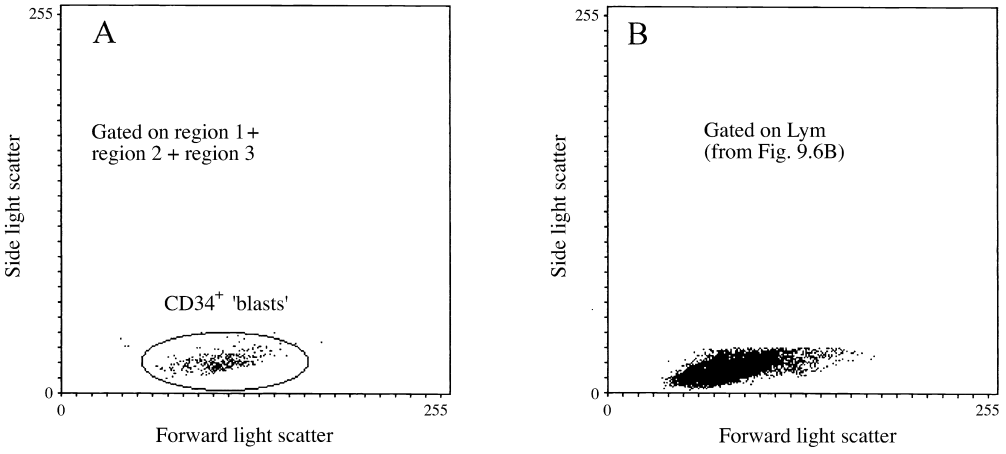

Fig. 9.8 Forward versus side light scatter profiles for the sample as for Fig. 9.6 and 9.7. (A) Events falling in region 3 of Fig. 9.7B, the final region shown is used to count $CD34^+$ blast cells. (B) Events falling in the region labelled 'Lym' in Fig. 9.6B; this provides a useful guide for the 'blast' region set in (A).

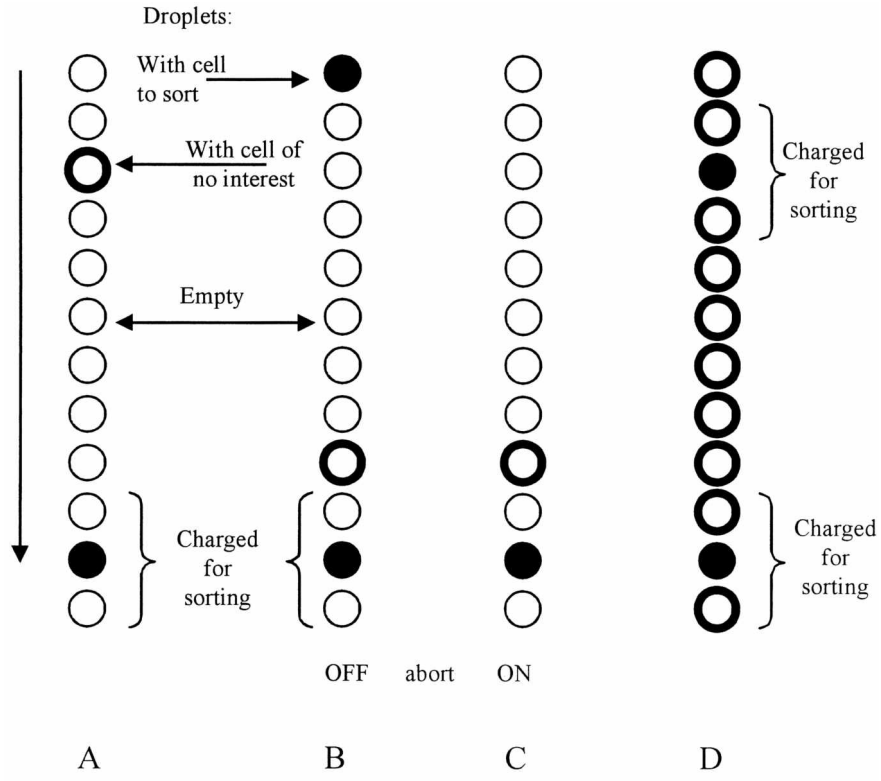

Fig. 9.9 Schematic representation of different situations encountered when sorting cells with a stream-in-air system. (A) high purity and recovery; (B) good recovery, risk of contamination; (C) lower recovery, high purity; (D) arrangement for optimum enrichment of low frequency events.

These are concerned with decisions regarding whether to sort a cell or not after taking into account the importance of purity and recovery. They apply equally to sorting electrostatically (stream in air) or mechanically (within a flow chamber). After identifying an event that satisfies a desired criterion, decisions then have to be made when it arrives at the correct position for sorting. With reference to stream-in-air sorting, there is an uncertainty as to exactly which droplet will contain a particular event. Some will occupy a position in the continuous stream that eventually forms a boundary between two droplets and the event could appear in either. Traditionally, three droplets were sorted to overcome this uncertainty. More recently, cytometers with 'phase sorting' are able to predict with more confidence exactly which droplet will contain an event and single-droplet sorting is feasible on these instruments. Consider a typical flow rate of 3000 events per second on a stream-in-air sorter with a drop frequency of 27 000 s^{-1}. The average occupancy of a droplet will be 0.09 and, if the events were spaced evenly, eight empty ones (Fig. 9.9A), would follow each droplet containing a cell. Sorting this idealised distribution would present few problems; a good recovery would be expected of highly purified material. However, not only are the events distributed at random amongst themselves they will also be spaced at random time intervals.

The spacing of events with time will be governed by Poisson distributions. There will be a probability of two events, or more, being placed in the same

droplet and of sequential droplets being occupied. These events may be both of interest or not of interest or, alternatively, there may be one of each. The calculation of these distributions is beyond the scope of this chapter (see Watson, 1992) but it should be obvious that these coincidence effects increase with the flow rate relative to the drop frequency. The example above with a conventional three-droplet sort would produce a coincidence event with a frequency of 0.16; if these were not sorted (aborted) in the interests of purity, the recovery immediately drops to a maximum of 84%. Flow sorters usually give the operator some control over the abort decision, for example, the situation shown in Fig. 9.9C would normally abort any sort decision and the desired cell would be lost. Overriding the abort mechanism as shown in Fig. 9.9B allows this cell to be collected but with an increased risk of also sorting the unwanted event, which, for the reasons explained above, may actually be in the intermediate droplet and be charged for sorting. Hence, recovery can be improved, with the penalty of increased contamination, by not aborting coincidence events. The only way to improve recovery and maintain high purity is to slow down the flow rate, decreasing the average drop occupancy and thereby reducing the coincidence frequency and abort rate.

9.5.1 Sorting at conventional speeds

As a useful guide, a flow cytometer operating at 3000 events per second processes about 10^7 events per hour, not taking any abort decisions into account. For typical 'biochemical' experiments, large numbers of cells are required and flow sorting has its limitations in these areas because it is too time consuming. The arrival of techniques based on the polymerase chain reaction has restimulated interest in flow sorting, as experimentation with individual and low numbers of cells has become a practical reality. An example is provided in the area of flow karyotyping and chromosome sorting, where the early 'libraries' were produced after several days sorting for each individual chromosome (Gray and Cram, 1990). It is now possible to flow sort a few hundred chromosomes within a short time and to use this material to produce an almost unlimited supply of 'paint' for that particular chromosome. This methodology has enabled marker chromosomes to be defined that were not resolved by conventional banding techniques (Arkesteinjn et al., 1999). Attempts to sort fetal cells from maternal blood for prenatal diagnosis have also been made since the early days of flow cytometry (Herzenberg et al., 1979). These have exploited the multiparameter approach of flow cytometry on individual cells over other immunoselection methods and have recently been reviewed by Bianchi (1999).

9.5.2 Sorting subpopulations of less than 5%

Low-frequency subpopulations are sorted at only a few events per second. These need careful collection. Being of like charge, the droplets repel each other and have a tendency to evaporate before coalescing; collecting into a tube already containing liquid is essential. Recoveries tend to fall dramatically as smaller subpopulations are investigated.

A useful strategy when attempting to isolate significant numbers of cells from subpopulations comprising less than 5% of the whole is to adopt a two-stage procedure. After a preliminary estimate of the frequency of the subpopulation, the flow rate is adjusted to give, on average, one cell per droplet, as shown in Fig. 9.9D. The required analytical rate would now be that of the drop drive frequency, i.e. up to 50 000 s^{-1}; which is well above the capabilities of conventional flow cytometers and sorters. However, if the required cells are fluorescently labelled it is then possible to trigger the machine such that it only detects positive cells at a frequency it can then process. The unwanted cells are then treated in the same way as debris below a conventional scatter threshold, that is to say ignored. If three droplets are charged and sorted we would expect a 33% purity and high recovery (Fig. 9.9D); the sort decisions will not be aborted as the unwanted cells are not detected. This strategy becomes more effective as the sorted population gets smaller.

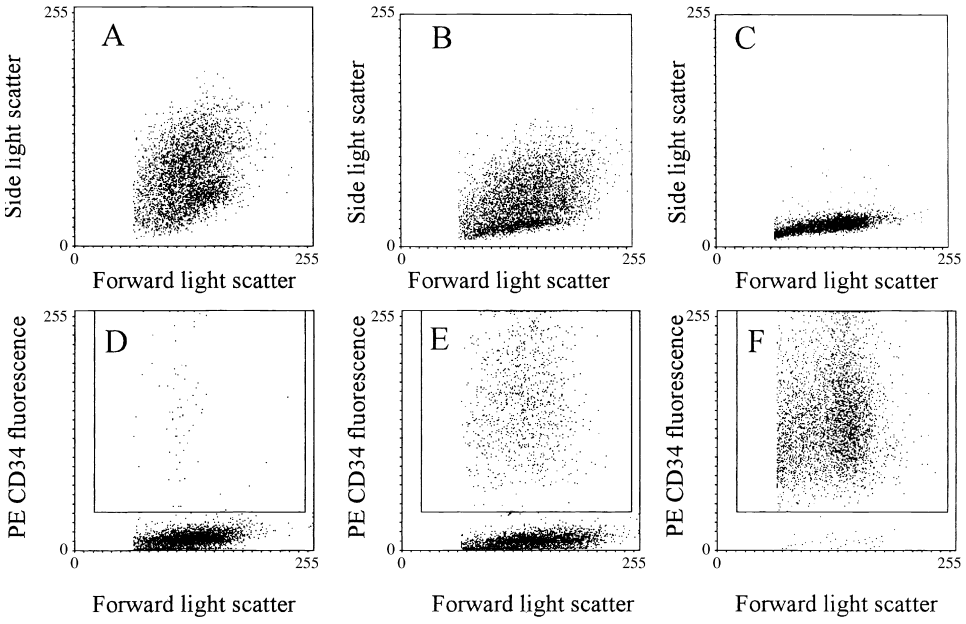

Fig. 9.10 Application of two-stage sorting to the purification of $CD34^+$ cells from a peripheral blood stem cell harvest. (A–C) Light scattering profiles; (D–F) forward light scatter versus PE–CD34 fluorescence. The unsorted sample initially comprised 1.45% positive cells. (B,E) Enrichment by fluorescence threshold sorting increased the purity to 22.3% positives. (C,F) Final purification by conventional sorting, produced 99% pure $CD34^+$ cells. PE, phycoerythrin.

An example of this procedure is shown in Fig. 9.10 where $CD34^+$ cells were selected from a peripheral blood stem cell harvest. Figure 9.10A,D illustrates the starting material with 1.45% positive cells with the sample running on a cytometer fitted with a 70 μm diameter nozzle and drop drive frequency of 27 000 s^{-1}. After switching the trigger to fluorescence and adjusting the threshold such that only the positive cells were detected, the flow rate was adjusted to $27\,000 \times 1.45/100$ or about 400 events per second, which places one cell in each droplet on average. A total of 3×10^8 cells were processed in 4 h and the sorted cells appeared as shown in Fig. 9.10B,E; the $CD34^+$ cells now form 22.3% of the total with a recovery of 60%. This material was then resorted with a conventional scatter threshold taking 1.5 h to produce the material shown in Fig. 9.10C,F. The result was 99% pure CD34 cells and for this stage the recovery was 80%. The total time taken was less than 5 h with a net recovery of 48%. Conventional sorting would have taken 40 h, probably with a somewhat lower recovery as collecting material under these conditions is notoriously difficult. This procedure is also amenable to subset sorting, the enrichment being produced with a key parameter; any other fluorescent probes can be utilised at the purification stage. Cells sorted twice by this process have been used for various assays (Baines et al., 1994; Roberts et al., 1995) and any adverse effects are thought to be minimal. The combination of magnetic or other immune-based separation followed by flow sorting opens up a similar possibility of rapid enrichment combined with the high purity obtainable by flow sorting. High-speed sorters now exist that operate at higher pressures and frequencies than conventional stream-in-air machines, but the potential of these machines has yet to be established. In many applications, the functional com-

petence of a cell is a key concern after sorting; for example, it may not be enough that the cells are 'alive' by dye exclusion tests but instead they may need to be cloned or differentiated in vitro in response to cytokines. The main factors affecting cell survival seem to be the nozzle diameter and the pressure. Cells such as dendritic cells and microglia, which are particularly fragile, may need to be sorted relatively slowly at low pressures (~1.03–1.38 Bar; ~15–20 lb in^{-2}), using a large diameter nozzle (≥ 80 μm) to preserve their expected functions, whereas smaller more robust cells can be subjected to faster sort rates using higher pressures and smaller nozzles.

9.5.3 Flow sorting single cells (cloning)

One of the earliest applications of flow sorting was the isolation of individual hybridoma cells for the purposes of monoclonal antibody production. This was achieved by incubating fluorescently labelled beads coupled to specific antigens with hybridoma cells to detect those cells actively excreting antibodies to that antigen (Dangl and Herzenberg, 1982; Parks et al., 1979). Applying the arguments above, it has been established that high purity can be achieved by operating sorters well below their theoretical limits, with appropriate gating to eliminate doublets and with the abort mechanisms in operation to eliminate other coincident events. If single cells are required, the time element also becomes insignificant. For example, if a cytometer is operating at a low flow rate, individual cells from very small subpopulations will be detected at a reasonable rate. For a flow rate of 1000 s^{-1} and a subpopulation of 0.1%, one of the desired cells would be detected every second, which is probably faster than the time taken to reposition any collection device sorting between events. Even at a frequency of 0.01%, a typical 96-well microtitre plate could be filled within 20 min. The subsequent stages in monitoring monoclonal antibody production by cultures of hybridoma cells are far more time consuming than the time taken to clone the cultures by flow sorting. Multiparameter flow cytometry has also been utilised to monitor antibody production by hybridomas at this stage of batch culture (Al-Rubeai et al., 1991).

9.6 Conclusions

An understanding of the statistics of individual flow cytometry datasets enables the user to appreciate the need to collect sufficient data to justify the total time spent on any experimental procedure. As smaller populations have come under investigation, this has often been overlooked and has produced errors that are considerably larger than the normal biological and experimental variations. The power of flow cytometry undoubtedly lies in the area of multiparametric correlated measurements on individual events. As these data can now be acquired at high speed, the time taken to collect statistically reliable information on these minor populations is often only a small price to pay. As flow cytometers have become tools for processes such as collecting viable cells, so the requirements for cleaning and sterilising the instruments have become more stringent. Protocol 9.4 has been adopted in my laboratory for many years with very few unresolved problems relating to contamination. Many of these aspects have been utilised recently in the study of dendritic cells by flow cytometry. A significant number of papers have appeared investigating these antigen-presenting cells from a variety of sources, with an overwhelming battery of monoclonal antibodies being used to further their characterisation. It would be difficult to do justice to this topic as part of this chapter; the publication of Macey et al. (1998) is typical, employing many of the procedures already described in this chapter: multiparameter measurements to identify cells, the inclusion of nuclear stains to aid gating, sorting at slow rates to reduce coincidence events (aborts), etc. They also justify their findings with morphological evidence obtained by electron microscopy of the sorted cells, reminding us that such confirmation is necessary when pursuing these complex multidimensional exercises. Finally, a

re-iteration of the golden rule of rare event analysis. It is the number of rare events observed that determines the precision of their measurement, not the total size of the dataset.

Protocol 9.4 Cleaning and sterilising flow sorters in preparation for collecting viable cells

Daily shutdown

1. Flush thoroughly with sheath fluid and fill sample lines with a non-ionic detergent (1 : 250 dilution of 7 × stock solution).
2. Spray sample unit and collection chamber with hard surface disinfectant.

Weekly shutdown

Fill all fluidic lines with the detergent.

Preparation for sterile sorting

1. Flush all lines with the detergent for 1 h.
2. Spray the sample unit and collection chamber with hard surface disinfectant.
3. Flush all lines for 10 min with a 'sample' of 70% ethanol in place.
4. Flush all lines with sterile sheath fluid for 30 min.

Sorting

Follow normal good microbiological practice for handling samples aseptically.

Acknowledgements

The author is grateful to Janet Fisher and Sarah Phillips for providing information on the FMH and CD34 assays, respectively.

9.7 REFERENCES

Al-Rubeai, M., Emery, A.N., Chalder, S. (1991) Flow cytometric study of cultured mammalian cells. Journal of Biotechnology **1**, 67–81.

Altman, D.G. (1991) *Practical Statistics for Medical Research*. Chapman & Hall, London.

Arkesteinjn, G., Jumelet, E., Hagenbeek, A., Smit, E., Slater, R., Martens, A. (1999) Reverse chromosome painting for the identification of marker chromosomes and complex translocations in leukaemia. *Cytometry* **35**, 117–24.

Armitage, P., Berry, G. (1987) *Statistical Methods in Medical Research*. Blackwell Scientific, Oxford, UK.

Baines, P., Truran, L., Bailey-Wood, R., Hoy, T., Lake, H., Poynton, C.H., Burnett, A. (1994) Haemopoietic colony-forming cells from peripheral blood stem cell harvests: cytokine requirements and lineage potential. *British Journal of Haematology* **88**, 472–80.

Barnett, D., Granger,V., Whitby, L., Storie, I., Reilly, J.T. (1999) Absolute $CD4^+$ T-lymphocyte and $CD34^+$ stem cell counts by single-platform flow cytometry: the way forward. *British Journal of Haematology* **106**, 1059–62.

Bianchi, D.W. (1999) Fetal cells in the maternal circulation: feasibility for prenatal diagnosis. *British Journal of Haematology* **105**, 574–83.

Chapman, J.F., Bain, B.J., Bates, S.C., Knowles, S.M., Shwe, K.H., Parker-Williams, J., Robson, L., Robson, S.C. (1999) The estimation of fetomaternal hemorrhage. *Transfusion Medicine* **9**, 87–92.

Dangl, J.L., Herzenberg, L.A. (1982) Selection of hybridomas and hybridoma variants using the fluorescent activated cell sorter. *Journal of Immunological Methods* **52**, 1–14.

Davis, B.H., Bigelow, N. (1989) Flow cytometric quantification using thiazole orange provides clinically useful reticulocyte maturity index. *Archives of Pathology and Laboratory Medicine* **113**, 684–9.

Gray, J.W., Cram, L.S. (1990) Flow karyotyping and chromosome sorting. In: Melamed, M.R., Lindmo, T., Mendelsohn, M.L. (eds.), *Flow Cytometry and Sorting*, 2nd edn, pp. 503–29. Wiley-Liss, New York.

Herzenberg, L.A., Bianchi, D.W., Schhroder, J., Cann, H.M., Iverson, G.M. (1979) Fetal cells in the blood of pregnant women: detection and enrichment by fluorescence-activated cell sorting. *Proceedings of the National Academy of Sciences of the USA* **76**, 1453–5.

Holyoake, T.L., & Alcorn, M.J. (1994) CD34 positive hemopoietic cells: biology and clinical applications. *Blood Reviews* **8**, 113–24.

Keeney, M., Chin-Yee, I., Weir, K., Popma, J., Nayar, R., Sutherland, D.R. (1998) Single platform flow cytometric absolute counts based on the ISHAGE guidelines. *Cytometry* **34**, 61–70.

Lee, L.G., Chen, C.H., Chiu, L.A. (1986) Thiazole orange: a new dye for reticulocyte analysis. *Cytometry* **7**, 508–17.

Lloyd-Evans, P., Guest, A.R., Austin, E.B., Scott, M.L. (1999) Use of phycoerythrin-conjugated anti-glycophorin A monoclonal antibody as a double label to improve the accuracy of FMH quantification by flow cytometry. *Transfusion Medicine* **9**, 155–60.

Macey, M.G., McCarthy, D.A., Vogiatzi, D., Brown, K.A., Newland, A.C. (1998) Rapid flow cytometric identification of putative $CD14^-$ and $CD64^-$ dendritic cells in whole blood. *Cytometry* **31**, 199–207.

Parks, D.R., Bryan, V.M., Oi, V.T., Herzenberg, L.A. (1979) Antigen-specific identification and cloning of hybridomas with a Fluorescence Activated Cell Sorter. *Proceedings of the National Academy of Sciences of the USA* **76**, 1962–6.

Roberts, G.M., Hoy, T., Hallet, M.B. (1995) The production of large 'signalling competent' myeloid cells from circulating $CD34^+$ cells in neonatal blood. *Journal of Immunological Methods* **179**, 187–92.

Schmitz, F.J., Werner, E. (1986) Optimization of flow-cytometric discrimination between reticulocytes and erythrocytes. *Cytometry* **7**, 439–44.

Sutherland, D.R., Keating, A., Nayar, R., Anania, S., Stewart, A.K. (1994) Sensitive detection and enumeration of $CD34^+$ cells in peripheral and cord blood by flow cytometry. *Experimental Hematology* **22**, 1003–10.

Sutherland, D.R., Anderson, L., Keeney, M., Nayar, R., Chin-Yee, I. (1996) The ISHAGE guidelines for $CD34^+$ cell determination by flow cytometry. *Journal of Hematotherapy* **5**, 213–26.

Tanke, H.J., Nieuwenhuis, I.A.B., Koper, G.J.M., Ploem, J.S. (1980) Flow cytometry of reticulocytes based on RNA fluorescence. *Cytometry* **1**, 313–20.

Watson, J.V. (1992) *Flow Cytometry Data Analysis: Basic Concepts and Statistics*. Cambridge University Press, Cambridge, UK.

10

Cell cycle, DNA and DNA ploidy analysis

Paul D. Allen and Adrian C. Newland

St Bartholomew's and Royal London School of Medicine and Dentistry, Queen Mary and Westfield College, London

10.1 Introduction

Cells enter the cell cycle from a state of quiescence following mitogenic stimulation, duplicate their genetic information faithfully and distribute it equally to two daughter cells. To achieve this end, a cycling cell passes through a series of tightly regulated cell cycle phases and checkpoints that ensure complete DNA replication occurs before chromosomal segregation and cytokinesis at mitosis.

Successful cell replication requires mitogen-induced cell cycle entry from the quiescent resting stage G_0, into the first gap phase G_1. If the extracellular mitogenic signals persist, the cell will commit itself to progress further towards cell replication. Alternatively, withdrawal of these signals (e.g. nutrient withdrawal) results in a return to G_0. The point of no return for the cell, with respect to commitment to cell cycle progression, is the restriction point, found late in G_1. Once this point has been passed, the decision to replicate DNA, and subsequently undergo cell division, has been made already and becomes independent of mitogenic signalling. DNA synthesis then occurs in S phase and on its completion, cells enter the second gap phase, G_2, before the initiation of mitosis (M phase).

Transition from one cell cycle phase to the next is tightly controlled such that progress to any given phase of the cell cycle will occur only if the previous phase has been completed. The cell cycle machinery ensures that this happens by a series of positive and negative feedback circuits, some of which will be mentioned below.

The cell cycle proceeds via induction of a series of cyclins, which are expressed at the prerequisite stages of the cell cycle. For each cyclin, there is a cyclin-dependent kinase (CDK) partner, which must bind to the cyclin to form a functional complex. Cyclin/CDK complexes can also be regulated by cyclin-dependent kinase inhibitors (CDKi), which can bind to the cyclin/CDK complex and inhibit its function.

10.2 Cell cycling

In the presence of mitogen, a cell leaves G_0 as a result of the induction of one or more of the D-type cyclins. Cyclin D binds either CDK4 or CDK6 as a CDK-binding partner and in the continued presence of growth stimulation the cyclin D/CDK complex activity increases during G_1 and peaks towards the G_1–S phase transition. If, for example, nutrients are withdrawn at this stage cyclin D synthesis ceases; it is rapidly degraded and cells return to G_0. However, when growth conditions are maintained, cyclin D complexes persist throughout the cell cycle and hence subsequent cell cycle events. Therefore, although the initial cyclin D expression is mitogen dependent, once cells have passed the restriction point, cyclinD/CDK activity is no longer essential for cell cycle progression. This is because the cyclin D/CDK4 or cyclin D/CDK6 complex triggers, by phosphorylation, the activation of further substrates responsible for cell cycle continuity beyond the mitogen-dependent stage. One such substrate is the retinoblastoma protein, pRb, which is present normally in a state of hypophosphorylation and holds the cell cycle in check at G_1. pRb binds the transcription factor E2F/DP-1 and keeps it inactive. In-

duction of the cyclin D/CDK complexes induces phosphorylation of pRb and the release of E2F/DP-1, resulting in the transcription of cyclin E. Cyclin E binds CDK2 and the active complex, usually maximal at the G_1–S transition, induces further pRb phosphorylation and further E2F/DP-1 release in a positive feedback loop. The cell cycle is now cyclin E driven. Continued release of E2F from the phosphorylated pRb results in transcriptional activation of cyclin A, which also binds CDK2, at the protein level, as its CDK-binding partner. Cyclins A and E appear to be essential for transition of the cell cycle from G_1 to S, probably because substrates for cyclin A/CDK2 and cyclin E/CDK2 complexes include proteins at the origin of DNA replication. Cyclin E is rapidly degraded in early S phase following ubiquitination and proteosomal degradation triggered by CDK2 phosphorylation. The E2F transcription factor is also inactivated by binding of the cyclin A/CDK2 to the E2F heterodimer binding partner DP-1, and its subsequent phosphorylation. However, it has been shown recently that phosphorylation per se is not sufficient to block E2F/DP-1 DNA-binding properties.

As S phase progresses, cyclin A switches CDK-binding partners and binds CDK1. Cyclin B begins to accumulate during late S phase and into G_2. Its transcriptional regulation is not fully understood. Two CCAAT boxes sited in the proximal promoter region have been shown to be essential for S phase induction of cyclin B, which is also shown to bind the nuclear factor Y (NF-Y) transcription factor. Also, cyclin A/CDK2, cyclin E/CDK2 and cyclin D/CDK4 have been shown to activate the cyclin B_1 promoter in certain cell models. However, it is clear that cyclin B/CDK1 complexes are essential for passage of cells from G_2 into mitosis, thus completing the cell cycle. Subsequent ubiquitination and proteosomal degradation of cyclin B occurs as cells leave mitosis as daughter cells. pRb remains hyperphosphorylated throughout the S and G_2 phases of the cell cycle and is not dephosphorylated until completion of mitosis.

10.3 Cell cycle regulation

Under certain circumstances, it is necessary to apply a brake to the cell cycle. This may be to prevent unwanted proliferation or to induce a cell cycle arrest for running repairs to be made following errors in replicative processes or following DNA damage induced by extracellular stress. The former process is mediated by a series of CDKi that bind to and inhibit the activity of cyclin/CDK complexes and the latter by checkpoint control mechanisms that subsequently activate the CDKi to cause cell cycle arrest (Fig. 10.1).

One family of CDKi is the INK4 family. The known members are p15, p16, p18 and p19 (i.e. INK4b, INK4a, INK4c and INK4d, respectively), which exhibit a certain amount of tissue specificity. These proteins bind to and inhibit the kinase activity of CDK4 and CDK6 and render the cyclinD/CDK4 and cyclin D/CDK6 complexes inactive. As pRb is a substrate for cyclin D/CDK complexes, it remains in the hypophosphorylated form and E2F/DP-1 is not released to initiate transcription of cyclins E or A. Thus the cell remains in G_1 and will not pass the restriction point even in the presence of mitogenic growth factors.

Another family of CDKi includes $p21^{waf1/cip1/sdi}$, $p27^{kip1}$, $p57^{kip2}$ and p107. This family of CDKi has the greatest affinity for CDK2; consequently it blocks the activity of cyclinE/CDK2 and cyclinA/CDK2 complexes and constrains the cell cycle at the late G_1 and G–S transition phases of the cell cycle. Evidence suggests that $p27^{kip-1}$ influences the restriction point since quiescent cells express high levels of $p27^{kip-1}$ that fall upon induction of the cell cycle through nontranscriptional regulation.

Another way of retarding the cell cycle is through cell cycle checkpoint mechanisms, which monitor the progress of the cell cycle and can induce cell cycle arrest at G_1–S, G_2–M transitions and can also influence S phase progression. For example, in yeast, a series of negative feedback loops will prevent entry into S phase if mitosis is not complete but also entry into mitosis will not occur if S phase is not completed. In mammalian cells, the best

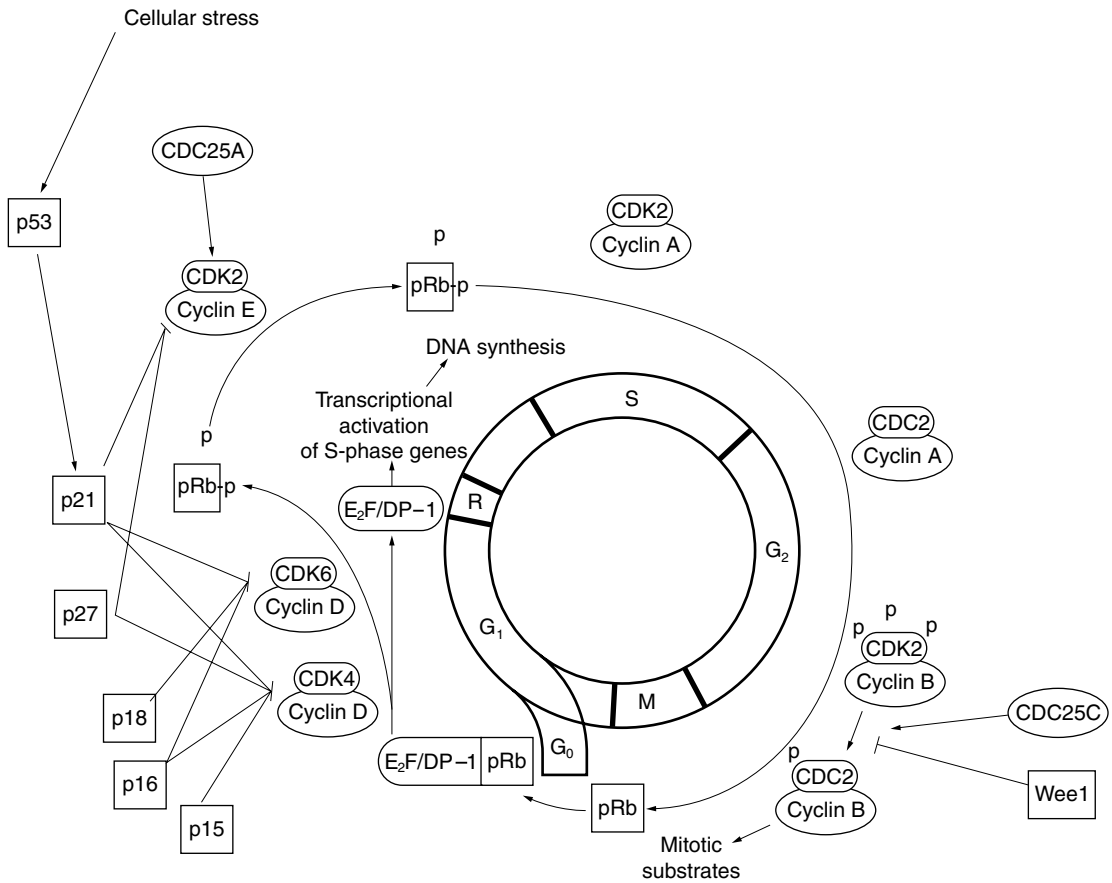

Fig. 10.1 Cell cycle phases and the proteins involved in their regulation, indicating when the requirement for the different cyclins occurs, which cyclin-dependent kinase (CDK) they bind to and two of the potential inhibitors of cyclin/CDK complexes (see text for more details). |——, signifies inhibition. (From Op de Beeck, A., Caillet-Fauquet, P. (1997) Viruses and the cell cycle. *Progress in Cell Cycle Research* **3,** 1–19, with permission from Kluwer Academic/Plenum Publishers.)

characterised checkpoint control is that orchestrated through the tumour suppressor gene p53.

p53 accummulates following DNA damage. A functional ataxia telangiectasia gene product is essential for this process and this product is constitutively expressed throughout the cell cycle. Patients with mutated nonfunctional product suffer enhanced susceptibility to radiation and defects in G_1 and G_2 regulation as well as altered p53 and $p21^{waf\text{-}1}$ expression. p53 encodes for a nuclear phosphoprotein of 393 amino acid residues that regulates transcription control of a broad spectrum of genes. Amongst these are the murine double minute (MDM-2) chromosomal gene product, which can act in a negative feedback loop to block p53-mediated transcription. The interaction between MDM-2 and p53, therefore, determines the duration of p53 activity. p53 also regulates the transcription of $p21^{waf\text{-}1}$. $p21^{waf\text{-}1}$ preferentially binds to and inhibits CDK2 activity and, therefore, is instrumental in blocking the cell cycle. If CDK2 activity is inhibited, pRb is not maintained in the phosphorylated form and will not release E2F/DP-1 for active transcription of cyclin E, thus imposing a G_1

cell cycle arrest and a failure to proceed into S phase, along the same lines as the $p27^{kip-1}$-mediated cell cycle arrest.

Another gene transactivated by p53 is the growth arrest and DNA damage gene GADD45. This gene is induced by ultraviolet and gamma irradiation but is also seen at times of cell cycle arrest. Both GADD45 and $p21^{waf-1}$ will bind to the 37 kDa proliferating cell nuclear antigen, which is required for DNA synthesis by polymerases δ and ε and is also important for postreplicative DNA repair. Binding of $p21^{waf-1}$ to this proliferation antigen has been shown to inhibit both its replicative and its repair activity.

There is now increasing evidence to show that p21 also contributes to the regulation of the G_2–M transition. In transformed fibroblasts, p21 accummulated in the nucleus during the G_2–M transition and was associated with cyclin A/CDK and cyclin B/CDK complexes. When p21 was expressed in cell lines, cells that contained pRb functional arrested in G_1 whereas pRb-negative cells arrested at G_2. These observations did not correlate with p53 status.

The G_2–M transition can be also regulated by phosphorylation of tyrosine and threonine residues on CDK1. Phosphorylation is mediated by Wee1 kinase and inactivates CDK1 irrespective of whether it is bound to cyclin B. This process is reversed by the phosphatase activity of *cdc*25.

Cell cycle regulation is clearly important in organ and tissue development and in the initiation and progress of cancer (Sherr, 1996). Mutations in the cell cycle engine (i.e. the cyclins and CDKs) are, by their nature, lethal to the cell. However, mutations in the cell cycle regulatory proteins, or failure of checkpoint control mechanisms, leads to unwanted proliferation or genomic instability. Therefore, cell biologists and clinicians require to investigate both the cell cycle and the components that control it (Darzynkiewicz et al., 1996; Duque et al., 1993; Shankey et al., 1993). A basic flow cytometric procedure suitable for studying cyclins and other nuclear proteins is described in Protocol 10.1

Protocol 10.1 Detection of cyclins and other nuclear proteins

1. Harvest approximately 1×10^6 cells and wash once in phosphate-buffered saline (PBS).
2. Resuspend the cells in 0.5 ml ice-cold 70% ethanol and incubate on ice for 45 min. Substitute ethanol for ice-cold pure methanol for cyclin D studies.
3. Wash once in PBS.
4. Add a 1 ml of 0.9% Triton® X-100 in 150 mmol l^{-1} sodium chloride, 1 mmol l^{-1} Hepes pH 7.4 and 4% fetal bovine serum. Incubate for 10 min at room temperature.
5. Wash once in PBS and resuspend the pellet in 100 μl PBS.
6. Add 90 μl of the suspension to 10 μl of a 1 : 20 dilution of primary antibody (i.e. a final dilution of 1 : 200). Incubate for 2 h at room temperature or overnight at 4°C.
7. Wash once in PBS. If the primary antibody was not directly conjugated add 100 μl of 1 : 10 or 1 : 20 dilution of FITC-conjugated goat anti-mouse $F(ab')_2$ fragments and incubate for 1 h at room temperature.
8. Wash once in PBS and analyse.
9. If simultaneous bivariate analysis of cell cycle distribution is required then counterstain with a 1 ml volume of 50 μg ml^{-1} propidium iodide (PI) and 200 μg ml^{-1} RNAase and incubate for 30 min at 37°C. Do *not* wash the cells prior to analysis, as illustrated in Fig. 10.5, below.

Notes: This protocol cites 70% ethanol as the permeabilisation/fixation agent in conjunction with a Triton® X-100 step. In certain circumstances, the Triton® X-100 stage may not be required and, therefore, can be omitted from the protocol. Also 1% paraformaldehyde for 2 h at 4°C represents an alternative for cyclin studies, although it is not recommended if DNA staining for bivariate cyclin/DNA content is to be performed, as paraformaldehyde impairs PI staining of DNA (Juan and Darzynkiewicz, 1998).

Cyclin D studies should be carried out using pure methanol rather than 70% ethanol although 1% paraformaldehyde can again be used if there is to be no simultaneous DNA staining. Variation from the predicted cyclin distribution about the cell cycle may be observed under certain circumstances, particularly as a result of cell cycle pertubation (e.g. following drug treatment) and in various tumour cell lines. Readers are referred to the excellent review by Darzynkiewicz et al. (1996) on this subject.

10.4 Flow cytometric analysis of the cell cycle

The flow cytometer is ideally suited for determining the cell cycle distribution of an asynchronous population of cells. Generating histograms of DNA content against cell numbers gives an accurate assessment of the percentage of cells in each phase of the cell cycle. Dual fluorescence is an easy adaptation to make to quantify antigen expression in each phase of the cell cycle and with new advances in fluorochromes, various types of multiparameter analysis are now possible (see also Ch. 13). Additional data such as the proliferative state of the population can be assessed by measuring the percentage of cells in S phase. Numerical chromosomal abnormalities can also be obtained from histograms of DNA content.

A disadvantage of flow cytometry is the requirement for a suspension of single cells. This can be a problem when analysing solid tissue. Either physical disaggregation can be attempted or, where the tissue contains fibrous material, enzymic digest using a cocktail based on collagenase can be used. However, this can be labour intensive and hence time consuming. A final filtration through a 35 μm nylon mesh is strongly recommended whichever method is used.

Pulse processing is a prerequisite for accurate analysis of DNA content during the cell cycle. Two adjoining diploid cells (i.e. clumped together) with a $2n$ DNA content have exactly the same DNA content as a single cell with a $4n$ DNA content. Distinguishing between the two possibilities is important for cell cycle analysis and in studies involving the determination of ploidy. The pulse-processing capability on flow cytometers enables the simultaneous measurement of height, area and width of the pulse generated by a fluorescent cell as it passes through the laser. Pulse height indicates the highest intensity of the pulse; area indicates the total amount of signal for the pulse, and width indicates the size of the cell by the amount of time that it was in the beam. They are measured as three independent entities even though they are derived from the same signal. In DNA experiments, the cytometer must provide resolution, linearity and the ability to distinguish aggregates. The first two criteria are achieved by correctly calibrating the cytometer usually using the manufacturers' DNA quality control particle calibration kits and procedures. Resolving singlet cells from aggregates is based on the fact that aggregates are larger than singlet cells and, therefore, will have a greater pulse width signal than singlet cells. Pulse area is the most accurate measurement of total cell fluorescence. Therefore, as cells replicate their DNA during S phase, there is an increase in the pulse area for a population of proliferating cells. There will also be an increase in cell size and so the pulse width will also increase. When a dot plot of pulse area against pulse width is created for a population of singlet cells, area and width increase as cells increase DNA content. An aggregate of two cells in G_1 will have the same pulse area as a single cell in G_2–M transition but the pulse width will be greater, thus enabling a distinction to be made between singlets and aggregated cells (Fig. 10.2).

An alternative is to plot pulse area against pulse height on a dot plot since in singlet cells an increase in pulse intensity (height) is proportional to the size of the cell (area). This is not true of aggregates. The gains can be adjusted so that a relationship of one is displayed for area against height. Singlet cells will fall in a population forming a 45° angle from bottom left (G_0–G_1) to top right (G_2–M). Cells outside this population will be aggregated cells (Fig. 10.3).

10.5 DNA content to determine cell cycle distribution

The use of DNA measurement to determine cell cycle distribution is based on the premise that cells in G_0 or G_1 phases of the cell cycle possess a normal diploid chromosomal, and hence DNA content ($2n$), whereas cells in G_2 and just prior to mitosis (M) contain exactly twice this amount ($4n$). As DNA is synthesised during S phase, cells are found with a DNA content ranging between $2n$ and $4n$ (Protocol 10.2).

A range of dyes are available for determining DNA content. Dyes widely used are the phenanthridinium nucleic acid intercalators propidium iodide (PI) and ethidium bromide. They are both excited by argon lasers. Photobleaching of complexes of ethidium bromide and DNA has meant that PI is usually the dye of choice. Both dyes are impermeant for viable cells, necessitating cell permeabilisation. These dyes will also bind to RNA, so RNAase is used to ensure only DNA is measured. Both dyes have a large enough Stokes' shift to allow multiparameter analysis using, for example, FITC-labelled antibodies.

Other dyes used to determine DNA content include Hoechst 33258, Hoechst 33342 and 7-aminoactinomycin D. The Hoecsht dyes are cell permeant and bind to the minor groove of DNA; Hoecsht 33342 has a slightly higher permeability than Hoecsht 33258. Hoechst dyes are excited by the ultraviolet range of an helium–cadmium laser and the Stokes' shift is sufficient for multiparameter analyses. Their high affinity for poly-d(A-T) sequences means they can displace DNA intercalators. 7-Aminoactinomycin D is impermeant for viable cells. It undergoes a spectral shift on binding to DNA. It is excited by an argon laser and emits beyond 610 nm, again making it useful for multiparameter analyses.

More recently, a series of cyanine dyes have been developed. These include the SYTO® dyes. They exhibit large fluorescent enhancement on binding to DNA, giving quantum yields of >0.4 and have extremely low intrinsic fluorescence. They are also

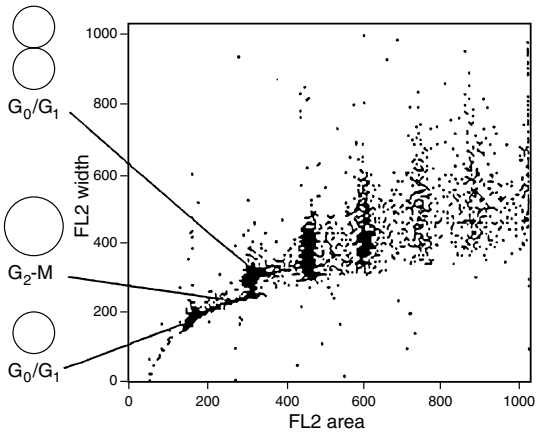

Fig. 10.2 Pulse processing produces a dot blot of pulse area against pulse width. Doublet cells with a $2n$ DNA content each possess the same DNA content as $4n$ singlet cells but have a greater pulse width. (Reprinted from CellQuest Software, Becton Dickinson FacsVantage Users Manual (1995) with the permission of BD Biosciences.)

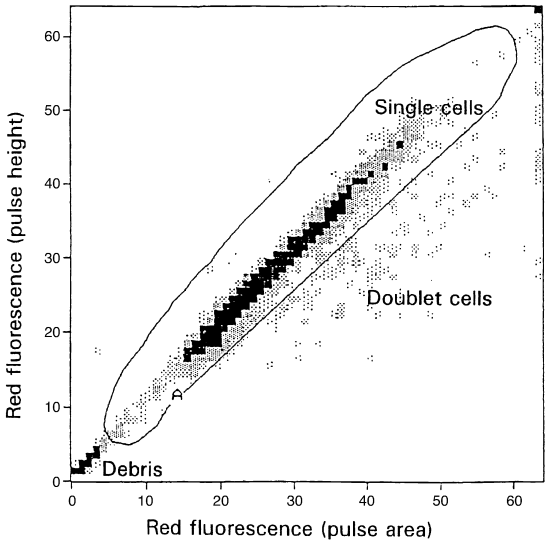

Fig. 10.3 Pulse processing produces a dot blot of pulse area against pulse height for an asynchronous proliferating cell line stained with propidium iodide. Gains have been adjusted so that the pulse height and area are directly proportional to each other. Cells falling out of gate A will be clumped or aggregated cells.

cell permeant and, therefore, stain viable cells. A histogram plot of DNA content against cell numbers gives the classical DNA profile for a proliferating cell culture (Fig. 10.4).

Protocol 10.2 Cell cycle distribution by DNA content

1. Harvest approximately 2×10^5 cells and wash once in PBS.
2. Resuspend the cells in 0.5 ml of ice-cold 70% ethanol and incubate on ice for >2 h.
3. Wash cells three times by centrifugation in PBS and resuspend in a 1 ml mix of 50 μg ml^{-1} PI and 200 μg ml^{-1} RNAase in PBS, for 30 min at 37°C.
4. Do *not* wash cells prior to analysis on the flow cytometer. PI is an intercalating agent and will leak out of the cell if the population is resuspended in buffer not containing PI.
5. Cells are analysed as illustrated in Fig. 10.3.

Note: DNA content alone will not distinguish between G_0 and G_1 nor G_2 and premitotic cells (Steck and El-Nagger, 1998).

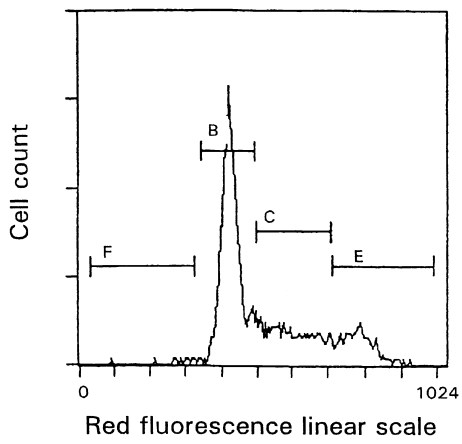

Fig. 10.4 DNA histogram of an asynchronous cycling cell population stained with propidium iodide. Gate B is cells in G_0 plus G_1 phases; gate C is cells in S phase and gate E represents cells in G_2 plus M phases. Any cells falling in gate F would be considered to be apoptotic (see text for details).

DNA content may be measured in association with other nuclear or cellular components such as cyclins by dual fluorescence analysis in which PI is used to stain the DNA and an antibody conjugated to fluorescein isothiocyanate (FITC) or phycoerythrin (PE) is used to define the antigen of interest (see also Ch. 13). An example of this type of analysis is shown in Fig. 10.5.

10.6 S phase analysis using bromodeoxyuridine uptake

The determination of the percentage of cells in S phase is dependent upon the detection of a thymidine analogue, bromodeoxyuridine (BrdU), which is incorporated into DNA during DNA replication. Bivariate analysis of total DNA content uses PI (see Section 10.9) staining along the *x*-axis plotted against BrdU incorporation detected via FITC-labelled antibodies to BrdU on the *y*-axis. Immediately following a pulse of BrdU labelling, the green fluorescence (BrdU content) is observed in S phase. If the population is sampled every 1–2 h, the passage of labelled cells into G_2 can be observed, followed by the appearance of green fluorescence in G_1 as the cells pass through mitosis. The fluorescence intensity is halved as the cells divide because the average amount of BrdU per cell is halved. Green fluorescence reappearing in S phase is indicative of a complete cell cycle and the time taken is indicative of the cell cycle kinetics for the cell population sampled (Fig. 10.6). Depending on the cell type, the BrdU pulse can be as short as 6 min and still be detectable by flow cytometry.

A method for S phase analysis using BrdU uptake is described in Protocol 10.3. Alternatively, a kit for measuring cell proliferation (ABSOLUTE-S; Alexis Biochemicals) is commercially available. This is based on the method published by Li et al. (1995), which involves no heat or acid denaturation step.

Protocol 10.3 S phase analysis in proliferating cells using bromodeoxyuridine uptake

1. Add BrdU to an exponentially growing population of cells to a final concentration of 10 μmol l^{-1} and incubate for 1 h at 37°C.
2. Harvest the cells and centrifuge at 400 × *g* for 5 min.
3. Resuspend the pellet in ice-cold 70% ethanol to a final concentration of 1×10^6 cells in 100 μl volume and incubate on ice for 45 min.
4. Wash 1×10^6 cells in PBS and resuspend the pellet in 1 ml volume of a denaturing buffer (2 mol l^{-1} HCl plus 0.5% bovine serum albumin) and incubate for 20 min at room temperature.
5. Wash once in PBS and resuspend the pellet in a 1 ml volume of a neutralising buffer of 0.1 mol l^{-1} sodium borate pH 8.5 for 2 min at room temperature.
6. Wash once in PBS and resuspend the pellet in 100 μl PBS.
7. Add 90 μl of cells to 10 μl of anti-BrdU monoclonal antibody diluted to a predetermined optimal concentration and incubate for 1 h at room temperature.
8. Wash in PBS. If the anti-BrdU antibody was not directly conjugated then add 100 μl of a 1 : 10 or 1 : 20 dilution of FITC-conjugated goat anti-mouse $F(ab')_2$ fragments for 1 h at room temperature.
9. Wash once in PBS and resuspend in a 1 ml volume of 50 μg ml^{-1} PI and 200 μg ml^{-1} RNAase for 30 min at 37°C.
10. Do *not* wash prior to analysis.

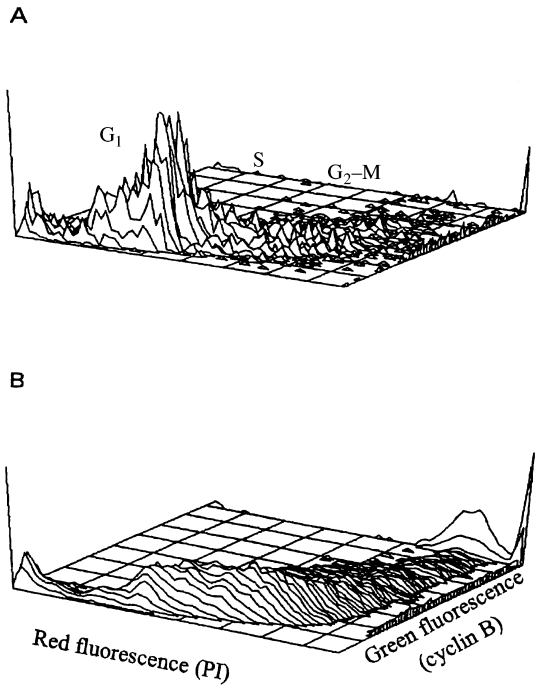

Fig. 10.5 A three-dimensional histogram plot of proliferating K562 cells stained for cyclin B_1 (fluorescein isothiocyanate (FITC)-conjugated final antibody, green) and propidium iodide (PI, red) for DNA content. (A) The majority of cells in G_1 and S phase have not stained positive for cyclin B_1. (B) An imposed G_2–M cell cycle arrest (1 μg ml^{-1} etoposide for 24 h) results in cells in G_2–M staining strongly for cyclin B_1.

10.7 Numerical chromosomal aberrations

All species have a characteristic number of chromosomes. In humans, the diploid number (2*n*) is 46 and hence the haploid number (*n*) is 23. Any number of chromosomes that is an exact multiple of the haploid number is a state known as polyploidy. Although triploid (3*n*) and tetraploid (4*n*) chromosomal numbers are very rarely seen in humans, polyploidisation (e.g. 32*n* to 128*n*) is seen during the development of megakaryocytes, the precursors of platelets. Any number of chromosomes that is not an exact multiple of *n* is termed aneuploidy. This refers, for example, to situations where there are three copies of a given chromosome (trisomy) or only a single copy of a given chromosome (monosomy). Aneuploid and triploid cells are seen in fetal tissue from spontaneous miscarriages and still births. Survival after birth with a triploid autosomal chromosome number in every cell of the body is

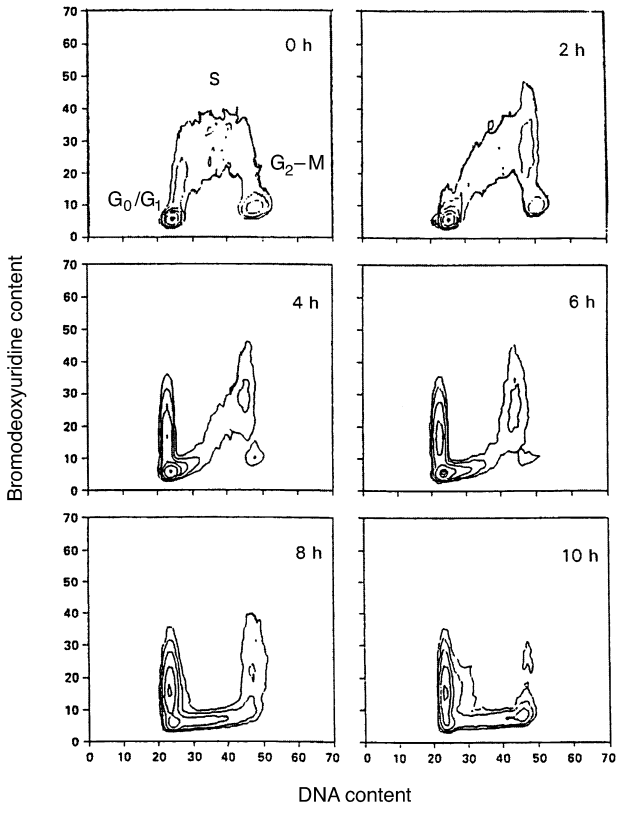

Fig. 10.6 Cell cycle analysis of Chinese hamster ovary (CHO) cells pulsed with 10 μmol l^{-1} bromodeoxyuridine (BrdU) for 30 min and resuspended in fresh medium. Samples of the cell suspension were removed every 2 h, fixed and then stained with fluorescein isothiocyanate (FITC)-conjugated goat anti-mouse antibody following primary antibody staining with anti-BrdU antibody. Propidium iodide was used to determine DNA content. Labelled cells are seen to pass out of S phase at time zero and into G_2–M transition at 2 h. At 4 h, mitosis has occurred in a proportion of the population leaving some labelled cells in G_2–M and others in G_0–G_1. This is also observed at 6 and 8 h but by 10 h the majority of cells have passed through G_2–M into G_0–G_1 with a small percentage of cells re-entering S phase. (Reprinted by permission of the copyright holder, from Dolbeare, F., Gratzner, H.G., Pallavicini, M.G., Gray, J.W. (1983) Flow cytometric measurement of total DNA content and incorporated bromodeoxyuridine. *Proceedings of the National Academy of Sciences of the USA* **80**, 5573–7.)

extremely rare. Monosomy, the loss of a single chromosome, also appears lethal in humans but, in contrast, trisomy is observed in several human disorders, for example, trisomy 21 in children with Down's syndrome, trisomy 18 in Edwards' syndrome and trisomy 13 in Patau's syndrome.

However, chromosomal number aberrations can occur in single cells; in neoplastic disease such a single cell is clonally expanded. Therefore, it is only the diseased cells that exhibit aneuploidy. An estimate of chromosomal number (i.e. ploidy) can be made by an analysis of DNA content of the neoplastic cell population. This can be used as both a diagnostic and prognostic tool. Guidelines for the implementation of DNA cytometry for clinical diagnosis have been published (Shankey et al., 1993). Abnormalities in DNA content have been used to identify high- and low-risk groups of patients in a range of malignancies including breast and bladder carcinomas, non-small cell lung cancer, and cervical, ovarian and colorectal carcinomas. In this way low-risk patients may be spared the trauma of high-dose, intensive therapeutic regimens.

The prognostic relevance of DNA content is firmly established in hematological malignancies. Abnormal DNA content is determined by establishing a DNA index (DI). Cells are stained with PI based on Protocol 10.2. (It is not within the scope of this chapter to outline a protocol for diagnostic purposes. Interested parties should refer to published standard operating procedures from recognised service centres.) The DI is expressed as the ratio of the DNA content of the G_0 plus G_1 cells in the abnormal population to the G_0 plus G_1 DNA content of a normal diploid population. The abnormal peak is identified by comparing its position with either normal lymphocytes or nucleated chicken erythrocytes. (These can be mixed in with the test sample and analysed together.) Often, in diseases such as acute lymphocytic leukaemias (also called acute lymphoblastic leukaemia and acute lymphoid leukaemia) a residual normal population can be perceived to verify the position of the normal control sample G_0 plus G_1 peak. Clearly the DI for a diploid population is 1.00 and, therefore, hyperdiploid cells

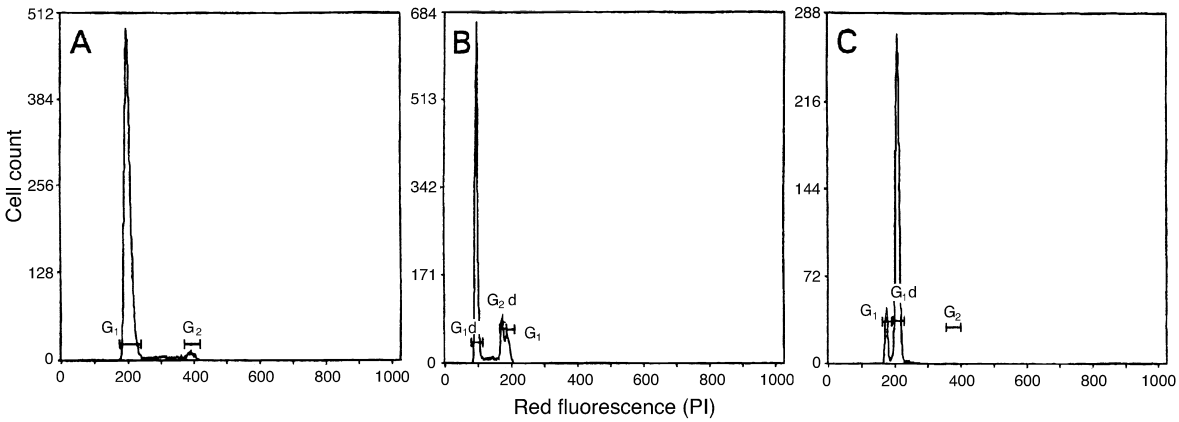

Fig. 10.7 Ploidy studies. (A) A histogram was generated from peripheral blood lymphocytes of a normal subject, which would have a DNA index (DI) of 1.00. (B) The analysis of cells from a patient with hypodiploid lymphocytes (G_0d and G_1d) with a DI of 0.55. N.B. There is also a normal population of diploid cells in this sample. (C) The analysis of cells from a patient with hyperdiploid lymphocytes and a DI of 1.23. There is also a normal population (G_1) in this sample but the hypodiploid population is clearly visible in gate G_1d. PI, propidium iodide.

have a DI >1.00 and hypodiploid populations have a DNA index <1.00. Tetraploid ($4n$) tumours have a DI of 2.0. Figure 10.7 illustrates the flow cytometric analysis of hypodiploid and hyperdiploid lymphocytes from patients with acute lymphocytic leukaemia.

In order to resolve either abnormal peaks from normal peaks or the possibility of more than one abnormal stem line, flow cytometric optimisation is essential. Broad G_0 plus G_1 peaks will not provide the resolution required and coefficients of variation (CVs) of <5.0 have been quoted by Merkel et al. (1987) as being essential for accurate data interpretation.

The calculation of a DI has been used in the identification of high- and low-risk patients in many hematological malignancies and guidelines for this analysis have been proposed (Duque et al., 1993; Ormerod et al., 1998; Shankey, et al., 1993). This has been refined particularly for childhood acute lymphocytic leukaemias, where leukaemic cell hyperploidy with a modal chromosomal number >50 (i.e. a DI >1.16) is consistent with a favourable prognosis whereas a DI <1.16, including diploid patients, identifies those who do less well. Age and white cell count also contibuted to the overall assessment of these patients (Trueworthy et al., 1992). A kit is available commercially, CYCLOSCOPE™ B-ALL (Exalpha Biologicals), that facilitates the detection of hyperdiploid leukaemic blast cells identified by the expression of CD19, cytoplasmic CD79a or cytoplasmic CD22. The kit may be used to monitor minimal residual disease in patients who had blasts with DNA aneuploidy at diagnosis (Cuidad et al., 1997).

10.8 Conclusions

The methods described in this chapter represent basic starter protocols for the analysis of the cell cycle and some of the components that drive it. Each method should be adapted to requirements. Flow cytometric analysis requires fixation and permeabilisation of the cell. The fixation process should not destroy antigen epitopes and permeabilisation should be sufficient to enable antibody penetration, particularly when staining for nuclear antigens such as the cyclins. Optimal conditions and antibody concentrations should be assessed for each experimental situation. Likewise for the permeabilisation/fixation procedures.

Acknowledgements

The authors would like to thank Tim Milne for his assistance and advice with the section on ploidy studies and for making the flow cytometry data available.

10.9 REFERENCES

Cuidad, J., San Miguel, J.F., Lopez-Berges, M.C., Valverde, B., Orfao, A. (1997) Immunophenotypic detection of minimal residual disease in acute lymphoblastic leukaemia. In: Buchner, T. (ed.), *Acute Leukaemias VI. Prognosis Factors and Treatment Strategies*. pp. 321–7. Springer-Verlag, Berlin.

Darzynkiewicz, Z., Gong, J., Juan, G., Ardelt, B., Traganos, F. (1996) Cytometry of cyclin proteins. *Cytometry* **25**, 1–13.

Dolbeare, F., Gratzner, H.G., Pallavicini, M.G., Gray, J.W. (1983) Flow cytometric measurement of total DNA content and incorporated bromodeoxyuridine. *Proceedings of the National Academy of Sciences of the USA* **80**, 5573–7.

Duque, R.E., Andreeff, M., Braylan, R.C., Diamond, L.W., Peiper. S.C. (1993) Consensus review of the clinical utility of DNA flow cytometry in neoplastic hematopathology. *Cytometry* **14**, 492–6.

Juan, G., Darzynkiewicz, Z. (1998) Detection of cyclins in individual cells by flow and laser scanning cytometry. In: Jaroszeski, M.J., Heller, R. (eds.), *Flow Cytometry Protocols. Methods in Molecular Biology* pp. 67–83. Humana Press, Totowa, NJ.

Li, X., Traganos, F., Melamed, M.R., Darzynkiewicz, Z. (1995) Single step procedure for labeling DNA strand breaks with fluorescein or BODIPY-conjugated deoxynucleotides: detection of apoptosis and bromodeoxyuridine incorporation. *Cytometry* **20**, 172–80.

Merkel, D.E., Dressler, L.G., McGuire, W.L. (1987) Flow cytometry, cellular DNA content and prognosis in human malignancy. *Journal of Clinical Oncology* **5**, 1690–703.

Op de Beeck, A., Caillet-Fauquet, P. (1997) Viruses and the cell cycle. *Progress in Cell Cycle Research* **3**, 1–19.

Ormerod, M.G., Tribukait, B., Giaretti, W. (1998) Consensus report of the task force on standardisation of DNA flow cytometry in clinical pathology. DNA Flow Cytometry Task Force of the European Society for Analytical Cellular Pathology. *Analytical Cell Pathology* **17**, 103–10.

Shankey, T.V., Robinovitch, P.S., Bagwell, B., Bauer, K.D., Duque, R.E., Hedley, D., Mayall, B.H., Wheeless, L.L. (1993) Guidelines for implementation of clinical DNA cytometry. *Cytometry* **14**, 472–7.

Sherr, C.J. (1996) Cancer cell cycles. *Science*, **274**, 1672–77.

Steck, K., El-Nagger, A. (1998) Solid tumor DNA analysis. In: Jaroszeski, M.J., Heller, R. (eds.), *Flow Cytometry Protocols. Methods in Molecular Biology*, pp. 181–195. Humana Press, Totowa, NJ.

Trueworthy, R., Schuster, J., Look, T., Crist, W., Borowitz, M., Carroll, A., Frankel, L., Harris, M., Wagner, H., Haggard, M., Mosijczuk, A., Steuber, P., Land, V. (1992) Ploidy of lymphoblasts is the strongest predictor of treatment outcome in B-cell progenitor cell acute lymhoblastic leukemia of childhood: a pediatric oncology group study. *Journal of Clinical Oncology* **10**, 606–13.

11

Cell viability, necrosis and apoptosis

Paul D. Allen and Adrian C. Newland

St Bartholomew's and Royal London School of Medicine and Dentistry, Queen Mary and Westfield College, London

11.1 Introduction

The very existence of multicellular organisms is dependent upon a balance between life and death. Starting with fetal development, through to tissue and organ regeneration in adulthood, events are determined by the timely activation of proliferation, differentiation and cell death. To maintain tissue and organ homeostasis, proliferation must be countered by cell death. For decades the emphasis of research in cell biology lay with investigations into proliferative responses and differentiation, but the importance of cell death is now well established as an active cellular process.

11.2 Apoptosis

Apoptosis is a series of sequential events under genetic control resulting in cell death (Darzynkiewicz et al., 1998; Penninger and Kroemer, 1998). It is seen during fetal development (e.g. loss of interdigitating membranes and synaptogenesis in the nervous system), thymic selection to eliminate self-reactive lymphoid cells, elimination of cancer and virally infected cells, and in cell and tissue renewal in the bone marrow, gut and skin. Morphological changes associated with an apoptotic cell include cell and nuclear condensation, accumulation of chromatin around the inner nuclear envelope and segregation of nuclear and cytoplasmic material into membrane-bound apoptotic bodies. In vivo, cytoplasmic membrane changes during apoptosis lead to recognition of cells undergoing apoptosis, resulting in phagocytosis by surrounding cells. The bottom line is that large amounts of cell death can occur without the spillage of cellular contents into the cellular environment, thus avoiding the induction of inflammatory responses. Biochemically, apoptosis is epitomised by the loss of the inner mitochondrial membrane potential ($\Delta\psi m$) and release of cytochrome *c* into the cytosol. The apoptotic machinery, consisting of a cascade of cysteine proteases, or caspases, is then activated; this, in turn, triggers the cleavage of the inhibitor of the caspase-activated deoxyribonuclease. The caspase-activated deoxyribonuclease is then released to cleave DNA into the 182 base pair DNA multimers, which when separated by agarose gel electrophoresis gives the characteristic DNA 'ladder' pattern; the hallmark of apoptosis. Caspase activation during apoptosis also cleaves various cellular substrates such as actin, fodrin and lamins, which play a role in the morphological changes seen in apoptosis, as well as certain anti-apoptotic gene products.

11.3 Genetic control of apoptosis

Genetic changes occurring through mutation, chromosomal translocation or viral activation can cause aberrations in the control of apoptosis and can clearly lead to disease. Inappropriate induction of apoptosis can result in the degenerative diseases, e.g. Alzheimer's and Parkinsons' diseases, whereas blockade of apoptosis or failure to induce it can lead to cancer and the autoimmune diseases.

That apoptosis is genetically controlled as a programmed event became evident from the original studies performed on the nematode worm

Caenorhabditis elegans. This worm contains 1090 somatic cells of which 131 are programmed to die. Three genes were identified as essential to the regulation of apoptosis in these cells and were named the cell death (*ced*) genes. The three genes in question were *ced-3*, *ced-4* and *ced-9*. *ced-3* and *ced-4* were found to be essential for cell death to proceed whereas *ced-9* promoted cell survival. Extended genetic studies in *C. elegans* showed that *ced-9* inhibited the activity of *ced-4*, which in turn activated the pro-apoptotic functions of *ced-3*. Human homologues of all three genes have now been identified. *ced-3* showed sequence homology with mammalian interleukin 1β converting enzyme (ICE). This was the first member identified of the family of caspases, which were found to constitute the driving force of the morphological and biochemical changes seen in apoptotic cells. However, whether there is a direct role for ICE (caspase 1) per se in apoptosis remains debatable. The human homologue of *ced-4* has recently been found to be Apaf-1 (apoptosis activation factor 1, an apoptosis-inducing factor), a crucial partner of cytochrome *c* and caspase 9 in the formation of the apoptosome (see below). The human homologue of the survival gene, *ced-9*, was identified as *BCL-2*. At the time, *BCL-2* was known as a gene aberrantly expressed in patients with follicular B-cell lymphoma following the characteristic t(14:18) chromosomal translocation seen in this disease. This novel aspect of promoting cell survival, rather than proliferation, renders cells expressing *BCL-2* resistant to a wide range of death-inducing procedures including growth factor withdrawal, treatment with cytotoxic drugs, metabolic toxins and viral infections. It is clear that inappropriate expression of *BCL-2* and its effects of promoting cell survival contributes considerably to oncogenesis in neoplastic disease.

11.4 Bcl-2 expression and apoptosis

It transpires that Bcl-2 is only one protein of a relatively large family, based on sequence homology of four Bcl-2 homology regions designated BH1 to BH4. Moreover, some members of the Bcl-2 family antagonise apoptosis whereas others promote cell death. Members that inhibit cell death include Bcl-2, Bcl-XL, Bcl-w, A1 and MCL-1. This spectrum of death antagonists reflects tissue and cell development specificity in their expression. Those members of the Bcl-2 family that promote cell death include BAX, BCL-Xs, BAD, BAK and BIK. If BAX is coexpressed with either Bcl-2 or Bcl-XL, then the pro-apoptotic activity of BAX is negated. BAX can form homodimers or it can heterodimerise with Bcl-2 or Bcl-XL. It has been proposed that the proportion of BAX *not* heterodimerised to Bcl-2 or Bcl-XL determines an apoptotic threshold that, if exceeded, promotes apoptosis. BIK works in a similar way to BAX in terms of interaction with apoptosis antagonists and, again like BAX, can induce apoptosis directly if overexpressed in certain cell models. Both Bcl-2 and Bcl-XL have been found localise to the outer membrane of mitochondria, which plays a pivotal role in determining the outcome of death-inducing signals (see below).

11.5 Necrosis

Traditionally, necrosis has been exemplified by the morphology observed following accidental cell death, e.g. as seen in burns. Cells are destroyed by membrane fracture and cell contents are spilled into the interstitial spaces causing inflammation. If the stimulus is less pronounced, e.g. plasma membrane damage by complement or by lytic viruses or interference of energy-dependent ion pumps by poisons such as sodium azide, then cellular swelling is seen as necrotic morphology. This morphology results from water uptake by the cell to compensate for Na^+, K^+, Ca^{2+} and Mg^{2+} moving down their respective concentration gradients. There is a decline in protein synthesis and the mitochondrial membrane swells; if the stimulation persists, lysosomal enzymes are released and there is activation of degrading phospholipases, a fall in pH and a switch to anaerobic glycolysis. These changes result in plasma membrane rupture and the induction of

inflammation in surviving surrounding cells.

Historically, apoptosis and necrosis have represented two possible but separate responses of a cell to cell death induction. The former is induced not only as a genetically programmed cell death in response to DNA damage and to mild changes in the environment but also by physiological inducers such as tumour necrosis factor α and Fas ligand (Fas-L). The latter is induced in response to extreme or prolonged stimuli or accidental rupture of cell membranes. But when does a 'short' stimulus become a 'prolonged' stimulus? When does a 'weak' stimulus become a 'strong' stimulus? There are several observations that suggest that apoptosis and necrosis are not separate processes but rather that they represent two extremes of a continuum. First, necrosis is often seen following primary induction of apoptosis; second, the same inducer can induce either apoptosis or necrosis; third, in some cell types inhibition of caspases will block apoptosis only for necrosis to proceed; and fourth, loss of $\Delta\psi m$ and cytochrome *c* release is observed in both apoptosis and necrosis. This last point is critical to the outcome of the cell death process and is most probably cell dependent.

11.6 Mitochondrial membrane potential, cytochrome *c* and cell death

The $\Delta\psi m$ results from a differential distribution of proteins on either side of the impermeable inner mitochondrial membrane. This produces an electrical gradient across the membrane that is crucial for mitochondrial function, with the inner side of the membrane maintaining a net negative charge. There is now evidence to show that in apoptosis, loss of $\Delta\psi m$ occurs through the formation of a mitochondrial permeability transition (PT) pore or mitochondrial megachannel (Green and Reed, 1998). The PT pore is a dynamic multiprotein complex that contacts with both the inner and outer mitochondrial membranes. Opening of the pore not only disrupts the $\Delta\psi m$ but also provides a channel for the uptake of solutes and water into the mitochondrion. This has numerous effects on mitochondrial function, including release of Ca^{2+} and glutathione from the mitochondrial matrix, uncoupling of oxidative phosphorylation, shutdown of ATP synthesis and increased superoxide production from the uncoupled electron transport chain. Therefore, opening of the PT pore can in itself induce necrosis. Central to apoptosis being triggered is the release of cytochrome *c* from the intermembrane space into the cytosol, presumably because inner membrane swelling following water and solute uptake eventually ruptures the outer mitochondrial membrane. In apoptosis, the release of cytochrome *c* initiates activation of the 'apoptosome'; a complex of Apaf-1, cytochrome *c* (Apaf-2) and procaspase 9 (Apaf-3). Cytochrome *c* binding to WD-40, 40 amino acid residue repeat regions on Apaf-1, allows recruitment of caspase 9 to the caspase recruitment domain on Apaf-1 with the subsequent activation of caspase 9. The apoptotic protease cascade is thus activated by the cleavage and activation of procaspase 3 by the activated form of caspase 9. Consequently, cytochrome *c* release by mitochondria commits a cell to cell death.

However, another caspase-activating protein released from the mitochondria is the apoptosis-inducing factor (AIF), which has also been shown to activate procaspase 3 and cause apoptotic changes in cell nuclei. Inhibition of PT pore (e.g. by bongkrekic acid) prevents the release of AIF. As Bcl-2 is located in the outer mitochondrial membrane, it has been proposed that Bcl-2 inhibits the release of cytochrome *c* and/or AIF either directly or by inhibiting the generation of a PT pore (Minn et al., 1998). Consistent with this theory is that BAX overexpression causes PT pore formation in some systems. However, other possible roles of Bcl-2, Bcl-XL and BAX in modulating mitochondrial physiology, other than PT pore regulation and release of AIF or cytochrome *c,* have been proposed. One is that the outer mitochondrial membrane can be disrupted through transient hyperpolarisation of the inner mitochondrial membrane, precisely the opposite to the hypopolarisation seen with opening of the PT pore. This process can be inhibited by Bcl-XL.

Alternatively, it has been shown that Bcl-2, Bcl-XL and BAX molecules can themselves form ion channels in synthetic membranes, which could subsequently govern ion transport, affect pH or interact with components of the PT pore.

Whether a cell proceeds down the apoptotic or necrotic pathways is cell dependent. It has been proposed that in cells that have high cytochrome *c* levels, enough may remain inside the mitochondria to maintain electron transport and ATP production. The release of cytochrome *c* activates downstream caspases to go on to cleave cytoplasmic and nuclear substrates. Necrosis occurs on cytochrome *c* release if endogenous caspase inhibitors block the apoptotic response. In this scenario, the eventual loss of cytochrome *c* from the inner mitochondrial compartment results in a slow non-apoptotic cell death.

11.7 Flow cytometry

11.7.1 Viability and necrosis

A dot plot of forward light scatter versus side scatter is a measure of cell size and cell granularity, respectively (see Ch. 1), the latter being dependent upon the presence of intracellular structures that change the refractive index of light. Cell condensation during early apoptosis is seen as a decrease in forward light scatter only. As apoptosis proceeds, both forward and side scatter diminish. In necrotic death, cells swell initially, and then cellular contents are rapidly released. This is seen on the flow cytometer as an initial increase in forward light scatter followed by a rapid decrease in both forward and side scatter. Changes in cell size can be used in conjunction with surface phenotypic markers to identify the dying population.

Protocol 11.1 Detection of apoptosis using a propidium iodide DNA content assay

1. Harvest approximately 2×10^5 cells and wash once in phosphate-buffered saline (PBS).
2. Resuspend the cells in 0.5 ml of ice-cold 70% ethanol and incubate on ice for >2 h.
3. Wash cells three times in PBS and resuspend in a 1 ml mix of 50 μg ml^{-1} PI and 200 μg ml^{-1} RNAase in PBS for 30 min at 37°C.
4. Do *not* wash cells prior to analysis on the flow cytometer. PI is an intercalating agent and will leak out of the cell if the population is resuspended in buffer not containing PI.
5. Analyse using pulse processing to gate out aggregated cells and cell debris. On a histogram plot of red fluorescence against cell numbers, the apoptotic cells fall to the left of the G_0 plus G_1 peak.

A more discriminatory characteristic of dying cells is the changes in the permeability of the membrane on the induction of death. Cationic dyes such as propidium iodide (PI) or 7-aminoactinomycin D (7-AAD) are excluded from viable cells (Philpott et al., 1996). For example, membrane rupture seen in necrosis and the very late stages of apoptosis permeabilises cells to PI (Protocol 11.1). However, certain changes in energy-dependent ionic membrane transport during apoptosis allows a degree of fluorochrome uptake for a dye such as 7-AAD (Protocol 11.2). This permits a discrimination of viable cells, which exclude the dye totally, from apoptotic cells, which fluoresce dimly, and necrotic and late apoptotic cells, which fluoresce brightly.

Protocol 11.2 Detection of apoptosis using uptake of 7-aminoactinomycin D

1. Wash cells in PBS and resuspend at 1×10^6 ml^{-1} in PBS.
2. Add 7-AAD to 1 ml of cells, i.e. 10^6 cells, to give a final 7-AAD concentration of 20 μg ml^{-1}.
3. Incubate the cells at 4°C for 20 min.
4. Pellet the cells and resuspend in 500 μl of 2% paraformaldehyde.
5. Analyse the cells within 30 min of fixation with a dot plot using forward light scatter on the *x*-axis

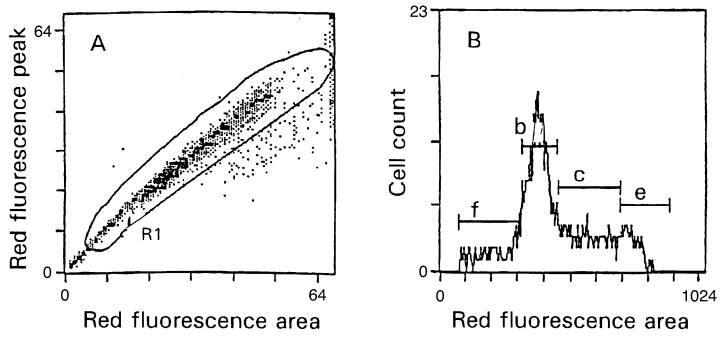

Fig. 11.1 Pulse processing for analysis of cells for apoptosis. (A) A dot plot of pulse area against pulse height of an asynchronous population of cells stained for DNA content with propidium iodide. Region R1 omits aggregated cells, seen below the region, and cell debris, which is seen in the extreme bottom left-hand corner. (B) A further analysis of the cells in gate R1 shows gate f, which represents a background of apoptotic cells in an untreated cell population and does not include cell debris.

and 7-AAD fluorescence intensity on the *y*-axis.

6. Three distinct populations should be observed, consisting of a population with 7-AAD fluorescence equivalent to the negative control (non-stained paraformaldhyde-fixed cells), which are the viable cells, 7-AAD bright cells, which are the dead or late apoptotic cells, and 7-AAD dim cells, which are the apoptotic population.

Hoescht 33342 is taken up by both viable and dead cells but the rate of uptake is far slower in viable cells. Apoptotic cells also stain strongly with Hoescht 33342 so, when used in conjunction with PI, viable cells (no dye uptake), necrotic cells (PI, red staining) and apoptotic cells (Hoescht, blue staining) can all be detected on the flow cytometer following a short staining period (Protocol 11.3). The emission spectra of these dyes also allows for a third fluorochrome to be used (e.g. fluorescein isothiocyanate (FITC)) for a phenotypic identification of the dying cell population.

Protocol 11.3 Detection of apoptosis and necrosis using Hoechst 33342 and propidium iodide

1. Harvest 1×10^6 cells and resuspend in 1 ml of PBS.
2. Add Hoechst 33342 to a final concentration of 1 μg ml^{-1} (e.g add 100 μl of a stock solution of Hoechst 33342 (10 μg ml^{-1}) to 900 μl of cell suspension).
3. Add PI to a final concentration of 5 μg ml^{-1} (e.g. one drop of PI from a stock of 50 μg ml^{-1} using a Pastette).
4. Incubate for 5 min and analyse using a dot plot of PI fluorescence intensity on the *x*-axis and Hoechst 33342 fluorescence intensity on the *y*-axis.

Note: Hoechst 33342 emission spectra shifts towards the red in apoptotic cells. To avoid loss of Hoechst fluorescence use a 400 nm long-pass filter instead of the usual Hoechst DNA filter combination of 400 nm long-pass and a 480 nm short-pass filters.

11.7.2 Apoptosis

There are certain characteristics of apoptotic cells that can be identified and used to detect apoptotic

cells in an otherwise healthy population of cells. Technically, the easiest characteristic to detect is loss of DNA from permeabilised cells owing to DNA fragmentation. When cells are permeabilised, for example by 70% ethanol, the fragmented 182 bp DNA multimers leak out of the cell. The result is a population of cells with a reduced DNA content. If the cells are then stained with a DNA intercalating dye such as PI, then a DNA profile representing cells in G_1, S and G_2 plus M phases will be observed, with apoptotic cells being represented by a sub-G_0–G_1 population seen to the left of the G_0–G_1 peak (Protocol 11.1 and Figs. 11.1 and 11.2).

Internucleosomal DNA fragmentation (to produce the 182 bp DNA multimers) is preceded by fragmentation into 300 kb and/or 55 kb fragments. In certain cells with some apoptotic stimuli, fragmentation goes no further. Such large fragments can only be resolved electrophoretically using pulsed field gel electrophoresis. They will not leak out of permeabilised cells and therefore the cells would appear to be non-apoptotic in terms of DNA content assays on the flow cytometer. However, the nicks (or strand breaks) can be detected using the terminal deoxynucleotidyl transferase (TdT) dUTP nick end labelling technique (TUNEL), which is based on the ability TdT to end-label nicks in the DNA brought about by the caspase-activated deoxyribonuclease with the nucleotide deoxyuridine trisphosphate (dUTP). TdT has the ability to label 3' blunt ends of double-stranded DNA independently of a template (Protocol 11.4).

Protocol 11.4 Detection of apoptosis by a terminal deoxynucleotidyl transferase, deoxyuridine trisphosphate, nick-end labelling (TUNEL) technique

1. Harvest 1.5×10^6 cells and wash in PBS.
2. Resuspend in 1 ml of PBS and add 1 ml 2% (w/v) paraformaldehyde and place on ice for 15 min.
3. Wash twice by centrifugation in PBS and resuspend the pellet in 2 ml of 70% ethanol.
4. Place at –20°C for at least 30 min but overnight (approx. 16 h) may give better results. Cells can be stored for up to 3 days at this stage.
5. Rehydrate the cells in PBS by pelleting the cells, aspirating the ethanol and resuspending the cells in 1 ml PBS.
6. Pellet and resuspend the cells in 50 μl cacodylate buffer (0.2 mol l^{-1} potassium cacodylate, 2.5 mmol l^{-1} Tris-HCl pH 6.6, 2.5 mmol l^{-1} $CoCl_2$, 0.25 mg ml^{-1} bovine serum albumin, 5 U TdT and 0.5 nmol l^{-1} FITC–dUTP) and incubate for 60 min at 37°C.
7. Wash twice by centrifugation in PBS.
8. Analyse on a histogram plot of green fluorescence against cell numbers.

Note: Control is as in step 6 but omitting the TdT.

There are various techniques to detect the incorporated dUTP. These include using dUTP conjugated with either biotin or digoxygenin. For flow cytometry, the former is labelled with FITC–avidin and the latter by using FITC–conjugated antibody to digoxygenin. Another variation is to use bromodeoxyuridine (BrdU), as a thymidine analogue that is again visualised using FITC-conjugated anti-BrdU antibodies. More recently, a direct protocol has been made available by labelling dUTP with FITC. This eliminates the requirement for secondary reagents and, therefore, is less labour intensive. Moreover, nonspecific binding of secondary reagents is eliminated, thus maintaining sensitivity. This method remains the method of choice when using TUNEL techniques for flow cytometry. Nicks occur at a far higher rate in apoptosis than necrosis.

An alternative to following DNA fragmentation for the detection of apoptosis is to examine morphological changes in the cell membrane of apoptotic cells. There are many alterations in the constitution and distribution of membrane proteins, glycoproteins and phospholipids, but one change in particular has proven useful; this involves phosphatidylserine (PS). In viable cells, its distribution about the membrane is asymmetric, with the inner membrane layer containing the anionic phos-

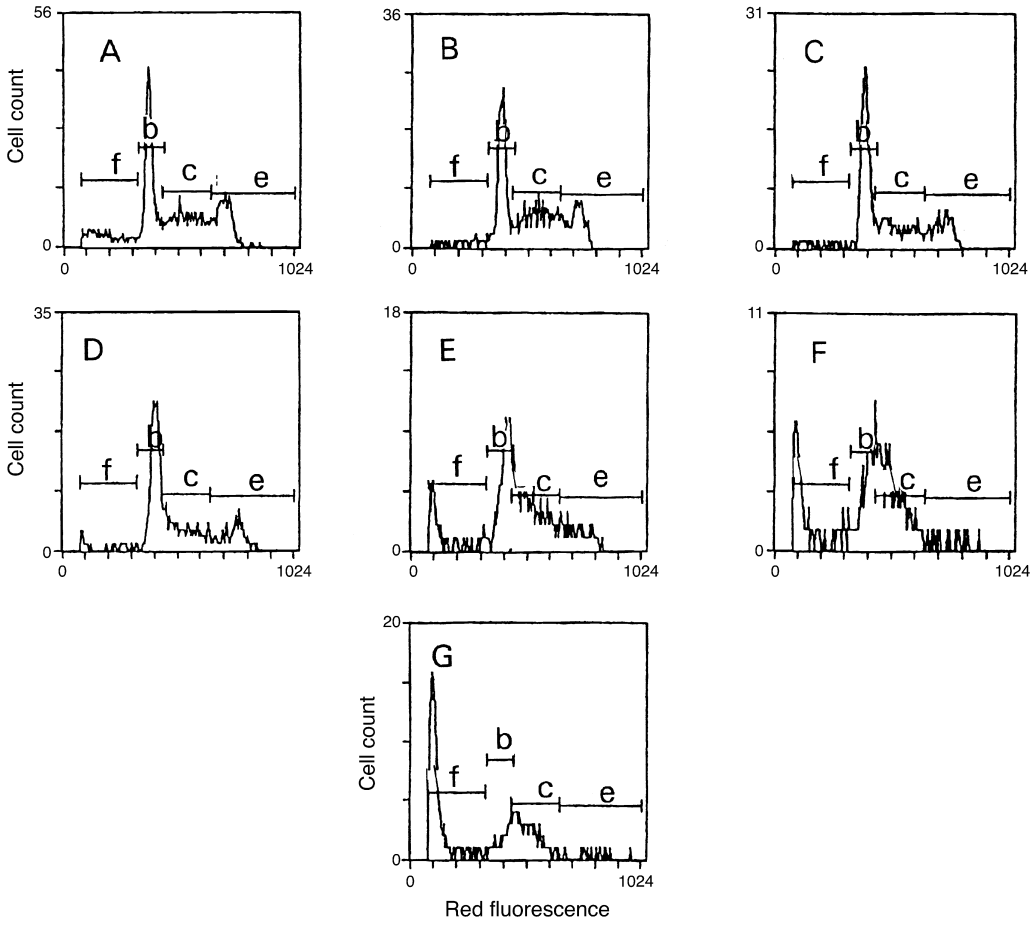

Fig. 11.2 A T lymphoblastic cell line treated with increasing concentrations of an apoptosis-inducing drug and then stained for DNA content with propidium iodide. The population (gate f) with less DNA than that found in G_0–G_1 is indicative of DNA loss owing to DNA cleavage during apoptosis. (A) The control population; (B–G) increasing concentrations of the apoptosis-inducing drug.

pholipids (i.e. PS) and the outer layer neutral phospholipids. During apoptosis, the distribution of anionic phospholipids flips and PS is exposed on the outer phospholipid membrane layer. This is then detectable on apoptotic cells. The Ca^{2+}-dependent phospholipid-binding protein annexin V has a high affinity for PS. When annexin V is conjugated to a fluorochrome such as FITC or PE, PS can be detected flow cytometrically (Protocol 11.5 and Fig. 11.3).

Protocol 11.5 Detection of phosphatidylserine as a marker of apoptosis using annexin V

1. Wash 1×10^6 cells in PBS and resuspend in 1 ml incubation buffer (10 mmol l^{-1} Hepes, pH 7.4, 150 mmol l^{-1} NaCl, 5 mmol l^{-1} $CaCl_2$).
2. Add FITC-labelled annexin V to a final concentration of 2.5 μg ml^{-1}.
3. Wash once in incubation buffer, resuspend in 1 ml incubation buffer and analyse cells using a

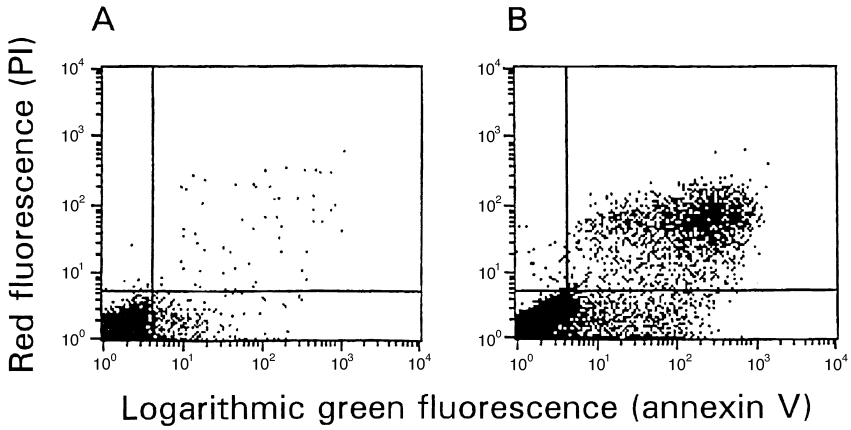

Fig. 11.3 A quadrant dot blot analysis of peripheral blood mononuclear cells stained for apoptosis using an annexin V detection of phosphatidylserine expression along the *x*-axis, counterstained with propidium iodide (PI) to detect late apoptotic or necrotic cells. Control cells are represented in (A) and cells undergoing apoptosis are represented in (B). The lower left quadrant are viable non-apoptotic cells; the lower right is apoptotic cells binding annexin V; the upper right are late apoptotic cells that are binding annexin V and taking up PI. The upper left would contain cells that take up PI but do not bind annexin V. These cells would most likely be necrotic.

histogram of green fluorescence on the x-axis and cell numbers on the *y*-axis.

4. Use nonstained cells as a negative control.
5. Alternatively, if PI (5 μg ml^{-1}) is incorporated in the incubation buffer at step 3, then a dot blot of PI on the *x*-axis against annexin V on the *y*-axis can be used to distinguish viable cells, which are negative for both PI and annexin V, apoptotic cells, which are annexin V positive but exclude PI and are therefore PI negative, and late apoptotic or necrotic cells, which are double positive for PI uptake and annexin V staining.

The fall in $\Delta\psi m$ can also be measured flow cytometrically. Normal mitochondrial function has a requirement for a negative charge on the inner side of the mitochondrial inner membrane. This is maintained by the asymmetrical distribution of H^+ across the membrane, giving rise to both a potential difference and a chemical pH gradient. Cationic lipophilic dyes such as CMXRos (chloromethyl-X-rosamine), JC-1 (5,5'6,6'-tetrachloro-1,1',3,3'-tetraethylbenzimidazol carbocyanide iodide), $DiOC_6(3)$ (3,3'-dihexyloxacarbocyanide iodide) and rhodamine 123 are taken up and distributed across the inner membrane in a way that is dependent on the H^+ distribution, i.e. to the inner membrane matrix (Macho et al., 1996). Methods using these dyes are dependent on the fact that the effects of $\Delta\psi m$ greatly exceed the effect of the plasma membrane potential in terms of cationic dye uptake. This is demonstrated by the observation that 137 mmol l^{-1} KCl, which disrupts plasma membrane potential, causes only a small drop in fluorescence whereas disruption of $\Delta\psi m$ by the protonophore carbonyl-cyanide *m*-chlorophenylhydrazone (mClCCP) induces a far greater drop in fluorescence.

Loss of $\Delta\psi m$ is detected in dying cells by measuring either the concomitant loss of dye from the inner mitochondrial matrix, caused by the redistribution of H^+ as the PT pore opens, or the change in fluorescence caused by the conformational change in the dye as the $\Delta\psi m$ falls. The former approach is typified by use of $DiOC_6(3)$, which is lost from the mitochondrial inner membrane matrix when the $\Delta\psi m$ falls. The latter is typified by JC-1(Protocol 11.6). At high membrane potential, JC-1 forms aggregates and emits fluorescence in the red

region at 590 nm. When the $\Delta\psi$m falls, JC-1 forms monomers that emit green fluorescence at 527 nm. A plot of green fluorescence against red fluorescence (i.e. JC-1 monomers against JC-1 aggregates) will give a population of cells that is positive for both red and green in untreated cells. This reflects the heterogeneity of mitochondria in individual cells, some have a high $\Delta\psi$m whereas in others $\Delta\psi$m can be low. Overall loss of $\Delta\psi$m, as seen in cell death, is visualised flow cytometrically as a loss of red fluorescence (JC-1 aggregates) while green fluorescence is maintained.

Protocol 11.6 Detection of changes in inner mitochondrial membrane potential using nonfixable dyes

1. Harvest 1×10^5 cells and wash once by centrifugation in PBS.
2. Resuspend cells in 1 ml medium containing 40 nmol l^{-1} $DiOC_6(3)$ or alternatively 1 μmol l^{-1} JC-1.
3. Incubate cells for 15 min at 37°C.
4. Wash once by centrifugation in PBS.
5. Resuspend in 1 ml PBS and analyse immediately.
6. $DiOC_6(3)$-stained cells can be analysed using green fluorescence on the *x*-axis against cell numbers on the *y*-axis. A fall in green fluorescence indicates a loss of $\Delta\psi$m.
7. JC-1-stained cells can be analysed using red fluorescence (590 nm) on the *x*-axis against cell numbers on the *y*-axis. A fall in red fluorescence indicates a loss of $\Delta\psi$m. Alternatively, two-colour fluorescence can be used with a dot plot of green fluorescence on the *x*-axis and red fluorescence on the *y*-axis.

11.7.3 Methodological advantages and disadvantages

The flow cytometer is an important tool for the analysis of cell death. The rapidity with which large numbers of cells can be analysed gives flow cytometry a great advantage over other techniques. The range of fluorochromes and the different characteristics of apoptotic and necrotic cells renders multiparameter analyses possible, if and when required.

For example, screening of large numbers of samples for viability is easily performed because nonpermeabilised cells will not take up cell-impermeant dyes such as PI; such cells are, therefore, viable or in the early stages of apoptosis. Detection of PS expression coupled with a counter stain of PI on permeabilised cells allows a bivariate analysis to determine which phase of the cell cycle contains the apoptotic cells. Analysis using TUNEL followed by PI staining will provide a similar analysis. Annexin V or TUNEL identification of apoptotic populations can be used together with staining for specific phenotypic markers or other antigens of interest.

There are certain problems associated with data interpretation. The percentage apoptosis is not indicative of the rate of apoptosis. It is a 'freeze frame' view of the population showing how many cells are apoptotic/necrotic *at the time of sampling*. It is not a cumulative assessment of the total number of dead cells: 30% apoptosis every 8 h will produce twice as much cell death as 30% every 16 h yet the flow cytometer will register 30% in both circumstances. Or to put it another way, there is no way of knowing whether the cells detected as apoptotic at 16 h are the same as the ones detected as apoptotic at 8 h or whether they are a different population of cells. These problems are best resolved using technology other than flow cytometry, for example time-lapse video microscopy.

11.7.4 Problems associated with DNA content assays

Measurement of the loss of fragmented DNA from apoptotic cells is not always reproducible. It will depend on time of permeabilisation, cell type and washing procedures. Indeed, it is reported that washing the cells in 0.2 mol l^{-1} phosphocitrate buffer (pH 7.8) greatly enhances extraction of fragmented DNA. Identification of apoptotic cells as

containing less DNA than cells in the G_0–G_1 peak may also be misleading since mechanically damaged cells, or normal non-apoptotic hypodiploid cells, would fall into this population on the cytometer, giving an artifically high assessment of the percentage of apoptotic cells in the population. An overestimation of apoptotic cells will also be obtained if the primary gate does not exclude cell debris, as this is seen as poorly stained events that indicate less DNA than possessed by cells in the G_0 plus G_1 region. Alternatively, this assessment can be artificially low if the apoptotic cells are generated from the G_2 plus M population because loss of DNA from a premitotic cell could give a DNA content similar to that of an S or G_1 phase cell. Also the requirement for cell permeabilisation does not allow discrimination of apoptotic cells from necrotic. Clearly the use of 7-AAD, with or without Hoescht 33342, on nonpermeabilised cells solves this problem.

11.7.5 Problems associated with the TUNEL and phosphatidylserine techniques

Nicks in DNA are not specific for apoptosis as they can be induced mechanically or in necrosis. Also, complete DNA degradation does not always occur in apoptosis, although in human cells this is rare. However, nicks should be detectable when fragmentation into 300 kb and 55 kb sections has occurred in apoptotic cells even if complete degradation does not take place. Exposure of PS on the outer leaflet of the cell membrane is not specific for apoptotic cells since PS has been reported to be exposed in some instances of necrosis.

11.7.6 Problems associated with the detection of the inner mitochondrial membrane potential

The use of cationic dye to detect loss of transmembrane potential in dying cells can be the subject of misinterpretation. Artifacts occur because of autoquenching of these dyes at high intramitochondrial concentrations; oxidation of the fluorochromes also leads to loss of fluorescence, and dye uptake can be dependent upon changes in mitochondrial size rather than changes in transmembrane potential. In addition, dyes such as $DiOC_6$ and JC-1 do not lend themselves to fixation, which can be a problem when investigating metabolically active cells because cells must be analysed immediately after staining. However, chloromethyl-X-rosamine (CMXRos) can be fixed with paraformaldehyde, which means that cells can be stored and that membrane integrity postfixation does not have to be maintained (Protocol 11.7). This enables, for example, staining for either mitochondrial membrane proteins or for those proteins found in the nucleus (Macho et al., 1996).

Protocol 11.7 Detection of changes in inner mitochondrial membrane potential using a fixable dye

1. Harvest 1×10^5 cells and wash once by centrifugation in PBS.
2. Resuspend cells in 1 ml medium containing 30 mmol l^{-1} CMXRos (stock solutions of CMXRos can be made in dimethyl sulphoxide at concentrations 100–200-fold more concentrated than required and stored at –20°C).
3. Incubate cells at 37°C for 15 min.
4. Analyse cells using green fluorescence against cell numbers.
5. Alternatively, cells can be resuspended in medium containing 150 mmol l^{-1} CMXRos and after incubation they can be fixed by resuspending the CMXRos-stained cell pellet in 4% paraformaldehyde in PBS for 15 min at room temperature.
6. Cells can be stored at 4°C and/or stained for a second antigen of interest using membrane permeabilisation procedures such as acetone, ethanol or detergents.

Note: A positive control for these experiments is to treat cells with an uncoupling agent, e.g. 50 μmol l^{-1} mClCCP, which completely abolishes the transmembrane potential.

Table 11.1 *Emission wavelengths of some dyes used for monitoring viability, apoptosis and necrosis*

Fluorochrome	Emission wavelength (nm)
Hoescht 33342	460
Propidium iodide (PI)	617
Fluorescein isothiocyanate (FITC)	520
Phycoerythrin (PE)	525
7-Aminoactinomycin D (7-AAD)	647
5,5'6,6'-Tetrachloro-1,1',3,3'-tetraethylbenzimidazol carbocyanide iodide (JC-1)	
Aggregates	590
Monomers	527
3,3'-Dihexyloxacarbocyanide iodide ($DiOC_6(3)$)	525
Chloromethyl-X-rosamine (CMXRos)	630

11.8 Protocols

All of the protocols outlined in this chapter, except those using Hoecsht 33342, can be performed using flow cytometers with a 488 nm argon laser. Hoechst 33342 is best excited by the 325 nm line from a helium–cadmium laser but it can also be excited by light at 350 nm to 360 nm from an argon laser if 325 nm excitation is not available. Emission wavelengths of the fluorochromes described in this chapter for monitoring viability, apoptosis and necrosis are given in Table 11.1 so that the appropriate choice of band-pass filters can be made. As usual, cytometer alignment and colour compensation when two or more fluorochromes are in use should be optimised before analyses are carried out.

Acknowledgements

The authors would like to thank Leah Krukowski who provided the quadrant analyses of annexin V and propidium iodide stained mononuclear cells.

11.9 REFERENCES

Darzynkiewicz, Z., Juan, G., Li, X., Gorczyca, W., Murakami, T., Traganos, F. (1998) Cytometry in cell necrobiology: analysis of apoptosis and accidental cell death (necrosis). *Cytometry* **27**, 1–20.

Green, D.R., Reed, J.C. (1998) Mitochondria and apoptosis. *Science*, **281**, 1309–12.

Macho, A., Decaudin, D., Castedo, M., Hirsch, T., Susin, S.A., Zamzani, N., Kroemer, G. (1996) Chloromethyl-X-rosamine is an aldehyde fixable potential-sensitive fluorochrome for the detection of early apoptosis. *Cytometry* **25**, 333–40.

Minn, A.J., Swain, R.E., Ma, A., Thompson, C.B. (1998) Recent progress on the regulation of apoptosis by Bcl-2 family members. *Advances in Immunology* **70**, 245–79.

Penninger, J.M., Kroemer, G. (1998) Molecular and cellular mechanisms of T lymphocytic apoptosis. *Advances in Immunology* **68**, 51–144.

Philpott, N.J., Turner, A.J., Scopes, J., Westby, M., Marsh, J.C., Gordon-Smith, E.C., Dalgleish, A.G., Gibson, F.M. (1996) The use of 7-aminoactinomycin D in identifying apoptosis: simplicity of use and broad spectrum of application compared with other techniques. *Blood* **87**, 2244–51.

12

Phagocyte biology and function

Marion G. Macey

St Bartholomew's and Royal London School of Medicine and Dentistry,
Queen Mary and Westfield College, London

12.1 Introduction to phagocyte biology

Neutrophils, monocytes and macrophages are important in the immune surveillance of microorganisms and malignant cells. All three cell types are capable of secreting a variety of chemical mediators and of phagocytosing particulate matter. Neutrophil and monocyte recruitment to sites of infection is guided by complex phenomena that involve microbial emanations, cytokines, interleukins and microenvironment modifications of the vascular endothelium. The interaction between molecules on the surface of the phagocyte (CD11b and CD62L) with those on the endothelium (intercellular adhesion molecule 1, CD62P and CD62E) is critical for the recruitment and attachment. Following adherence to endothelium and prior to vascular emigration, the phagocytes undergo a rapid cytoskeleton rearrangement, which is necessary for chemotaxis and for exertion of their phagocytic properties against microorganisms. This latter step depends on the expression of specific receptors (FcRs, CD11b, CD14, CD35) that recognise opsonised (immunoglobulin- and/or complement-coated) microorganisms and particles.

Micoorganisms are phagocytosed into phagolysosomal vacuoles, where they are subjected to strong oxygen-dependent microbicidal systems that are characterisd by the so-called NADPH-dependent respiratory burst and oxygen-independent systems including degrading enzymes, defensins (peptide antibiotics) and cathepsin G.

In addition to their beneficial role, phagocytes may also be involved in the pathogenesis of several noninfectious diseases such as acute and chronic myocardial ischaemia, idiopathic pulmonary fibrosis, emphysema, rheumatoid arthritis and certain forms of glomerulonephritis. The tissue-damaging properties arise when phagocytes are activated; this results in the upregulation of certain membrane molecules, degranulation, with release of myeloperoxidase, elastase and other proteases, and the production of reactive oxygen species, including intermediate oxygen radicals.

The evaluation of phagocyte function is important in the diagnosis of patients who present with recurrent infections, suspected chronic granulomatous disease, suspected leukocyte adhesion deficiency (LAD) 1 and 2 or immunodeficiency states. It is also useful to monitor diseases that can be mediated by an excessive and uncontrolled phagocyte activation and to monitor the clinical use of hematopoietic growth factors, such as recombinant granulocyte colony-stimulating factor (G-CSF) and recombinant granulocyte–monocyte colony-stimulating factor (GM-CSF), and other molecules such as interferon-γ (IFN-γ), which modify the function of monocytes and neutrophils. The main obstacles in studying phagocytes have been the difficulties encountered in (i) the transport of samples that require immediate analysis; (ii) the rapid handling of cells from peripheral blood and other sources such synovial fluid, bronchiolar lavage and cerebrospinal fluid; (iii) working with small volumes of blood or with blood from leukopenic patients; (iv) the complexity of some tests; and (v) processing several samples in a single work session. Many of these problems may be overcome by bringing the patient to the proximity of the laboratory and by using simple rapid assays to investigate the

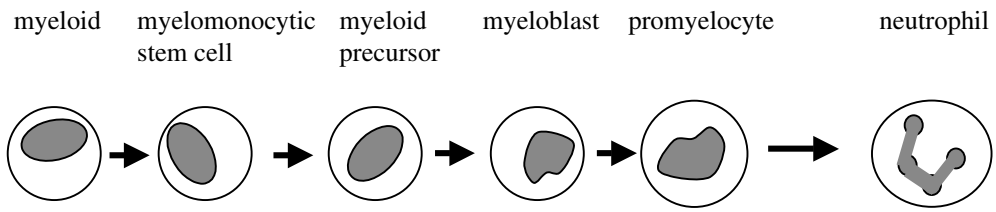

myeloid	myelomonocytic stem cell	myeloid precursor	myeloblast	promyelocyte	neutrophil		
CD33	CD13	CD13	CD13	CD13	CD10	CD52	CD132
CD34	CD33	CD15	CD15	CD15	CD11b	CD66a	CD139
CD117	CD34	CD33	CD33	CD33	CD11c	CD66c	CD141
CD123	CD115	CD116	CD38	CD116	CD12	CD66d	CD147
CD131	CD116	CD123	CD116	CD123	CD13	CD87	CD148
CD135	CD123	CD131	CD123	CD131	CD15	CD89	CD149
CD151	CD131	CD131			CD16b	CD92	CD151
	CD135	HLA-DR			CD17	CD93	CD153
	HLA-DR				CD24	CD101	CD156
					CD31	CD116	CD162
					CD32	CD123	CD14[a]
					CD35	CD128	CD63[a]
					CD43	CD131	CD64[a]

Fig. 12.1 Antigen expression during myeloid maturation. [a]Expressed on activation.

phagocytes. Flow cytometry allows rapid assessment of phagocyte maturational stages; expression of functional antigens, adhesion molecules and receptors; priming; response to cytokines, chemoattractants and activators; and phagocytosis.

12.2 Maturational states of neutrophils and monocytes

12.2.1 Antigen expression during myeloid maturation

The expression of membrane receptors on developing myeloid cells in the bone marrow is illustrated in Fig. 12.1. Myelopoiesis may be followed both morphologically and immunologically by flow cytometry. In a scattergram of a low-density mononuclear cell bone marrow population, early myeloid precursor cells (colony-forming unit, granulocyte macrophage) and myeloblasts are found in the blast gate; metamyelocytes, stab cells and segmented neutrophils are found in the myeloid gate and promyelocytes and myelocytes are variably split between these two gates (Civin and Loken, 1987). Immunological maturation within these gates can be followed by dual-fluorescence immunofluorocytometry, for instance by the gradual loss of membrane CD33 and gain of CD16 expression, which occurs with maturation towards a segmented neutrophil.

12.2.2 Antigen expression during monocytoid maturation

Monocytic cells also occur within the blast gate, and cultured monocytic cells, which express $CD16^{+/++}CD33^{++}$, can be phenotypically distinguished from developing myeloid cells $CD16^{+/++}CD33^{+}$ (Fig. 12.2). Dual-fluorescence flow cytometry has also shown that the acquisition of membrane CD16 late in myeloid development occurs simultaneously with that of decay accelerating factor (CD55), a complement regulatory protein, probably as a result of attachment of both preformed proteins to the membrane via a common phosphatidylinositol glycosyl phospholipid (PIG) anchor (Veys et al., 1990). Acquisition of these

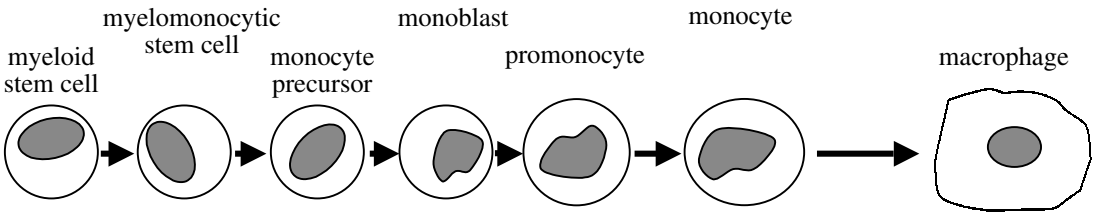

myeloid stem cell	myelomonocytic stem cell	monocyte precursor	monoblast	promonocyte	monocyte			macrophage	
CD33	CD13	CD13	CD13	CD13	CD4	CD49f	CD121	CD11c	CD23[a]
CD34	CD33	CD15	CD14	CD14	CD9	CD63	CD123	CD14	CD25[a]
CD117	CD34	CD33	CD15	CD15	CD11b	CD64	CD127	CD16	CD69[a]
CD123	CD115	CD115	CD33	CD33	CD11c	CD65	CD128	CD26	CD105[a]
CD131	CD116	CD116	CD115	CD115	CD12	CD68	CD132	CD31	CD153[a]
CD135	CD123	CD123	CD116	CD116	CD13	CD74	CD137	CD32	
CD151	CD131	HLA-DR	CD123	CD123	CD14	CD84	CD139	CD36	
HLA-DR	CD135				CD17	CD85	CD141	CD45RO	
	HLA-DR				CD31	CD86	CD148	CD45RB	
					CD32	CD87	CD149	CD63	
					CD33	CD89	CD155	CD68	
					CD35	CD91	CD156	CD71	
					CD36	CD92	CD162	CD74	
					CD38	CD93	CD164	CD87	
					CD40	CD98	CD165	CD88	
					CD43	CD101	HLA-DR	CD101	
					CD45	CD102	CD142[a]	CD119	
					CD49b	CD115	CD163[a]	CD121b	
					CD49e	CD119		CD163	

Fig. 12.2 Antigen expression during monocytoid maturation. [a]Expressed on activation.

membrane proteins may differentiate peripheral blood from bone marrow neutrophils (Civin and Loken, 1987).

12.3 Expression of functional antigens and receptors on the cell surface

The final array of mature phagocyte membrane receptors is by no means static; monocytes and neutrophils possess a great number of surface antigens. The baseline expression of these antigens and the modifications that they undergo regulate the interaction of the phagocyte with other cells, its recruitment to sites of inflammation, chemotaxis and its reactivity towards agonists and degranulation. Monocytes and neutrophils express numerous receptors including those for growth factors (G-CSF, GM-CSF), for interleukins (e.g IL-1, IL-6, IL-8), for cytokines (e.g IFN-γ, tumour necrosis factor α (TNF-α)), for complement components (C3b, C3bi C5a), for agonists including *N*-formylmethionylleucylphenylalanine (fMLP), leukotriene B_4 (LTB_4), platelet-activating factor (PAF), histamine, adenosine, lipopolysaccharide (LPS) and for the Fc regions of IgG and IgA (CD16, CD32, CD64, CD89). Monoclonal antibodies are available to most of these molecules and to other antigens such as those associated with adhesion; these antibodies allow recognition of the presence and level of expression of these cell surface receptors. Such molecules may be easily identified in whole blood preparations by the method first described by McCarthy and Macey (1993). In this procedure samples (20–40 μl) of anticoagulated whole blood are incubated at 4°C with a red fluorescent nuclear dye (LDS-751) and either monoclonal antibodies specific for adhesion molecules or receptors conjugated to fluorescein iso-

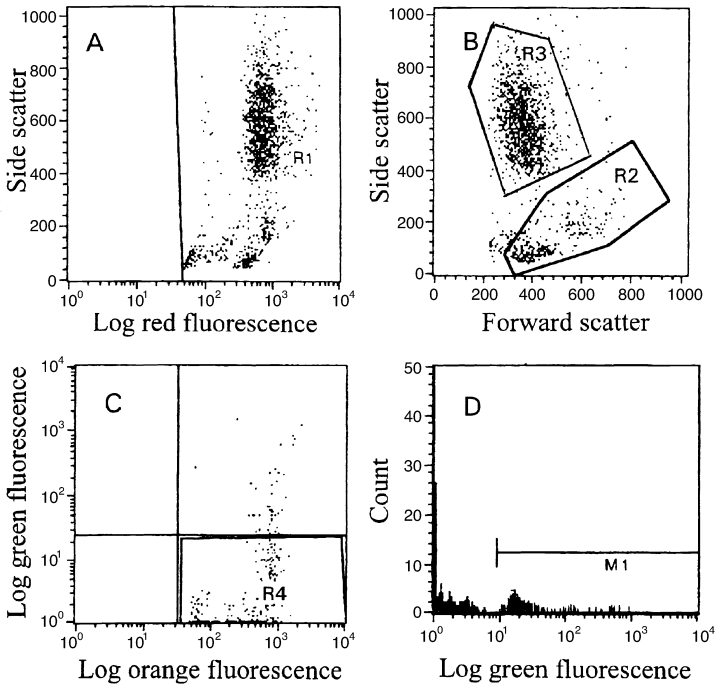

Fig. 12.3 Analysis of cells in whole blood. (A) Nucleated cells in whole blood labelled with the red fluorescent nuclear dye LDS-751 are identified in a plot of side scatter versus log red fluorescence region R1. Events falling outside R1 are excluded from analysis. (B) Leukocytes falling within R1 are back-gated to a histogram of forward scatter versus side scatter in which mononuclear cells and neutrophils may be distinguished, regions R2 and R3, respectively. (C, D) The fluorescence associated with cells in each region may be assessed in dual- or single-parameter histograms (C and D, respectively).

thiocyanate (FITC) or phycoerythrin (PE). After incubation for 5–10 min, the blood is diluted to 1 ml with Hanks' balanced salt solution (HBSS) buffered with 10 mmol l^{-1} HEPES (HHBSS) and analysed by flow cytometry immediately. Leukocytes are identified in a dual-parameter dot plot of side scatter (*y*-axis) and log red fluorescence (*x*-axis); neutrophils and monocytes may be gated and the expression of the molecule of interest analysed (Fig. 12.3). This method is extremely rapid (10–15 min from venesection to analysis) and also avoids the influences of isolation procedures (Macey et al., 1992, 1994, 1995, 1997, 1999; McCarthy and Macey 1993, 1996; McCarthy et al., 1994), which can result in artefactual changes in antigens such as increases in expression of the integrin CD11b or loss of expression of the selectin CD62L (see Protocol 2.1, pp. 18).

12.4 Receptor signalling

Phagocytes express a variety of plasma membrane receptors that allow the recognition of and response to a variety of compounds in an inflammatory environment including bacterial products such as formyl peptides and LPS, components of the complement and clotting cascades and soluble factors such as cytokines released by other cells. Receptors can be divided into several groups based on their structure and on the signalling pathways to which they are linked (Table 12.1). Upon ligand binding, the

Table 12.1 *Membrane receptors in phagocytes that may participate in signalling*

Receptor grouping	Examples	Structural characteristics	Comments
Group 1: G-protein linked	fMLP, C5a, PAF, LTB_4, IL-8, chemokines	Seven membrane-spanning domains (serpentine)	Linked to heterodimeric GTP-binding proteins, α- and βγ-subunits of G-proteins may transduce signals
Group 2: membrane tyrosine kinase	PDGF	Integral membrane proteins, intrinsic tyrosine kinase activity	Ligation leads to receptor dimerisation, cross-dimerisation and cross-(auto)phosphorylation; adaptor molecules involved via SH2 domains
Group 3: tyrosine kinase-linked	RcγRIIa, GM-CSF	RcγRII is a member of the immunoglobulin family of receptors	Linked to cytosolic tyrosine kinases (Src family including Hck, Fgr and perhaps Janus family kinases (JAK))
Group 4: glycosylphosphatidylinositol-linked	RcγRIIIb, decay accelerating factor	These receptors have no intracellular domain	RcγRIIIb is involved in phagocytosis
Group 5: adhesion molecules, selectins	β_2-Integrins, (CD11a/CD18, CD11b/CD18, CD11c/CD18), L-selectin	β-Integrins have a heterodimeric structure with relatively long cytoplasmic tails; L-selectin has an extracellular lectin-binding domain and a very short cytoplasmic tail	Potentiation of the oxidative burst and phagocytosis in adherent cells, intracellular Ca^{2+} levels, actin cytoskeletal changes, mitogen activated protein kinase activation, gene expression
Group 6: ceramide-linked	TNF	Two TNF receptors have been cloned, both single membrane-spanning glycoproteins with homology to receptors for nerve growth factor and Fas (CD95)	Tyrosine phosphorylation, activation of membrane-bound sphingomyelinase with generation of ceramide, which in turn activates a 96 kDa protein kinase

C5a, complement component 5a; fMLP, *N*-formylmethionylleucylphenylalanine; GM-CSF, granulocyte–macrophage colony-stimulating factor; IL-8, interleukin 8; LTB_4, leukotriene B_4; PAF platelet-activating factor; PDGF, platelet-derived growth factor; TNF, tumour necrosis factor.

receptor is activated and a signal is transmitted to the cell interior resulting in the initiation of a cascade of intracellular events.

Receptors for the classical 'chemoattractants' (named for their ability to stimulate chemotaxis) such as bacterial products (formyl peptides), products of the complement cascade (C5a), phospholipid metabolites (PAF and LTB_4), and cytokines such as IL-8 possess seven membrane-spanning domains and are functionally linked to heterodimeric G-proteins. These receptors usually mediate more than chemotaxis, including degranulation and activation of NADPH oxidase. Binding of ligand to this class of receptor leads to activation of the closely associated G-proteins, which in turn activate downstream effector pathways involving an array of intracellular enzymes including kinases and phosphatases (Fig. 12.4).

In contrast to the receptors with seven membrane-spanning domains described above, other phagocyte receptors such as those for growth factors and cytokines and those involved in phagocytosis are linked to the cell interior by pathways primarily involving tyrosine phosphorylation (Fig. 12.4). The receptor for platelet-derived growth factor has intrinsic tyrosine kinase activity and receptors such as that for GM-CSF may be closely associated with cytosolic tyrosine kinases such as $p72^{syk}$

that localise to the cytosolic side of the plasma membrane (Downey et al., 1995).

Despite the diversity of receptors, the basic activating mechanisms used are limited in number and shared by various receptors. Often the binding of ligands leads to dimerisation or clustering of receptors especially for multivalent ligands on surfaces. Receptor dimerisation exposes the receptor or associated proteins to the enzymatic activity of the other receptor (or associated kinase) of the dimer. This is the mechanism involved in growth factor and cytokine receptor signalling. Other receptors undergo a conformational change upon ligand binding that activates enzymatic activity of the receptor or associated proteins (such as heterodimeric G-proteins for the fMLP receptor). Occupation of receptors that are themselves ion channels or are closely associated with ion channels can lead to activation of ion fluxes. This is a common mechanism in excitable tissues such as neurons but may also be relevant to phagocytes.

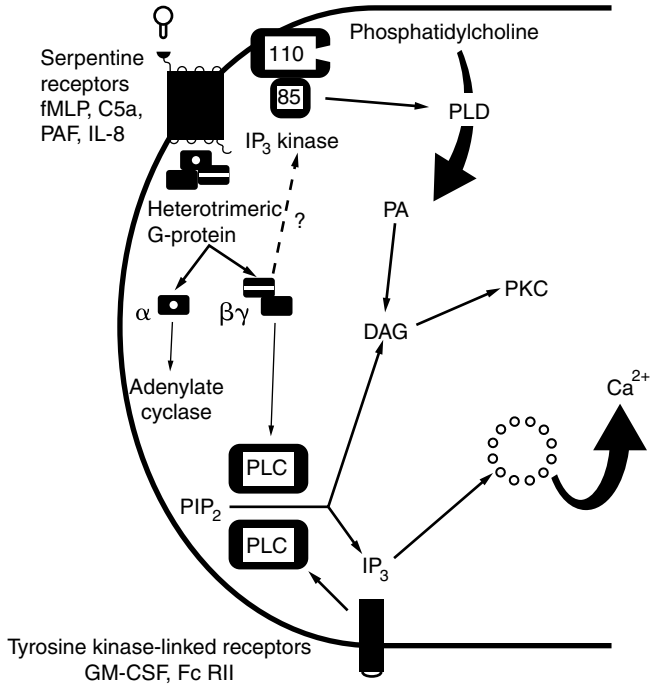

Fig. 12.4 Activation of intracellular pathways may proceed by receptors linked to heterodimeric GTP-binding proteins (serpentine receptors) or by receptors linked more directly to tyrosine kinases and Fc receptors. These pathways appear to share some common elements. DAG, diacylglycerol; PA, phosphatidic acid; fMLP, formylmethionylleucylphenylalanine; GM-CSF, granulocyte–monocyte colony-stimulating factor; IL, interleukin; PAF, platelet-activating factor; PIP_2, phosphotidylinositol bisphosphonate; IP_3, inositol trisphosphate; PKC, protein kinase C; PLC, phospholipase C; PLD, phospholipase D. (Reprinted from Downey, G.P., Fukushima, T., Failkow, L., Waddell, T.K. (1995) Intracellular signaling in neutrophil priming and activation. *Cell Biology* **6**, 345–56, with the permission of the publisher, Academic Press.)

12.5 Priming and activation

Priming refers to a process whereby the response of cells to an activating stimulus is potentiated, sometimes greatly, by prior exposure to a priming agent (Table 12.2). Neutrophil and monocyte priming by agents such as TNF-α, G-CSF, GM-CSF and LPS causes a dramatic increase in the response of these cells to an activating agent; this process has been shown to be critical for phagocyte-mediated tissue damage both in vitro and in vivo. The principal consequence of priming, aside from direct effects on cell polarisation, deformability and integrin/selectin expression, is to permit secretogogue-induced superoxide anion generation, degranulation and release of lipid-derived mediators such as LTB_4 and PAF. It is now recognised that most priming agents also serve an additional function of delaying apoptosis and hence increasing the functional longevity of these cells at sites of inflammation. The mechanisms underlying priming include changes in receptor number and/or affinity, G-protein expression, phospholipase C and phospholipase A_2 activation, changes in intracellular Ca^{2+} concentration, protein tyrosine phosphorylation, and enhanced phospholipase D and phosphoinositide 3-kinase activity. Recent studies have also revealed that it is possible for neutrophils to de-prime spontaneously

Table 12.2 *Priming agents*

Priming agent	Time to induce maximal priming	Reference
ATP	15 s	Kuhns et al. (1988)
Substance P	1 min	Lloyds and Hallett (1993)
Ionomycin	2 min	Finkel et al. (1987)
Inositol hexakisphosphate	2 min	Eggleston et al. (1991)
L-selectin crosslinking	3 min	Waddell et al. (1994)
PAF	5 min	Vircellotti et al. (1988)
CD18 crosslinking	5 min	Liles et al. (1995)
TNF-α	10 min	Berkow et al. (1987)
Interleukin 8	10 min	Daniels et al. (1992)
Orthovanadate	10 min	Lloyds and Hallett (1994)
Influenza A virus	30 min	Busse et al. (1991)
LPS	120 min	Guthrie et al. (1984)
GM-CSF	120 min	Weisbert et al. (1986)
IFN-γ	120 min	Tennenberg et al. (1993)

ATP, adenosine trisphosphate; GM-CSF, granulocyte–monocyte colony-stimulating factor; IFN-γ, interferon-γ; LPS, lipopolysaccharide; PAF, platelet-activating factor; TNF-α, tumour necrosis factor α.

and fully after an initial challenge with, for example, PAF.

Although priming was initially described as an in vitro phenomenon, many priming agents have clear biological relevance in vivo and are released in response to infection, trauma and hemorrhage. For example, circulating endotoxin has been associated with the development of adult respiratory distress syndrome (Parsons et al., 1989) and persistent high levels of plasma TNF-α and IL-6 have been linked to poor outcome in septic shock (Pinsky et al., 1993). Although such cytokines are detectable in the blood stream only in extreme circumstances, locally generated mediators serve to upregulate the functional responses of extravasated neutrophils or monocytes; indeed crosslinking adhesion molecules is itself a priming stimulus (Finkel et al., 1987; Liles et al., 1995) and the process of extravasation per se may result in a degree of priming (Condliffe et al., 1998). Priming may be investigated by flow cytometry by assessing changes in adhesion molecule expression (Condliffe et al., 1996; Macey et al., 1993a).

12.6 Prolonged responses to cytokines and/or hormones

Phagocytic cells produce a number of proinflammatory cytokines (TNF-α, IL-1α, IL-1β, IL-12, IFN-α, IFN-γ, IL-6) and anti-inflammatory cytokines (IL-1RA, transforming growth factor β) in response to various agonists, including some of these cytokines. Studies of how IL-10 and IFN-γ affect cytokine and chemokine production in LPS-stimulated neutrophils have revealed two distinct phases. In the early phase, there is a low level of chemokine release, directly induced by the LPS. This is followed by a second delayed phase, in which endogenous TNF-α and Il-1α synergise with LPS in producing dramatically elevated levels of IL-8, macrophage inhibitory protein 1α and 1β and growth-related gene product-α. This sequential production of chemokines by LPS-activated neutrophils, regulated by the cytokines TNF-α and IL-1β, may serve to amplify the recruitment and activation of neutrophils and other leukocytes in vivo during an inflammatory response to LPS. Il-10 has also been shown to be a potent

inhibitor of the cytokine known as MIG (monokine induced by gamma interferon) which can be induced by both IFN-γ and LPS. By regulating neutrophil-derived cytokine production, IL-10 may have an important regulatory role in limiting the duration and extent of acute inflammatory responses, for instance in lethal endotoxaemia. Marie et al. (1998) suggest that IL-10 produced during sepsis (Freidman et al., 1997) reduces the production of IL-8 and may render neutrophils unresponsive to further stimulation by LPS. IL-4 and IL-13 have also been shown to have an inhibitory affect on neutrophil IL-8 production in the presence of LPS (Marie et al., 1996). The intracellular production of cytokines induced by culturing granulocytes with cytokines may be analysed by flow cytometry and is discussed further in Ch. 13. The presence of cytokines both in vitro and in vivo also influences the expression of certain cell surface molecules such as CD14 and CD64 on neutrophils, CD143 and CD163 on monocytes and CD23, CD25, CD69, CD105 and CD153 on macrophages.

Hormones such as growth hormone have been shown to reduce phagocytic and metabolic function in neutrophils. This is the result of reduced TNF production (Balteskard et al., 1997). Glucocorticoids have also been shown to block PAF-induced downregulation of CD62L and upregulation of CD11/CD18 on neutrophils. This suggests that ligation of glucocorticoid receptors has an anti-inflammatory effect on cells by the inhibition of leukocyte accumulation at sites of tissue injury (Filep et al., 1997).

12.7 Chemoattractant binding and rapid responses to chemotaxins/activators

Monocytes and neutrophils are activated by, and respond by moving towards, molecules termed chemotactic factors; these include the complement component C5a, fMLP, LTB_4, PAF, the neuropeptide substance P, the phorbol ester phorbol myristate acetate (PMA) and also phagocytic particles and substances released by microorganisms such as fungi, bacteria and viruses. The magnitude and time of response depends on the agonist used, but for most of these the response time is minutes rather than hours. Interaction of the cell with these agonists may be investigated through the analysis of the binding of fluorochrome-labelled molecules or by determining features of cellular activation such as cytokine production, surface antigen changes, shape change or metabolic burst. Figure 12.5 illustrates the effect of fMLP on the size, metabolic burst and CD62L expression on neutrophils.

12.8 Shape changes

Several aspects of phagocyte physiology, such as motility, phagocytosis, translocation of granules, degranulation and recycling of receptors, and their regulation are associated with changes in the organisation of the cytoskeleton. Upon activation, changes in the cytoskeleton arrangements occur, and actin polymerisation (G-actin assembly to form F-actin filaments) represents one of the most dynamic phenomenon that characterise phagocyte activation (Howard and Watts, 1994). Actin polymerisation may be measured by flow cytometry using phalloidin, a fluorescent peptide with a high affinity for polymerised actin (Mineshita et al., 1997; Wulf et al., 1979). Phallacidin conjugated to both nitroblue diazonium (NBD) and FITC facilitate the measurement of the global amount of F-actin with high sensitivity. Flow cytometry does not, however, make a distinction between the two pools of F-actin molecules that are described as Triton® soluble and Triton® insoluble (Watts and Howard, 1993). Before staining with phalloidin, phagocytes have to be permeabilised.

Forward scatter and side scatter may also be used to detect shape changes. Forward scatter is proportional to size, and when neutrophils are activated in suspension they swell and exhibit increased forward scatter (Macey et al., 1998). Keller et al. (1995) showed that there is a direct relationship between light scattering in flow cytometry and changes in

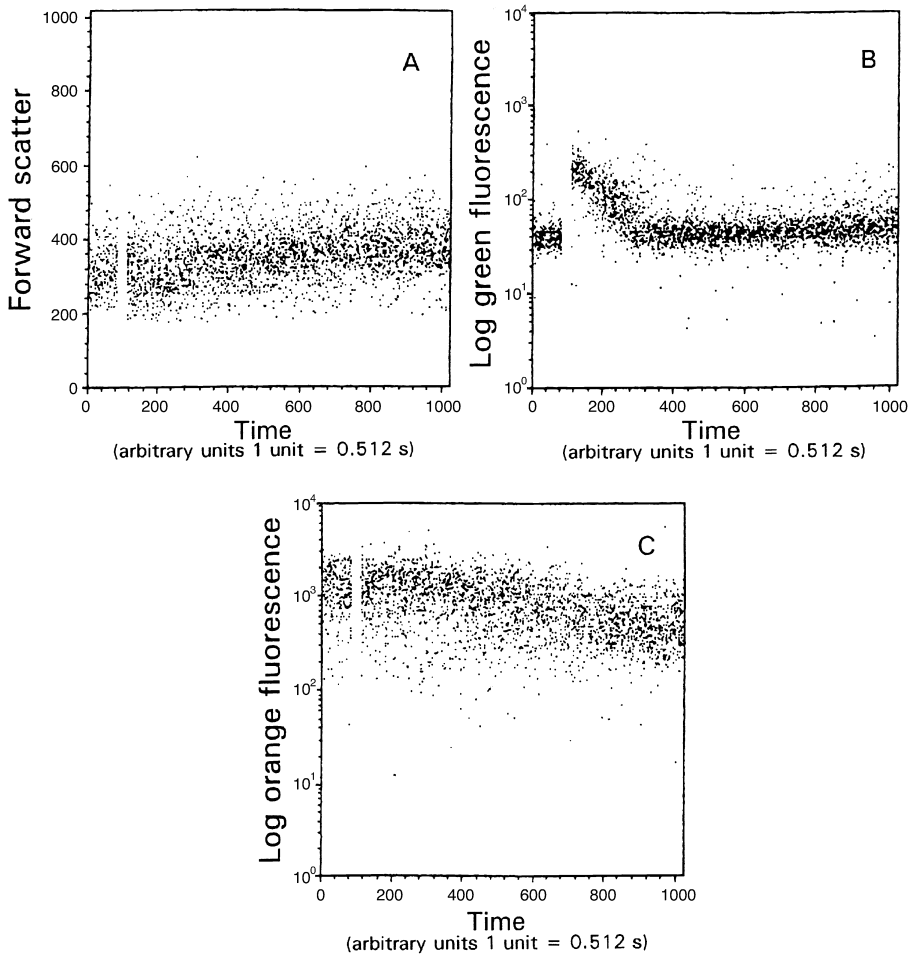

Fig. 12.5 The simultaneous continuous measurement of changes in size, Ca^{2+} concentration and L-selectin expression in neutrophils stimulated with the chemoattractant *N*-formylmethionylleucylphenylalanine (fMLP). Cells were labelled with Fluo-3, LDS-751 and phycoerythrin (PE)-conjugated anti-L-selectin (CD62L). Fluo-3 is a Ca^{2+} indicator that is excitable at 488 nm and that exhibits an increase in green fluoresecence upon binding with free Ca^{2+}. Neutrophils were identified as in Fig. 12.3A,B. Baseline levels of forward scatter (A), Fluo-3 (B) and PE (C) fluorescence were established in dual-parameter plots with time on the *x*-axis. At 60 s, fMLP was added, so producing a small gap in the histogram trace. (A) There is a small but gradual increase in size after addition of the fMLP. (B) A marked increase in fluorescence is seen after addition of fMLP because of the release of free Ca^{2+}, which binds to Fluo-3 and results in a greater fluorescence emission. The green fluorescence rapidly falls back to the baseline level, producing the characteristic 'Ca^{2+} spike' associated with signal transduction. (C) After activation, L-selectin is shed from the surface of the cell and this leads to a gradual loss of PE fluorescence as antibody bound to this adhesion molecule is also lost from the cell surface.

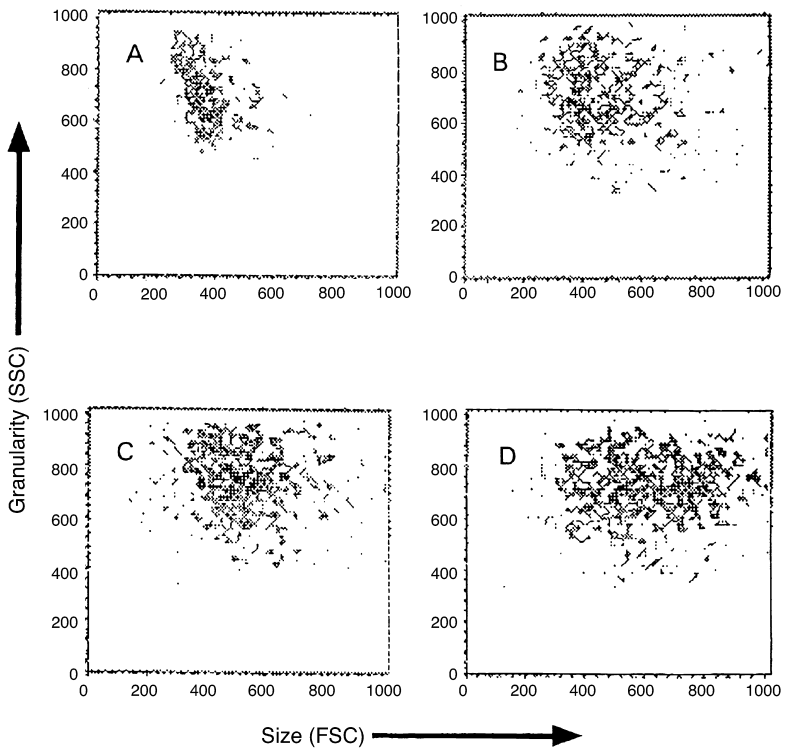

Fig. 12.6 The effect on cell size of *N*-formylmethionylleucylphenylalanine (fMLP) and a peptide that activates the protease-activated receptor (PAR) 2. Neutrophils were identified as in Fig. 12.3A and back-gated to a histogram of forward scatter and side scatter. (A) The light scattering properties of resting unstimulated neutrophils. (B) Upon addition of fMLP, these swell and have increased forward scatter. (C) Addition of the peptide that activates PAR-2 also stimulates an increase in size and forward scatter, (D) Priming the neutrophils with fMLP before addition of the activating peptide results in an augmented increase in size and forward light scatter.

shape, volume and actin polymerisation. Shape change has been used to measure the effect of a variety of chemokines on the polarisation of eosinophils (Sabroe et al., 1999).

Figure 12.6 shows the effect of using fMLP to prime neutrophils prior to the addition of a peptide that activated the protease-activated receptor 2, which is expressed by neutrophils.

12.9 Membrane potential and changes in ion permeability

The generation of intermediate oxygen radicals after monocyte and neutrophil stimulation is accompanied by changes in membrane potential. Lipophilic dyes such as the cyanine compounds 3,3'-dipentyloxacarbocyanine iodide ($DiOC_5(3)$) and dipropylthiocarbocyanine ($DiSC_5(3)$) can be used to measure this aspect of cellular activation. These dyes diffuse into the cell with different localisation patterns depending on their concentration. Cellular activation is followed by a loss of cell-associated fluorescence, which is related to changes in membrane potential. Stimulation with PMA results in an irreversible loss of fluorescence caused by an irreversible membrane depolarisation; however, stimulation with the chemotactic agents fMLP or C5a result in a initial loss of fluorescence with a nadir at about 2 min, followed by a gradual return to

the baseline level. A dose-dependent reduction in fluorescence during the initial phases of stimulation can be observed with increasing concentrations of the chemotactic stimuli. When fMLP is used, a small proportion of neutrophils do not respond or do not show the biphasic response to the stimulus because of the heterogeneity of the response to this peptide. These potentiometric cyanine dyes have been shown to be independent of the action of oxygen radicals and of mitochondrial activity, although they accumulate into mitochondria.

The activation of phagocytic cells leads to an initial cytoplasmic acidification because of the generation of large amounts of protons by NADPH oxidase. As a consequence, proton-conducting channels and the Na^{2+}–K^{+} antiport are activated, leading to sustained intracellular acidification. These two aspect of intracellular pH changes may be measured by flow cytometry. Intracellular changes of pH in response to either soluble or particulate stimuli may be monitored by means of the fluorochrome carboxyseminapthorhodafluor-1 (SNARF-1) and its acetoxy-methyl ester (SNARF-1/AM) (Rothe and Valet, 1994a). This dye, which is modified by elastase, is loaded into the cell and fluoresces in the orange region of the light spectrum. However, with increasing pH, the fluorescence moves to the red region of the spectrum. A ratio of the red to orange fluorescence is calculated through the calibration of cells with high K^{+} buffers of defined pH in the presence of nigericin, a polyether ionophore that carries monovalent cations across membranes with high specificity for K^{+}. A 575–595 nm band-pass filter and a 620 nm long-pass filter have to be used to evaluate acidic orange SNARF-1/AM and basic SNARF-1, respectively.

12.10 Phagocytosis, endocytosis and oxidative burst

The phagocytosis of fluorochrome-labelled bacteria, yeast, zymosan or beads may be readily assessed by flow cytometry. The particles should be opsonised with human serum immunoglobulins and phagocytosis is evaluated by measuring the change in fluorescence of the neutrophil after introduction of the target particle. This evaluation is based on both the calculation of the percentage of neutrophils with intracellular fluorescence and the intensity of fluorescence, which has been shown to correlate with the number of phagocytosed particles.

General variables that can affect this assay are the incubation temperature and the agitation frequency. Different times of incubation can be used to study the kinetics of the phagocytic process and its initial rate (first 10 min). Opsonisation with either homologous or heterologous serum may be carried out to distinguish between defects that are cellular or plasma related. FITC-conjugated non-opsonised *Escherichia coli* are now commercially available to facilitate such studies. A specific variable is bacteria to neutrophil ratio, as the rate of phagocytosis is dependent on the number of targets available. Quenching performed by trypan blue or other dyes is useful to distinguish between internalised and cell-bound fluorescent particles, since the fluoresecence from the latter is quenched in the presence of trypan blue.

Uptake by pinocytosis and trafficking through the endocytic pathways may be facilitated by using fluorescent dextran conjugates, which are inert sugar polymers that are readily endocytosed (Waters et al., 1996). Localising lysosomes in live cells is made possible by staining with dyes termed LysoTrackers™, which are dyes with high selectivity for acidic organelles (Demo et al., 1999).

An increased oxygen uptake accompanies phagocytosis when this is stimulated by a number of agonists. The various metabolic changes that oxygen undergoes after reduction by a single electron bring about the so-called respiratory or oxidative burst. The reactions of this oxygen pathway are catalysed by a membrane-bound NADPH oxidase that is formed from the assembly of membrane (cytochrome) and cytoplasmic components. Several intermediate, highly reactive oxygen radicals are produced, such as superoxide anion, hydrogen peroxide, hypochlorous acid, hydroxyl radical and

singlet oxygen (Hampton et al., 1998). These radicals are important effectors of both the antimicrobial activity and the tissue-damaging properties displayed by human neutrophils. Therefore, assessing the production of these radicals appears to be important in the diagnosis of chronic granulomatous disease, myeloperoxidase deficiency, sepsis possibly caused by immunosuppression, hematological diseases, and the metabolic changes that neutrophils undergo in the course of diseases that are caused by excessive and uncontrolled neutrophil activation. Flow cytometry allows a rapid and sensitive intracellular measurement of some of these components of the oxidative burst, such as superoxide anion and hydrogen peroxide. Intracellular superoxide production may be measured by the analysis of the direct action of this radical on hydroethidine (Rothe and Valet, 1990). This blue fluorochrome is oxidised by superoxide anion to red fluorescent ethidium bromide (EB). Substrate loading must be analysed at 420–460 nm and so requires a laser that emits in the ultraviolet region of the spectrum. The resultant EB emits at 600 nm (Rothe and Valet, 1994b). Upon stimulation and production of superoxide anions, there is an 8- to 20-fold increase in fluorescence in cells from normal individuals. Hydrogen peroxide can also oxidise EB and its activity may, therefore, interfere with superoxide measurement. Intracellular hydrogen peroxide production has been measured by utilising the oxidation-dependent fluorescence of several dyes. Brandt and Keston (1965) first described the formation of highly fluorescent 2',7'-dichlorofluorescein (DCF) from nonfluorescent 2',7'-dichlorofluorescin (DCFH), which is the product of the hydrolysis of nonfluorescent 2',7'-dichlorofluorescin diacetate (DCFH-DA). The substrate DCFH-DA is a stable nonpolar molecule that readily diffuses through the cell membrane of the neutrophil. Once inside the cell, the acetyl groups are cleaved by enzymes in the cytoplasm to produce the polar molecule DCFH, which is trapped within the cell. DCFH is nonfluorescent but becomes highly fluorescent when oxidised by hydrogen peroxide, which is produced during the oxidative burst in neutrophils. The increase in fluorescence associated with the oxidation of DCFH is, therefore, a direct measure of the oxidative burst.

Dihydrorhodamine 123 has also been used to analyse hydrogen peroxide generation. Upon oxidation by peroxide, this nonfluorescent dye transforms to the highly fluorescent green rhodamine 123, with maximum emission at 525 nm (Rothe and Valet, 1994c).

The oxidative burst associated with stimulation by Texas Red®-labelled, opsonised bacteria has been described for dual laser flow cytometry (Bass et al., 1983; Szejda et al., 1984). This was modified for use on a single laser flow cytometer (Macey et al., 1990) and two assays were used to measure the functional ability of the isolated neutrophils: first the rate of uptake of IgG-opsonised bacteria labelled with propidium iodide (PI) and, second, the oxidative burst associated with stimulation by either opsonised bacteria or PMA. In the latter assay, the oxidative burst was measured by the increase in fluorescence associated with oxidation of DCFH-DA to the highly fluorescent DCF (Protocol 12.1).

Protocol 12.1 Assay procedure for phagocytosis and the oxidative burst

Bacterial culture

1. *Staphylococcus aureus* strain Wood 45 (protein A negative, Central Public Health Laboratory National Collection of Type Cultures (CPHL NCTC) Colindale, London, Code NCo7121) are maintained on agar slopes, plated on blood agar and the colonies picked off into peptone water.
2. Cultures are agitated at 37°C overnight.
3. The cells are washed three times by centrifugation in HBSS without phenol red (Gibco) and fixed with 70% ethanol at 4°C for 30 min.
4. The fixed cells are then washed twice by centrifugation in phosphate-buffered saline (PBS) containing 1% gelatine and 1% glucose (Sigma) (PBSg) pH 7.2 and resuspended to a final

concentration of 1×10^8 organisms ml^{-1} as determined by optical density measurement at 580 nm in a spectrophotometer.

Opsonisation of bacteria

1. Bacteria 10^8 in 1 ml PBSg are mixed with 1 ml (30 mg ml^{-1}) human serum and 1 ml 0.2 mol l^{-1} carbonate buffer pH 8.6 then incubated with vigorous agitation at 37°C for 30 min.
2. The bacteria are washed twice by centrifugation in PBSg and resuspended to a final concentration of 1×10^8 ml^{-1}.

Propidium iodide labelling of bacteria

1. Bacteria 10^8 in PBSg are incubated with PI (Sigma) at a final concentration of 50 μg ml^{-1} at 37°C for 30 min then washed twice by centrifugation with PBSg.
2. The labelled bacteria are resuspended in PBSg to a final concentration of 10^8 ml^{-1}.

Preparation of phorbol myristate acetate (PMA)

1. A stock solution of PMA (Sigma) 1 mg ml^{-1} is made in absolute ethanol and stored in portions at –20°C.
2. Immediately prior to use, the PMA is diluted in PBSg to a final concentration of 100 ng ml^{-1}.

Preparation of 2',7'-dichlorofluorescin diacetate

1. A stock solution (10 mmol l^{-1}) of DCFH-DA (Molecular Probes) is made in absolute ethanol and stored in the dark at 4°C.
2. Immediately prior to use, the DCFH-DA is diluted in PBSg to a final concentration of 5μmol l^{-1}.

Assay of oxidative product formation

1. Neutrophils in whole blood (1 ml) are preincubated for 15 min with 5 μmol l^{-1}M DCFH-DA in PBSg with agitation at 37°C.
2. After 15 min incubation, 100 μl samples of cells are incubated in sterile round-bottom tubes with 100 μl PBSg (negative control), opsonised bacteria at a bacteria to cell ratio of 500 : 1 (test), non-opsonised bacteria at the same ratio (test control), and PMA at a final concentration of 100ng ml^{-1} (positive control).
3. The tubes are incubated at 37°C with vigorous agitation.
4. The reaction is stopped by the addition of 2 ml FACS™-Lysing Solution (BD Biosciences) for 10 min. The cells are then washed twice in PBSg, resuspended and analysed by flow cytometry.
5. Samples from each type of stimulation are set up in quadruple such that samples can be removed at times from 0 to 60 min after commencement of the assay.

Assay of bacterial uptake

1. Samples (100 μl) of blood are incubated in round-bottom tubes with 100 μl of PBSg (negative control), opsonised PI-labelled bacteria at a cell to bacteria ratio of 1 : 500 (test) and non-opsonised labelled bacteria (test control).
2. Assays are set up in triplicate and samples removed, diluted 1 : 5 in PBSg and analysed by flow cytometry at 10, 20 and 30 min.
3. The reaction is stopped as above.
4. The rate of increase in red fluorescence per minute is taken to be directly related to the rate of uptake of bacteria.

Flow cytometry

1. All studies are performed on a flow cytometer equipped with an argon laser (488 nm emission).
2. Forward angle light scatter, 90° side light scatter, green (510–550 nm) and red (>580 nm) fluorescence are recorded.
3. The assay for neutrophil stimulation is performed in parallel with that for bacterial uptake.
4. Typical results for a metabolic burst assay are shown in Fig. 12.7.

12.10.1 Alternative assays

A number of assays have been described for measurement of neutrophil phagocytosis by other techniques. The important point of distinction be-

tween internalised and membrane-bound particles was addressed by Fattorossi et al. (1989). In this assay, fluorescein-conjugated heat-killed *Candida albicans* was opsonised by purified antibodies and used as targets for human polymorphonuclear granulocytes (PMN). The procedure is based on the observation that the target cells lose their green fluorescence upon incubation with EB through the resonance energy transfer phenomenon occurring between the two fluorochromes. PMN are incubated with the opsonised target for 20 min at 4 or 37°C, in the presence of cytochalsin B, an inhibitor of the phagocytic process that does not affect membrane binding of fluorescein. EB is added and the green and red fluorescence associated with PMN is evaluated. EB does not penetrate intact cell membranes so internalised particles are not affected by EB and remain green, whereas membrane-bound particles assume an intense red stain. By dual-fluorescence analysis, the number of PMN containing and/or binding fluorescein-labelled targets can be assessed.

The oxidation of hydroethidine to EB has been used to measure the oxidative metabolic burst in neutrophils stimulated with opsonised fluorescein-labelled bacteria (Perticarari et al., 1991). Dual-fluorescence analysis was used to measure the red EB emission together with the green fluorescence associated with ingested bacteria. In this assay, crystal violet was added to quench the fluorescence associated with membrane-bound bacteria such that only internalised bacteria were assayed.

The relative involvement, in phagocytosis, of receptors for the Fc portion of IgG and the complement components C3b and C4b has also been studied (Andoh et al., 1991). Fluorescent latex beads coated specifically with IgG or complement components were used in this study. To evaluate bead attachment, the phagocytic assay was performed with cells treated with 3 μmol l^{-1} cytochalasin D, which inhibited internalisation. The percentage of cells with ingested beads and the number of ingested beads per 100 cells was assessed. This allowed quantitative analysis of the function of cell surface receptors for IgG and complement components.

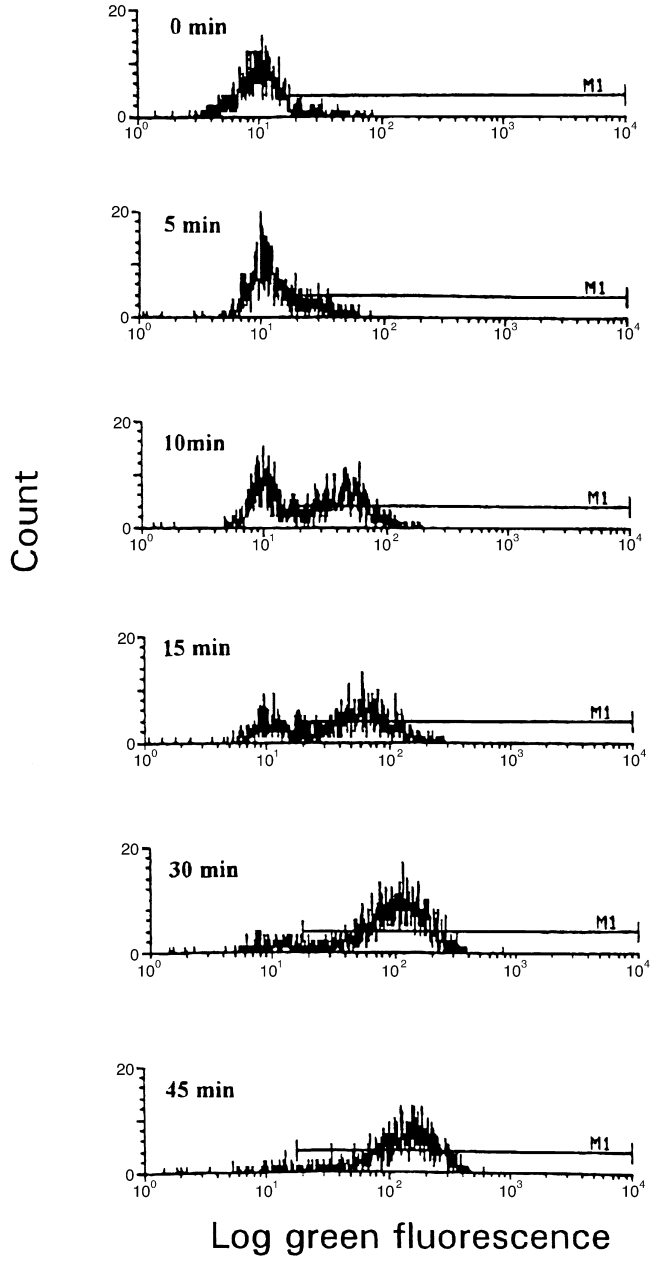

Fig. 12.7 The increase in fluorescence associated with the oxidation of 2',7'-dichlorofluorescin diacetate in neutrophils stimulated with *Staphylococcus aureus* over a 45 min time period.

The fluorescent dye LDS-751 is specific for nucleated cells and has been used in whole blood assays to eliminate erythrocytes from analysis of granulocyte oxidative metabolic burst (Himmelfarb et al., 1992; Macey et al., 1998). The detection of reactive oxygen species is facilitated by oxidation of DCFH-DA (as above). The effect of LPS on phagocytosis and metabolic burst has also been assessed in whole blood (Bohmer et al., 1992). Rothe and Valet (1988) developed a method based on the evaluation of green fluorescence emitted by acridine orange during phagocytosis as a measure of ingested bacterial DNA and, indirectly, the amount of ingested bacteria.

12.11 Nitric oxide release

Nitric oxide (NO) plays a critical role as a molecular mediator of a variety of physiological processes including blood pressure regulation and neurotransmission. However, because free NO is a transient species with a half-life of about 5 s, investigations of this gaseous molecule have relied largely on studies of nitric oxide synthase (NOS). This enzyme catalyses the NADPH- and O_2-dependent oxidation of L-arginine to NO and L-citrulline. Specific inhibitors of NOS isoforms are available that may be used to investigate the biological effects of NO. NO is a highly reactive species that in the presence of oxygen is also reported to release superoxide anion. Under physiological conditions, NO is oxidised to nitrite and nitrate. The dye 2,3-diaminonaphthalene reacts with nitrite to form the fluorescent product ^{1}H-naphthotriazole and this dye has been used to detect nitrite at concentrations between 10 nmol l^{-1} and 10 μmol l^{-1}. The dihydofluoresceins, dihydrorhodamines and dihydrorosamines, which are used extensively to detect various forms of oxygen, are known to react with NO, yielding the same oxidation products. NO also reacts with superoxide or hydrogen peroxide to produce the peroxynitrite anion, which oxidises dihydrorhodamine 123. Continuous fluorimetric detection of NO in the presence of other reactive oxygen species has recently become feasible. 1,2-Diaminoanthraquinone is nonfluorescent until it reacts with NO to produce a red fluorescent precipitate (Heiduschka and Thanos, 1998).

12.12 Multiparameter techniques to assess function and phenotype

The simultaneous evaluation of two or more parameters is readily achieved with flow cytometry. Phagocytosis, hydrogen peroxide production and L-selectin shedding can be simultaneously measured using PI-labelled bacteria, DCFH-DA and PE–CD62L (Macey et al., 1998). Hydroethidine and DCFH-DA can be used together to measure superoxide anion and hydrogen peroxide at the same time (Rothe and Valet, 1990), and the simultaneous measurement of intracellular phagosomal pH changes, phagocytosis, ingestion and degradation of bacteria has also been reported (Bassoe and Bjerknes, 1985; Rothe et al., 1990).

12.13 Clinical applications of phagocyte function assays

Flow cytometric assays for actin polymerisation have been shown to correlate with gel scanning measurements of F-actin and have been successfully employed in the detection of actin polymerisation defects in patients with human immunodeficiency virus (HIV) infections (Elbim et al., 1994), chronic myeloid leukaemia (Naik et al., 1990), rare cases of inherited defects of neutrophil motility (Roos et al., 1993) and in children with severe congenital neutropenia (Elsner et al., 1993).

Flow cytometric assays for the measurement of membrane potential changes have been used to evaluate the metabolic abnormalities that can be found in the neutrophils from patients with chronic granulomatous disease (Seligmann and Gallin, 1980).

Applications of flow cytometric evaluation of hydrogen peroxide have been reported in a number of

Table 12.3 *The effects of granulocyte colony-stimulating factor and granulocyte–macrophage colony-stimulating factor on mature phagocytic cells*

	Neutrophils		Monocyte/macrophage	
Characteristic	G-CSF	GM-CSF	G-CSF	GM-CSF
Expression of CD11b/CD18	Increased	Increased	None	–
Expression of CD64	Increased	–	–	–
Expression of CD14	Increased	–	–	–
Expression of IgA FcR	–	Increased	–	–
Expression of fMLPR	–	Increased	–	–
Expression of LTB_4R	–	Increased	–	–
Chemotactic activity	Enhanced	Enhanced	–	–
Phagocytic activity	Enhanced	Enhanced	–	Enhanced
Microbicidal activity	Enhanced	Enhanced	–	–
ADCC	Enhanced	Enhanced	–	Enhanced
Oxidative activity	Enhanced	Enhanced	–	Enhanced
IL-1 induction	–	Enhanced	–	Enhanced
Intracellular killing	–	–	–	Enhanced

–, no data; ADCC, antibody-dependent cellular cytotoxicity; fMLP *N*-formylmethionylleucylphenylalanine; IL-1, interleukin 1; LTB_4R, leukotriene B_4 receptor.
From: Root and Dale, 1999.

clinical settings. Neutrophils from patients with chronic granulomatous disease have been shown to fail to produce hydrogen peroxide in assays using DCFH-DA and dihydrorhodamine (Crockard et al., 1997; Emmendorffer et al., 1994). Subpopulations of neutrophils with different hydrogen peroxide production have been found in patients with chronic granulomatous disease (Emmendorffer et al., 1994) and with acute bacterial infections (Bass et al., 1986). Intracellular production of hydrogen peroxide has also been measured in myeloproliferative diseases (Samuelsson et al., 1994).

Flow cytometric assessment of both up- and downregulation of neutrophil and monocyte adhesive receptors have been studied to explain rapid movements in body pools of these cells following infusion of various compounds including GM-CSF (Macey et al., 1993b) and G-CSF. Mature neutrophils express receptors for both G-CSF and GM-CSF, and exposure of these cells to either cytokine in vivo or in vitro induces a number of functional and phenotypic changes (Table 12.3). Both G-CSF and GM-CSF can participate in the enhancement of a number of functions of neutrophils that are important to their role in antibacterial and antifungal defence. In addition, GM-CSF has a number of actions directed at monocytes and macrophages, which are involved in their role both in inflammation and the cellular immune response.

Disorders of neutrophil membrane receptors that have been elucidated by flow cytometry can be divided into inherent neutrophil and monocyte abnormalities and abnormalities induced by in vivo stimulation of normal cells. An example of the latter is the upregulation of the adhesive receptor CD11b by GM-CSF. The neutrophil CD11/CD18 receptor is upregulated severalfold in response to chemotactic factors and this is clinically relevant in neutropenia occurring during dialysis, induced by the generation of C5a (Mazzucchelli et al., 1992).

Inherent abnormalities in antigen expression also exist and include diminished expression of CD11b in congenital LAD, which is caused by a biosynthetic defect of the common β-subunit of CD18

(Harlan et al., 1992). This is an autosomal recessive disorder resulting in neutrophilia, defective neutrophil mobilisation and recurrent bacterial infection without pus formation. Although deficiencies of this type are rare, about 50 patients with LAD have been reported worldwide. Patients with LAD-1 lack β_2-integrin (CD18), which associates with CD11a–c. These patients, therefore, have nonfunctional leukocyte adhesion molecules and these cells cannot bind to endothelium at sites of inflammation. Recently a LAD-1-like case was reported in which a child had 50% expression of CD18 but the integrin had a functional defect (Hogg et al., 1999). Etzioni et al. (1992) report two patients who have normal adhesion molecules but whose neutrophils have a deficiency of sialyl-Lewis X (CD15s). This molecule is the ligand for the selectins. A deficiency of this molecule results in failure of cell–cell interaction, specifically neutrophil adhesion to endothelial cells and platelets. These patients both had otherwise unexplained recurrent severe infections and were classified as having LAD-2.

Reduced upregulation of CD11b from intracellular pools on neonatal neutrophils results in reduced neutrophil migration in vitro and is believed to contribute to infectious morbidity and mortality among neonatal populations (Jones et al., 1990). Similarly, reduced expression of C5a receptors, as determined by FITC-labelled recombinant C5a, on neutrophils from neonates has been related to reduced exocytosis of myeloperoxidase and reduced C5a-stimulated chemotaxis (Nybo et al., 1998). Other inherent abnormalities include isolated CD16 deficiency in otherwise normal individuals (Fromont et al., 1992; Huizinga et al., 1988).

Paroxysmal nocturnal hemoglobinuria is an acquired hematopoietic stem cell disorder in which a somatic mutation of X-linked *PIG-A* results in a partial or absolute lack of synthesis of PIG linkage that anchors proteins to the cell membrane. There are more than 40 surface protein molecules that have a PIG linkage in the membrane of different cells. These include the FcγRIIIb receptor for human IgG (CD16) on neutrophils, decay accelerating factor (CD55) on erythrocytes and the receptor for LPS (CD14) on monocytes. Deficiency in these molecules will, therefore, affect the function of a variety of cells. The hemolytic anaemia associated with paroxysmal nocturnal hemoglobinuria results from a lack of CD55 in the red cell membrane, which renders the cells susceptible to complement-mediated lysis. Most if not all patients have evidence of underlying bone marrow failure.

12.14 Neutrophil antibodies

Neutrophil specific alloantibodies have been implicated in a number of clinical disorders including febrile transfusion reactions (de Rie et al., 1985; Verheugt et al., 1977), severe pulmonary reactions following blood transfusion (Schiffer et al., 1979; Thompson et al., 1971), isoimmune neonatal neutropenia (Lalezari et al., 1986) and failure of effective granulocyte transfusion (Cairo et al., 1992; Schiffer, 1980).

Neutrophil specific autoantibodies have been identified in autoimmune neutropenia (AIN) in adults (Bux et al., 1991a; Welte and Dale, 1996) and children (Bux et al., 1998; Lyall et al., 1992). The antigens identified by these granulocyte-specific antibodies were designated the 'N' series (Lalezari and Radel, 1974). McCullough (1983) analysed the clinical significance of this antigen system. The neutrophil NA antigen system has two alleles NA1 and NA2, which have a phenotypic frequency of 46% and 88%, respectively, in the Caucasian population (Hartman et al., 1990). The granulocyte antigens NA1 and NA2 are two allelic gene products of the gene for FcγRIIIb (CD16). These antigens are frequently targets of granulocyte-specific allo- and autoantibodies that cause neutropenia. Different distributions of these antigens have been found in population studies. Recently a third alloantigen, SH, of FcγRIIIb was identified (Bux et al., 1997). Some individuals have been found to lack one or more of these antigens and this appears to influence a number of immune functions. FcγRIIIb is the low-affinity receptor for the Fc region of complexed IgG antibodies and preferentially removes immune

complexes from the circulation. It is released from the neutrophil membrane during apoptosis and soluble FcγRIIIb can inhibit proliferation and production of stimulated B-cells. Antibodies are available that are specific for the different alloantigens: monoclonal antibodies GRM1 and PEN1 are specific for NA2 but the reactivity of PEN1 is sixfold higher on cells that are SH^+. The use of these antibodies allows the flow cytometric detection of the different antigens in individuals within the population (Koene et al., 1998). Studies have provided evidence for the relevance of FcγRIIIb polymorphisms as risk factors for a number of infectious and autoimmune diseases (van der Pol and van de Winkel, 1998). Antibodies to FcγRIIIb have been described in numerous patients with AIN (Bux et al., 1991a,b; Cartron et al., 1992; Fromont et al., 1992; Rios et al., 1991; Stroncek et al., 1991). The FcγRIIIb seems to be very immunogenic, because the clinically most important granulocyte-specific antigens NA1 and NA2, as well as the recently described SH antigens, are also located on this neutrophil-restricted glycoprotein. Hartman et al. (1990) found that in many patients with AIN the autoantibodies were reactive with a 45 kDa antigen that was probably the cytoskeletal, intracellular component actin. Neutrophil autoantibodies specific for CD11b/CD18 have also been found in patients with AIN (Hartman and Wright, 1991). This finding suggests that in some patients with AIN the presence of antibodies to the functionally important adhesion proteins CD11b/CD18 may interfere with neutrophil function, thereby amplifying the risk of infection associated with neutropenia. Antibodies specific for FcRII (CD32) and the complement component CR1 (CD35) may also be found in the sera of these patients (Welte and Dale, 1996).

Anti-neutrophil antibodies may also be found in drug-induced agranulocytosis (Walbreohl and John, 1992; Weitzman and Stossel, 1978). The realisation that drug-induced antibodies are involved in the mechanism of agranulocytosis is important as rechallenge with the offending drug may lead to a dramatic and severe recurrence of neutropenia. In addition to isolated AIN, the presence of neutrophil-associated immunoglobulin (NAIg) has been demonstrated in many other diseases where neutropenia may occur, such as the generalised autoimmune diseases systemic lupus erythematosus, rheumatoid arthritis and Felty's syndrome (Goldschmeding et al., 1988; Lasito and Lorusso, 1979; McCullough et al., 1987). Sera from patients with these diseases has been reported to contain both anti-neutrophil antibodies of various isotypes and immune complexes (Lasito and Lorusso, 1979; Zubler et al., 1976), which may or may not be associated with the neutropenia. Consequently it is not known whether NAIg in these diseases has an antibody nature or represents immune complexes that have bound to the Fc receptors and complement receptors on the neutrophil membrane. However either or both may be responsible for inducing neutropenia.

NAIg is also present in chronic infections such as HIV infection (Klaassmen et al., 1990; Murphy et al., 1987) and immune complexes have also been implicated in the pathophysiology of neutropenia in this disease (Bowen et al., 1985). However, evidence suggests that NAIg in HIV infections is autoimmune in nature (Klaassmen et al., 1991a). Neutrophil-associated antibodies have also been implicated in a number of conditions including Hodgkins's disease (Gordon et al., 1991), Crohn's disease (Stevens et al., 1991), primary bilary cirrhosis (Bux et al., 1991a), ulcerative colitis (Shanahan et al., 1992), inflammatory bowel disease (Cambridge et al., 1992) and nutritional copper deficiency (Higuchi et al., 1991).

12.14.1 Detection of anti-neutrophil antibodies

The study of anti-neutrophil antibodies by fluorescence techniques became possible in 1976 with the development of a method to overcome the non-specific binding of IgG from normal serum to neutrophils (Verheugt et al., 1977). The method involves the paraformaldehyde fixation of the neutrophil membrane prior to incubation with the test serum. This prevents the binding of normal IgG but permits the binding of most anti-neutrophil antibodies and some immune complexes (Engelfreit et al., 1984).

However, certain specific anti-neutrophil antibodies cannot be detected by immunofluorescence, for example those specific for NB2 antigens (Verheugt et al., 1977). In contrast to the study of neutrophil membrane receptors, neutrophil preparation without the use of red cell lysis steps (by Ficoll®–Paque or dextran red cell sedimentation) have been found to give better results (Clay and Kline, 1985). Anti-neutrophil antibodies are usually either HLA or neutrophil specific. This distinction requires an additional lymphocytotoxicity test or chloroquine stripping of antigens prior to testing (Minchinton and Waters, 1984).

The differentiation between immune complex and antibody binding may be difficult; a polymorphic pattern of reactivity favours the presence of an antibody as does a positive eluate prepared from the test neutrophils when incubated with control cells. Immune complexes tend to be pan-reactive and can be detected by alternative techniques (Clay and Kline, 1985). Both immune complexes and antibodies may be clinically relevant in the setting of immune neutropenia (Caligaris-Capio et al., 1979). The detection of IgG bound to the neutrophil membrane in vivo is also difficult to interpret as this may reflect anti-neutrophil antibody, immune complex or nonspecific IgG binding, as discussed above, although the absence of neutrophil-associated IgG may help to exclude an immune mechanism. Again elution techniques may provide an answer (Klaassmen et al., 1991b).

Flow cytometric methods for the detection of anti-neutrophil antibodies have been described and compare favourably with light microscopy (Minchinton et al., 1989). A major concern has been whether flow cytometric methods would be able to exclude from the analysis neutrophils that had been damaged during preparation. These cells fluoresce brightly but with an abnormal fluorescence pattern, which can be discerned by light microscopy (Clay and Kline, 1985). In fact, these cells are also excluded by flow cytometry as their light scattering properties are altered (McMann et al., 1988). Flow cytometry enables the use of lymphocytes and monocytes as well as neutrophils as target cells and this permits, in a single test, the distinction between HLA or other antigens and neutrophil-specific antibodies (Veys et al., 1988a). However, it is possible that very weak antibodies may be adsorbed onto other cells and missed using this technique (Minchinton et al., 1984). The pattern of fluorescence in the flow cytometric histograms may give some indication as to the presence of antibody or immune complex (Veys et al., 1988b). Flow cytometry also gives slightly superior results with chloroquine-stripped neutrophils (Minchinton et al., 1984).

Flow cytometry has provided a ready tool for the study of neutrophil disorders. Some of these techniques are now used on a routine basis, while other research applications promise to unravel the further role of neutrophils in both body defence and disease mechanisms.

12.14.2 Assay of neutrophil-associated immunoglobulins and anti-neutrophil antibodies

Protocol 12.2 describes a procedure suitable for the detection of neutrophil-associated immunoglobulin and anti-neutrophil antibodies. It involves a single-step separation of mononuclear cells, neutrophils and erythrocytes using a discontinuous Histopaque (Sigma) gradient centrifugation assay (English and Anderson, 1974). This method eliminates the need for hypotonic lysis of red cells, which may cause damage to the neutrophil membrane (Clay and Kline, 1985). It is also the preferred method for preparation of leukocytes for functional assays because it results in minimal activation of granulocytes (Macey and McCarthy, 1993).

Protocol 12.2 Assay of neutrophil-associated immunoglobulins and anti-neutrophil antibodies

1. Whole blood (10 ml) anticoagulated with Na_2EDTA (ethylenediamintetraacetic acid disodium salt; 5 mg ml^{-1}, Sigma) is diluted with an equal volume of HBSS without phenol red (Sigma).
2. Histopaque 1119 (3 ml) (Sigma) is added to 15 ml round-bottom tubes and 3 ml Histopaque 1077 is carefully layered onto it. Blood (6 ml) is layered

on top of the upper Histopaque layer.
3. The tube is centrifuged at $700 \times g$ for 30 min at room temperature (RT) after which the mononuclear cells are harvested from the plasma/1077 interface and the neutrophils are collected from the 1077/1119 interface. Erythrocytes are pelleted to the bottom of the tube.
4. The granulocytes and mononuclear cells are then washed separately twice in HBSS containing 0.2% globulin-free bovine serum albumin (HBSS-BSA) (Sigma) by centrifugation at $250 \times g$ for 5 min at RT.
5. The cells are then fixed with filtered 1% paraformaldehyde (Sigma) in HBSS pH 7.2 for 5 min at RT. Paraformaldehyde should be freshly prepared from a stock 4% solution which should be made monthly and stored frozen in portions.
6. After fixation, the cells are washed twice in HBSS-BSA and neutrophils and mononuclear cells are mixed in equal numbers to give a leukocyte suspension of 2×10^6 ml^{-1} to 4×10^6 ml^{-1} in HBSS-BSA. The average platelet contamination is 5×10^6 ml^{-1}.
7. Leukocytes (100 μl) are then incubated with 5 μl FITC-conjugated rabbit F(ab')$_2$ anti-human IgG, IgM and control serum (Dako) for 30 min at 4°C. After a final wash in HBSS-BSA the cells are resuspended in the same ready for analysis.

Note: For indirect antibody testing, 100 μl leukocyte suspension is incubated with 100 μl test serum for 30 min at 37°C, washed twice in HBSS-BSA and labelled as above. Negative controls (serum from nontransfused, blood group AB healthy males) and positive controls (anti-NA1, multispecific anti-HLA or serum from patients with immune complex disorders such as rheumatoid arthritis) should be included in the study.

Flow cytometric analysis

1. Cell populations are separated by analysis of their light scattering properties.
2. Adequate separation of the cells is confirmed by labelling the cells with monoclonal antibodies, CD2, CD14 and CD16. Lymphocytes are $CD2^+CD14^-CD16^-$, monocytes are $CD2^-CD14^+CD16^-$ and neutrophils are $CD2^-CD14^-CD16^+$.

Protocol 12.3 describes a procedure for the short-term liquid culture of bone marrow cells and their use in the detection of drug-induced autoantibodies to myeloid precursor cells.

Protocol 12.3 Short-term liquid bone marrow cultures for autoantibody detection

This is from a method described by Nagler et al. (1990).

1. Bone marrow (10 ml) is collected into 300 U preservative-free heparin (Monoparin) and mixed with 10 ml Iscoves modified Dulbecco's medium (IMDM, Gibco).
2. The cells are layered over an equal volume of Ficoll®–Hypaque (density 1.077 g ml^{-1}) and the gradient centrifuged at $400 \times g$ for 30 min at RT.
3. Mononuclear cells at the interface of the medium and Ficoll® are collected then washed twice and resuspended in IMDM supplemented with 5% fetal bovine serum (FBS, Gibco) (IMDM-FBS).
4. The cells are then incubated for 1 h at 37°C in 3.5 cm petri dishes (Nunc) to allow adherence of monocytic cells.
5. The nonadherent cells are collected, washed and resuspended in IMDM-FBS and counted.
6. Samples (2×10^7 cells ml^{-1}) are incubated with 65 μl My8 antiserum (Beckman Coulter) or 5 μl anti-glycophorin A (Dako) at 4°C for 20 min. The cells are washed in cold medium, resuspended in 3 ml IMDM-FBS and poured into prepared goat anti-mouse-coated petri dishes (see below).
7. The cells are incubated for 70 min at 4°C. The dishes are then washed with IMDM to recover unbound cells, which are washed and resuspended in IMDM-FBS containing 10 ng G-CSF (Amgen).

Goat anti-mouse petri dishes

1. To prepare the goat anti-mouse petri dishes, 0.05 mol l^{-1} tris-buffered saline (TBS) pH 9.5 is filtered onto 100 mm × 15 mm Nunc petri dishes.
2. Goat anti-mouse immunoglobulin (500 μl) is added and the dishes are incubated at 23°C for 40 min.
3. After which the TBS is decanted and the dishes

are washed four times in PBS prior to addition of IMDM-FBS for 15 min at 4°C.

Detection of anti-myeloid precursor antibodies and/or drug-associated anti-myeloid precursor antibodies

1. Cells are prepared as above then incubated with a predetermined nontoxic concentration of the suspect drug together with either 10% control serum that has had complement inactivated by heating at 56°C for 30 min or 10% test serum (heat treated as above).
2. The cells are then cultured in IMDM-FBS containing 10 ng G-CSF at 37°C in an atmosphere of 5% CO_2. The expression of CD33 and CD16 is monitored at 132 h.

Detection of drug-associated complement-dependent anti-myeloid precursor antibodies

1. Cells prepared as above are incubated with a predetermined, nontoxic concentration of the suspect drug.
2. After 12 h, the cells are pelleted and resuspended in IMDM containing either 5% control serum (heat treated) plus 5% test serum or 5% test serum (heat treated) plus 5% control serum.
3. The cells are incubated for 1 h at 37°C, washed twice and resuspended in IMDM containing 15% FBS with 10 ng G-CSF.
4. The cells are then cultured and hematopoiesis monitored at 132 h by determining the percentage of $CD33^+$ and $CD16^+$ cells.

12.15 Clinical applications of flow cytometry to the study of autoimmune neutropenia

The combination of a flow cytometric phagocytosis assay with flow cytometric assay of oxidative metabolism has been used to determine the functional abilities of neutrophils from patients with AIN (Macey et al., 1990). These patients inherently have low numbers of neutrophils; consequently, flow cytometry, which is a highly sensitive system, is greatly beneficial. In this study, the finding of a weak correlation between the neutrophil count and the NAIgG was contradictory to previous reports (Hadley et al., 1987) and was perhaps a result of the increased sensitivity of the flow cytometric assay compared with light microscopy.

The data presented showed that neutropenic patients do have a reduced ability to respond to opsonised bacteria compared with normal controls and patients with other autoimmune disorders. Also the data confirmed that the degree of metabolic burst is related to the rate of uptake of bacteria. The rate of bacterial uptake was not found to be related to the amount of IgG on the neutrophil surface or the number of neutrophils circulating in the patient. However the rate of phagocytosis was found to correlate with the expression of FcRII and FcRIII. The expression of these receptors was found to be lower than normal, which would be consistent with the presence of increased numbers of immature cells. These findings suggest that the functional ability of neutrophils in patients with AIN is influenced by IgG Fc receptor expression (Veys et al., 1988b). Neutrophil function may also be influenced by C3b receptor expression (Fearon and Collins, 1983). Reduced IgG Fc receptor expression has also been found on neutrophils from patients after bone marrow transplantation. These cells also have reduced functional abilities (Macey et al., 1990).

12.16 Neutrophil IgG Fc receptor expression and function

Neutrophils express three receptors for the Fc portion of human IgG, termed FcγRI, FcγRII and FcγRIII (Deo et al., 1997). FcγRI is normally expressed in low numbers; however, in the presence of IFN-γ there is a marked increase in the expression of FcγRI (Buckle et al., 1990). These receptors are necessary for the phagocytosis of IgG-opsonised particles. The expression of these receptors is, therefore, useful as a measure of potential function, as a diagnostic indicator of infection or systemic

inflammatory response (Davis, 1996) and for therapeutic monitoring of IFN-γ therapy (Davis et al., 1995) (Protocol 12.4).

Protocol 12.4 Assay of Fc receptor expression

1. Neutrophils in anticoagulated whole blood (100 μl) are incubated with 20 μl FITC–CD16, FITC–CD32 and FITC–CD64 (Beckman Coulter) for 10 min at 4°C. Appropriate negative controls are included in each assay.
2. The cells are resuspended in cold (4°C) HHBSS-BSA containing 0.01% of a saturated solution of LDS-751 (Molecular Probes) prior to flow cytometric analysis.
3. Cells are gated in a dual-parameter histogram of side light scatter versus log red fluorescence.
4. The percentage fluorescence positivity above the negative control is determined and the mean channel fluorescence recorded for the expression of each Fc receptor on neutrophils.

12.17 Conclusions

Many of the assays described here have been used primarily as research tools but recently they have begun to be utilised in clinical settings. Their use for clinical applications has been limited by those factors referred to at the beginning of this chapter, relating to the requirement of rapid transport and handling of the sample. However, if flow cytometry is to be used on a more routine basis in clinical laboratories there is one further problem that requires to be addressed, that of standardisation. Recently, an initiative was started by a group of clinical laboratories using flow cytometry in different European countries to elaborate the current consensus on flow cytometric methods for the clinical laboratory as a basis for future quality assurance and control procedures. At present this group has not considered the numerous leukocyte function assays that may be performed by flow cytometry but it is anticipated that these will be examined in the near future.

12.18 REFERENCES

Andoh, A., Fujiyama, Y., Kitoh, K., Hodohara, K., Bamba, T., Hosada, S. (1991) Flow cytometric assay for phagocytosis of human monocytes mediated via Fc-gamma receptors and complement receptor CR1 (CD35). *Cytometry* **12**, 677–86.

Balteskard, L., Unneberg, K., Halvorsen, D., Ytrebo, L.M., Waage, A., Sjursen, H., Revhaug, A. (1997) The influence of growth hormone on tumour necrosis factor and leucocyte function in sepsis. *Scandinavian Journal of Infectious Disease* **29**, 393–9.

Bass, D.A., Parce, J.W., Dechatelet, L.R., Sjejda, P., Seeds, M.C., Thomas, M. (1983) Flow cytometric studies of oxidative product formation by neutrophils. A graded response to membrane stimulation. *Journal of Immunology* **130**, 1910–17.

Bass, D.A., Olbrandtz, P., Szejda, P., Seeds, M.C., McCall, C.E. (1986) Subpopulations of neutrophils with increased oxidative product formation in blood of patients with infection. *Journal of Immunology* **136**, 860–8.

Bassoe, C.F., Bjerknes, R. (1985) Phagocytosis by human leukocytes. Phagosomal pH and degradation of seven species of bacteria measured by flow cytometry. *Journal of Medical Microbiology* **19**, 37–43.

Berkow, R.L., Wang, D., Larrick, J.W., Dodson, R.W., Howard, T.H. (1987) Enhancement of neutrophil superoxide production by preincubation with recombinant human tumor necrosis factor. *Journal of Immunology* **139**, 3783–91.

Bohmer, R.H., Trinkle, L.S., Staneck, J.L. (1992) Dose effect of LPS on neutrophils in whole blood flow cytometric assay of phagocytosis and oxidative burst. *Cytometry* **13**, 525–31.

Bowen, D.L., Lane, H.C., Fauci, A.S. (1985) Immunopathogenesis of the aquired immunodeficiency syndrome. *Annals Internal Medicine* **103**, 704–9.

Brandt, R., Keston, A.S. (1965) Synthesis of diacetyldichlorofluorescein: a stable reagent for fluorometric analysis. *Analytical Biochemistry* **11**, 6–10.

Buckle, A.M., Jagaram, Y., Hogg, N. (1990) Colony stimulating factors and interferon gamma differentiating effect on cell surface molecules shared by monocytes and neutrophils. *Clinical and Experimental Immunology* **81**, 339–45.

Busse, W.W., Vrtis, R.F., Steiner, R., Dick, E.C. (1991) In vitro incubation with influenza virus primes human polymorphonuclear leucocyte generation of superoxide. *American*

Journal of Respiratory Cell Molecular Biology **4**, 347–54.

Bux, J., Kissel, K., Nowak, K., Spengel, U., Mueller-Eckhardt, C. (1991a) Autoimmune neutropenia: clinical and laboratory studies in 143 patients. *Annals of Haematology* **63**, 249–52.

Bux, J., Robertz, Vaupel, G.M., Glasmacher, A., Dengler, H.J., Meuller-Eckhardt, C. (1991b) Autoimmune neutropenia due to NA1 specific antibodies in primary biliary cirrhosis. *British Journal of Haematology* **77**, 121–2.

Bux, J., Stein E.L., Bierling, P., Fromont, P., Clay, M., Stoncek, D., Santoso, S. (1997) Characterisation of a new alloantigen (SH) on the human neutrophil Fcγ receptor IIIb. *Blood* **89**, 1027–34.

Bux, J., Behrens, G., Jaeger, G., Welte, K. (1998) Diagnosis and clinical course of autoimmune neutropenia in infancy: analysis of 240 cases. *Blood* **91**, 181–6.

Cairo, M.S., Worcester, C.C., Rucker, R.W., Hanten, S., Amlie, R.N., Sender, L, Hicks, D.A. (1992) Randomised trial of granulocyte transfusion versus intravenous immunoglobulin therapy for neonatal neutropenia and sepsis. *Journal of Pediatrics* **120**, 281–5.

Caligaris-Cappio, F., Gamussi, G., Gavosto, A. (1979) Idiopathic neutropenia with normocellular bone marrow: An immune complex disease. *British Journal of Haematology* **43**, 595–605.

Cambridge, G., Rampton, D.S., Stevens, T.R., McCarthy, D.A., Kamm, M., Laeker, B. (1992) Anti-neutrophil antibodies in inflammatory bowel disease: prevalence and diagnosic role. *Gut* **33**, 668–74.

Cartron, J., Celton, J.L., Gane, P., Astier, A., Fridman, W.H., Boissinot, G., Cartron, J.P. (1992) Iso-immune neonatal neutropenia due to an anti-Fc receptor III (CD16) antibody. *European Journal of Pediatrics* **151**, 438–41.

Civin, C.L., Loken, M.R. (1987) Cell surface antigens on human marrow cells: dissection of haematopoietic development using monoclonal antibodies and multiparameter flow cytometry. *International Journal of Cell Cloning* **5**, 267–86.

Clay, M.E., Kline, W.E. (1985) Detection of granulocyte antigens and antibodies: current perspectives and approaches. In: Garratty, G. (ed.), *Current Concepts in Transfusion Therapy*, pp. 183–265. American Association of Blood Banks, Arlington, VA.

Condliffe, A.M., Chilvers, E.R., Haslett, C., Dransfield, I. (1996) Priming differentially regulates neutrophil adhesion molecule expression/function. *Immunology* **89**, 105–11.

Condliffe, A.M., Kitchen, E, Chilvers, E.R. (1998) Neutrophil priming: pathophysiological consequences and underlying mechanisms. *Clinical Science* **94**, 461–71.

Crockard, A.D., Thompson, J.M., Boyd, N.A., Haughton, D.J., McCluskey, D.R., Turner, C.P. (1997) Diagnosis and carrier detection of chronic granulomatous disease in five families by flow cytometry. *International Archives of Allergy and Immunology* **114**, 144–52.

Daniels, R.H., Finnen, M.J., Hill, M.E., Lackie, J.M. (1992) Recombinant human monocyte IL-8 primes NADPH-oxidase and phospholipase A_2 activation in human neutrophils. *Immunology* **75**, 157–63.

Davis, B.H. (1996) Quantitative neutrophil CD64 expression: promising diagnostic indicator of infection or systemic acute inflammatory response. *Clinical Immunology* **16**, 121–36.

Davis, B.H., Bigelow, N.C., Curnutte, J.T., Ornvold, K. (1995) Neutrophil CD64 expression: potential diagnostic indicator of acute inflammation and therapeutic monitor of interferon-γ therapy. *Laboratory Hematology* **1**, 2–12.

Demo, S.D., Masuda, E., Rossi, A.B., Throndset, B.T., Gerard, A.L., Chan, A.L., Armstrong, R.J., Fox, B.P., Lorens, J.B., Payan, D.G., Scheller, R.H., Fisher, J.M. (1999) Quantitative measurement of mast cell degranulation using a novel flow cytometric annexin-V binding assay. *Cytometry* **36**, 340–8.

Deo, Y.M., Graziano, R.F., Repp, R., van de Winkel, J.G.J. (1997) Clinical significance of IgG Fc receptors and FcγR-directed immunotherapies. *Immunology Today* **18**, 127–35.

de Rie, M.A., van des Plas-van Dalen, C.M., Engelfriet, C.P., von dem Borne, A.E.G.Kr. (1985) Serology of febrile transfusion-reactions. *Vox Sanguinis* **49**, 126–34.

Downey, G.P., Fukushima, T., Failkow, L., Waddell, T.K. (1995) Intracellular signaling in neutrophil priming and activation. *Cell Biology* **6**, 345–56.

Eggleston, P., Penhallow, J., Crawford, N. (1991) Priming action of inositol hexakisphosphate ($InsP_6$) on the stimulated respiratory burst in human neutrophils. *Biochimica et Biophysica Acta* **1094**, 309–16.

Elbim, C., Prevot, M.H., Bouscarat, F., Franzini, E., Chollet-Martin, S., Hakim, J., Gougerot-Pocidalo, M.A. (1994) Polymorphonuclear neutrophils from human immunodeficiency virus infected patients show enhanced activation, diminished fMLP induced L-selectin shedding and an impaired oxidative burst after cytokine priming. *Blood* **84**, 2759–64.

Elsner, J., Roesler, J., Emmendorffer, A, Lohmann-Matthes, M.L., Welte, K. (1993) Abnormal regulation in the signal transduction in neutrophils from patients with severe congenital neutropenia: relation of impaired mobilization of cytosolic free calcium to altered chemotaxis, superoxide anion generation and F-actin content. *Experimental Hematology* **21**, 38–44.

Emmendorffer, A., Nakamura, M., Rothe, G., Spiekerman, K., Lohman-Matthes, M.L., Roesler, J. (1994) Evaluation of flow cytometric methods for the diagnosis of chronic granulomatous disease variants under routine laboratory

conditions. *Cytometry* **18**, 147–55.

Engelfreit, C.P., Tetteroo, J.P.W., van der Veen, J.P.W., Werner, W.F., van Plas-van Dalen, C., von dem Borne, A.E.G.Kr. (1984) Granulocyte-specific antigens and methods for their detection. In: McCullogh, J.J., Sandler, R.M. (eds.), *Advances in Immunobiology*: *Blood Cell Antigens and Bone Marrow Transplantation, Progress in Clinical and Biological Research*, pp. 121–54. Liss, New York.

English, D., Anderson, B.R. (1974) Single-step separation of red blood cells, granulocytes and mononuclear leukocytes on discontinous density gradients of Ficoll Hypaque. *Journal of Immunological Methods* **5**, 249–52.

Etzioni, A., Frydman, M., Pollack, S., Avidor, I. (1992) Recurrent severe infections caused by a novel leucocyte adhesion deficiency. *New England Journal of Medicine* **327**, 1789–92.

Fattorossi, F., Nisini, R., Pizzola, J.G., D'Amelio, R. (1989) New, simple flow cytometry technique to discriminate between internalized and membrane-bound particles in phagocytosis. *Cytometry* **10**, 320–5.

Fearon, D., Collins, L. (1983) Increased expression of C3b receptors on polymorphonuclear leukocytes induced by chemotactic factors and by purification procedures. *Journal of Immunology* **130**, 370–5.

Filep, J.G., Delalandre, A., Payette, Y., Foldes-Filep, E. (1997) Glucocorticoid receptor regulates expression of L-selectin and CD11/CD18 on human neutrophils. *Circulation* **96**, 295–301.

Finkel, T.H., Pabst, M.J., Suzuli, H. (1987) Priming of neutrophils and macrophages for enhanced release of superoxide anion by the calcium ionophore ionomycin: implications for regulation of the respiratory burst. *Journal of Biological Chemistry* **262**, 12589–96.

Freidman, G., Jankowski, S., Marchant, A., Goldman, M., Kahn, R.J., Vincent, J.L. (1997) Blood interleukin-10 levels parallel the severity of septic shock. *Journal of Critical Care* **12**, 183–7.

Fromont, P., Bettaieb, A., Skouri, H., Floch, C., Poulet, E., Duedari, N., Bierling, P. (1992) Frequency of the polymorphonuclear neutrophil Fc gamma receptor III deficiency in the French population and its involvement in the development of neonatal alloimmune neutropenia. *Blood* **79**, 2131–4.

Goldschmeding, R., Breedveld, F.C., Engelfreit, C.P., von dem Borne, A.E.G.Kr. (1988) Lack of evidence for the presence of neutrophil autoantibodies in the serum of patients with Felty's syndrome. *British Journal of Haematology* **68**, 37–40.

Gordon, B.G., Kiwauka, J., Kadushin, J. (1991) Autoimmune neutropenia and Hodgkin's disease: successful treatment with intravenous immunoglobulin. *American Journal of Pediatric Hematology and Oncolology* **13**, 164–7.

Guthrie, L.A., McPhail, L.C., Henson, P.M. (1984) Priming of neutrophils for enhanced release of oxygen metabolites: evidence for increased activity of the superoxide-producing enzyme. *Journal of Experimental Medicine* **160**, 1656–71.

Hadley, A.G., Byran, M.A., Chapel, H.M., Bunch, C., Holburn, A.M. (1987). Anti-granulocyte opsonic activity in sera from patients with systemic lupus erythematosus. *British Journal of Haematology* **65**, 61–5.

Harlan, J.M., Winn, R.K., Vedder, N.B., Doershuk, C.M., Rice, C.L. (1992) In vivo models of leukocyte adherence to endothelium. In: Harlan, J.M. (ed.), *Adhesion: its Role in Inflammatory Disease*, pp. 117–50. Freeman, New York.

Hampton, M.B., Kettle, A.J., Winterbourn, C.C. (1998) Inside the neutrophil phagosome: oxidants, myeloperoxidase, and bacterial killing. *Blood* **92**, 3007–17.

Hartman, K.R., Wright, D.G. (1991) Identification of autoantibodies specific for the neutrophil adhesion glycoproteins CD11b/CD18 in patients with autoimmune neutropenia. *Blood* **78**, 1096–104.

Hartman, K.R., Mallet, M.K., Nath, J., Wright, D.G. (1990) Antibodies to actin in autoimmune neutropenia. *Blood* **75**, 736–43.

Heiduschka, P., Thanos, S. (1998) NO production during neuronal cell death can be directly assessed by a chemical reaction in vivo. *NeuroReport* **9**, 4051–7.

Higuchi, S., Higashi, A., Nakamura, T., Yanabe, Y., Matsuda, I. (1991) Anti-neutrophil antibodies in patients with nutritional copper deficiency. *European Journal of Pediatrics* **150**, 327–30.

Himmelfarb, J., Hakim, R.M., Holbrook, D.G., Leeber, D.A., Ault, K.A. (1992) Detection of granulocyte reactive oxygen species formation in whole blood using flow cytometry. *Cytometry* **13**, 83–9.

Hogg, N., Stewart, M.P., Scark, S.L. (1999) A novel leucocyte adhesion deficiency caused by expressed but non functional β_2 integrins MAC-1 and LFA-1. *Journal of Clinical Investigation* **109**, 97–106.

Howard, T.H., Watts, R.G. (1994) Actin polymerisation and leucocyte function. *Current Opinion in Hematology* **1**, 61–6.

Huizinga, T.W., van der Schoot, C.E., Jost, C., Klaassen, R., Kleijer, M., von dem Borne, A.E.G.Kr., Roos, D., Tetteroo, P.A.T. (1988) The PI-linked receptor for FcR III is released on stimulation of neutrophils. *Nature* **333**, 667–9.

Jones, D.H., Schmalsteig, F.C., Dempsey, K., Krater, S.S., Nannen, D.D., Wayne Smith. C., Anderson, D.C. (1990) Subcellular distribution and mobilisation of MAC-1 (CD11b/CD18) in neonatal neutrophils. *Blood* **75**, 488–98.

Keller, H.U., Fedier, A., Rohner, R. (1995) Relationship between light scattering in flow cytometry and changes in shape,

volume, and actin polymerisation in human polymorphonuclear leucocytes. *Journal of Leucocyte Biology* **57**, 519–25.

Klaassmen, R.J.L., Mulder, J.W., Vlekke, A.B.J., Eftinck, Schattenkerk, J.K.M., Weigel, H.M., Lange, J.M.A., von dem Borne, A.E.G.Kr. (1990) Autoantibodies against peripheral blood cells appear early in HIV infection and their prevalance increases with disease progression. *Clinical and Experimental Immunology* **81**, 11–17.

Klaassmen, R.J.L., Vlekke, A.B.J., von dem Borne, A.E.G.Kr. (1991a) Neutrophil-bound immunoglobulin in HIV infection is of autoantibody nature. *British Journal of Haematology* **77**, 403–9.

Klaassmen, R.J.L., Goldschmeding, R., Vlekke, A.B.J., Rozendaal, R., von dem Borne, A.E.G.Kr. (1991b) Differentiation between neutrophil-bound antibodies and immune complexes. *British Journal of Haematology* **77**, 398–402.

Koene, H.R., Kleijer, M., Roos, D., de Haas, M., von dem Borne, A.E.G.K. (1998) FrγRIIIB gene duplication: evidence for presence and expression of three distinct FrγRIIIB genes in NA(1$^+$,2$^+$)SH$^+$ individuals. *Blood* **91**, 673–9.

Kuhns, D.B., Wright, D.G., Nath, J., Kaplan, S.S., Basford, R.E. (1988) ATP induces transient elevations of [Ca^{2+}] in human neutrophils and primes these cells for enhanced O_2^- generation. *Laboratory Investigation* **58**, 488–93.

Lalezari, P., Radel, E. (1974) Neutrophil specific antigens: immunologic and clinical significance. *Seminars in Hematology* **11**, 281–90.

Lalezari, A.P., Khorshidi, M., Petrosova, M. (1986) Autoimmune neutropenia of infancy. *Journal of Pediatrics* **109**, 764–9.

Lasito, A., Lorusso, L. (1979) Polymorphonuclear leukocyte fluorescence and cryoglobulin phagocytosis in systemic lupus erythematosus. *Clinical and Experimental Immunology* **35**, 376–9.

Liles, W.C., Ledbetter, J.A., Waltersdorph, A.W., Klebanhoff, S.J. (1995) Crosslinking CD18 primes human neutrophils for activation of the respiratory burst in response to specific stimuli: implications for adhesion-dependent physiological responses in neutrophils. *Journal of Leucocyte Biology* **58**, 690–7.

Lloyds, D., Hallett, M.B. (1993) Activation and priming of the human neutrophil oxidase response by substance P: distinct signal transduction pathways. *Biochimica et Biophysica Acta* **1175**, 207–13.

Lloyds, D., Hallett, M.B. (1994) Neutrophil priming induced by orthovanadate: evidence of a role for tyrosine phosphorylation. *Biochemical Pharmacology* **48**, 15–21.

Lyall, E.G., Lucas, G.F., Eden, O.B. (1992) Autoimmune neutropenia of infancy. *Journal of Clinical Pathology* **45**, 431–4.

Macey, M.G., McCarthy, D. (1993) The quantitation of adhesion molecules and other function associated antigens on human peripheral blood leucocytes. *Cytometry* **14**, 898–908.

Macey, M.G., Sangster, J., Veys, P., Newland, A. (1990) Flow cytometric analysis of the functional ability of neutrophils from patients with autoimmune neutropenia. *Journal of Microscopy* **159**, 277–83.

Macey, M.G., Jiang, X.P., Veys, P., McCarthy, D., Newland, A.C. (1992) Expression of functional antigens on neutrophils. Effects of preparation. *Journal of Immunological Methods* **149**, 37–42.

Macey, M.G., Wilton, J.M.A., Carbon, R., Edmonds, S., Perry, J.D., McCarthy, D. (1993a) Leukocyte activation and function-associated antigens in inflammatory disease. *Agents and Actions* **38**, 39–40.

Macey, M.G., Sangster, J., Kelsey, S., Newland, A.C. (1993b) Pilot study: effect of G-CSF on neutrophil *ex-vivo* function post bone marrow transplantation. *Clinical and Laboratory Haematology* **15**, 79–85.

Macey, M.G., McCarthy, D.A., Newland, A.C. (1994) The *ex vivo* function and expression of function associated antigens on peripheral blood neutrophils and monocytes. *Experimental Hematology* **22**, 967–72.

Macey, M.G., McCarthy, D.A., Vordermeier, S., Newland A.C., Brown K.A. (1995) Effects of cell purification methods on CD11b and L-selectin expression as well as the adherence of activated leucocytes. *Journal of Immunological Methods* **181**, 211–19.

Macey, M.G., Davies, C.A., McCarthy, D.A., Newland, A.C. (1997) The Coulter Q-Prep system: effect on the apparent expression of leucocyte cell surface antigens. *Cytometry* **30**, 67–71.

Macey, M.G., McCarthy, D.A., Howells, M.A., Curtis, M.A., King, G., Newland, A.C. (1998) Multiparameter flow cytometric analysis of polymorphonuclear leucocytes in whole blood from patients with adult rapidly progressive periodontitis reveals low expression of the adhesion molecule L-selectin (CD62L). *Cytometry* **34**, 152–8.

Macey, M.G., McCarthy, D.A., Milne, T., Cavenagh, J.D., Newland, A.C. (1999) Comparative study of five commercial reagents for preparing normal and leukaemic lymphocytes for immunophenotypic analysis by flow cytometry. *Cytometry* **38**, 153–60.

Marie, C., Pitton, C., Fitting, C., Cavaillon, J.M. (1996) Regulation by antiinflammatory cytokines (IL-4, IL-10, IL-13 and TGFβ) of IL-8 production by LPS and or TNF-α activated human polymorphonuclear cells. *Mediators of Inflammation* **5**, 334–40.

Marie, C., Muret, J., Fitting, C., Losser, M.R., Payen, D., Cavaillon, J.M. (1998) Reduced *ex-vivo* interleukin-8 production by neutrophils in septic and nonseptic systemic inflammatory

response syndrome. *Blood* **91**, 3439–46.

Mazzucchelli, I., Mazzone, A., Pasotti, D., Fossati, G., Cavigliano, P., Ricevuti, G., Notario, A. (1992) Role of hemostasis and inflammation in increase of adhesion molecule of phagocytes. *24th Congress of the International Society for Hematology British Journal of Haematology* p. 208.

McCarthy, D.A., Macey, M.G. (1993) A simple flow cytometric procedure for the determination of surface antigens on unfixed leucocytes in whole blood. *Journal of Immunological Methods* **163**, 155–60.

McCarthy, D.A., Macey, M.G. (1996) Novel anticoagulants for flow cytometric analysis of live leucocytes in whole blood. *Cytometry* **23**, 196–204.

McCarthy, D.A., Macey, M.G., Cahill, M.R., Newland, A.C. (1994) The effect of fixation on quantification of the expression of leucocyte function-associated surface antigens. *Cytometry* **17**, 39–49.

McCullough, J.J. (1983) Granulocyte antigen systems and their clinical significance. *Human Pathology* **14**, 228–34.

McCullough, J.J., Clay, M.E., Thompson, H.W. (1987) Autoimmune granulocytopenia. In: Engelfreit, C.P., von dem Borne, A.E.G.K. (eds.), *Ballière's Clinical Immunology and Allergy*, Vol. 1, No. 2, pp. 303–13. Ballière-Tindall, London.

McMann, L.E., Walterson, M.L., Hogg, L.M. (1988) Light scattering and cell volumes in osmotically stressed and frozen-thawed cells. *Cytometry* **9**, 33–8.

Minchinton R.M, Waters A.H (1984) Chloroquine stripping of HLA antigens from neutrophils without removal of neutrophil specific antigens. *British Journal of Haematology* **57**, 703–6.

Minchinton, R.M., Rockman, S., McGrath, K.M. (1989) Evaluation and callibration of a fluorescence-activated cell sorter for the interpretation of the granulocyte immunofluorescence test (GIFT). *Clinical and Laboratory Haematology* **11**, 349–59.

Mineshita, M., Kimura, T., Murai, H., Moritani, C., Ishioka, S., Kambe, M., Yamakido, M. (1997) Whole blood incubation method to study neutrophil cytoskeletal dynamics. *Journal of Immunological Methods* **202**, 59–66.

Murphy, M.F., Metcalf, P., Waters, A.H., Carne, C.A., Weller, I.V.D., Linch, D.A., Smith, A. (1987) Incidence and mechanism of neutropenia and thrombocytopenia in patients with human immunodeficiency virus infection. *British Journal of Haematology* **66**, 22–4.

Nagler, A., Binet, C., Mickichan, M., Negrin, R., Bangs, C., Donlon, T., Greenberg, P. (1990) Impact of marrow cytogenetics and morphology on in vitro hematopoiesis in the myelodysplastic syndromes: comparison between recombinant human granulocyte colony stimulating factor and granulocyte-monocyte CSF. *Blood* **76**, 1299–307.

Naik, N.R., Bhisey, A.N., Advani, S.H., Lichtman, M.A. (1990) Flow cytometric studies on actin polymerisation in PMN cells from chronic myeloid leukaemia (CML) patients. *Leukocyte Research* **14**, 921–6.

Nybo, M., Sorensen, O., Leslie, R., Wang, P. (1998) Reduced expression of C5a receptors on neutrophils from cord blood. *Archives of the Diseased Child, Fetal and Neonatal Education* **78**, 129–33.

Parsons, P.E., Worthen, G.S., Moore, E.E., Tate, R.M., Henson, P.M. (1989) The association of circulating endotoxin with the development of the adult respiratory distress syndrome. *American Review of Respiratory Disease* **140**, 294–301.

Perticarari, S., Presani, G., Mangiarotti, M.A., Banfi, E. (1991) Simultaneous flow cytometric method to measure phagocytosis and oxidative products by neutrophils. *Cytometry* **12**, 687–93.

Pinsky, M.R., Vincent, J.L., Deviere, J., Alegre, M., Kahn, R.J., Dupont, E. (1993) Serum cytokine levels in human septic shock: relation to multiple organ failure and mortality. *Chest* **103**, 565–75.

Rios, E., Heresi, G., Arevalo, M. (1991) Familial alloimmune neutropenia of NA-2 specificity. *American Journal of Pediatric Hematology and Oncology* **13**, 296–9.

Roos, D., Kuijpers, T.W., Mascart-Lemone, F., Koenderman, L., de Beer, M., van Zweiten, R., Verhhoeen, A.J. (1993) A novel syndrome of severe neutrophil dysfunction: unresponsiveness confined to chemotaxin-induced functions. *Blood* **81**, 2735–40.

Root, R.K., Dale, D.C. (1999) Granulcyte colony stimulating factor and granulocyte-macrophage colony stimulating factor: comparisons and potential for use in the treatment of infections in nonneutropenic patients. *Journal of Infectious Diseases* **179**, S342–52.

Rothe, G., Valet, G. (1988) Phagocytosis, intracellular pH and cell volume in the multifunctional analysis of granulocytes by flow cytometry. *Cytometry* **9**, 316–24.

Rothe, G., Valet, G. (1990) Flow cytometric analysis of respiratory burst activity in phagocytes with hydroethidine and 2',7'-dichlorofuorescein. *Journal of Leucocyte Biology* **47**, 440–5.

Rothe, G., Valet, G. (1994a) Measurement of intracellular pH of leucocytes with SNARF-1/AM. In: Robinson, J.P. (ed.), *Handbook of Flow Cytometry Methods*, pp. 175–6. Wiley-Liss, New York.

Rothe, G., Valet, G. (1994b) Measurement of NADPH oxidase activity with hydroethidine. In: Robinson, J.P. (ed.), *Handbook of Flow Cytometry Methods*, pp. 159–60. Wiley-Liss, New York.

Rothe, G., Valet, G. (1994c) Measurement of phagosomal hydrogen peroxide production with dihydrorhodamine 123. In:

Robinson, J.P. (ed.), *Handbook of Flow Cytometry Methods*, pp. 155–6. Wiley-Liss, New York.

Rothe, G., Kellerman, W., Valet, G. (1990) Flow cytometric parameters of neutrophil function as early indicators of sepsis- or trauma-related pulmonary or cardiac organ failure. *Journal of Laboratory and Clinical Medicine* **115**, 52–6.

Sabroe, I., Hartnell, A., Jopling, L.A., Bel, S., Ponath, P.D., Pease, J.R., Collons, P.D., Williams, T.J. (1999) Differential regulation of eosinophil chemokine signalling via CCR3 and non-CCR3 pathways. *Journal of Immunology* **162**, 2946–55.

Samuelsson, J., Forslid, J., Hed, J., Palmblad, J. (1994) Studies of neutrophil and monocyte oxidative responses in polycythemia vera and related myeloproliferative disorders. *British Journal of Haematology* **87**, 464–8.

Seligmann, B., Gallin, J.I. (1980) Use of lipophilic probes of membrane potential to assess human neutrophil activation: abnormality in chronic granulomatous disease. *Journal of Clinical Investigation* **66**, 493–6.

Schiffer, C.A., Aisner, J., Daly, P.A., Schimpff, S.C., Wiernik, P.H. (1979) Alloimmunisation following prophylactic granulocyte transfusion. *Blood* **54**, 766–74.

Schiffer, C.A. (1980) Granulocyte transfusions: an established or still experimental therapeutic procedure. *Vox Sanguinis* **38**, 56–8.

Shanahan, F., Duerr, R.H., Rotter, J.I., Yang, H., Sutherland, L.R., McElree, C., Landers, C.J., Targan, S.R. (1992) Neutrophil autoantibodies in ulcerative colitis: familial aggregation and genetic heterogeneity. *Gastroenterology* **103**, 456–61.

Stevens, C., Peppercorn, M.A., Grand, R.J. (1991) Crohn's disease associated with autoimmune neutropenia. *Journal of Clinical Gastroenterology* **13**, 328–30.

Stroncek, D.F., Skubitz, K.M., Plachta, L.B., Shankar, R.A., Clay, M.E., Herman, J., Fleit, H.B., McCullough, J. (1991) Alloimmune neonatal neutropenia due to an antibody to the neutrophil Fc-gamma receptor III with maternal deficiency of CD16 antigen. *Blood* **77**, 1572–80.

Szejda, P., Paerce, J.W., Seeds, M.S., Bass, D.A. (1984). Flow cytometric quantitation of oxidative product formation by polymorphonuclear leukocytes during phagocytosis. *Journal of Immunology* **133**, 3303–7.

Tennenberg, S.D., Fey, D.E., Lieser, M.J. (1993) Oxidative priming of neutrophils by interferon-γ. *Journal of Leucocyte Biology* **53**, 301–8.

Thompson, J.S., Severon, C.D., Parmley, M.J., Marmorstein, B.L., Simmons, A. (1971) Pulmonary 'hypersensitivity' reactions induced by transfusion of non-HLA leukoagglutinins. *New England Journal of Medicine* **284**, 1120–5.

van der Pol, W., van de Winkel, J.G. (1998) IgG receptor polymorphisms: risk factors for disease. *Immunogenetics* **48**, 222–32.

Verheugt, F.W.A., von dem Borne, A.E.G.Kr., Decary, F., Engelfreit, C.P. (1977) The detection of granulocyte alloantibodies with an indirect immunofluorescent test. *British Journal of Haematology* **36**, 533–44.

Veys, P.A., Macey, M.G., Newland, A.C. (1988a) Detection of granulocyte antibodies using flow cytometric analysis of leucocyte immunofluorescence. *Vox Sanguinis* **56**, 42–7.

Veys, P.A., Macey, M.G., Newland, A.C. (1988b) Autoimmune neutropenia and the neutrophil FcR. *Biochememical Society Transactions* **16**, 732.

Veys, P.A., Wilkes, S., Ellis, G., Hoffbrand, A.V. (1990) Deficiency in DAF and CD16 on PNH neutrophils. *British Journal of Haematology* **76**, 318.

Vircellotti, G.M., Yin, H.Q., Gustafson, K.S., Nelson, R.D., Jacobs, H.S. (1988) Platelet activating factor primes neutrophil responses to agonists: role in promoting neutrophil-mediated endothelial damage. *Blood* **71**, 1100–7.

Walbroehl, G.S., John, P.G. (1992) Antibiotic associated neutropenia. *American Family Physician* **45**, 2237–41.

Waddell, T.K., Failkow, L., Chan, C.K., Kishimoto, T.K., Downey, G.P. (1994) Potentiation of the oxidative burst of human neutrophils: a signalling role for L-selectin oxide anion by the calcium ionophore ionomycin: implications for regulation of the respiratory burst. *Journal of Biological Chemistry* **269**, 18485–91.

Waters, JB., Oldstone, M.B.A., Hahn, KM. (1996) Changes in cytoplasmic structure of CTLs during target cell recognition and killing. *Journal of Immunology* **157**, 3396–402.

Watts, R.G., Howard, T.H. (1993) Mechanism of actin reorganisation in chemotactic factor-activated polymorphonuclear leucocytes. *Blood* **81**, 2750–5.

Weisbart, R.H., Kwan, L., Golde, D.W., Basson, J. (1986) Human GM-CSF primes neutrophils for enhanced oxidative metabolism in response to the major physiological chemoattractants. *Blood* **69**, 18–21.

Weitzman, S.A., Stossel, T.P. (1978) Drug-induced immunological neutropenia. *Lancet* **i**, 1068–71.

Welte, K., Dale, D. (1996) Pathophysiology and treatment of severe chronic neutropenia. *Annals of Hematology* **72**, 158–64.

Wulf, E., Deboden, A., Bautz, F.A., Faulisch, H., Wieland, T.H. (1979) The fluorescent phallotoxin, a tool for the visualisation of cellular actin. *Proceedings of the National Academy of Sciences of the USA* **76**, 1979–84.

Zubler, R.H., Nydegger, U.E., Perrin, L.H., Fehr, K., McCormick, J., Lambert, P.H., Meischer, P.A. (1976) Circulating and intraarticular immune complexes in patients with rheumatoid arthritis. *Journal of Clinical Investigation* **57**, 1308–19.

13

Intracellular measures of signalling pathways

James W. Jacobberger[1] and David W. Hedley[2]

[1]Case Western Reserve University, Ohio, USA
[2]Ontario Cancer Institute, Princess Margaret Hospital, Ontario, Canada

13.1 Introduction

This chapter reviews and discusses two different flow cytometric approaches to the study of cellular physiology (defined as studies of the dynamic state of a cell population). The first approach uses fixed and permeabilised cells to detect and quantify epitopes on important regulatory molecules as a function of cell cycle phase or stage in the cell death process at a single time point per sample. This approach is static and the time domain, and consequently the physiological state, is inferred. The second approach uses live, dying or dead cells in a native state that have been stained with fluorescent molecules that 'report' the physiological state. These measurements are dynamic and fluctuate in real time.

The discussion and examples herein are biased towards the signalling pathways in cancer cells that, in aggregate, define the oncogenic phenotype. Published studies of signalling pathways have increased steadily since the early 1980s, but advances that provide a more complete picture of pathways as interacting nodal networks are more recent. At present, the exact definition of a pathway/network is not very precise. The following is a definition within the context of this chapter: 'the aggregate biochemical process by which some particular cell behaviour (phenotype) is regulated that includes all chemical changes in the ''resting state'' that affect the cell phenotype significantly when components of the pathway are modulated.'

Logically, all components within the cell are interconnected to some degree; therefore, modulating one component will probably have some effect on all others. If the regulatory pathways are a multidimensional set of interconnected reactions, one area can only be viewed in isolation by invoking an arbitrary cut-off where the magnitude of an effect on another reaction is deemed insignificant. Many of the key nodes of regulation are proteins and measurement of the level, activity and associations of these protein components as a function of two different states may provide an outline of a particular pathway. This is one of the main goals of static cytometric methodology. However, a more complete pathway picture is dynamic and involves enzyme reactions, ion movements, molecule synthesis and breakdown, organelle and structure movement, and global cell behaviour. The dynamic methods discussed in this chapter attempt to describe pathways in that way. Together, these approaches comprise an effort to define more comprehensively what we mean when we use the word 'cell'.

A tenet of analytical cytology is that correlated quantitative measurements on cells provide better understanding of the state of the underlying population than does any single measurement; consequently, this chapter is restricted to a description of multiparametric flow cytometry. One area where multiparametric analysis will play an important role is in the development of cancer therapeutics. This derives directly from the ability to measure cellular physiological state and the molecules that drive that state for a single population among many. This approach can provide detailed and immediate assessment of drug action, especially for drugs targeted to specific pathway molecules. It can also measure molecules of the signalling pathway by immunofluorescence and analyse apoptosis utilising

physiological probes. Some specific examples where these approaches may currently provide useful therapeutic information are provided. Since the emphasis of this chapter is directed to future trends, its content may be somewhat speculative in places.

Extensive referencing has been avoided. References to a number of books that contain detailed methods can be found in Section 13.8. However, all of these methods should be regarded as a starting point and (in our opinion) individual investigators are obligated to evaluate and optimise protocols in their own laboratories for their particular purpose.

13.2 Regulatory pathways

Initially the essential features of the regulatory pathways of cell proliferation are described with an emphasis on proteins and omitting details about most of the second messenger signals generated by lipids, ions, etc. Both positive and negative feedback and crosstalk are ignored. Within this context, cell proliferation can be divided into two processes: cell cycling and cell death.

Resting, undamaged, somatic cells receive signals from at least three sources:

- extracellular soluble molecules
- extracellular insoluble matrix molecules
- cell–cell binding molecules.

Each signal begins with interaction of an extracellular molecule (the ligand) with a cell receptor. Activated receptors initiate a signal intracellularly by creating a chemical cascade that is propagated through scaffolding and adaptor molecules, transducers and transcription factors. The transcription factors can be suppressive or activating and can initiate the transcription of genes encoding effector molecules, additional regulatory proteins, or both. Figure 13.1 shows three well-studied signalling systems.

One example of a pathway would be activation of the cell cycle by binding of a peptide ligand (e.g. epidermal growth factor (EGF)) to a tyrosine kinase receptor (ErbB1), signalling through the Ras, Raf, MEK1 (a mitogen-activated protein kinase (MAPK)/ERK activating kinase, also known as MAPKK), ERK1 and ERK2 (extracellular-signal-regulated kinases) transduction system to ETS transcription factors among others (Garrington and Johnson, 1999; Hackel et al., 1999, Moghal and Sternberg, 1999). One central end product in this pathway is transcription of D-type cyclins (Albanese et al., 1995; Roussel, 1998; Yan et al., 1997) and formation of active cyclin D-dependent kinase complexes. These complexes are one component of a signalling system that ultimately activates transcription of cyclin E, which is part of the next downstream regulatory component (formation of cyclin E-dependent kinase complexes). These maintain a central negative regulator of G_1 phase, the retinoblastoma protein (pRb or p105), in a state that does not restrict active E2F transcription factors. Effector enzymes needed for DNA synthesis are transcribed in an E2F-dependent manner. For static or dynamic analysis of this system in epithelial cells, one might be tempted to measure cyclin D_1. And indeed, the levels of cyclin D_1 in a population should reflect the activity of specific tyrosine kinase receptor systems. However, since there is significant crosstalk between signalling systems that serve to modify the downstream products, measurement of a single entity will not carry much meaning for an unknown sample (e.g. a tumour biopsy). Since MAPK may be an integrating node, the levels of MAPK, active MAPK (phosphorylated on tyrosine and threonine) and cyclin D_1 referenced to a standard might possibly determine the distribution of activity of cell cycle-stimulating tyrosine kinase receptors.

Cell death involves signalling in much the same manner as cell cycling; indeed, cell death pathways are activated by growth factors. In the example presented above, cell death is invoked when active E2F is inappropriately present in S phase, for example through infection by mutant DNA viruses that fail to inactivate p53. A difference in cell death pathways is that the balance toward cell death can arise from intracellular signals such as incorrect cell cycle regulatory gene expression, high reactive oxygen species or DNA damage.

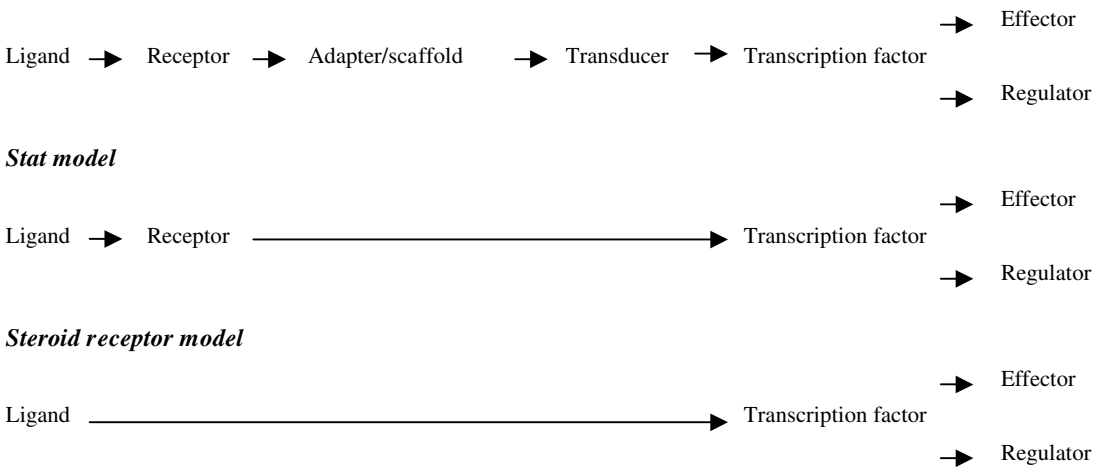

Fig. 13.1 An outline of the main features of signalling systems. Each model from top to the bottom requires less interactions to get from the initiating extracellular molecule (ligand) to the activation of a transcription factor. Cell signalling is obviously much more complex than depicted here.

13.3 Detection of intracellular protein epitopes

13.3.1 Cell preparation

Flow cytometry requires single cell suspensions and microscopy requires the deposition of cells onto a slide, preferably as a single cell layer or less (sections). Although confocal systems can handle cell layers that are thicker, quantification of confocal images from thick sections has not become popular.

For blood, spleen, bone marrow or other loosely aggregated cells, preparation of a single cell suspension involves mincing and pipetting. For tissue culture cells, chelation of divalent cations alone is often sufficient, otherwise chelation and protease treatment can be used. For solid tissues, treatment with Ca^{2+} chelators coupled with proteases provides the best suspensions (Bauer and Jacobberger, 1994; Hitchcock and Ensley, 1993; Pallavicini, 1987; Visscher and Crissman, 1994).

Once single cell suspensions have been made, it is necessary to permeabilise the cell membranes so that immunological probes can be introduced. This can be done by treatment with mild detergents or organic solvents. Both remove lipids. Organic solvents also denature proteins; consequently, they inactivate the enzymes that would otherwise degrade cellular constituents and, thus, fix or preserve the cells. A method of fixation without permeabilisation uses chemically reactive compounds that form covalent substitutions in, and crosslinks between, molecules such as proteins and nucleic acids. The single most used and useful of these agents is formaldehyde. Fixation and permeabilisation are thoroughly reviewed by Jacobberger, (1991, 2000), Clevenger and Shankey (1993), Bauer and Jacobberger (1994) and Camplejohn (1994). The best preparations of cells for flow cytometry are those that have been fixed using a low concentration of formaldehyde and then resuspended in detergent or low-molecular-weight alcohols to permeabilise them. Important points to consider are that:

- the stoichiometry of dye binding to DNA is inversely proportional to the formaldehyde concentration
- the target molecules may be extracted by alcohol or detergent
- alcohol may denature the target molecule(s) and render it (them) immunologically nonreactive
- dependent on the epitope structure and the anti-

body, formaldehyde can react with critical amino acids in the target epitope(s) and render the cells immunologically nonreactive
- the preservation of higher order structure by formaldehyde and detergents may mask epitopes
- alcohol-fixed cells stick to plastic surfaces – especially at room temperature.

Because of these factors, the strategy used by most investigators is to compare several fixation procedures quantitatively for maximisation of the epitope-specific fluorescence (Jacobberger, 2000).

13.3.2 Immunological staining

The comments in this section pertain to high-quality staining defined by maximum sensitivity and ease of quantification; they do not necessarily pertain to 'quick and dirty' procedures. For comprehensive reviews on staining see Jacobberger (1991, 2000), Clevenger and Shankey (1993), Bauer and Jacobberger (1994), Camplejohn (1994), Prussin (1997) and Maino and Picker (1998).

Antibodies can bind to cells nonspecifically. Aside from the intended specific reaction and any cross-reactions or binding to Fc receptors, antibodies will also bind to cellular constituents with low affinity. This becomes a problem when staining intracellularly because there are a large number of potential binding sites. For example, the fluorescence of antigen-negative cells stained with preimmune serum can be brighter than antigen-positive cells stained with immune serum (Jacobberger et al., 1986). To minimise this problem, permeable cells are usually incubated with a buffered solution of protein. These solutions vary, but bovine serum albumin (BSA, 0.1–10%) and dilutions of serum (1–50%) are common. Many investigators scrimp on the use of these reagents but it is false economy. One effective strategy is to make the wash solutions and the antibody diluent the same. If 2% BSA in phosphate-buffered saline (PBS) is used as the blocking buffer then it can be used throughout a procedure to ensure that maximum inhibition of nonspecific binding is achieved.

Antibodies diffuse into cells in approximately 5–15 min (Jacobberger, 1989); consequently, incubations with antibodies are usually for 30–90 min. For reactions with primary antibodies, a balance between washing away bound nonspecific antibody and eluting bound specific antibody is necessary. One procedure that works well is to wash twice at 4°C. However, the exact conditions may depend on each antibody–antigen pair. For primary labelling, monovalent binding may predominate, whereas it is likely that secondary reactions include significant amounts of bivalent binding. In addition, secondary reagents usually have a higher affinity (or avidity) for their antigen than do primary reagents. In any case, more stringent washing conditions can be used with good effect. One method is to wash three times at 37°C. Since antibodies diffuse to equilibrium in ~15 min, washes should be for at least that long. Also, as the laws of mass action are followed, large washing volumes are beneficial. However, this needs to be balanced against minimising the area of plastic surface with which the cells can interact.

Reagents should not be used without assurances that the fluorescence reported is proportional to the target molecule that it is intended to detect. Monoclonal antibodies may often demonstrate significant cross-reaction. The best controls are a negative and positive cell line of the same species and tissue type that one is probing. With or without validating data of this type, an isotype control antibody (nonreactive antibody of the same species and class as the reactive antibody) is often used to estimate background, nonspecific binding plus any other source of unrelated light. However, additional validating data such as Western blot, functional modulation of the target molecule concentration, correct tissue staining pattern, etc. are necessary if positive/negative cell controls are not available.

Direct staining has only recently become available for revealing intracellular antigens rather than lineage-restricted surface antigens. Permeabilised cells are incubated with the probe, washed then analysed. The number of directly labelled probes is relatively few and the majority are conjugated to fluorescein isothiocyanate (FITC). Most of the human cluster of differentiation (CD) antibodies are

Table 13.1 *Commercially available fluorochrome-labelled monoclonal antibodies to intracellular antigens*[a]

Target	Fluorochrome	Company
Cyclins D_1, D_2, D_3, A, and/or B_1	FITC	PharMingen, Oncogene Science, BioSource
CDK1	FITC	Oncogene Science
$p21^{WAF1}$	FITC	Oncogene Science, Biosource
$p27^{KIP1}$	FITC	Biosource
p16	FITC	PharMingen
p16	PE	PharMingen
c-Myc	FITC	Oncogene Science
pRb	FITC	PharMingen
pRb	PE	PharMingen
pRb	Cy-chrome	PharMingen
p53	FITC	PharMingen, Oncogene Science, Biosource, Serotec, DAKO
Bcl-2	FITC	PharMingen, Serotech, DAKO
Bcl-2	PE	PharMingen
PCNA	FITC	PharMingen, Oncogene Science, CalTag, Serotec
PCNA	R-PE	CalTag
Ki-67	FITC	PharMingen
MIP-1α	FITC	R&D Systems
MIP-1β	FITC	R&D Systems
TdT	FITC	Serotec
Vimentin	FITC	Serotec
Cytokeratin	FITC	DAKO
EGFR	FITC	Serotec

CDK1, cyclin-dependent kinase 1; EGFR, epidermal growth factor receptor; FITC, fluorescein isothiocyanate; MIP, macrophage inhibitory protein; PCNA, proliferating cell nuclear antigen; PE, phycoerythrin; pRb, retinoblastoma protein; R-PE, Rhodophycae phycoerythrin; TdT, terminal deoxynucleotidyl transferase.

[a]This table was generated by a Web search of catalogues. Sites that were difficult to fathom or slow were omitted. Widely available probes like labelled anti-CD3 are not listed. Contact details for the companies can be found in the Appendix.

available conjugated to several different reporter molecules. Clinically, some of these are important as intracellular probes in the diagnosis of leukaemias and lymphomas as lineage markers (Jacobberger, 2000). Anti-human cytokine antibodies are also widely available. Some companies that sell directly conjugated monoclonal antibodies to key intracellular target molecules are listed in Table 13.1.

Indirect staining is more complicated than direct staining. It involves incubating permeabilised cells with a primary antibody, washing, incubating with a labelled secondary antibody reactive with the species and class of the primary antibody, washing, then analysis. An advantage is that cells can be probed with any monoclonal antibody but a disadvantage is that the staining procedure is lengthy. To obtain information on the expression of cell cycle-related antigens, cells are typically incubated for 10 min with wash solution, centrifuged, incubated with primary antibody for 1 h, washed twice for 15 min each, incubated with secondary antibody for 1 h, washed three times for 15 min each, incubated with RNAase for 30 min, then resuspended in a propidium iodide (PI) solution and incubated for 1 h. Variations on this type of staining are incubation with a biotinylated primary and labelled streptavidin or avidin secondary reagent, or incubation with primary, biotinylated secondary and labelled streptavidin or avidin tertiary reagent. The last procedure can provide a small enhancement of signal (two- to threefold) (Srivastava et al., 1992).

13.3.3 Multiparametric epitope detection

The drive in the development of quantitative cytometric assays for intracellular antigens has been towards the use of multiple probes. The reasoning behind this is that multiparametric static information not only improves the reliability of inferences about the physiological state of a cell population but is also an essential prerequisite for any acceptable degree of accuracy. In the last few years, several papers have demonstrated that the better availability of interesting or important antibody probes and a wide array of fluorescence reporter molecules have resulted in high-quality staining of more than one antigen plus DNA. An excellent example of this strategy is the study by Juan et al. (1998) in which the expression of cyclin B_1 or cyclin A, phosphorylated histone H3 (H3P) and DNA content were probed simultaneously with antibodies directly labelled with FITC or phycoerythrin (PE) and with 4,6-diamino-2-phenylindole (DAPI) to stain DNA. High levels of phosphorylated histone H3 are normally present only in mitotic cells that are in M phase. Bivariate analysis with cyclin A unequivocally determined the total number of mitotic cells (H3P positive) and subdivided M into prophase through metaphase (cyclin A positive, H3P positive) and anaphase through telophase (cyclin A negative, H3P positive). Similarly, bivariate analysis with cyclin B_1 determined the mitotic cells in prophase through anaphase (cyclin B_1 positive, H3P positive) and telophase cells (cyclin B_1 negative, H3P positive). This suggests a method for measuring the kinetics of mitosis by quantifying the percentage of cells in each of these compartments (hypothesised in Jacobberger (2000)). Since cell cycle regulation involves checkpoints (Osmani and Ye, 1997; Russell, 1998) in the mitotic phase, this approach could provide insights into the actions of drugs that directly or indirectly affect the rate at which cells pass these checkpoints.

Recently Sramkoski et al. (1999) demonstrated the use of indirect plus direct staining to mark mitotic cells with a monoclonal antibody reactive with pRb/p105 (Clevenger et al., 1987) (developed with secondary antibody labelled with cyanin™ 5 (Cy™5)) and the G_2–M cells with an FITC-conjugate anti-cyclin B_1 antibody. DNA was stained with Hoechst 33342. Since both of the probes in this study produce highly specific patterns that have been previously validated independently, the highly reproducible patterns validated the use of an indirect/direct procedure. There was a possibility that the secondary antibody used in the first reaction could be present with a high level of unbound combining sites such that the incoming directly labelled probe bound to it in amounts sufficient to obscure the direct specific (cyclin B_1) signal. This information has been recently used to demonstrate that two indirect procedures could be coupled (J.W. Jacobberger, R.M. Sramkoski and K.E. Shults, unpublished data). In this case, there may be significant binding of the second secondary to the initial primary. However, the extent appears to be manageable (at least in specific cases); consequently it may be possible to determine whether certain combinations of unlabelled primary antibodies will be useful, before fluorochrome-conjugated versions of them become commercially available.

This particular area is critically important because cytometric analyses that will be truly insightful and not simply utilitarian may need to probe several molecules simultaneously (see above). So far, it is known that the following combinations of fluors: FITC/PE/DAPI, FITC/Cy™5/DAPI, Alexa™-350/FITC/PI, and FITC/PE/Cy™5/DAPI can be used to detect up to three antigens coupled with DNA (DAPI, Hoechst 33342, and Hoechst 33258 can be used interchangeably). Overlap in the emission spectra of FITC and PE can be a problem, but acceptable FITC–anti-cyclin B_1 patterns and PE–anti-p16 can be obtained (unpublished observations). It should be possible to bring antibodies labelled with peridinin–chlorophyll *a* complex (PerCP) into this milieu and if so, four epitopes and DNA content might be measured at the same time with currently configured three-laser commercial cytometers (ultraviolet, 488 nm, 633 nm excitations). It is possible that, for many studies, DNA can be dispensed with and an ultraviolet or 410 nm excited probe

used, thereby providing enough signal for the detection of five epitopes. While this number may be too few to be ideal, it should provide useful information on the cell population.

13.4 Determination of DNA and protein content

13.4.1 DNA content

Much of the work aimed at detecting and quantifying intracellular antigens by cytometry has been coupled with analysis of DNA content because of the investigator's interest in cell cycle, apoptosis or solid tumour phenotype. The most obvious exception to this is the detection of intracellular cytokines in lymphoid cells by investigators interested in immunology. This makes sense because the dominant theme in cytometry within the immunology community is the categorisation of cells into subsets or unique populations by virtue of the presence or absence, rather than the level of expression, of a particular protein. The need or desire to assess DNA content has always been problematic. As mentioned earlier, formaldehyde-fixed cells stain poorly for DNA, alcohol-fixed cells are sticky and difficult to work with and DNA dyes have broad excitation and emission spectra, thus limiting the number of immunofluorescent probes that can be used in conjunction with any particular DNA dye. There does not appear to be any solution at present for this problem and compromises must be made. However, recent papers describing probes that mark mitotic cells well (Anderson et al., 1998; Di Vinci et al., 1993; Friedrich et al., 1998; Juan et al., 1998; Sramkoski et al., 1999) demonstrate that a mitotic index may be determined by immunological probes. When it is necessary to obtain only a relative index of cell proliferation, then one of these probes might be used and the DNA dye eliminated. An example of this might be clinical analysis of solid tumour cells where a mitotic index, or a determination of the percentage of cells in S phase, may provide the same information. However, the low frequency of mitotic cells relative to S phase may be a problem. If not, DNA ploidy assays could be carried out independently. Needless to say, if the cell cycle pattern of expression is important, then there is no substitute for a DNA dye at present (see also Ch. 10 for DNA quantification).

13.4.2 Total protein

Some investigators have coupled measurement of total protein content with measurement of specific proteins by immunological means. Reactive dyes like FITC can be used or the noncovalent dye SR101 can be used (Engelhard et al., 1991). In the most basic type of analysis, total protein content provides a baseline with which to compare movement of expression levels in the specific protein. Thus, if a specific protein increases or decreases in line with movement of total protein, then the effect on the specific protein might be nonspecific at first glance. In contrast, if the effect on the specific protein deviates from that on total protein content, then the effect might be more direct. Inherently, for cell proliferation studies and inferences, this makes a lot of sense because cell cycle progression is at the most basic level tied to cell metabolism and energy levels. The value of this measurement in clinical assays is untested to our knowledge but seems worth investigating (see also Ch. 3 for fluorochrome staining of total protein).

13.5 Assessing the physiological status of cells

Alterations in the intracellular environment can be monitored using fluorescent probes for live cell function. In contrast to static measurements of proteins, the important applications here include the measurement of transmembrane potentials, ion concentrations, the generation of reactive oxygen intermediates (ROI) or species (ROS) and the maintenance of the cellular redox environment. Individually, these techniques are often informative. For example, reactive oxygen probes are used in the clinic to assess neutrophil function in conditions such as chronic granulomatous disease, while the

measurement of Ca^{2+} fluxes is widely used in immunology and pharmacology research to determine cellular reactivity. It is possible to combine several probes that have different excitation and emission spectra, and examples of this approach are given below. As with the multicolour immunofluorescence techniques described elsewhere in this chapter, the simultaneous measurement of inter-related biochemical changes can be used to study complex cellular processes.

13.5.1 Membrane potential

Measurements of membrane potential are made using fluorigenic probes that readily cross an intact outer membrane and introduce minimal perturbations to live cell function. With the exception of equilibrium dyes used to measure membrane potential, the fluorescent product is retained as a result of chemical modifications that occur intracellularly. This is usually achieved by loading the dye in the form of a membrane-permeant ester that can be hydrolysed to a polar, nonpermeant form by intracellular esterases.

Stains that are sensitive to membrane potential have the chemical properties of being cationic and amphipathic; consequently, dye molecules passively accumulate in membrane-bound compartments that carry a negative charge on the inner surface. Although these techniques are sensitive to the surface membrane potential, most of the signal strength detected by flow cytometry reflects the mitochondrial inner membrane potential (see also Chs. 3, 12 and 16 for dyes to monitor transmembrane potential).

13.5.2 Intracellular ion concentrations

Ion probes incorporate chelating groups with affinities such that at physiological concentrations some dye molecules are ion bound, and some are ion free. The probes are designed so that the two forms have different spectral properties. Ideally, this involves a shift in the peak emission wavelength so that the ratio of the bound to free emissions gives a measure of ion concentration that is independent of the number of dye molecules inside the cell. For some ions, such as Na^+, K^+ and Zn^{2+}, 'ratiometric' probes are not yet available, but useful information can still be obtained using probes that show changes in peak fluorescence intensity in the ion-bound form. Ion probes are loaded into cells as membrane-permeant esters (see also Chs. 3 and 7 for dye monitoring of intracellular ions).

13.5.3 Reactive oxygen and nitrogen species

Assessment of the oxidising/reducing environment uses stains that are irreversibly modified by redox reactions. Reactive oxygen intermediates such as hydrogen peroxide and superoxide can be readily detected using dyes that are chemically reduced forms of fluorescent stains such as ethidium and dichlorofluorescein. As these become oxidised, the generation of fluorescence gives a measurement of intracellular reactive oxygen generation. Nitric oxide generation can be measured using diaminofluorescein, which works on a similar principle (see also Chs. 3 and 7 for monitoring oxidative metabolism).

13.5.4 Glutathione content

The tripeptide glutathione (GSH) is the most significant intracellular reducing agent in terms of the molar concentration. Cells increase GSH in response to external stimuli or mild oxidative stress, whereas decreases occur during overwhelming oxidative stress or apoptosis, when the redox balance shifts from the normal reducing state to an oxidising intracellular environment. These changes can be monitored at the single cell level using the reactive probes monochlorobimane or monobromobimane, which form fluorescent complexes with GSH.

13.6 Monitoring physiological changes during cell death

Aberrant regulation of cell death plays a key role in a

wide range of pathological conditions, including neurodegenerative diseases, disorders of the immune system and cancer. At the molecular level, these abnormalities appear to alter a balance between death effector mechanisms and cell survival pathways. However, at the present time, it is difficult to fit all of the individual genes involved in apoptosis regulation into a single unifying scheme. An alternative viewpoint is to examine programmed cell death in terms of the critical physiological changes that occur during this process, such as alterations in the cellular redox states, loss of mitochondrial membrane potential and deregulation of intracellular Ca^{2+} levels. The genes involved in apoptosis regulation can then be examined for their impact on this death sequence. For this approach, multiparametric flow cytometry is an extremely powerful technique because of its ability to examine complex physiological processes occurring in subpopulations of cells.

13.6.1 Mitochondrial permeability transition

One of the key physiological events during early apoptosis is the loss of mitochondrial membrane potential as a result of the opening of a pore complex centred on the ADP/ATP translocator in the inner membrane (Heiden et al., 1999; Kroemer, 1998). In addition to dissipating the electrochemical gradient used to drive ATP synthase, the permeability transition results in osmotic swelling of the mitochondria and rupture of the outer membrane. This releases mediators of the late stages of apoptosis, several of which are located in the intermembrane space (Granville et al., 1998; Kroemer, 1998). The electron carrier cytochrome *c* is the best characterised of these. Upon release into the cytoplasm, cytochrome *c* binds to the docking protein apoptosis-inducing factor 1 (Apaf-1), which is then able to activate caspase-9; this activates the executioner caspase-3, which is responsible for many of the structural and morphological changes that characterise apoptotic cell death (Barinaga, 1998).

13.6.2 Metabolic consequences of the permeability transition

In addition to activating of the executioner phase of apoptosis, the mitochondrial permeability transition has major metabolic consequences (Marchetti et al., 1996). Dissipation of the inner mitochondrial membrane potential prevents the synthesis of ATP by oxidative phosphorylation. Intracellular Ca^{2+} homeostasis is disrupted, partly because ATP is needed to drive Ca^{2+} pumps and also because energised mitochondria are used to sequester Ca^{2+} and provide a buffer for short-term Ca^{2+} fluctuations. The loss of cytochrome *c* results in electron carriers in the respiratory chain being held in their reduced state, where the energy can be dissipated by reductions of molecular oxygen (Cai and Jones, 1998). Reactive oxygen intermediates generated by this process are a major source of the oxidative stress that characterises late phases of cell death. Because of this accumulation of severe metabolic changes, the permeability transition is a lethal event, regardless of whether late caspases are activated. In the presence of broad-specificity caspase inhibitors such as benzyloxycarbonyl-valinyl-alaninyl-aspartyl-(*O*-methyl)- fluoromethylketone (zVAD-fmk), the cellular features following the mitochondrial permeability transition resemble those of necrosis (Xiang et al., 1996).

13.6.3 Oxidative stress and maintenance of cellular redox balance

The high levels of reactive oxygen generation following cytochrome *c* release are associated with severe, irreversible metabolic damage. Oxidative stress can also occur earlier in the apoptosis pathway, through to inefficiencies in mitochondrial respiration or the increased generation of reactive oxygen by intracellular enzyme systems such as the p53-dependent oxidoreductase phosphatidylinositol glycosyl phospholipid 3 (PIG3) (Polyak et al., 1997). Reactive oxygen intermediates such as hydrogen peroxide can modify protein thiol redox states by producing disulphide bonding between

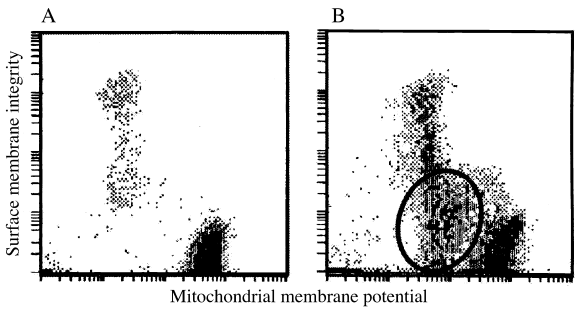

Fig. 13.2 Dual-parameter plots of mitochondrial membrane potential (fluorescence intensity of the octadecyl indocarbocyanin dye $DiIC_1{}^8(5)$: abscissa; logarithmic scale) and surface membrane integrity potential (fluorescence intensity of propidium iodide: ordinate; logarithmic scale). (A) Untreated cells from a patient with acute myeloid leukaemia stage 2 (AML-2). (B) Cells after treatment for 24 h with cytosine arabinoside. The circle indicates a population of drug-treated cells that has lost mitochondrial membrane potential but still retains an intact outer membrane.

adjacent cysteine residues. This can be injurious to cells; for example, thiol oxidation in the ADP/ATP translocator can trigger the permeability transition. However, many genes that code for cellular antioxidants are under redox-sensitive promoters such as the transcription factor NFB, thus providing a feedback mechanism that allows cells to adapt to oxidative stress by upregulating antioxidant defences (Aslund and Beckwith, 1999).

13.6.4 Mapping the death sequence by multiparametric flow cytometry

The following series of multiparameter flow cytometry data illustrate the potential for mapping the sequence of physiological events that occur during apoptosis. Although fluorescence probes for live cell function are used, the general approach is similar to that described in this chapter for studying cell cycle regulation using multiple fluorescent antibodies. The example used here is a well-characterised human leukaemia model in which apoptosis is triggered by the anti-leukaemic agent cytosine arabinoside (Miyauchi et al., 1989). The events shown are consistent with an extensive literature that deals with the subject using a wide range of model systems.

By labelling apoptotic cells with a membrane potential-sensitive stain, such as the octadecyl indocarbocyanine dye ($DiIC_{18}(5)$), in the presence of the DNA intercalating stain PI, which is excluded by an intact surface membrane, it is possible to demonstrate that the permeability transition occurs in cells that retain an intact outer membrane (Fig. 13.2). Note that all cells that have lost their surface membrane integrity have a low mitochondrial membrane potential, and that all cells with energised mitochondria retain an intact outer membrane. A population of cells, marked as a circle in Fig. 13.2B, has lost mitochondrial membrane potential but retains an intact outer membrane. A sequence of cellular viability to loss of mitochondrial membrane potential to loss of outer membrane integrity is suggested by this simple dual-labelling technique.

Because the ionised Ca^{2+} probe indo-1 has excitation and emission characteristics that are compatible with PI and the mitochondrial membrane potential probe, it is possible to examine the relationship between Ca^{2+} regulation and the permeability transition using a triple labelling technique. As seen in Fig. 13.3, cells that retain energised mitochondria also maintain a low level of intracellular Ca^{2+}. Some of the cells in Fig. 13.2 with low mitochondrial membrane potential and an intact outer membrane have increased their intracellular Ca^{2+}, consistent with a key role of mitochondria in normal Ca^{2+} regulation. However, note that intracellular Ca^{2+} levels are still regulated in a proportion of cells that have lost mitochondrial membrane potential (circled). This suggests that for a short period of time, cells are able to regulate intracellular Ca^{2+} despite the loss of mitochondrial membrane potential. Possibly this is achieved using ATP generated by glycolysis.

Using the same experimental model, complex alterations in the cellular redox environment can be demonstrated by simultaneously labelling cells with a reactive oxygen probe such as dichlorofluorescein, and the glutathione stain monobromobimane

(Hedley and McCulloch, 1996). As seen in Fig. 13.4, considerable intracellular heterogeneity is generated in the levels of ROI and GSH during drug exposure, with distinct subpopulations of cells appearing. Since an identical drug treatment is being given to genetically homogenous cells, the likeliest explanation for this heterogeneity is that the subpopulations represent transition states in a pathway. The population labelled 1 shows elevations in both ROI and GSH, consistent with an early increase in reactive oxygen generation, and adaptation to this by upregulation of the antioxidant glutathione. Population 2 cells show much greater levels of ROI, with loss of GSH. Since there are relatively few transitional events seen in the figure, progression from population 1 to population 2 is likely to proceed rapidly. In terms of redox systems, this shift is consistent with a transition to an overall oxidising intracellular redox state. From this state, a second transition can be seen in Fig. 13.4, where cells show a further reduction of GSH, and a decrease in ROI generation (population 3). Although not illustrated in this dataset, this second transition is correlated with the increases in intracellular Ca^{2+} shown in Fig. 13.3. Since reactive oxygen generation is an active metabolic process, the transition to this low ROI/GSH, high Ca^{2+} state is indicative of metabolic death, which precedes the ultimate loss of outer membrane integrity.

When the mitochondrial membrane potential dye is introduced to the combined ROI plus GSH plus PI uptake-staining protocol, it can now be seen that the transition to high ROI and loss of GSH coincides with the mitochondrial permeability transition (Backway et al., 1997). These inter-relations are shown as a series of bivariate plots in Fig. 13.5.

The alterations in cellular redox balance can be interpreted as indicating increases in mitochondrial reactive oxygen generation, caused by the loss of cytochrome *c*, coupled with the inability to maintain GSH levels because of the severe energy deficit that occurs with the loss of oxidative phosphorylation as a source of ATP. This detailed description of the physiological changes that occur during apoptosis, obtained by multiparametric flow cytometry,

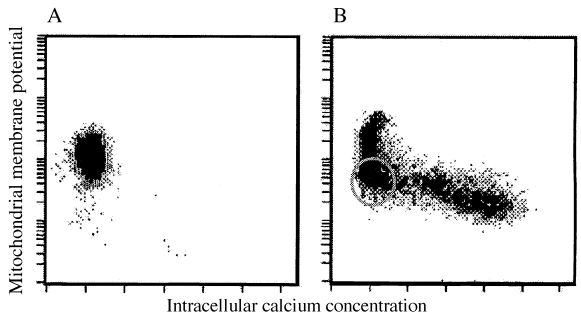

Fig. 13.3 Relationship between loss of mitochondrial membrane potential (fluorescence intensity of the octadecyl indocarbocyanin dye $DiIC_1{}^8(5)$: ordinate; logarithmic scale) and deregulation of intracellular Ca^{2+} (fluorescence intensity of indo-1: abscissa; linear scale).
(A) Untreated cells from a patient with acute myeloid leukaemia stage 2 (AML-2). (B) Cells after treatment for 24 h with cytosine arabinoside. The circle indicates a population of drug-treated cells that has lost mitochondrial membrane potential but is still able to maintain a low Ca^{2+} level. Plotted from same data set as Fig. 13.2.

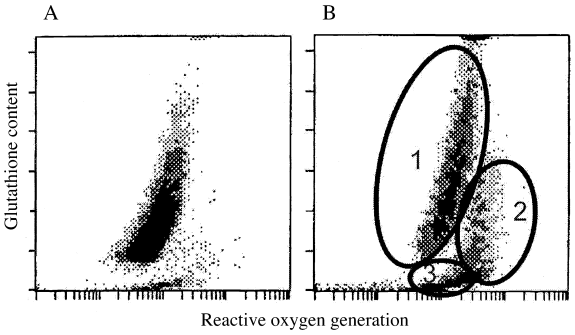

Fig. 13.4 Dual-parameter plots of glutathione content (monobromobimane fluorescence: ordinate; linear scale) versus reactive oxygen generation (dichlorofluorescin fluorescence: abscissa; logarithmic scale) in cells from a patient with acute myeloid leukaemia stage 2 (AML-2).
(A) Untreated cells and (B) cells after treatment with cytosine arabinoside. The data are gated to exclude propidium iodide-positive cells. Note the complex alterations in cellular redox state that occur during apoptosis. See text for an explanation of populations 1–3.

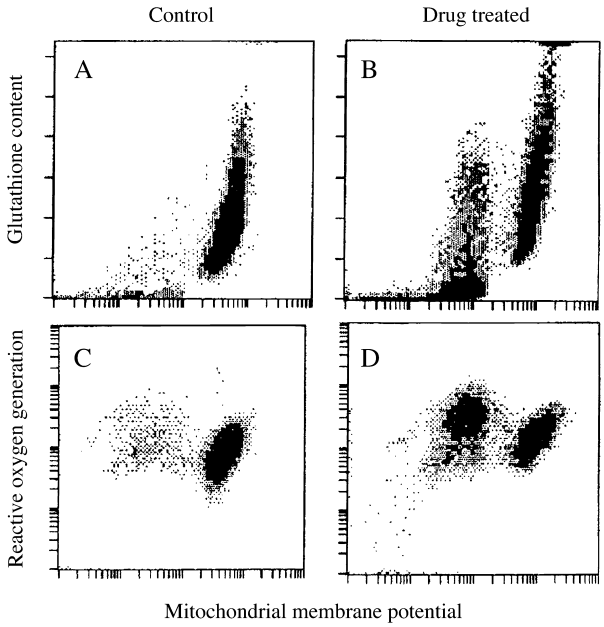

Fig. 13.5 Relationships between oxidative stress parameters and mitochondrial membrane potential in cells from a patient with acute myeloid leukaemia. (A,C) Untreated (control) cells and (B,D) during drug-induced apoptosis. Plotted from the same dataset used in Fig. 13.4. See Figs. 13.3 and 13.4 for staining details.

supports the idea of the permeability transition as a key coordinating feature of apoptosis.

There remain several outstanding questions concerning the 'death pathway' outlined above. Early-phase caspases, activated at the cell surface by signalling pathways, can precipitate the permeability transition, thus providing an amplification step that releases activators of late caspases. However, in some experimental models, the permeability transition appears not be an essential feature of apoptosis, since early-phase caspases are able to activate the executioner phase directly. Cytochrome *c* can be released from mitochondria prior to the loss of membrane potential, suggesting that osmotic rupture of the outer membrane is not an essential feature of the mitochondrial phase of apoptosis (Heiden et al., 1999; Saikumar et al., 1998a,b). The various members of the Bcl-2 family of proteins play complex roles in the control of apoptosis that are not completely understood (Reed, 1998). However, it is likely that differences in their expression levels between cell lines help to explain some of the apparent inconsistencies in our current picture of the mitochondrial phase of apoptosis. (Additional aspects of apoptosis are discussed in Ch. 11.)

13.7 Immunodetection of target molecules and pathways

13.7.1 Diagnosis

An excellent example by Shackney and Shankey (1997) of the multiparametric analysis of clinical material is illustrative of what might be achieved in elucidating gene expression. In this study, primary tumours from 94 patients with breast cancer were evaluated for DNA content and expression of the EGF receptor (EGFR), Her2 (a surface membrane protein) and $p21^{ras}$ by correlated flow cytometry. The relative flow cytometric results of EGFR and Her2 were reported in absolute numbers of molecules by a method employing a standard cell line and enzyme-linked immunosorbent assay (ELISA) to obtain the conversion.

When the data were treated separately (i.e. when the mean of each parameter was treated as an independent measure), there was no statistically supported correlation between the expression of any of these three markers. The significant findings were that the diploid tumours did not overexpress the three genes and that aneuploid tumours overexpressed Her2, which might be expected. However, when the data were analysed in a correlated fashion on a per cell basis, 96% of the tumours contained a cell population in which the expression of Her2 was directly correlated with that of EGFR. The ratio (Her2 : EGFR) was >1 for most DNA tetraploid and aneuploid tumours and <1 for most DNA diploid tumours. Overexpresssion of $p21^{ras}$ occurred in cells that overexpressed Her2, EGFR, or both, but rarely in cells that did not overexpress one or the other.

The authors state that the data are consistent with a model in which EGFR and Her2 heterodimerise and upregulate Ras expression. (However, the Her2 :

EGFR ratios suggest a distinct imbalance where a significant number of molecules of Her2 or EGFR would not have a heteropartner.) The tumours fell neatly into two patterns: (i) DNA aneuploid (including tetraploid and aneuploid) with high Her2/high Her2 : EGFR (59 of 94 tumours) or (ii) DNA diploid with high EGFR/low Her2 : EGFR (19 of 94 tumours). Therefore, it was speculated that these represent two different evolutionary sequences (Shackney and Shankey, 1997). Additionally it was shown that tumours with Her2 : EGFR >2 contained infiltrating ductal carcinoma, while infiltrating pure lobular carcinomas had Her2 : EGFR <2. This paper is a landmark because:

- a cell-based multiparameter study of regulatory proteins and stem line identification has been applied to clinical samples on a large scale
- the results were expressed in absolute numbers of molecules so that better sense could be made of the multiparametric data
- ratios between components were used to reduce the complexity of the data
- DNA content was used to remove proliferation-related expression from the analysis.

However, the paper is not without problems. For example, it is arguable that genetic evolution data can be derived from studies of gene expression where the gene expression levels are highly modulated and the data are continuous distributions rather than discontinuities like the mutations themselves. The exact significance of the measurements is not known; that is, the percentage of each distribution caused by error or by biological variation is unknown. The unknown percentage of error could get amplified by deriving ratios. Finally, the many data transformations that were necessary make it difficult to understand the relationship of the initial measurement to the final datum. However, none of these potential problems diminish the importance of this paper. It shows both the power of cellular-based assays and the complexity that monitoring four parameters produces when three of those parameters are regulatory molecules. For a longer version of this evaluation, see Jacobberger (2000) from which this section was derived.

13.7.2 Therapeutic monitoring

More recently, Jacobberger et al. (1999) developed an assay to monitor tumour suppressor (p53) reconstitution in the gene therapy of ovarian carcinoma. In this work, cells were stained with FITC–DO7, an anti-p53 antibody and unconjugated IF-2, a monoclonal antibody to the murine double minute 2 protein (Mdm2), in an indirect/direct assay. PE–goat anti-mouse was used for the second label probe. When prostate or ovarian carcinoma cell lines were infected with a recombinant, replication-defective adenovirus vector encoding wild-type human p53 (ad-p53), the number of cells that expressed p53 above resting state were quantified as well as the expression level of induced p53 and Mdm2. Thus, this two-parameter flow cytometry assay permitted:

- quantification of the percentage of cells that were infected and expressed p53
- determination that the expressed p53 was active by virtue of Mdm2 expression.

Figure 13.6 shows some typical data for a cell line infection.

The data suggest that the transcriptional power of p53 (at least for Mdm2) is saturated in the cells expressing the p53 at the highest levels. This type of inference could not be made from a single sample utilising a 'bulk' assay like an ELISA or Western blot. However, this assay might be much less meaningful for clinical samples with cellular heterogeneity. To address this, the assay has been coupled with CD45 staining and is currently being used in a meaningful way to monitor nonimmune ascites cells from patients undergoing ad-p53 treatment in phase I clinical trials. This is an example of utilising pathways (in this case a p53 segment) to assist evaluation of therapeutic efficacy and using quantitative and multiparametric cytometry to reduce the complexity of clinical samples with high cellular heterogeneity.

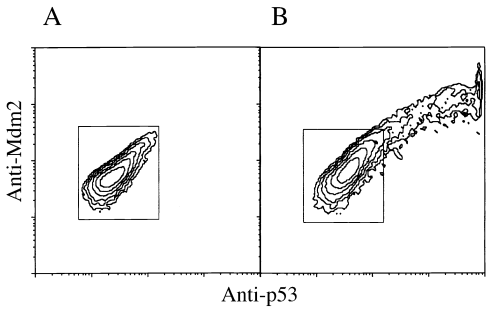

Fig. 13.6 p53 gene transfer. An ovarian carcinoma cell line, PA1, was infected with an adenovirus vector encoding wild-type human p53 at 300 infectious units per cell. At 24 h, cells were trypsinised, fixed and stained for p53 and Mdm2 as described in the text. (A) The 'uninfected or resting state'. (B) The 'Ad-p53 treated or transfected state'. The results show that Mdm2 is transcriptionally activated by p53.

13.8 Protocols

It should by now be apparent that no 'basic/starter' protocols have been included in this chapter. This omission is deliberate because there are so many different variables that need to be optimised for a particular intracellular labelling application. Researchers who need to assay intracellular components are recommended to read the general reference texts by Robinson (1993, 1997) and Darzynkiewicz et al. (1994) and then to optimise the variables described for their own system.

13.9 Authors' comments

When we were first asked to write this chapter, it was not clear to us that a subject termed 'intracellular cellular components: metabolism and signalling' could be put together with any continuity. First, the subject is very broad and, second, it can be approached from several angles. We have reduced the complexity somewhat by mentally focusing on cytometry related to cancer and cancer therapeutics, which was convenient since this is colinear with our interests. A second mental exercise was to view both immunocytochemical approaches and fluorescence reporter approaches as assays of cellular physiology. We employed this for the sake of continuity; however, the exercise was not difficult since, explicitly conveyed or not, gaining knowledge of the cellular physiological state at the time of assay is almost always at the heart of most cytometric assays of cell regulatory and signalling molecules. Although space was limited, we hope that we conveyed the wealth of tools that can be brought to bear when solving a problem, testing a hypothesis or simply exploring a part of the nature of a cell population in a 'resting state' and an 'altered state' after interaction with an exogenous stimulus. In the near future, it may be that successful treatment of cancer and other diseases will become more rooted in science and less rooted in physician experience and unknown factors. We believe (based on the principle that we hope we have conveyed here) that the snapshots that cytometry gives us of both population complexity and the physiological state of each subpopulation will play a significant role in that transition.

13.10 REFERENCES

Albanese, C., Johnson, L., Watanabe, G., Eklund, N., Vu, D., Arnold, A., Pestell, R.G. (1995) Transforming p21 ras mutants and c-Ets-2 activate the cyclin D_1 promoter through distinguishable regions. *Journal of Biological Chemistry* **270**, 23589–97.

Anderson, H.L, de Jong, G., Vincent, I., Roberge, M. (1998) Flow cytometry of mitotic cells. *Experimental Cell Research* **238**, 498–502.

Aslund, R., Beckwith, J. (1999) Bridge over troubled waters: sensing stress by disulfide bond formation. *Cell* **96**, 751–3.

Backway, K.L., McCulloch, E.A., Chow, S., Hedley, D.W. (1997) Relationships between the mitochondrial permeability transition and oxidative stress during ara-C toxicity. *Cancer Research* **57**, 2446–51.

Barinaga, M. (1998) Death by dozens of cuts. [News] *Science* **280**, 32–4.

Bauer, K.D., Jacobberger, J.W. (1994) Analysis of intracellular proteins. In: Darzynkiewicz, Z., Robinson, J.P., Crissman, H.A. (eds.), *Flow Cytometry, Methods in Cell Biology,* Vol. 41, pp. 351–76. Academic Press, San Diego, CA.

Cai, J., Jones, D.P. (1998) Superoxide in apoptosis. Mitochondrial generation triggered by cytochrome *c* loss. *Journal of Biological Chemistry* **273**, 11401–4.

Camplejohn, R.S. (1994) The measurement of intracellular antigens and DNA by multiparametric flow cytometry. *Journal of Microscopy* **176**, 1–7.

Clevenger, C.V., Shankey, T.V. (1993) Cytochemistry II: immunofluorescence measurement of intracellular antigens. In: Bauer, K.D., Duque, R.E., Shankey, T.V. (eds.), *Clinical Flow Cytometry,* pp. 157–76. Williams & Wilkins, Baltimore, MD.

Clevenger, C.V., Epstein, A.L., Bauer, K.D. (1987) Modulation of the nuclear antigen p105 as a function of cell-cycle progression. *Journal of Cellular Physiology* **130**, 336–43.

Darzynkiewicz, Z., Robinson, J.P., Crissman, H.A. (eds.) (1994) *Flow Cytometry, Methods in Cell Biology,* Vols. 41, 42. Academic Press, San Diego, CA.

Di Vinci, A., Geido, E., Keffer, U., Vidali, G., Glaretti, W. (1993) Quantitative analysis of mitotic and early-G_1 cells using monoclonal antibodies against the AF-2 protein. *Cytometry* **14**, 421–7.

Engelhard, H.H.D., Krupka, J.L., Bauer, K.D. (1991) Simultaneous quantification of c-Myc oncoprotein, total cellular protein, and DNA content using multiparameter flow cytometry. *Cytometry* **12**, 68–76.

Friedrich, T.D., Okubo, E., Laffin, J., Leliman, J.M. (1998) Okadaic acid induces appearance of the mitotic epitope MPM-2 in SV40-infected CV-1 cells with a >G2-phase DNA content. *Cytometry* **31**, 260–4.

Garrington, T.P., Johnson, G.L. (1999) Organization and regulation of mitogenactivated protein kinase signaling pathways. *Current Opinion in Cell Biology* **11**, 211–18.

Granville, D.J, Carthy, C.M., Hunt, D.W., McManus, B.M. (1998) Apoptosis: molecular aspects of cell death and disease. *Laboratory Investigation* **78**, 893–913.

Hackel, P.O., Zwick, E., Prenzel, N., Ullrich, A. (1999) Epidermal growth factor receptors: critical mediators of multiple receptor pathways. *Current Opinion in Cell Biology* **11**, 184–9.

Hedley, D.W., McCulloch, E.A. (1996) Generation of reactive oxygen intermediates after treatment of blasts of acute myeloblastic leukemia with cytosine arabinoside: role of *bcl*-2. *Leukemia* **10**, 1143–9.

Heiden, M.G., Chandel, N.S., Schumacker, P.T., Thompson, C.B. (1999) Bcl-xL prevents cell death following growth factor withdrawal by facilitating mitochondrial ATP/ADP exchange. *Molecular Cell* **3**, 159–67.

Hitchcock, C.L., Ensley, J.F. (1993) Technical considerations for dissociation of fresh and archival tumors. In: Bauer, K.D., Duque, R.E., Shankey, T.V. (eds.), *Clinical Flow Cytometry, Principles and Application,* pp. 93–110. Williams & Wilkins, Baltimore, MD.

Jacobberger, J.W. (1989) Cell cycle expression of nuclear proteins. In: Yen, A. (ed.), *Flow Cytometry: Advanced Research and Applications,* Vol. 1, pp. 305–26. CRC Press, Boca Raton, FL.

Jacobberger, J.W. (1991) Intracellular antigen staining: quantitative immunofluorescence. *Methods* **2**, 207–18.

Jacobberger, J.W. (2000) Flow cytometric analysis of intracellular protein epitopes. In: Stewart, C.C., Nicholson, J.K.A. (eds.), *Immunophenotyping, Cytometric Cellular Analysis*, pp. 361–406. John Wiley & Sons, New York.

Jacobberger, J.W, Fogleman, D., Lichman, J.M. (1986) Analysis of intracellular antigens by flow cytometry. *Cytometry* **7**, 356–64.

Jacobberger, J.W., Sramkoski, R.M., Zhang, D., Zumstein, L.A., Doerksen, L.D., Merritt, J.A., Wright, S.A., Shults, K.E. (1999) Bivariate analysis of the p53 pathway to evaluate Ad-p53 gene therapy efficacy. *Cytometry* **38**, 201–13.

Juan, G., Traganos, F., James, W.M., Ray, J.M., Roberge, M., Sauve, D.M., Anderson, H., Darzynkiewicz, Z. (1998) Histone H3 phosphorylation and expression of cyclins A and B1 measured in individual cells during their progression through G2 and mitosis. *Cytometry* **32**, 71–7.

Kroemer, G. (1998) The mitochondrion as an integrator/coordinator of cell death pathways. *Cell Death and Differentiation* **5**, 547.

Maino, V.C., Picker, L.J. (1998) Identification of functional subsets by flow cytometry: intracellular detection of cytokine expression. *Cytometry* **34**, 207–15.

Marchetti, P., Castedo, M., Susin, S.A., Zanizami, N., Hirsch, T., Macho, A., Haeffner, A., Hirsch, R., Geuskens, M., Kroemer, G. (1996) Mitochondrial permeability transition is a central coordinating event of apoptosis. *Journal of Experimental Medicine* **184**, 1155–60.

Miyauchi, L., Kellcher, C.A., Wang, C., Minkin, S., McCulloch, E.A. (1989) Growth factors influence the sensitivity of leukemic stem cells to cytosine arabinoside in culture. *Blood* **73**, 1272–8.

Moghal, N., Stemberg, P.W. (1999) Multiple positive and negative regulators of signaling by the EGF-receptor. *Current Opinion in Cell Biology* **11**, 190–6.

Osmani, S.A., Ye, X.S. (1997) Targets of checkpoints controlling mitosis: lessons from lower eukaryotes. *Trends in Cell Biology* **7**, 283–8.

Pallavicini, M.G. (1987) Solid tissue dispersal for cytokinetic analyses. In: Gray, J.W., Darzynkiewicz, Z. (eds.), *Techniques in Cell Cycle Analysis Series: Biological Methods,* pp. 139–62. Humana Press, Clifton, NJ.

Polyak, K., Xia, Y., Zweier, J.L., Kinzler, K.W., Vogelstein, B. (1997) A model for p53-induced apoptosis. [See comments] *Nature* **389**, 300–5.

Prussin, C. (1997) Cytokine flow cytometry: understanding cytokine biology at the single-cell level. *Journal of Clinical Immunology* **17**, 195–204.

Reed, J.C. (1998) Bcl-2 family proteins. *Oncogene* **17**, 3225–36.

Robinson, J.P. (ed.) (1993) *Handbook of Flow Cytometry Methods*. Wiley-Liss, New York.

Robinson, J.P. (ed.) (1997) *Current Protocols in Cytometry*, Vol. 11. Wiley-Liss, New York.

Roussel, M.F. (1998) Key effectors of signal transduction and G_1 progression. *Advances in Cancer Research* **74**, 1–24.

Russell, P. (1998) Checkpoints on the road to mitosis. *Trends in Biochemical Sciences* **23**, 399–402.

Saikumar, P., Dong, Z., Patel, Y., Hall, K., Hopfer, U., Weinberg, J.M., Venkatachalam, M.A. (1998a) Role of hypoxia-induced Bax translocation and cytochrome *c* release in reoxygenation injury. *Oncogene* **17**, 3401–15.

Saikumar, P., Dong, Z., Weinberg, J.M., Venkatachalam, M.A. (1998b) Mechanisms of cell death in hypoxia/reoxygenation injury. *Oncogene* **17**, 3341–9.

Shackney, S.E., Shankey, T.V. (1997) Common patterns of genetic evolution in human solid tumors. *Cytometry* **29**, 1–27.

Sramkoski, R.M., Wormsley, S.W., Bolton, W.E., Crumpler, D.C., Jacobberger, J.W. (1999) Simultaneous detection of cyclin B_1, p105, and DNA content provides complete cell cycle phase fraction analysis of cells that endoreduplicate. *Cytometry* **35**, 274–83.

Srivastava, P., Sladek, T.L., Goodman, M.N., Jacobberger, J.W. (1992) Streptavidin-based quantitative staining of intracellular antigens for flow cytometric analysis. *Cytometry* **13**, 711–21.

Visscher, D.W., Crissman, J.D. (1994) Dissociation of intact cells from tumors and normal tissues. In: Darzynkiewicz, Z., Robinson, J.P., Crissman, H.A. (eds.), *Flow Cytometry: Methods in Cell Biology*, 2nd edn, Vol. 41, pp. 1–13. Academic Press, San Diego, CA.

Xiang, L., Chao, D.T., Korsmeyer, S.J. (1996) BAX-induced cell death may not require interleukin 1 beta-converting enzyme-like proteases. *Proceedings of the National Academy of Science of the USA* **93**, 14559–63.

Yan, Y.X., Nakagawa, H., Lee, M.H., Rustgi, A.K. (1997) Transforming growth factor-alpha enhances cyclin D_1 transcription through the binding of early growth response protein to a *cis*-regulatory element in the cyclin D_1 promoter. *Journal of Biological Chemistry* **272**, 33181–90.

14

Cell–cell interactions

Marion G. Macey[1] and Mary R. Cahill[2]

[1]St Bartholomew's and Royal London School of Medicine and Dentistry, Queen Mary and Westfield College, London

[2]Regional General Hospital, Dooradyle, Limerick, Republic of Ireland

14.1 Adhesion molecules in cell–cell interactions

14.1.1 Introduction

Cell–cell interactions are a feature and function of all living cells. Examples include interactions of mobile cells such as ova and sperm and the solid coalescence of skin cells to form a watertight epidermis. Cell–cell interactions are of importance both in cell structure and cell function. Cell–cell interactions provide physical barriers (skin), boundaries (organ capsules) and tissue cohesion. They provide a mechanism of communication between cells (nervous tissue) and are the means of reproduction (the cell–cell interaction of ova and sperm). When these interactions occur in mobile cells, for example in the blood, they are the means of switching on, spreading or regulating fundamental processes such as inflammation and coagulation.

Many cell–cell interactions are mediated via cell adhesion molecules (CAMs). CAMs are surface membrane structures designed or adaptable to binding with similar structures, termed ligands, on other cells. Many CAMs have now been identified and their molecular structures have been elucidated. Based on structural homology, to date, six families of CAMs have been defined but there are a number of new adhesion molecules that are yet to be grouped.

The families so far known are the immunoglobulin family, the cadherin family, the integrin family, the selectins, the surface proteoglycan family and the sialomucin family. CAMs play an important role in signal transduction as well as mediating adhesion with other cells and matrix components. Most CAMs may also be found as soluble circulating proteins, and levels of these soluble CAMs have been found to be raised in inflammatory conditions.

14.1.2 The immunoglobulin superfamily

Members of the immunoglobulin (Ig) superfamily are cell surface proteins that are defined by the presence of one or more Ig domains comprising approximately 100 amino acid residues arranged in a 'sandwich' of two sheets of antiparallel β-strands. Important examples of this group include the leukocyte function-associated antigen 2 (LFA-2, CD2) and 3 (CD58), neuronal cell adhesion molecule 1 (NCAM-1, CD56) and carcinoembryonic antigen family (CEA, CD66). CD66 is characterised as a granulocyte-specific activation antigen. It is predominantly expressed by granulocytes but may also be expressed by activated T-cells and natural killer cells. On granulocytes, CD66 plays a role in cell adhesion and migration.

Furthermore, several members of this family are important molecules involved in leukocyte–endothelial adhesion. These include the platelet/endothelial cell adhesion molecule 1 (PECAM-1, CD31), the intercellular adhesion molecules 1 and 2 (ICAM-1 (CD54) and ICAM-2 (CD102)), vascular cell adhesion molecule 1 (VCAM-1, CD106) and the mucosal addressin cell adhesion molecule 1 (MAdCAM-1). The melanoma cell adhesion molecule (MCAM, CD146) is constitutively expressed in all types of human endothelial cell. CD166, or activated leukocyte cell adhesion molecule (ALCAM), has

recently been characterised in the human system as the ligand for CD6.

14.1.3 The cadherin family

Cadherins are Ca^{2+}-dependent, transmembrane intercellular adhesion proteins. They control the development and maintenance of tissues both in vertebrates and in invertebrates. Classic cadherins can be grouped based on their primary structures. The cadherin superfamily is divided into several families according to the number of repeats in the extracellular domains. The family of classic cadherins are typically composed of five extracellular repeats (domains) and serve cell–cell adhesion functions. Others, including desmosomal cadherins and the protooncogene product RET (rearranged during transfection), may serve as adhesion molecules but could also have other biological roles.

Cadherin molecules possess functional sites for adhesive recognition, Ca^{2+} binding, membrane integration, cytoskeletal interactions and post-translational modifications such as glycosylation, phosphorylation and proteolysis. Classic cadherins have extracellular domains located in the N-terminal part of the molecule. The intracellular domain is linked to actin filaments via α- and β-catenin and is involved in signal transduction (Alattia et al., 1999). The extracellular domains are folded and have been shown to be similar to the variable and constant domains of the immunoglobulin superfamily although there are no sequence homologies.

Some, notably the epithelial (E) cadherins, have been implicated in the metastases of tumour cells. Loss of cell–cell adhesiveness contributes to the process of metastasis whereby tumour cells can invade surrounding tissues and disseminate to distant organs. The cell adhesion system mediated by E-cadherins has been shown to be critical in maintaining cell–cell adhesion and is often inactive in epithelial cancers. This inactivation may result from mutations that directly affect the genes for E-cadherin or may occur in those genes that code for the catenins. Loss of E-cadherin expression is an adverse prognostic indicator in several carcinomas including those of the colon, stomach, prostate and breast (Beavon, 1999). In some situations, as in the development of oesophageal cancer, changes in adhesion molecule expression correlate with tumour progression (Jankowski et al., 1999)

14.1.4 The integrin superfamily

The integrins were originally named because they integrate the extracellular environment with the cytoskeleton. Initially, these membrane glycoproteins were given Roman numeral designations based on their relative mobilities in sodium dodecylsulphate polyacrylamide gels but they have been further classified recently based on subunit analysis. An integrin molecule is a heterodimer consisting of a single α- and a single β-transmembrane protein chain held in noncovalent linkage (Garrod, 1993). To date 15 α-chains and eight β-chains have been described, resulting in a very large number of potential combinations. A particular β-chain may associate with several different α-chains forming several integrin subfamilies. The ligands for integrin are most often extracellular matrix proteins, or occasionally soluble proteins such as fibrinogen or other CAMs (ICAM-1, VCAM-1, MAdCAM-1). Many integrins can bind to the same extracellular matrix molecule and each has more than one ligand (Table 14.1). The ligand-binding region is formed by components of both chains and several integrins recognise the same short peptide sequence Arg-Gly-Asp (RGD in the single letter code for amino acids) present in a variety of extracellular matrix molecules such as fibronectin and vitronectin. Integrin binding is dependent on the presence of divalent metallic cations, and ligand specificity can be modulated by the cations present and indeed by the surrounding lipid microenvironment. This is important to note when investigating the expression of integrins and their ligands by immunofluorescence, as conformational changes in these molecules may adversely affect the binding of some fluorochrome-conjugated antibodies.

Integrins are expressed by almost all cell types except mature erythrocytes. Some are found on

Table 14.1 *The integrin superfamily*

β-Subunit	α-Subunit	Other names	Ligands	Cellular distribution
β_1 (CD29)	α_1	VLA-1	Collagen, laminin	Activated T-cells, monocytes, neuronal cells, melanoma cells and smooth muscle cells
	α_2	VLA-2	Collagen, laminin	Expressed on platelets, megakaryocytes, activated T- and B-cells, monocytes, epithelial cells, neuronal cells, thymocytes, endothelial cells, fibroblasts, melanoma cells, osteoclasts and mesangial cells
	α_3	VLA-3	Collagen, laminin, fibronectin	Nearly all adherent cell lines, kidney glomerulus, thyroid, some basement membranes, B-cells
	α_4	VLA-4	Fibronectin, VCAM-1	Wide reactivity; not expressed on platelets or neutrophils
	α_5	VLA-5, GPIcIIa	Fibronectin	A variety of cells and tissues
	α_6	VLA-6	Laminin	A variety of cells/tissues including platelets, epithelium, endothelium, monocytes and T-cells
	α_7	VLA-7	Laminin	
	α_7	VLA-8		
	α_v		Vitronectin, fibronectin	
β_2 (CD18)	αL (CD11a)	LFA-1	ICAM-1,2,3	Expressed on all leukocytes; absent from nonhemopoietic tissues and platelets
	αM (CD11b)	Mac-1	ICAM-1, C3bi, factor X, fibrinogen, heparin	Expressed on subsets of T- and B-cells, monocytes granulocytes and natural killer cells
	αX (CD11c)	p150,95	Platelet-bound fibrinogen	Expressed on subsets of T- and B-cells, monocytes, macrophages, granulocytes and natural killer cells
β_3	α_{11b}	GPIIbIIIa	Fibrinogen, fibronectin, von Willebrand factor, vitronectin, thrombospondin	Expressed on platelets and platelet precursors
	α_v (CD51)		Fibrinogen, fibronectin, von Willebrand factor, vitronectin, thrombospondin, osteopontin, collagen	Endothelial cells, osteoclasts, some B-cells, activated T-cells and monocytes, macrophages, platelets and melanoma cells
β_4	α_6		Laminin	Leukocytes
β_5	α_v		Vitronectin	Leukocytes
β_6	α_v		Fibronectin	Leukocytes
β_7	α_4		MAdCAM-1, VCAM-1	Lymphocytes
β_7	α_E	HML-1	E-cadherin	$CD8^+$ intraepithelial T-cells of the gut mucosa

HML-1, human mucosal lymphocyte 1; ICAM, intercellular adhesion molecule; LFA-1, leukocyte function-associated antigen 1; VCAM, vascular cell adhesion molecule; VLA, very late antigen.

numerous cell types, while $\alpha_{IIb}\beta_3$-integrin is restricted to platelets and the β_2-integrins to leukocytes. The importance of these molecules for normal cell function is demonstrated by the observation that deficiencies result in significant disease states (Nurden and Caen, 1975). Although the greater portion of the integrin chain is extracellular, they also possess short intracytoplasmic domains that serve as signal transducers for transmembrane signalling (Clarke and Brugge, 1995).

Integrins are subclassified according to their β-subunit. The β_1-integrins mediate cell–matrix adhesion and β_2-integrins are cell–cell adhesion receptors. The β_1-integrins (or very late activation antigens, VLA) have widespread expression and are involved in the organisation of lymphoid tissue. The β_2-integrins (leukocyte integrins) are central to leukocyte function and to leukocyte–endothelial interactions.

14.1.5 The selectins

There are three selectin family members, E-selectin, L-selectin and P-selectin (Bevilacqua et al., 1987; Vestweber, 1992). Each member comprises a single-chain molecule that has three transmembrane loops. They all possess an N-terminal Ca^{2+}-type (C-type) lectin domain, an epidermal growth factor (EGF) domain and a variable number (two to nine) of complement regulatory domains, the archetypes of which bind C3b and C4b. Proximal to the complement regulatory domain is a transmembrane sequence and short intracytoplasmic tail. Lectin and EGF domains are highly homologous between selectins. In contrast to other adhesion molecules, they bind not to protein but to carbohydrate. Selectins and their ligands are concentrated at the tips of microvilli, where they mediate leukocyte rolling on endothelium. Selectins participate in adhesive and inflammatory responses (Moore et al., 1991) and have a role in signal transduction pathways (Weyrich et al., 1995).

E-selectin (CD62E) is found on endothelial cells and was previously designated ELAM-1 (endothelial leukocyte adhesion molecule 1). It becomes slowly upregulated on the cell surface after exposure to inflammatory mediators. It mediates the binding of neutrophils, monocytes, eosinophils, basophils and a subpopulation of T-cells to vascular endothelium. Cellular expression of E-selectin is restricted to activated endothelial cells after tumour necrosis factor γ or interleukin 1 stimulation and peaks at 4–6 h before declining to basal levels by 24 h.

L-selectin (CD62L) mediates lymphocyte and neutrophil adhesion to endothelium and was previously designated LAM-1 (leukocyte adhesion molecule 1). It is expressed by most leukocytes and functions in both homophilic and heterophilic neutrophil adhesion. L-selectin is constitutively expressed and is not dependent on cellular activation. Upon cellular activation, however, the molecule undergoes proteolytic cleavage as it is shed from the cell surface.

The third member of the selectin family, P-selectin (CD62P), is stored in platelet alpha granules and endothelial cell Wiebel–Palade bodies. It is rapidly released and/or translocated to the cell surface on cellular activation. P-selectin (Hsu-Lin et al., 1984; McEver and Martin, 1984) of the platelet alpha granule was previously called GMP 140 (granule membrane protein 140) and PADGEM (platelet activation-dependent granule external membrane protein; Coller, 1989). It has a molecular weight of 140 kDa and is composed of a single polypeptide chain (Johnston et al., 1989). It is a measure of platelet activation used in many clinical studies (Cahill et al., 1996a,b; Collins et al., 1994). It is important that it should be measured with minimal manipulation and no fixation as exposure is easily provoked in vitro (Cahill et al., 1993). The functions of P-selectin include acting as a ligand to tether activated neutrophils to sites of damaged endothelium, which is enhanced by the presence of activated platelets (Evangelista et al., 1993; Lorant et al., 1993).

14.1.6 The cell surface proteoglycan family

Cell surface heparan sulphate proteoglycans possess the unique capacity to bind a variety of growth/angiogenic factors and chemokines via their hepa-

ran sulphate side-chains. Important members of this family are the isoforms of the hyaluronan receptor CD44. The family of CD44 isoforms are derived from spliced variants of CD44 mRNA and are widely expressed on most cell types. CD44 has structural similarity to the selectins and is involved in leukocyte attachment to and rolling on endothelial cells, homing to peripheral lymphoid organs and to sites of inflammation, and leukocyte aggregation, as well as regulation of hemopoiesis.

Abnormalities in the CD44 cell adhesion molecule have been intensively investigated in many types of cancer. Variants of the CD44 protein created by alternative splicing are expressed by cancer cells and are associated with the ability of these cells to metastasise and with a poor prognosis (Goodison et al., 1999). Also soluble forms of CD44 may be detected in the serum of patients with cancer and in some settings correlate with clinical outcome. In nonHodgkin's lymphomas, for example, high serum levels of soluble CD44 at diagnosis are associated with a high prognostic index score, poor response to treatment and an unfavourable outcome (Ristamaki et al., 1997).

14.1.7 The sialomucin family

Members of the endothelial mucins include MAdCAM-1, GlyCAM-1 (glycosylation-dependent cell adhesion molecule 1) and CD34. Leukocyte mucins include PSGL-1 (P-selectin glycoprotein ligand 1), CD43, CD45, CD68 and CD93. Mucins have multiple serine and threonine residues, which occur in clusters along the peptide backbone. Linked to these are carbohydrate chains that are typically heavily sialylated and so negatively charged. They can, therefore, act as anti-adhesive molecules through their charge or as adhesive molecules with their specific ligands.

14.1.8 Other adhesion molecules

A number of other adhesion molecules have been described that do not fit into the above families. CD73 possesses 5'-nucleotidase activity and catalyses the dephosphorylation of purine and pyrimidine ribo- and deoxyribonucleoside monophosphates to their corresponding nucleosides. It has been shown to have a role in mediating lymphocyte adhesion to endothelium. CD99 was first described as a T-cell surface molecule that could modulate T-cell adhesion phenomena and was termed E2, an antigen present at high density on Ewing sarcoma cells. Its gene was the first discovered human pseudoautosomal gene, which was termed *MIC2*. CD99 is present on many cell types in addition to hemopoietic cells. CD151 (platelet-endothelial tetraspan antigen 3 (PETA-3)) is a member of the tetraspan family with amino acid homology with CD9, CD63 and CD53. It has wide tissue distribution and like CD9 and CD63 is associated with β_1-integrins on the cell surface. CD164 (MGC-24, multiglycosylated core protein of 24 000 M_r) is a mucin-like molecule rich in serine and threonine residues, originally identified as a peanut agglutinin-binding glycoprotein expressed by a variety of normal and neoplastic epithelial cells. Functionally, CD164 is thought to play a role in mediating adhesion between hemopoietic and bone marrow stromal cells. CD165 is believed to be an adhesion molecule involved in the adhesion of thymocytes to thymic epithelial cells. It is a cell surface glycoprotein, but its precise structure is unknown. It is expressed on subsets of lymphocytes, monocytes and platelets.

14.2 Analysis of cell–cell interactions

Our ability to examine adhesion molecules involved in cell–cell interactions in cells is greatly enhanced by flow cytometry (Table 14.2).

It is not possible to discuss comprehensively every adhesion molecule on every cell in which cell–cell interactions matter. Some of the most important cell–cell interactions in the human body involve platelets. Platelet–platelet interactions and platelet–leukocyte interactions will, therefore, be discussed in some detail below followed by an assessment of

Table 14.2 *Cell adhesion molecules that may be measured by flow cytometry*

CD number	Molecule	Cellular expression
CD9	Motility-related protein 1 (MRP-1)	Platelets
CD11a	Leukocyte function antigen 1 (LFA-1)	Leukocytes
CD11b	Receptor for the C3bi complement component (C3biR)	Leukocytes
CD11c	Receptor for the C3 complement component (CR4)	Leukocytes
CD15	Lewis X	Leukocytes
CD15s	Sialyl-Lewis X	Leukocytes
CD29	GPIIa	Platelets, leukocytes, endothelial cells
CD31	Platelet endothelial cell adhesion molecule 1 (PECAM-1)	Leukocytes, endothelial cells
CD34	L-selectin ligand	Leukocytes
CD35	Receptor for the C1 complement component (CR1)	Leukocytes
CD41	GPIIb	Platelets
CD42a	GPIX	Platelets
CD42b	GPIb	Endothelial cells
CD43	Sialophorin	Leukocytes
CD44	Hyaladherin (H-CAM)	Leukocytes
CD47	Integrin-associated protein	Platelets, leukocytes, endothelium
CD49	Very late antigens (VLA)	Platelets, leukocytes, endothelium
CD50	Intercellular adhesion molecule 3 (ICAM-3)	Leukocytes
CD51	Integrin α_v-chain	Platelets, leukocytes, endothelium
CD54	Intercellular adhesion molecule 1 (ICAM-1)	Leukocytes, endothelial cells
CD56	Neuronal cell adhesion molecule (NCAM)	Leukocytes
CD58	Leukocyte function-associated antigen 3 (LFA-3)	Leukocytes
CD61	GPIIIa	Platelets
CD62E	E-selectin	Endothelial cells
CD62L	L-selectin	Leukocytes
CD62P	P-selectin	Platelets
CD66	Biliary glycoprotein	Leukocytes
CD73	Ecto-5'-nucleotidase	Leukocytes
CD99	E2	Leukocytes, endothelial cells
CD104	Integrin β_4-chain	Leukocytes, endothelial cells
CD106	Vascular cell adhesion molecule 1 (VCAM-1)	Leukocytes, endothelial cells
CD144	VE-cadherin	Endothelial cells
CD146	Melanoma cell adhesion molecule (MCAM)	Leukocytes, endothelial cells
CD147	Intracellular matrix metalloproteinase inducer (EMMPRIN)	Platelets, leukocytes, endothelial cells
CD151	Platelet-endothelial tetraspan antigen 3 (PETA-3)	Platelets, leukocytes, endothelium
CD162	P-selectin glycoprotein ligand 1 (PSGL-1)	Leukocytes
CD164	MGC-24	Leukocytes
CD165	Gp137	Platelets, leukocytes
CD166	Activated leukocyte adhesion molecule (ALCAM)	Leukocytes

Table 14.3 *Molecules involved in the adhesion and aggregation of platelets*

Molecule	Classification	CD	Ligand
Platelet endothelial cell adhesion molecule 1 (PECAM-1)	Immunoglobulin superfamily	CD31	Heparan sulphate, glycosaminoglycan, $\alpha_v\beta_3$-integrin, CD31
FcγRIIa	Fc receptor	CD32	Immunoglobulin cell adhesion molecules
GPIIIb GPIV	Membrane glycoprotein	CD36	Thrombospondin
GPIIb/IIIa	$\alpha_{IIb}\beta_3$-Integrin	CD41a	Fibrinogen, fibronectin, von Willebrand factor, vitronectin
GPIX	Leucine-rich glycoprotein	CD42a	von Willebrand factor
GPIbα	Leucine-rich glycoprotein	CD42b	Filamin, thrombin, von Willebrand factor
GPIbβ	Leucine-rich glycoprotein	CD42c	Von Willebrand factor, thrombin
GPV	Leucine-rich glycoprotein	CD42d	Thrombin
GPIa/Iia	$\alpha_2\beta_1$-Integrin, VLA-2	CD49b	Collagen, laminin
GPIc/Iia	$\alpha_5\beta_1$–Integrin VLA-5	CD49e	Fibronectin
GPIc/Iia	$\alpha_6\beta_1$-Integrin VLA-6	CD49f	Laminin
Vitronectin receptor	$\alpha_V\beta_3$-Integrin	CD51	Vitronectin
P-selectin	Selectin	CD62P	Sialyated carbohydrates including Lewis-X (CD15), P-selectin glycoprotein ligand 1 (CD24)

leukocyte–leukocyte and leukocyte–endothelial interactions.

14.3 Platelet–platelet interactions

Increased platelet activation may lead to platelet aggregation and thrombosis. This can result in clinical syndromes such as myocardial infarction and stroke, both of which are major causes of morbidity and mortality. Reduced platelet–platelet interaction can result in bleeding problems, which although much rarer can also be serious.

Flow cytometry is increasingly used to characterise accurately the phenotypic alterations of platelets that are related to their cellular activation, hemostatic function and to maturation of precursor cells. More than 40 molecules (Clemetson and McGregor, 1987) have been identified on the surface membrane of platelets, many of which change in relation to the activation state and function of the cell. Many of these are adhesion molecules and the principal platelet adhesion molecules belong to the integrin and selectin families. They are shown together with their ligands in Table 14.3. The process of platelet activation is a receptor-mediated response of resting platelets to a variety of specific stimuli originating from activated proteins of the coagulation cascade (thrombin), subendothelial matrix proteins (collagen) or specific mediators such as ADP or platelet-activating factor (PAF).

One of the most important platelet glycoproteins is $\alpha_{IIb}\beta_3$-integrin (GPIIb/IIIa, CD41a), which functions as the fibrinogen receptor but also binds less avidly to fibronectin, von Willebrand factor and vitronectin. This molecule is the most abundant glycoprotein on the platelet surface membrane and is present with a copy number of 20 000–40 000 (Mistry et al., 1991). GPIIb has two subunits of 123 and 140 kDa. It is unique to megakaryocytes and platelets. GPIIIa has a molecular mass of 108 kDa under reduced conditions. It forms the common subunit of a number of nonplatelet specific integrins.

The glycoprotein $\alpha_{IIb}\beta_3$-integrin is a transmembrane protein and it is postulated that the intracytoplasmic portion is associated with cytoskeletal and cytoplasmic actin and connected to

the platelet cytoskeleton via a protein called talin (Clemenson, 1988). After crosslinking, transmembrane signalling occurs both from outside in and from inside out using signalling mechanisms such as G-peptides, protein kinase C and calpain (Siess, 1990). Exposure of activated $\alpha_{IIb}\beta_3$-integrin is therefore preceded by a chain of membrane and intracellular molecular events (Shattil et al., 1987) that link platelet activation, shape change and aggregation. These changes are important precursors to cell–cell interaction: $\alpha_{IIb}\beta_3$-integrin is an externally orientated Ca^{2+}-dependent heterodimer and fibrinogen is a dimeric molecule that can bind two platelets at a time. It is through the binding of the dimeric fibrinogen molecule that platelets are linked together and the platelet plug grows.

Because $\alpha_{IIb}\beta_3$-integrin is present on the platelet membrane in its resting (inactivated) form, it must change its conformation to the activated form (Coller, 1989; Sims et al., 1991) to function effectively to bind fibrinogen. The exposure of $\alpha_{IIb}\beta_3$-integrin is the final common pathway leading to platelet aggregation (Coller, 1989; Plow and Ginsberg, 1988), hence the importance of preserving inactive $\alpha_{IIb}\beta_3$-integrin on resting platelets. In contrast, other platelet glycoprotein receptors (e.g. GPIb) can bind to their ligands on resting platelets without modification. This essential step in the powerful process of platelet aggregation (and therefore thrombosis) is tightly regulated, but the exact regulatory pathways are currently unknown.

Exposure of $\alpha_{IIb}\beta_3$-integrin in vitro can be brought about by a number of agonists such as thrombin, ADP or ristocetin. A differential response to these agonists may be seen in terms of numbers of receptors exposed after activation. Thrombin is the most potent agonist, exposing the greatest number of receptors. Agonists can activate the receptor by a variety of different means (Siess, 1990). The generation of thromboxane A_2 is not essential to effect a conformation change in $\alpha_{IIb}\beta_3$-integrin. This point is of practical significance because platelet aggregation can occur in the presence of blockade of the arachidonic acid pathway, for example in patients taking aspirin.

14.4 Platelet activation in clinical disorders

Abnormal platelet behaviour has been identified in several disorders characterised by vascular pathology including coronary artery disease (Cahill et al., 1996a; Knight et al., 1997), Alzheimer's disease (Davies et al., 1997), myeloproliferative disorders (Thibert et al., 1995), diabetes (Tschoepe et al., 1997a,b), pre-eclampsia (Konijnenberg et al., 1997) and glomerular disease (Barnes, 1997). Activated platelets have been identified in the majority of these disorders and antiplatelet therapy has been valuable in the management of some of these conditions, including ischaemic heart disease (Antiplatelet Trialists' Collaborative Study, 1994), diabetic vascular disease (ETDRS Investigators, 1992), cerebrovascular disease (CAPRIE Study Steering Committee, 1996), and pre-eclampsia (Sibai et al., 1993). Platelet activation has been shown to be increased in myeloproliferative disorders (Cahill et al., 1996b) and in inflammatory bowel disease (Collins et al., 1994). The use of pharmacological inhibitors of platelet function has increased with the development of anti-$\alpha_{IIb}\beta_3$-integrin inhibitory antibody and ADP-blocking drugs, such as clopidogrel, which render platelets less susceptible to activation.

As well as their vital role in hemostasis, platelets have been shown in recent research to have a role in inflammation (Andrews et al., 1997). Activated platelets release a number of molecules that are potent amplifiers of basophil, mast cell and neutrophil activity, including platelet factor 4, β-thromboglobulin, platelet-derived growth factor and histamine-releasing factor. Platelets also release a number of inflammatory mediators such as oxygen free radicals, PAF, thromboxane, 12-hydroxyeicosatetraenoic acid, serotonin, platelet factor 4, and transforming growth factor β (Deuel et al., 1981, 1982; Goetzl et al., 1977; Wahl et al., 1987). Recently, platelets have also been shown to release nitric oxide (Okada et al., 1996). As well as contributing to chemoattraction and activation of other inflammatory cells, some of these platelet-derived mediators may increase vascular permeability and

moderate vascular tone (Berk et al., 1986; Braque et al., 1987).

14.5 Flow cytometric analysis of platelet activation

14.5.1 Intracellular events

One of the earliest responses in the initial phase of platelet activation is an increase in cytosolic free Ca^{2+}, which can be measured in the altered fluorescence intensity of the ion-sensitive intracellular probe Fluo-3 (Dachary-Prigent et al., 1995; Monteiro et al., 1999). Another early event induced by agonists is the polymerisation of G-actin into long F-actin filaments during the reorganisation of the cytoskeleton. An increase in F-actin content can be detected with fluorescent phalladin or phalloidin derivatives following permeabilisation of the platelets (Oda et al., 1992).

14.5.2 Shape change

Upon reorganisation of the cytoskeleton, platelets lose their discoid form and this reversible shape change is associated with changes in cellular forward and side scatter characteristics. Standardised flow cytometric measurement of this shape change has proved difficult (Ruf and Patscheke, 1995); however, more recently, instrumentation has been developed that allows more sensitive assessment of this phenomenon (Macey et al., 1999).

14.5.3 Surface membrane changes

Platelets express a variety of glycoproteins that are involved in adhesion and aggregation (Table 14.3). Not all of these molecules are expressed on resting cells. It is functionally advantageous for some receptors to become expressed only on activated platelets, for example $\alpha_{IIb}\beta_3$-integrin, which once expressed alters its molecular configuration to facilitate fibrinogen binding and platelet–platelet interaction and leads to thrombosis if sustained.

Platelet activation in vitro is associated with a decrease in the number of GPIb/IX complexes on the platelet surface, which are redistributed into the platelet canalicular system (Michelson et al., 1994) and an increase in the number of $\alpha_{IIb}\beta_3$-integrin complexes on the platelet surface owing to redistribution from intracellular pools such as storage organelle membranes (Woods et al., 1986). Exposure of the procoagulant surface is the result of a flip-flop in anionic phospholipids, predominantly phophatidylserine, from the inner to the outer leaflet of the membrane bilayer, which forms a binding substrate for the prothrombinase complex. This change can be detected either by using antibodies to clotting factors Va or VIIIa (Hoffman et al., 1992) or by the binding of fluorochrome-labelled annexin V (Dachary-Prigent et al., 1993).

Upon activation, platelet surface $\alpha_{IIb}\beta_3$-integrin complexes undergo conformational changes that generate neoepitopes detectable by using monoclonal antibodies such as PAC1 (Shattil et al., 1987). The consequent changes in conformation can also be detected by monitoring changes in fluorescence energy resonance produced when two different monoclonal antibodies directed against epitopes on the glycoprotein are either brought together or move apart (Sims et al., 1991). Binding of specific ligands such as fibrinogen to $\alpha_{IIb}\beta_3$-integrin following activation can also be detected using monoclonal antibodies or fluorochrome-conjugated fibrinogen (Frojmovic et al., 1996; Ugarova et al., 1993).

14.5.4 Organisational events

Three membrane glycoproteins have been characterised in platelet lysosomes: the lysosomal integral membrane protein CD63 antigen (also designated gp53, ME491 antigen, pltgp40 or granulophysin) (Metzelaar and Clevers, 1992) and the lysosome-associated membrane proteins (LAMP) LAMP-1 (CD107a) (Febbraio and Silverstein, 1990) and LAMP-2 (CD107b) (Silverstein and Febbraio, 1992). So far, three dense body integral membrane proteins have been identified: the CD63 antigen, a

LAMP-2 protein primarily associated with lysosomes and P-selectin associated with the alpha granules (Israels et al., 1992). Three major GMPs have been identified: P-selectin (CD62P), GMP-33 and $\alpha_{IIb}\beta_3$-integrin (Metzelaar et al., 1992). Following platelet activation, CD62P and GMP-33 are expressed on the plasma membrane by fusion of the granule with the plasma membrane. Several alpha granule membrane receptors, CD9, CD31, CD36 and GPIIb/IX/V complex, may also be detected by flow cytometry (Zagursky et al., 1995). Release of dense granules may be detected by a decrease in mepacrine staining (Wall et al., 1995).

14.6 Methods for the analysis of platelet adhesion and activation molecules

14.6.1 Preanalytical variables: anticoagulant

Accurate assessment of in vivo or in vitro cellular expression of molecules requires optimal preanalytical conditions to prevent in vitro artefactual activation. The choice of anticoagulant for collected blood is one of the critical preanalytical conditions, as anticoagulants exert different effects on the activation of cells ex vivo. Historically, sodium citrate has been the favoured anticoagulant for use in the studies of platelet activation and function, including aggregation and adherence (Protocol 14.1). However, recent studies have suggested that the anticoagulant CTAD, a mixture of sodium citrate, theophylline, adenosine and dipyridamole, may be better for retaining the ex vivo status of platelets (Mody et al., 1999). It should be noted that this anticoagulant is light sensitive and only stable for up to 4 h (Kuhne et al., 1995).

Protocol 14.1 Venepuncture for flow cytometry samples

1. The patient should be seated with the arm extended and comfortably supported. Only a light tourniquet positioned above the antecubital fossa for a brief period should be used.
2. A 19 gauge needle is inserted into the antecubital veins, the tourniquet released and blood venesected into a standard plastic syringe. The first 2 ml of blood is discarded. Vacutainers® (BD Biosciences) may be used.
3. The blood is immediately transferred to a glass tube containing citrate by gently dripping it down the side of the tube. The formation of bubbles is avoided at all stages. Samples should be placed in an upright rack and transported to the laboratory within 5 min.

14.6.2 Analysis of platelet surface activation antigens $\alpha_{IIb}\beta_3$-integrin

The first antibody that recognised the activated conformation of $\alpha_{IIb}\beta_3$-integrin was developed in 1994. This antibody, PAC1, is an IgM antibody that recognises a sequence on the $\alpha_{IIb}\beta_3$-integrin that is exposed on activation (Protocol 14.2). It may not be used with samples that have been fixed with formaldehyde (Shattil et al., 1985). The normal conformation of $\alpha_{IIb}\beta_3$-integrin is dependent on the presence of divalent ions (predominantly Ca^{2+}) at physiological concentrations (Shattil et al., 1987). Removal of divalent ions results in an altered conformation; therefore blood samples in ethylenediamine tetraacetic acid (EDTA) are unsuitable for study of the activated form of this molecule. EDTA may in itself cause dissociation of the $\alpha_{IIb}\beta_3$-integrin complex (Shattil et al., 1987).

The monoclonal antibodies against $\alpha_{IIb}\beta_3$-integrin may be conjugated to fluorescent molecules and analysed flow cytometrically. There are now directly conjugated IgG antibodies available, such as RUU-SP2.41 (Immunotech). These reduce the manipulation needed to measure antibody binding to activated $\alpha_{IIb}\beta_3$-integrin on platelets because a directly conjugated antibody obviates the need for a washing step. P-selectin can be measured in whole blood using a similar procedure (Protocol 14.3).

Protocol 14.2 Measurement of activated $\alpha_{IIb}\beta_3$-integrin on the platelet surface using PAC1

Antibody preparation

1. PAC1 (500 μg) reconstituted with 500 μl of sterile water should be divided into 5 μl amounts at a concentration of 1 mg ml^{-1} as recommended by Shattil et al. (1985) and stored at –70°C.
2. These samples are then diluted in 78 μl Tyrode's solution immediately prior to use (62 μg ml^{-1}). PAC1 displays linear platelet binding with a platelet count in the range 50×10^9 to 100×10^9 cells l^{-1} at a concentration (working solution) of 30 μg ml^{-1}.

Method

1. Fresh citrated samples are required, diluted one in ten in Tyrode's solution with added 0.1% bovine serum albumin (BSA).
2. Whole blood is diluted in filtered Tyrode's solution at room temperature and PAC1 added at the working concentration of 30 μg ml^{-1} followed by incubation for 15–20 min at 21°C.
3. Samples are washed in Tyrode's solution and centrifuged at $2000 \times g$ for 10 min.
4. The platelet pellet is resuspended in Tyrode's solution and a fluorescent conjugate (either phycoerythrin (PE) or Red 613) anti-mouse antibody added.
5. After a further 5 min incubation, the samples are diluted to 1000 μl volume with Tyrode's solution and analysed immediately by flow cytometry. Platelets are identified in a histogram of logarithmic forward scatter (*x*-axis) and side scatter (*y*-axis). (Fig. 14.1). Platelets have light scattering properties that allow them to be easily distinguished from erythrocytes and other leukocytes. The platelets may be gated and their fluorescence analysed.

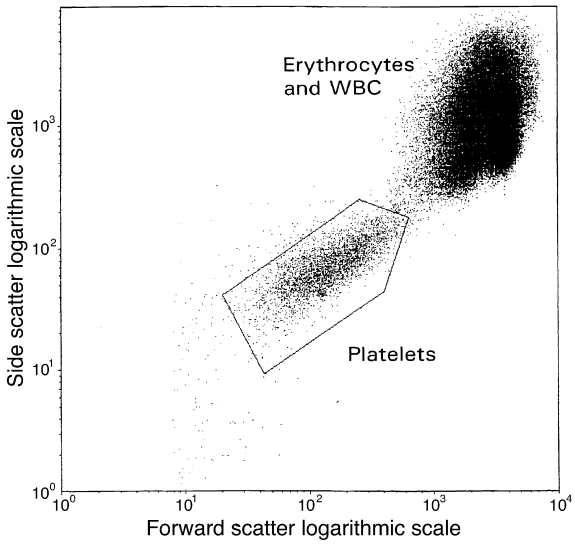

Fig. 14.1 The light scattering properties of platelets in diluted whole blood. WBC, white blood cells.

Protocol 14.3 Analysis of P-selectin in whole blood

1. Blood (4.5 ml in citrate) is drawn using the standardised techniques described in Protocol 14.1.
2. Within a maximum of 10 min after venesection, 30 μl of blood is added to 270 μl Tyrode's solution with 0.1% BSA (1 : 10 dilution).
3. The diluted blood (5 μl) is added to tubes already containing 10 μl of antibody (anti-P-selectin is commercially available). The final concentration of platelets is approximately 10×10^9 l^{-1} to 20×10^9 l^{-1}, and the final concentration of antibody is 6 μg ml^{-1}.
4. The agonist (at a final volume of 3 μl) is reconstituted at varying concentrations and added to each tube. This serves to maintain a constant concentration of antibody.
5. Blood is incubated for 10 min, after which it is diluted for analysis with Tyrode's solution.
6. Appropriate positive and negative controls are used in each experiment.
7. Analysis is then performed immediately as described in Protocol 14.2.

14.7 Platelet–leukocyte interactions

Although most blood cells circulate as single cells, a small number can also exist in the form of aggregates. These can be homotypic or heterotypic, such as platelet–platelet aggregates or platelet–leukocyte aggregates. Platelet–leukocyte aggregates may be important in thrombotic (Li et al., 1997, 1999) and inflammatory disease states (Gawaz et al., 1994; Peters et al., 1999; Tschoepe et al., 1997a,b). Li et al. (1999) have developed a rapid reliable procedure for measuring platelet–leukocyte aggregates in whole blood, which is consistent with the recommendations of the European Working Group on clinical cell analysis (Schmitz et al., 1998) (Protocol 14.4).

Protocol 14.4 Procedure for measuring platelet–leukocyte aggregates

1. Blood is collected by venepuncture, without stasis, into siliconised Vacutainer® tubes (Becton Dickinson) containing 1/10 volume of 3.8% trisodium citrate.
2. Within 3 min of collection, 5 μl of blood is added to 45 μl HEPES-buffered saline (150 mmol l^{-1} NaCl, 5 mmol l^{-1} KCl, 1 mmol l^{-1} $MgSO_4$, 10 mmol l^{-1} HEPES, pH 7.4) containing appropriately diluted fluorescein isothiocyanate (FITC)-conjugated CD42a (Beb1, Becton Dickinson) and Rhodophycae phycoerythrin (R-PE)-conjugated CD45 (T29/33, Dako) monoclonal antibodies (final concentration 1.25 and 20 μg ml^{-1}, respectively).
3. The blood is incubated for 2 min at room temperature without agitation then diluted by mild fixation with 0.5% formaldehyde in saline and analysed by flow cytometry within 3 h (Fig. 14.2).

14.8 Leukocyte–leukocyte interactions

Methods for leukocyte–leukocyte interactions have been developed to investigate various processes in the immune response such as antigen presentation and natural killer cell function (Hatam et al., 1994). Protocol 14.5 was developed to detect specific cell-mediated cytotoxicity (Lowdell et al., 1997). The target cells are labelled with an orange fluorescent membrane dye PKH-26; effector cells may be identified by the addition of fluorescein-conjugated monoclonal antibodies and cell death is detected by the differential uptake of the red fluorescent dye propidium iodide (PI).

Protocol 14.5 Method for measuring leukocyte–leukocyte interaction

1. Target cells K562 are washed once in RPMI 1640 supplemented with l-glutamine (0.3 g l^{-1}), penicillin (100 U ml^{-1}) and streptomycin (100 μg ml^{-1}) and resuspended in PKH cell labelling buffer (Sigma).
2. The cells are mixed with an equal volume of 4 mmol l^{-1} PKH-26 (Sigma) for 2 min at 21°C. The labelling reaction is stopped by the addition of an equal volume of fetal bovine serum (FBS) for 1 min and the cells are washed twice in RPMI 1640 supplemented with 10% FBS and resuspended to 1×10^5 ml^{-1}.
3. Peripheral blood mononuclear effector cells (100 μl) at a concentration of 0.6×10^6 to 10.0×10^6 cells ml^{-1} are mixed with 100 μl PKH-26 labelled target cells and 25 μl of Pl solution (1 μg $ml^{-1;}$, Sigma) in tubes and gently mixed.
4. The tubes are centrifuged at $50 \times g$ for 5 min then incubated at 37°C in 5% CO_2 in air.
5. After 1 h, the tubes are placed on ice until analysed.
6. Spontaneous cell death is determined by incubating both targets or effectors alone. Samples are run in duplicate.
7. The targets and effector cells are identified on a two-parameter histogram of forward and side scatter and the proportions of red and orange fluorescent cells are determined in a histogram of log orange and log red fluorescence. This allows the enumeration of four subpopulations:

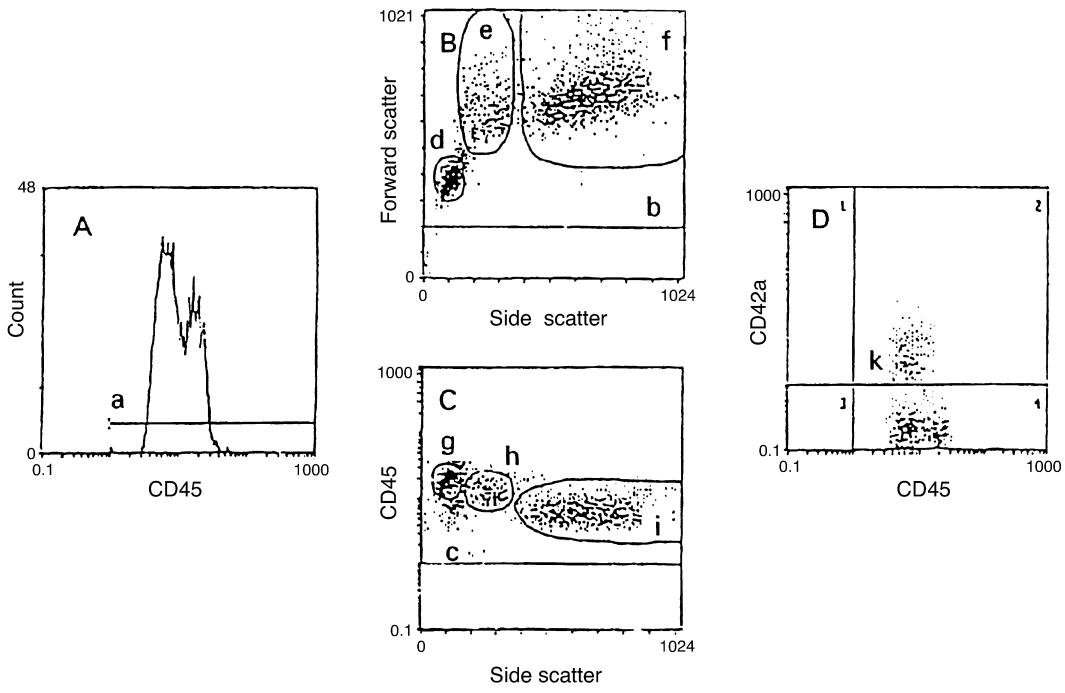

Fig. 14.2 The flow cytometric analysis of platelet–leukocyte aggregates in whole blood. (A) The cells in blood are analysed for R-PE–CD45 expression and leukocytes positive for CD45 are gated. (B) These events are then backgated to a histogram of forward scatter and side scatter, in which a rectangular region b is defined to separate leukocytes from debris. Amorphous regions d, e and f are set around the lymphocytes, monocytes and neutrophils, respectively. (C) R-PE–CD45 events in region a are also backgated to a histogram of side scatter and CD45 in which regions c, g, h and i are drawn to define all leukocytes, lymphocytes, monocytes and neutrophils, respectively. Events occurring in both regions b and c are considered to be intact leukocytes. (D) Regions b and c are then analysed in a dual-fluorescence histogram of R-PE–CD45 and FITC–CD42a. Dual positive events in region k are considered to be platelet–leukocyte conjugates. Single positive events are considered to be platelet-free leukocytes. The relative percentage of platelet–leukocyte conjugates may then be determined. Similarly events occurring in both d and g are considered to be lymphocytes; those in e and h are monocytes and those in f and i are neutrophils. Quantum Red™-conjugated CD3, CD14 and CD16 may also be used to identify lymphocytes, monocytes and neutrophils, respectively. FITC, fluorescein isothiocyanate; R-PE, Rhodophycae phycoerythrin. (Reprinted by permission of Wiley-Liss, Inc., a subsidiary of John Wiley & Sons, Inc., from Li, N., Goodall, A.H., Hjemdahl, P. (1999) Efficient flow cytometric assay for platelet–leukocyte aggregates in whole blood using fluorescence signal triggering. *Cytometry* **35**, 145–61.)

(i) live targets (orange fluorescent only), (ii) killed targets (orange and red fluorescent) (iii) live effector (nonfluorescent) and (iv) dead effectors (red fluorescent only) (Fig. 14.3).

8. The effector to target ratio can then be calculated. At least 2000 target events should be enumerated.
9. The spectral overlap of the fluorochromes is electronically compensated using PKH-26-labelled targets alone and unstained targets with membranes that have been permeabilised by treatment with 0.1% Tween® 20 detergent (Sigma) in phosphate-buffered saline (PBS; Sigma) for 10 min at 37°C. These Tween-treated targets are then washed twice and incubated with PI (0.1 μg ml^{-1}). This preparation contains both live and dead targets.
10. The cell-mediated cytotoxicity is determined by

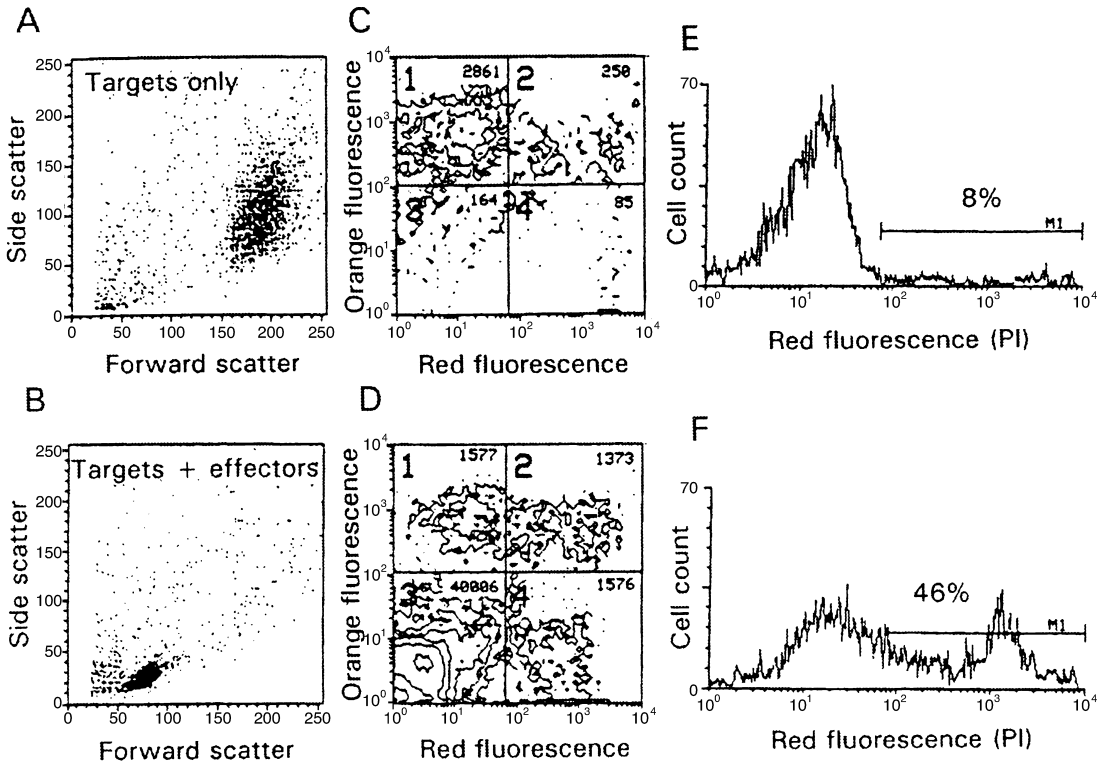

Fig. 14.3 Flow cytometric analysis of leukocyte–leukocyte interactions. The targets and effector cells are identified on a two-parameter histogram of forward and side scatter (A, B) and the proportions of red and orange fluorescent cells are determined in a histogram of log orange and log red fluorescence (C, D). This allows the enumeration of four subpopulations: (i) live targets (orange fluorescent only), (ii) killed targets (orange and red fluorescent) (iii) live effector (nonfluorescent) and (iv) dead effectors (red fluorescent only) (E, F). The relative proportion of live and dead target cells are determined from the subpopulations l and 2. (Reprinted by permission of Wiley-Liss, Inc., a subsidiary of John Wiley & Sons, Inc., from Hatam, L., Schuval, S., Bonagura, V.R. (1994) Flow cytometric analysis of natural killer cell function as a clinical assay. *Cytometry* **16**, 59–68.)

subtracting the percentage of background cell death from the percentage of specific cell death.

14.9 Leukocyte–endothelial cell interactions

Epithelial cells and endothelial cells express high levels of adhesion molecules and assays to quantify the adhesive interactions between leukocytes and activated epithelial and endothelial cells have been developed. Protocol 14.6 was developed to identify different subpopulations of lymphocytes adhering to cultured parenchymal cells treated with proinflammatory cytokines (Korlipara et al., 1996).

Protocol 14.6 Procedure for measuring leukocyte–endothelial cell interactions

1. Confluent endothelial or epithelial cells in 24-well plates are washed and 500 μl of RPMI 1640 medium without phenol red is added to each well.
2. Then 5×10^5 resting peripheral blood lymphocytes or mitogen-activated T-cells are added

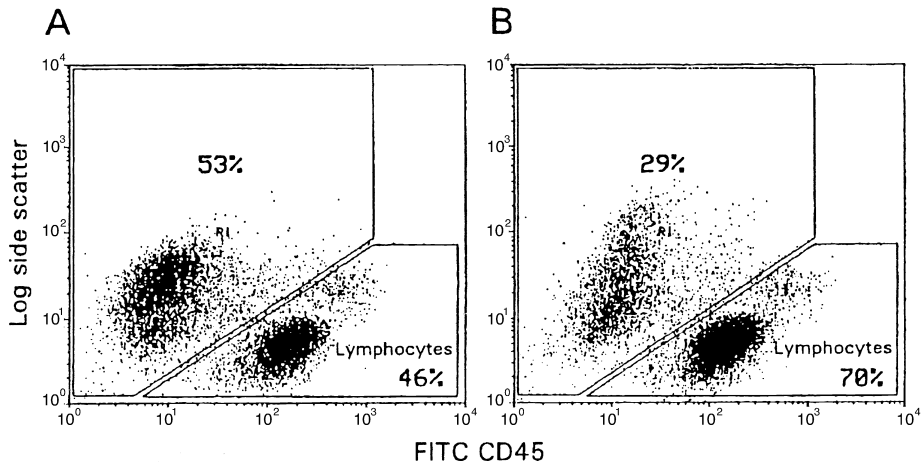

Fig. 14.4 Flow cytometric analysis of leukocyte–endothelial cell interactions using fluorescein isothiocyanate (FITC). Cells are analysed in a histogram of log green fluorescence and log side scatter. The results are expressed as a ratio of the number of FITC–CD45$^+$ lymphocytes to the number of FITC–CD45$^-$ parenchymal cells. The analysis is shown for cells incubated without stimulation (A) and for endothelial cells stimulated with tumour necrosis factor (B). (Reprinted from *Journal of Immunological Methods* **191**, Korlipara, L.V., Leon, M.P., Rix, D.A., Douglas, M.S., Gibbs, P., Bassendine, M.F., Kirby, J.A., Development of a flow cytometric assay to quantify lymphocyte adhesion to cytokine-stimulated human endothelial and biliary epithelial cells, pages 121–30 (1996) with permission from Elsevier Science.)

in a further 500 μl of medium. The plates are incubated for 1 h at 37°C in an humidified chamber with 5% CO_2.

3. Nonadherent cells are resuspended by mechanical plate shaking for 3 min at 150 oscillations min^{-1} and the wells washed gently three times with PBS containing 5% serum.
4. The remaining cells are detached from the plastic and completely dissociated by treatment with trypsin-EDTA. The cell suspensions are washed and labelled with an optimum concentration of FITC–CD45.
5. Cells are analysed in a histogram of log green fluorescence and log side scatter (Fig. 14.4). The results are expressed as a ratio of the number CD45 lymphocytes to the number of CD45$^-$ parenchymal cells.
6. The phenotype of the adherent cells may be further characterised by the addition of PE-conjugated CD4, CD8 or CD56. The proportion of each lymphocyte subset in the adherent population is then compared with the proportion in the original cell preparation and the results are expressed as a ratio. Values over 1.0 indicate preferential adhesion.

14.10 Dysregulated cell–cell interactions and adhesion molecule deficiency states

Cell–cell interactions are of basic importance in the genesis and maintenance of organ structure and integrity and in the initiation and regulation of numerous vital bodily functions. Dysregulated cell–cell interactions lead to organ dysfunction and disease (Cavenagh et al., 1998) (Table 14.4).

14.11 Defects in human integrins

The in vivo importance of cell adhesion molecules may be appreciated by the study of those rare patients who have a specific inherited defect of the integrin molecules (Table 14.5).

Table 14.4 *Pathological results of dysregulated cell–cell interactions*

Pathological reduction in cell–cell interaction (adhesion)	Pathological increase in cell–cell interaction
Abnormal vascular development	Inappropriate inflammation
Developmental cardiac defects	Inappropriate thrombosis
Impaired chemotaxis	
Susceptibility to infection, metastatic carcinoma and bleeding	

Table 14.5 *Inherited defects of integrin molecules*

Type of integrin	Disease	Infections	Molecule expression
β_2	LAD-1	Severe	0–1% CD18
		Moderate	2–5% CD18
	LAD-1-like	Moderate/severe	50% CD18 (functional defect)
β_3	Glanzmann's	Mucosal bleeding	Abnormal $\alpha_{IIb}\beta_3$ -integrin
	Glanzmann's-like	Mucosal bleeding	Normal $\alpha_{IIb}\beta_3$-integrin
$\beta_2 + \beta_3$	LAD-1 variant	Moderate LAD-1 and thrombasthenia	CD18 and $\alpha_{IIb}\beta_3$-integrin normal

LAD, leukocyte adhesion deficiency.

14.11.1 Leukocyte adhesion deficiencies

The importance of cell–cell interactions and the adhesion molecules on which they depend is demonstrated when such molecules are deficient. Although deficiencies of adhesion molecules are rare, about 50 patients with leukocyte adhesion molecule deficiency (LAD) have been reported worldwide. Patients with LAD-1 lack β_2-integrin (CD18), which associates with CD11a–c. These patients, therefore, have nonfunctional leukocyte adhesion molecules and these cells cannot bind to endothelium at sites of inflammation. Recently a LAD-1-like case was reported in which a child had 50% expression of CD18 but the integrin had a functional defect (Hogg et al., 1999). Etzioni et al. (1992) reported two patients who had normal adhesion molecules but whose neutrophils had a deficiency of sialyl-Lewis X (CD15s). This molecule is the ligand for the selectins. A deficiency of this molecule results in failure of cell–cell interaction, specifically neutrophil adhesion to endothelial cells and platelets. These patients both had otherwise unexplained recurrent severe infections and were classified as having LAD-2.

14.11.2 Glanzmann's thrombasthenia

The importance of the $\alpha_{IIb}\beta_3$-integrin is highlighted by the effects of a naturally occurring deficiency in Glanzmann's disease (French and Seligsohn, 2000). In this condition, quantitative (type 1) or qualitative (type 2) abnormalities of $\alpha_{IIb}\beta_3$-integrin on the platelet surface render aggregation impossible (George et al. 1984; George and Shattil, 1991). Afflicted individuals are prone to mucocutaneous and gastrointestinal bleeding of variable severity. Bleeding time is prolonged and platelet count is normal (Larrieu et al., 1968).

Tako Kuijpers and colleagues (1997) have described a patient with defective function of both β_2-(LAD-1) and $\alpha_{IIb}\beta_3$-integrins (Glanzmannn's thrombasthenia). Although both molecules were structurally expressed on the cell surfaces, they did not become activated, and leukocyte adhesion and platelet aggregation were impaired.

14.12 Defects in other human adhesion molecules

14.12.1 Bernard–Soulier syndrome

Bernard–Soulier syndrome (Bernard and Soulier,

1948) has classically been regarded as a deficiency of membrane glycoprotein Ib (Nurden and Caen, 1975). It is now known that there are roughly parallel deficiencies of GPIb and GPIX (Clemetson et al., 1982) and that these glycoproteins are complexed together on platelet membranes. There is also a deficiency of GPV (the thrombin 'receptor') on these platelets (Clemetson and McGregor, 1987). Clinically, a platelet-type bleeding disorder of variable severity is accompanied by a normal number of large platelets on blood films, markedly prolonged bleeding times and abnormal platelet aggregation response to ristocetin.

14.12.2 The gray platelet syndrome

The gray platelet syndrome, where platelets lack the alpha granules that normally store P-selectin, are rare but much studied. Families with these syndromes manifest a bleeding disorder of variable severity. The platelets may contain abnormal vesicles that store some P-selectin. In addition, other important granule proteins are lacking and so the symptoms cannot be attributed to the reduction in P-selectin alone (Rosa et al., 1987).

14.13 Pharmacologically induced deficiency states

Because of the pivotal importance of $\alpha_{IIb}\beta_3$-integrins in producing platelet aggregation and thrombosis, methods of blocking the function of the $\alpha_{IIb}\beta_3$-integrin complex have been sought for decades. A temporary state of functional 'thrombasthenia', a sort of reversible Glanzmann's, has been demonstrated to be advantageous in a variety of situations in which thrombosis is life threatening.

In recent years, the rapid development of such drugs began with the development of $\alpha_{IIb}\beta_3$-integrin receptor blockers, with a monoclonal antibody that could abolish in vivo platelet thrombus formation (Coller et al., 1989). They were initially used therapeutically with success in patients with unstable angina (Gold et al., 1990) and have undergone large-scale clinical studies in patients with myocardial infarctions and postcoronary angioplasty (EPIC Investigators, 1994; Topol et al., 1994). A reduction in the combined endpoints of death, reinfarction or need for revascularisation has been demonstrated in these studies. Bleeding time was prolonged and significant bleeding complications were noted. The ability to define the resting and activated states of this molecule by flow cytometry have significantly contributed to our understanding of the function and therapeutic manipulations that are possible.

14.14 Analysis of platelet-directed antibodies

Anti-platelet antibodies are a major mechanism for accelerated elimination of platelets in diseases such as autoimmune thrombocytopenia, neonatal alloimmune thrombocytopenia, post-transfusion purpura, refractoriness to platelet transfusion and drug-induced thrombocytopenia. Platelet-reactive antibodies may be directed against allogeneic structures on glycoproteins thought to be platelet-specific antigens and which have been classified as human platelet antigens (HPA) 1–9 (von dem Borne et al., 1996), against human leukocyte antigen (HLA) class I molecules, drug-dependent structures and the platelet Fcγ-II receptor (CD32). In neonatal alloimmune thrombocytopenia and post-transfusion purpura, the platelet destruction is induced by anti-HPA antibodies, while autoimmune thrombocytopenia is caused by autoantibodies reacting with glycoproteins (mainly $\alpha_{IIb}\beta_3$-integrin), and platelet refractoriness is mainly caused by anti-HLA antibodies (Schmitz et al., 1998). Evaluation/quantification of platelet-bound immunoglobulins (Protocol 14.7) and measurement of antibody-induced platelet activation are two strategies for the detection of anti-platelet antibodies.

Protocol 14.7 Method for the detection of platelet-associated immunoglobulin

Sera

Sera from normal healthy volunteers who have not received blood transfusions are used as negative controls. Test sera are from patients with autoimmune thrombocytopenia diagnosed by standard criteria.

Antisera

FITC rabbit $F(ab')_2$ fragments, anti-human IgG and anti-human IgM are used to identify the platelet-associated immunoglobulin. FITC-conjugated mouse anti-GPIb or anti-GPIIIa is used as the positive control. FITC-conjugated rabbit anti-mouse immunoglobulin is used as a negative control. For analysis of indirect platelet-associated immunoglobulin, the optimal antiserum dilution may be determined by a chequer-board titration with various dilutions of antibody-containing and normal sera. The optimum dilution is that which gives maximal fluorescence with the antibody-containing serum and minimal fluorescence with the normal serum.

Blood collection and analysis

Blood should be analysed as soon after collection as possible. Storage of platelets results in activation, degranulation and expression of increased amounts of internalised IgG on the platelet surface (Fijnheer et al., 1990). Blood that has been stored for more than 24 h should not be analysed as the results will be spurious.

Preparation of a suspension of platelets

1. Blood is collected in liquid K_3EDTA (5 mg ml^{-1} blood). Platelet-rich plasma is obtained by centrifugation of EDTA-anticoagulated blood at $80 \times g$ for 20 min at room temperature.
2. The platelets are obtained by centrifugation of the platelet-rich plasma, at $640 \times g$ for 10 min at room temperature and then are washed three times with filtered (0.22 μm filter) 9 mmol l^{-1} EDTA in PBS (EDTA-PBS).
3. The platelets are resuspended in the same buffer containing 1% BSA (this should be greater than 99% globulin free) to a final concentration of 1×10^7 to 2×10^7 ml^{-1}.
4. Contamination by erythrocytes and other leukocytes should be less than 0.01×10^9 l^{-1}, as determined by a hematology differential counter.

Direct immunofluorescence test

1. A suspension of the patient's platelets (0.1 ml) is incubated with the optimum amount of (i) FITC-conjugated rabbit anti-human IgG or IgM, (ii) FITC-conjugated rabbit anti-mouse Ig, and (iii) FITC-conjugated mouse anti-human GP IIIa, for 20 min at room temperature.
2. The platelets are then washed twice with EDTA-PBS by centrifugation at $800 \times g$ and resuspended to 1 ml in EDTA-PBS and analysed by flow cytometry.
3. Cells examined by flow cytometry are analysed on a histogram of log forward angle light scatter and log 90° side light scatter; this allows distinction by size and granularity of contaminating red cells and platelet aggregates or fragments. Only single intact platelets are gated.
4. Confirmation of platelet gating is established using the positive control antibody with greater than 99% of gated events being positive. Background immunofluorescence is determined with the negative control cells for each patient; then all settings are retained unchanged during subsequent analysis. At least 10 000 gated events are analysed.

Indirect immunofluorescence test

1. A suspension (0.1 ml) of pooled blood group O platelets is incubated with 0.1 ml of patient's or control serum for 30 min at room temperature.
2. After incubation, the platelets are washed twice in filtered EDTA-PBS and then incubated with FITC-conjugated rabbit anti-human IgG or IgM at room temperature for 30 min.
3. Platelets are resuspended and analysed as above.

The fluorescence associated with platelets incubated with the control and test sera are compared and may be reported as a ratio of test fluorescence to control fluorescence.

Note: Platelets should be analysed fresh because paraformaldehyde-fixed or liquid nitrogen-frozen platelets exhibit high levels of nonspecific antibody binding and/or autofluorescence. The wash buffer used is at pH 6.5 to reduce binding of immune complexes (Myllyla, 1973) and prevent platelet activation (Lagarden et al., 1980).

Analysis of platelets in whole blood

It is possible to detect immunoglobulin directly on platelets in whole blood.

1. Anticoagulated whole blood (1 ml) is washed three times by centrifugation in 20 ml EDTA-PBS buffer then resuspended in buffer containing 1% BSA.
2. Portions (100 μl) are then incubated with antisera as described above and resuspended in 2 ml buffer containing 1% BSA and 0.0002% LDS-751 for analysis.
3. Cells are analysed in a histogram of log side light scatter and log red fluorescence (LDS-751 is a red nuclear dye that emits light maximally at 650 nm).

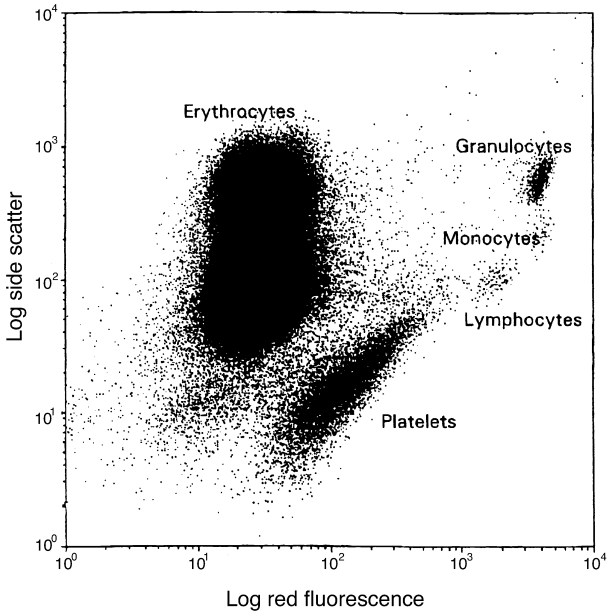

Fig. 14.5 The analysis of whole blood in which erythrocytes, platelets, lymphocytes, monocytes and granulocytes may be distinguished. Cells are analysed in a histogram of log side light scatter and log red fluorescence associated with LDS-751, a red nuclear dye that emits light maximally at 650 nm.

Figure 14.5 shows the analysis of whole blood in which erythrocytes, platelets, lymphocytes, monocytes and granulocytes may be distinguished. This method is not faster than Protocol 14.7 but does have the advantage that more than one cell type may be analysed for the presence of surface immunoglobulin binding. This is useful for the distinction of platelet-specific antibodies from those such as HLA or nonspecific antibodies that bind to other leukocytes. The presence of platelet-bound HLA antibodies may be important in certain situations such as transplantation.

14.15 Fluorescence resonance energy transfer

The analysis of fluorescence energy transfer (FRET) between anti-human antibodies detecting platelet-bound allo- or autoantibodies and monoclonal antibodies directed against specific target glycoproteins provides a novel flow cytometric technique. This method permits the epitope-specific characterisation of human antibodies directed against different target structures on platelets. It is based on the nonradiating energy transfer from a primary excited fluorophore to a second fluorophore not directly excited by the monochromatic light source. The critical dependence of FRET efficiency on the distance between both the fluorochromes permits the discrimination between epitopes within a distinct glycoprotein complex. Compared with the capture-based assays, this technique is faster, simpler and of clinical use, especially in patients refractory to platelet transfusion (Koksch et al., 1995).

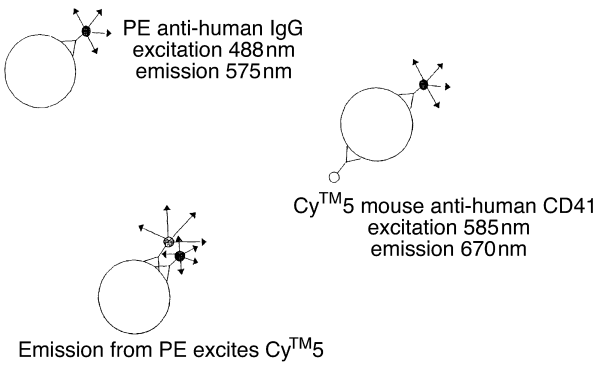

Fig. 14.6 Fluorescence resonance energy transfer involves transfer of energy from an excited fluorochrome to a second fluorochrome that then emits light. Here phycoerythrin (PE) is used as the donor and cyanin™5 (Cy™5) as the acceptor. PE but not Cy™5 is excited at 488 nm. PE transmits energy in a nonradiative manner to Cy™5 which emits light at 650 nm. Fluorescence from Cy™5 is only detectable if the PE is bound to the same, or nearby, site.

14.15.1 Direct fluorescence resonance energy transfer assay

In the direct FRET procedure, PE is used as the donor and cyanin™5 (Cy™5) as the acceptor fluorophore. Platelet suspensions (0.5 ml) are incubated with PE-conjugated goat anti-human IgG or IgM and mouse anti-human CD32 (FcγRII), CD41 (GPIIbIIIa), CD42b (GPIbβ), HLA-ABC or HLA-DR followed by incubation with Cy™5-conjugated goat anti-mouse antibodies. The cells are analysed on a flow cytometer equipped with an argon ion laser that emits light at 488 nm. PE but not Cy™5 is excited at 488 nm. PE transmits energy in a nonradiative manner to Cy™5, which emits light at 650 nm (Fig. 14.6). Fluorescence from Cy™5 is only detectable if the autoantibody is bound to the same site as the mouse monoclonal antibodies. This facilitates identification of the site of autoantibody binding.

14.16 Clinical relevance of platelet-directed antibodies

The flow cytometric quantification of platelet-bound immunoglobulin using anti-human IgG and IgM antisera (platelet immunofluorescence test, PIFT) is frequently used to detect anti-platelet antibodies and is regarded as sensitive (although sometimes it may not detect antibodies to low density antigens such as HPA-5). This test may either be performed directly, for detection of anti-platelet antibodies bound in vivo, or indirectly where patient serum is incubated with test platelets. The PIFT does not discriminate anti-HPA from anti-HLA antibodies and the nonspecific bound immunoglobulins. Direct PIFT in comparison with monoclonal antibody capture assays seem to identify a different group of patients, which in part may result from the detection of internalised antibodies in the latter assay (Joutsi and Kekomaki, 1997). The indirect PIFT when used as a crossmatching assay before platelet transfusion is well suited as a routine diagnostic assay.

The alternative measurement involving antibody-induced platelet activation has only a low practical value since only a subset of anti-platelet antibodies cause platelet activation. Flow cytometric analysis of platelet activation induced by antibodies to platelet factor 4–heparin complexes may be diagnostically helpful in patients with immune-mediated type II heparin-induced thrombocytopenia (Greinacher et al., 1994).

14.17 REFERENCES

Alattia, J.R., Kurokawa, H., Ikura, M. (1999) Structural veiw of cadherin mediated cell–cell adhesion. *Cellular and Molecular Life Science* **55**, 359–67.

Andrews, R.K., Lopez, J.A., Berndt, M.C. (1997) Molecular mechanisms of platelet adhesion and activation. *International Journal of Biochemical Cell Biology* **29**, 91–105.

Anti-platelet Trialist's Collaborative Study (1994) Collaborative overview of randomised trials of anti-platelet therapy 1. Prevention of death, myocardial infarction and stroke by prolonged anti-platelet therapy in various categories of patients. *British Medical Journal* **308**, 81–106.

Barnes, J.L. (1997) Platelets in glomerular disease. *Nephron* **77**, 378–93.

Beavon, R.G. (1999) Regulation of E-cadherin: does hypoxia

initiate the metastatic cascade. *Molecular Pathology* **52**, 179–88.

Berk, B.C., Alexander, R.W., Brock, T.A., Gimbrone, M.A. Jr, Webb, R.C. (1986) Vasoconstriction: a new activity for platelet derived growth factor. *Science* **232**, 87–90.

Bernard, J., Soulier, J.P. (1948) Sur une nouvelle variete de dystrophie thrombocytaire-hemorragipare congenitale. *Seminars d'Hôpital Paris* **24**, 3217–23.

Bevilacqua, M.P., Pober, D.L., Mendrick, R.S., Cotran, R.S., Gimbrone, M.A. Jr (1987) Identification of an inducible endothelial–leucocyte adhesion molecule. *Proceeding of the National Academy of Science of the USA* **84**, 9238–42.

Braque, P., Touqui, L., Shen, T.S., Vargaftig, B.B. (1987) Perspectives in platelet activating research. *Pharmaceutical Reviews* **39**, 97–145.

Cahill, M.R., Macey, M.G., Newland, A.C. (1993) Fixation with formaldehyde induces expression of activation dependent platelet membrane glycoproteins. *British Journal of Haematology* **84**, 527–9.

Cahill, M.R., Dawson, J.R., Newland, A.C. (1996a) Platelet surface activation antigen expression at baseline and during elective angioplasty in patients with mild to moderate coronary artery disease. *Blood Coagulation and Fibrinolysis* **7**, 165–8.

Cahill, M.R., Macey, M.G., Newland, A.C. (1996b) Correlation of GP53 and P-selectin expression in myeloproliferative disorders and normal controls. *Blood Coagulation and Fibrinolysis* **7**, 169–71.

CAPRIE Study Steering Committee (1996) A randomised blinded trial of clopidogrel versus aspirin in patients at risk of ischaemic events. *Lancet* **348**, 1329–39.

Cavenagh, J.D., Cahill, M.R., Kelsey, S.M. (1998) Adhesion molecules in clinical medicine. *Critical Reviews in Clinical Laboratory Sciences* **34**, 415–59.

Clarke, E.A., Brugge, J.S. (1995) Integrins and signal transduction pathways: the road taken. *Science* **168**, 233–39.

Clemenson, K.J. (1988) Biochemistry of platelet membrane glycoproteins In: Jamieson, G.A. (ed.), *Progress in Clinical and Biological Research: Platelet Membrane Receptors; Molecular Biology, Immunology, Biochemistry, and Pathology,* Vol. 282, pp. 33–75. Liss, New York.

Clemetson, K.J., McGregor, J.L. (1987) Characterisation of platelet membrane glycoproteins. In: MacIntyre, D.E., Gordon, J.L. (eds.), *Platelets in Biology and Pathology III*, pp. 1–32. Elsevier, Amsterdam.

Clemetson, K.J., McGregor, J.L., James, E. (1982) Characterization of the platelet membrane glycprotein abnormalities in Bernard–Soulier syndrome and comparison with normal by surface labelling techniques and high-resolution two dimensional gel electrophoresis. *Journal of Clinical Investigation* **70**, 304–11.

Coller, B.S. (1989) Activation-specific platelet antigens. In: Kunicki, T.J. (ed.), *Platelet Immunobiology: Molecular and Clinical Aspects,* pp. 166–89. Lippincott, Philadelphia, PA.

Coller, B.S., Folts, J.D., Smith, S.R., Scudder, L.E., Jordan, R. (1989) Abolition of *in vivo* platelet thrombus formation in primates with monoclonal antibodies to platelet GPIIb/IIIa receptor. *Circulation* **80**, 1766–74.

Collins, C.E., Cahill, M.R., Newland, A.C., Rampton, D.S. (1994) Platelets circulate in an activated state in inflammatory bowel disease. *Gastroenterology* **106**, 840–5.

Dachary-Prigent, J., Pasquet, J.M., Freyssinet, J.M., Carron, J.C., Nurden, A.T. (1993) Annexin V as a probe of aminophospholipid exposure and platelet membrane vesiculation: a flow cytometry study showing a role for free sufhydryl groups. *Blood* **81**, 2554–65.

Dachary-Prigent, J., Pasquet, J.M., Freyssinet, J.M., Nurden, A.T. (1995) Calcium involvement in aminophospholipid exposure and microparticle formation during platelet activation: a study using Ca^{2+}-ATPase inhibitors. *Biochemistry* **34**, 11625–34.

Davies, T.A., Long, H.J., Tibbles, H.E., Sgro, K.R., Wells, J.M., Rathbun, W.H., Seetoo, K.F., McMenamin, M.E., Smith, S.J., Feldman, R.G., Levesque, C.A., Fine, R.E., Simons, E.R. (1997) Moderate and advanced Alzheimer's patients exhibit platelet activation differences. *Neurobiology and Ageing* **18**, 155–62.

Deuel, T.F., Senior, R.M., Chang, D., Griffin, G.L., Heinrikson, R.L., Kaiser, E.T. (1981) Platelet factor 4 is chemotactic for neutrophils and monocytes. *Proceedings of the National Academy of Science of the USA* **78**, 4584–7.

Deuel, T.F., Senior, R.M., Huang, J.S., Griffin, G.L. (1982) Chemotaxis of monocytes and neutrophils to platelet derived growth factor. *Journal of Clinical Investigation* **69**, 1046–9.

EPIC Investigators (1994) Use of a monoclonal antibody directed against the platelet glycoprotein IIb/IIIa receptor in high risk coronary angioplasty. *New England Journal of Medicine* **330**, 956–61.

ETDRS Investigators (1992) Aspirin effects on mortality and morbidity in patients with diabetes mellitus. Early Treatment Diabetic Retinopathy Study, Report 14. *Journal of the American Medical Association* **268**, 1291–1300.

Etzioni, A., Frydman, M., Pollack, S., Avidor, I., Phillips, M.L., Paulson, J.C., Gershoni-Baruch, R. (1992) Recurrent severe infections caused by a novel leucocyte adhesion deficiency. *New England Journal of Medicine* **327**, 1789–92.

Evangelista, V., Piccardoni, P., White, J.G., de Gaetano, G., Cerletti, C. (1993) Cathepsin G-dependent platelet stimulation by activated polymorphonuclear leucocytes and its inhibi-

tion by antiproteinases: role of P-selectin mediated cell-cell adhesion. *Blood* **81**, 2947–57.

Febbraio, M., Silverstein, R.L. (1990) Identification and characterisation of LAMP-1 as an activation-dependent platelet surface glycoprotein. *Journal of Biological Chemistry* **256**, 18531–7.

Fijnheer, R., Modderman, P.W., Veldman, Ouwehand, W.H., Nieuwenhuis, H.K., Roos, D., de Korte, D. (1990) Detection of platelet activation with monoclonal antibodies and flow cytometry. Changes during platelet storage. *Transfusion* **30**, 20–5.

French, D.L., Seligsohn, U. (2000) Platelet glycoprotein IIb/IIIa receptors and Glanzmann's thrombasthenia. *Arteriosclerosis, Thrombosis and Vascular Biology* **20**, 607–10.

Frojmovic, M.M. (1996) Flow cytometric analysis of platelet activation and fibrinogen binding. *Platelets* **7**, 9–21.

Garrod, D.R. (1993) Cell to cell and cell to matrix adhesion. *British Medical Journal* **306**, 703–5.

Gawaz, M.P., Mujais, S.K., Schmidt, B., Gurland, H.J. (1994) Platelet–leucocyte aggregation during hemodialysis. *Kidney* **46**, 489–95.

George, J.N., Shattil, S.J. (1991) The clinical importance of acquired abnormalities of platelet function. *New England Journal of Medicine* **324**, 27–39.

George, J.N., Nurden, A.T., Philips, D.R. (1984) Molecular defects in interactions of platelets with the vessel wall. *New England Journal of Medicine* **311**, 1084–98.

Goetzl, E.J., Woods, J.M., Gorman, R.R. (1977) Stimulation of human eosinophils and neutrophil polymorphonuclear leukocyte chemotaxis and random migration by 12-L-hydroxy-5,8,10,14-eicosatetraenoic acid. *Journal of Clinical Investigation* **59**, 179–81.

Gold, H.K., Gimple, L., Yasuda, T., Leinbach, R.S., Werner, W., Holt, R., Jordan, R., Berger, J.H., Collen, D., Coller, B.S. (1990) Pharmacodynamic study of $F(ab')_2$ fragments of murine monoclonal antibody directed against human platelet glycoproteins GPIIb/IIIa in patients with unstable angina pectoris. *Journal of Clinical Investigation* **86**, 651–59.

Goodison, S., Urquidi, V., Tarin, D. (1999) CD44 cell adhesion molecules. *Molecular Pathology* **52**, 189–96.

Greinacher, A., Admiral, J., Dummel, V., Vissac, A., Kiefel, V., Mueller-Eckhardt, C. (1994) Laboratory diagnosis of heparin-associated thrombocytopenia and comparison of platelet aggregation test, and platelet factor 4/heparin enzyme linked immunosorbent assay. *Transfusion* **34**, 381–5.

Hatam, L., Schuval, S., Bonagura, V.R. (1994) Flow cytometric analysis of natural killer cell function as a clinical assay. *Cytometry* **16**, 59–68.

Hoffman, M., Monroe, D.M., Roberts, H.R. (1992) Coagulation factor Ixa binding to activated platelets and platelet derived microparticles: a flow cytometric study. *Thrombosis and Haemostasis* **68**, 74–8.

Hogg, N., Stewart, M.P., Scark, S.L. (1999) A novel leucocyte adhesion deficiency caused by expressed but non functional α_2 integrins MAC-1 and LFA-1. *Journal of Clinical Investigation* **109**, 97–106.

Hsu-Lin, S.C., Berman, C.L., Furie, B.C., August, D., Furie, B. (1984) A platelet membrane protein expressed during platelet activation and secretion. Studies using a monoclonal antibody specific for thrombin activated platelets. *Journal of Biological Chemistry* **259**, 9121–6.

Israels, S.J., Gerrard, J.M., Jaques, Y.V., McNicol, A., Cham, B., Nishibori, M., Bainton, D.F. (1992) Platelet dense granule membranes contain both granulophysin and P-selectin (GMP-140) *Blood* **101**, 880–6.

Jankowski, J.A., Wright, N.A., Metzler, S.J. (1999) Molecular evolution of the metaplasia–dysplasia–adenocarcinoma sequence in the eosophagus. *American Journal of Pathology* **154**, 965–73.

Johnston, G.I., Cook, R.G., McEver, R.P. (1989) Cloning of GMP-140, α granule membrane protein of platelets and endothelium: sequence similarity to proteins involved in cell adhesion and inflammation. *Cell* **56**, 1033–44.

Jousti, L., KeKomaki, R. (1997) Comparison of the platelet immunofluorescence test (direct PIFT) with a modified direct monoclonal antibody specific immobilization of platelet antigens (direct MAIPA) in detection of platelet associated IgG. *British Journal of Haematology* **96**, 204–9.

Knight, C.J., Panesar, M., Wright, C., Clarke, D., Butowski, P.S., Patel, D., Patrineli, A., Fox, K., Goodall, A.H. (1997) Altered platelet function detected by flow cytometry. Effects of coronary artery disease and age. *Arteriosclerosis, Thrombosis and Vascular Biology* **17**, 2044–53.

Koksch, M., Rothe, G., Keifel, V., Schmitz, G. (1995) Fluorescence resonance energy transfer as a new method for the epitope-specific characterisation of antiplatelet antibodies. *Journal of Immunological Methods* **187**, 53–67.

Konijnenberg, A., van der Post, J.A., Mol, B.W., Schaap, M.C., Lazarov, R., Bleker, O.P., Boer, K., Sturk, A. (1997) Can flow cytometric detection of platelet activation early in pregnancy predict the occurrence of preeclampsia? A prospective study. *American Journal of Obstetrics and Gynecology* **177**, 434–42.

Korlipara, L.V., Leon, M.P., Rix, D.A., Douglas, M.S., Gibbs, P., Bassendine, M.F., Kirby, J.A. (1996) Development of a flow cytometric assay to quantify lymphocyte adhesion to cytokine-stimulated human endothelial and biliary epithelial cells. *Journal of Immunological Methods* **191**, 121–30.

Kuhne, T., Hornstein, A., Semple, J., Chang, W., Blanchette, V.,

Freedman, J. (1995) Flow cytometric evaluation of platelet activation in blood collected into EDTA vs Diatube-H, a sodium citrate solution supplemented with theophylline, adenosine and dipyridamole. *American Journal of Haematology* **50**, 40–5.

Kuijpers, T.W., van Lier, R.A.W., Hamann, D. (1997) Leucocyte adhesion type 1 (LAD-1) variant. *Journal of Clinical Investigation* **100**, 1725–33.

Lagarden, M., Bryon, P.A., Guichardant, M., Dechavanne, M. (1980) A simple and efficient method for platelet isolation from their plasma. *Thrombosis Research* **17**, 581–8.

Larrieu, M.J., Caen, J.P., Meyer, D.O., Vainer, H., Sultan, Y., Bernard, J. (1968) Congenital bleeding disorders with long bleeding time and normal platelet count. *American Journal of Medicine* **45**, 354–72.

Li, N., Goodall, A.H., Hjemdahl, P. (1997) A sensitive flow cytometric assay for circulating platelet–leucocyte aggregates. *British Journal of Haematology* **99**, 808–16.

Li, N., Goodall, A.H., Hjemdahl, P. (1999) Efficient flow cytometric assay for platelet–leucocyte aggregates in whole blood using fluorescence signal triggering. *Cytometry* **35**, 145–61.

Lorant, D.E., Topham, K.M., Whatley, R.E., McEver, R.P., McIntyre, T.M., Prescott, S.M., Zimmerman, G.A. (1993) Inflammatory roles of P selectin. *Journal of Clinical Investigation* **92**, 559–70.

Lowdell, M.W., Ray, N., Crastin, R., Corbett, T., Deane, M., Prentice, H.G. (1997) The in vitro detection of anti-leukaemia-specific cytotoxicity after autologous bone marrow transplantation for acute leukaemia. *Bone Marrow Transplantation* **19**, 891–7.

Macey, M.G., Carty, E., Webb, L., Chapman, E.S., Zelmanovic, D., Okrongly, D., Rampton, D.S., Newland, A.C. (1999) Use of mean platelet component to measure platelet activation on the Advia 120 haematology system. *Cytometry* **38**, 250–5.

McEver, R.P., Martin, M.N. (1984) A monoclonal antibody to a membrane glycoprotein binds only to activated platelets. *Journal of Biological Chemistry* **259**, 9799–804.

Metzelaar, M.J., Clevers, H.C. (1992) Lysosomal membrane glycoproteins in platelets. *Thrombosis and Haemostasis* **68**, 378–82.

Metzelaar, M.J., Heijnen, H.F.G., Sixma, J.J., Niewenhuis, H.K. (1992) Identification of a 33 kDa protein associated with the β-granule membrane (GMP-33) that is expressed on the surface of activated platelets. *Blood* **79**, 372–9.

Michelson, A.D., Benoit, S.E., Kroll, M.H., Li, J.M., Rohrer, M.J., Kestin, A.S., Barnard, M.R. (1994) The activation induced decrease in platelet surface expression of the glycoprotein Ib–IX complex is reversible. *Blood* **83**, 3562–73.

Mistry, R., Cahill, M., Chapman, C., Wood, J.K., Barnett, D.B. (1991) ^{125}I-Fibrinogen binding to platelet in myeloproliferative disorders. *Thrombosis and Haemostasis* **66**, 329–33.

Mody, M., Lazarus, A.H., Semple, J.W., Freedman, J. (1999) Preanalytical requirements for flow cytometric evaluation of platelet activation: choice of anticoagulant. *Transplantation Medicine* **9**, 147–54.

Monteiro, M., Sansonetty, F., Goncalves, M.J., O'Connor, J.E. (1999) Flow cytometric kinetic assay of calcium mobilization in whole blood platelets using fluo-3 and CD41. *Cytometry* **35**, 302–10.

Moore, K.L., Varki, A., McEver, R.P. (1991) GMP140 binds to a glycoprotein receptor on human neutrophils: evidence for a lectin like interaction. *Journal of Cell Biology* **112**, 491–9.

Myllyla, G. (1973) Aggregation of human blood platelets by immune complexes in the sedimentation pattern test. *Scandinavian Journal of Haematology* **19**, 50.

Nurden, A.T., Caen, J.P. (1975) Specific roles for platelet surface glycoprotein in platelet function. *Nature* **255**, 720–22.

Oda, A., Daley, J.F., Cabral, C., Kang, J., Smith, M., Salzman, E.W. (1992) Heterogeneity in filament actin content among individual human blood platelets. *Blood* **79**, 920–7.

Okada, M., Sagawa, T., Tominaga, A., Kodama, T., Hitsumoto, Y. (1996) Two mechanisms for platelet-mediated killing of tumour cells: one cyclo-oxygenase dependent and the other nitric oxide dependent. *Immunology* **89**, 158–64.

Peters, M.J., Dixon, G., Kotowicz, K.T., Hatch, D.J., Heyderman, R.S., Klein, N.J. (1999) Circulating platelet–neutrophil complexes represent a subpopulation of activated neutrophils primed for adhesion, phagocytosis and intracellular killing. *British Journal of Haematology* **106**, 391–9.

Plow, E.F., Ginsberg, M.H. (1988) Cellular adhesion: GPIIb/IIIa as a prototypic adhesion receptor. *Progress in Hemostasis and Thrombosis* **296**, 320–31.

Ristamaki, R., Joesuu, H., Lappalainen, K. (1997) Elevated serum CD44 level is associated with unfavourable outcome in non-Hodgkin's lymphoma. *Blood* **90**, 4039–45.

Rosa, J.P., George, J.N., Bainton, D.F. (1987) Gray platelet syndrome. Demonstration of alpha granule membranes that can fuse with the cell surface. *Journal of Clinical Investigation* **80**, 1138.

Ruf, A., Patscheke, H. (1995) Flow cytometric detection of activated platelets: comparison of determining shape change, fibrinogen binding and P-selectin expression. *Seminars in Thrombosis and Hemostasis* **21**, 146–51.

Schmitz, G., Rothe, G., Ruf, A., Barlage, S., Tschope, D., Clemetson, K.J., Goodall, A.H., Michelson, A.D., Nurden, A.T., Shankey, V.T. (1998) European working group on clinical cell analysis: consensus protocol for the flow cytometric charac-

terisation of platelet function. *Thrombosis and Haemostasis* **79**, 885–96.

Shattil, S.J., Cunningham, N., Hoxie, J.A., Brass, L.F. (1985) Changes in the platelet membrane glycoprotein IIb/IIIa complex during platelet activation. *Journal of Biological Chemistry* **260**, 11107–14.

Shattil, S.J., Cunningham, N., Hoxie, J.A. (1987) Detection of activated human platelets in whole blood using activation-dependent monoclonal antibodies and flow cytometry. *Blood* **70**, 307–15.

Sibai, B.M., Caritis, S.N., Thom, E., Klebanoff, M., McNellis, D., Rocco, L., Paul, R.H., Romero, R., Witter, F., Rosen, M. (1993) Prevention of pre-eclampsia with low-dose aspirin in healthy nulliparous pregnant women. The National Institute of Child Health and Human Development Network of Maternal Fetal Medicine Units. *New England Journal of Medicine* **329**, 1213–18.

Siess, W. (1990) Platelets in the pathogenesis of atherosclerosis. *Advances in Experimental Medicine and Biology* **273**, 119–27.

Silverstein, R.L., Febbraio, M. (1992) Identification of lysosomal membrane associated protein-2 as an activation dependent platelet surface glycoprotein. *Blood* **80**, 1470–5.

Sims, P.J., Ginsberg, M.H., Plow, E.F., Shattil, S.J. (1991) Effect of platelet activation on the conformation of the plasma membrane glycoprotein GPIIb/IIIa complex. *Journal of Biological Chemistry* **266**, 7345–52.

Thibert, V., Bellucci, S., Cristofari, M., Gluckman, E., Legrand, C. (1995) Increased platelet CD36 constitutes a common marker in myeloproliferative disorders. *British Journal of Haematology* **91**, 618–24.

Topol, E.J., Califf, R.M., Weisman, H.F., and the EPIC Investigators. (1994) Randomised trial of coronary intervention with antibody against platelet IIb/IIIa integrin for reduction of clinical restenosis: results at six months. *Lancet* **343**, 881–6.

Tschoepe, D., Driesch, E., Schwippert, B., Lampeter, E.F. (1997a) Activated platelets in subjects at increased risk of IDDM. *Diabetologia* **40**, 573–7.

Tscheope, D., Rauch, U., Schwippen, B. (1997b) Platelet–leucocyte cross-talk in diabetes mellitus. *Hormone and Metabolic Research* **29**, 631–5.

Ugarova, T.P., Budzynski, A.Z., Shattil, S.J., Ruggeri, Z.M., Ginsberg, M.H., Plow, E.F. (1993) Conformational changes in fibrinogen elicited by its interaction with platelet membrane glycoprotein GpIIb/IIIa. *Journal of Biological Chemistry* **268**, 21080–7.

Wahl, S.M., Hunt, D.A., Wakefield, L.M. (1987) Transforming growth factor type beta induces monocyte chemotaxis and growth factor production. *Proceedings of the National Academy of Sciences of the USA* **63**, 943–5.

Wall, J.E., Buijs, Wilt, M., Arnold, J.T., Wang, W., White, M.M., Jennings, L.K., Kackson, C.W. (1995) A flow cytometric assay using mepacrine for study of uptake and release of platelet dense granule contents. *British Journal of Haematology* **89**, 380–5.

Weyrich, A.S., McIntyre, T.M., McEver, R.P. (1995) Monocyte tethering by P-selectin regulates monocyte chemotactic protein-1 and tumor necrosis factor-α secretion. Signal integration and NF-κB transduction. *Journal of Clinical Investigation* **95**, 2297–303.

Woods, V.L. Jr, Wolff, L.E., Keller, D.M. (1986) Resting platelets contain a substantial centrally located pool of glycoprotein IIb–IIIa complex which may be accessible to some but not other extracellular proteins. *Journal of Biological Chemistry* **261**, 15242–51.

Vestweber, D. (1992) Selectins: cell surface lectins which mediate the binding of leucocytes to endothelial cells. *Seminars in Cell Biology* **3**, 211–20.

von dem Borne, A.E.G.K., de Haas, M., Simcek, S., Porcelijn, L., van der Schoot, C.E. (1996) Platelet and neutrophil alloantigens in clinical medicine. *Vox Sanguinis* **70**, 34–40.

Zagursky, R.J., Sharp, D., Solomon, K.A., Schwartz, A. (1995) Quantitation of cellular receptors by a new immunocytochemical flow cytometry technique. *Biotechniques* **18**, 504–9.

15

Nucleic acids

Charles L. Goolsby

Northwest University Medical School, Chicago, USA

15.1 Introduction

Although much remains to be elucidated, the molecular mechanisms underlying or associated with a number of human diseases have, in the 1990s, become better understood. With the completion of the Human Genome Project, we can expect human disease-associated loci or genes to be discovered with greater frequency. The accompanying paradigm shift in laboratory medicine to a wider use of molecular techniques in the diagnosis of human disease is clearly reflected in the new proposed World Health Organization classification of acute leukaemias. At the same time there is a move to use of molecular detection methods for the determination of antibiotic resistance genes in bacterial infections. Clinicians will increasingly be expected to understand the genetic basis of disease and to interpret the results of laboratory tests aimed at detecting or reflecting events at the genetic level.

Where there is a strong correlation and specificity between an underlying genetic alteration and cellular immunophenotype, cytometry may be a cost-effective and powerful screening tool. However, combined genetic and immunophenotypic analysis at the single cell level can provide information that is essential to a better understanding of the role of cellular heterogeneity in disease onset and progression and of the response to therapy. This can be facilitated by linking sequence-specific nucleic acid detection techniques with classical cell-based quantitative, multiparameter approaches such as flow cytometry or laser scanning cytometry. Thus subpopulations that are positive for a specific genetic sequence, genetic alteration or infectious organism can be detected within cell populations of a given immunophenotype; conversely, immunophenotypic heterogeneity can be determined within cell populations containing a particular nucleic acid sequence.

In infectious disease, the potential utility of cell-based molecular cytometry approaches has already been demonstrated in the analysis of human immunodeficiency virus (HIV) associated disease (Borzi et al., 1996; Patterson et al., 1993, 1995, 1998). Cell-based flow cytometry assays employing the polymerase chain reaction (PCR) and the reverse transcriptase polymerase chain reaction (RT-PCR) coupled with immunophenotyping have clarified which cell populations are latently and actively infected (Patterson et al., 1993) and have detected altered cellular characteristics accompanying infection (Patterson et al., 1995). Furthermore, data from flow cytometry fluorescence in situ hybridisation (FISH) detection of HIV RNA, coupled with immunophenotypic analysis, suggest that cell-based measurements of viral load may offer additional prognostic information to plasma viral load determinations in monitoring the emergence of drug-resistant populations (Patterson et al., 1998). Clearly, knowledge of the cellular reservoirs for both latent and active viral infection is important in understanding the dynamics of virus populations during both early infection and disease progression. Monitoring how therapy alters the active and latent virus reservoirs and cellular characteristics, such as the receptors or co-receptors, that are necessary for infection may be critical in optimising therapeutic responses. Similar potential obviously exists for the *in situ* detection of other viruses such as human

cytomegalovirus, Epstein–Barr virus (EBV), and human papilloma virus (HPV) (Imbert-Marcille et al., 1997; Just et al., 1998; Komminoth et al., 1994; Lizard et al., 1993; Montone et al., 1996), particularly where the wealth of surrogate markers seen in HIV does not exist.

Strong associations with specific chromosomal abnormalities are seen in a number of hematopoietic malignancies. In the classic examples of chronic myeloid leukaemia (CML) (Lee et al., 1992; Nowell and Hungerford, 1960; Rowley, 1973) and acute promyelocytic leukaemia (APML) (Larson et al., 1984; LoCoco et al., 1992), documentation of the presence of the t(9;22) and t(15;17) transclocations, respectively, or their molecular counterparts, is becoming mandatory for confirmation of the diagnosis. In addition to these classic examples, numerous leukaemias (Borkhardt et al., 1997; Claxton et al., 1994; Gauwerky and Croce, 1993; Harbott et al., 1997; Kita et al., 1994; Nucifora and Rowley, 1994; Taub et al., 1982; Thirman et al., 1993) and lymphomas (Gauwerky and Croce, 1993; Lambrechts et al., 1993; Soubeyran et al., 1993; Taub et al., 1982) are now highly associated with specific chromosomal abnormalities. In addition to the diagnostic importance of cytogenetic data, important prognostic subgroups are also frequently defined; for example, patients with B-cell acute lymphoblastic leukaemia (B-ALL) and positive for t(1;19) have a significantly poorer prognosis (Hunger et al., 1991; Izraeli et al., 1993) than others. As mentioned above, in some cases immunophenotypic features may correlate with the same group that is defined by an underlying cytogenetic abnormality, in this case, cytoplasmic μ expression. A very interesting family, or group, of translocations, all involving the genes for either the α- or β-chains of the core-binding transcription factor (Borkhardt et al., 1997; Claxton et al., 1994; Harbott et al., 1997; Kita et al., 1994; Nucifora and Rowley, 1994), has come to light. These include t(12;21) in childhood B-ALL (Borkhardt et al., 1997; Harbott et al., 1997), t(8;21) in the M2 category of patients with acute myeloid leukaemia (AML M2) (Kita et al., 1994; Nucifora and Rowley, 1994), and inv(16) in AML M4 with eosinophilia (Claxton et al., 1994). Abnormalities in the genes coding for this single transcription factor are involved in approximately 15 to 20% of all acute leukaemias and, although a diverse group of malignancies, they all carry a relatively good prognosis. Therefore, for both diagnostic and prognostic reasons, it is clearly appealing to be able to provide data on genetic aberrations at the same time as that on the immunophenotype of hematopoietic malignancies.

Molecular techniques such as PCR and RT-PCR can be quite sensitive at detecting the presence of cells of minimum residual disease in many malignancies. However, a more complete understanding than simply the presence or absence of residual disease cells is needed in order to identify those patients in whom disease is going to recur and who, therefore, may require more intensive therapy or follow-up, as opposed to those in whom recurrence is less likely and who may be spared unnecessary additional therapy, which itself carries an increased risk of morbidity. For example, in APML (LoCoco et al., 1992), other than in the short interval following *all-trans*-retinoic acid therapy, the detection of residual disease at any level is a bad prognostic sign indicative of recurrence. By comparison, in CML (Lee et al., 1992; Zhao et al., 1993), detectable residual disease is seen in a significant fraction of patients in long-term clinical remission. Westbrook (1992) has suggested that it may be the number of CML residual cells, not just presence or absence, that may be important in whether a patient relapses or not. Once 'molecular cytometry' techniques with adequate sensitivity have been developed, they will provide important information not only on the number of residual cells (tumour burden) but also on critical cellular features, such as proliferation, drug resistance status and other prognostic markers. These data and an understanding of the heterogeneity in dysregulation of proliferation/apoptosis and of the activation of drug resistance mechanisms within the residual disease cells in response to therapy will be key to predicting in which patients disease is going to recur. Excitingly, this will allow a patient-specific evaluation of who does, and does not, require more intensive therapy.

Although the cytogenetics of most solid tumours

is considerably more complex than that of haematopoietic diseases and, as yet, few disease-defining abnormalities have been identified, the application of nucleic acid-based molecular cytometry techniques is still relevant. The most obvious current application would be in the identification of the amplification of relevant genes such as *HER2/neu* (Szollosi et al., 1995). Amplification of *HER2/neu* carries prognostic significance in breast cancer but the heterogeneity within the tumour cell population of this amplification and the relationship to protein expression remains to be elucidated. It is also clear that the pattern and nature of underlying genomic instability is reflected in the phenotype and characteristics of the tumour population (Shackney and Shankey, 1997). The key to a more complete understanding of this relationship will be the development of techniques to assess these connections more directly.

Lastly, the translocations and genetic alterations that underlie many human malignancies result in the production of altered proteins, or even new fusion proteins, that are important in disease initiation, progression and response to therapy, and which may, therefore, serve as relevant targets for development of new therapeutics, as has been seen in APML (Huang et al., 1988; Warrell et al., 1991) and CML (Thiesing et al., 1999). Additionally, the chromosomal and genetic changes that underlie cancer development are taking place in a background of cellular regulatory processes, which are controlled by multiple and, in some instances, redundant pathways. The regulation of cell proliferation, apoptosis, differentiation and response to therapy is influenced not only by alterations in the tumour cells but also by surrounding normal cells, and vice versa. This reinforces the need for advances in the development of techniques to detect these abnormalities and their associated protein products at the cellular level. Consequently, as more sophisticated multiparameter molecular cytometry techniques are developed, an exciting realm of new studies in a number of areas will unfold both in the clinical and basic research areas.

In this chapter, the current state of cell-based 'molecular cytometry' techniques will be discussed.

15.2 Flow karyotyping

Before discussing the detection of specific nucleic acid sequences in individual cells, it is appropriate to consider briefly the flow cytometric analysis of chromosomes isolated in suspension. Many genetic alterations relevant in cancer were originally identified by classical cytogenetic analysis and these studies frequently point to relevant targets for in situ or molecular detection even when changes are not seen at the chromosome level. Additionally, the development of flow cytometry techniques for identifying individual chromosomes (Jensen et al., 1977; Langlois et al., 1982) preceded the development of those for *in situ* nucleic acid hybridisation (Trask et al., 1985) by some years.

For the flow cytometric analyses of chromosomes in suspension, chromosomes are isolated from exponentially growing cultures of cells that have been enriched for mitotic cells by employing mitotic blocking agents such as colcemid. The mitotic cells are then 'shaken' off and the chromosomes isolated by resuspending the cells in a hypotonic solution along with agents to stabilise the chromosomes when they are released. Disruption of the mitotic cells is accomplished using detergents and/or physical shearing forces. Reviews of these techniques can be found in publications by Bartholdi et al. (1987a) and Cram et al. (1990). Chromosomes are stained either with a single fluorescent dye that binds stochiometrically to the DNA (Bartholdi et al., 1987a,b; Cram et al., 1990) or with two fluorescent DNA-binding dyes, one which preferentially binds to AT-rich regions and one that preferentially binds to GC-rich regions (Bartholdi et al., 1987a; Cram, 1990; Gray et al., 1986; Langlois et al., 1982). The latter technique enables chromosomes to be distinguished not only by their total DNA content but also by differences in their AT and GC content (Protocol 15.1). An example of this type of bivariate analysis of chromosomes from a human foreskin fibroblast cell strain culture is shown in Fig. 15.1, in which it is possible to resolve all but the 9–12 group of human chromosomes. Alternative staining techniques developed by Meyne et al. (1984) enable chromosome 9 from this group to be

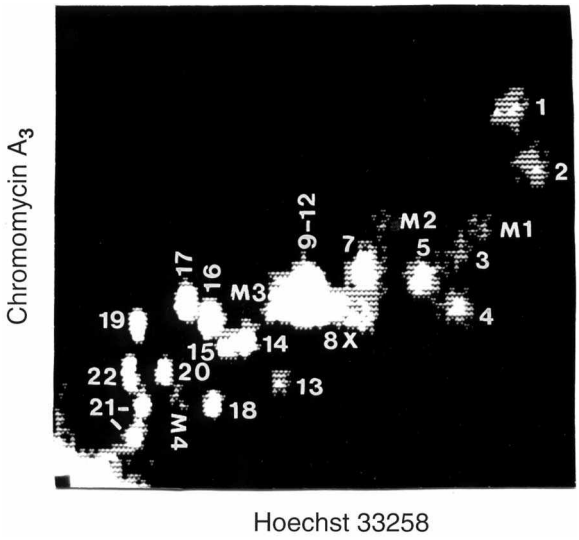

Fig. 15.1 Bivariate histogram of chromomycin A_3 versus Hoechst 33258 staining of chromosomes isolated from an SV40-transformed human cell line after 136 population doublings in tissue culture, demonstrating resolution of all the normal chromosomes (all but 9–12 are numbered individually) as well as abnormal marker chromosomes (M1–4). (Reprinted from *Cancer Genetics and Cytogenetics* **50**, Goolsby, C.L., Wiley, J.E., Steiner, M., Bartholdi, M.F., Cram, L.S., Kraemer, P.M., Karyotype evolution in a simian virus 40-transformed tumorigenic human cell line, pages 231–48 (1990) with permission from Elsevier Science.)

resolved although resolution of other chromosomes is lost.

Protocol 15.1 Bivariate staining of chromosome preparations

Reagents

Chromosome isolation buffer containing spermine and spermidine: 15 mmol l^{-1} tris-HCl, 2 mmol l^{-1} ethylenediamine tetraacetic acid (EDTA), 0.5 mmol l^{-1} EGTA (ethylene glycol-bis(β-aminoethyl ether)-*N,N,N',N'*-tetraacetic acid), 80 mmol l^{-1} KCl, 20 mmol l^{-1} NaCl, 0.1% (v/v) β-mercaptoethanol, 1.2 mg ml^{-1} digitonin, 0.2 mmol l^{-1} spermine, 0.5 mmol l^{-1} spermidine). The first five ingredients in buffer are mixed, the pH adjusted to 7.2 and β-mercaptoethanol added. The digitonin is then added and solution incubated at 37°C for 45 min followed by filtering (0.22 μm). Then spermine and spermidine are added

- Chromomycin A_3 stock solution: chromomycin A_3 at 0.5 mg ml^{-1} (520 μmol l^{-1}) prepared in McIlvane's buffer (a solution of 0.1 mol l^{-1} citric acid mixed with 0.2 mol l^{-1} Na_2HPO_4 to give a pH of 7.0) mixed with equal volume of 5 mmol l^{-1} $MgCl_2$
- Hoechst 33258 stock solution: 0.5 mg ml^{-1} (49 μmol l^{-1}) in deionised water

Protocol

1. Add 0.1 mg ml^{-1} colcemid to exponentially growing cultures of cells.
2. Incubate for 10–14 h (approximately 40–50% of population doubling time) under optimum growth conditions. The length of the colcemid block and the colcemid concentration needed will vary with different cell types.
3. Concentrate mitotic cells by mitotic shake off.
4. Wash the mitotic-enriched cell suspension in phosphte-buffered saline (PBS).
5. Resuspend 5×10^6 to 7×10^6 cells in 0.5 ml 40 mmol l^{-1} KCl.
6. Incubate at room temperature for 10 min. The length of this hypotonic step, temperature, and KCl concentration will vary with different cell types.
7. Add an equal volume of chromosome isolation buffer.
8. Incubate on ice for 1 min.
9. Release chromosomes by vortexing for 30–45 s. The speed and time of vortexing required will be dependent on the individual preparation as well as the cell type. Chromosome release and quality during this step must be checked by examining small samples of the suspension stained

with a DNA fluorescent dye such as propidium iodide (PI).
10. Add chromomycin A_3 stock solution to a final concentration of 120 μmol l^{-1}.
11. Incubate at 4°C for 12–24 h.
12. Add Hoechst 33258 stock solution to a final concentration of 1.7 μmol l^{-1}.

Analysis

Chromosomes are then analysed on a dual laser flow cytometer with ultraviolet (either argon or krypton laser) and violet (457.9 nm) excitation. Sheath fluid should be same as chromosome isolation buffer minus digitonin, spermine and spermidine.

Flow cytometric bivariate chromosome analysis can clearly detect or identify anomalies in chromosome number, reciprocal translocations and other chromosomal aberrations within a cell population (Gray et al., 1988; Lebo et al., 1986). It is important to point out that flow cytometric analysis of chromosomes in suspension yields information on the relative frequency of specific chromosomes within the whole cell population and not of individual cells. For example, a perfect tetraploid population would look no different from a diploid population and, likewise, a population containing 40% of the cells diploid for a given chromosome and 60% trisomic for the same chromosome would look identical to a population that was 70% diploid and 30% tetrasomic for that chromosome.

Nonetheless, the flow karyotyping information does carry significant data on how well cells carrying specific abnormalities are competing or surviving within an evolving population such as a tumour. For example, in studies of karyotype instability in cancer, flow karyotyping coupled with traditional G-banded analyses were particularly useful in monitoring the evolution of specific chromosomal abnormalities during neoplastic progression (Bartholdi et al., 1987b; Goolsby et al., 1990). Reproducible flow cytometric analyses, particularly the detection of anomalies in chromosome number and of reciprocal translocations, requires very careful preparation and analysis of material. The complexity of these analyses and their susceptibility to loss of specific chromosomes, particularly the larger ones, has prevented wider use of these techniques in a clinical setting. However, sorting of specific chromosomes based on these techniques was crucial to the generation of the chromosome-specific libraries essential for the Human Genome Project (Deaven et al., 1986).

One application that has proved useful with clinical material has been the sorting of marker chromosomes that could not be completely characterised by chromosome banding techniques (Blennow et al., 1992). DNA isolated from these complex marker chromosomes is used in PCR to generate labelled probes, which are employed in multicolour FISH analyses on normal metaphase spreads to identify the make-up of the complex marker chromosome. Rapid localisation of a gene can also be accomplished in a technique termed 'spot blot analysis' (Lebo et al., 1985). Individual chromosomes are sorted onto nitrocellulose filters (one type per filter) followed by hybridisation employing a labelled probe specific for the gene of interest (Protocol 15.2). An example of these analyses is shown in Fig. 15.2 where the chromosomal localisation of SV40 (simian virus 40) viral sequences was determined in an SV40-transformed cell line.

Protocol 15.2 Spot blot analyses

Reagents and equipment

- Chromosome suspension prepared as described above
- Filter holder that can be mated to output from flow sorter: these are available commercially but can be easily made using a reusable syringe filter holder of appropriate size. A small wire bracket can be fabricated to hold the half of the syringe filter holder to which a vacuum can be applied in a position to catch the deflected sort stream. A

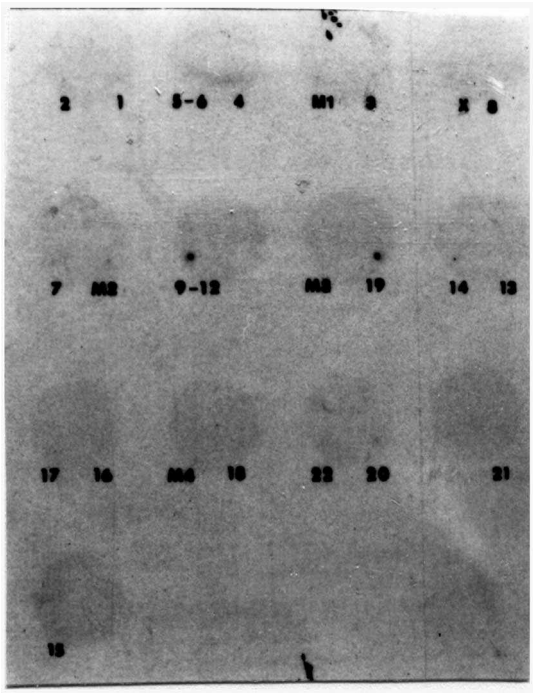

Fig. 15.2 Spot blot analyses of chromosomes isolated from an SV40-transformed human cell line at 136 population doublings in tissue culture. Each of the chromosomes shown in Fig. 15.1 was sorted individually into spots on nitrocellulose filters (visible as the larger, low contrast circles in the autoradiograph). Filters were hybridised using an α-^{32}P-labelled probe specific for the SV40 sequences used in the transformation of the cells and homologous nucleic acid sequences allowed to hybridise. The two small intense black spots that are visible immediately above the labels '19' and '9–12' demonstrate that the SV40 sequences were integrated on chromosome 19 and within the 9–12 group, later shown to be chromosome 9.

gentle vacuum is then applied to this and the filter placed on top. The gentle vacuum carries away the liquid from the sort droplets and leaves the chromosomes on the filter

- Denaturing solution: 0.5 mol l^{-1} NaOH, 1.5 mol l^{-1} NaCl
- Neutralisation solution: 1.5 mol l^{-1} NaCl, 0.5 mol l^{-1} tris-HCl pH 8.0
- Saline sodium citrate* (S-SC): single strength (1 ×) is 150 mmol l^{-1} NaCl, 15 mmol l^{-1} sodium citrate, pH 7.4
- Denhardt's solution* single strength (1 ×) is 20 μg ml^{-1} Ficoll®, 20 μg ml^{-1} polyvinylpyrrolidone, 20 μg ml^{-1} bovine serum albumin (BSA)
- Prehybridisation/hybridisation solution*: 5 × S-SC, 1 × Denhardt's, 20 mmol l^{-1} $NaPO_4$ pH 6.7, 10% dextran sulphate, 40% formamide, 100 μg ml^{-1} sonicated salmon sperm DNA
- An α-P^{32} labelled probe prepared by standard techniques (either random primer extension or nick translation procedure)
- 2 × S-SC-SDS solution: double strength (2 ×) S-SC containing 0.1% sodium dodecyl sulphate (SDS)
- 0.1 × S-SC-SDS solution: one tenth strength (0.1 ×) S-SC containing 0.1% SDS

*Pre-mixed reagents are available from Sigma.

Protocol

1. Flow sort individual chromosomes or chromosome groups onto nitrocellulose filters.
2. Mark filters as to chromosome(s) in spot and circle area where sorted chromosome spot is located. Use only special filter marking pens designed for labelling nitrocellulose filters that are going to be used in radioactive hybridisations.
3. Denature filters by laying on Whatman 3MM paper that has been saturated with denaturing solution for 5 min.
4. Neutralise filters by laying on Whatman 3MM paper that has been saturated with neutralisation solution for 5 min.
5. Place filters between sheets of Whatman 3MM paper and air dry at room temperature for 1–2 h.
6. Dry filters in sleeve of Whatman 3MM paper at 80°C in a vacuum oven.
7. Rehydrate filters in 2 × S-SC buffer.
8. Incubate filters in prehybridisation/hybridisation solution for 4 h at 42°C. The formamide concentration, salt concentration, time and temperature may need to be varied depending on the probe/target sequence being studied.
9. Remove 1 ml of prehybridisation/hybridisation

solution and add sufficient labelled probe to give 10^6 counts min^{-1} ml^{-1} in the total volume of prehybridisation/hybridisation buffer.
10. Denature probe mixture at 100°C for 10 min. Place on ice immediately.
11. Add denatured probe mixture to hybridisation buffer containing filters.
12. Incubate filters for 24–36 h at 42°C. The hybridisation temperature may need to be varied depending on the probe/target sequence being studied.
13. Remove hybridisation solution.
14. Wash filters in 2 × S-SC-SDS for 15 min at room temperature.
15. Remove 2 × S-SC-SDS.
16. Incubate filters in 2 × S-SC-SDS at room temperature for 15 min.
17. Remove 2 × S-SC-SDS.
18. Incubate filters in 0.1 × S-SC-SDS at room temperature for 15 min.
19. Remove 0.1 × S-SC-SDS.
20. Incubate filters in 0.1 × S-SC-SDS at 48°C for 30 min. Salt concentration and temperature may need to be varied depending on probe/target sequence being studied.
21. Remove 0.1 × S-SC-SDS.
22. Repeat stringency wash steps 17 and 18.
23. Dry filters between sheets of Whatman 3MM paper.
24. Place filters on an old sheet of X-ray film. Tape down with small pieces of tape on just edge of each filter.
25. Place film with filters in X-ray cassette with fresh undeveloped X-ray film on top.
26. Expose film at −70°C until adequate hybridisation signal is seen on developed film (typically 24–96 h).

15.3 Fluorescence in situ hybridisation analyses with cells in suspension

Numerous reports of flow cytometric detection of specific DNA and RNA sequences (as opposed to total DNA or RNA) employing FISH techniques have been published (Arkesteijn et al., 1995; Bauman and Bentvelzen, 1988; Bayer and Bauman, 1990; Belloc et al., 1993; Borzi et al., 1996; Crouch et al., 1997; Donovan et al., 1997; Imbert-Marcille et al., 1997; Just et al., 1998; Lalli et al., 1992; Lizard et al., 1993; Pajor and Bauman, 1991; Patterson et al., 1998; Pennline et al., 1992; Pinkel et al., 1986; Ravichandran et al., 1992; Stowe et al., 1998; Timm and Stewart, 1992; Trask et al., 1985, van Dekken et al., 1990; Yu et al., 1992). In these techniques, a labelled nucleic acid probe or probes homologous to a specific DNA or RNA sequence within the cell is used in in situ hybridisation reactions adapted for cells in suspension. The ability to couple FISH analyses in multiparameter protocols with antibody staining of cell surface and intracellular antigens significantly increases the power and utility of these assays for the characterisation of cells within a heterogeneous population specific for a given DNA or RNA sequence (Crouch et al., 1997; Patterson et al., 1998; Stowe et al., 1998). A schematic representation of cell-based FISH procedures is shown in Fig. 15.3 and a basic procedure is described in Protocol 15.3. Typically, cells are first stained with antibodies directed against any cell surface epitopes of interest. In many FISH applications, hybridisation temperatures can be kept below 55°C, facilitating the use of directly labelled fluorescent antibodies. For temperatures above 55°C, an indirect antibody detection method may be used, such as a biotinylated primary antibody revealed with fluorochrome-labelled streptavidin, which is added only after the hybridisation and stringency washes. Following incubation with antibody, cells are fixed and permeabilised. Obviously, for detection of intracellular antigens, antibody would need to be added concurrently with, or after, permeabilisation. Fixation and permeabilisation is a critical aspect of these analyses, the optimum conditions of which can be dependent on cell type. Cells must be sufficiently permeabilised to facilitate the free diffusion of labelled nucleic acid probe(s) into the cell, with adequate denaturation, or breathing, of the target sequences to allow specific hybridisation between probe(s)

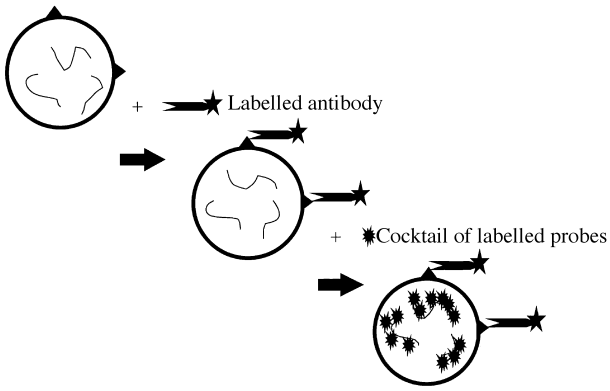

Fig. 15.3 Schematic representation of the fluorescent in situ hybridisation procedure. Filled triangles represent cell surface antigen and the thin solid line represents an intracellular nucleic acid target. Cells are first stained with labelled antibody(ies) followed by hybridisation with a probe(s) directed against the target sequence of interest as described in the text.

and target(s). At the same time, the antigenicity of the relevant antigens and the ultrastructure that confers the cell's characteristic light scattering properties must be preserved. This is a sensitive balance requiring some attention to provide reproducible results. Although a number of fixation/permeabilisation combinations have been tried, satisfactory results can be obtained using Ortho PermeaFix, a commercially available one step fixation/permeabilisation reagent (Patterson et al., 1995, 1998). Typical conditions would be for 18 h at 4°C, although shorter times may be employed. Other commercially available fixation/permeabilisation systems might work as well but they would need to be tested. Alternatively, 1–4% paraformaldehyde followed by 0.1% Triton® X-100 or saponin for permeabilisation may be employed (Goolsby et al., 2000; Mosiman and Goolsby, 2000).

After fixation and permeabilisation, cells are resuspended in hybridisation buffer containing the labelled nucleic acid probe(s). Probes may be made in a variety of ways. For targets with high numbers of copies per cell, such as repetitive alpha-satellite-like chromosome-specific centromeric sequences, a single labelled oligonucleotide probe may be adequate. For low numbers of copies per cell, a pool or cocktail of oligonucleotide probes (several to well over a hundred in some applications) having nonoverlapping homologies to regions along the target of interest may be required. In this way, a large number of labelled probes are bound to each target nucleic acid molecule. Since labelling of the probe can affect the melting temperature of the probe–target complex as well as nonspecific binding of the probe, oligonucleotide probes need to be manufactured to high standards. Even changing the specific derivative of the labelling fluorophore can dramatically alter the characteristics of the probe(s). It has been found that probes synthesised using phosphoramidite chemistry followed by a three-step purification using high-pressure liquid chromatography (HPLC) work well. However, many commercial organisations that offer custom synthesis facilities are not familiar with making probes for in situ cellular applications and their performance in flow cytometric FISH applications varies. Therefore, one must carefully screen batches of probes for adequate performance.

Consistency in manufacture is critical, particularly when constructing cocktails of multiple probes. Probes must be labelled in an identical manner and purified so that they are homogeneous in terms of labelling and nonspecific binding characteristics. Additionally, they must have very low nonspecific binding as even minor nonspecific binding of each probe when summed over tens to hundreds of probes in the cocktail can easily overwhelm any specific hybridisation signal. Individual probes in the cocktail should have very similar melting temperatures (T_m). The control of stringency is dependent on the ability to 'melt' off probes that are not closely base pair matched and consequently have a lower T_m. If probes in the cocktail have a wide range of T_m values then adequate control of stringency will be difficult. Probes generated by random primer extension or nick translation labelling of nucleic acid inserts in molecular constructs, such as plasmids or cosmids, can be used. However, these procedures can generate a heterogeneous mix of probes in terms of labelling, GC/AT ratio/distribu-

tion, and size, resulting in a probe mixture with a wide range of T_m values. Use of oligonucleotide probes allows tight control of these probe characteristics and and they have been found to be more sensitive when using probe cocktails. Nonetheless, probes generated by labelling from long DNA templates have been used successfully in this setting (Borzi et al., 1996; Pennline et al., 1992; Trask et al., 1988; van Dekken et al., 1990). Lastly, it should be re-emphasised that, for detection of higher copy number targets, one may need to pool only several oligonucleotide probes to obtain adequate sensitivity; cocktails containing as few as five probes having been utilised for detection of viral RNA and DNA sequences (Lizard et al., 1993; Stowe et al., 1998). Other labels and types of probes, such as peptide–nucleic acid probes or probes designed to quench except when bound to target, also have potential.

The make-up and exact concentrations of components in the hybridisation buffer varies with different probe–target combinations. Typical hybridisation buffers for FISH with cells in suspension contain S-SC, formamide, blocking unlabelled nucleic acid and labelled probe. The T_m of probe–target complexes varies with salt and formamide concentration, with the T_m increasing with increasing salt and decreasing with increasing formamide. Thus, for a given probe–target complex, the salt, formamide and hybridisation temperature are adjusted such that the hybridisation reaction is carried out at a few degrees below the theoretical T_m of the probe–target complex. Since the calculated T_m assumes that the nucleic acids are isolated free of cellular protein and in situ structure, the theoretical values are only estimates for cellular in situ hybridisation. Optimum temperatures are determined empirically by optimising the specific bound probe signal above background (signal to noise) using the theoretical values as a starting point. Hybridisation buffers should also contain high concentrations of a blocking reagent to inhibit nonspecific binding of probe(s). Typically, 500 $\mu g\ ml^{-1}$ of sheared single-strand salmon sperm or herring testes DNA is used. Other reagents, such as Denhardt's and dextran sulphate, are not generally employed in FISH procedures with cells in suspension. The high viscosity of these reagents makes handling (centrifugation, washing, etc.) of cell suspensions difficult. Following hybridisation, one (or more) incubation or wash is (are) carried out at, or slightly above, the temperature used for hybridisation. This increases the stringency of the hybridisation reaction by washing, or melting off, those probes with lower numbers of base pairs matched to the target, thereby increasing the specificity of the reaction. Detection chemistry follows the stringency washes if an indirect antibody approach was utilised. If direct antibody staining was performed, cells are resuspended in PBS for flow cytometric analysis. Significant increases in autofluorescence background frequently occur following the hybridisation step and techniques to correct for, or to suppress, this background may need to be employed (Mosiman et al., 1997; Roederer and Murphy, 1986; Steinkamp and Crissman, 1993; Steinkamp and Stewart, 1986). A simple, instrumentation-independent technique is the addition of trypan blue to the analysis buffer (Mosiman et al., 1997). For reasons that as yet are not totally clear, this can also quench some nonspecifically bound fluorescence signal as well.

The flow cytometric detection of cells stained employing FISH techniques utilising a probe generated from total genomic DNA was first reported by Trask et al. (1985). These 'proof of principle' experiments were soon followed by the successful detection of highly repetitive alpha satellite-like chromosome-specific sequences in individual cells (Pinkel et al., 1986; Trask et al., 1988; van Dekken et al., 1990) which could be coupled with measurement of other cellular features, such as DNA content, and were able to resolve differences in chromosome number. More recently, these techniques for the flow cytometric detection of chromosome-specific sequences have been used in analysis of transplant recipients to evaluate allogeneic engraftment and chimerism in sex-mismatched bone marrow transplants (Arkesteijn et al., 1995; van Tol et al., 1998). An exciting, more recent, report has been the use of flow cytometric FISH to detect telomeric repetitive sequences (Hultdin et al., 1998; Rufer et al., 1998).

Detection of targets at low copy number has also been reported. Lizard et al. (1993) reported detection of 600 copies of the HPV genome in CaSki cells, although the 20–50 copies harboured in HeLa cells could not be detected. It should be noted, however, that the 20–50 copies of HPV DNA per cell could be detected by confocal microscopy in the same experiments. As mentioned above, sensitivity was limited in these analyses employing fluorescein-labelled probes by autofluorescence, which has also been reported by others (Mosiman et al., 1997; Yu et al., 1992).

Soon after the report of Trask et al. (1985), parallel 'proof of principle' experiments detecting specific ribosmal RNA sequences (rRNA) in FISH flow cytometric experiments were reported by Bauman and Bentvelzen (1988). Thereafter, Pajor and Bauman (1991) used FISH-based analyses to monitor rRNA levels in differentiating cells and quantitative measurements of poly(A)$^+$ messenger RNA (mRNA) were demonstrated by Belloc et al. (1993). The application of flow cytometric FISH analyses to the detection of cellular RNA sequences has covered a wide area (Bayer and Bauman, 1990; Crouch et al., 1997; Lalli et al., 1992; Patterson et al., 1998; Pennline et al., 1992; Ravichandran et al., 1992; Timm and Stewart, 1992; Yu et al., 1992; Stowe et al., 1998) ranging from low to high copy number targets. These have included detection of abundant messages such as cytokine mRNA (Pennline et al., 1992) and actin mRNA (Timm and Stewart, 1995) as well as lower copy number targets. Lalli et al. (1992) reported detection of 1200 copies of glyceraldehyde 3-phosphate dehydrogenase mRNA that was in good quantitative agreement with parallel spot blot results. Other reports of detection of RNAs in the low to intermediate range of copies per cell include measurement of histone H4 (1800 copies per cell), 18S rRNA and 28S rRNA (Yu et al., 1992), 500 copies of β-globin mRNA (Bayer and Bauman, 1990) and 150–300 copies of a V_H sequence in immunoglobulin heavy chain mRNAs (Ravichandran et al., 1992).

Using the techniques described, pools of oligonucleotide probes that in aggregate spanned most of the HIV *gag* sequence could detect as few as 30 copies of HIV RNA per cell in an ACH-2 cell model system (Patterson et al., 1998). ACH-2 cells carry integrated HIV DNA but under normal culture conditions have very low levels, less than several copies per cell, of HIV RNA. However, when the cells are stimulated with tumour necrosis factor α, HIV RNA expression is rapidly upregulated to thousands of copies per cell. Figure 15.4 shows the results for a typical experiment in which unstimulated and stimulated ACH-2 cells were mixed in varying concentrations. At this level of expression (several thousand copies of RNA per cell), a small percentage of positive cells within a mixed population can be detected. Obviously, with appropriate choice of immunophenotypic markers to select a subpopulation of cells from a heterogeneous mix, the overall detection limit can be significantly less than 1% of the cells within a sample. Additionally, even without benefit of immunophenotype to select a subpopulation of cells, for higher numbers of targets per cell, less than 1% positive cells can be detected. In a model EBV system with higher levels of viral RNA than in the HIV ACH-2 model, it is possible to detect $<1\%$ positive cells in a heterogeneous sample, an example of which is shown in Fig. 15.5. Moreover, examination of hybridisation median fluorescence intensity versus time following stimulation of ACH-2 cells (Fig. 15.6) demonstrated the ability of these assays to monitor modulation of cellular RNA expression at least in a semiquantitative manner. Further, comparison of mean fluorescence intensity with quantitative RT-PCR estimates of number of copies of HIV RNA per cell (Patterson et al., 1998) showed that as few as 30 copies of RNA per cell produced a detectable, significant increase in hybridisation signal. A number of other investigators have used flow cytometric FISH techniques in the study of viral disease including HIV (Borzi et al., 1996), HPV (Lizard et al., 1993) and EBV (Crouch et al., 1997; Stowe et al., 1998).

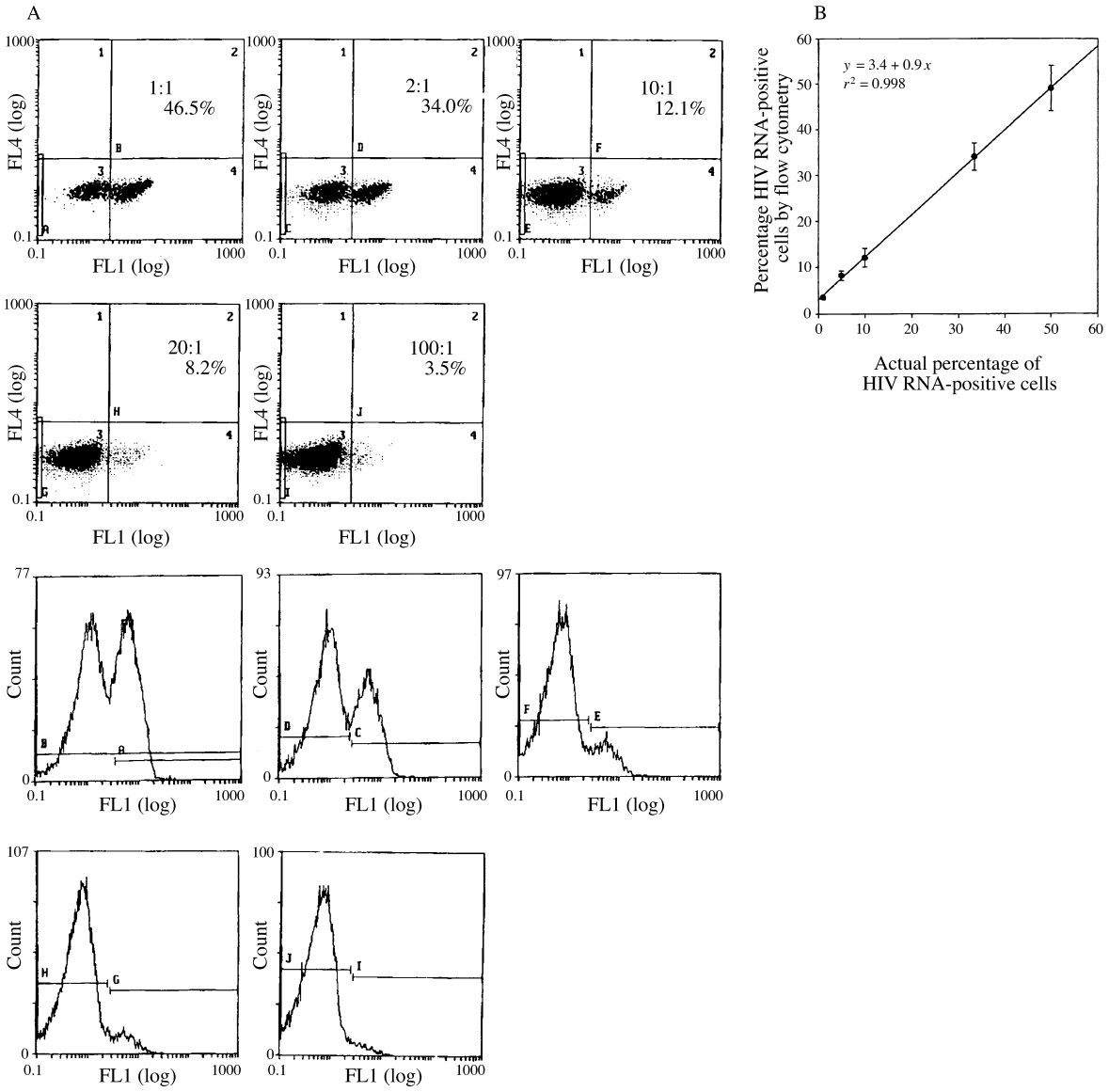

Fig. 15.4 Representative example of experimental results for mixing of unstimulated ACH-2 cells and cells stimulated with tumour necrosis factor α for 24 h. Cells were then hybridised as described in the text using a cocktail of directly labelled oligonucleotide probes specific for HIV RNA sequences (see Patterson et al., 1998). (A) Two-parameter distributions of trypan blue counterstain fluorescence (FL4, ordinate; logarithmic scale) versus HIV RNA probe (fluorescein isothiocyanate (FITC)) fluorescence intensity (FL1, abscissa; logarithmic scale) (upper row) or number of cells (ordinate; linear scale) versus HIV RNA probe fluorescence intensity (FL1, abscissa; logarithmic scale) (lower row) for various mixes of stimulated and unstimulated cells. The ratios shown are unstimulated cells to stimulated cells and the percentages shown are the percentages of positive cells as detected in the flow cytometric FISH assay. (B) The results of multiple experiments comparing the actual percentage of HIV RNA-positive cells (stimulated ACH-2) versus the measured percentage of HIV RNA-positive cells are shown. (Reprinted by permission of Wiley-Liss, Inc., a subsidiary of John Wiley & Sons, Inc., from Patterson, B.K., Mosiman, V.L., Cantarero, L., Furtado, M., Bhattacharya, M., Goolsby, C. (1998) Detection of persistently productive infection of monocytes in the peripheral blood of HIV-positive patients using a flow cytometry based FISH assay. *Cytometry* **31**, 265–74.)

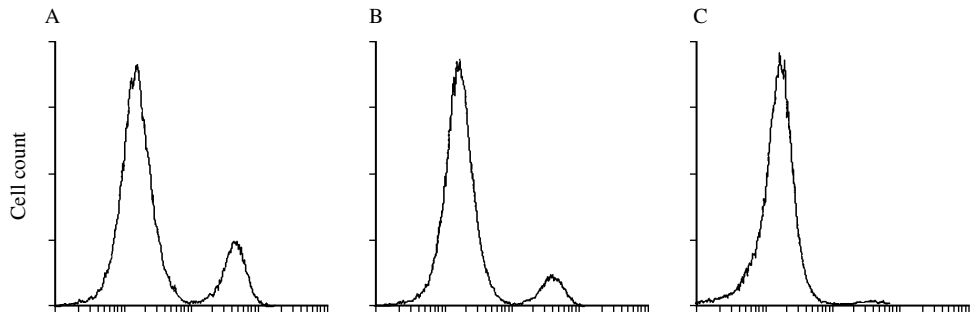

Fig. 15.5 Representative results of hybridisation experiments employing a cocktail of five oligonucleotide direct-labelled probes specific for Epstein–Barr virus (EBV) RNA (Stowe, 1998). Mixtures of EBV RNA-positive cells (Raji) and peripheral blood mononuclear cells (EBV RNA negative) were made followed by fluorescence in situ hybridisation as described in the text. Distributions of number of cells (ordinate) versus EBV RNA probe fluorescence intensity (FL1, abscissa; logarithmic scale) are shown for mixtures containing 25% (A), 10% (B) and 0.5% (C) EBV-positive cells.

Protocol 15.3 Fluorescence in situ hybridisation (FISH)

Reagents

- Hybridisation buffer: 2 × S-SC, 50% formamide, 500 μg ml^{-1} sonicated salmon sperm DNA
- A preparation of cultured cells, peripheral blood mononuclear cells obtained by standard Ficoll®-Hypaque methods (see Ch. 2), or other single cell suspension
- Direct labelled fluorescent probe, which can be manufactured by standard synthesis methods. Best results have been obtained with phosphoramidite synthesis chemistry and multistep HPLC purification. (See Goolsby et al. (2000) and Mosiman and Goolsby (2000) for more details and for considerations when using multiple probes)

Protocol

1. Wash cells in Ca^{2+}-, Mg^{2+}-free PBS.
2. Resuspend 10^6 cells in 100 μl PBS.
3. Add manufacturers recommended or optimised concentration of antibody directed against surface antigen(s) of interest.
4. Wash cells by centrifuging (typically 400 × *g* for 5–10 min) in PBS.
5. Resuspend cells in 100 μl Ortho Permeafix. Incubate at 4°C for 18 h. The time of fixation is cell type dependent. Alternative fixation is 2–4% *fresh* paraformaldehyde followed by saponin permeabilisation.
6. Wash cells by centrifuging twice in PBS.
7. Resuspend in 1 ml 2 × S-SC.
8. Centrifuge cells at 400 × *g* for 10 min, aspirate off supernatant.
9. Resuspend cells in 30 μl hybridisation buffer. The formamide and salt concentration may need to be varied with different target/probe sequences.
10. Add 10 μl of a direct fluorescently labelled probe(s), that has been resuspended in 2 × S-SC to the cell suspension and mix.
11. Incubate at 44°C for 1 h. The hybridisation temperature and length (time) of hybridisation may need to be varied with different target/probe sequences.
12. Add 1 ml 2 × S-SC (pre-warmed to 44°C), mix.
13. Centrifuge cells at 400 × *g* for 10 min, aspirate off supernatant.
14. Resuspend cells in 1 ml 0.1 × S-SC/0.1% Triton® X-100 (pre-warmed to 44°C).
15. Incubate suspension at 44°C for 20 min.

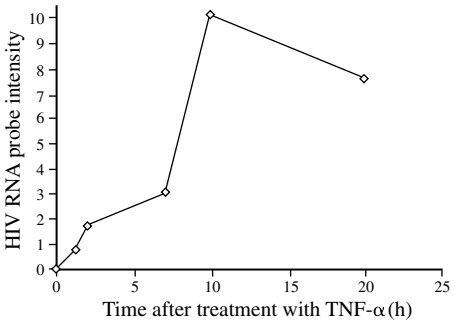

Fig. 15.6 Use of fluorescence intensity to follow the rapid upregulation of HIV RNA in ACH-2 cells stimulated with tumour necrosis factor α (TNF-α). Cells were collected at the times indicated, hybridised as described in the text using a cocktail of direct labelled oligonucleotide probes specific for HIV RNA and fluorescence intensity determined. (Reprinted by permission of Wiley-Liss, Inc., a subsidiary of John Wiley & Sons, Inc., from Patterson, B.K., Mosiman, V.L., Cantarero, L., Furtado, M., Bhattacharya, M., Goolsby, C. (1998) Detection of persistently productive infection of monocytes in the peripheral blood of HIV positive patients using a flow cytometry based FISH assay. *Cytometry* **31**, 265–74.)

16. Centrifuge cells at $400 \times g$ for 10 min. Aspirate off supernatant. For different target/probe sequences, steps 16–18 may need to be repeated multiple times. Salt concentration, incubation temperature and length of incubation may also need to be varied.
17. Resuspend cells in 0.5–1.0 ml PBS.
18. Add highly purified trypan blue to a final concentration of 1 μg ml^{-1}. Trypan blue concentration may need to be varied in order to optimise signal to noise.

Analysis

Analyse on flow cytometer using an appropriate strategy, e.g. light scatter and/or fluorescence to gate the cells of interest and the relevant fluorescence channels to detect the antibody and/or probe used.

These techniques have also been adapted for the detection of viral sequences in patient samples (Patterson et al., 1998; Stowe et al., 1998). Examples of the detection of HIV RNA within the monocyte population in the peripheral blood of an HIV-positive patient are shown in Fig. 15.7. Preliminary results suggest that, in HIV disease, these measurements of cellular viral load may add additional prognostic information to classical measurements of plasma viral load (Patterson et al., 1998). In this report on a cohort of 39 HIV-positive patients, seven showed a significant increase in their plasma viral load levels during the course of the study. For six of the seven, the increase in the plasma viral load levels was preceded by increases in the numbers of HIV-positive monocytes in their peripheral blood. Whether cellular viral load measurements may add to prognostic information on the emergence of drug-resistant populations in HIV-positive patients remains to be seen but it is enticing.

15.4 Approaches using in situ polymerase chain reaction or reverse transcriptase polymerase chain reaction with cells in suspension

As discussed above, in flow cytometric FISH analyses, detection of targets at high copy number could be accomplished using a single fluorescently labelled probe; however, detection of targets at low to intermediate copy numbers required amplification of the fluorescence hybridisation signal. This could be accomplished by amplifying the amount of fluorescence associated with each bound probe or by using multiple probes that bound to nonoverlapping regions of the target. Although low levels of RNA per cell (30 copies) can be detected in homogeneous populations of cells using the latter technique, only sequences present in significantly higher copy numbers can be detected in heterogeneous populations. Even in homogeneous cell populations, detection of less than 30 copies per cell may be required in many instances.

To increase the sensitivity of flow cytometric detection of nucleic acid targets in cells, several laboratories have adapted in situ PCR (RT-PCR) assays for use with cells in suspension (Bains et al., 1993;

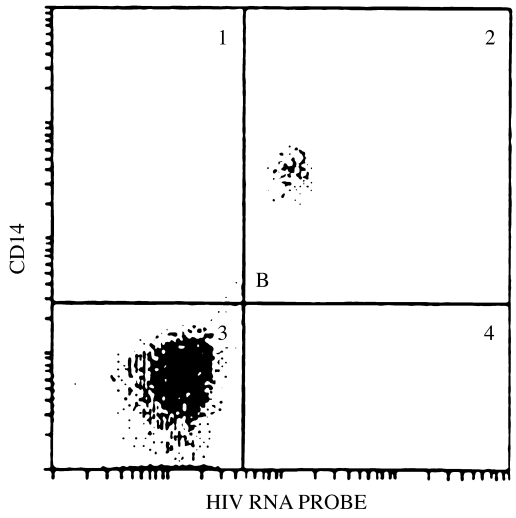

Fig. 15.7 Bivariate distribution of CD14 staining versus HIV RNA probe fluorescence intensity. Peripheral blood mononuclear cells were isolated from an HIV-positive patient by Ficoll®–Hypaque separation. Cells were then stained with a phycoerythrin-labelled CD14 antibody followed by fixation/permeabilisation and hybridisation using a cocktail of directly labelled oligonucleotide probes specific for HIV RNA, as described in the text. Cells were counterstained with trypan blue. (Reprinted by permission from Goolsby, C.L., Thompson, E., Mosiman, V. (2000) Combined immunophenotyping and molecular phenotyping. In: Stewart, C., Nicholoson, J. (eds.), *Immunophenotyping*. Wiley, New York.)

Embleton et al., 1992; Patterson et al., 1993, 1995; Testoni et al., 1996; Timm et al., 1995). A schematic representation of the in situ PCR technique is shown in Fig. 15.8 and a basic procedure is described in Protocol 15.4. In this case, the cellular nucleic acid target of interest is amplified to a very high copy number using primers that span the target of interest. As in the FISH-based techniques, cells are first stained with antibody(ies) directed against cell surface antigens of interest; however, because of the higher temperatures associated with thermal cycling, and depending on the antigen and the choice of labelling fluorophore used, an indirect labelling method, such as biotin–avidin, may be necessary (Patterson et al., 1993, 1995). Even for fluorophores that are thermally stable, one must verify that the labelled complex is stable. Presently, for RT-PCR procedures, a wholesale digestion of cellular protein is required for the RT step (Goolsby et al., 2000; Mosiman and Goolsby, 2000; Patterson et al., 1993). This wholesale digestion of cellular protein precludes doing simultaneous antigen detection and limits the usefulness of cell-based RT-PCR techniques. Future refinements that more selectively remove cellular proteins responsible for inhibiting the RT reaction may circumvent this restriction. Preliminary studies, using an acidic extraction procedure to remove proteins, have shown promise (Goolsby et al., 2000).

Following antibody incubation, or as a first step for RT-PCR, cells are fixed and permeabilised as described for the FISH techniques above. Cells are then carried through the PCR (RT-PCR) procedure. Although quite similar to PCR (RT-PCR) with isolated nucleic acids, there are several key differences for the successful application to cells in suspension. The first is the inclusion of a bulky nucleotide such as digoxigenin- or biotin-labelled dUTP as substrate during the amplification reaction to aid with retention of the amplified product inside the cell. Without incorporation of a bulky nucleotide into the amplified product, the majority of the product diffuses out of the cell (Frumkin et al., 1995; Goolsby et al., 2000; Patterson et al., 1993, 1995; Timm and Stewart, 1992). In the worst case, without use of a bulky nucleotide, all detectable positive signal is lost to the solution; even in the best case, the signal to noise ratio is greatly reduced. Amplification conditions are similar to those used for isolated nucleic acids, except that, in general, the Mg^{2+} and the polymerase concentrations are higher (two- to threefold and twofold, respectively) compared with optimised concentrations for isolated nucleic acids. The annealing and elongation times generally need to be extended as well. For optimum results with RT-PCR, typically, the duration of the reverse transcription step needs to be extended compared with that used for isolated nucleic acids. A bulky nucleotide should be included as substrate during this step as well. These extended times probably reflect, at least par-

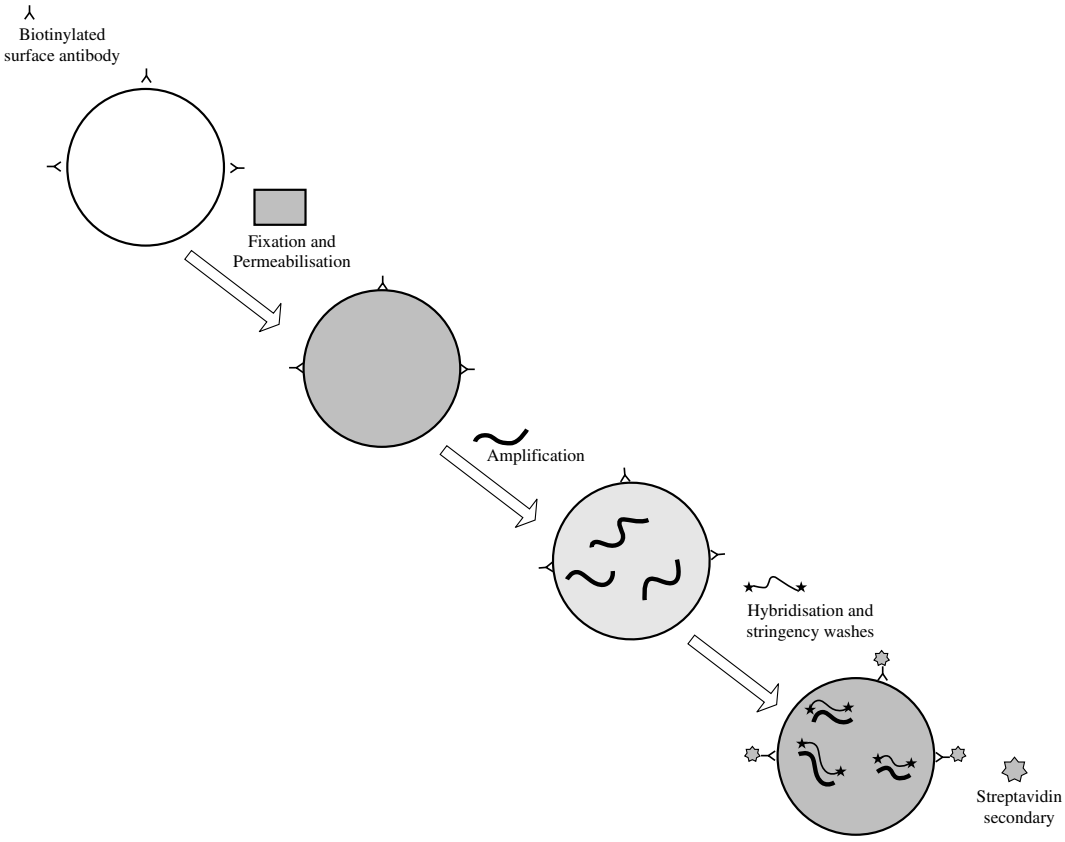

Fig. 15.8 Schematic representation of the polymerase chain reaction/fluorescence in situ hybridisation technique coupled with surface antigen detection. Thick solid line represents amplified sequence of interest inside the cell. Thin line with stars represents a direct labelled oligonucleotide probe specific for the amplified sequence. (Reprinted by permission from Goolsby, C.L., Thompson, E., Mosiman, V. (2000) Combined immunophenotyping and molecular phenotyping. In: Stewart, C., Nicholoson, J. (eds.), *Immunophenotyping*. John Wiley & Sons, Inc., New York.)

tially, the difficulties encountered by the enzymes working around the structure of nucleic acids in situ within the cell as opposed to isolated nucleic acids stripped of all protein in suspension (Goolsby et al., 2000). Optimisation of all of these parameters will need to be done for each target and primer set. Following amplification of the target of interest, fluorescent detection of the amplified target must be achieved. Although one can detect the amplified product directly by detection of the bulky nucleotide that was incorporated into the product, or alternatively by incorporating a fluorescent-labelled nucleotide into the product during amplification, this is not optimum. High copy number targets have been detected successfully using this approach (Bains et al., 1993). However, for lower copy number targets, significant increases in signal to noise, and in reproducibility, have been seen in both suspension and slide-based in situ PCR (RT-PCR) if FISH is used to detect the amplified product (Goolsby et al., 2000; Komminoth et al., 1994; Long et al., 1993; Mosiman and Goolsby, 2000; Patterson et al., 1993,

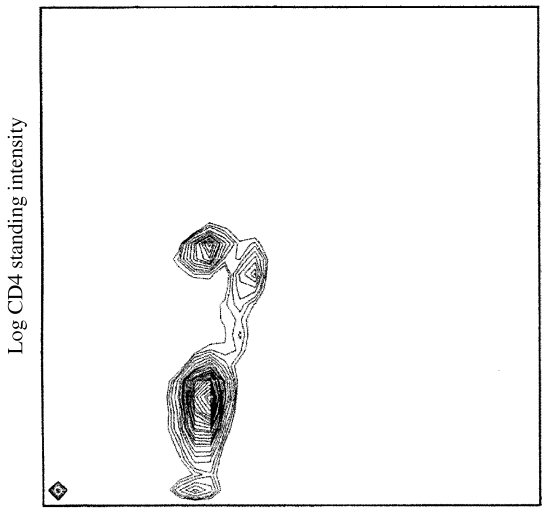

Fig. 15.9 Bivariate distribution of CD4 staining (three decade logarithmic scale) versus HIV DNA probe fluorescence intensity (three decade logarithmic scale). Peripheral blood mononuclear cells were isolated from a HIV-positive patient by Ficoll®–Hypaque separation. Monocytes were depleted using a CD14 magnetic bead system. Cells were then stained with a biotinylated CD4 antibody followed by fixation/permeabilisation and in situ polymerase chain reaction using primers specific for HIV DNA (see Patterson et al., 1993; 1995). Following amplification, fluorescence in situ hybridisation was performed using a directly labelled oligonucleotide probe directed against the amplified HIV DNA sequence. The biotinylated antibody was then detected with a phycoerythrin-labelled streptavidin. Note the reduced CD4 staining in the HIV DNA-positive cells compared with the HIV DNA-negative cells. (Reprinted by permission from Goolsby, C.L., Thompson, E., Mosiman, V. (2000) Combined immunophenotyping and molecular phenotyping. In: Stewart, C., Nicholoson, J. (eds.), *Immunophenotyping*. John Wiley & Sons, Inc., New York.)

1995). Significant amounts of nonspecific amplified material are generated in cell-based in situ PCR (RT-PCR) reactions (Long et al., 1993), at least partially because of the lack of stringency in primer binding to cellular targets in the first rounds of amplification. If the amplified product is detected directly, then both the specific and nonspecifically amplified product will be detected. Employing a FISH detection of the amplified material helps in detecting only the specifically amplified material. The FISH step is carried out as described above. In general, it is adequate to employ only a single labelled oligonucleotide probe homologous to the amplified product in this step. Following the FISH procedure, the appropriate techniques using secondary detection reagents for surface antibody visualisation are carried out. Although, at present the correction techniques described above for reducing the significant increases in autofluorescence background that accompany thermal cycling have not been employed, increases in the sensitivity and reproducibility of these assays might be achieved if they are used.

These approaches can detect single copy DNA sequences (Patterson et al., 1993, 1995) and very low RNA levels (Patterson et al., 1993) in individual cells. These cell-based techniques have been employed in the study of HIV disease as well as to detect higher copy number chromosome-specific DNA targets in individual cells (Timm et al., 1995). Figure 15.9 shows a typical result of PCR/FISH detection of cellular HIV DNA coupled with CD4 staining in peripheral blood mononuclear cells isolated from an HIV-positive patient. It was consistently found that the staining for the CD4 antigen using antibodies recognising a conformation-dependent epitope in the HIV-binding site was dimmer in the $CD4^+$ cells that were positive for HIV DNA than in those that were negative (Patterson et al., 1995). Further study using CD4 antibodies recognising a linear epitope on the CD4 antigen that was independent of the HIV-binding site showed this to be most likely because of epitope alteration/deletion or masking, and not from downregulation of the CD4 antigen. Cellular *in situ* RT-PCR/FISH detection of HIV RNA coupled in parallel with the PCR/FISH analysis of HIV DNA was able to demonstrate that the majority of peripheral blood lymphocytes in HIV-positive patients are latently infected (Patterson et al., 1993). Other exciting applications of flow cytometric in situ RT-PCR cellular assays have included studies of immunoglobulin gene rearrangements (Embleton

et al., 1992) and the detection of the *bcr:abl* translocation mRNA resultant from the t(9;22) translocation in both cell lines (Embleton et al., 1992) and in cells from patients with CML (Testoni et al., 1996).

Protocol 15.4 Polymerase chain reaction-fluorescence in situ hybridisation

Reagents and equipment

- Prepare peripheral blood mononuclear cells by standard Ficoll®–Hypaque methods (see Ch. 2)
- PCR reaction mixture: 10 mmol l^{-1} tris-HCl pH 8.3, 50 mmol l^{-1} KCl, 1.5 mmol l^{-1} $MgCl_2$, 0.25 mmol l^{-1} each dATP, dCTP and dGTP, 0.14 mmol l^{-1} dTTP, 4.3 μmmol l^{-1} dUTP-11-digoxigenin, 100 pmol l^{-1} each forward and reverse primer (for primers used in Fig. 15.9, see Patterson et al., 1995), 5 U Taq polymerase, 0.001% (w/v) gelatin
- 2 × S-SC
- Hybridisation buffer: 2 × S-SC, 50% formamide, 500 μg ml^{-1} sonicated salmon sperm DNA
- A single direct fluorescently labelled probe specific for the amplified product is usually adequate. The probe can be manufactured by standard synthesis methods. Best results have been obtained with phosphoramidite synthesis chemistry and multi-step HPLC purification. See Goolsby et al. (2000) and Mosiman and Goolsby (2000) for more details
- PCR thermocycler

Protocol

1. Wash cells by centrifuging (typically 400 × *g* for 5–10 min) in Ca^{2+}-, Mg^{2+}-free PBS.
2. Resuspend 10^6 cells in 100 μl PBS.
3. Add manufacturers recommended, or optimised, concentration of biotinylated antibody specific for surface antigen of interest.
4. Incubate for 30 min at room temperature. Optimum time may vary.
5. Wash cells by centrifuging in PBS.
6. Resuspend in 100 μl Ortho Permeafix. Incubate at 4°C for 18 h. The time of fixation is cell type dependent. Alternative fixation is 2–4% *fresh* paraformaldehyde followed by saponin permeabilisation.
7. Wash cells by centrifuging twice in PBS.
8. Resuspend cells in 190 μl PCR reaction mixture. The exact conditions, particularly the Mg^{2+} concentration, will need to be varied for different primers.
9. Thermocycle as for standard PCR. The PCR conditions are similar to those used for standard PCR, although increased Taq concentration as well as increased annealing and extension times may be needed (see Goolsby et al., 2000; Mosiman and Goolsby, 2000). As an example, the conditions for data in Fig. 15.9 were 25 cycles of 94°C for 1 min, 58°C for 2 min, and 74°C for 1.5 min.
10. Centrifuge cells at 400 × *g* for 10 min. Aspirate off supernatant.
11. Resuspend in 1 ml 2 × S-SC.
12. Centrifuge cells at 400 × *g* for 10 min. Aspirate off supernatant.
13. Resuspend cells in 30 μl hybridisation buffer. The formamide and salt concentration may need to be varied with different target/probe sequences.
14. Add 10 μl probe(s) resuspended in 2 × S-SC to cell suspension, mix.
15. Incubate at 44°C for 1 h. The hybridisation temperature and length (time) of hybridisation may need to be varied with different target/probe sequences.
16. Add 1 ml 2 × S-SC (pre-warmed to 44°C), mix.
17. Centrifuge cells at 400 × *g* for 10 min. Aspirate off supernatant.
18. Resuspend cells in 1 ml 0.1 × S-SC/0.1% Triton® X-100 (pre-warmed to 44°C).
19. Incubate suspension at 44°C for 20 min.
20. Centrifuge cells at 400 × *g* for 10 min. Aspirate off supernatant. For different target/probe sequences, steps 17–19 may need to be repeated multiple times. Salt concentration, incubation temperature and length of incubation may also need to be varied.
21. Wash by centrifuging in PBS.

22. Resuspend in 100 μl PBS.
23. Add manufacturer's recommended, or optimised, concentration of fluorescently labelled streptavidin. (Phycoerythrin–streptavidin was used in Fig. 15.9.)
24. Incubate for 20 min at room temperature.
25. Wash by centrifuging in PBS.
26. Resuspend in 0.5–1.0 ml of PBS.

Analysis

Analyse by flow cytometry using a strategy and instrument settings appropriate to the sample and fluorochromes used. Although it was not utilised in the data presented in Fig. 15.9, trypan blue may be added to a final concentration of 1 $\mu g\ ml^{-1}$ to help to reduce autofluorescence background. The optimum trypan blue concentration may vary and should be adjusted to optimise signal to noise.

15.5 Conclusions

The development of flow cytometry-based assays coupling detection of specific genetic or expression information at the nucleic acids level with other relevant cellular characteristics in sophisticated multiparametric analyses is at an early stage. The first reports appeared at the end of the 1980s. In the intervening years, the assays have been difficult for many laboratories to implement. This has generally been caused by the lack of adequate reagents, which must be prepared and screened carefully, as well as the failure to recognise the importance of key critical steps in the procedures and to appreciate the potential artefacts and background problems when analysing the data (Goolsby et al., 2000; Mosiman and Goolsby, 2000). Nonetheless, from a meagre beginning representing four publications as of 1988, the field has grown to over 35 publications with application in infectious disease, cancer, transplant medicine, immunology and cell biology. Clearly, an exciting future lies ahead as these techniques are employed in more sophisticated multiparametric analyses designed to understand the basic biology of human disease. This may provide more relevant monitors of disease and aid, in a patient-specific manner, in treatment decisions and therapeutic monitoring.

15.6 REFERENCES

Arkesteijn, G.J., Erpelinck, S.L., Martens, A.C., Hagenbeek, A. (1995) Chromosome specific DNA hybridization in suspension for flow cytometric detection of chimerism in bone marrow transplantation and leukemia. *Cytometry* **19**, 353–60.

Bains, M.A., Agarwal, R., Pringle, J.H., Hutchinson, R.M., Lauder, I. (1993) Flow cytometric quantitation of sequence-specific mRNA in hemopoietic cell suspensions by primer-induced in situ (PRINS) fluorescent nucleotide labeling. *Experimental Cell Research* **208**, 321–6.

Bartholdi, M., Meyne, J., Albright, K., Luedemann, M., Campbell, E., Chritton, D., Deaven, L.L., Cram, L.S. (1987a) Chromosome sorting by flow cytometry. *Methods in Enzymology* **151**, 252–67.

Bartholdi, M.F., Ray, F.A., Cram, L.S., Kraemer, P.M. (1987b) Karyotype instability of Chinese hamster cells during tumor progression. *Somatic Cell and Molecular Genetics* **13**, 1–10.

Bauman, J.G.J., Bentvelzen, P. (1988) Flow cytometric detection of ribosomal RNA in suspended cells by fluorescent in situ hybridization. *Cytometry* **9**, 517–24.

Bayer, J.A., Bauman, J.G.J. (1990) Flow cytometric detection of beta-globin mRNA in murinehaemopoietic tissues using fluorescent in situ hybridization. *Cytometry* **11**, 132–43.

Belloc, F., Lacombe, F., Dumain, P., Mergny, J.L., Lopez, F., Bernard, P., Reiffers, J., Boisseau, M.R. (1993) Flow cytometric estimation of Poly(A)+RNA by fluorescent in situ hybridization. *Cytometry* **14**, 339–43.

Blennow, E., Telenius, H., Larsson, C., de Vos, D., Bajalica, S., Ponder, B.A., Nordenskjold, M. (1992) Complete characterization of a large marker chromosome by reverse and forward chromosome painting. *Human Genetics* **90**, 371–4.

Borkhardt, A., Cazzaniga, G., Viehmann, S., Valsecchi, M.G., Ludwig, W.D., Burci, L., Mangioni, S., Schrappe, M., Riehm, H., Lampert, F., Basso, G., Masera, G., Harbott, J., Biondi, A. (1997) Incidence and clinical relevance of TEL/AML1 fusion genes in children with acute lymphoblastic leukemia enrolled in the German and Italian multicenter therapy trials. *Blood* **90**, 571–7.

Borzi, R.M., Piacentini, A., Monaco, M.C., Lisignoli, G., Degrassi, A., Cattini, L., Santi, S., Facchini, A. (1996) A fluorescent in situ hybridization method in flow cytometry to

detect HIV-1 specific RNA. *Journal of Immunological Methods* **193**, 167–76.

Claxton, D.F., Liu, P., Hsu, H.B., Marlton, P., Hester, J., Collins, F., Deisseroth, A.B., Rowley, J.D., Siciliano, M.J. (1994) Detection of fusion transcripts generated by the inversion 16 chromosome in acute myelogenous leukemia. *Blood* **83**, 1750–6.

Cram L.S. (1990) Flow cytogenetics and chromosome sorting. *Human Cell* **3**, 99–106.

Crouch, J., Leitenberg, D., Smith, B.R., Howe, J.G. (1997) Epstein–Barr virus suspension cell assay using in situ hybridization and flow cytometry. *Cytometry* **29**, 50–7.

Deaven, L.L., van Dilla, M.A., Bartholdi, M.F., Carrano, A.V., Cram, L.S., Fuscoe, J.C., Gray, J.W., Hildebrand, C.E., Moyzis, R.K., Perlman, J. (1986) Construction of human chromosome-specific DNA libraries from flow-sorted chromosomes. *Cold Spring Harbor Symposia on Quantitative Biology* **LI**, 159–67.

Donovan, J.A., Simmons, F.A., Esrason, K.T., Jamehdor, M., Busuttil, R.W., Novak, J.M., Grody, W.W. (1997) Donor origin of a post-transplant liver allograft malignancy identified by fluorescence in situ hybridization for the Y chromosome and DNA genotyping. *Transplantation* **63**, 80–4.

Embleton, M.J., Gorochov, G., Jones, P.T., Winter, G. (1992) In-cell PCR from mRNA: amplifying and linking the rearranged immunoglobulin heavy and light chain V-genes within single cells. *Nucleic Acids Research* **20**, 3831–7.

Frumkin, L.R., Patterson, B.K., Leverenz, J.B., Agy, M.B., Wolinsky, S.M., Morton, W.R., Corey, L. (1995) Infection of *Macaca numestrina* brain with human immunodeficiency virus type 1. *Journal of General Virology* **76**, 2467–76.

Gauwerky, C.E., Croce, C.M. (1993) Chromosomal translocations in leukemia. *Seminars in Cancer Biology* **4**, 333–40.

Goolsby, C.L., Wiley, J.E., Steiner, M., Bartholdi, M.F., Cram, L.S., Kraemer, P.M. (1990) Karyotype evolution in a simian virus 40-transformed tumorigenic human cell line. *Cancer Genetics and Cytogenetics* **50**, 231–48.

Goolsby, C.L., Thompson, E., Mosiman, V. (2000) Combined immunophenotyping and molecular phenotyping. In: Stewart, C., Nicholoson, J. (eds.), *Immunophenotyping*, pp. 407–28. John Wiley, New York.

Gray, J.W., Lucas, J., Peters, D., Pinkel, D., Trask, B., van den Engh, G., Van Dilla, M. (1986) Flow karyotyping and sorting of human chromosomes. *Cold Spring Harbor Symposia on Quantitative Biology* **LI**, 141–9.

Gray, J.W., Trask, B., van den Engh, G., Silva, A., Lozes, C., Grell, S., Schonberg, S., Yu, L.C., Golbus, M.S. (1988) Application of flow karyotyping in prenatal detection of chromosome aberrations. *American Journal of Human Genetics* **42**, 49–59.

Harbott, J., Viehmann, S., Borkhardt, A., Henze, G., Lampert, F. (1997) Incidence of TEL/AML1 fusion gene analyzed consecutively in children with acute lymphoblastic leukemia in relapse. *Blood* **90**, 4933–7.

Huang, M.E., Ye, Y.C., Chen, S.R., Chai, J.R., Lu, J.X., Zhoa, L., Gu, L.J., Wang, Z.Y. (1988) Use of *all-trans*-retinoic acid in the treatment of acute promyelocytic leukemia. *Blood* **72**, 567–72.

Hultdin, M., Gronlund, E., Norrback, K.-F., Norrback, K., Eriksson-Lindstrom, E., Just, T., Roos, G. (1998) Telomere analysis by fluorescence in situ hybridization and flow cytometry. *Nucleic Acids Research* **26**, 3651–6.

Hunger, S.P., Galili, N., Carroll, A.J., Crist, W.M., Link, M.P., Cleary, M.L. (1991) The t(1;19)(q23;p13) results in consistent fusion of E2A and PBX1 coding sequences in acute lymphoblastic leukemias. *Blood* **77**, 687–93.

Imbert-Marcille, B.M., Robillard, N., Poirier, A.S., Coste-Burel, M., Cantarovich, D., Milpied, N., Billaudel, S. (1997) Development of a method for direct quantification of cyto-megalovirus antigenemia by flow cytometry. *Journal of Clinical Microbiology* **35**, 2665–9.

Izraeli, S., Janssen, J.W.G., Haas, O.A., Harbott, J., Brok-Simoni, F., Walther, J.U., Kovar, H., Henn, T., Ludwig, W.D., Reiter, A. (1993) Detection and clinical relevance of genetic abnormalities in pediatric acute lymphoblastic leukemia: a comparison between cytogenetic and polymerase chain reaction analyses. *Leukemia* **7**, 671–8.

Jensen, R.H., Langlois, R.G., Mayall, B.H. (1977) Strategies for choosing a deoxyribonucleic acid stain for flow cytometry of metaphase chromosomes. *Journal of Histochemistry and Cytochemistry* **25**, 954.

Just, T., Burgwald, H., Broe, M.K. (1998) Flow cytometric detection of EBV (EBER snRNA) using peptide nucleic acid probes. *Journal of Virological Methods* **73**, 163–74.

Kita K., Shirakawa, S., Kamada, N. and the Japanese Cooperative Group of Leukemia/Lymphoma. (1994) Cellular characteristics of acute myeloblastic leukemia associated with t(8;21)(q22;q22*). Leukemia and Lymphoma* **13**, 158–65.

Komminoth, P., Adams, V., Long, A.A., Roth, J., Saremaslani, P., Flury, R., Schmid, M., Heitz, P.U. (1994) Evaluation of methods for hepatitis C virus detection in archival liver biopsies. *Pathology Research and Practice* **190**, 1017–25.

Lalli, E., Gibellini, D., Santi, S., Facchini, A. (1992) In situ hybridization in suspension and flow cytometry as a tool for the study of gene expression. *Analytical Biochemistry* **207**, 298–303.

Lambrechts, A.C., Hupkes, P.E., Dorssers, L.C.J., van't Veer, M.B. (1993) Translocation (14;18)-positive cells are present in the circulation of the majority of patients with localized (stage I and II) follicular non-Hodgkin's lymphoma. *Blood*

82, 2510–16.

Langlois, R.G., Yu, L-C., Gray, J.W., Carrano, A.V. (1982) Quantitative karyotyping of human chromosomes by dual beam flow cytometry. *Proceedings of the National Academy of Sciences of the USA* **79**, 7876–80.

Larson, R.A., Kondo, K., Vardiman, J.M., Butler, A.E., Golomb, H.M., Rowley, J.D. (1984) Evidence for a 15;17 translocation in every patient with acute promyelocytic leukemia. *American Journal of Medicine* **76**, 827–41.

Lebo, R.V., Tolan, D.R., Bruce, B.D., Cheung, M.C., Kan, Y.W. (1985) Spot blot analysis of sorted chromosomes assigns a fructose intolerance gene locus to chromosome 9. *Cytometry* **6**, 478–83.

Lebo, R.V., Golbus, M.S., Cheung, M.C. (1986) Detecting abnormal human chromosome constitutions by dual laser flow cytogenetics. *American Journal of Medical Genetics* **25**, 519–29.

Lee, M-S., Kantarjian, H.M., Talpaz, M., Freireich, E.J., Deisseroth, A., Trujillo, J.M., Stass, S.A. (1992) Detection of minimal residual disease by polymerase chain reaction in Philadelphia-chromosome-positive chronic myelogenous leukemia following interferon therapy. *Blood* **79**, 1920–3.

Lizard, G., Chignol, M.C., Chardonnet, Y., Souchier, C., Bordes, M., Schmitt, D., Revillard, J.P. (1993) Detection of human papillomavirus DNA in CaSki and HeLa cells by fluorescent in situ hybridization. *Journal of Immunological Methods* **157**, 31–8.

LoCoco, F., Diverio, D., Pandolfi, P.P., Biondi, A., Rossi, V., Avvisati, G., Rambaldi, A., Arcese, W., Petti, M.C., Meloni, G. (1992) Molecular evaluation of residual disease as a predictor of relapse in acute promyelocytic leukemia. *Lancet* **340**, 1437–8.

Long, A.A., Komminoth, P., Lee, E., Wolfe, H.J. (1993) Comparison of indirect and direct in-situ polymerase chain reaction in cell preparations and tissue sections. Detection of viral DNA, gene rearrangements and chromosomal translocations. *Histochemistry* **99**, 151–62.

Meyne, J., Bartholdi, M.F., Travis, G.L., Cram, L.S. (1984) Counterstaining human chromosomes for flow karyology. *Cytometry* **5**, 580–3.

Montone, K.T., Lizky, L.A., Wurster, A., Kaiser, L., Bavaria, J., Kotloff, R., Palevsky, H., Pietra, G.G., Tomaszewski, J.E. (1996) Analysis of Epstein–Barr virus associated posttransplantation lymphoproliferative disorder after lung transplantation. *Surgery* **119**, 544–51.

Mosiman, V.L., Goolsby, C.L. (2000) In situ hybridization in flow cytometry. In: Faguet, G. (ed.), *Hematologic Malignancies*. CRC Press, Boca Raton, FL.

Mosiman, V.L., Patterson, B.K., Canterero, L. (1997) Reducing cellular autofluorescence in flow cytometry: an in situ method. *Cytometry* (*Communications in Clinical Cytometry*) **30**, 151–6.

Nowell, P.C., Hungerford, D.A. (1960) A minute chromosome in human chronic granulocytic leukemia. *Science* **132**, 1497.

Nucifora, G., Rowley, J.D. (1994) The AML1 and ETO genes in acute myeloid leukemia with a t(8;21). *Leukemia and Lymphoma* **14**, 353–62.

Pajor, L., Bauman, J.G.J. (1991) Flow cytometric measurement of rRNA levels detected by fluorescent in situ hybridization in differentiating K-562 cells. *Histochemistry* **96**, 73–81.

Patterson, B.K., Till, M., Otto, P., Goolsby, C., Furtado, M.R., McBride, L.J., Wolinsky, S.M. (1993) Detection of HIV-1 DNA and messenger RNA in individual cells by PCR-driven in situ hybridization and flow cytometry. *Science* **260**, 976–9.

Patterson, B.K., Goolsby, C.L., Hodara, V., Lohman, K.L., Wolinsky, S.M. (1995) Detection of decreased CD4 expression in CD4 positive HIV-1 DNA positive cells by dual immunophenotyping and fluorescence in situ polymerase chain reaction. *Journal of Virology* **69**, 4316–22.

Patterson, B.K., Mosiman, V.L., Cantarero, L., Furtado, M., Bhattacharya, M., Goolsby, C. (1998) Detection of persistently productive infection of monocytes in the peripheral blood of HIV positive patients using a flow cytometry based FISH assay. *Cytometry* **31**, 265–74.

Pennline, K.J., Pellerito-Bessette, F., Umland, S.P., Siegel, M.I., Smith, S.R. (1992) Detection of in vivo-induced IL-1 mRNA in murine cells by flow cytometry (FC) and fluorescent in situ hybridization (FISH). *Lymphocyte and Cytokine Research* **11**, 65–71.

Pinkel, D., Gray, J.W., Trask, B., van den Engh, G., Fuscoe, J., van Dekken, H. (1986) Cytogenetic analysis by in situ hybridization with fluorescently labeled nucleic acid probes. *Cold Spring Harbor Symposia on Quantitative Biology* **LI**, 151–7.

Ravichandran, K.S., Semproni, A.R., Goldsby, R.A., Osborne, B.A. (1992) Immunoglobulin V_H usage analysis by fluorescent in situ hybridization and flow cytometry. *Journal of Immunological Methods* **153**, 249–59.

Roederer, M., Murphy, R.F. (1986) Cell-by-cell autofluorescence correction for low signal-to-noise systems: application to epidermal growth factor endocytosis by 3T3 fibroblasts. *Cytometry* **7**, 558–65.

Rowley, J.D. (1973) A new consistent chromosomal abnormality in chronic myelogenous leukemia identified by quinacrine fluorescence and Giemsa staining. *Nature* **243**, 290–3.

Rufer, N., Dragowska, W., Thornbury, G., Roosnek, E., Lansdorp, P.M. (1998) Telomere length dynamics in human lymphocyte subpopulations measured by flow cytometry. *Nature Biotechnology* **16**, 743–7.

Shackney, S., Shankey, T. (1997) Common patterns of genetic evolution in human solid tumors. *Cytometry* **29**, 1–27.

Soubeyran, P., Cabanillas, F., Lee, M.S. (1993) Analysis of the expression of the hybrid gene *bcl-2/IgH* in follicular lymphoma. *Blood* **81**, 122–7.

Steinkamp, J.A., Crissman, H.A. (1993) Resolution of fluorescence signals from cells labeled with fluorochromes having different lifetimes by phase-sensitive flow cytometry. *Cytometry* **14**, 210–16.

Steinkamp, J.A., Stewart, C.C. (1986) Dual-laser differential fluorescence correction method for reducing cellular background autofluorescence. *Cytometry* **7**, 566–74.

Stowe, R.P., Cubbage, M.L., Sams, C.F., Pierson, D.L., Barrett, A.D. (1998) Detection and quantification of Epstein–Barr virus EBER1 in EBV-infected cells by fluorescent in situ hybridization and flow cytometry. *Journal of Virological Methods* **75**, 83–91.

Szollosi, J., Balazs, M., Feuerstein, B., Benz, C.C., Waldman, F.M. (1995) ERBB-2 (HER2/neu) gene copy number, p185 HER-2 overexpression, and intratumor heterogeneity in human breast cancer. *Cancer Research* **55**, 5400–7.

Taub, R., Krisch, L., Morton, C., Lenoir, G., Swan, D., Tronick, S., Aaronson, S., Leder, P. (1982) Translocation of the c-myc gene into the immunoglobulin heavy chain locus in human Burkitt lymphoma and murine plasmacytoma cells. *Proceedings of the National Academy of Sciences of the USA* **79**, 7837–41.

Testoni, N., Marinelli, G., Farabegoli, P., Zaccaria, A., Amabile, M., Raspadori, D., Pelliconi, S., Zuffa, E., Carboni, C., Tura, S. (1996) A new method of 'in-cell reverse transcriptase-polymerase chain reaction' for the detection of *bcr/abl* transcript in chronic myeloid leukemia patients. *Blood* **87**, 3822–7.

Thiesing, J.T., Ohno-Jones, S., Kolibaba, K.S., Druker, B.J. (1999) Efficacy of an ABL tyrosine kinase inhibitorin conjunction with other anti-neoplastic agents against BCR-ABL positive cells. *Blood* **94**(suppl), 100a.

Thirman, M.J., Gill, H.J., Burnett, R.C., Mbangkollo, D., McCabe, N.R., Kobayashi, H., Ziemin-van der Poel, S., Kaneko, Y., Morgan, R., Sandberg, A.A. (1993) Rearrangement of the MLL gene in acute lymphoblastic and acute myeloid leukemias with 11q23 chromosomal translocations. *New England Journal of Medicine* **329**, 909–14.

Timm, E.A. Jr, Stewart, C.C. (1992) Fluorescent in situ hybridization in suspension (FISHES) using digoxigenin-labeled probes and flow cytometry. *BioTechniques* **12**, 363–6.

Timm, E.A. Jr, Podniesinske, E., Duckett, L., Cardott, J., Stewart, C.C. (1995) Amplification and detection of a Y-chromosome DNA sequence by fluorescence in situ polymerase chain reaction and flow cytometry using cells in suspension. *Cytometry* **22**, 250–5.

Trask, B., van den Engh, G., Landegent, J., in de Wal, N.J., van der Ploeg, M. (1985) Detection of DNA sequences in nuclei in suspension by in situ hybridization and dual beam flow cytometry. *Science* **230**, 1401–3.

Trask, B., van den Engh, G., Pinkel, D., Mullikin, J., Waldman, F., van Dekken, H., Gray, J. (1988) Fluorescence in situ hybridization to interphase cell nuclei in suspension allows flow cytometric analysis of chromosome content and microscopic analysis of nuclear organization. *Human Genetics* **78**, 251–9.

van Dekken, H., Arkesteijn, G.J.A., Visser, J.W.M., Bauman, J.G. (1990) Flow cytometric quantification of human chromosome specific repetitive DNA sequences by single and bicolor fluorescent in situ hybridization to lymphocyte interphase nuclei. *Cytometry* **11**, 153–64.

van Tol, M.J., Langlois van den Bergh, W., Mesker, W., Ouwerkerk-van Velzen, M.C., Vossen, J.M., Tanke, H.J. (1998) Simultaneous detection of X and Y chromosomes by two-color fluorescence in situ hybridization in combination with immunophenotyping of single cells to document chimaerism after sex-mismatched bone marrow transplantation. *Bone Marrow Transplantation* **21**, 497–503.

Warrell, R.P. Jr, Frankel, S.R., Miller, W.H. Jr, Scheinberg, D.A., Itri, L.M., Hittelman, W.N., Vyas, R., Andreeff, M., Tafuri, A., Jakubowski, A. (1991) Differentiation therapy of acute promyelocytic leukemia with tretinoin. *New England Journal of Medicine* **324**, 1385–93.

Westbrook, C.A. (1992) The role of molecular techniques in the clinical management of leukemia: lessons from the Philadelphia chromosome. *Cancer* **70**, 1695–700.

Yu, H., Ernst, L., Wagner, M., Waggoner, A. (1992) Sensitive detection of RNAs in single cells by flow cytometry. *Nucleic Acids Research* **20**, 83–8.

Zhao, L., Kantarjian, H.M., van Oort, J.V., Cork, A., Trujillo, J.M., Liang, J.C. (1993) Detection of residual proliferating leukemic cells by fluorescence in situ hybridization in CML patients in complete remission after interferon treatment. *Leukemia* **7**, 168–71.

16

Microbial infections

David Lloyd[1], David J. Mason[2] and Marc T. E. Suller[1]

[1]University of Cardiff, Cardiff, UK
[2]University of Warwick, Coventry, UK

16.1 Introduction

Flow cytometry is as yet a relatively unexploited but potentially extremely valuable method for the study of microorganisms and microbial infections. The light scattering signal produced by most viruses is beyond the detection limit of commercial flow cytometers, but bacteria and other larger microorganisms produce signals that can readily be detected. Consequently, studies involving viruses have been primarily concerned with infected cells rather than virions. Studies involving microorganisms have been directed not only at the cells, both infected and phagocytic, in which they might occur but also at the microorganisms themselves. This chapter summarises recent achievements and the potential uses of flow cytometry in the study of viruses, bacteria, yeasts and protozoa, and of the diseases caused by these microorganisms.

16.2 Viruses

Cytometric techniques have so far been applied mainly to:

- studies of virus replication
- the detection of virus-infected cells
- the assay of antiviral compounds.

16.2.1 Studies of virus replication

Virus infection is initiated by attachment sites on the virion surface binding to complementary structures on the surface of susceptible host cells. The cellular receptors are normal host components that the virus has usurped solely for the purpose of gaining entry to the cell. In many instances, only certain cells of a host are susceptible to infection and the limited distribution of receptor and/or coreceptor molecules is one determinant of tissue tropisms. Therefore, the identification of cells bearing suitable receptors is one goal in understanding the molecular aspects of pathogenicity. Fluorochrome-labelled virus particles have been used in at least one instance to identify cells bearing virus-specific receptors and it is likely that this technique will find wider application.

Infection of cells by all viruses results in the production of novel virus-coded nucleic acids and proteins that accumulate within the cell. In addition, infection by some enveloped viruses is associated with the expression of virus-coded envelope glycoproteins on the cell surface. In situ hybridisation with virus-specific probes, or immunolabelling with fluorochrome-conjugated antibodies directed against virus-coded products, followed by flow cytometric analysis provides a useful technique for the detection and quantification of virus-related macromolecules that are found in, or on, infected cells (McSharry, 1994).

Virus infection is also frequently associated with alterations in the patterns of host macromolecular biosynthesis. Sometimes these changes are caused directly by virus-coded components, perhaps to facilitate virus biosynthesis, as in the 'shut off' in host protein synthesis that accompanies picornavirus infection. In other instances, they are a response of the host cell to infection. In animal cells, virus infection normally induces the synthesis of interferons, which in turn regulate the expression of interferon-

responsive genes and the production of many cellular proteins. Many animal viruses have developed strategies to evade host defence mechanisms, for example by inhibiting apoptosis and interfering with the expression of the major histocompatibility complex (MHC) antigens. Irrespective of how they are induced, the changes in host cell metabolism that accompany virus infection can be monitored using probes or antibodies specific to the particular components.

The immunodetection of virus antigens on the surface of infected cells in suspension is straightforward but the detection of cytoplasmic or nuclear antigens requires that the infected cell first be permeabilised. This can be done using methanol, methanol/paraformaldehyde combinations or commercially available products such as Permeafix (see Ch. 2). The DNA intercalating dye propidium iodide (PI) provides a convenient method of identifying certain cellular DNA changes associated with viral infection. Both procedures have been used extensively to monitor the changes in host and virus-coded components that occur during the virus replication cycle.

A summary of the approaches used, and of the results obtained, in some important flow cytometric studies of virus replication is given in Table 16.1.

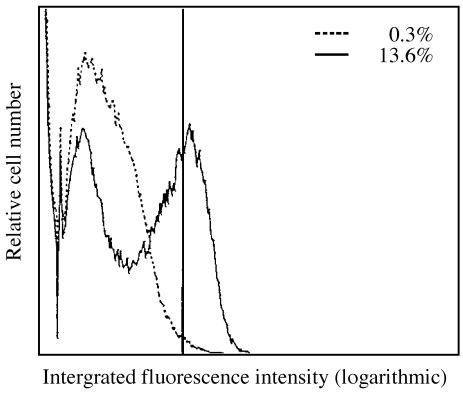

Fig. 16.1 Histogram quantifying green fluorescence from binding of HIV p24-specific monoclonal antibody revealed with affinity-purified $F(ab')_2$ fragments of goat anti-mouse immunoglobulin antibody conjugated with fluorescein isothiocyanate. Signals were processed using logarithmic amplifiers and are presented on a three-decade logarithmic axis. The cursor is placed in a position such that 0.1% of lymphocytes from random blood bank donors, run on the same day, would lie to the right. Results are shown from two individuals in whom 0.3% and 13.6% of lymphocytes were p24 positive. (Reprinted from Ohlsson-Wilhelm, B.M., Cory, J.M., Kessler, H.A., Eyster, M.E., Rapp, F., Landay, A. (1990) Circulating human immunodeficiency virus (HIV) p24 antigen-positive lymphocytes: a flow cytometric measure of HIV infection. *Journal of Infectious Diseases* **162**, 1018–24, with the permission of the University of Chicago Press.)

16.2.2 The detection of virus-infected cells

In both clinical diagnostic virology and in virus research it is frequently necessary to be able to distinguish and score infected cells. In situ hybridisation with virus-specific probes or, more frequently, immunolabelling with virus-specific antibodies followed by flow cytometry has been used to count infected cells in suspension. Similarly, labelled infected cells in monolayers could also be counted using laser scanning cytometry (see Ch. 6) but we are not aware of any reports in which this technique has been employed. In principle, it is possible to immunolabel infected cells with antibodies directed either against the virus-coded structural proteins or glycoproteins (virion components) or against the virus-coded nonstructural proteins. As antibodies to the virion components are readily available and the corresponding antigens usually accumulate to higher levels than do the virus-coded nonstructural antigens, it is these antibodies that are normally used. However, antibodies to nonstructural proteins, such as the human immunodeficiency virus (HIV) Nef protein, have been used when warranted.

There are already, reliable, long-established procedures for the laboratory diagnosis of most of the important human virus infections; consequently, flow cytometric assays have been developed only where they are likely to offer advantages over other procedures. For this reason, many studies have focused on HIV, particularly as monitoring the number of infected peripheral blood leukocytes might be clinically useful (Fig. 16.1).

Table 16.1 *Studies of virus replication by flow cytometry*

Virus and study	Method	Results	Author(s)
Infection of mouse fibroblasts with herpes simplex virus	Indirect immunofluorescence	MHC class I antigen expression was downregulated upon infection. This is an important mechanism involved in reducing the susceptibility of infected cells to killing by cytotoxic T-cells	Jennings et al. (1985)
Simian virus 40 (SV40) infection of Chinese hamster embryo (CHE) cells	Cellular DNA measured with PI and SV40 T antigen with FITC-labelled antibody in methanol fixed cells	The level of T antigen (a DNA-binding nuclear phosphoprotein involved in the induction of cellular DNA synthesis, which, in turn, is required to initiate cellular transformation) correlated with the amount of cellular DNA during the cell cycle	Jacobberger et al. (1986)
Herpes simplex virus (HSV) type I in murine, simian and human cells	Binding of monoclonal antibodies for each major glycoproteins B, C, D, and E revealed by an indirect labelling procedure	Each of the major glycoproteins was expressed on the surface of murine, simian and human cells at different levels depending on the stage of the infectious cycle	Jennings et al. (1987)
Infection of cells of a human diploid fibroblast strain (FLOW2000) by human cytomegalovirus	Dual colour flow cytometry using immunofluorescence and PI	An early viral antigen was detected within 30 min of infection; its level of expression increased with time and viral inoculum	Elmendorf et al. (1988)
Binding of Epstein–Barr virus (EBV) to lymphocytes	FITC-labelled EBV particles	Binding of EBV to the CR2 receptor of a range of B lymphocyte subpopulations was observed	Harabuchi et al. (1988)
Herpes simplex virus-infected endothelial cells	Indirect immunofluorescence	Expression of GMP140 (P-selectin) adhesion protein was dependent on expression of viral glycoprotein C; this mediates increased platelet adherence, which is thought to contribute to virus-induced cell injury	Etingin et al. (1991)
The mobility of influenza hemagglutinin (HA) on the surface of host cells	Indirect immunofluorescence	Redistribution of the HA glycoprotein resulted from the interactions of bivalent antibodies, cytoplasmic domains of the viral glycoprotein, and host–cell components	Lydy and Compans (1993)
Effects of interferons on the expression of measles virus glycoproteins in the human monocytic cell line U937	Indirect immunofluorescence after fixation and permeabilisation	The human MxA protein, which is inducible by interferons α and β, inhibits the expression of glycoproteins F and H, and subsequent release of infectious virus; this may contribute to the establishment of a persistent infection in human cells	Schnorr et al. (1993)

FITC , fluorescein isothiocyanate; PI, propidium iodide.

Table 16.2 *The detection of virus-infected cells by flow cytometry*

Virus and study	Method	Results	Author(s)
Human immunodeficiency virus (HIV)-infected lymphoid cells	Monoclonal antibodies to HIV p24 antigen	Infected cells could be counted at a frequency of 10^{-4} and p24 levels could be quantified within the cell; infected cultures could be identified 3 days earlier than by using the conventional reverse transcriptase assay	Cory et al. (1987)
Human bronchoalveolar lavage and cytomegalovirus	Immunofluorescence of an early viral antigen	Detection of virus-infected cells compared favourably with conventional procedures	Elmendorf et al. (1988)
Peripheral blood mononuclear cells from HIV-seropositive patients	Intracellular HIV Nef and p24 antigens detected by indirect immunofluorescence; DNA detected by PI	Asymptomatic patients (i.e. those not showing the clinical symptoms of acquired immunodeficiency (AIDS)) did not express p24 antigens	McSharry et al. (1990)
Monitoring the progression of disease and response to therapy in patients with HIV	Antibody to HIV p24	A rapid flow cytometric assay for p24 devised to monitor disease progression (see Fig. 16.1)	Ohlsson-Wilhelm et al. (1990)
Blue tongue virus (BTV)	Simultaneous measurements of FITC-labelled monoclonal antibody to BTV surface antigens and PE-labelled monoclonal antibody to BTV internal antigens	Able to detect infected cells within 2–4 h of inoculation; furthermore, viral replication was confirmed 24 h earlier than by infectivity assays	Barratt Boyes et al. (1992)
Hepatitis C virus (HCV)	Monoclonal antibodies directed against a specific 73 amino acid residue sequence of the HCV core antigen	Core antigen was located within the cytoplasm but not on the surface of the infected cell	Bouffard et al. (1992)
HIV	Polyclonal rabbit antibody HIV in an indirect immunofluorescence assay	The level of viral antigens expressed on the surface of the host cells was shown to correlate with the viral dose; the technique was more sensitive than determination of reverse transcriptase activity in supernatants	Bohm et al. (1992)
Monitoring disease and the presence of HIV in peripheral blood mononuclear cells	HIV proviral DNA detected using an in situ polymerase chain reaction in the presence of digoxigenin-labelled dUTP to obtain a digoxigenin-labelled amplicon able to react with anti-digoxigenin FITC-conjugated antibody	Demonstrated the potential of in situ hybridisation in conjunction with flow cytometry for disease monitoring	Re et al. (1994)

FITC, fluorescein isothiocyanate; PE, phycoerythrin; PI, propidium iodide.

In general, the detection of virus-infected cells by flow cytometry can be more sensitive, simpler and quicker than conventional techniques. A summary of the approaches used and the results obtained in flow cytometric studies for the detection of virus infection is given in Table 16.2.

16.2.3 The assay of antiviral compounds

The efficiency of antiviral compounds has also been assessed by flow cytometry. Fluorescein diacetate, an indicator of cell viability, provided a rapid viability assay for HIV-infected lymphocytes treated with zidovudine (Schols et al., 1988). The level of herpes simplex virus glycoprotein C was used as an indicator of the susceptibility of the virus to aciclovir, ganciclovir and foscarnet (Pavic et al., 1997). This flow cytometric assay, which was fast and reproducible, compared well with a test based on inhibition of the cytopathic effect; it also had the advantage of being able to detect low numbers of drug-resistant viruses in mixtures of resistant and sensitive strains.

16.3 Bacteria

To date, flow cytometric techniques have been applied mainly to:

- the detection, identification and characterisation of bacteria
- studies of bacterial multiplication and antibiotic susceptibility
- the elucidation of bacterium–host interactions.

They have been used less often to detect foreign genes and plasmids in genetically modified bacteria.

16.3.1 The detection, identification and characterisation of bacteria

Immunolabelling monitored by flow cytometry has been used successfully to detect, identify and count rapidly a number of clinically important bacteria in a variety of samples (e.g. in cultures and food) and to characterise their surface antigens. Bacterial suspensions can be directly counted at 5×10^4 organisms min^{-1} and direct detection at 10^3 organisms ml^{-1} is possible. The limit of detection using fluorochrome-labelled antibodies is claimed to be 10 bacteria ml^{-1}; the availability of reagents for this specific application is continually increasing. It is anticipated that routine rather than research implementation of these methods in diagnostic microbiology will accompany the introduction of simple, cheap, laser-diode-based instruments. Where only low numbers of organisms are present, it has proved advantageous to include an enrichment step, for example by using immunomagnetic beads, prior to analysis. The possibility of using fluorescent ribosomal RNA (rRNA) targeted probes to identify and count organisms in mixed populations has also been established (Table 16.3).

Flow sorting has been used to isolate *Staphylococcus aureus* labelled with fluorochrome-conjugated antibodies from mixed bacterial populations (Porter et al., 1993). With this method, *S. aureus* was recovered at a purity in excess of 90% even when present in low numbers.

16.3.2 Bacterial multiplication and antibiotic susceptibility

During the multiplication of bacteria, there are changes in cell size, shape and internal complexity, which would be expected to have effects on the light scattering properties of the cells. There are also changes in DNA content that are directly related to the cell cycle and can be assessed by methods to quantify DNA. Consequently, both of these parameters have been measured frequently (sometimes simultaneously) in studies of bacterial multiplication (Table 16.4).

It should be remembered, that particle counts represent the 'total' rather than the 'viable' count of the microorganism. There are instances, however, where it is important to assess viability and vitality in bacterial cultures; consequently many flow cytometric techniques have been developed for this purpose. These techniques involve the use of fluor-

Table 16.3 *The detection, identification and characterisation of bacteria by flow cytometry*

Organism and study	Method	Results	Authors
Detection of specific antigenic determinants of outer membrane proteins of *Haemophilus influenzae*	Indirect detection of bound mouse monoclonal anti-Hib porin antibodies using anti-mouse antibodies conjugated to fluorescein	Increases in fluorescence seen on binding of monoclonal antibodies	Srikumar et al. (1992)
Rapid identification and enumeration of *Escherichia coli* in mixed microbial populations	Direct labelling using fluorescent conjugated antibodies	*E. coli* was recovered at $> 90\%$ purity by cell sorting	Porter et al. (1993)
E. coli	Fluorescent rRNA-targeted oligonucleotide probes	Successful rapid identification and enumeration in mixed microbial populations	Wallner et al. (1993)
Rapid detection of *Salmonella* spp. in food products	Monoclonal antibodies directly conjugated to FITC together with unlabelled monoclonal antibodies revealed by PE-conjugated goat anti-mouse immunoglobulin	Changes in fluorescence profiles	McClelland and Pinder (1994a–c)
Detection of low numbers of *Listeria monocytogenes* in cultures	Paramagnetic labelling with 50 nm iron particles	Cells successfully separated using high gradient column and analysed using flow cytometry	Jacobsen et al.(1997a)
Pseudomonas aeruginosa	Fluorescence in situ hybridisation combined with flow cytometry	Successful rapid identification in bioaerosols without measurable nonspecific binding	Lange et al. (1997)
Detection of *Salmonella typhimurium* in food products	Dual labelling with the viability stain ChemChrome B (Chemunex) and fluorescent-conjugated monoclonal antibodies	Detection down to 10^2 cells ml^{-1} possible	Clarke and Pinder (1998)

FITC, fluorescein isothiocyanate; PE, phycoerythrin.

escent dyes to probe changes in membrane potential (Table 16.5), membrane integrity (Table 16.6), or intracellular metabolic activity (Table 16.7). Because successful antibiotics can affect vitality and/or viability and will ultimately inhibit bacterial multiplication, many of these techniques have proved particularly useful in studies of antibiotic susceptibility (Fig. 16.2).

As yet there have been relatively few objective studies of the efficacy of the various possible indicators of bacterial vitality and viability. The available results suggest that some indicators may perform better than others in given situations. Protocol 16.1 gives one method. Exclusion of the oxonol dye bis-(1,3-dibutylbarbituric acid) trimethine oxonol ($DiBAC_4(3)$) gives reliable indication of bacterial viability in all Gram-positive and Gram-negative strains investigated to date; however, before any indicator is used extensively, it would seem worthwhile investigating how the results obtained with it correlate with those given by other procedures, e.g. viable counts. Dual- and multiparameter flow cytometry studies have allowed changes to be monitored simultaneously in, for instance, membrane integrity and membrane potential, or membrane potential and respiratory activity. They have

Table 16.4 *Studies of bacterial multiplication using flow cytometric methods*

Organism and study	Method	Results	Author(s)
DNA content during the cell cycle of *Escherichia coli*	DNA content measured using mithramycin–EB	Permeabilisation to mithramycin–EB was originally achieved by fixation but more recently by the use of cold shock; fluorescence and theoretical values agreed closely	Steen and Boye (1980), Walberg et al. (1997)
DNA content during the cell cycle of *E. coli*	Quantitative measurement of DNA content using mithramycin–EB, DAPI–PI or Hoechst 33258	Changes in fluorescence profiles monitored	Akerlund et al. (1995), Allman et al. (1991), Boye and Lobner-Olesen (1991), Sgorbati et al. (1996)
Salmonella typhimurium during starvation	Light scatter and DNA content (Hoechst 33342)	Changes in scatter profiles and DNA content monitored	Joux et al. (1997), Lebaron and Joux, (1994), Monfort and Baleux (1994)
Cell size analysis of *E. coli*	Light scatter	Changes in profiles monitored	Lopéz-Amorós et al. (1994), Vives-Rego et al. (1994), Wold et al. (1994)
Mycobacterium bovis and *M. smegmatis*	Microencapsulation technology combined with flow cytometry	This technique allowed colony growth of these normally intracellular organisms to be quantified within just 1–3 days after encapsulation	Ryan et al. (1995)
M. avium following exposure to isoniazid	SYTO® 16 (a cell-permeant nucleic acid dye)	Changes in fluorescence profiles monitored	Ibrahim et al. (1997)
DNA content during the cell cycle of *E. coli*	DNA-specific dye SYBR® green I	Does not require cell permeabilisation for staining	Mason et al. (1999)

DAPI–PI, 4',6-diamidino-2-phenylindole dihydrochloride and propidium iodide; EB, ethidium bromide.

also allowed subpopulations of an organism to be defined on the basis of physiological criteria. Light scatter is a complex function of cell size, shape, refractility and granularity. Perturbation of any one of these characteristics is likely to be detectable but usually in a nonlinear manner, making quantification difficult. An example (Allman et al., 1990) where calibration of bacterial size determined by forward light scatter correlated well with cell volume determined with a Coulter counter suggests that even the simplest instruments can be used for this purpose (Table 16.8).

Protocol 16.1 Enumeration of bacteria and assessing culture viability

Specimen requirements and reagents

- A 1 mg ml^{-1} stock solution of PI (Sigma or Molecular Probes) in deionised water, which can be stored at –20°C for up to 1 year if protected from light
- Working strength PI solution (100 μg ml^{-1}) made by diluting stock solution with deionised water
- Control bacteria in suspension (approximately 10^8 cells ml^{-1})
- Test bacteria in suspension (growth medium or buffer)

Table 16.5 *The assessment of bacterial viability or vitality based on membrane potential*

Organism and study	Method	Results	Author(s)
Penicillin-treated *Staphylococcus aureus*	Uptake of $DiOC_6(3)$ (a cationic dye)	Results closely matched minimum inhibitory concentration (MIC) penicillin sensitivity data obtained by traditional methods	Ordóñez and Wehman (1993)
S. aureus	Fluorescent dyes sensitive to changes in membrane potential: $DiBAC_4(3)$ or rhodamine 123	The dyes were successful indicators of membrane perturbation	Diaper and Edwards (1994), Suller and Lloyd (1998), Suller et al. (1997)
Antimicrobial susceptibility testing in *Escherichia coli* and other bacteria	Bacteria labelled with $DiBAC_4(3)$ (an anionic probe) or calcafluor white	Susceptible bacteria exhibited an increase in fluorescence upon addition of $DiBAC_4(3)$	Jepras et al. (1995, 1997), Mason et al. (1994, 1995a,b, 1997), Sheppard et al. (1997)
Salmonella typhimurium	Uptake of rhodamine 123	Fluorescence intensity of stained cells was correlated with the viable counts	Lopéz-Amorós et al. (1995)
Pseudomonas fluorescens	Uptake of rhodamine 123	Rhodamine 123 cell-associated fluorescence increased upon hyperpolarisation with valinomycin	Porter et al. (1995a)
Several *Listeria* strains treated with antimicrobial peptides	Uptake of $DiOC_6(3)$	Optimum staining conditions were found to be 0.1 μmol l^{-1} $DiOC_6(3)$ for 5×10^6 cells ml^{-1} and the resulting data were found to be as sensitive as ATP bioluminescence	Ratinaud and Revidon (1996)
Methicillin- and vancomycin-treated *S. aureus*	Uptake of $DiBAC_4(3)$	See Fig. 16.2.	Suller et al. (1997)

$DiBAC_4(3)$, bis-(1,3 dibutylbarbituric acid) trimethine oxonol; $DiOC_6(3)$, 3,3'-dihexyloxacarbocyanine iodide.

Method

1. Prepare a positive control for PI uptake by adding 900 μl ice-cold ethanol (80%v/v) to 100 μl control bacteria. Incubate for 60 min at 4 °C and resuspend bacteria in 1 ml sterile growth medium or buffer.
2. Add 900 μl control suspension or test suspension to 100 μl working strength PI solution and incubate samples for 3–5 min at room temperature prior to analysis.

Aquiring data on the flow cytometer

1. Set-up flow cytometer for excitation at 488 nm with a band-pass filter at 605 nm. Monitor dye emission using the red fluorescence detector gated by light scatter parameters. Use light scatter and fluorescence detectors with logarithmic amplification.
2. Analyse an unstained suspension of cells prior to stained samples.
3. Collect data from at least 3×10^3 cells on each acquisition.

Analysing the data

1. Display a cytogram of forward versus side scatter and place a region around the bacterial population. (Note: there is some shrinkage when cells are alcohol-fixed, which may reduce the light scatter signal from this population compared

Table 16.6 *The assessment of bacterial viability or vitality based on membrane integrity*

Organism and study	Method	Results	Author
Antibiotic-induced damage in *Escherichia coli*	Uptake of PI	Changes in cell-associated fluorescence	Gant et al. (1993)
Antibiotic-induced changes in *E. coli*	SYTOX® green	Changes in cell-associated fluorescence	Roth et al. (1997)
Antibiotic sensitivity of *Listeria monocytogenes*	*Bac*Light™ viability kit (Molecular Probes)	Successful cytometric determination of defined proportions of live and dead cell mixtures	Swarts et al. (1998)

PI, propidium iodide.

Table 16.7 *The assessment of bacterial viability or vitality by the detection of metabolic activity*

Organism and study	Method	Results	Author(s)
Efflux pumps in *Escherichia coli*	EB	An alternative use for this nucleic acid dye	Jernaes and Steen (1994)
Ciprofloxacin-treated *E. coli*	CTC (a redox dye)	CTC was reduced by active cells to a fluorescent formazan	Mason et al. (1995b)
Rapid susceptibility testing of *Mycobacterium tuberculosis* to various antimycobacterial agents	FDA	Only live cells hydrolyse FDA to produce fluorescent bacteria	Kirk et al. (1998), Norden et al. (1995)
Antibiotic susceptibility in nontuberculosis mycobacterial strains	Hydrolysis of FDA	Antibiotic-treated cells hydrolysed less FDA than untreated cells	Bownds et al. (1996)
Metabolic activity in *Staphylococcus aureus*	Calcein AM	Calcein fluorescence used to assess metabolic activity	Comas and Vives-Rego (1998)
Methicillin-exposed *S. aureus*	CTC	CTC was reduced by active cells to a fluorescent formazan	Suller and Lloyd (1998)

Calcein AM, calcein acetoxy-methyl ester; CTC, cyano-2,3-ditolyl tetrazolium chloride; FDA, fluorescein diacetate.

with unfixed organisms.) Use this region to gate a histogram of red fluorescence.
2. Adjust the photomultiplier voltage on the red fluorescence detector to fit unstained cells within the first decade and mark this second region.
3. Use the ethanol-fixed cells to identify a third region of interest in the red fluorescence histogram corresponding to PI-stained cells; these should be at least one decade higher in fluorescence intensity than the unstained cells.
4. Obtain a total particle count from statistics relating to the region of interest in the light scatter histogram. Estimate viable count by observing the size of population in the second region of interest. The size of the population in the third region of interest relates to the number of nonviable bacteria in a sample.

16.3.3 Bacterium–host interactions

Pathogenic bacteria or their extracellular products frequently need to attach to particular host cells or structures in order to initiate or propagate an infection. Simiarly, host phagocytic cells need to attach

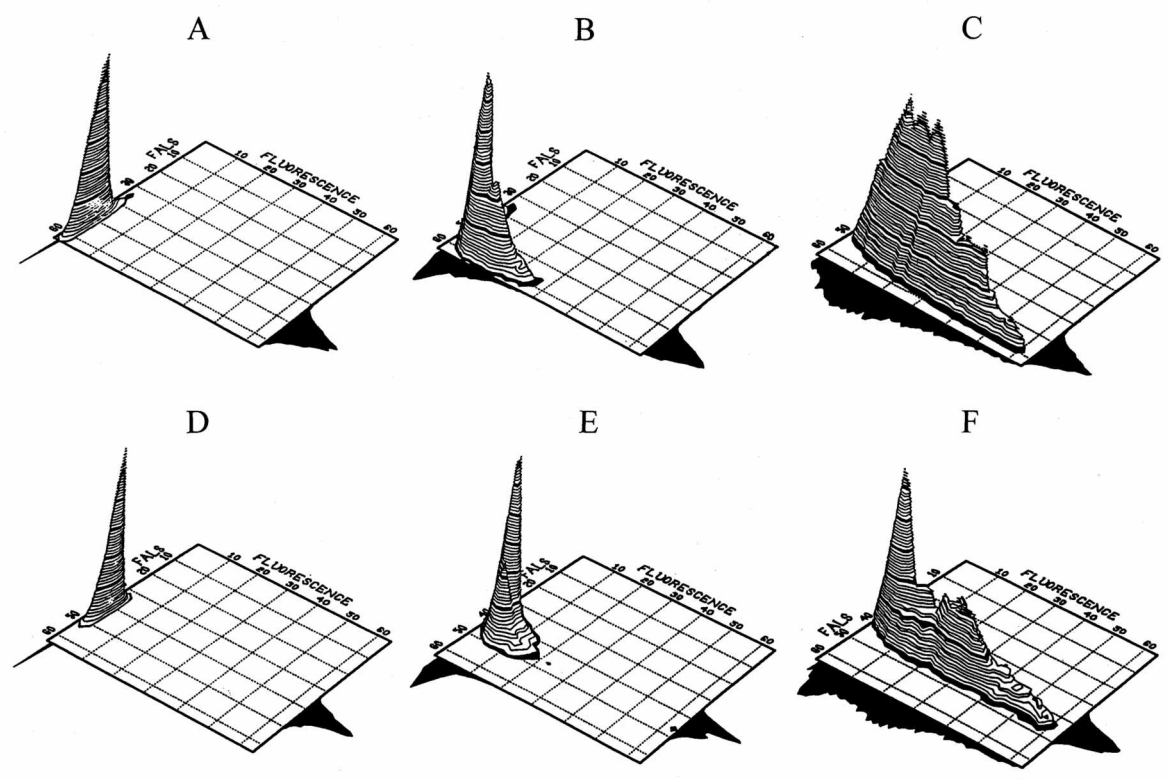

Fig. 16.2 Dual-parameter histograms of forward light scatter against bis-(1,3-dibutylbarbituric acid) trimethine oxonol ($DiBAC_4(3)$) fluorescence for the effect of methicillin (4 μg ml^{-1}) on antibiotic-sensitive *Staphylococcus aureus* strain NCTC 6571 (AC), and vancomycin (4 g ml^{-1}) on a methicillin-resistant (MRSA) strain NCTC 11353 (D–F) after 0 min (A, D), 30 min (B, E), and 120 min (C, F). (Reproduced from Suller, M.T.E., Stark, J.M., Lloyd, D. (1997) *Journal of Antimicrobial Chemotherapy* **40**, 77–83, with the permission of the Oxford University Press.)

to bacteria prior to engulfing and killing them as part of the immune response to infection. Flow cytometry has proved particularly useful in studies of these interactions. It has been possible, for instance, to label host and bacterial cells or structures separately and to follow attachment and engulfment by monitoring changes in light scattering and/or fluorescence. An interesting recent development in this respect is the use of genetic modification techniques for producing bacteria that become biosynthetically labelled with the green fluorescent protein during their growth. Because phagocytosis elicits a respiratory burst that is associated with transient increases in several signalling molecules, including cytoplasmic Ca^{2+}, and a more prolonged production of reactive oxygen species, these parameters have often been monitored alongside the uptake of labelled bacteria. There is increasing interest in the development of techniques for the quantification of phagocytosis-related events in whole blood ex vivo, because of their relevance to events in vivo (Table 16.9; see also Ch. 12).

16.3.4 The detection of foreign genes and plasmids

Tombolini et al. (1997) have described the chromosomal tagging of *Pseudomonas fluorescens* with the gene for the green fluorescent protein. They found

Table 16.8 *Comparative and multiparameter flow cytometry studies of bacterial viability or vitality*

Organism and study	Method	Results	Author(s)
The effects of different classes of antibiotic on *Escherichia coli*	Monitoring of the ratio of protein content, as measured by FITC fluorescence, to forward light scatter	Antimicrobial activity detectable within 2 h of treatment	Durodie et al. (1995)
Rapid susceptibility testing of *Pseudomonas* spp. to a quaternary ammonium compound	Rhodamine 123, the *Bac*Light™ viability kit and uptake of SYTOX® green	Staining was poor with rhodamine 123 and the *Bac*Light™ viability kit; good correlation established between SYTOX® green uptake and colony counts	Langsrud and Sundheim (1996)
Listeria monocytogenes	CFDA, ChemChrome B, (Chemunex), the *Bac*Light™ viability kit, BCECF-AM and rhodamine 123	The most reproducible results, which also correlated well with estimates of colony-forming units, were achieved using CFDA and ChemChrome B. Results obtained with the *Bac*Light™ viability kit varied with the growth phase. Only low fluorescence activity was detected from organisms labelled with either BCECF-AM or rhodamine 123	Jacobsen et al. (1997b)
Salmonella typhimurium	Uptake of $DiBAC_4(3)$ and CTC reduction	Close agreement between uptake of $DiBAC_4(3)$ and respiratory activity as detected by CTC reduction	Lopéz-Amorós et al. (1997)
Postantibiotic effects of imipenem and ciprofloxacin on *Pseudomonas aeruginosa*	Light scatter and PI	Changes monitored in light scatter and fluorescence profiles	Gottfredsson et al. (1998)
Characterisation of *Salmonella typhimurium*	$DiBAC_4(3)$, EB and PI	Populations divisible into four physiological states characterised by labelling with the three probes	Nebe-von Caron et al. (1998)

BCECF-AM, 2',7'-bis-(2-carboxyethyl-5-(and-6)-carboxyfluorescein acetoxy-methyl ester; CFDA, carboxyfluorescein diacetate; CTC, cyano-2,3-ditolyl tetrazolium chloride; $DiBAC_4(3)$, bis-(1,3 dibutylbarbituric acid) trimethine oxonol; EB, ethidium bromide; FITC, fluorescein isothiocyanate; PI, propidium iodide.

that expression of a single copy of the gene was sufficient to be detected by flow cytometry. Flow cytometry has been also used to monitor green fluorescent protein fluorescence following its incorporation into *Mycobacterium* spp. as a reporter molecule for gene expression (Dhandayuthapani et al., 1995; Kremer et al., 1995).

An in situ polymerase chain reaction that yields a fluorescently labelled product was used in conjunction with flow cytometry by Porter et al. (1995b) for the detection of a plasmid-encoded gene (*xy1E*) in *Ps. fluorescens*.

16.4 Yeasts

Eosin Y selectively stains nonviable blastospores of *Candida albicans* without affecting the viability of competent yeast cells. This provides a more precise counting method than the enumeration of colony-forming units (Constantino et al., 1995).

Table 16.9 *Flow cytometry in the study of bacteria–host interactions*

Organism and study	Method	Results	Author(s)
Helicobacter pylori adhesion to human gastric carcinoma cells	Indirect detection of bound bacteria using rabbit whole cell antibody raised against *H. pylori* and FITC-conjugated goat anti-rabbit IgG	Gastric adenocarcinoma cells, with *H. pylori* attached, were rendered fluorescent following labelling with antibodies	Dunn et al. (1991)
Phagocytosis of *Haemophilus influenzae*	FITC-labelled *H. influenzae*	Quantification of phagocytosis	Bredius et al. (1993), Vogel et al. (1994)
H. influenzae attachment to human epithelial cells	FITC-labelled *H. influenzae*	Attachment of labelled *H. influenzae* to unlabelled epithelial cells detected by monitoring fluorescence profiles of epithelial cells	Raza et al. (1993)
Platelet binding and aggregation by *Streptococcus salavarius* exopolysaccharide	*S. salavarius* stained with Hoechst 33342; platelets labelled with FITC-conjugated antibodies	Dual-labelled particles represented bacteria bound to platelets	Sullam et al. (1993)
Staphylococcus aureus	FITC-labelled *S. aureus*	Quantification of phagocytosis	Perschel et al. (1994)
Mycobacterium spp. interactions with host cell	FITC-labelled *Mycobacterium* spp.	Quantification of phagocytosis by monocytes	Hewish et al. (1996)
		Binding and internalisation by epithelial cells	de Boer et al. (1996)
	Mycobacterium spp. expressing the green fluorescent protein	Bacteria expressing green fluorescent protein could be detected alone or in association with mammalian cells	Valdivia et al. (1996)
Salmonella typhimurium binding to epithelial cells or macrophages	Green fluorescent protein incorporated into bacterium	*Salmonella* spp. could be readily detected	Valdivia et al. (1996)
Helicobacter pylori attachment to human epithelial cells	Bacteria labelled with CFDA-SE	Attachment of labelled *H. pylori* to unlabelled epithelial cells detected by monitoring fluorescence profiles of epithelial cells	Logan et al. (1998)
H. pylori adherence to human gastric carcinoma cells	Polyclonal antibody to heat shock protein, HSP60, in *H. pylori*	Intensity of HSP60 expression correlated with adherence to human cells	Yamaguchi et al. (1996)
Binding of *Streptococcus suis* to albumin	Indirect detection of bound albumin using rabbit polyclonal antibody against albumin and FITC-conjugated monoclonal antibodies raised against rabbit immunoglobulins	Changes in fluorescence profiles	Quessy et al. (1997)

CFDA-SE, carboxyfluorescein diacetate succinimidyl ester; FITC, fluorescein isothiocyanate.

The sensitivity of *Candida* strains to amphotericin has been distinguished by the use of the membrane-potential sensitive dye 3,3'dipentyloxacarbocyanine iodide $DiOC_5(3)$ (Ordóñez and Wehman, 1995). Incubation in the presence of the antibiotic for 30 min was sufficient to perturb dye uptake in sensitive strains, and the effect was dose dependent (Fig. 16.3). PI, ChemChrome Y and oxonol have also been used to study the interaction between amphotericin and *C. albicans* (Carter et al., 1993); ethidium bromide (EB) also shows promise in this respect (O'Goreman and Hopfer, 1991).

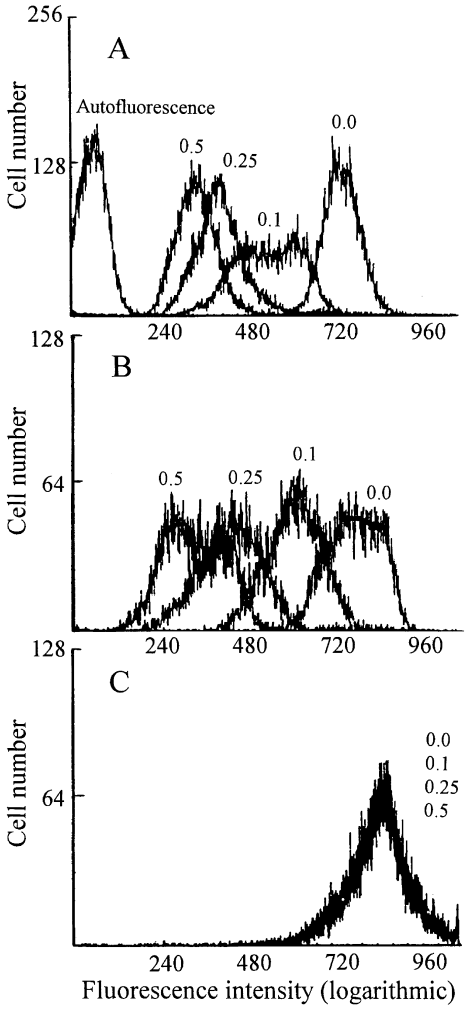

Fig. 16.3 The effect of amphotericin on three strains of *Candida* monitored by the fluorescence of 3,3'-dipentyloxacarbocyanine iodide ($DiOC_5(3)$). Histogram peaks are labelled with the doses ($\mu g\ ml^{-1}$) of amphotericin used. (A) *C. albicans* ATCC 14053 is susceptible (a sample without $DiOC_5(3)$ treatment, aut fluorescence also included). (B) *C. tropicalis* ATCC 13803 is susceptible. (C) *C. tropicalis* ATCC 28707 is resistant. The fluorescence intensity of the resistant strain remained unchanged over the full range of antibiotic concentrations used. (Reprinted by permission of Wiley-Liss, Inc., a subsidiary of John Wiley & Sons, Inc., from Ordóñez, J. V., Wehman, N.M. (1995) Amphotericin B susceptibility of *Candida* spp. assessed by rapid flow cytometric membrane potential assay. *Cytometry* **22**, 154–7.)

16.5 Protozoa

Flow cytometry provides a rapid procedure for differential counting of viable and nonviable *Trichomonas vaginalis*. It also gives results that are of greater statistical significance than the traditional method, which distinguishes motile from nonmotile cells microscopically (Humphreys et al., 1994). Two different methods – live/dead fluorescein diacetate (FDA)/PI staining and $DiBAC_4(3)$ oxonol exclusion criterion – gave similar results. Moreover, there was good agreement between the flow cytometric and microscopical counting methods for assessment of sensitivity to killing by metronidazole (Fig. 16.4).

Pneumocystis carinii cysts and trophozoites in lung homogenates from an animal (rat) model have been counted using PI (de Stefano et al., 1992; Lapinsky et al., 1991). Flow cytometry enabled the pathogen and the larger animal cells, with their higher nucleic acid content, to be clearly distinguished. Exclusion of the dye from organisms with an intact plasma membrane provided a method for identifying viable cells, while total numbers were estimated after formaldehyde fixation. Fluorescence activated cell sorting of cysts has also been described (Libertin et al., 1984). Calcein acetoxymethyl ester can be used as a fluorophore for this organism after freeze–thaw treatment (Kanishiro et al., 1993).

The susceptibility of *Leishmania infantum* promastigotes to amphotericin has been measured using the principle that any perturbant of the plasma membrane potential will affect cyanine dye uptake (Azas et al., 1997). The use of this test for predicting the clinical outcome of leishmaniasis has yet to be reported.

The long-term culture of *Leishmania donovani* amastigotes has been facilitated by cytofluorometric methods (Doyle et al., 1991) and determination of the plasticity of chromosome numbers and targeting of essential genes has been described (Cruz et al., 1993). Other in vitro studies include differentiation of promastigotes (Darcy et al., 1987) and the characterisation of species-specific antibodies (Jaffe

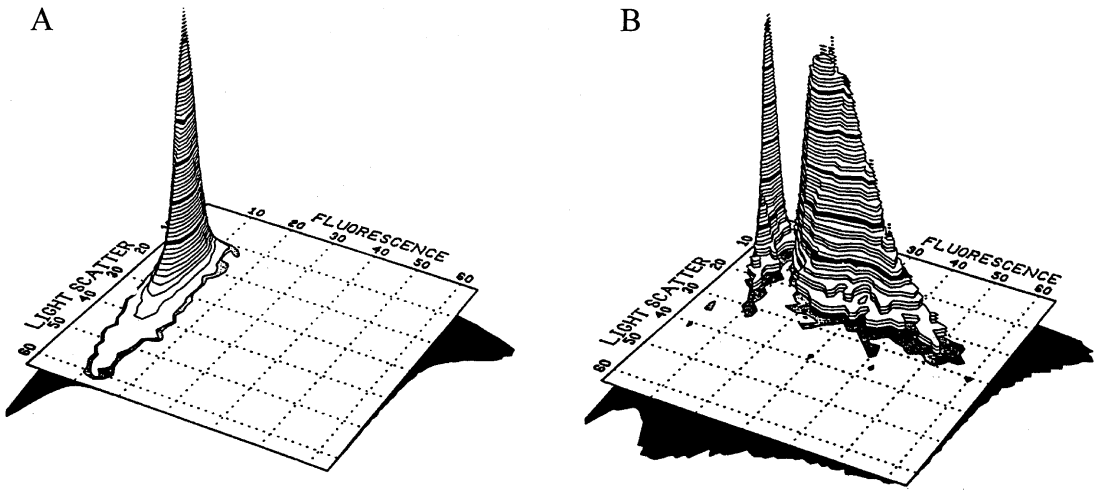

Fig. 16.4 Light scatter versus fluorescence cytograms for *Trichomonas vaginalis* incubated in the absence (A) and in the presence (B) of 2 μg ml^{-1} metronidazole. Cultures were stained with bis-(1,3-dibutylbarbituric acid) trimethine oxonol ($DiBAC_4(3)$) (1 μg ml^{-1}). (Reprinted by permission of Wiley-Liss, Inc., a subsidiary of John Wiley & Sons, Inc., from Humphreys, M., Allman, R., Lloyd, D. (1994) Determination of the viability of *Trichomonas vaginalis* using flow cytometry. *Cytometry* **15**, 343–8.)

et al., 1990). The interaction between murine macrophages and *Leishmania* spp. has also been studied using flow cytometry (Bertho et al., 1992; Butcher et al., 1992).

Staining of red blood cells infected with *Plasmodium falciparum* using streptavidin–fluorescein isothiocyanate (FITC) and staining intra-erythrocytic parasitic DNA with hydroethidium enabled simultaneous flow cytometric analysis of parasitaemias (Protocol 16.2); this approach has been used to quantify the culture of the malaria parasites (Pattanapanyasat et al., 1993, 1996). Parasitaemia has been monitored using flow cytometry (Bunyaratvej et al., 1993; Kadjoian et al., 1992) as has the treatment of severe malaria by exchange transfusion (Wernli et al., 1991). Screening of blood samples for malaria parasites by cytofluorimetry has been described by van Vianen et al. (1993). Asexual multiplication (Janse et al., 1987, 1989) of the parasite and generation of chromosome size polymorphism has been monitored (Ponzi et al., 1990).

Protocol 16.2 Flow cytometric detection of malaria parasites

- A 1 mg ml^{-1} stock solution of PI (Sigma or Molecular Probes) in deionised water is stable for a long period of time if kept dark at 4°C; final concentration for cell staining is 1 μg ml^{-1} in phosphate buffered saline (PBS)
- Hydroethidine (Polysciences) is dissolved in *N*,*N*-dimethylacetamide at a stock concentration of 7 mg ml^{-1}; a working strength solution is prepared by adding 20 μ1 of the stock hydroethidine solution to 10 ml PBS
- Glutaraldehyde (Sigma) diluted with PBS at a stock concentration of 25% and stored at –20°C; final strength solution is made by diluting the stock 1/100 with PBS (to 0.25%) and storing at 4°C

Specimens

- Blood samples are collected from infected humans or laboratory animals as described by van Vianen et al. (1993). (This protocol deals with samples obtained from in vitro culture of the

blood stages of *Plasmodium falciparum* (Trager and Jensen, 1976))
- Samples from the culture are centrifuged for 10 s at 15 000 × *g* in an Eppendorf centrifuge or at 500 × *g* for 10 min in a bench centrifuge to remove culture medium

Cell fixation

1. Packed infected blood cell samples (1–2 μl) obtained from cultures are washed once in 5 ml cold PBS before fixation.
2. Subsequently 1 ml of 0.25% glutaraldehyde in PBS is added and the sample is mixed vigorously.
3. Fixation can be done at 4 °C for 15 min or at room temperature for 10 min.
4. Fixed cells can be kept at 4°C for many months.
5. Before staining, cells are washed twice with 5 ml PBS.

Staining

1. Fixed blood samples are stained for at least 30 min at room temperature in the dark with 1 ml of working strength PI.
2. Alternatively, fresh cultured blood samples can be vitally stained without fixation using hydroethidine: 1–2 μl of infected blood cells are washed twice in PBS, and the cell pellet is stained with 1 ml working strength hydroethidine solution for at least 30 min at 37°C before flow cytometric analysis.

Acquiring data on the flow cytometer

1. The PI- or hydroethidine-stained cells are excited with 488 nm light in a flow cytometer equipped with an argon ion laser.
2. Red blood cells are gated on the basis of their logarithmic amplification of the forward scatter and 90° side light scatter signals.
3. Red fluorescence of PI or ethidine is measured through a 585 nm band-pass filter.
4. A total of 30 000 red blood cells are analysed. Percentage parasitaemia and fluorescent intensity are obtained from an integrated fluorescence histogram between the infected and the control uninfected samples.

Note: a fuller account of flow cytometry in malaria detection can be found in the article by Janse and van Vianen (1994).

The diagnosis of giardiasis by the identification of *Giardia intestinalis* in faecal samples relies on filtration and centrifugation followed by fluorogenic staining with FDA and PI (Jones and Senft, 1985; Schupp and Erlandsen, 1987), eosin (Kasprzak and Majewska, 1983) or 4', 6-diamidino-2-phenylindole (DAPI) (Thiriat et al., 1998). Flow cytometric methods have been perfected for detection of *Giardia* spp. in water supplies after novel flocculation techniques (Vesey et al., 1993); a comprehensive review (Vesey et al., 1994) includes methods using antibodies, lectins, DNA stains, vital staining and fluorescent in situ hybridisation.

The burgeoning problems of corneal keratitis in contact lens users caused by *Acanthamoeba castellanii* has led to a flurry of activity in the diagnosis and prophylaxis of this condition, which can lead to blindness. Flow cytometry has provided a powerful approach to the study of loss of viability of trophozoites and cysts in vitro, and hence to the development of efficient amoebicidal and cysticidal agents (e.g. chlorohexidine and polyhexamethylene biguanide) (Khunkitti et al. 1996, 1997a,b, 1998a,b). Turner et al. (1999) provide the most recent review.

16.6 The immune response to infection

Microbial infections in animals provoke an acquired immune response that is manifest by the production of pathogen-specific lymphocytes and/or antibodies. The ability to detect and to measure the concentration of antibodies produced against microbes is important when studying the specific immune response that occurs following either natural infection or prophylactic immunisation. It is often crucial to distinguish between seropositive and seronegative individuals for diagnostic purposes, while monitoring the level of serum antibody can sometimes provide clinically useful information on the progress of infection. There are already well-

established conventional immunoassays available for the detection of antibodies to many pathogenic microorganisms; however, antimicrobial antibodies can also be detected and quantified by flow cytometric procedures. Immunoassays, in essence, enable the complexes (immune complexes) that are formed between microbial antigen(s) and antibody molecules to be selectively detected and/or quantified. Depending on the circumstances, immune complexes may vary in size from little more than a few antibody molecules attached to a soluble antigen molecule to large precipitates comprising countless antibody molecules and large particulate antigens. Consequently, in flow cytometric procedures, the reaction conditions are usually arranged so that the immune complexes that are formed are of a size to produce a signal that lies within the range of the light scattering detectors. The bound primary antibody, which is normally unlabelled (e.g. contained in a patient serum sample), is then detected by an indirect immunofluorescence procedure using fluorochrome-conjugated F(ab') or $F(ab')_2$ fragments of an antispecies immunoglobulin antibody. Where the target antigen occurs on, or within, a microorganism such as a bacterium, the microorganism itself can be detected by light scattering. Small soluble antigens, which generate only very weak light scattering signals, are usually first bound covalently to polystyrene or latex beads of a size that can readily be detected.

16.6.1 Viruses

Various research groups have employed flow cytometry to detect antibodies to HIV. Sligh et al. (1989) incubated infected cells from seropositive patients with FITC-conjugated $F(ab')_2$ fragments of goat anti-human IgG and fetal bovine serum (to decrease nonspecific binding) (Fig. 16.5).

This procedure was used to measure antibody induced by vaccination with recombinant HIV envelope glycoprotein gp160, which had been produced in insect tissue culture cells infected with a baculovirus vector (Gorse et al., 1992). The early

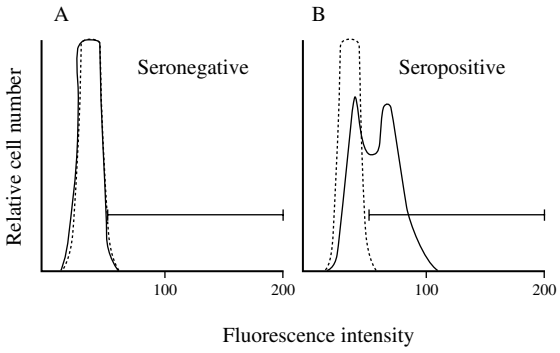

Fig. 16.5 Flow cytometric histograms of HIV-seronegative (A) and HIV-seropositive sera (B). Dotted lines indicate H9 cells; solid lines indicate HIV-H9 cells. The bar represents the positive fluorescence region. (Reprinted from Sligh, J.M., Roodman, S.T., Tsai, C.C. (1989) Flow cytometric indirect immunofluorescence assay with high sensitivity and specificity for detection of antibodies to human immunodeficiency virus (HIV). *American Journal of Clinical Pathology* **91**, 210–4, with permission from the American Society for Clinical Pathology.)

period of HIV infection is associated with a low level of antibody, which is difficult to detect. Hu et al. (1996) used insoluble recombinant HIV Gag p45, Gag gp41, gp160 and Pol 97 polyprotein as antigens and carriers to detect HIV antibodies in patient's plasma together with FITC or phycoerythrin (PE)-labelled goat antibody against human λ-, μ- or α-chains. The presence of antibody was detected earlier than achieved with the enzyme-linked immunosorbant assay (ELISA) or the Western blot assay that are currently used. This provides new opportunities for studies on immune responses and immunopathogenesis in the early period of infection by HIV.

Flow cytometry has been used to assess the ability of antibodies to prevent the binding of viral antigens to cell surface receptors. For example, vaccination with a recombinant HIV envelope protein resulted in an increase in neutralising antibody in serum, the level of which correlated with the prevention of cell binding in vitro and protection in vivo (Rosa et al., 1996).

The ability of flow cytometry to distinguish between two populations based on their light scatter

has allowed for the simultaneous detection of antibodies to more than one virus. McHugh et al. (1988) used two sizes of polystyrene microsphere coated with viral antigen to detect anti-cytomegalovirus and anti-herpes simplex virus antibodies using biotinylated goat anti-human IgG plus a streptavidin–PE label.

16.6.2 Bacteria

Helicobacter pylori is linked to gastritis and peptic ulcers and is a major healthcare problem. Serum IgG antibodies to *H. pylori* were detected using antigen-coated polystyrene and indirect immunofluorescence (Best et al., 1997). This technique successfully distinguishes between positive and negative patients and, because the level of blood antibody decreases with effective treatment, it allows monitoring of the disease.

Brucella abortus and *S. aureus* are problematic within the dairy industry because they infect cows and contaminate the milk they produce. Flow cytometry has provided a sensitive and reliable method for the detection of antibodies to these organisms in blood or milk using antigen-coated latex and indirect immunofluorescence (Iannelli et al., 1998).

In a flow cytometric serodiagnostic test for the causative agent of Lyme disease, *Borrelia burgdorferi,* the spirochaete cells and complement were incubated with sera from patients with symptoms of the disease and indirect immunofluorescence was performed (Callister et al., 1994; Creson et al., 1996). Lim et al. (1994) modified this procedure by using acridine orange (an indicator of viability) to detect the presence of anti-borrelial antibodies by measuring the loss of viability of the bacterial cells, as indicated by a reduction in intracellular fluorescence.

Passive immunisation with antisera to *Streptococcus pneumoniae* facilitates phagocytosis of these invading organisms. Human prevaccination sera already contain high levels of C polysaccharide antibodies, which are not protective in humans but which may produce false-positive results in a flow cytometric assay to evaluate antibody-induced phagocytosis. This problem was overcome by the development of a highly encapsulated strain for serotypes 6A, 6B, 14, 19F and 23S (Jansen et al., 1998). Only antibodies specific to these antigens initiated phagocytosis. This technique provided similar results to the ELISA usually employed for these studies.

16.6.3 Protozoa

Antibodies to the protozoan *Toxoplasma gondii* were detected and quantified by incubating fixed tachyzoites with serum samples from the patient and following this with indirect immunofluorescence (Cozon et al. 1993). Detection of these antibodies has traditionally been achieved by indirect immunofluorescence microscopy but flow cytometry is quicker and allows for quantitative measurements.

Sera from patients with Chagas' disease, caused by *Trypanosoma cruzi*, contain membrane-bound lytic antibodies that bind to the protozoal cells. Using an indirect immunofluorescence procedure followed by flow cytometry, Martins et al. (1995) could distinguish between sera from chronically untreated, treated but not cured, and cured patients based on the presence of anti-trypomastigote antibodies.

16.7 Conclusions

Flow cytometry shows great potential for the study of microbes and various aspects of microbial infections. It is somewhat disappointing that, despite its greater sensitivity and speed when compared with the tests currently used, this technique, as yet, has not made great inroads into diagnostic microbiology.

Acknowledgements

The authors wish to thank Dr Kovit Pattanapanyasat for expert help with the protocol for *Plasmodium* quantification.

16.8 INTERNET SITES

http://www.cyto.purdue.edu/flowcyt/research/microflow/
Purdue University flow cytometry and microbiology site contains several interesting articles and useful protocols of particular relevance to bacteriology.

16.9 REFERENCES

Akerlund, T., Nordstrom, K., Bernander, R. (1995) Analysis of cell size and DNA content in exponentially growing and stationary phase batch cultures of *Escherichia coli*. *Journal of Bacteriology* **177**, 6791–7.

Allman, R., Hann, A.C., Phillips, A.P., Martin, K.L., Lloyd, D. (1990) Growth of *Azotobacter vinelandii*: correlation of Coulter cell size, flow cytometric parameters and ultrastructure. *Cytometry* **11**, 822–31.

Allman, R., Schjerven, T., Boye, E. (1991) Cell cycle parameters of *Escherichia coli* K-12. *Journal of Bacteriology* **173**, 7970–4.

Azas, N., Di Giorgio, C., Delmas, F., Timon-David, P. (1997) Assessment of amphotericin B susceptibility in *Leishmania infantum* promastigotes by flow cytometric membrane potential assay. *Cytometry* **28**, 165–9.

Barratt Boyes, S.M., Rossitto, P.V., Stott, J.L., Maclachlan, N.J. (1992) Flow cytometric analysis of *in vitro* blue tongue virus infection of bovine blood mononuclear cells. *Journal of General Virology* **73**, 1953–60.

Bertho, A.L., Cysne, L., Coutinho, S.G. (1992) Flow cytometry in the study of the interaction between murine macrophages and the protozoan parasite *Leishmania amazonensis*. *Journal of Parasitology* **78**, 666–71.

Best, L.M., Haldane, D.J., Bezanson, G.S., van Zanten, S.J. (1997) *Helicobacter pylori*: primary susceptibility to clarithromycin *in vitro* in Nova Scotia. *Canadian Journal of Gastroenterology* **11**, 298–300.

Bohm, D., Nick, S., Voss, G., Hunsmann, G. (1992) Detection of viral surface antigens on HIV-2_{ben} infected human tumor cell lines by flow cytometry. *Cytometry* **13**, 259–66.

Bouffard, P., Hayashi, P.H., Acevedo, N., Levy, N., Zeldis, J.B. (1992) Hepatitis C virus is detected in a monocyte/macrophage subpopulation of peripheral blood mononuclear cells of infected patients. *Journal of Infectious Diseases* **166**, 1276–80.

Bownds, S., Kurzynski, T.A., Norden, M.A., Dufek, J.L., Schell, R.F. (1996) Rapid susceptibility testing for nontuberculosis mycobacteria using flow cytometry. *Journal of Clinical Microbiology* **34**, 1386–90.

Boye, E., Lobner-Olesen, A. (1991) Bacterial growth control studied by flow cytometry. *Research Microbiology* **142**, 131–5.

Bredius, R.G., de Vries, C.E., Troelstra, A., van Alphen, L., Weening, R.S., van de Winkel, J.G., Out, T.A. (1993) Phagocytosis of *Staphylococcus aureus* and *Haemophilus influenzae* type B opsonised with polyclonal human IgG1 and IgG2 antibodies. Functional hFc gamma RIIa polymorphism to IgG_2. *Journal of Immunology* **151**, 1463–72.

Bunyaratvej, A., Butthep, P., Bunyaratvej, P. (1993) Cytometric analysis of blood cells from malaria-infected patients and *in vitro* infected blood. *Cytometry* **14**, 81–5.

Butcher, B., Sklar, L.A., Seamer, L.C., Glew, R.H. (1992) Heparin enhances the interaction of infective *Leishmania donovani* promastigotes with mouse peritoneal macrophages. A fluorescence flow cytometric analysis. *Journal of Immunology* **148**, 2879–86.

Callister, S.M., Schell, R.F., Lim, L.C.L., Jobe, D.A., Case, K.L., Bryant, G.L., Molling, P.E. (1994) Detection of borreliacidal antibodies by flow cytometry – an accurate, highly specific serodiagnostic test for lyme disease. *Archives of Internal Medicine* **154**, 1625–32.

Carter, E.A., Paul, F., Hunter, P.A. (1993) Cytometric evaluation of antifungal agents. In: Lloyd, D. (ed.), *Flow Cytometry in Microbiology*, pp. 111–120. Springer-Verlag, London.

Clarke, R.G., Pinder, A.C. (1998) Improved detection of bacteria by flow cytometry using a combination of antibody and viability markers. *Journal of Applied Microbiology* **84**, 577–84.

Comas, J., Vives-Rego, J. (1998) Enumeration, viability and heterogeneity in *Staphylococcus aureus* cultures by flow cytometry. *Journal of Microbiological Methods* **32**, 45–53.

Constantino, P.J., Budd, D.E., Gare, N.F. (1995) Enumeration of viable *Candida albicans* blastospores using tetrabromofluorescein (Eosin Y) and flow cytometry. *Cytometry* **19**, 370–5.

Cory, J.M., Ohlsson-Wilhelm, B.M., Brock, E.J., Shaeffer, N.A., Steck, M.E., Eyster, M.E., Rapp, F. (1987) Detection of human immunodeficiency virus-infected lymphoid cells at low frequency by flow cytometry. *Journal of Immunological Methods* **105**, 71–8.

Cozon, G., Roure, C., Lizard, G., Greenland, T., Larget-Piet, D., Gandilhon, F., Peyron, F. (1993) An improved assay for the detection of *Toxoplasma gondii* antibodies in human serum by flow cytometry. *Cytometry* **14**, 569–75.

Creson, J.R., Lim, L.C.L., Glowacki, N.J., Callister, S.M., Schell, R.F. (1996) Detection of anti-*Borrelia burgdorferi* antibody responses with the borreliacidal antibody test, indirect fluorescent antibody assay performed by flow cytometry, and Western immunoblotting. *Clinical and Diagnostic Laboratory Immunology* **3**, 184–90.

Cruz, A., Titus, R., Beverly, S.M. (1993) Plasticity in chromosome number and testing of essential genes in *Leishmanii* by targeting. *Proceedings of the National Academy of Sciences of the USA* **90**, 1599–1603.

Darcy, F., Torpier, G., Kausnierz, J P., Rizvi, F.S., Santoro, F. (1987) In vitro differentiation of promastigotes monitored by flow cytometry. *Experimental Parasitology* **64**, 376–84.

de Boer, E.C., Bevers, R.F.M., Kurth, K.H., Schamhart, D.H.J. (1996) Double fluorescent flow cytometric assessment of bacterial internalization and binding by epithelial cells. *Cytometry* **4**, 381–7.

de Stefano, J.A., Sleight, R., Babcock, C.F., Stamkoski, R.M., Walzer, P.D. (1992) Isolation of *Pneumocystis carinii* cysts by flow cytometry. *Parasitology Research* **78**, 179–82.

Dhandayuthapani, S., Via, L.E., Thomas, C., Horowitz, P.M., Deretic, D., Deretic, V. (1995) Green fluorescent protein as a marker for gene-expression and cell biology of mycobacterial interactions with macrophages. *Molecular Microbiology* **5**, 901–12.

Diaper, J.P., Edwards, C. (1994) Survival of *Staphylococcus aureus* in lakewater monitored by flow cytometry. *Microbiology* **140**, 35–42.

Doyle, P.S., Engel, J.C., Pimenta, P.F., da Silva, P.P., Dwyer, D.M. (1991) *Leishmania donovani* long-term axenic culture of amastigotes at 37°C. *Experimental Parasitology* **73**, 326–34.

Dunn, B.E., Altmann, M., Cambell, G.P. (1991) Adherence of *Helicobacter pylori* to gastric carcinoma cells: analysis by flow cytometry. *Reviews of Infectious Diseases* **13**, S657–64.

Durodie, J., Coleman, K., Simpson, I.N., Loughborough, S.H., Winstanley, D.W. (1995) Rapid detection of antimicrobial activity using flow cytometry. *Cytometry* **21**, 374–7.

Elmendorf, S., McSharry, J.J., Laffin, J.A., Fogleman, D., Lehman, J.M. (1988) Detection of early cytomegalovirus with 2-color quantitative flow cytometry. *Cytometry* **9**, 254–60.

Etingin, O.R., Silverstein, R.L., Hajjar, D. (1991) Identification of a monocyte receptor on herpes virus-infected endothelial cells. *Proceedings of the National Academy of Science of the USA* **88**, 7200–3.

Gant, V.A., Warnes, G., Phillips, I., Savidge, G.F. (1993) The application of flow cytometry to the study of bacterial responses to antibiotics. *Journal of Medical Microbiology* **39**, 147–54.

Gorse, G.J., Frey, S.E., Newman, F.K., Belshe, R.B. (1992) Detection of binding antibodies to native and recombinant human immunodeficiency virus type 1 envelope glycoproteins following recombinant gp160 immunization measured by flow cytometry and enzyme immunoassays. *Journal of Clinical Microbiology* **30**, 2606–12.

Gottfredsson, M., Erlendsdottir, H., Sigfusson, A., Gudmundsson, S. (1998) Characteristics and dynamics of bacterial populations during postantibiotic effect determined by flow cytometry. *Antimicrobial Agents and Chemotherapy* **42**, 1005–11.

Harabuchi, Y., Koizumi, S., Osato, T., Yamanaka, N., Kataura, A. (1988) Flow cytometric analysis of Epstein Barr virus receptor among the different B cell subpopulations using simultaneous two-color immunofluorescence. *Virology* **165**, 278–81.

Hewish, M.J., Meikle, A.M., Hunter, S.D., Crowe, S.M. (1996) Quantifying phagocytosis of *Mycobacterium avium* complex by human monocytes in whole blood. *Immunology and Cell Biology* **74**, 306–12.

Hu, Y.W., Birch, P., Balaskas, E., Zeibdawi, A., Scalia, V., Theriault-Valin, S.A., Gill, P., Aye, M.T. (1996) Flow cytometric immunofluorescence assay for detection of antibodies to human immunodeficiency virus type 1 using insoluble precursor forms of recombinant polyproteins as carriers and antigens. *Journal of Clinical Microbiology* **34**, 1412–19.

Humphreys, M., Allman, R., Lloyd, D. (1994) Determination of the viability of *Trichomonas vaginalis* using flow cytometry. *Cytometry* **15**, 343–8.

Iannelli, D., Dapice, L., Fenizia, D., Serpe, L., Cottone, C., Viscardi, M., Capparelli, R. (1998) Simultaneous identification of antibodies to *Brucella abortus* and *Staphylococcus aureus* in milk samples by flow cytometry. *Journal of Clinical Microbiology* **36**, 802–6.

Ibrahim, P., Whiteley, A.S., Barer, M.R. (1997) SYTO16 labelling and flow cytometry of *Mycobacterium avium*. *Letters in Applied Microbiology* **25**, 437–41.

Jacobberger, J.W., Fogleman, D. and Lehman, J.M. (1986) Analysis of intracellular antigens by flow cytometry. *Cytometry* **7**, 356–64.

Jacobsen, C. Fremming, C., Jakobsen, M. (1997a) Immunomagnetic separation of *Listeria monocytogenes* for cytometric determination of viable cells in liquid. *Journal of Microbiological Methods* **31**, 35–43.

Jacobsen, C. N., Rasmussen, J., Jakobsen, M. (1997b) Viability staining and flow cytometric detection of *Listeria monocytogenes*. *Journal of Microbiological Methods* **28**, 35–43.

Jaffe, C.L., Perez, M.L., Sarfstein, R. (1990) *Leishmania tropica*: characterisation of a lipophosphoglycan-like antigen recognised by species-specific monoclonal antibodies. *Experimental Parasitology* **70**, 12–24.

Janse, C.J., van Vianen, P.H. (1994) Flow cytometry in malaria detection. In: Darzynkiewicz, Z., Robinson, J.P., Crissman, H.A. (eds.), *Methods in Cell Biology,* Vol. 42, Part B: pp. 295–318. Academic Press, San Diego, CA.

Janse, C.J., van Vianen, P.H., Tanke, H.J., Mons, B., Ponnudurai,

T., Overdulve, J.P. (1987) *Plasmodium* species: flow cytometry and microfluorimetry assessments of DNA content and synthesis. *Experimental Parasitology* **64**, 88–94.

Janse, C.J., Boorsma, E.G., Ramesar, J., van Vianen, P., van der Meer, R., Zenobi, P., Casaglia, O., Mons, B., van der Berg, F.M. (1989) *Plasmodium berghei*: gametocyte production, DNA content, and chromosome-size polymorphisms during asexual multiplication *in vivo*. *Experimental Parasitology* **68**, 274–82.

Jansen, W.T.M., Gootjes, J., Zelle, M., Madone, D.V., Verhoef, J., Snipe, H., Verhaul, A.F.M. (1998) Use of highly encapsulated *Streptococcus pneumoniae* strains in a flow cytometric assay for assessment of the phagocytic capacity of serotype-specific antibodies. *Clinical and Diagnostic Laboratory Immunology* **5**, 703–10.

Jennings, S.R., Rice, P.L., Kloszewski, E.D., Anderson, R.W., Thompson, D.L., Tevethia, S.S. (1985) Effect of herpes simplex virus types 1 and 2 on surface expression of class 1 major histocompatibility complex antigens on infected cells. *Journal of Virology* **56**, 757–66.

Jennings, S.R., Lippe, P.A., Pauza, K.J., Spear, P.J., Pereira, L., Trevethia, S.S. (1987) Kinetics of expression of herpes simplex virus type 1-specific glycoprotein species on the surfaces of infected murine, simian, and human cells: flow cytometric analysis. *Journal of Virology* **61**, 104–12.

Jepras, R.I., Carter, J., Pearson, S.C., Paul, F.E., Wilkinson, M. J. (1995) Development of a robust flow cytometric assay for estimating numbers of viable bacteria. *Applied and Environmental Microbiology* **61**, 2696–701.

Jepras, R.I., Paul, F.E., Pearson, S.C., Wilkinson, M.J. (1997) Rapid assessment of antibiotic effects on *Escherichia coli* by bis-(1,3-dibutylbarbituric acid) trimethine oxonol and flow cytometry. *Antimicrobial Agents Chemotherapy* **41**, 2001–5.

Jernaes, M.W., Steen, H. B. (1994) Staining of *Escherichia coli* – influx and efflux of ethidium bromide. *Cytometry* **17**, 302–9.

Jones, K.H., Senft, J.A. (1985) An improved method to determine cell viability by simultaneously staining with fluorescein diacetate and propidium iodide. *Journal of Histochemistry and Cytochemistry* **33**, 77–9.

Joux, F., Lebaron, P., Troussellier, M. (1997) Succession of cellular states in a *Salmonella typhimurium* population during starvation in artificial seawater microcosms. *FEMS Microbiology Ecology* **22**, 65–76.

Kadjoian, V., Gasquet, M., Delmas, F., Guiraud, H., DeMeo, M., Langet, M., Timon-David, P. (1992) Flow cytometry to evaluate the parasitemia of *Plasmodium falciparum*. *Journal de Pharmacie Belgique* **47**, 499–543.

Kanishiro, E.S., Wyder, M.A., Wu, Y-P., Cushion, M.T. (1993) Reliability of calcein acetoxy methyl ester and ethidium homodimer or propidium iodide for viability assessment of microbes. *Journal of Microbiological Methods* **17**, 1–16.

Kasprzak, W., Majewka, A.C. (1983) Infectivity of *Giardia* sp. cysts in relation to eosin exclusion and excystation *in vitro*. *Tropenmedizine und Parasitologie* **3**, 70–2.

Khunkitti, W., Lloyd, D., Furr, J.R., Russell, A.D. (1996) The lethal effects of biguanides on cysts and trophozoites of *Acanthamoeba castellanii*. *Journal of Applied Bacteriology* **81**, 73–7.

Khunkitti, W., Lloyd, D., Furr, J.R., Russell, A.D. (1997a) Aspects of the mechanisms of action of biguanides on trophozoites and cysts of *Acanthamoeba castellanii*. *Journal of Applied Bacteriology* **82**, 107–14.

Khunkitti, W., Avery, S.V., Lloyd, D., Furr, J.R., Russell, A.D. (1997b) Effects of biocides on *Acanthamoeba castellanii* as measured by flow cytometry and plaque assay. *Journal of Antimicrobial Chemotherapy* **40**, 227–33.

Khunkitti, W., Hann, A.C., Lloyd, D., Furr, J.R., Russell, A.D. (1998a) Biguanide-induced changes in *Acanthamoeba castellanii*: an electron microscopy study. *Journal of Applied Microbiology* **84**, 53–62.

Khunkitti, W., Lloyd, W., Furr, D.J.F., Russell, A.D. (1998b) *Acanthamoeba castellanii*: growth encystment, excystment and biocide suseptibility. *Journal of Infection* **36**, 43–68.

Kirk, S.M., Schell, R.F., Moore, A.V., Callister, S.M., Mazurek, G.H. (1998) Flow cytometric testing of susceptibilities of *Mycobacterium tuberculosis* isolates to ethambutol, isoniazid, and rifampin in 24 hours. *Journal of Clinical Microbiology* **36**, 1568–73.

Kremer, I., Baulard, A., Estaquier, J., Poulaingodefroy, O., Locht, A. (1995) Green fluorescent protein as a new expression marker in mycobacteria. *Molecular Microbiology* **17**, 913–22.

Lange, J.L., Thorne, P.S., Lynch, N. (1997) Application of flow cytometry and fluorescent in-situ hybridisation for assessment of exposures to airborne bacteria. *Applied and Environmental Microbiology* **63**, 1557–63.

Langsrud, S., Sundheim, G. (1996) Flow cytometry for rapid assessment of viability after exposure to a quaternary ammonium compound. *Journal of Applied Bacteriology* **81**, 411–18.

Lapinsky, S.E., Glencross, D., Car, N.G., Kallenbach, J.M., Zwi, S. (1991) Quantification and assessment of viability of *Pneumocystis carinii* organisms by flow cytometry. *Journal of Clinical Microbiology* **29**, 911–15.

Lebaron, P., Joux F. (1994) Flow cytometric analysis of the cellular DNA content of *Salmonella typhimurium* and *Alteromonas haloplanktis* during starvation and recovery in seawater. *Applied and Environmental Microbiology* **60**, 4345–50.

Libertin, C.R., Woloschak, G.E., Wilson, W.R., Smith, T.F. (1984)

Analysis of *Pneumocystis carinii* cysts with a fluorescence-activated cell sorter. *Journal of Clinical Microbiology* **20**, 877–80.

Lim, L.C.L., Liu, Y.F., Schell, K., Lovrich, S.D., Callister, S.M., Schell, R.F. (1994) Detection of borreliacidal antibody by using acridine orange and flow cytometry. *Clinical and Diagnostic Laboratory Immunology* **1**, 44–50.

Logan, R.P.H., Robins, A., Turner, G.A., Cockayne, A., Borriello, S.P., Hawkey, C.J. (1998) A novel flow cytometric assay for quantitating adherence of *Helicobacter pylori* to gastric epithelial cells. *Journal of Immunological Methods* **213**, 19–30.

Lopéz-Amorós, R., Comas, J., Carulla, C., Vives-Rego, J. (1994) Variations in flow cytometric forward scatter signals and cell-size in batch cultures of *Escherichia coli*. *FEMS Microbiology Letters* **117**, 225–30.

Lopéz-Amorós, R., Comas, J., Vives-Rego, J. (1995) Flow cytometric assessment of *Escherichia coli* and *Salmonella typhimurium* starvation survival in seawater using rhodamine 123, propidium iodide and oxonol. *Applied and Environmental Microbiology* **61**, 2521–6.

Lopéz-Amorós, R., Castel, S., Comas-Riu, J., Vives-Rego, J. (1997) Assessment of *E. coli* and *Salmonella* viability and starvation by confocal laser microscopy and flow cytometry using rhodamine 123, $DiBAC_4(3)$, propidium iodide, and CTC. *Cytometry* **29**, 298–305.

Lydy, S.L., Compans, R.W. (1993) Role of the cytoplasmic domains of viral glycoproteins in antibody-induced cell surface mobility. *Journal of Virology* **67**, 6289–94.

Martins, O.A., Pereira, M.E.S., Carvalho, J.F., Cancado, J.R., Brener, Z. (1995) Flow cytometry, a new approach to detect anti-live trypomastigote antibodies and monitor the efficacy of specific treatment in human Chagas disease. *Clinical and Diagnostic Laboratory Immunology* **2**, 569–73.

Mason, D.J., Allman, R., Stark, J.M., Lloyd, D. (1994) Rapid estimation of bacterial antibiotic susceptibility with flow cytometry. *Journal of Microscopy* **176**, 8–16.

Mason, D.J., Lopéz-Amorós, R., Allman, R., Stark, J.M., Lloyd, D. (1995a) The ability of membrane potential dyes and calcafluor white to distinguish between viable and non viable bacteria. *Journal of Applied Bacteriology* **78**, 309–15.

Mason, D.J., Power, E.G.M., Talsania, H., Phillips, I., Gant, V.A. (1995b) Antibacterial action of ciprofloxacin. *Antimicrobial Agents and Chemotherapy* **39**, 2752–8.

Mason, D.J., Dybowski, R., Larrick J.W., Gant, V.A. (1997) Antimicrobial action of rabbit leukocyte $CAP18_{(106–137)}$. *Antimicrobial Agents and Chemotherapy* **41**, 624–9.

Mason, D.J., Mortimer, F.C., Gant, V.A. (1999) Flow cytometric antibiotic susceptibility testing. In: Robinson, J. P. (ed.), *Current Protocols in Flow Cytometry*. John Wiley, New York.

McClelland, R.G., Pinder, A.C. (1994a) Detection of low-levels of specific *Salmonella* species by fluorescent antibodies and flow cytometry. *Journal of Applied Bacteriology* **77**, 440–7.

McClelland, R.G., Pinder, A.C. (1994b) Detection of *Salmonella typhimurium* in dairy products with flow cytometry and monoclonal antibodies. *Applied and Environmental Microbiology* **60**, 4255–62.

McClelland, R.G., Pinder, A.C. (1994c) Rapid assay for pathogenic *Salmonella* organisms by immunofluorescence flow cytometry. *Journal of Microscopy* **176**, 17–22.

McHugh, T.M., Miner, R.C., Logan, L.H., Stites, D.P. (1988) Simultaneous detection of antibodies to cytomegalovirus and herpes simplex virus by using flow cytometry and a microsphere-based fluorescence immunoassay. *Journal of Clinical Microbiology* **26**, 1957–61.

McSharry, J.J. (1994) Uses of flow cytometry in virology. *Clinical Microbiology Reviews* **7**, 576–604.

McSharry, J.J., Costantino, R., Robbiano, E., Echols, R., Stevens, R., Lehman, J.M. (1990) Detection and quantification of human immunodeficiency virus-infected peripheral blood mononuclear cells by flow cytometry. *Journal of Clinical Microbiology* **28**, 724–33.

Monfort, P., Baleux, B. (1994) Effects of environmental factors present in the St. Lawrence Estuary (Québec, Canada) on experimental survival of *Salmonella salamae* as determined by flow cytometry. *Canadian Journal of Microbiology* **40**, 712–19.

Nebe-von Caron, G., Stephens, P., Badley, R.A. (1998) Assessment of bacterial viability status by flow cytometry and single cell sorting. *Journal of Applied Microbiology* **84**, 988–98.

Norden, M.A., Kurzynski, T.A., Bownds, S.E., Callister, S.M., Schell, R.F. (1995) Rapid susceptibility testing of *Mycobacterium tuberculosis* (H37RA) by flow cytometry. *Journal of Clinical Microbiology* **33**, 1231–7.

O'Goreman, M.R.G., Hopfer, R.L. (1991) Amphotericin B susceptibility testing of *Candida* species. *Cytometry* **12**, 734–47.

Ohlsson-Wilhelm, B.M., Cory, J.M., Kessler, H.A., Eyster, M.E., Rapp, F., Landay, A. (1990) Circulating human immunodeficiency virus (HIV) p24 antigen-positive lymphocytes: a flow cytometric measure of HIV infection. *Journal of Infectious Diseases* **162**, 1018–24.

Ordóñez, J.V., Wehman, N.M. (1993) Rapid flow cytometric antibiotic susceptibility assay for *Staphylococcus aureus*. *Cytometry* **14**, 811–18.

Ordóñez, J. V., Wehman, N.M. (1995) Amphotericin B susceptibility of *Candida* species assessed by rapid flow cytometric membrane potential assay. *Cytometry* **22**, 154–7.

Pattanapanyasat, K., Udomsangpetch, R., Webster, H.K. (1993)

Two colour flow cytometric analysis of intraerythrocytic malaria parasite DNA and surface membrane-associated antigen in erythrocytes infected with *Plasmodium falciparum*. *Cytometry* **14**, 449–54.

Pattanapanyasat, K., Yongvanitchit, D., Heppner, D.G., Tongtawe, P., Kyle, D.E., Webster, H.K. (1996) Culture of malaria parasites in two different red blood cell populations using biotin and flow cytometry. *Cytometry* **25**, 287–94.

Pavic, I., Hartmann, A., Zimmermann, A., Michel, D., Hampl, W., Schleyer, I., Mertens, T. (1997) Flow cytometric analysis of herpes simplex virus type 1 susceptibility to acyclovir, ganciclovir and foscarnet. *Antimicrobial Agents and Chemotherapy* **41**, 2686–92.

Perschel, W.T., Langefeld, T., Yildiz, M. (1994) How to quantify phagocytosis of *Staphylococcus aureus* K807 by PMN in a flow cytometer. *Medizinische Welt* **45**, 100–5.

Ponzi, M., Janse, C.J., Dore, E., Scotti, R., Pace, T., Reterink, T.J., van der Berg, F.M., Mons, B. (1990) Generation of chromosome size polymorphisms during *in vivo* mitotic multiplication of *Plasmodium berghei* involves both loss and addition of subtelomeric repeat sequences. *Molecular and Biochemical Parasitology* **41**, 73–82.

Porter, J., Edwards, C., Morgan, J.A.W., Pickup, R.W. (1993) Rapid, automated separation of specific bacteria from lake water and sewage by flow cytometry and cell sorting. *Applied and Environmental Microbiology* **59**, 3327–33.

Porter, J., Pickup, R., Edwards, C. (1995a) Membrane hyperpolarization by valinomycin and its limitations for bacterial viability assessment using rhodamine 123 and flow-cytometry. *FEMS Microbiology Letters* **132**, 259–62.

Porter, J., Pickup, R., Edwards, C. (1995b) Flow cytometric detection of specific genes in genetically-modified bacteria using in-situ polymerase chain-reaction. *FEMS Microbiology Letters* **134**, 51–6.

Quessy, S., Busque, P., Higgins, R., Jacques, M., Dubreuil, J.D. (1997) Description of an albumin binding activity for *Streptococcus suis* serotype 2. *FEMS Microbiology Letters* **147**, 245–50.

Ratinaud, M.H., Revidon, S. (1996) Flow cytometric method to assess functional state of the *Listeria* membrane. *Journal of Microbiological Methods* **25**, 71–7.

Raza, M.W., Ogilvie, M.M., Blackwell, C.C., Stewart, J., Elton, R.A., Weir, D.M. (1993) Effect of respiratory syncytial virus-infection on binding of *Neisseria meningitidis* and *Haemophilus influenzae* type-B to a human epithelial cell line (Hep-2) *Epidemiology and Infection* **110**, 339–47.

Re, M.C., Furlini, G., Gibellini, D., Vignoli, M., Ramazzoti, E., Lolli, S., Raniera, S., LaPlaca, M. (1994) Quantification of human immunodeficiency virus type 1-infected mononuclear cells in peripheral blood of seropositive subjects by newly developed flow cytometry analysis of the product of an *in situ* PCR assay. *Journal of Clinical Microbiology* **32**, 2152–7.

Rosa, D., Campagnoli, S., Moretto, C., Guenzi, E., Cousens, L., Chin, M., Dong, C., Weiner, A.J., Lau, J.Y.N., Choo, Q.L., Chien, D., Pileri, P., Houghton, M., Abrignani, S. (1996) A quantitative test to estimate neutralizing antibodies to the hepatitis C virus: cytofluorimetric assessment of envelope glycoprotein 2 binding to target cells. *Proceedings of the National Academy of Science of the USA* **91**, 1759–63.

Roth, B.L., Poot, M., Yue, S.T., Millard, P.J. (1997). Bacterial viability and antibiotic susceptibility testing with SYTOX green nucleic acid stain. *Applied and Environmental Microbiology* **63**, 2421–31.

Ryan, C., Nguyen, B.T., Sullivan, S.J. (1995) Rapid assay for mycobacterial growth and antibiotic susceptibility using gel microdrop encapsulation. *Journal of Clinical Microbiology* **33**, 1720–6.

Schnorr, J.J., Schneider-Schaulies, S., Simon-Jodicke, A., Pablovic, J., Horisberger, M.A., Ter Meulen, V. (1993) MxA-dependent inhibition of measles virus glycoprotein synthesis in a stably transfected human monocytic cell line. *Journal of Virology* **67**, 4760–8.

Schols, D., Pauwels, R., Vanlangendonck, F., Balzarini, J., de Clercq, E. (1988) A highly reliable, sensitive flow cytometric/fluorimetric assay for the evaluation of the anti-HIV activity of antiviral compounds in MT-4 cells. *Journal of Immunological Methods* **114**, 27–32.

Schupp, D.G., Erlandsen, S.L. (1987) A new method to determine *Giardia* cyst viability: correlation of fluorescein diacetate and propidium iodide staining with animal infectivity. *Applied and Environmental Microbiology* **53**, 704–7.

Sgorbati, S., Barbesti, S., Citterio, S., Bestetti, G., DeVecchi, R. (1996) Characterization of number, DNA content, viability and cell size of bacteria from natural environments using DAPI/PI dual staining and flow cytometry. *Minerva Biotechnologica* **8**, 9–15.

Sheppard, F.C., Mason, D.J., Bloomfield, S.F., Gant, V.A. (1997) Flow cytometric analysis of chlorhexidine action. *FEMS Microbiology Letters* **154**, 283–8.

Sligh, J.M., Roodman, S.T., Tsai, C.C. (1989) Flow cytometric indirect immunofluorescence assay with high sensitivity and specificity for detection of antibodies to human immunodeficiency virus (HIV). *American Journal of Clinical Pathology* **91**, 210–14.

Srikumar, R., Chin, A.C., Vachon, V., Richardson, C.D., Ratcliffe, M.J.H., Saarinen, L., Kayhty, H., Makela, P.H., Coulton, J.W. (1992) Monoclonal antibodies specific to porin of *Haemophilus influenzae* type-B – localization of their cognate epi-

topes and tests of their biological-activities. *Molecular Microbiology* **6**, 665–76.

Steen, H.B., Boye, E. (1980) *Escherichia coli* growth studied by dual-parameter flow cytophotometry. *Journal of Bacteriology* **145**, 1091–4.

Sullam, P.M., Costerton, J.W., Yamasaki, R., Dazin, P.F., Mills, J. (1993) Inhibition of platelet binding and aggregation by streptococcal exopolysaccharide. *Journal of Infectious Diseases* **167**, 1123–30.

Suller, M.T.E., Stark, J.M., Lloyd, D. (1997) A flow cytometric study of antibiotic-induced damage and evaluation as a rapid antibiotic susceptibility test for methicillin-resistant *Staphylococcus aureus*. *Journal of Antimicrobial Chemotherapy* **40**, 77–83.

Suller, M.T.E., Lloyd, D. (1998) Flow cytometric assessment of the postantibiotic effect of methicillin on *Staphylococcus aureus*. *Antimicrobial Agents and Chemotherapy* **42**, 1195–9.

Swarts, A.J., Hastings, J.W., Roberts, R.F., von Holy, A. (1998) Flow cytometry demonstrates bacteriocin-induced injury to *Listeria moncytogenes*. *Current Microbiology* **36**, 266–70.

Thiriat, L., Sidaner, F., Schwartzbrod, J. (1998) Determination of *Giardia* cyst viability in environmental and faecal samples by immunofluorescence, fluorogenic dye staining, and differential interference contrast microscopy. *Letters in Applied Microbiology* **26**, 237–42.

Tombolini, R., Unge, A., Davey, M.E., deBruijn, F.J., Jansson, J.K. (1997) Flow cytometric and microscopic analysis of GFP-tagged *Pseudomonas fluorescens* bacteria. *FEMS Microbiology Ecology* **22**, 17–28.

Trager, W., Jensen, J.B. (1976) Human malaria parasites in continuous culture. *Science* **193**, 673–5.

Turner, N.A., Russell, A.D., Furr, J.R., Lloyd, D. (1999) Control, prevention and treatment of *Acanthamoeba keratitis*. *Science Progress* **82**, 1–8.

Valdivia, R.H., Hromockyj, A.E., Monack, D., Ramakrishnan, L., Falkow, S. (1996) Applications for green fluorescent protein (GFP) in the study of host–pathogen interactions. *Gene* **173**, 47–52.

van Vianen, P.H., van Engen, A., Thaithong, S., van der Keur, M., Tanke, H.J., van der Kuy, H.J., Mons, B., Janse, C. J. (1993) Flow cytometric screening of blood samples for malaria parasites. *Cytometry* **14**, 276–80.

Vesey, G., Narai, J., Ashbolt, N., Williams, K., Veal, D. (1994) Detection of specific microorganisms in environmental samples using flow cytometry. *Methods in Cell Biology* **42**, 489–522.

Vesey, G., Slade, J.S., Bryne, M., Shepherd, K., Dennis, P.J., Fricker, C.R. (1993) A new method for the concentration of *Cryptosporidium* oocysts from water. *Journal of Applied Bacteriology* **75**, 82–6.

Vives-Rego, J., Lopéz-Amorós, R., Comas, J. (1994) Flow cytometric narrow-angle light scatter and cell size during starvation of *Escherichia coli* in artificial sea water. *Letters in Applied Microbiology* **19**, 374–6.

Vogel, L., van Alphen, L., Geluk, F., Troelstra, A., Martin, E., Bredius, R., Eijk, P., Jansen, H., Dankert, J. (1994) Quantitative flow cytometric analysis of opsonophagocytosis and killing of nonencapsulated *Haemophilus influenzae* by human polymorphonuclear leukocytes. *Clinical and Diagnostic Laboratory Immunology* **1**, 394–400.

Walberg, M., Gaustad, P., Steen, H.B. (1997) Rapid assessment of ceftazidime, ciporofloxacin, and gentamicin susceptibility in exponentially-growing *E. coli* cells by means of flow cytometry. *Cytometry* **27**, 169–78.

Wallner, G., Amann, R., Beisker, W. (1993) Optimizing fluorescent in situ hybridization with ribosomal-RNA-targeted oligonucleotide probes for flow cytometric identification of microorganisms. *Cytometry* **14**, 136–43.

Wernli, M., Tichelli, A., von Planta, M., Gratwohl, A., Speck, B. (1991) Flow cytometric monitoring of parasitaemia during the treatment of severe malaria by exchange transfusion. *European Journal of Haematology* **46**, 121–7.

Wold, S., Skarstad, K., Steen, H.B., Stokke, T., Boye, E. (1994) The initiation mass for DNA replication in *Escherichia coli* K-12 is dependent on growth rate. *EMBO Journal* **13**, 2097–102.

Yamaguchi, H., Osaki, T., Taguchi, H., Hanawa, T., Yamamoto, T., Kamiya, S. (1996) Flow cytometric analysis of the heat shock protein 60 expressed on the cell surface of *Helicobacter pylori*. *Journal of Medical Microbiology* **45**, 270–7.

17

Leukocyte cell surface antigens

Marion G. Macey

St Bartholomew's and Royal London School of Medicine and Dentistry,
Queen Mary and Westfield College, London

17.1 Introduction

Cells of the immune system have a large number of different glycoprotein receptors on their surfaces, with a wide range of biological functions. Most membrane glycoproteins are, however, constructed from a limited set of protein structural units, which are recognisable at the amino acid sequence level. The three-dimensional structure of many of these domains or modules is now known. For leukocytes a systematic approach to naming the surface molecules has been adopted and numbers have been assigned to surface proteins based upon the binding of groups of antibodies. These groups of antibodies have been used to define antigens associated with cell differentiation and have been termed clusters of differentiation or CDs. So far 247 CDs have been defined and a further 40 cell-surface proteins have been described in detail (Barclay et al., 1993, 1997; Campbell, 1998). A CD guide may be found on the worldwide web at http://www.ncbi.nlm.nih.gov/prow.

17.2 Modules and domains

The idea that most cell surface molecules are constructed from a limited repertoire of building blocks is now well established. For example, a domain is a spatially distinct structural unit that folds independently; the sequence need not be contiguous. Modules are a subset of domains that are contiguous in sequence and that are repeatedly used in functionally diverse proteins. They have identifiable amino acid patterns that can be described by a 'consensus' sequence. In the case of extracellular modules, compatible phases at the exon/intron boundaries are often observed. A repeat is a module unit that does not occur as a single copy and several repeats are needed to form a superstructure. An example is the leucine-rich repeat that occurs in CD42.

The various modules come in a range of sizes and they can appear in a variety of settings with different frequencies. They can be recognised at the amino acid sequence level in database searches using a consensus sequence. Table 17.1 lists common domains and modules and gives a brief summary of some of their properties; it does not necessarily include all the modules as new ones are still being found. Also, rare examples (e.g. the somatomedin B module found in a cell-surface phosphodiesterase PCI, galactin modules, the LY module found in the low-density lipoprotein (LDL) receptor, and the leucine-rich repeat), have been omitted. However, clearly, a great deal is now known about some structural features of most cell-surface receptors. Some idea of the overall structure of most receptors can now be deduced from the structure of the building blocks. The various structural building blocks have probably been conserved in evolution because they form stable structures that fold relatively quickly and efficiently and their use confers biological advantages to the receptors. A representative selection of molecules found at the leukocyte cell surface is illustrated in Fig. 17.1. These interact with a wide range of ligands some well characterised, others less so. The interactions are transient and often multivalent.

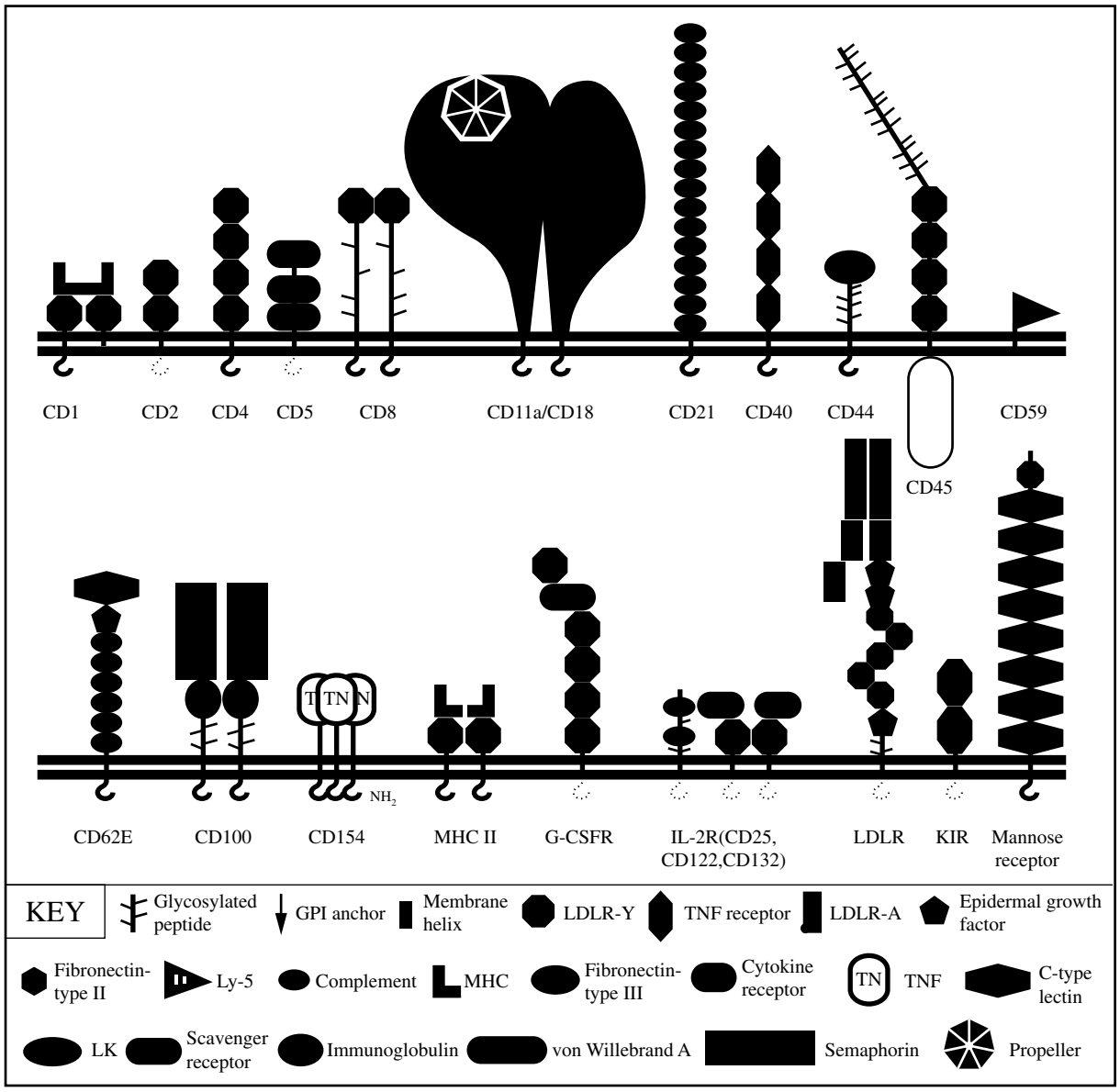

Fig. 17.1 Illustrative examples of leukocyte cell-surface molecules showing their domain architecture. Putative glycosylation sites on domains are not identified and the intracellular regions are not to scale. All the receptors shown, except CD154, are of the class I type, where the N-terminus is outside the cell and the C-terminus is inside. The nomenclature and symbols used are those proposed by Bork and Bairoch (1995). G-CSFR, receptor for granulocyte colony-stimulating factor; GPI, glycosyl phosphatidylinositol; IL-2R, receptor for interleukin 2; KIR, killer inhibitory receptor; LDLR, receptor for low density lipoprotein; Ly-5, a T-cell antigen; LK, lymphokine; MHC, major histocompatibility complex; TNF, tumour necrosis factor.

Table 17.1 *Modules and domains in cell surface receptors*

	Properties	Examples
Modules		
CL: C-type lectin	120 amino acid residues; occurs in about 6% of leukocyte receptor proteins	Selectins CD62 E, L and P
CP: complement control protein	60 amino acid residues; abundant in complement components, viruses, thyroxide peroxidase, mucins and selectins	The complement receptor CR2 (CD21)
CR: cytokine receptor	100 amino acid residues; occurs in about 8% of leukocyte receptors; structurally related to and grouped with the F3 module	
EG: epidermal growth factor	40 amino acid residues; occurs in 4% of leukocyte receptors including those involved in coagulation, complement and the extracellular matrix	Selectin family and low density lipoprotein (LDL) receptor
F2: fibronectin type II	60 amino acid residues; occurs in 1% of leukocyte receptors	Mannose receptor
F3: fibronectin type III	100 amino acid residues; occurs in 12% of leukocyte receptors	Hormone growth receptor
Ig: immunoglobulin superfamily	100 amino acid residues	CD2, CD49, CD106, sialoadhesin
LA: type A LDL receptor	40 amino acid residues; occurs in 1% of leukocyte receptors	LDL receptor
LK: link/proteoglycan tandem repeat	100 amino acid residues; occurs in less than 1% of leukocyte cell surface proteins	CD44, tumour necrosis factor stimulated gene 6 (TSG-6), aggrecan
LU: Ly-6	The precise function of these proteins is unknown	CD95
SR: scavenger receptor	110 amino acid residues; occurs in 3% of leukocyte receptor proteins	CD6
TR: tumour necrosis factor receptor	35 amino acid residues	Receptors for nerve growth factor, epidermal growth factor, insulin, CD40
VA: von Willebrand A	200 amino acid residues; found in numerous extracellular proteins	Collagen, integrins
Domains		
MHC: major histocompatibility complex	Occurs in 2% of leukocyte receptor proteins	MHC class I and II molecules
Sema: semaphorin	500 amino acid residues; involved in neuronal growth	CD100
TN: tumour necrosis factor	150 amino acid residues; occurs in 3% of leukocyte receptor proteins	TNF-α, lymphotoxin, CD40L, CD30L, FasL, OX40L

17.3 Clusters of differentiation

The list of CDs recognised at the 7th International Workshop on Human Leukocyte Differentiation Antigens (2000), together with a brief description of the molecular structure of the antigen, its biological function and relevance to disease, are given in Table 17.2.

Table 17.2 *The clusters of differentiation as designated at the 7th International Workshop on Human Leukocyte Differentiation Antigens (HLDA)*

Antigen	Other names	Molecular mass (kDa)	Molecular structure (family name)	Cellular distribution	Function	Disease relevance	Reference
CD1a CD1b CD1c CD1d CD1e	T6 gene product	49 45 43	Glycosylated type I transmembrane polypeptide α-chain noncovalently associated with β_2-microglobulin. (immunoglobulin superfamily)	Expressed on cortical thymocytes. Intracytoplasmic expression in activated mature T-cells. CD1a highly expressed on Langerhans cells	Soluble CD1 has been demonstrated to restrict T-cell responses to nonpeptide lipid and glycolipid antigens	Antimicrobial immunity	Sieling et al. (1999)
CD2	E-rosette receptor, T11, LFA-2	50	Single-chain type 1 transmembrane molecule with two Ig-like domains. CD2 has structural similarity and a genetic linkage to CD58 (immunoglobulin superfamily)	Thymic T-and B-cells; peripheral T- and NK cells	Role in alternative T-cell activation; regulation of T- or NK-mediated cytolysis; induction of apoptosis in T-cells; production of cytokines and regulation of T-cell anergy	In vivo administration of CD2 monoclonal antibody or CD2 ligand (CD58) induces immunosuppression and T-cell anergy	Rudd et al. (1999)
CD3γ CD3δ CD3ε CD3η CD3ζ	T3, CD3 complex	26 21 20 22 19	The CD3 complex has five invariant polypeptide chains that associate to form three dimers: γ/ε,δ/ε and ζ/ζ; or ζ/η; intracellular portion of the ζ chain contains ITAMs (unknown family)	Thymic T-cells upon maturation; all peripheral T-cells	Signal transduction after antigen recognition by the TCR; regulation of TCR expression	Used in immunosuppressive therapy in organ and bone marrow transplantation and autoimmune diseases	Bartlett and Longo (1999), Garner and Kearse (1999)
CD4	None	55	Monomeric molecule containing four Ig-fold domains (immunoglobulin superfamily)	T-cells, T-cell lines and thymocytes during maturation	Signal transduction in T-cell activation and maturation	Unknown	Speck et al. (1999)
CD5	T1	58	Extracellular region has three SRCR domains (SRCR family)	Low density on thymocytes; high density on mature T-cells; low density on a subset of B-cells	Modulates signalling through the antigen-specific receptor complex (TCR and BCR); modulates T- and B-cell interactions in antibody-mediated immune responses	Expressed in B-cell chronic lymphocytic leukaemia; downmodulation of CD5 leads to T-cell anergy in autoimmune disorders	Cabezudo et al. (1999), Perez-Villar et al. (1999)

CD6	T12	105	Single-chain type I transmembrane molecule containing three SRCR domains (SRCR family)	Low expression on immature thymocytes; high expression on mature thymocytes, most peripheral blood T-cells, a subset of B-cells and some neurons	CD6 is an adhesion molecule mediating adhesion of developing thymocytes to thymic epithelial cells; it is costimulatory with CD3; monoclonal antibodies belonging to CD6 inhibit autologous mixed lymphocyte reactions	May be involved in autoimmunity and graft-versus-host disease; CD6 monoclonal antibodies have been used to deplete T-cells from bone marrow transplants to prevent graft-versus-host disease: $CD6^-$ cells are less autoreactive than $CD6^+$ cells	Bowen and Aruffo (1999)
CD7	None	38	The extracellular region has a single IgV-like domain, a stalk region with four proline-rich repeats, a membrane-spanning region and a cytoplasmic tail (immunoglobulin superfamily)	Thymocytes, mature T-cells, NK cells and stem cells	CD7 can function as a costimulatory molecule that induces cytokine secretion and modifies cellular adhesion	A CD7-deficient patient with severe immune deficiency has been described. CD7 is used to classify T-cell acute lymphoblastic leukaemia	Lee et al. (1998)
CD8α, CD8β	T-cell coreceptor, T8	38	Disulphide-linked type I transmembrane glycoprotein composed of an α- and β-chain; CD8α can form a homodimer but CD8β cannot (T-cell coreceptor family)	Most thymocytes and T-cells that are specific for antigen presented by MHC class I molecules; some γ/δ T-cells and NK cells express CD8α/α homodimers	Coreceptor for TCR ligand binding and T-cell activation, which are critical for MHC class I-restricted antigen recognition	Critically important for positive selection of T-cells; used to identify killer T-cells	Cho et al. (1999), Wyer et al. (1999)
CD9	P_{24} MRP-1	24	CD9 is a type III tetraspan membrane protein (TM4 superfamily)	Platelets, early B-cells, activated T-cells, eosinophils, basophils, endothelial cells, brain, nerves, smooth and cardiac muscles and epithelia	CD9 monoclonal antibodies modulate cell adhesion and migration; ligands for CD9 include CD63, CD81, CD82, β_1-integrins and HLA-DR	CD9 monoclonal antibodies have been used for bone marrow purging in autologous transplants; CD9 expression correlates inversely with metastasis in melanoma and breast cancer	Aoyama et al. (1999), Uchida et al. (1999)

Table 17.2 (*cont.*)

Antigen	Other names	Molecular mass (kDa)	Molecular structure (family name)	Cellular distribution	Function	Disease relevance	Reference
CD10	CALLA, neutral endopeptidase	100	Type II integral membrane protein (zinc metalloprotease family)	Lymphoid precursors, germinal centre B-cells, mature neutrophils, brush border epithelium	Regulation of B-cell growth and proliferation; acts as a zinc metalloprotease	Used for phenotyping leukaemias; associated with hemopoietic differentiation	Fang et al. (1999), Nakajima et al. (1999)
CD11a	LFA-1α	170	Expressed as a heterodimer CD11a/CD18; noncovalently linked (integrin α-chain family)	Expressed on all leukocytes. Absent from nonhemopoietic tissues and human platelets	Intercellular adhesion and costimulatory function; ligands include ICAM-1 CD54, ICAM-2 CD102 and ICAM-3 CD50; antibodies to CD11a/CD18 block T-cell responses to antigen-presenting cells, T-cell help to B-cells, cytotoxic lymphocytes and NK-mediated killing, macrophage killing of tumour cells and leukocyte–endothelial adhesion/extravasation	Immune/ inflammatory responses are dependent upon leukocyte adhesion; lymphocyte recirculation through lymph nodes is CD11a/CD18 dependent. CD11a monoclonal antibodies reduce graft failure for bone marrow grafts in immunodeficient children. LAD-1 results from a lack of CD18	Ni et al. (1999)
CD11b	CR3, Mac-1 ($_H$-integrin), C3biR	165	Type 1 transmembrane protein (integrin α-chain family)	Expressed on subsets of T- and B-cells, monocytes, granulocytes and NK cells	Neutrophil and monocyte interactions with stimulated endothelium; phagocytosis of iC3b- or Ig-coated particles; neutrophil degranulation, respiratory burst, spreading, chemotaxis and apoptosis	Target for anti-inflammatory drug therapies; absent in leukocyte-deficient patients, resulting in recurrent bacterial infection	Todd and Petty (1997)
CD11c	P150, CR4	145	Type 1 transmembrane protein (integrin α-chain family)	Expressed on subsets of T- and B-cells, monocytes, macrophages, granulocytes and NK cells	Similar functions to CD11b/CD18 with which it cooperates; major CD11/CD18 receptor on macrophages	Absent in patients with LAD-1	Todd and Petty (1997)

CDw12	P90-120	150–160	Phosphoprotein structure unknown; (unknown family)	Expressed on monocytes, granulocytes and NK cells	Unknown	Unknown	Patel et al. (1995)
CD13	Aminopeptidase N	150	Type II integral membrane protein; expressed as a homodimer (unknown family)	Expressed on myeloid precursor and mature cells, some large granular lymphocytes, endothelial cells, epithelial cells, bone marrow stromal cells, oesteoclasts and cells lining bile duct canaliculi	Unknown	Receptor for strains of RNA coronaviruses; required for interaction between human cytomegalovirus and the target cells; the presence of CD13 autoantibodies is associated with the development of graft-versus-host disease following bone marrow transplantation	Kolb et al. (1998), Phillips et al. (1999)
CD14	LPS receptor	53	GPI-anchored glycoprotein	Expressed on monocytes, weakly on granulocytes and tissue macrophages	CD14 functions as receptor for endotoxin (LPS); LPS binds to serum lipoprotein, which facilitates the binding of LPS to CD14; this then results in cell activation, cytokine release and increased cell surface adhesion molecule expression; two soluble forms exist	Required for the production of cytokines in murine model if shock induced by endotoxin or live *Escherichia coli*; soluble forms of CD14 have a plasma concentration of about 3 $\mu g\ ml^{-1}$; in blood, the soluble form exceeds the membrane form of CD14 by 10^2- to 10^3-fold	Haziot et al. (1999)
CD15, CD15s, CD15su, CD15s/su	Lewis X, sialated Lewis X, sulphated Lewis X, sialated, sulphated Lewis X	Unknown	Oligosaccharide, carbohydrate antigen having type 2 chain polylactosamines	Expressed on precursor and mature granulocytes and monocytes, cells of lymphoid and myeloid leukaemias and lymphomas, Langerhans cells and many cancer cells especially adenocarcinoma	Possibly involved in adhesion	Target for anti-cancer therapies; CD15 monoclonal antibodies may be used for bone marrow purging prior to transplantation	Sanders et al. (1999)

Table 17.2 (*cont.*)

Antigen	Other names	Molecular mass (kDa)	Molecular structure (family name)	Cellular distribution	Function	Disease relevance	Reference
CD16	Low-affinity Fc receptor for IgG	50–65	Two truncated Ig-like domains, phosphatidylinositol linked and transmembranous forms; polymorphic on granulocytes. (immunoglobulin superfamily)	Highly expressed on NK cells, granulocytes and macrophages; low expression on subsets of both TCR α/β^+ and γ/δ^+ T-cells	Low-affinity Fc receptor for IgG, immune complexes, main receptor for antibody-dependent cellular cytotoxicity; cross-linked antibodies may activate cytotoxicity, cytokine production and receptor expression	Unknown	Ikura et al. (1999), Mandleboim et al. (1999)
CDw17	LacCer	150–160	Lactosyl disaccharide group of the glycosphingolipid lactosyl ceramide (LacCer family)	Expressed on monocytes, granulocytes, basophils, platelets, subset of B-cells, tonsilar dendritic cells and IL-2-activated T-cells	LacCer binds to bacteria and may function in phagocytsosis	Unknown	Zimmerman et al. (1998)
CD18	β_2 Subunit	90	Type I transmembrane protein (integrin family)	Expressed by all leukocytes	Unknown	Important in inflammatory responses; lacking in patients with LAD-1	Chavakis et al. (1999), Weber et al. (1999)
CD19	B4	120	Transmembrane protein with two extracellular C2-type Ig-like domains (immunoglobulin superfamily)	Expressed on B-cells, malignant B-cells and follicular dendritic cells; expression on B-cells lost at plasma cell stage	CD19 is a critical signal transduction molecule that regulates B lymphocyte development, activation and differentiation; interacts with CD21 (CR2) and CD81 (target for antiproliferative antigen 1, TAPA-1)	Loss of CD19 results in impaired humoral and cellular immune responses	Ciudad et al. (1998)
CD20	B1 antigen	33, 35, 37	Transmembrane protein (CD20 family)	Expressed on all maturational stages of B-cells	Regulation of B-cell activation and proliferation	B1 monoclonal antibodies used in the treatment of lymphoma	Davis et al. (1999)
CD21	CR2, C3d receptor, Epstein–Barr virus receptor	145	Transmembrane protein; regulator of complement activation (unknown family)	Expressed on B-cells from the stage of Ig expression, lost upon activation; follicular mantle zone and marginal zone B-cells, follicular dendritic cells, subset of immature thymocytes	Receptor for Epstein–Barr virus and for C3d, C3dg and iC3b; complement components may activate B-cells through CD21; involved in signal transduction with CD19, CD81 and Leu-13	Typing lymphomas	Huang et al. (1995)

CD22	B lymphocyte cell adhesion molecule	140	Single-chain type I transmembrane molecule that contains seven Ig-like domains (immunoglobulin superfamily)	B-cell-specific expression: surface expression on mature B-cells, cytoplasmic expression on late pro- and early pre-B-cells	Involved in adhesion and signalling	Antibody treatment of lymphoma/leukaemia	O'Keefe et al. (1999), van Horssen et al. (1999)
CD23	FcεRII, low-affinity IgE receptor	45	Type II integral membrane glycoprotein (C-type lectin family)	B cells, monocytes, follicular dendritic cells, apical light zone, T-cells, platelets, eosinophils, neutrophils, Langerhan's cells, platelets and megakaryocytes	Regulation of IgE synthesis; pro-inflammatory function: triggering of monokine release by activated monocytes; ligands include IgE, CD21, CD11b, CD11c	Allergy, negative feedback regulation of IgE synthesis, IgE-mediated antigen presentation. Soluble CD23 correlates with disease progression in chronic lymphocytic leukaemia	Hasegawa et al. (1999), Lorenzi et al. (1999)
CD24	B cell antigen-1	35-45	GPI-anchored glycoprotein (unknown family)	Expressed on B-cells except plasma cells, mature granulocytes and a variety of epithelial cells	Unknown	Identification of maturational stage in B-cells	Pass et al. (1998)
CD25	IL-2 receptor α-chain	55	Type I transmembrane molecule (unknown family)	Activated T- and B-cells, activated monocytes and macrophage and T-cell lines transformed by human T-cell leukaemia virus	IL-2 receptor α-chain	Control of autoimmunity	Cipres et al. (1999)
CD26	Dipeptidyl peptidase IV ectoenzyme	120,110	Single-chain type II transmembrane molecule (prolyl oligopeptidase, serine type exopeptidase family)	Mature thymocytes, activated T-, B- and NK cells, macrophages, variety of epithelia	Costimulatory molecule in T-cell activation	Associated with autoimmune disease, adenosine deaminase deficiency and HIV pathogenesis	van der Velden and Hulsmann (1999)
CD27	T14, S152	110–120	Type I transmembrane molecule (TNF receptor family)	Expressed on majority of peripheral blood T-cells, preferentially on $CD45RA^+$ T-cells after activation, medullary thymocytes, a subpopulation of B-cells and NK cells	Mediates a costimulatory signal for T- and B-cells; soluble CD27 produced after T-cell activation	Raised levels of soluble CD27 in patients with immunopathological diseases may be used as a measure of T-cell activation	Lens et al. (1998), Nagumo et al. (1999)
CD28	Tp44, T44	90	Homodimeric type I transmembrane glycoprotein (immunoglobulin superfamily)	Expressed on mature $CD3^+$ thymocytes, most peripheral blood T-cells and plasma cells	The binding of CD28 with its ligands CD80 or CD86 costimulates T-cell effector function and T-cell-dependent antibody production	Control of T-cell-mediated humoral immunity; monoclonal antibody blockade of CD80 and/or CD86 antigens induces T-cell anergy	Burgisser et al. (1999)

Table 17.2 (*cont.*)

Antigen	Other names	Molecular mass (kDa)	Molecular structure (family name)	Cellular distribution	Function	Disease relevance	Reference
CD29	Integrin β_1-chain, VLA β-chain, platelet GPIIa	110	Transmembrane glycoprotein (integrin family)	T- and B-cells, monocytes, platelets, fibroblasts, endothelial cells, mast cells, fat cells, hepatocytes, smooth muscle	Adhesion to VCAM-1, MAdCAM-1, collagen, laminin, fibronectin; costimulation of T-cells	CD29 is critical for embryogenesis, regulates lymphocyte migration, controls hemopoietic stem cell differentiation, is associated with tumour progression and metastasis	Ellerbroek et al. (1999), Schwartz et al. (1999)
CD30	Ki-1 antigen	120	Type I glycoprotein with five cysteine-rich repeats and a central hinge region (TNF receptor family)	Activated T-, B- and NK cells, monocytes, various cell lines, large lymphoid cells in lymph node, tonsil, thymus and decidua, Reed–Sternberg cells, Hodgkin cells, embryonal carcinoma cells	Involved in negative selection of T-cells in the thymus and TCR-mediated cell death; activates NFκB via TNF receptor associated factors 2 and 3	Used to identify lymphoproliferative disorders and lymphomas; elevated levels of soluble CD30 in patients with hepatitis B correlate with disease activity	Bauer et al. (1999), Kurts et al. (1999)
CD31	Platelet endothelial cell adhesion molecule 1 (PECAM-1)	130–140	Single-chain type I transmembrane protein (immunoglobulin superfamily)	Endothelial cells, platelets, monocytes, neutrophils, subset of T-cells and NK cells	CD31 is an adhesion molecule exhibiting both homophilic and heterophilic binding; CD31 ligation leads to increased integrin expression	CD31 monoclonal antibodies block diapedesis of neutrophils, monocytes and NK cells in vitro and in vivo	Wakeham et al. (1999)
CD32	FcγRIIa FcγRIIb1 FcγRIIb2	42 40 37	Transmembrane proteins; the extracellular region has two Ig-like domains and the cytoplasmic tail contains an ITAM or an immunoreceptor tyrosine-based inhibiton motif ITIM (Fc receptor family)	CD32 is expressed in one or more isoforms on most hemopoietic cells; FcγRIIa is found on neutrophils, platelets, monocytes and some T- and B-cells; FcγRIIb1 or 2 is found on B-cells, monocytes and mast cells	Regulates B-cell function when co-engaged with antigen receptor; mediates phagocytosis of Ig-coated particles and targets antigen into presenting pathways	Involved in immune complex-mediated tissue damage and destruction of antibody-coated cells in autoimmune diseases	Kim et al. (1999a)

CD33	P67	150	Glycoprotein with a signal peptide and an IgV domain (sialoadherin family (sialic acid-dependent cytoadhesion molecules))	Expressed on all myelo/monocytic cells; decreasing expression occurs upon maturation and differentiation. No expression outside hemopoietic system	Unknown; has carbohydrate/lectin activity	Used for the diagnosis of acute myeloid leukaemia and negative selection of human self-regenerating hemopoietic stem cells	Sievers et al. (1999), Taylor et al. (1999)
CD34	GP105–120	40	Heavily glycosylated type I transmembrane protein; two forms exist (sialomucin family)	Expressed on early lympho-hemopoietic stem and progenitor cells, small-vessel endothelial cells, embryonic fibroblasts and some nervous tissue; also expressed on cells in a number of fetal tissues	Cell–cell adhesion, CD34 ligand is L-selectin (CD62L); inhibition of hemopoietic differentiation	Required for hemopoietic differentiation; MAb have been used to quantify and purify stem/progenitor cells for transplantation	Pecora (1999)
CD35	CR1, C3b/C4b receptor	165–185	Type I single-chain membrane glycoprotein; (regulators of complement activation family)	Expressed on erythrocytes, neutrophils, monocytes, eosinophils, B-cells, 10–15% of T-cells, glomerular podocytes, follicular-dendritic cells and some astrocytes; the Knops, McCoy, Swain–Lagley and York blood groups antigens are located on CD35	On leukocytes, CD35 mediates adherence of C4b/C3b-coated particles in preparation for phagocytosis, which requires cooperation with CR3 (CD11/CD18) and the Fcγ receptors; on erythrocytes CD35 mediates adherence of targets coated with C4b/C3b and their transport to the phagocyte systems of the liver and spleen. CD35 facilitates C3b and C4b cleavage by factor 1 and accelerates the decay of C3 and C5 convertases and thus limits complement activation	Mediates removal and processing of immune complexes; a recombinant soluble CD35 has been used as a complement inhibitor. CD35 is required for B-cell response to T-cell-dependent antigens	Baiu et al. (1999)

Table 17.2 (*cont.*)

Antigen	Other names	Molecular mass (kDa)	Molecular structure (family name)	Cellular distribution	Function	Disease relevance	Reference
CD36	GPIV, GPIIIb	80–90	Transmembrane protein (unknown family)	Expressed on platelets, mature monocytes and macrophages, microvascular and mammary endothelial cells, during stages of erythroid cell development and on some macrophage-derived dendritic cells	Scavenger receptor for oxidised LDL and shed phosphoreceptor outer segments; recognition and phagocytosis of apoptotic cells; role in platelet adhesion and aggregation and platelet–monocyte interactions; cytoadherence of *Plasmodium falciparum*-infected erythrocytes	Mediates atherogenesis and macrophage foam cell formation. Is required for cytoadherence of *Plasmodium*-infected cells to microvascular endothelial cells in malaria; inflammation is resolved by phagocytosis of aged neutrophils; individuals who do not have the platelet associated alloantigen (designated naka) do not express CD36 but no physiological problems have been associated with this deficiency	Nakamura et al. (1999), Rutella et al. (1999)
CD37	Gp52–40	40–52	Polypeptide with three potential N-glycosylation sites (TM4 family)	Expressed on normal and neoplastic surface membrane immunoglobulin positive ($smIg^+$) B-cells; on resting and activated T-cells, neutrophils and monocytes	Involved in signal transduction; ligands include CD53, CD81, CD82 and MHC class II	Used for identification of malignancies derived from mature B-cells, chronic lymphocytic leukaemia, hairy cell leukaemia and non-Hodgkin's lymphoma	Ferrer et al. (1998)

CD38	T10	45	Single-chain type II transmembrane molecule (ADP-ribosyl cyclase family)	Expressed on hemopoietic cells during early differentiation and activation, high expression on plasma cells, variable expression in other tissues	Regulator of cell activation and proliferation, involved in adhesion between human lymphocytes and endothelium; ligands include CD31, TCR, BCR, CD16, CD73 and plasma cell membrane differentiation antigen 1 (PC-1)	Monitoring HIV infection and progression; plasma cell identification, targeting of immuno-toxin antibody in the treatment of myeloma, purging of acute promyelocytic leukaemia cells, post-transplant monitoring	Ferrero and Malavasi (1999)
CD39	None	80	Transmembrane protein enzyme (ectoapyrase family)	Mantle zone B-cells, activated T-cells, NK cells, macrophages, Langerhans cells and dendritic cells	May protect cells from the effects of extracellular ATP	First mammalian ectoapyrase identified	Dzhandzhugazy et al. (1998), Schulte et al. (1999)
CD40	Bp50	48	Single-chain type I transmembrane molecule (TNF/NGF family)	B-cell, pro-B through to plasma cells, basal epithelial cells, epithelial cell carcinoma, macrophages, follicular dendritic cells, endothelial cells, fibroblasts, keratinocytes, interdigitating cells, $CD34^+$ cells	On B-cells involved in growth, differentiation and isotype switching; promotes cytokine production in macrophages and dendritic cells; upregulates adhesion molecules on dendritic cells and keratinocytes; stimulates growth arrest in epithelial cells	Central to T-cell-dependent responses; may influence survival of B-cell lymphomas; ligands include CD40 ligand	Bachmann et al. (1999), Kosaka et al. (1999)

Table 17.2 (*cont.*)

Antigen	Other names	Molecular mass (kDa)	Molecular structure (family name)	Cellular distribution	Function	Disease relevance	Reference
CD41	GPIIb	135	CD41 is the α-subunit of CD41/CD61 complex, a Ca^{2+}-dependent, noncovalently associated heterodimer; CD41 is extracellular and contains four repeating segments that bind Ca^{2+} (integrin family)	Expressed on platelets and platelet precursors	CD41/CD61 plays a central role in platelet activation and aggregation	Glanzmann's thrombasthenia is an inherited bleeding disorder resulting from an absence of CD41/CD61; nine mutations have been identified within CD41. CD41 bears at least two alloantigenic determinants that can be induced in an alloimmune response, leading to thrombocytopenia. Some monoclonal antibodies may be used for diagnosis of Glanzmann's thrombasthenia, megakaryoblastic leukaemia, detection of alloantibodies and antithrombotic therapy	Clemetson and Clemetson, (1994), Vorchheimer et al. (1999)
CD42a	GPIX	22	Single-chain integral membrane glycoprotein forms a noncovalently linked complex with CD42b, c and d (LRG family)	Expressed on platelets and megakaryocytes	The CD42 complex mediates adhesion of platelets to subendothelial matrices under high shear rates and amplifies the platelet response to thrombin during thrombin-stimulated platelet activation	The CD42 complex is absent on platelets from patients with Bernard–Soullier syndrome, which is characterised by thrombocytopenia and giant platelets; CD42a monoclonal antibodies have been used for the detection of platelet autoantibodies	Slupsky et al. (1997)

CD42b	GPIbα	160	Heterodimer composed of an α-chain (CD42b) and a β-chain (CD42c) linked by a disulphide bond; it forms a noncovalently linked complex with CD42a and d (LRG family)	Expressed on platelets and megakaryocytes	See CD42a for function. The cytoplasmic domain is associated via actin-binding protein with the cytoskeleton	See CD42a for disease relevance. CD42b carries a single amino acid residue polymorphism resulting in the Ko alloantigen system	Walker and Green, (1999)
CD42c	GPIbβ	160	Heterodimer composed of an α-chain (CD42b) and a β-chain (CD42c) linked by a disulphide bond; it forms a noncovalently linked complex with CD42a and d (LRG family)	Expressed on platelets and megakaryocytes	See CD42a for function	See CD42a for disease relevance	de Cristofaro and de Candia (1999)
CD42d	Glycoprotein V	82	Single-chain integral membrane glycoprotein; forms a noncovalently linked complex with CD42a–c (LRG family)	Expressed on platelets and megakaryocytes	See CD42a for function	See CD42a for disease relevance	Koskela et al. (1998)
CD43	Sialophorin	95–135	Single-chain type I transmembrane molecule (sialomucin family)	Expressed on most leukocytes; proteolytic shedding occurs from lymphocytes and neutrophils upon activation	Adhesion molecule with ligand CD54; may also act as an anti-adhesive molecule because of the large number of negatively charged sialic acid residues	Low expression found as a secondary defect in Wiskott–Aldrich syndrome	Lai et al. (1999)
CD44 and CD44s (soluble CD44)	Homing-associated cell adhesion molecule (H-CAM), Hermes	85	Transmembrane protein (hyaladherin family)	Expressed on the surface of most cell types: not expressed on platelets, hepatocytes, certain lymphoid cell lines, cardiac muscle, kidney tubular epithelium, testis and portions of the skin	CD44 is involved in leukocyte attachment, rolling on endothelium and homing to peripheral lymphoid organs and to sites of inflammation; signalling through CD44 induces cytokine release and lymphoid activation	CD44 monoclonal antibodies inhibit inflammation in mouse models of athritis; CD44–hyaluronic acid interactions have a role in tumour metastasis	Kinoshita et al. (1999), Pilarski et al. (1999)
CD44R (CD44 receptor)	CD44v	85–250	Structure as for CD44; at least 18 isoforms have been reported (unknown family)	Expressed on epithelial cells and monocytic cells; may be upregulated on activated leukocytes	Involved in leukocyte attachment to endothelium and homing to peripheral lymphoid organs and sites of inflammation	Monoclonal antibodies belonging to CD44v6 inhibit metastasis	Levesque and Haynes (1997)

Table 17.2 (*cont.*)

Antigen	Other names	Molecular mass (kDa)	Molecular structure (family name)	Cellular distribution	Function	Disease relevance	Reference
CD45	Leukocyte common antigen (LCA)	180–220	Long single-chain type I molecule (protein tyrosine phosphatase PTPase family)	Expressed on all hemopoietic cells; a major component of the glycocalx. CD45RO and CD45RA isoforms expressed on different subsets of T-cell	Required for TCR and BCR-mediated activation; ligands include galectin-1, CD2, CD3, CD4 and lymphocyte phosphatase-associated phosphoprotein (LPAP)	Target for immunosuppressive therapy. Required for T-cell maturation and antigen receptor-mediated activation	Altin and Sloan (1997), Justman (1997)
CD46	Membrane cofactor protein (MCP)	35–52	Single-chain type I transmembrane protein; at least four isoforms exist (regulator of complement activation family)	Expressed on salivary gland ducts, lymphocytes, endothelium, interstitial tissues and muscle cells. Often increased expression on tumour cells. Not expressed on erythrocytes	Limits the formation and function of C3 convertase; crosslinking CD46 downregulates IL-12 production; ligands include serum factor I protease, C3b and C4b	Control of IL-12 production is important in immunosuppression	Devaux et al. (1999)
CD47	Integrin associated protein, Rhesus-related antigen	45–60	An extracellular IgV-like domain with five membrane-spanning segments (immunoglobulin superfamily)	Broad tissue distribution including hemopoietic cells, epithelial and endothelial cells, fibroblasts, brain, mesenchymal cells, tumour cell lines	Adhesion molecule, thrombospondin receptor	Required for host defence, for β_3-integrin-dependent ligand binding, cell migration and activation	Frazier et al. (1999)
CD48	Blast-1	45	CD48 is a GPI-linked cell surface molecule with two Ig-like domains (immunoglobulin superfamily)	Pan-leukocyte except neutrophils and platelets; upregulated on activated lymphocytes	Adhesion via its ligand CD2; acts as an accessory molecule in $\gamma\delta$ and $\alpha\beta$ T-cell recognition	The frequency of $CD48^+$ cells is decreased in patients with paroxysmal hemoglobinuria	Moran and Miceli (1998)
CD49a	VLA-1α, integrin α_1 chain	200	Long type I transmembrane molecule noncovalently associated with integrin β_1-chain (CD29) to form $\alpha_1\beta_1$-integrin VLA-1 (integrin family)	Activated T-cells, monocytes, neuronal cells, melanoma cells and smooth muscle cells	Adhesion receptor for collagen and laminin-1	CD49a is upregulated in a number of inflammatory diseases but its role is unclear	Gardner et al. (1999)

CD49b	VLA-2α, GPIa, integrin α_2-chain	150	Transmembrane glycoprotein, noncovalently associated with integrin β_1-chain (CD29) to form $\alpha_2\beta_1$-integrin (VLA-2) (integrin family)	Expressed on platelets, megakaryocytes, activated T- and B-cells, monocytes, epithelial cells, neuronal cells, thymocytes, endothelial cells, fibroblasts, melanoma cells, osteoclasts and mesangial cells	Mediates cell adhesion to collagen (type I, II, III and IV), laminin; receptor for echovirus 1	Required for wound healing through the contraction of type I collagen induced by its binding to CD49b	Thomas et al. (1998)
CD49c	VLA-3, integrin α_3-chain	145–150	Long type I transmembrane molecule noncovalently associated with integrin β_1-chain (CD29) to form $\alpha_3\beta_1$-integrin (VLA-3) (integrin family)	Nearly all adherent cell lines, kidney glomerulus, thyroid, some basement membranes, B-cells	A component of an adhesion receptor for laminin-5, fibronectin, laminin-1, collagen, invasin and entacin; may be associated with the TM4 family CD9, CD63 and CD81 for signal transduction	Regulatory role in cell fusion and may be involved in migration of cells into the epidermis	Berditchevski et al. (1996)
CD49d	VLA-4, integrin α_4-chain	145	Transmembrane molecule, the extracellular region includes more than three EF-hand like divalent cation-binding sites, which mediate adhesion noncovalently associated with integrin β_1-chain (CD29) to form $\alpha_4\beta_1$-integrin (VLA-4) (integrin α-chain family)	Broad cellular reactivity; not expressed on platelets or neutrophils	Adhesion to cell surface ligands VCAM-1 and MAdCAM-1, fibronectin and thrombospondin; assists tethering or rolling of T-cells, homing of T-cell subsets to Peyer's patches via MAdCAM-1; T-cell costimulation with TCR/CD3-mediated signalling	CD49d is involved in multiple inflammatory responses through regulation of lymphocyte migration and T-cell activation; it is essential for the differentiation and traffic of hemopoietic stem cells and is involved in tumour progression and metastasis	Arroyo et al. (1996)
CD49e	VLA-5α, integrin α_5-chain	160	Long type I transmembrane molecule noncovalently associated with integrin β_1-chain (CD29) to form $\alpha_5\beta_1$-integrin (VLA-5) (integrin family)	A variety of adherent and nonadherent cells	A component of an adhesion receptor heterodimer $\alpha_5\beta_1$-integrin to fibronectin	Binding of $\alpha_5\beta_1$-integrin to fibronectin induces apoptosis	Chon et al. (1998)

Table 17.2 (*cont.*)

Antigen	Other names	Molecular mass (kDa)	Molecular structure (family name)	Cellular distribution	Function	Disease relevance	Reference
CD49f	VLA-6α, GPIc, integrin α_6-chain	150	Long type I transmembrane molecule noncovalently associated with integrin β_1-chain (CD29) to form $\alpha_6\beta_1$-integrin (VLA-6) (integrin family)	A variety of cells and tissues	$\alpha_6\beta_1$- (CD49f/CD29) and $\alpha_6\beta_4$- (CD49f/CD104) integrins are receptors for laminins, facilitate adhesion to basement membranes and spreading of leukocytes and tumour cells; $\alpha_6\beta_1$ and $\alpha_6\beta_4$-integrins are important in embryogenesis and thymocyte development, respectively	$\alpha_6\beta_4$-Integrin facilitates wound healing in the interaction between epithelial cells and basement membrane. CD49f is involved in tumour metastasis. Bullous pemphigoid results from autoantibodies binding to CD49f in the basement membrane of skin	Tomatis et al. (1999)
CD50	ICAM-3	115–140	Type I membrane protein (immunoglobulin family)	Leukocytes of all lineages, epidermal Langerhans cells, endothelial cells	Provides costimulatory signal in immune responses, regulates leukocyte function associated antigen 1 (LFA-1)/ICAM-1 and β_1-integrin-dependent pathways	Unknown	Del Pozo et al. (1998)
CD51	α_v-Integrin subunit	150	Heterodimer with standard integrin α-chain structure (integrin family)	Endothelial cells, osteoclasts, some B-cells, activated T-cells and monocytes, macrophages, platelets and melanoma cells	Adhesion to matrix and cells, role in signal transduction, role in bone metabolism and apoptosis, possible role in infection because CD51 binds adenovirus and mycobacteria	$\alpha_V\beta_3$-Integrin is upregulated in some cancers and is a target for drug development in bone and vascular disease, angiogenesis and tumour metastasis	Cao et al. (1998)
CD52	CAMPATH-1 (Cambridge Pathology 1)	25–29	GPI-linked short peptide (CD52/CD24/heat stable antigen (HSA) family)	Expressed on thymocytes, malignant and normal lymphocytes, monocytes and macrophages	A monoclonal IgM anti-lymphocyte antibody that fixes complement; unknown	CD52 monoclonal antibodies used for immunodepletion in the treatment of lymphoid malignancies and as immunosuppressants in transplatation and autoimmune diseases	Novitzky et al. (1999)

CD53	None	32–42	Type III transmembrane protein (TM4 superfamily)	Leukocytes; not present on platelets, erythrocytes and nonhemopoietic cells	Signal transduction; CD53 crosslinking promotes B-cell activation; ligands include other tetraspans, VLA-4 and HLA-DR	Unknown	Lagaudriere-Gesbert et al. (1997), Mollinedo et al. (1998)
CD54	ICAM-1	75–115	Type I transmembrane molecule (immunoglobulin superfamily	Expressed on endothelial and epithelial cells, activated T- and B-cells, monocytes and some solid tumour cells; inducible by TNF, IL-I 1and IFN-γ	Reacts with CD11a or b/CD18 resulting in immune reaction/inflammation; involved in neutrophil endothelial cell binding; acts as a receptor for rhinovirus and erythrocytes infected with malarial parasites	Some CD54 monoclonal antibodies can reduce reperfusion injury; may be useful for preventing allograft rejection	Kim et al. (1999b), Ni et al. (1999)
CD55	Decay accelerating factor (DAF)	70	Single-chain GPI-anchored type I cell surface protein; (regulator of complement activation)	Widely expressed on cells throughout the body including erythrocytes; low expression on NK cells	Limits formation and half-life of C3 convertases; has been implicated as a ligand or protective molecule in fertilisation; crosslinking results in signal transduction	CD55 deficiency is found in paroxysmal nocturnal hemoglobinuria and in psoriatic skin lesions; expression may be related to tumourigenesis. Cytomegalovirus incorporates the CD55 antigen into its membrane	Sun et al. (1999)
CD56	Neuronal cell adhesion molecule (NCAM)	175–220	Transmembrane glycoprotein (immunoglobulin superfamily)	Expressed on NK cells and subsets of $CD4^+$ and $CD8^+$ T-cells; present in brain cerebellum and cortex and at neuromuscular junction. CD56 is also present on large granular lymphocytic leukaemia, small-cell lung carcinomas, neuronal derived tumours, myelomas and myeloid leukaemias	CD56 plays a role in homo- and heterophilic neural cell adhesion; ligands include heparin sulphate	Unknown	Rawstron et al. (1999)

Table 17.2 (*cont.*)

Antigen	Other names	Molecular mass (kDa)	Molecular structure (family name)	Cellular distribution	Function	Disease relevance	Reference
CD57	HNK1 (human natural killer 1)	110	Carbohydrate associated with several proteins and lipids (unknown family)	Expressed on NK cells and T-cell subsets, some B-cell lines, B-cell chronic lymphocytic leukaemia, melanoma lines and small-cell lung carcinoma lines	Unknown	Unknown	Mollet et al. (1999)
CD58	LFA-3	40–70	Transmembrane and GPI-anchored molecular forms (immunoglobulin superfamily)	Distributed over many tissues both hemopoietic and nonhemopoietic	CD58 mediates adhesion between killer and target cells, antigen-presenting cells and T-cells, thymocytes and thymic epithelial cells; it provides costimulatory signals in immune responses, activates killer cells and acts as the ligand for CD2	Unknown	Hoffman *et al* (1998), Itzhaky et al. (1998)
CD59	Membrane inhibitor of reactive lysis	18–25	Single-chain GPI-anchored cell surface protein structurally related to snake venom neurotoxins (Ly6 superfamily)	Widely expressed on cells in all tissues; expression on erythrocytes is required for their survival	Inhibits formation of membrane attack complex, thus protects cells from complement-mediated lysis; has a signalling role in T-cell activation; ligands include CD8, CD9, Lck and Fyn	CD59 is incorporated into the HIV envelope and protects virus and virus-infected cells against complement deposition	Zhang et al. (1999)
CD60a CD60b CD60c	Ganglioside D_3 7-*O*-acetyl GD_3 9-*O*-acetyl GD_3	120	9-*O*-Acetylated disialosyl group predominantly found on ganglioside D_3 (glycolipid family)	Thymic epithelium, activated keratinocytes, synovial fibroblasts, glomeruli, smooth muscle cells, astrocytes; CD60 expression seems to correlate with a $CD4^+$ T type helper-2-like cytokine profile; CD60c expression defines a helper population within the $CD8^+$ T-cells	CD60a/b antibodies provide costimulatory/comitogenic signals for T-cells	Unknown	Claus et al. (2000), Wada et al. (1998)

CD61	GPIIIa, β_3 integrin	90	Cysteine-rich single protein, common β-subunit of CD41/CD61 (GPIIb-IIIa) and CD51/CD61 (vitronectin receptor) (integrin family)	With CD41 on platelets and megakaryocytes; with CD51 on endothelium, smooth muscle, some B-cells, monocytes/macrophages, platelets, osteoclasts, mast cells, fibroblasts and tumour cells	CD41/CD61 mediates attachment of cells to diverse matrix proteins including immobilised fibrinogen, fibronectin and von Willebrand factor; CD51/CD61 binds in addition vitronectin; CD61 also interacts with α-actinin, paxillin and talin	CD41/CD61 is absent or dysfunctional in Glanzmann's thrombasthenia;. CD51/CD61 plays a role in tumour metastasis and adenovirus infection. Some monoclonal antibodies may be applicable for detection of alloantibodies and for antithrombotic therapy	Brezinchek et al. (1999)
CD62E	E-selectin, endothelial leukocyte adhesion molecule 1 (ELAM-1)	107–115	Transmembrane protein with one C-type lectin domain and one EGF-like domain (selectin family)	Expressed on activated endothelium	CD62E mediates leukocyte rolling on activated endothelium at inflammatory sites and may also support tumour cell adhesion during hematogenous metastasis and play a role in angiogenesis; ligands include sialyl-Lewis X, sialyl-Lewis A, cutaneous leukocyte antigen (CLA), PSGL-1	Required for leukocyte emigration to sites of inflammation; patients with LAD II who lack sialyl-Lewis X have recurrent pyogenic infections	He et al. (1998)
CD62L	L-selectin	65	Transmembrane protein with one C-type lectin domain and one EGF-like domain (selectin family)	Expressed on most peripheral blood B- and T-cells, monocytes, granulocytes, some NK cells, spleen lymphocytes, bone marrow myeloid and lymphoid cells	CD62L mediates lymphocyte homing to high endothelial venules of peripheral lymphoid tissue and leukocyte rolling on activated endothelium at inflammatory sites	Ligands include CD34, glycosylation-dependent cell adhesion molecule-1 and MAdCAM-1; monoclonal antibodies may be used to block inflammatory responses	Tu et al. (1999)

Table 17.2 (*cont.*)

Antigen	Other names	Molecular mass (kDa)	Molecular structure (family name)	Cellular distribution	Function	Disease relevance	Reference
CD62P	P-selectin, granule membrane protein 140 (GMP-140)	120	Long single-chain type 1 transmembrane molecule with one N-terminal lectin domain and one EGF-like domain (selectin C type lectin family)	CD62P is mobilised from storage granules to the cell surface of activated platelets and endothelial cells; it is also rapidly internalised from endothelial cell surfaces; ligands include P-selectin PSGL-1, CD24	Interaction of CD62P with PSGL-1 mediates tethering and rolling of leukocytes on the surface of activated endothelium at sites of inflammation; CD62P is also involved in platelet-mediated delivery of lymphocytes to high endothelial venules	Deficiency results in decreased neutrophil, monocyte and $CD4^+$ lymphocyte recruitment to sites of inflammation	Yang et al. (1999a)
CD63	Gp53	40–55	Transmembrane protein with a lysosomal targeting sequence (TM4 superfamily)	Intracellular lysosomal protein; activated platelets, degranulated neutrophils, monocytes, macrophages, endothelium, fibroblasts, osteoclasts, smooth muscle, nerve tissue and synovial lining cells	Function unknown; ligands include CD29/CD49c, CD29/CD49f, CD9 and CD81	CD63 monoclonal antibodies may be used to identify activated platelets and primary melanoma cells	Barrio et al. (1998)
CD64	FcγRI	72	Transmembrane protein with three Ig domains (immunoglobulin superfamily)	Monocytes, macrophage, dendritic cell subset, neutrophils activated by G-CSF	Endocytosis of IgG-antigen complexes; antigen capture for presentation to T-cells; antibody dependent cellular cytotoxicity; release of cytokine and reactive oxygen species	Increased neutrophil expression is associated with infectious diseases and therapy with IFN-γ or G-CSF	Ernst et al. (1998), van Spriel et al. (1999)
CD65	None	Unknown	Type 2 carbohydrate chain with four lactosamine repeats (poly-*N*-acetyllactosamines family)	Granulocytes, monocytes, myeloid leukaemia cells	Unknown	Unknown	Pui et al. (1998)
CD65s	Sialylated-C transmembrane protein with three IgC2-and one IgV-like domains, CEA, (immunoglobulin superfamily Dw65)	Unknown	Type 2 carbohydrate chain with four lactosamine repeats (poly-*N*-acetyllactosamines family)	Granulocytes, monocytes, some acute lymphatic leukaemia cells; in myeloid differentiation, soluble CD65 appears when CD34 disappears	Involved in phagocytsosis. Ligands include CD62E and CD62P	Monoclonal antibodies may be used to identify a subset of pre-B-type acute lymphoblastic leukaemia	Oehler et al. (1998)

CD66a	Biliary glycoprotein	140–180	Transmembrane protein with three IgC_2- and one IgV-like domains. GPI CEA linked (immunoglobulin superfamily)	Granulocytes and epithelial cells	Capable of homo- and heterophilic adhesion; CD62E binding, tumour suppression, type I fimbriae binding, transmembrane signalling, activating neutrophils	CD66a is a receptor for *Neisseria gonorroheae* and *N. meningitidis*; thought to have a tumour suppressive activity	Kammerer et al. (1999)
CD66b	CD67	95–100	Transmembrane protein with three IgC^2-and one IgV-like domains; GPI-linked CEA (immunoglobulin superfamily)	Granulocytes	Capable of homo- and heterophilic adhesion, transmembrane signalling, activating neutrophils	Unknown	Hansen et al. (1998)
CD66c	Nonspecific crossreacting antigen (NCA)	90	As for CD66a	Granulocytes and epithelial cells	As for CD66a	Neutrophil activation	Honnig et al. (1999)
CD66d	CEA gene family member-1	35	Transmembrane protein with one IgV-like domain. GPI-linked CEA (immunoglobulin superfamily)	Granulocytes	Capable of activating neutrophils; is a receptor for *N. gonorroheae* and *N. meningitidis*	CD66d may play a signalling role and regulate the adhesion activity of CD11/CD18 on neutrophils	Skubitz et al. (1997)
CD66e	CEA	180–200	Transmembrane protein with six IgC_2-and one IgV-like domains. GPI-linked CEA (immunoglobulin superfamily)	Epithelial cells	Capable of homo- and heterophilic adhesion	May play a role in metastasis of cancer cells; serum form used as an indicator of tumour burden	Obrink (1997)
CD66f	Pregnancy-specific glycoprotein (PSG)	54–72	Transmembrane protein with two or three IgC_2-and one IgV-like domains. GPI-linked CEA (immunoglobulin superfamily)	Produced in placenta (and released), fetal liver and myeloid cell lines	May be involved in immune regulation and protection of the fetus from maternal immune system	Necessary for successful pregnancy – low levels in maternal blood predict spontaneous abortion	Skubitz et al. (1999)
CD68	Gp110	110	Type I transmembrane glycoprotein (sialomucin family)	Expressed intracellularly in cytoplasmic granules but can be detected in small amounts on the surface; monocytes, macrophages, dendritic cells, neutrophils, basophils, mast cells, myeloid progenitors, $CD34^+$ subset, activated T-cells, subset of B-cells, some B-type acute lymphoblastic leukaemic cells	Unknown	Soluble forms found in serum and urine	Rittner et al. (1999)

Table 17.2 (*cont.*)

Antigen	Other names	Molecular mass (kDa)	Molecular structure (family name)	Cellular distribution	Function	Disease relevance	Reference
CD69	Activation inducer molecule (AIM)	60	Type II membrane protein with a C-type lectin domain (C-type lectin, group V family)	Expressed on activated T- and B-cells, thymocytes, NK cells, neutrophils and eosinophils; CD69 is constitutively expressed by a subset of medullary mature thymocytes, mantle B-cells and some $CD4^+$ T-cells in the germinal centres of normal lymph nodes, platelets and epidermal Langerhans cells	Signal-transmitting receptors in different cells; involved in the activation of T-cells, monocytes and platelets; also has a function in redirected lysis mediated by activated NK cells	Highly expressed on T-cells in inflammatory infiltrates in rheumatoid arthritis, viral hepatitis and autoimmune thyroiditis	Avra and Andersson (1999), Rea et al. (1999)
CD70	CD27 ligand	29	Type II membrane protein (TNF family)	Activated T- and B-cells	Costimulation of T- and B-cells	Unknown	Lens et al. (1998)
CD71	Transferrin receptor T9	190	Disulphide-bonded homodimeric type II transmembrane molecule (transferrin receptor family)	Expressed on all proliferating cells, reflecting need for iron; on reticulocytes and erythroid cells expression is related to heme synthesis	Iron uptake; ferrotransferrin binds to CD71 at neutral pH and is internalised to an acidic endosomal compartment where at pH 5 the iron is released and transported into the cytoplasm	Uptake of iron; monoclonal antibodies have also been used to target cytotoxic molecules to proliferating cells	Glasova et al. (1998)
CD72	Lyb-2	80–86	Type II transmembrane glycoprotein (C-type lectin family)	Expressed on all B-cell lineages except plasma cells; also found on spleen red pulp macrophages and liver Kupffer cells	CD72 monoclonal antibodies can induce proliferation of resting B-cells and augment the response to immobilised but not soluble anti-IgM antibody; CD72 monoclonal antibodies also increase the expression of MHC class II on resting B-cells	May be used to identify B lineage malignancies	Nadler et al. (1998)

CD73	Ecto-5'-nucleotidase	69–-72	GPI-linked protein	Expressed on subpopulations of T and B-cells, follicular dendritic cells, epithelial and endothelial cells	Possesses enzyme activity of an ecto-5'-nucleotidase and may regulate cell surface adenosine availability; can mediate lymphocyte adhesion to endothelium; has a role in B-cell interactions with dendritic cells	Associated with maturation of T- and B lymphocytes; reduced expression has been found on lymphocytes from patients with immunodeficiency caused by lymphoid maturation arrest; high expression of CD73 in lymphoid malignancies is a poor prognostic indicator	Chalmers (1999)
CD74	Invariant chain	33, 35, 41	Type II integral transmembrane molecule contains the class II binding site called CLIP (class II-associated invariant chain peptide) (unknown family)	Expressed on B-cells, activated T-cells, macrophages, activated endothelial and epithelial cells	Intracellular sorting of MHC class II molecules	Required for antigen processing	Ramachandra et al. (1999)
CD75	None	Not relevant	Carbohydrate (sialoglycan family)	Mature $smIg^+$ B-cells, germinal centre B-cells of lymphoid secondary follicle, subpopulation of T-cells, erythrocytes	Cell adhesion; ligands include CD22	Unknown	de Lau et al. (1998)
CD75s	None	Not relevant	Carbohydrate (sialoglycan sialated family)	Mature $smIg^+$ B-cells, mantal zone B-cells of lymphoid secondary follicle, subpopulation of T-cells, mature B lineage leukaemias, subset of endothelial and epithelial cells	Unknown	Unknown	Kniep et al. (1999)
CD77	Burkitt's lymphoma antigen (BLA), Gb3	1052	Neutral glycophosphingolipid	Germinal centre B lymphocytes; highly expressed on Burkitt's lymphoma cells and weakly expressed on some follicular centre lymphocytes	Crosslinking CD77 induces apoptosis in Burkitt's lymphoma cells	Unknown	Lingwood et al. (1998), Mylvaganam and Lingwood (1999)

Table 17.2 (*cont.*)

Antigen	Other names	Molecular mass (kDa)	Molecular structure (family name)	Cellular distribution	Function	Disease relevance	Reference
CDw78	None	Unknown	Unknown	Tissue macrophages, epithelium, B-cells	Antibodies	Unknown	Derbal et al. (1999)
CD79α and CD79β	Ig-a and Ig-b	82–95	Transmembrane heterodimer molecules (immunoglobulin superfamily)	B lymphocytes	Bind to Ig to constitute B-cell antigen receptors on B-cell surfaces; transmits signals into the cytoplasm on antigen binding to surface Ig; ligands include Ig, CD5, CD19 and CD22	Unknown	Alfarano et al. (1999), Dworzak et al. (1998)
CD80	B7	60	Transmembrane molecule containg one IgV and one C-type domain (immunoglobulin superfamily)	Activated T and B-cells, macrophages	Coregulator of T-cell activation with CD86; ligands include CD28 and CD152	Involved in the allo-activation of T-cells and has a critical role in autoimmune, humoral and transplant responses	Chambers and Allison (1999)
CD81	Target for antiproliferative antigen 1 (TAPA-1)	26	Molecule with four transmembrane domains (TM4 family)	Broadly expressed on hemopoietic cells; absent from erythrocytes, platelets and neutrophils. Expressed by endothelial and epithelial cells	Member of a CD19–CD21–leu-13 signal transduction complex	Regulation of cell growth	Rice (1999)
CD82	4F9, C33	45–90	Molecule with four transmembrane domains (TM4 family)	Broadly expressed on activated/differentiated hemopoietic cells; absent from erythrocytes; upregulated in T-cells by activation	Signal transduction, crosslinking promotes monocyte activation and stimulates T-cell proliferation; provides costimulatory signals for cytokine production	CD82 expression has been found to correlate with prostate cancer metastatic potential	Hammond et al. (1998), Uchida et al. (1999)
CD83	HB15	43	Transmembrane protein with a single extracellular IgV domain (immunoglobulin superfamily)	Subsets of dendritic cells and dendritic cells generated in vitro; weak expression on some lymphoblastoid cell lines and on some germinal centre B-cells in vivo	Unknown	Unknown	Cignetti et al. (1999)

CD84	None	68–80	Unknown	Mature B-cells, thymocytes and a subset of T-cells, monocytes, platelets, macrophages	Unknown	Unknown	de la Fuente et al. (1997)
CD85f CD85g CD85I CD85j	ILT2 ILT3 ILT4 ILT5	110	Immunoglobulin-like transcript (KIR family)	Plasma cells, mantle zone B-cells and germinal centre cells, hairy cell leukaemia, B-cell, subset of T-cell, monocytes, supopulation of NK cells and a few tissue macrophages	May inhibit or induce cell activation; allows immune cells to monitor class I expression on other cells and to respond to its absence; may contribute to homeostatsis	Diagnosis of hairy cell leukaemia and plasma cell neoplasms	Colonna et al. (1999)
CD86	B7-2, B70	80	Single chain transmembrane molecule with one IgV-like and one IgC_2-like domain (immunoglobulin superfamily)	Interdigitating dendritic cells in T zones of secondary lymphoid organs, Langerhans cells, memory B-cells and germinal centre B-cells, monocytes, activated T-cells and endothelial cells	CD86 acts as one of the ligands for the T-cell costimulatory molecule CD28; it also binds CD152 which transduces negative signals to T-cells	Signalling through CD28 and CD152 by engagement of CD80 and CD86 has a critical role in the induction and regulation of immune responses; blockade of CD28 signalling may have a role in the treatment of autoimmune diseases	Yu et al. (1998)
CD87	Urokinase plasminogen activator receptor (uPA)	35–59	Single-chain GPI-anchored receptor	T-cell, NK cell, monocytes, neutrophils after degranulation, vascular endothelial cells, fibroblasts, smooth muscle cells, keratinocytes, placental trophoblasts, hepatocytes and many types of tumour cell	Receptor-bound uPA can convert plasminogen to plasmin, which is bound to physically adjacent plasma membrane receptors; receptors for uPA and plasmin have been localised to the leading edge of migrating leukocytes and tumour cells, the enzyme activity of plasmin causing the pericellular hydrolysis of extracellular matrix proteins in the path of cellular invasion; CD87 may contribute to β_2-integrin-dependent adherence and chemotaxis	CD87 may contribute to the process of neoplastic and inflammatory cell invasion. In certain cancers high levels of expression of uPA content have been associated with poor prognosis	Miyake et al. (1999)

Table 17.2 (*cont.*)

Antigen	Other names	Molecular mass (kDa)	Molecular structure (family name)	Cellular distribution	Function	Disease relevance	Reference
CD88	C5a receptor	43	G-protein coupled receptor (rhodopsin family)	Granulocytes, monocytes, dendritic cells, hepatoma-derived cell line HepG2, astrocytes, microglia	C5a-mediated inflammation activation of granulocytes	CD88 appears to be necessary to protect against bacterial infections	Nataf et al. (1999)
CD89	IgA Fc receptor	45–100	Type I transmembrane glycoprotein with two extracellular IgG_2-like domains (Fc receptor, multichain immune recognition receptor family)	Myeloid lineage cells from promyelocytes to neutrophils and from promonocytes to monocytes, activated eosinophils, alveolar and splenic macrophages	Induces phagocytosis, degranulation, respiratory burst and killing of microorganisms	Binds both monomeric and polymeric forms of either IgA_1 or IgA_2 at boundary between Cα2 and Cα3 domains	Valerius et al. (1997), van Spriel et al. (1999)
CD90	Thy-1	25–35	Single Ig domain GPI-anchored (immunoglobulin superfamily)	Hemopoietic stem cells, neurons, fibroblasts, stromal cells, high endothelial venule endothelium but not other endothelia, some lymphoblastoid and leukaemic cell lines	May contribute to inhibition of proliferation differentiation of hemopoietic stem cells and neuron memory in the central nervous system; ligands include CD45, Lck, Fry, P100	May have potential for inhibiting hemopoietic development and for controlling neuron formation in the brain	Sandel and Monroe (1999)
CD91	α_2-Microglobulin receptor/LDL receptor-associated protein	600	Transmembrane molecule with two subunits (LDL receptor family)	Neurons, hepatocytes, fibroblasts, macrophages, synctiotrophoblasts, monocytes, erythroblasts/reticulocytes	Endocytosis-mediating receptor expressed in coated pits; ligands include α_2-microglobulin–proteinase complexes, plasminogen activator (free or complexed with inhibitors), lipoprotein lipase, β-amyloid precursor protein, thrombospondin, receptor-associated protein, which is required for normal processing of the receptor	Regulation of extracellular proteolytic activity and lipoprotein levels; receptor has a nutritional role; high expression of the receptor is seen in plaques in the brain of patients with Alzheimers's disease and atherosclerotic lesions. Knockout of genes in mice is lethal	

CDw92	None	70	(Unknown family)	Monocytes, granulocytes, myeloid cell lines, lymphocytes, fibroblasts, endothelial cells, epithelial cells	Unknown	Unknown	Ghannadan et al. (1998)
CDw93	None	110	*O*-Sialyglycoprotein (unknown family)	Monocytes, granulocytes, myeloid cell lines, endothelial cells, cells in acute myeloblastic leukaemia	Unknown	Unknown	Pickl et al. (1996)
CD94	Kp43	70	Type II transmembrane protein with an extracellular C-type lectin domain (C-type lectin family)	NK cells, subsets of $CD8^+$ $\alpha\beta^+$ and $\gamma\delta^+$ T-cells, activated NK cells	The CD94–natural killer glycoprotein 2-A (NKG2-A) complex is involved in inhibition of NK-cell function; ligands include NKG2-A (kp43) and p39	Unknown	Lopez-Botet et al. (1999)
CD95	Apolipoprotein 1 (APO-1), Fas	45, 90, >200	Type I transmembrane molecule with an intracytoplasmic death domain (TNF/NGF family)	Activated T- and B-cells	Mediation of apoptosis-inducing signals	One of the receptor molecules mediating apoptosis of targets by cytotoxic T-cells	Schwartz et al. (1999)
CD96	T-cell activation increased late expression (TACTILE)	160	Type I membrane glycoprotein (immunoglobulin superfamily)	Activated T- and NK cells, helper and cytotoxic T-cell lines and clones and some transformed T-cell lines	Adhesion of activated T- and NK cells during the late phase of the immune response	Unknown; ligands include CD55	Hamann et al. (1998), Kalden et al. (1998)
CD97	None	74–89	Transmembrane protein with three EGF domains with EGF (Glu-Gly-Asp) domains (seven-span transmembrane proteins (TM7) family)	Activated T- and B-cells, monocytes and granulocytes	Unknown; ligands include CD55	Unknown	Hoang-Vu et al. (1999)
CD98	4F2, FRP-1	125	Disulphide-linked heterodimer (unknown family)	Broad activity on activated and transformed cells; not hemopoietic specific and found at lower levels on quiescent cells	Involved in the regulation of cellular activation; ligands include actin; may act as an amino acid transporter	Upregulated on leukocytes in inflammatory lesions, strongly expressed by neoplastic cells	Tsurudome et al. (1999)
CD99 and CD99R	E2 (*MIC2* gene product)	32	Single-type transmembrane chain (no family established)	Expressed on all hemopoietic cells and many other cell types; not expressed on fetal B-cells	Modulation of T-cell adhesion, via CD2 pathway; induction of homotypic adhesion of corticothymocytes; induction of apoptosis of $CD4^+CD8^+$ $CD3^{int}CD69^+$ thymocytes	Allows differential diagnosis within round cell sarcomas in children; increased density on peripheral $CD8^+$ T-cells from HIV-positive patients	Waclavicek et al. (1998)

Table 17.2 (*cont.*)

Antigen	Other names	Molecular mass (kDa)	Molecular structure (family name)	Cellular distribution	Function	Disease relevance	Reference
CD100	None	120, 300	Homodimer (semaphorin, immunoglobulin family)	Most hemopoietic cells except immature bone marrow cell, erythrocytes and platelets; increase expression on activated T-cells; expressed on germinal centre B-cells but not mantle zone B-cells	Augments proliferative response of T-cells to mitogens; increases CD45-induced T-cell adhesion; induces B-cell homotypic adhesion and downregulates B-cell expression of CD23. Ligands include CD45	Unknown	Delaire et al. (1998), Dorfman et al. (1998)
CD101	V7, P126	240	Transmembrane molecule with seven extracellular IgV-like domains (immunoglobulin family)	Monocytes, granulocytes, dendritic cells; activated T-cells	Involved in allogeneic T-cell responses and T-cell proliferation	Unknown	Soares et al. (1998)
CD102	ICAM-2	55–65	Type I membrane protein with two extracellular IgG2-like domains (immunoglobulin family)	Vascular endotheial cells, some resting lymphocytes, monocytes, platelets	Providing costimulatory signal in immune response, lymphocyte recirculation	Unknown; ligands include LFA-1 and CD11b/CD18	Casasnovas et al. (1999), Salomon and Bluestone (1998)
CD103	HML-1, integrin α_E-chain	175	Type I transmembrane protein (integrin α-chain)	Expressed on 90% of intestinal intraepithelial lymphocytes, 40% of lamina propria T lymphocytes, majority of intraepithelial lymphocytes in extraintestinal sites, 0.5–5% of lymphocytes in peripheral blood and peripheral lymphoid organs, enteropathy-associated T-cell lymphomas, hairy B-cell leukaemia and adult T-cell leukaemias associated with human T-cell leukaemia virus; expression is induced by activation and TGF-β_1	Tissue-specific retention of lymphocytes at basolateral surface of intestinal epithelial cells, possible accessory function for activation of intraepithelial lymphocytes. Ligands include E-cadherin and β_7 integrin	Localisation of intestinal intraepithelial lymphocytes	Rostapshova et al. (1998)

CD104	Integrin β_4-chain	205	Transmembrane glycoprotein noncovalently associated with α_6-integrin (CD49f) to form $\alpha_6\beta_4$ -integrin (integrin family)	Epithelial cells, Schwann cells, keratinocytes, some tumour cells, some endothelial cells, neuronal cells, monocytes, $CD4^{-}CD8^{-}$ pre-T-cells and trophoblasts; also expressed in tonsil, spleen, breast, tongue, colon, lung, ovary and foreskin tissues, especially along the basement membrane	Cell adhesion to several laminins; hemidesmosome formation; cell migration toward basement membrane; stabilisation of dermal–epidermal junction; growth arrest of epithelial cells; differentiation of epithelial cells, Schwann cells and thymocytes; tumour metastasis and progression	Important role in wound healing, associated with embryogenesis/ development and tumour metastasis/ progression; CD104 knockout mice die soon after birth	Patel et al. (1995)
CD105	Endoglin	180	Type I integral membrane homodimeric protein (TGF-β receptor type III family)	Small and large vessel endothelial cells, activated monocytes and tissue macrophages, bone marrow stromal cells, pre-B-cells in fetal marrow, erythroid precursors in fetal and adult bone marrow, syncytiotrophoblast throughout pregnancy	Modulator of cellular responses to TGF-β_1; ligands include TGF-β_1 and TGF-β_3	Endoglin is the target gene for hereditary hemorrhagic talen-giectasia type 1	Barbara et al. (1999), Miller et al. (1999)
CD106	VCAM-1	110	Transmembrane molecule containing variable number of IgC_2-type domains (immunoglobulin superfamily)	Activated endothelium, follicular dendritic cells, some tissue macrophages, interdigitating cells, synoviocytes	Leukocyte adhesion, transmigration and costimulation of T-cell proliferation	Anti-VCAM monoclonal antibodies have been used as anti-inflammatory agents with some success	McCrohon et al. (1999)
CD107a	LAMP-1	100–120	Transmembrane protein (unknown family)	Lysosomal membrane, degranulated platelets; phytohaemagglutinin-activated T-cells, fMLP-activated neutrophils	Unknown	Highly metastatic tumour cells express more LAMP molecules on the cell surface than poorly metastatic cells	Ji et al. (1998)
CD107b	LAMP-2	100–120	Transmembrane protein (unknown family)	Lysosomal membrane, degranulated platelets, TNF-α-activated endothelium, fMLP-activated neutrophils	Unknown	Highly metastatic tumour cells express more LAMP molecules on the cell surface than poorly metastatic cells	Akasaki and Tsuji (1998)

Table 17.2 (*cont.*)

Antigen	Other names	Molecular mass (kDa)	Molecular structure (family name)	Cellular distribution	Function	Disease relevance	Reference
CDw108	John–Milton–Hagen (JMH) human blood group antigen	76	GPI-anchored protein (unknown family)	Erythrocytes, peripheral blood lymphocytes, lymphoblasts and lymphoblastic cell lines	Possible role in adhesion; ligands include tyrosine kinases	Deficiency of erythroid CDw108 has been associated with a rare form of congenital dyserythropoietic anaemia	Mudad et al. (1995)
CD109	8A3, 7D1	170	Single-chain GPI-anchored glycoprotein (unknown family)	Activated T-cells, activated platelets, vein and artery endothelial cells, megakaryocytes, $CD38^{+}CD34^{+}$ progenitors, some epithelial cells	Unknown	Reconstitution of hemopoiesis	Kelton et al. (1998)
CD110	Receptor for thrombopoietin (MPL)	35	Glycoprotein (unknown family)	Platelets and megakaryocytes	Product of the proto-oncogene c-*mpl*, receptor for thrombopoietin, which regulates platelet production and activation	Potential to manipulate blood cell development for therapeutic benefit	Kaushansky (1999)
CD114	G-CSFR	130	Single-chain type I transmembrane molecule; cytokine receptor, hematopoietin receptor (class I cytokine receptor family)	All stages of granulocyte differentiation, on monocytes and platelets at different levels, endothelial cells, placenta, trophoblastic cells, many cultured tumour cells	Specific regulator of myeloid proliferation and differentiation; ligands include G-CSF, Jak1, Jak2	Target for enhancing recovery of myelopoiesis in patients after chemotherapy. Target for hemopoietic stem cell and progenitor cell mobilisation for peripheral blood stem cell transplantation. Target of G-CSF treatment in patients with severe chronic neutropenia. G-CSF receptor mutations have been found in some patients with severe congenital neutropenia	Root and Dale (1999)

CD115	Macrophage colony-stimulating factor (M-CSF) receptor, c-Fms, colony-stimulating factor 1 (CSF-1)	150	A single polypeptide chain encoded by the c-*fms* proto-oncogene containing five Ig domains (subclass II receptor tyrosine kinase family; this family includes the PDGF receptor and c-Kit)	Mature and progenitor myeloid cells, osteoclasts, placental trophoblasts, choriocarcinoma and breast carcinoma cells in nonhemopoietic tissues; no expression detected on dendritic cells	Receptor for M-CSF (CSF-1)	Mutations of the gene for CD115 have been associated with hemopoietic malignancies	Terashi et al. (1999)
CD116	GM-CSF receptor α-subunit	80	Type I transmembrane protein (class I cytokine family)	Myeloid cells including macrophages, neutrophils, eosinophils, dendritic cells and their precursors	The primary binding subunit of the GM-CSF receptor; ligands include CDw131, IL-3 and IL-5	Unknown	Alexander and Nicola (1998)
CD117	Stem cell factor (SCF), receptor, c-Kit	145	Transmembrane protein containing five Ig-like domains; receptor for tyrosine kinase (type 3) immunoglobulin family)	Hemopoietic stem and progenitor cells, acute myeloid leukaemia cells, tissue mast cells, melanocytes, reproductive system, embryonic brain	Growth factor receptor; soluble form exists in serum, function unknown	CD117 loss results in piebaldism; CD117 is ectopically expressed in small-cell lung cancer and mutated and constitutively active in systemic mastocytosis	Nombedeu et al. (1999)
CDw119	INF-γ receptor α-chain, INF-γ receptor β chain	90	Type I transmembrane polypeptide (class II family of cytokine receptors)	Expressed on the surface of all cells and tissues examined	The IFN-γ receptor transduces IFN-γ-dependent biological signals; IFN-γ is a pleiotropic cytokine that plays important roles in promoting host defence and immunopathological processes	Mutations in the gene for the IFN-γ receptor α-chain result in enhanced susceptibility to mycobacterial infections	Bach et al. (1997)
CD120a, CD120b	TNF receptor type I/II (p55/p75)	55–75	Type I transmembrane molecule with a C-terminal death domain (TNF receptor superfamily)	Expressed on most cell types and tissues	Programmed cell death and antiviral activities	TNF induces fever, shock, tissue injury, tumour necrosis, anorexia, production of other cytokines and immunoregulatory molecules, cell proliferation, differentiation and apoptosis	Koubek et al. (1998)

Table 17.2 (*cont.*)

Antigen	Other names	Molecular mass (kDa)	Molecular structure (family name)	Cellular distribution	Function	Disease relevance	Reference
CD121a	IL-I receptor type I	75–85	Single-chain transmembrane molecule, (extracellular portion is in the immunoglobulin superfamily)	Expressed on virtually all cells	Mediates IL-1 signals	Unknown	Beil et al. (1998)
CDw121b	IL-I receptor type II	60–68	Single-chain transmembrane molecule (extracellular portion is in the immunoglobulin superfamily)	Expressed on B-cells, myeloid cells, some T-cells and some basal epithelial cells	Acts as a negative regulator of IL-1; it is often shed from the cell surface and can also bind IL-1 in the soluble form	Elevated levels of soluble CDw121b are found in sepsis	Yamada et al. (1997)
CD122	IL-2 receptor β-chain (IL-2Rβ)	70–75	Long single-chain type I transmembrane molecule (cytokine receptor family)	T- and B-cells, NK cells, monocytes and macrophages	Critical component of IL-2- and IL-15-mediated signalling	Involved in autoimmune disease and NK cell function	Cipres et al. (1999)
CD123	IL-3 receptor α-chain (IL-3Rα)	70	Single-chain type I transmembrane molecule (class I cytokine receptor family)	Most myeloid cell lineages including progenitors, endothelial cells	The primary binding subunit of the IL-3 receptor	Unknown	Koubek et al. (1998)
CD124	IL-4 receptor (IL-4R)	140	Single-chain transmembrane molecule (cytokine receptor family)	Hemopoietic and nonhemopoietic cells express IL-4; expression is increased upon activation	Receptor subunit for IL-4 and IL-13	IL-4, the ligand of CD124, plays an important role in the induction of T helper 2 cells and IgE class switch	Yamashita et al. (1999)
CDw125	IL-5 receptor α-chain (IL-5Rα)	60	Single-chain type I transmembrane protein (cytokine receptor family)	Eosinophils, activated B-cells and basophils	Low-affinity receptor for IL-5 α-subunit	Therapeutic target of eosinophilic inflammation involved in bronchial asthma	Toba et al. (1999)

CD126	IL-6 receptor (IL-6Rα)	80	Single-chain type I transmembrane molecule (class I cytokine receptor, immunoglobulin superfamily)	T-cells, monocytes, activated B-cells, hepatocytes and some other nonhematopoietic cells	Required in association with gp130 CD130 for mediating biological activities of IL-6; a soluble form exists which, when complexed to IL-6, is able to carry out trans-signalling	Dysregulated autocrine or paracrine stimulation of CD126 leads to myeloma and plasmacytoma; continuous expression of IL-6 causes hypergamma-globulinaemia, glomeruloproliferative nephritis, lymphoid infiltration in some organs, extramedullary hematopoiesis	Muller-Newen et al. (1998)
CD127	IL-7 receptor α-chain (IL-7Rα)	65–90	Single-chain transmembrane protein (cytokine receptor family)	B-cell precursors, majority of T-cells, expression on T-cells is downregulated following activation	Specific receptor for IL-7	Required for lymphoid differentiation and proliferation	Koubek et al. (1998)
CDw128	IL-8 receptor type A and B (IL-8R)	44–59	Transmembrane molecule (chemokine receptor family)	Neutrophils, monocytes, NK cells, astrocytes, microglia, a minor group of $CD8^+$ T-cells; type A expressed on endothelial cells, fibroblasts and platelets; type B expressed on melanocytes	Critical regulator of IL-8-mediated neutrophil chemotaxis and activation; a potential role in angiogenesis has been proposed	Targeted disruption of the IL-8 gene results in lymphadenopathy owing to increased B-cells, increased bone marrow cellularity and inhibition of neutrophil migration into the peritoneum	Koubek et al. (1998)
CD130	Gp130	130–140	Single-chain type I transmembrane molecule (class I of the cytokine receptor family)	Expressed at low level on almost all cell types	Required for inducing biological activities of IL-6, IL-11, leukaemia inhibitory factor (LIF) ciliary neutrophil factor (CNF), oncostatin M and cardiotrophin I	Activation of gp130, IL-6 and oncostatin M, has been shown to be involved in multiple myeloma	Koubek et al. (1999)
CDw131	Common β-subunit	120–140	Single-chain type I transmembrane molecule (class I of the cytokine receptor family)	Most myeloid cells including early progenitors, early B-cells	Signal-transducing molecule of the IL-3, IL5 and GM-CSF receptors	Involved in alveolar proteinosis and maintaining peripheral eosinophils	Hibi and Hirano (1998)

Table 17.2 (*cont.*)

Antigen	Other names	Molecular mass (kDa)	Molecular structure (family name)	Cellular distribution	Function	Disease relevance	Reference
CD132	Common γ-chain	65–70	Single-chain type I transmembrane molecule (class I of the cytokine receptor family)	T and B-cell, NK cells, monocytes, macrophages and neutrophils	Receptor for IL-2, IL-4, IL-7, IL-9 and IL-15; signalling for these cytokines, coupling to Jak3	Mutations cause X-linked severe combined immunodeficiency, a disease characterised by an absence of T and NK cells	Kumaki et al. (1999)
CD134	OX40	48–50	Type I integral membrane protein (TNF/NGF superfamily)	Activated $CD4^+$ T-cells, small populations of macrophages in Langerhan cell histocytosis and on a few blasts in B-cell nonHodgkin's lymphoma	Costimulatory signal transducer of TCR-mediated activation, cell adhesion	Marker of rheumatoid arthritis and acute graft-versus-host disease	Weinberg et al. (1999)
CD135	FLT3	130	Type III receptor tyrosine kinase (tyrosine kinase receptor family)	Expressed on multipotential, myelomonocytic and primitive B-cell progenitors	Growth factor receptor for early hemopoietic progenitors	Expressed on most acute myeloid leukaemia, acute lymphoblastic leukaemia and chronic myeloid leukaemia in blast phase. Expression is related to the risk of relapse in childhood ALL	Xiao et al. (1999)
CDw136	Macrophage-stimulating protein receptor (MSP-R)	180	Heterodimeric protein (tyrosine kinase receptor family)	Epithelial tissues, skin, kidney, lung, liver, intestine and colon; some established hemopoietic and neuroendocrine cells	Induction of migration, morphological change and proliferation in different target cells	Involved in wound healing and inflammation	Nanney et al. (1998), Willett et al. (1998)
CDw137	Induced by lymphocyte activation (ILA)	85	Type I transmembrane protein (TNF family)	Expression induced on T-cell, B-cells, monocytes, epithelial cells and hepatoma cells	Costimulator of T-cell proliferation	Unknown	Schwarz et al. (1997)

CD138	Syndecan-1, heparan sulphate proteoglycan	80–300	Membrane intercalated type I receptor (syndecans (1–4) family)	Expressed on various epithelia, pre-B-cells and plasma cells, sprouting capillaries of wound tissue and neuronal cells at injuries	Maintenance of cell morphology through interactions and receptor cooperation with extracellular matrix; coreceptor for growth factor signalling receptors	Syndecan-1 is lost when several stratified epithelia become malignant; this loss correlates with poor prognosis in patients	Gattei et al. (1999)
CD139	None	209	Unknown	Monocytes, granulocytes, erythrocytes, variable on B-cells, some myeloid cell lines, follicular dendritic cells, glomeruli and smooth muscle	Unknown	Expression in B-cell chronic lymphocytic leukaemia thought to indicate a good prognosis	Hadam (1998)
CD140a, CD140b	PDGF α-receptor	160–180	Single-chain transmembrane protein (split tyrosine kinase family)	CD140a is expressed on mesenchymal cells, fibroblasts, smooth muscle cells, numerous cancer cells and platelets; CD140b is expressed on mesenchymal cells, fibroblasts, smooth muscle cells, numerous cancer cells, monocytes, neutrophils and some microvascular endothelial cells	The PDGF receptors are involved in signal transduction associated with PDGF ligand binding; primary functions include stimulation of cell proliferation and migration	Involved in the development of intimal hyperplasia associated with acute injury; stimulator of wound healing; thought to play a role in cancer development	Valgeirsdottir et al. (1998)
CD141	Thrombomodulin (TM)	75	Single-chain type I membrane glycoprotein (C-type lectin family)	Endothelial cells, keratinocytes, megakaryocytes, platelets, monocytes, neutrophils, smooth muscle cells and synovial lining cells	Cofactor for thrombin-mediated activation of protein C and for thrombin activation of template-activating factor 1 (TAF-1) complete activating factor-1 which allows cleavage of C-terminal lysines from fibrin which decreases activation of plasminogen to plasmin	Plasma CD141 levels are indicative of endothelial cell damage; a few families with hypercoagulation disorders have been identified with CD141 gene mutations	Mutin et al. (1997)

Table 17.2 (*cont.*)

Antigen	Other names	Molecular mass (kDa)	Molecular structure (family name)	Cellular distribution	Function	Disease relevance	Reference
CD142	Tissue factor, thromboplastin, coagulation factor III	45–47	Single chain type I transmembrane protein (serine protease cofactor family)	Epidermal keratinocytes, glomerular epithelial cells, adventitial cells of blood vessels, astrocytes, myocardium, Schwann cells of peripheral nerves and stromal cells of organs such as liver, pancreas, spleen and thyroid	The 1 : 1 complex of CD142 and factor VIIa is the enzyme that initiates the clotting cascade; expression on the cell surface confers a procoagulant phenotype	CD142 is the major initiator of clotting in normal hemostasis and thrombotic diseases; antibodies to CD142 protect animals against lethality of septic shock	Brauner et al.(1998), Vickers et al. (1998)
CD143	Angiotensin-converting enzyme (ACE)	90–180	Type I transmembrane polpeptide (gluzincin, peptidylpeptidase family)	Endothelial cells, epithelial cells, neuronal cells, mesenchymal tissue, fibroblasts, adventitia of vessels, activated macrophages, histiocytes, Kupffer cells in liver, some T-cells and immature chondrocytes	CD143 acts as a peptidyl dipeptide hydrolase and is involved in the metabolism of two major vasoactive peptides, angiotensin II and bradykinin; CD143 also cleaves C-terminal dipeptides from various oligopeptides and protected tri-peptides from substance P and luteinising hormone releasing hormone (LH-RH)	There is a polymorphism in the gene for CD143 consisting of the insertion (I) or deletion (D) of a 287 bp DNA fragment in intron 16. The DD genotype is associated with myocardial infarction, strokes, diabetic nephropathy and other cardiovascular complications	Hagaman et al. (1998)
CD144	VE-cadherin	135	Transmembrane molecule (cadherin family)	Expressed only in endothelium	VE-cadherin organises adherent junctions in endothelial cells with control endothelial cell–cell adhesion and permeability migration and are responsible in part for contact inhibition of cell growth	Expression is reduced in human angiosarcomas	Yang et al. (1999b)

CDw145	None	110, 90, 25	Unknown	Expressed on endothelial cells, on THP-1 and some stromal cells	Unknown	Unknown	Mutin et al. (1997)
CD146	Melanoma cell adhesion molecule (MCAM) , Muc 18, S-ENDO, Mel-CAM	118	Transmembrane molecule with five Ig-like domains (immunoglobulin superfamily)	Endothelial cells, melanoma, smooth muscle, intermediate trophoblast, subpopulation of activated T-cells	Potential adhesion molecule	Marker of melanoma progression: expression confers increased tumourigenicity	Neidhart et al. (1999)
CD147	Intracellular matrix metalloproteinase inducer (EMMPRIN)	50–60	Single-chain type I transmembrane molecule containing two Ig-like domains (immunoglobulin superfamily)	All leukocytes, erythrocytes, platelets and endothelial cells	Potential adhesion molecule, some monoclonal antibodies inhibit MCF-7 cell aggregation and adhesion to type IV collagen, laminin and fibronectin	Expression is upregulated on granulocytes from rheumatoid and reactive arthritis patients	Guo et al. (1998)
CD148	High cell density enhanced protein tyrosine phosphatase (RPTPase)	200–260	Single-chain type I transmembrane protein (RPTPase type III phosphatase family)	Granulocytes, monocytes, resting T-cells, dendritic cells, platelets, fibroblasts, nerve cells, Kupffer cells; upregulated upon activation	Inhibition of CD3-mediated T-cell activation	May be involved in contact inhibition of cell growth	Koch et al. (1999)
CDw149	MEM-133	120	Unknown	Peripheral blood lymphocytes, monocytes, neutrophils, eosinophils, various hemopoietic cell lines	Unknown	Unknown	Ghannadan et al. (1998)
CD150	Signalling lymphocyte activation molecule (SLAM)	65–85	Single-chain type I transmembrane molecule with three Ig-like domains (immunoglobulin superfamily)	Thymocytes, $CD45RO^+$ T-cells, B-cells, dendritic cells, endothelial cells; upregulated after activation	Costimulatory molecule on B-cells and dendritic cells; ligand binding to B-cells enhances proliferation and Ig production	Unknown	De Vries et al. (1999), Sayos et al. (1998)
CD151	Platelet-endothelial tetrasspan antigen 3 (PETA-3), SFA-1	32	Transmembrane molecule (TM4 superfamily)	Endothelial cells, platelets, megakaryocytes, immature hemopoietic cells, epithelial cells	Homotypic adhesion, may modify integrin function or signalling	Some monoclonal antibodies cause platelet activation and aggregation	Sincock et al. (1999)
CD152	Cytotoxic lymphocyte-associated protein 4 (CTLA-4)	46–50	Transmembrane disulphide linked homodimer (immunoglobulin superfamily)	Activated T- and B-cells, not resting cells	High avidity receptor for CD80 and CD86 molecules, which are also ligands for CD28; CTLA-4 is believed to be a negative regulator of T-cell activation	May play a role in autoimmune diseases	Chambers and Allison (1999)

Table 17.2 (*cont.*)

Antigen	Other names	Molecular mass (kDa)	Molecular structure (family name)	Cellular distribution	Function	Disease relevance	Reference
CD153	CD30 ligand, CD30L	70–75	Transmembrane molecule (TNF superfamily)	Activated T-cell, activated macrophages, neutrophils, normal and malignant B-cells	Costimulates T-cell proliferation, enhances antigen specific cytokine production	CD30L may play a role in the maintenance of Reed–Sternberg cells in Hodgkin's lymphoma. Plays a role in thymic selection Fas-independent cell death	Shimozato et al. (1999)
CD154	CD40 ligand (CD40L)	28, 30, 33	Type II integral membrane glycoprotein (TNF/NGF ligand superfamily)	Expressed on activated $CD4^+$ T-cells	Inducer of B-cell proliferation and activation; is essential for Ig secretion and class switching in the presence of cytokines, notably IgE; regulates T-cell dependent IL-12 production by antibody-presenting cells and the development of T helper type 1 effector cells	Mutations in the gene for CD40L cause a rare X-linked immunodeficiency syndrome with humoral and cellular defects	Weinberg et al. (1999)
CD155	Polio virus receptor (PVR)	80–90	Transmembrane protein with tyrosine activation motif (immunoglobulin superfamily)	Monocytes	Negative regulation of CD44 mediates hyaluronan binding in monocytes	Unknown	Lopez et al. (1998)
CD156h CD156q	A disintegrin and metalloprotease (ADAM8/DNAM-1, ADAM17/TACE)	65 69	Long single-chain type I transmembrane molecule; a disintegrin and metalloproteinase	Neutrophils and monocytes; upregulated by retinoic acid and vitamin D_3	Possible involvement in extravasation of leukocytes	Inflammation	Yoshiyama et al. (1997)

CD157	Mo5	42–50	Single-chain GPI-anchored molecule (ADP-ribosyl cyclase family)	Granulocytes, monocytes, lymphoid progenitors, bone marrow stromal cells, myelomonocytic leukaemia, umbilical vein endothelial cells, synovial cells, follicular dendritic cells and reticular cells of peripheral lymphoid tissues	Supports the growth and development of progenitor cells	The level of CD157 on bone marrow stromal cells is higher in rheumatoid arthritis than in normals; high levels of serum soluble CD157 have also been detected in patients with severe rheumatoid arthritis	Sato et al. (1999)
CD158a	MHC class I specific receptors, p58.1, p50.1, (NKG2A)	50, 58	Type I glycoproteins with two Ig-like domains (immunoglobulin superfamily)	NK cell subsets and rare T-cells	Regulation of NK cell-mediated cytolytic activity upon interaction with the appropriate HLA-C alleles	Unknown	Colonna et al. (1999), Frohn et al. (1997)
CD158b	P58.2, p50.2	50, 58	Type I glycoproteins with two Ig-like domains (immunoglobulin superfamily (KIR))	NK cell subsets and rare T-cells	Regulation of NK cell-mediated cytolytic activity upon interaction with the appropriate HLA-C alleles	Unknown	Poggi et al. (1999)
CD158e	KIR3DL1/SS		As CD158a				
CD158h	KIR2DS4		As CD158a				
CD158k	KIR3DL2		As CD158a				
CD160	BY55/MHC-1 ligand	27 and 80 dimer	GPI-linked transmembrane protein (immunoglobulin superfamily)	NK cells, $CD8^+$ T-cell subset, intestinal intraepithelial T-cells	Ligand for classical and nonclassical MHC class I molecules	Important for host immune responses and cell-mediated cytotoxicity	Agrawal et al. (1999)
CD161	NK receptor PIA	80	Type II membrane glycoprotein expressed as a disulphide-bonded homodimer (C-type lectin group V family)	NK cells, subsets of $CD4^+$ and $CD8^+$ T-cells, preferentially expressed on T-cells with 'memory' phenotype, also on thymocytes and fetal liver T-cells	Undefined CD161 monoclonal antibodies have been reported either to augment or to inhibit NK cell-mediated cytotoxicity against certain Fc receptor-bearing targets and to induce immature thymocyte proliferation	Unknown	Azzoni et al. (1998)
CD162	P-selectin glycoprotein ligand 1 (PSGL-1)	160–250	Transmembrane molecule that forms a disulphide bonded homodimer (sialomucin, mucin family)	Most peripheral blood T-cells, monocytes, granulocytes, some B-cells and some $CD34^+$ bone marrow cells	PSGL-1 mediates rolling of leukocytes on activated endothelium, on activated platelets and on other leukocytes at inflammatory sites; ligands include CD62P, CD62E, CD62L	PSGL-1 plays a role in trafficking of T-cells and neutrophils	Moore (1998)

Table 17.2 (*cont.*)

Antigen	Other names	Molecular mass (kDa)	Molecular structure (family name)	Cellular distribution	Function	Disease relevance	Reference
CD162R	PEN5 epitope	120–170, 210–245	Sulphated polylactosamine carbohydrate (unknown family)	Subpopulation of mature NK cells, neuronal cells, astrocytes	Protein carrier is P-selectin glycoprotein ligand-1 (PSGL-1)	Differentiation of oligodendrocytes	Figarella-Branger et al. (1999)
CD163	M130	110	Single chain transmembrane protein (scavenger receptor superfamily)	Expressed by the majority of tissue macrophages but is absent from dendritic cells, interdigitating reticulum cells, Langerhans cells, tingible body macrophages and macrophages in the mantle and marginal zones of lymphoid tissue	CD163 is believed to be involved in differentiation and/or activation	CD163 may be of value in diagnosis of myeloid leukaemia	Droste et al. (1999)
CD164	Multiglycosylated core protein of 24 000 M_r (MGC-24)	160	Type I integral membrane glycoprotein (unknown family)	Monocytes, bone marrow stromal cells, a variety of normal and neoplastic epithelial tissues	CD164 is thought to mediate adhesion between bone marrow stromal cells and hemopoietic progenitor cells	Negative regulator of hematopoiesis	Watt et al. (1998)
CD165	AD2, gp37	37	Membrane glycoprotein (unknown family)	Subset of peripheral lymphocytes, immature thymocytes, monocytes, the majority of platelets, many T-cell type acute lymphoblastic leukaemias, neurons, islet cells and Bowman's capsule	Mediates adhesion between thymocytes and thymic epithelial cells	Highly expressed on many T-cell leukaemias; CD165 monoclonal antibodies may have therapeutic potential	Bruggers et al. (1995)
CD166	Activated leukocyte adhesion molecule (ALCAM)	100–105	Transmembrane protein with five Ig-like domains (immunoglobulin superfamily)	Neurons, activated T-cells, activated monocytes, epithelial cells and fibroblasts	Adhesion molecule that binds to CD6; involved in neurite extension by neurons via hetero- and homophilic interactions	May have a role in neurodegenerative diseases such as multiple sclerosis	Bowen and Aruffo (1999)

CD167a	Discoidin domain receptor	67	Glycoprotein (tyrosine kinase family)	Lymph node epithelia	Binds and is activated by collagen; adhesion and ordered cell migration during aggregation	Control of cellular responses to the extracellular matrix	Vogel et al. (1997)
CD168	Receptor for hyaluronan-mediated motility (RHAMM)	85–90	Filamentous protein, receptor for hyaluronan (unknown family)	Progenitor cells and B-cell lineage cells	Controls motility of cells	Increased expression on B-cells in various types of malignancies including chronic lymphoblastic leukaemia, myeloma, and Crohn's disease	Till et al. (1999)
CD169	Sialoadhesin, sheep erythrocyte receptor	65	(Immunoglobulin superfamily)	Bone marrow stromal macrophage	Binding to sialylated ligands	Control of signal transduction in tumour cells	Kusmartsev et al. (1999)
CD170	Sialic acid-binding Ig-like lectin 5 (Siglec 5)	140	(Immunoglobulin superfamily)	Neutrophils	Binding to sialylated ligands		Cornish et al. (1998)
CD171	Neural cell adhesion molecule L1	220	(Immunoglobulin superfamily)	Neuronal cells	Homophilic binding and neurite out growth	Impaired neuron development	Hortsch (2000)
CD172a	Signal regulatory protein (SIRP) α and β	40–50	Glycoprotein (unknown family)	SIRPα on lymphoid cells; SIRPα myeloid and neural cells; heterophilic adhesion ligands include CD47	Cellular activation tyrosine kinase signalling at neuronal synapses	Integrin function, host defence and neutrophil migration	Seiffert et al. (1999)
CD173	Histo blood group H type 2	148	Blood group antigen (unknown family)	Erythrocytes, $CD34^+$ progenitor cells	May be involved in hematopoiesis	Expressed in basal cell type carcinomas	Cao et al. (2000a)
CD174	Lewis y	52	Blood group antigen (unknown family)	Variety of cells	Function unknown; expression may be associated with viral infection	Associated with outcome of various malignancies	Mehdi et al. (1998)
CD175	Tumour-associated antigen (TN) TN	110	Apomucin (unknown family)	Cancer-associated carbohydrate	Derived from aberrant glycosylation of apomucins, allows invasion of tumour cells	Associated with the aggressiveness of malignant neoplasms	Sasaki et al. (1999)

Table 17.2 (*cont.*)

Antigen	Other names	Molecular mass (kDa)	Molecular structure (family name)	Cellular distribution	Function	Disease relevance	Reference
CD175s	Sialyl-TN (tumour-associated antigen)	110	Apomucin (unknown family)	Cancer-associated carbohydrate	As CD175	As CD175	Sasaki et al. (1999)
CD176	Thomsen–Friedenreich (TF)-related carbohydrate antigen	68–79	Oligosaccharide (unknown family)	Malignant cells, including leukaemia, lymphoma, epithilium, normal tonsillar lymphocytes	Unknown	Metaplastic differentiation is associated with sialyation of TF	Cao et al. (2000b)
CD176s	Sialyl-TF (Thomsen–Friedenreich (TF)-related carbohydrate antigen)	116–56	Oligosaccharide (unknown family)	As CD176	Unknown	As CD176	Cao et al. (2000b)
CD177	Neutrophil B1 antigen (NB1)	58–64	Neutrophil-specific antigen (unknown family)	Myelocytes, metamyelocytes, band cells and a subpopulation of mature neutrophils	Associated with myeloid differentiation	Antigenic determinant for antibodies in allo- and autoimmune neutropenia	Stroncek et al. (1998)
CD178	Fas ligand	45	Neutrophil-specific antigen (unknown family)	T and B lymphoid cells	Role in apoptosis	May play a role in autoimmune disorders such as diabetes mellitus	Sainio-Pollanen et al. (1998)
CD179a	Vpre-beta	18	Pre-BCR (unknown family)	B-lineage cells	The pre-BCR is composed of VpreB, λ_5, surrogate light chain (SL) and μ_H-chain and plays a critical role in B-cell development	B-lineage acute lymphoblastic leukaemia may be divided into five subtypes based on the differential expression of SL chain, μ_H chain, pre-BCR and light chain	Karusuyama et al. (2000)
CD179b	∝5	20	Pre-BCR (unknown family)	B-lineage cells	See CD179a	See CD179a	Karusuyama et al. (2000)

CD180	Rp105/αpg95	105	Type I transmembrane protein with LRG (Toll-like receptors family)	B-cells, monocytes	The LLG associates with a molecule MD-1 and this complex may have a role in LPS recognition and signalling in monocytes and B-cells	Recognition of pathogens	Miyake et al. (2000)
CD183	CXCR3	45–55	(G-protein-coupled cytokine receptor family)	T-cells, B-cell subset	Receptor for IFN-α inducible protein 10; monokine induced by IFN-α, secondary lymphoid tissue chemokine	Diagnosis of chronic lymphocytic leukaemia	Jones et al. (2000)
CD184	CXCR4	90	(G-protein-coupled cytokine receptor family)	Dendritic cells, monocytes, macrophages	Receptor for pulmonary and activation-regulated cytokine (PARC)	Receptor for HIV-1	Lapham et al. (1999)
CD185	CCR5	42	(G-protein coupled cytokine receptor family)	Peripheral blood lymphocytes, monocytes, NK cells, dendritic cells, macrophages	RANTES/macrophage inhibitory protein (MIP) 1α/MIP-1β receptor	Involved in the binding of HIV-1	Rabehi et al. (1999)
CDw197	CCR7	45	(G-protein coupled cytokine receptor family)	$CD8\alpha^+$ dendritic cells, T-cells	MIP-3β receptor	Involved in dendritic cell control of immune responses	Hasegawa et al. (2000)
CD200	OX-2	43	(Immunoglobulin superfamily)	Thymocytes, lymphocyte subset, neurons, endothelial cells	OX2 binds to a ligand receptor (OX2R) on macrophages	Possible role in controlling macrophages in a wide range of tissues	Wright et al. (2000)
CD201	Endothelial protein C receptor (EPCR)	49, 43 (soluble form)	Transmembrane protein	Endothelial cells	Receptor for protein C; facilitates activation by the thrombin–thrombomodulin complex	Critical role in the negative regulation of the blood clotting process	Esmon et al. (1999)
CD202b	Tie 2, Tek receptor tyrosine kinase	28–55	(Angiopoietin receptor family)	Endothelial cells, trophoblasts	Receptor for angiopoietin	Involved in tumour angiogenesis	Papapetropoulos et al. (1999)
CD203c	NPP3/PDNP3		Ectonucleotidase, type II transmembrane protein (unknown)	Basophils, mast cells and their precursors	Pyrophosphatase ectoenzyme associated with phosphodiesterase/ nucleotide	May play an important role in allergic disease	Buhring et al. (2000)
CD204	Macrophage scavenger receptor	85–97	(Scavenger receptor family)	Subsets of macrophages	Involved in foam cell formation, mediates influx of lipids into macrophages	Plays a role in the pathological deposition of cholesterol during the atherosclerotic process; involved in host defence	Elshourbagy et al. (2000)

Table 17.2 (*cont.*)

Antigen	Other names	Molecular mass (kDa)	Molecular structure (family name)	Cellular distribution	Function	Disease relevance	Reference
CD205	DEC205	202	Glycoprotein (unknown family)	Dendritic cells, lymphoid tissues	Antigen recognition molecule; homologous to the macrophage mannose receptor		Kato et al. (2000)
CD206	Macrophage mannose receptor	175, 165 (soluble form)	Multi-lectin receptor protein (unknown family)	Dendritic cells, Langerhans cells, monocytes, macrophages	Important in the innate immune response and for antigen processing by dendritic cells	Key role in host defence against pathogens	Jordens et al. (1999)
CD207	Langerin	40	(C-type lectin family)	Langerhan's cells	Receptor for mannose induces formation of Birbeck granules	Important role in antigen processing	Valladeau et al. (2000)
CD208	Dendritic cell (DC-LAMP)	110	Glycoprotein (unknown family)	Dendritic cells	Lysosome-associated homologous to CD68	Possible role in antigen presentation	de Saint-Vis et al. (1998)
CD209	Dendritic cell (DC-SIGN)	120	Type II membrane protein with C-type lectin domain (unknown family)	Dendritic cells	Mannose binding receptor; ligand for ICAM-3; receptor for viruses	Promotes binding and transmission of HIV-1 to T-cells	Teunis et al. (2000)
CDw210	IL-10 receptor (IL-10R)	97	(Class I cytokine receptor family)	T-cells	IL-10R plays a role in the functioning of regulatory T-cells that control inflammatory responses	The potential immunosuppressive activities of human recombinant IL-10 suggest that modulation of IL-10R may be clinically useful for treating autoimmune diseases	Syto et al. (1998)
CD212	IL-12 receptor (IL-12R)	110	Glycoprotein, high-affinity cytokine receptor composed of IL-12(R)β_1- and IL-12Rβ_2-chains (hemopoietin receptor superfamily)	Primarily on T- and NK cells	The expression of IL-12Rβ_2-chain on $CD4^+$ T-cells in mouse and humans appears to be differentially regulated by IFN-γ and IFN-α, respectively	The differentiation of $CD4^+$ T-cells into T helper type 1 cells is driven by IL-12 through the IL-12R β_2-chain	Nishikomori et al. (2000)

CD213a$_1$ and CD213a$_2$	IL-13 receptor (IL-13R) IL13Rα_1-chain, IL-13Rα-chain	130, 45–50 soluble form	(Cytokine receptor family)	T-cells, B-cells and NK cells	A functional IL-13R involves at least two cell surface proteins; the α_1-and α_2-chain	Soluble form of IL-13R may be used to modulate the fuction of IL-13 in vivo	Zhang et al. (1997)
CDw217	IL-17 receptor (IL-17R)	50–60	(Cytokine receptor family)	IL-17R is widely expressed, a finding consistent with the pleiotropic activities	Modulates expression of ICAM-1 and the synthesis of numerous proinflammatory mediators	Involvement of IL-17R in various proinflammatory processes	Fossiez et al. (1998)
CD220	Insulin receptor	190	Dimeric transmembrane protein (unknown family)	Muscle, liver and fat tissues	Regulation of cell metabolism, proliferation and growth	Insulin resistance is associated with aging, polycystic ovarian disease, syndrome X, cancer, trauma, obesity and type 2 diabetes mellitus	Hotamisligil (1999)
CD221	Insulin-like growth factor receptor 1 (IGFR1)	175	Glycoprotein (unknown family)	Epithelial cells in a variety of tissues	Mitogenic, cell survival and insulin-like actions that are essential for embryogenesis, postnatal growth physiology and breast development	Breast cancer has been associated with an increased expression of IGFR1	Ellis et al. (1998)
CD222	Insulin-like growth factor receptor 2 (IGF2R)	31–36	Glycoprotein (unknown family)	Epithelial cells in a variety of tissues	Mitogenic, cell survival and insulin-like actions that are essential for embryogenesis, postnatal growth physiology and breast development	Role in prostate cancer	Rajaram et al. (1997)
CD223	Lymphocyte activation gene 3 product (LAG 3)	70	Homology with CD4 (unknown family)	Activated T-cells and NK cells	Ligand for MHC class II, important in controlling T-cell reactivity	LAG3 is a receptor or coreceptor that defines different modes of natural killing for tumour cells	Miyazaki et al. (1996)
CD224	Gamma-glutamyl transferase	78–105	Transferase (unknown family)	Hepatocytes		Commonly measured to detect hepatic disfunction	Pfeifer et al. (2000)
CD225	Leu13	16	Type III transmembrane glycoprotein (unknown family)	Expressed strongly on B-, T- and NK cells and weakly on monocytes; it is not present on granulocytes, red blood cells or platelets	Leu13 appears to be a member of a multimeric cell surface signal transduction complex that contains CD19, CD21 (when expressed) and CD81 as well as a number of unidentified proteins	CD81 antibodies have proliferative effects on lymphoid cell lines, particularly those derived from large cell lymphomas	Levy et al. (1998)

Table 17.2 (*cont.*)

Antigen	Other names	Molecular mass (kDa)	Molecular structure (family name)	Cellular distribution	Function	Disease relevance	Reference
CD226	DNAX accessory molecule 1 (DNAM-1), platelet and T-cell activation antigen 1 (PTA-1)	65–67	Transmembrane glycoprotein (immunoglobulin super family)	Activated T-cells and NK cells, platelets/megakaryocytes and activated endothelial cells	DNAM-1 is a signal-transducing adhesion molecule involved in the cytolytic function mediated by cytotoxic T-cells and NK cells; platelet activation and aggregation	Involved in control of tumourigenesis	Jin et al. (2000)
CD227	Mucin constituent 1 (MUC1)	40–97	Transmembrane and secreted mucin (unknown family)	Epithelial cells, variety of malignant tumours of epithelial origin, activated T-cells	May play a role in immune responses	Expression of MUC1 may be predictive of the invasive/metastatic potential of tumours	McGuckin et al. (2000)
CD228	Melanotransferrin	90	Membrane-bound transferrin (unknown family)	Numerous adult and fetal tissues; tumour cells	Iron-binding protein involved in cell growth	Tumour-associated antigen	Richardson (2000)
CD229	Ly9	100–120	(Immunoglobulin superfamily)	Thymocyte, mature T- and B-cells	Role in leukocyte activation and differentiation	Cellular immune response mediator	de la Fuente et al. (1997)
CD230	Prion protein	33–38	Oligomeric β-sheet structure	Associated with neurons and the brain	Pathogenic protein. The 37 kDa laminin receptor precursor (LRP) is the interactor of the cellular prion protein	Role in Creutzfeldt–Jakob disease (CJD)	Rieger et al. (1999)
CD231	T-cell acute lymphoblastic antigen-1 (TALLA-1/A15)	28	(TM4 family)	T-cells, brain cells	Associates with β_1 integrins and MHC antigens	Involved in immune response modification	Serru et al. (1999)
CD232	Viral-encoded/ vascular endothelial semaphorin receptor (VESPR)	130–220	(Plexin family)	B-cell, monocytes, neutrophils, some NKs	Receptor binding results in upregulation of ICAM-1 and cytokine secretion	Receptor of vaccinia virus semaphorin protein	Comeau et al. (1998)
CD233	Band 3 blood group antigen	90–100	Multispanning membrane glycoprotein (unknown family)	Red cells	Red cell anion exchanger	Involved in glycolysis on the red cell surface	Groves and Tanner (1999)

CD234	Fy-glycoprotein, Duffy antigen/receptor for chemokines (DARC)	35–46	Chemokine receptor, homology to IL-8 (unknown family)	Red cells	DARC belongs to a family of erythrocyte chemokine receptors that bind C-X-C and C-C chemokines such as IL-8, monocyte chemoattractant protein 1 (MCP-1) and RANTES	DARC has been identified as a receptor for malaria parasites *Plasmodium vivax* and *P. knowlesi* and for HIV-1	Jaureguiberry et al. (1998), Daniels (1999)
CD235a, CD235b, CD235ab	Glycophorin A, glycophorin B, glycophorin A/B crossreactive monoclonal antibodies	90	Glycoprotein (unknown family)	Red cells	*Plasmodium falciparum* uses sialic acid residues on glycophorin A as receptors to invade human erythrocytes; *Vibrio cholerae* El Tor hemolysin binds to glycophorin B	Involved in malarial infection	Ranjan and Chitnis (1999)
CD236	Glycophorin C/D	32, 24	Sialoglycoprotein (unknown family)	Red cells	A single copy of a PDZ domain in human erythrocyte p55 binds to the C-terminus of the cytoplasmic domain of human erythroid glycophorin C	Regulation of cytoskeleton–membrane interactions	Marfatia et al. (1997)
CD238	Kell blood group antigen	93	Membrane glycoprotein (M13 subfamily of neutral endopeptidases family)	Red cells	Neutral endopeptidase, assembled in the endoplasmic reticulum and transported to the plasma membrane in association with XK a 444 amino acid residue membrane protein	Proteolytic enzyme that cleaves endothelin-3 to produce a ligand with multiple biological roles	Lee et al. (1999)
CD239	B-cell adhesion molecule (B-CAM)	52–59	(Immunoglobulin superfamily)	Red cells	Adhesion molecule similar to Lutheran blood group glycoprotein, roles in normal erythropoiesis, as well as in the pathophysiology of human disease	Implicated in tumourigenesis	Telen (2000)
CD240	CERh30CE, DRh30D, DCERh30D/CE, crossreactive monoclonal antibodies	32–34	Glycoprotein (unknown family)	Red cells	Component of the Rhesus blood system	Associated with a variety of Rhesus deficiency syndromes and diseases	Huang et al. (2000)

Table 17.2 (*cont.*)

Antigen	Other names	Molecular mass (kDa)	Molecular structure (family name)	Cellular distribution	Function	Disease relevance	Reference
CD241	Rhesus-associated glycoprotein (RhAg or Rh50)	45–100	Glycoprotein (unknown family)	Red cells	In the Rhesus blood system, RhAg (Rh-associated glycoprotein, or Rh50) is thought to be involved in Rh30 (D, CE) expression by forming a protein complex on the red cell surface	Associated with a variety of Rhesus deficiency syndromes and diseases	Avent and Read (2000)
CD242	ICAM-4, LW	37–47	Type I membrane protein (immunoglobulin family)	Red cells	May contribute to the adhesive interactions involved in the formation of erythroblastic islands and attachment to stroma cells and the extracellular matrix	Unknown	Bony et al. (1999)
CD243	P-glycoprotein product of the multidrug resistance gene 1 (*MDR-1*)	170	Glycoprotein (unknown family)	Parenchymal cells in several normal tissues	ATP-dependent transporter	Following upregulation of *MDR-1* energy-dependent transmembrane Pgp overexpression results in diminished intracellular concentrations of anthracyclins, vinca-alkaloids and epipodophyllotoxins	van den Heuvel-Eibrink et al. (2000)
CD244	2B4	60	(immunoglobulin superfamily)	Nk CELLS, T-cell subset, myeloid cells	Structurally related to CD2 like molecules. Binds to CD48. Mediates non-MHC-restricted cytotoxicity by NK cells	Regulation of a variety of immune responses	Nakajima and Colonna (2000)

CD245	p220/240	220–240	Glycoprotein (unknown family)	B-cell, $CD8^+$ T-cells, $CD45R^+/CD4^+$ T-cells, NK cells	The p220 antigen is found on the high-molecular-weight form of the T200 common leukocyte antigen family CD45; p220 is lost from the surface upon T-cell activation	May play a role in T-cell activation and inflammatory responses	Mimura et al. (1990)
CD246	Anaplastic lymphoma kinase	80–113	Tyrosine kinase (unknown family)	Lymphoma cells	Associated with the t(2;5)(p23;q35) translocation, which results in expression of a fusion protein, nucleophosmin-anaplastic lymphoma kinase (NPM-ALK)	ALK protein expression is an independent predictor of survival	Aoun et al. (1999)
CD247	Zeta chain	66	Transmembrane protein (unknown family)	T-cells	Intracellular signalling domain of the human CD3 complex	Target for immunotherapy	Jensen et al. (1998)

BCR, B-cell receptor; CEA, carcinoembryonic antigen; EGF, epidermal growth factor; fMLP, *N*- formyl methione leucylphenylalanine; G-CSF, granulocyte colony-stimulating factor; GM-CSF, granulocyte–macrophage colony-stimulating factor; GPI, glycosyl phosphatidylinositol; HIV, human immunodeficiency virus; ICAM, intercellular adhesion molecule; IFN, interferon; IL, interleukin; ITAM, immunoreceptor tyrosine-based activation motif; KIR, killer inhibitory receptor; LacCer, lactosyl ceramide; LAD, leukocyte adhesion deficiency; LAMP, lysosomal-associated membrane protein; LDL, low density lipoprotein; LFA, lymphocyte function-associated antigen; LPS, lipopolysaccharide; LRG, leucine-rich repeat; MAdCAM, mucosal addressin cell adhesion molecule; NGF, nerve growth factor; NK, natural killer; PDGF, platelet-derived growth factor; PSGL, P-selectin glycoprotein ligand; RANTES, regulated on activation normal T-cell expressed and secreted; s, soluble; sm, surface membrane; SRCR, scavenger receptor cysteine-rich; TAPA, target for antiproliferative antigen; TCR, T-cell receptor; TGF, transforming growth factor; TM, tetraspan; TNF, tumour necrosis factor; VCAM, vascular cell adhesion molecule; VLA, very late antigen.

17.4 REFERENCES

Agrawal, S., Marquet, J., Freeman, G.J., Tawab, A., Bouteiller, P.L., Roth, P., Bolton, W., Ogg, G., Boumsell, L., Bensussan, A. (1999) Cutting edge: MHC class I triggering by a novel cell surface ligand costimulates proliferation of activated human T cells. *Journal of Immunology* **162**, 1223–6.

Akasaki, K., Tsuji, H. (1998) Purification and characterization of a soluble form of lysosome-associated membrane glycoprotein-2 (lamp-2) from rat lysosomal contents. *Biochemical Molecular Biology International* **46**, 197–206.

Alexander, W.S., Nicola, N.A. (1998) Hemopoietic growth factor receptor abnormalities in leukemia. *Leukaemia Research* **22**, 1097–111.

Alfarano, A., Indraccolo, S., Circosta, P., Minuzzo, S., Valerio, A., Zamarchi, R., Fregonese, A., Calderazzo, F., Faldella, A., Aragno, M., Camaschella, C., Amedori, A., Caligaris-Coppia, F. (1999) An alternatively spliced form of CD79b gene may account for altered B-cell receptor expression in B-chronic lymphocytic leukemia. *Blood* **93**, 2327–35.

Altin, J.G., Sloan, E.K. (1997) The role of CD45 and CD45 related molecules in T cell activation. *Immunology Cell Biology* **75**, 430–45.

Aoun, P., Wu, D., Chanabhai, M., Skinnider, B.F., Greiner, T.C., Morris, S.W., Connors, J.M., Vose, J.M., Viswanatha, D., Coldman, A., Weisenburger, D.D. (1999) Prognostic significance of anaplastic lymphoma kinase (ALK) protein expression in adults with anaplastic large cell lymphoma. *Blood* **93**, 3913–21.

Aoyama, K., Oritani, K., Yokota, T., Ishikawa, J., Nishiura, T., Miyake, K., Kanakura, T., Tomiyama, Y., Kinkade, P.W., Matsuzawa, Y. (1999) Stromal cell CD9 regulates differentiation of hematopoietic stem/progenitor cells. *Blood* **93**, 2586–94.

Arroyo, A.G., Yang, J.T., Rayburn, H., Haynes, R.O. (1996) Differential requirement for alpha4 integrins during fetal and adult hematopoiesis. *Cell* **85**, 997–1008.

Avent, N.D., Reid, M.E. (2000) The Rh blood group system: a review. [Published erratum appears in *Blood* 2000 **95**, 2197] *Blood* **95**, 375–87.

Avra, E., Andersson, B. (1999) Kinetics of cytokine release and expression of lymphocyte cell-surface activation markers after in vitro stimulation of human peripheral blood mononuclear cells with *Streptococcus pneumoniae*. *Journal of Immunology* **49**, 237–43.

Azzoni, L., Zatsepina, O., Abebe, B., Bennett, I.M., Kanakaraj, P., Perussia, B. (1998) Differential transcriptional regulation of CD161 and a novel gene, 197/15s, by IL-2, IL-15, and IL-12 in NK and T cells. *Journal of Immunology* **161**, 3493–500.

Bach, B.A., Aquet, M., Schreiber, R.D. (1997) The IFN gamma receptor: a paradigm for cytokine receptor signaling. *Annual Review of Immunology* **15**, 563–91.

Bachmann, M.F., Wong, B.R., Josien, R., Steinman, R.M., Oxenius, A., Choi, Y. (1999) TRANCE, a tumor necrosis factor family member critical for CD40 ligand independent T helper cell activation. *Journal of Experimental Medicine* **189**, 1025–31.

Baiu, D.C., Prechi, J., Tchorbanov, A., Molina, H.D., Erdie, A., Sulica, A., Capel, P.J., Hazenbos, W.L. (1999) Modulation of the humoral immune response by antibody-mediated antigen targeting to complement receptors by Fc receptors. *Journal of Immunology* **162**, 3125–30.

Barbara, N.P., Wrana, J.L., Letarte, M. (1999) Endoglin is an accessory protein that interacts with the signalling receptor complex of multiple members of the transforming growth factor-beta superfamily. *Journal of Biological Chemistry* **274**, 584–94.

Barclay, A.N., Birkeland, M.L., Brown, M.H., Beyers, A.D., Davis, S.J., Somoza, C., Williams, A.F. (1993) *The Leucocyte Antigen Facts Book*. Academic Press, San Diego, CA.

Barclay, A.N., Brown, M.H., Law, S.K.A., McKnight, A.J., Tomlinson, M.G., van der Merwe, P. (1997) *The Leucocyte Antigen Facts Book*, 2nd edn. Academic Press, San Diego, CA.

Barrio, M.M., Bravo, A.I., Portela, P., Hersey, P., Mordoh, J. (1998) A new epitope on human melanoma-associated antigen CD63/ME491 expressed by both primary and metastatic melanoma. *Hybridoma* **17**, 355–64.

Bartlett, N.L., Longo, D.L. (1999) T-small lymphocyte disorders. *Seminars in Hematology* **36**, 264–70.

Bauer, S., Renner, C., Jawana, J.P., Hels, G., Ohnesorge, S., Gerlach, K., Pferudschuh, A. (1999) Immunotherapy of human tumors with T cell-activating bispecific antibodies: stimulation of cytotoxic pathways *in vivo*. *Cancer Research* **59**, 1961–5.

Beil, W.J., Fureder, W., Weiner, H., Grosschmidt, K., Maier, U., Schedle, A., Bankl, H.C., Lechner, K., Valent, P. (1998) Phenotypic and functional characterization of mast cells derived from renal tumor tissue. *Experimental Hematology* **26**, 158–63.

Berditchevski, F., Zutter, M.M., Hemler, M.E. (1996) Characterisation of novel complex on the cell surface between integrins and proteins with 4 transmembrane domains (TM4 proteins). *Molecular Biology Cell* **7**, 193–207.

Bony, V., Gane, P., Bailly, P., Cartron, J.P. (1999) Time-course expression of polypeptides carrying blood group antigens during human erythroid differentiation. *British Journal of Haematology* **107**, 263–74.

Bork, P., Bairoch, A. (1995) Extracellular protein modules. *Trends in Biochemical Science* **2**(suppl.).

Bowen, M.A., Aruffo, A. (1999) Adhesion molecules, their receptors and their regulation: analysis of CD6-activated leucocyte cell adhesion molecule (ALCAM/CD166) interactions. *Transplantation Proceedings* **31**, 795–6.

Brauner, A., Lu, Y., Hallden, G., Hylander, B., Lundahl, J. (1998) Difference in the blood monocyte phenotype between uremic patients and healthy controls: its relation to monocyte differentiation into macrophages in the peritoneal cavity. *Inflammation* **22**, 55–66.

Brezinchek, R.I., Oppenheimer-Marks, N., Lipsky, P.E. (1999) Activated T cells acquire endothelial cell surface determinants during transendothelial migration. *Journal of Immunology* **162**, 1677–84.

Bruggers, C.S., Patel, D.D., Scearce, R.M., Whichard, L.P., Haynes, B.F., Singer, K.H. (1995) AD2, a human molecule involved in the interaction of T cells with epidermal keratinocytes and thymic epithelial cells. *Journal of Immunology* **154**, 2012–22.

Buhring, H.J., Seiffert, M., Sano, K., Valent, P. (2000) The workshop antibody 97A6 recognizes NPP3, an ectonucleotidase primarily expressed on human basophils and mast cells. *Tissue Antigen* **55**(suppl. 1), 68.

Burgisser, P., Hamman, C., Kaufmann, D., Battegay, M., Rutschmann, O.T. (1999) Expression of CD28 and CD38 by $CD8^+$ T lymphocytes in HIV-1 infection correlates with markers of disease severity and changes towards normalization under treatment. *Clinical and Experimental Immunology* **115**, 458–63.

Cabezudo, E., Carrar, P., Morilla, R., Matutes, E. (1999) Quantitative analysis of CD79b, CD5 and CD19 in mature B-cell lymphoproliferative disorders. *Haematologica* **84**, 413–18.

Campbell, I.D. (1998) The modular architecture of leucocyte cell-surface receptors. *Immunological Reviews* **163**, 11–18.

Cao, Z., Huang, K., Horwitz, A.F. (1998) Identification of a domain on the integrin alpha5 subunit implicated in cell spreading and signalling. *Journal of Biological Chemistry* **237**, 670–9.

Cao, Y., Karsten, U., Schwartz-Albiez, R. (2000a) Expression of Thomsen–Friedenreich-related carbohydrate antigen on human leukaemia cells. *Tissue Antigen* **55**(suppl. 1), 26.

Cao, Y., Merling, A., Karsten, U., Schwartz-Albiez, R. (2000b) The carbohydrate blood group antigen H type 2 (blood group O) is expressed on $CD34^+$ hematopoietic progenitors. *Tissue Antigen* **55**(suppl. 1), 27.

Casasnovas, JM., Pieroni, C., Springer, T.A. (1999) Lymphocyte function-associated antigen-1 binding residues in intercellular adhesion molecule-2 (ICAM-2) and the integrin binding surface in the ICAM subfamily. *Proceedings of the National Academy of Science of the USA* **96**, 3017–22.

Chalmers, A.H. (1999) 5'-Ectonucleosidase in chronic lymphocytic leukaemia. *Clinical Biochemistry* **32**, 91–3.

Chambers, C.A., Allison, J.P. (1999) Costimulatory regulation of T cell function. *Current Opinion in Cell Biology* **11**, 203–10.

Chavakis, T., May, A.E., Preissner, K.T., Kanse, S.M. (1999) Molecular mechanisms of zinc–dependent leucocyte adhesion involving the urokinase receptor and beta2-integrins. *Blood* **93**, 2976–83.

Cho, B.K., Wang, C., Sugawa, S., Eisen, H.N., Chen, J. (1999) Functional differences between memory and naive CD8 T cells. *Proceedings of the National Academy of Science of the USA* **96**, 2976–81.

Chon, J.H., Netzel, R., Rock, B.M., Chaikof, E.L. (1998) Alpha4beta1 and alpha5beta 1 control cell migration on fibronectin by differentially regulating cell speed and motile cell phenotype. *Annals of Biomedical Engineering* **26**, 1091–101.

Cignetti, A., Bryant, E., Allione, B., Vitale, A., Foa, R., Cheever, M.A. (1999) CD34(+) acute myeloid and lymphoid leukemic blasts can be induced to differentiate into dendritic cells. *Blood* **94**, 2048–55.

Cipres, A., Gala, S., Martinez, A.C., Merida, I., Williamson, P. (1999) An IL-2 receptor beta subdomain that controls Bcl-X(L) expression and cell survival. *European Journal of Immunology* **29**, 1158–67.

Ciudad, J., Orfao, A., Vidriales, B., Macedo, A., Martinez, A., Gonzalez, M., Lopez-Berges, M.C., Valverde, B., San Miguel, J.F. (1998) Immunophenotypic analysis of $CD19^+$ precursors in normal human adult bone marrow: implications for minimal residual disease detection. *Haematologica* **83**, 1069–75.

Claus, C., Gocht, A., Schwartz-Albiez, R., Kniep, B. (2000) CDw60: specificity of the antibodies, distribution of the antigens and functional aspects. *Tissue Antigens* **55**(suppl.1), 28.

Clemetson, K.J., Clemetson, J.M. (1994) Molecular abnormalities in Glanzmann's thrombasthenia, Bernard–Soulier syndrome, and platelet-type von Willebrand's disease. *Current Opinion in Haematology* **1**, 388–93.

Colonna, M., Nakajima, H., Navarro, F., Lopez-Botet, M. (1999) A novel family of Ig-like receptors for HLA class I molecules that modulate function of lymphoid and myeloid cells. *Journal of Leucocyte Biology* **66**, 375–81.

Comeau, M.R., Johnson, R., DuBose, R.F., Petersen, M., Gearing, P., van den Bos, T., Park, L., Farrah, T., Buller, R.M., Cohen, J.I., Strockbine, L.D., Rauch, C., Spriggs, M.K. (1998) A poxvirus-encoded semaphorin induces cytokine production from monocytes and binds to a novel cellular semaphorin receptor, VESPR. *Immunity* **8**, 473–82.

Cornish, A.L., Freeman, S., Forbes, C., Zhang, M., Cepeda, M., Gentz, R., Augustus, M., Carter, K.C., Crocker, P.R. (1998)

Characterization of siglec-5, a novel glycoprotein expressed on myeloid cells related to CD33. *Blood* **92**, 2123–32.

Daniels, G. (1999) Functional aspects of red cell antigens. *Blood Reviews* **13**, 14–35.

Davis, T.A., Czerwinski, D.K., Levy, R. (1999) Therapy of B-cell lymphoma with anti-CD20 antibodies can result in the loss of CD20 antigen expression. *Clinical Cancer Research* **5**, 611–15.

de Cristofaro, R., de Candia, E. (1999) Thrombin interaction with platelet GpIb: structural mapping and effects on platelet activation. *International Journal of Molecular Medicine* **3**, 353–71.

de la Fuente, M.A., Pizcueta, P., Nadal, M., Bosch, J., Engel, P. (1997) CD84 leucocyte antigen is a new member of the Ig superfamily. *Blood* **90**, 2398–405.

Delaire, S., Elhabizi, A., Bensussan, A., Boumsell, L. (1998) CD100 is a leucocyte semaphorin. *Cellular and Molecular Life Science* **54**, 1265–76.

de Lau, W.B., Kuipers, J., Peters, P.J., Lokhurst, H.M., Clevers, H., Bast, B.J. (1998) Putative myeloma precursor cells expressing 2,6 sialic acid-modified antigens actually belong to the erythroid lineage. *Leukaemia Research* **22**, 163–73.

Del Pozo, M.A., Nieto, M., Serrador, J.M., Sancho, D., Vocente-Manzanares, M., Martinez, C., Sanchez-Madrid, F. (1998) *Cell Adhesion Communication* **6**, 125–33.

Derbal, K., Angelisova, P., Rasmussen, A.M., Hilgert, I., Funderud, S., Horejsi, V. (1999) The nature of the subset of MHC class II molecules carrying CDw78 epitopes. *International Immunology* **11**, 491–8.

de Saint-Vis, B., Vincent, J., Vandenabeele, S., Vanbervliet, B., Pin, J.J., Ait-Yahia, S., Patel, S., Mattei, M.G., Banchereau, J., Zurawski, S., Davoust, J., Caux, C., Lebecque, S. (1998) A novel lysosome-associated membrane glycoprotein, DC-LAMP, induced upon DC maturation, is transiently expressed in MHC class II compartment. *Immunity* **9**, 325–36.

Devaux, P., Christiansen, D., Fontaine, M., Gerlier, D. (1999) Control of C3b and C5b deposition by CD46 after alternative but not classical complement activation. *European Journal of Immunology* **29**, 815–22.

De Vries, J.E., Carbillido, J.M., Aversa, G. (1999) Receptors and cytokines involved in allergic TH2 T cell responses. *Journal of Allergy* **103**, S492–6.

Dorfman, D.M., Shahsafaei, A., Nadler, L.M., Freeman, G.J. (1998) The leucocyte semaphorin CD100 is expressed in most T-cell, but few B-cell, non-Hodgkin's lymphomas. *American Journal of Pathology* **153**, 255–62.

Droste, A., Sorg, C., Hogger, P. (1999) Shedding of CD163, a novel regulatory mechanism for a member of the scavenger receptor cysteine-rich family. *Biochemical Biophysical Research* **256**, 110–13.

Dworzak, M.N., Fritsch, G., Froschl, G., Printz, D., Gadner, H. (1998) Four-color flow cytometric investigation of terminal deoxynucleotidyl transferase-positive lymphoid precursors in paediatric bone marrow: CD79a expression precedes CD19 in early B-cell ontology. *Blood* **92**, 3203–9.

Dzhandzhugazyan, K.N., Kirkin, A.F., Straten, P., Zeuthen, J. (1998) Ecto-ATP diphosphohydrolase/CD39 is over expressed in differentiated human melanomas. *FEBS Letters* **430**, 227–30.

Ellerbroek, S.M., Fisher, D.A., Kearns, A.S., Bafetti, L.M., Stack, M.S. (1999) Ovarian carcinoma regulation of matrix metalloproteinase-2 and membrane type 1 matrix metalloproteinase through beta1 integrin. *Cancer Research* **59**, 1635–41.

Ellis, M.J., Jenkins, S., Hanfelt, J., Redington M.E., Taylor, M., Leek, R., Siddle, K., Harris, A. (1998) Insulin-like growth factors in human breast cancer. *Breast Cancer Research and Treatment* **52**, 175–84.

Elshourbagy, N.A., Li, X., Terret, J., Vanhorn, S., Gross, M.S., Adamou, J.E., Anderson, K.M., Webb, C.L., Lysko, P.G. (2000) Molecular characterization of the human scavenger receptor, human MARCO. *European Journal of Biochemistry* **267**, 919–26.

Ernst, L.K., Duchemin, A.M., Miller, K.L., Anderson, C.L. (1998) Molecular characterisation of six variant Fcgamma receptor class I (CD64) transcripts. *Molecular Immunology* **35**, 945–54.

Esmon, C.T., Gu, J.M., Xu, J., Qu, D., Stearn-Kurosawa, D.J., Kurosawa, S. (1999) Regulation and functions of the protein C anticoagulant pathway. *Haematologica* **84**, 363–8.

Fang, J.M., Finn, W.G., Hussong, J.W., Goolsby, C.L., Cubbon, A.R., Variakojis, D. (1999) CD10 antigen expression correlates with the t(14;18)(q32;q21) major breakpoint region in diffuse large B-cell lymphoma. *Modern Pathology* **12**, 295–300.

Ferrer, M., Yunta, M., Lazo, P.A. (1998) Pattern of expression of tetraspan genes in Burkitt lymphoma cell lines. *Clinical Experimental Immunology* **113**, 346–52.

Figarella-Branger, D., Daniel, L., Andre, P., Guia, S., Renaud, W., Monti, G., Vivier, E., Rougon, G. (1999) The PEN5 epitope identifies an oligodendrocyte precursor cell population and pilocytic astrocytomas. *American Journal of Pathology* **155**, 1261–9.

Ferrero, E., Malavasi, F. (1999) The metamorphosis of a molecule: from soluble enzyme to the leucocyte receptor CD38. *Journal of Leukocyte Biology* **65**, 151–61.

Fossiez, F., Banchereau, J., Murray, R., van Kooten, C., Garrone, P., Lebecque, S. (1998) Interleukin-17. *International Reviews of Immunology* **16**, 541–51.

Frazier, W.A., Gao, A.G., Dimitry, J., Chung, J., Brown, E.J., Lindberg, F.P., Linder, M.E. (1999) The thrombospondin receptor integrin-associated protein (CD47) functionally couples to heterodimeric Gi. *Journal of Biological Chemistry* **274**, 8554–60.

Frohn, C., Schlenke, P., Kirchner, H. (1997) The repertoire of HLA-Cw-specific NK cell receptors CD158 a/b (EB6 and GL183) in individuals with different HLA phenotypes. *Immunology* **92**, 567–70.

Gardner, H., Broberg, A., Pozzi, A., Laato, M., Heino, J. (1999) Absence of integrin alpha1beta1 in the mouse causes loss of feedback regulation of collagen in normal and wounded dermis. *Journal of Cell Science* **112**, 263–72.

Garner, T.G., Kearse, K.P. (1999) Modification of the T cell antigen receptor (TCR) complex by UDP-glucose: glycoprotein glucosyltransferase. TCR folding is finalised convergent with formation of alphabetadeltaepsilongammaepsilon complexes. *Journal of Biological Chemistry* **274**, 14094–9.

Gattei, V., Godeas, C., Degan, M., Rossi, F.M., Aldinucci, D., Pinto, A. (1999) Characterization of anti-CD138 monoclonal antibodies as tools for investigating the molecular polymorphisms of syndecan-1 in human lymphoma cells. *British Journal of Haematology* **104**, 152–62.

Ghannadan, S., Baghestanian, M., Wimazal, F., Eisenmenger, M., Latal, D., Kargul, G., Walchsofer, S., Sillaber, C., Lechner, K., Valent, P. (1998) Phenotypic characterization of human skin mast cells by combined staining with toluidine blue and CD antibodies. *Journal of Investigative Dermatology* **111**, 689–95.

Glasova, M., Konikova, E., Stasakova, J., Babusikova, O. (1998) the relationship of HLA-DR, CD38 and CD71 markers to activation, proliferation and differentiation of some leukemia and lymphoma cells. *Neoplasm* **45**, 88–95.

Groves, J.D., Tanner, M.J. (1999) Topology studies with biosynthetic fragments identify interacting transmembrane regions of the human red-cell anion exchanger (band 3, AE1). *Biochemical Journal* **344**, 687–97.

Guo, H., Majmudar, G., Jensen, T.C., Biswas, C., Toole, B.P., Gordon, M.K. (1998) Characterisation of the gene for human EMMPRIN, a tumor cell surface inducer of matrix metalloproteinases. *Gene* **220**, 99–108.

Hadam, M.R. (1998) CD139 workshop panel report. In: Kishimoto, T. (ed.), *Leucocyte Typing VI*, pp. 245–55. Garland, New York.

Hagaman, J.R., Moyer, J.S., Bachman, E.S., Sibony, M., Magyar, P.L., Welch, J.E., Smithies, O., Krege, J.H., O'Brien, D.A. (1998) Angiotensin-converting enzyme and male fertility. *Proceedings of the National Academy of Science of the USA* **95**, 2552–7.

Hamann, J., Stortelers, C., Kiss-Toth, E., Vogel, B., Eichler, W., van Lier, R.A. (1998) Characterization of the CD55 (DAF)-binding site on the seven-span transmembrane receptor CD97. *Journal of Immunology* **28**, 1701–7.

Hammond, C., Denzin, L.K., Pan, M., Griffith, J.M., Geuze, H.J., Cresswell, P. (1998) The tetraspan protein CD82 is a resident of MHC class II compartments where it associates with HLA-DR, -DM, and -DO molecules. *Journal of Immunology* **161**, 3282–91.

Hansen, I., Meyer, K., Hokland, P. (1998) Flow cytometric identification of myeloid disorders by asynchronous expression of the CD14 and CD66 antigens. *European Journal of Haematology* **61**, 339–46.

Hasagawa, S., Pawanker, R., Suzukki, K., Nakahata, T., Furuhata, T., Furukawa, S., Okumura, K., Ra, C. (1999) Functional expression of the high affinity receptor for IgE in human platelets and its intracellular expression in human megakaryocytes. *Blood* **93**, 2543–51.

Hasegawa, H., Kohno, M., Nomura, T., Sasaki, M., Yoshie, O., Fujita, S. (2000) CCR7 chemokine receptor expression on normal lymphocyte subsets and adult T cell leukaemia cells. *Tissue Antigens* **55**,(suppl. 1), 47.

Haziot, A., Hijita, N., Schultz, K., Zhang, F., Gangloff, S.C., Goyert, S.M. (1999) CD14 plays no major role in shock induced by *Staphylococcus aureus* but down-regulates TNF-alpha production. *Journal of Immunology* **162**, 4801–5.

He, X.Y., Zu, Z., Melrose, J., Mullowney, A., Vasquez, M., Queen, C., Vexler, V., Klingbeil, C., Co, M.S., Berg, E.L. (1998) Humanization and pharmacokinetics of a monoclonal antibody with specificity for both E- and P-selectin. *Journal of Immunology* **160**, 1029–35.

Hibi, M., Hirano, T. (1998) Signal transduction through cytokine receptors. *International Review of Immunology* **17**, 75–102.

Hoang-Vu, C., Bull, K., Schwarz, I., Krause, G., Schmutzler, C., Aust, G., Kohrle, J., Dralle, H. (1999) Regulation of CD97 protein in thyroid carcinoma. *Journal of Clinical Endocrine Metabolism* **84**, 1104–9.

Hoffmann, J.C., Kruger, R., Zeilen, S., Bayer, B., Zeilden, H. (1998) Human B cell differentiation: dependence on interactions with monocytes and T lymphocytes via CD40, CD80 (B7.1), and the CD2-ligands CD48 and CD58 (LFA-3). *Cell Biology International* **22**, 21–9.

Honig, M., Peter, H.H., Jantscheff, P., Grunert, F. (1999) Synovial PMN show a coordinated up-regulation of CD66 molecules. *Journal of Leukocyte Biology* **66**, 429–36.

Hotamisligil, G.S. (1999) The role of TNFalpha and TNF receptors in obesity and insulin resistance. *Journal of International Medicine* **245**, 621–5.

Hortsch, M. (2000) Structural and functional evolution of the

L1 family: are four adhesion molecules better than one? *Molecular and Cellular Neuroscience* **15**, 1–10.

Huang, C.H., Liu, P.Z., Cheng, J.G. (2000) Molecular biology and genetics of the Rh blood group system. *Seminars in Hematology* **37**, 150–65.

Huang, N., Kawano, M.M., Mahmoud, M.S., Mihara, K., Tsujimoto, T., Niwa, O., Kuramoto, A. (1995) Expression of CD21 antigen on myeloma cells and its involvement in their adhesion to bone marrow stromal cells. *Blood* **85**, 3704–12.

Ikura, S., Terao, K., Matszaki, I., Inoue-Murayama, M., Murayama, Y. (1999) U5 monoclonal antibody identifies a novel lymphocyte surface antigen preferentially expressed in human circulating natural killer cells with high cytotoxic activity. *Immunology* **96**, 485–90.

Itzhaky, D., Raz, N., Hollander, N. (1998) The glycosylphosphatidylinositol-anchored form and the transmembrane form of CD58 are released from the cell surface upon antibody binding. *Cellular Immunology* **187**, 151–7.

Jaureguiberry, G., Le Buenac, H., Bizzini, B., Zagury, J.F., Rappaport, J., Zagury, D. (1998) Binding of HIV-1 to RBCs involves the Duffy antigen receptors for chemokines. *Biomedicine and Pharmacotherapy* **52**, 436–9.

Jensen, M., Tan, G., Forman, S., Wu, A.M., Raubitschek, A. (1998) CD20 is a molecular target for scFvFc:zeta receptor redirected T cells: implications for cellular immunotherapy of CD20+ malignancy. *Biology of Blood and Marrow Transplantation* **4**, 75–83.

Ji, H., Chang, E.Y., Lin, K.Y., Kurman, R.J., Pardoll, D.M., Wu, T.C. (1998) Antigen-specific immunotherapy for murine lung metastastic tumors expressing human papillomavirus type 16 E7 oncoprotein. *International Journal of Cancer* **78**, 41–5.

Jin, B., Li, D., Jia, W., Tian, F., Ralston, K.J., Lui, X., Sun, C., Sun, K., Burns, G.F. (2000) Platelet and T cell activation antigen 1 (PTA1) is a novel member of the immunoglobulin superfamily involved in multiple lineage functions. *Tissue Antigens* **55**(suppl. 1), 107.

Jones, D., Benjamin, R.J., Shahsafaei, A., Dorfman, D.M. (2000) The chemokine receptor CXCR3is expressed in a subset of B-cell lymphomas and is a marker of B-cell chronic lymphocytic leukemia. *Blood* **95**, 627–32.

Jordens, R., Thompson, A., Amos, R., Koning, F. (1999) Human dendritic cells shed a functional, soluble form of the mannose receptor. *International Immunology* **11**, 1775–80.

Justman, L.B. (1997) The role of CD45 in signal transduction. *Advances in Immunology* **66**, 1–65.

Kalden, J.R., Andreesen, R., Henschke, F., Moldenhauer, G. (1998) Antibodies TC-12 and TH-111 (CD96) characterize T-cell acute lymphoblastic leukaemia and a subgroup of acute myeloid leukaemia. *Experimental Hematology* **26**, 1209–14.

Kammerer, R., Hahn, S., Singer, B.B., Luo, J.S., von Kleist, S. (1999) Biliary glycoprotein (CD66a), a cell adhesion molecule of the immunoglobulin superfamily, on human lymphocytes: structure, expression and involvement in T cell activation. *European Journal of Immunology* **28**, 3664–74.

Karusuyama, H., Tsuganezawa, K., Kiyokawa, Y., Matsuo, F., Kitamura, F., Toyama-Sorimachi, N., Kuida, K., Fujimot, J. (2000) Expression profile of pre-B cell receptor components in acute lymphoblastic leukaemia and its application to the diagnosis and classification of the disease. *Tissue Antigens* **55**(suppl. 1), 20.

Kato, M., MacDonald, K., Vuckovic, S., Hart, D.N.J. (2000) Expression of DEC-205 by human dendritic cells. *Tissue Antigens* **55**, 58.

Kaushansky, K. (1999) The enigmatic megakaryocyte gradually reveals its secrets. *Bioassays* **21**, 353–60.

Kelton, J.G., Smith, J.W., Horsewood, P., Warner, M.N., Warkentin, T.E., Finberg, R.W., Hayward, C.P. (1998) ABH antigens on platelets: expression on the glycosyl phosphatidylinositol-anchored protein CD109. *Journal of Laboratory and Clinical Medicine* **132**, 142–8.

Kim, J.J., Tsai, A., Nottingham, L.K., Morrison, L., Cunning, D.M., Oh, D.M., Lee, D.L., Dang, K., Dentchev, T., Chalian, A.A., Agadjanyan, M.G., Weiner, D.B. (1999a) Intracellular adhesion molecule-1 modulates beta-chemokines and directly costimulates T cells *in vivo*. *Journal of Clinical Investigation* **103**, 869–77.

Kim, J.T., Schimming, A.W., Kita, H. (1999b) Ligation of Fc gamma RII (CD32) pivotally regulates survival of human eosinophils. *Journal of Immunology* **162**, 4253–9.

Kinoshita, J., Haga, S., Shimizu, H., Watenabe, O., Kajiwara, T. (1999) The expression of variant exon v7-v8 CD44 in relation to lymphatic metastasis of human breast cancer. *Breast Cancer Research and Treatment* **53**, 177–83.

Kniep, B., Schakel, K., Nimtz, M., Schwartz-Albiez, R., Schmidt, M., Northoff, H., Vilella, R., Gramatzki, M., Reiber, E.P. (1999) Differential expression of alpha2–6 sialylated polylactosamine structures by human B and T cells. *Glycobiology* **9**, 399–406.

Koch, C., Staffler, G., Huttinger, R., Higert, I., Prager, E., Cerny, J., Steinlein, P., Majdic, O., Horejsi, V., Stockinger, H. (1999) T cell activation-associated epitopes of CD147 in regulation of the T cell response, and their definition by antibody affinity and antigen density. *International Immunology* **11**, 777–86.

Kolb, A.F., Hegyi, A., Maile, J., Heister, A., Hagemann, M., Siddell, S.G. (1998) Molecular analysis of the coronavirus-

receptor function of aminopeptidase N. *Advances in Experimental Medical Biology* **440**, 61–7.

Kosaka, Y., Calderhead, D.M., Manning, E.M., Hambor, J.E., Black, A., Geleziunas, R., Marcu, K.B., Noelle, R.J. (1999) Activation and regulation of the kappaB kinase in human B cells by CD40 signaling. *European Journal of Immunology* **29**, 1353–62.

Koskela, S., Kekomaki, R., Partanen, J. (1998) Genetic polymorphism in human platelet glycoprotein GPIb/IX/V complex is enriched in GPV (CD42d). *Tissue Antigens* **52**, 236–41.

Koubek, K., Kumberova, A., Stary, J., Babusikova, O., Klamova, H., Filipec, M. (1998) Expression of cytokine receptors on different myeloid leukemic cells. *Neoplasm* **45**, 198–203.

Koubek, K., Stary, J., Kumberova, A., Klamova, H., Filipec, M. (1999) Occurrence of cytokine receptors on different lymphoid leukaemic cells. *European Journal of Haematology* **63**, 1–10.

Kumaki, S., Ishii, N., Minegishi, M., Tsuchiya, S., Cosman, D., Sugamura, K., Konno, T. (1999) Functional role of interleukin-4 (IL-4) and IL-7 in the development of X-linked severe combined immunodeficiency. *Blood* **93**, 607–12.

Kurts, C., Carbone, F.R., Krummel, M.F., Koch, K.M., Miller, J.F., Heath, W.R. (1999) Signaling through CD30 protects autoimmune diabetes mediated by CD8 T cells. *Nature* **398**, 341–4.

Kusmartsev, S., Ruiz de Morales, J.M., Rullas, J., Danilets, M.G., Subiza, S.L. (1999) Sialoadhesin expression by bone marrow macrophages derived from Ehrlich-tumor-bearing mice. *Cancer Immunology and Immunotherapy* **48**, 493–8.

Lagaudriere-Gesbert, C., La Naour, F., Lebel-Binay, S., Billard, M., Lemichez, E., Boquet, P., Boucheix, C., Conjeaud, H., Rubinstein, E. (1997) Functional analysis of four tetraspans, CD9, CD53, CD81, and CD82, suggests a common role in costimulation, cell adhesion and migration: only CD9 upregulates HB-EGF activity. *Cellular Immunology* **182**, 105–12.

Lage, H., Christmann, M., Kern, M.A., Dietel, M., Pick, M., Kaina, B., Schadendorf, D. (1999) Expression of DNA repair proteins hMSH2, hMSH6, hMLH1 in melanoma cells with acquired drug resistance. *International Journal of Cancer* **80**, 744–50.

Lai, R., Weiss, L.M., Chang, K.L., Arber, D.A. (1999) Frequency of CD43 expression in non-Hodgkin lymphoma. A survey of 742 cases and further characterization of rare $CD43^+$ follicular lymphomas. *American Journal of Clinical Pathology* **111**, 488–94.

Lapham, C.K., Zaitseva, M.B., Lee, S., Romanstseva, T., Golding, H. (1999) Fusion of monocytes and macrophages with HIV-1 correlates with biochemical properties of CXCR4 and CCR5. [Published erratum appears in *Nature Medicine* 1999 **5**, 590]. *Nature Medicine* **5**, 303–8.

Lee, D.M., Staats, H.F., Sundy, J.S., Patel, D.D., Sempowski, G.D., Scearce, R.M., Jones, D.M., Haynes, B.F. (1998) Immunological characterisation of CD7-deficient mice. *Journal of Immunology* **160**, 5749–56.

Lee, S., Lin, M., Mele, A., Cao, Y., Russo, D., Redman, C. (1999) Proteolytic processing of big endothelin-3 by the kell blood group protein. *Blood* **94**, 1440–50.

Lens, S.M., Tesselaar, K., van Oers, M.H., van Lier, R.A. (1998) Control of lymphocyte function through CD27–CD70 interactions. *Seminars in Immunology* **10**, 491–9.

Levesque, M.C., Haynes, B.F. (1997) Cytokine induction of the ability of human monocyte CD44 to bind to hyaluronan is mediated primarily by TNF-alpha and is inhibited by IL-4 and IL-13. *Journal of Immunology* **159**, 6184–94.

Levy, S., Todd, S.C., Maecker, H.T. (1998) CD81 (TAPA-1): a molecule involved in signal transduction and cell adhesion in the immune system. *Annual Review of Immunology* **16**, 89–109.

Lingwood, C.A., Khine, A.A., Arab, S. (1998) Globotriaosyl ceramide (Gb3) expression in human tumor cells: intracellular trafficking defines a new retrograde transport pathway from the cell surface to the nucleus, which correlates with sensitivity to verotoxin. *Acta Biochimica Polonica* **45**, 351–9.

Lopez, M., Aoubala, M., Jordier, F., Isnardon, D., Gomez, S., Dubreuil, P. (1998) The human poliovirus receptor related 2 protein is a new hematopoietic/endothelial homophilic adhesion molecule. *Blood* **92**, 4602–11.

Lopez-Botet, M., Navarro, F., Llano, M. (1999) How do NK cells sense the expression of HLA-G class Ib molecules? *Seminars in Cancer Biology* **9**, 19–26.

Lorenzi, R., Jouvin, M.H., Burrone, O.R. (1999) Functional Fc epsilonRI engagement by a second secretory IgE isoform detected in humans. *European Journal of Immunology* **29**, 936–45.

Mandelboim, O., Malik, P., Davis, D.M., Jo, C.H., Boyson, J.E., Strominger, J.L. (1999) Human CD16 as a lysis receptor mediating direct natural killer cell cytotoxicity. *Proceedings of the National Academy of Science of the USA* **96**, 5640–4.

Marfatia, S.M., Morais-Cabral, J.H., Kim, A.C., Byron, O., Chishti, A.H. (1997) The PDZ domain of human erythrocyte p55 mediates its binding to the cytoplasmic carboxyl terminus of glycophorin C. Analysis of the binding interface by in vitro mutagenesis. *Journal of Biological Chemistry* **272**, 24191–7.

McCrohon, J.A., Jessup, W., Handelsman, D.J., Celermajer, D.S. (1999) Androgen exposure increases human monocyte adhesion to vascular endothelium and endothelial cell expression of vascular cell adhesion molecule 1. *Circulation* **99**, 2317–22.

McGuckin, M., MacDonald, K.P.A., Tran, M., Wykes, M., Hart, D.N.J. (2000) MUC1 epithelial mucin: expression by normal hematopoietic cells. *Tissue Antigens* **55(suppl**. 1), 87.

Mehdi, S.A., Tatum, A.H., Newman, N.B., Imperato, A., Daucher, J., Kohman, L.J., Graziano, S.L. (1998) Prognostic significance of Lewis y antigen in resected stage I and II non-small cell lung cancer. *Chest* **114**, 1309–15.

Miller, D.W., Graulich, W., Karges, B., Stahl, S., Ernst, M., Ramaswamy, A., Sedacek, H.H., Muller, R., Adamkiewicz, J. (1999) Elevated expression of endoglin, a component of the TGF-beta-receptor complex, correlates with proliferation of tumor endothelial cells. *International Journal of Cancer* **81**, 568–72.

Mimura, T., Fernsten, P., Jarjour, W., Winfield, J.B. (1990) Autoantibodies specific for different isoforms of CD45 in systemic lupus erythematosus. *Journal of Experimental Medicine* **172**, 653–6.

Miyake, H., Hara, I., Yamanaka, K., Gohji, K., Arakawa, S., Kamidono, S. (1999) Elevation of serum levels of urokinase-type plasminogen activator and its receptor is associated with disease progression and prognosis in patients with prostate cancer. *Prostate* **39**, 123–9.

Miyake, K., Ogata, S., Akashi, Y., Nagal, Y., Kimoto, M. (2000) Expression of RP105 and Toll-like receptor 4 on B cells and their possible cooperation in LPS recognition. *Tissue Antigens* **55**(suppl. 1), 22.

Miyazaki, T., Dierich, A., Benoist, C., Mathi, S.D. (1996) Independent modes of natural killing distinguished in mice lacking Lag3. *Science* **272**, 405–8.

Mollet, L., Fautrel, B., Leblond, V., Bergeron, F., Marie-Beral, H., Baumelou, E., Hubert, P., Debre, P., Autran, B. (1999) Leukemic $CD3^+$ LGL share functional properties with their $CD3^+$ $CD57^+$ cell counterpart expanded after BMT. *Leukemia* **13**, 230–40.

Mollinedo, F., Martin-Martin, B., Gajate, C., Lazo, P.A. (1998) Physiological activation of human neutrophils down-regulates CD53 cell surface antigen. *Journal of Leukocyte Biology* **63**, 699–706.

Moore, K.L. (1998) Structure and function of P-selectin glycoprotein ligand-1. *Leukemia and Lymphoma* **29**, 1–15.

Moran, M., Miceli, M.C. (1998) Engagement of GPI-linked CD48 contributes to TCR signals and cytoskeletal reorganization: a role for lipid rafts in T cell activation. *Immunity* **9**, 787–96.

Mudad, R., Rao, N., Angelisova, P., Horejsi, V., Telen, M.J. (1995) Evidence that CDw108 membrane protein bears the JMH blood group antigen. *Transfusion* **35**, 566–70.

Muller-Newen, G., Kuster, A., Hammann, U., Keul, R., Horsten, U., Martens, A., Graeve, L., Wijdenes, J., Heinrich, P.C. (1998) Soluble IL-6 receptor potentiates the antagonistic activity of soluble gp130 on IL-6 responses. *Journal of Immunology* **161**, 6347–55.

Mutin, M., Dignat-George, F., Sempol, J. (1997) Immunologic phenotype of cultured endothelial cells: quantitative analysis of cell surface molecules. *Tissue Antigens* **50**, 449–58.

Mylvaganam, M., Lingwood, C.A. (1999) Adamantyl globotriaosyl ceramide: a monovalent soluble mimic which inhibits verotoxin binding to its glycolipid receptor. *Biochemical and Biophysical Research Communications* **257**, 391–4.

Nadler, M.J., Brennan, L.A., Gish, G.D., Timms, J.F., Fusaki, N., Jongstra-Bilen, J., Tada, N., Pawson, T., Wither, J., Neel, B.G., Hozumi, N. (1998) B-cell transmembrane protein CD72 binds to and is an in vivo substrate of the protein tyrosine phosphatase SHP-1. *Current Biology* **10**, 1009–17.

Nagumo, H., Agematsu, K., Shinozaki, K., Hokibara, S., Ito, S., Takmoto, M., Nikaido, T., Yasui, K., Uehara, Y., Yachie, K., Komijama, A. (1999) CD27/CD70 interaction augments IgE secretion by promoting the differentiation of memory B cells into plasma cells. *Journal of Immunology* **162**, 4464–71.

Nakajima, H., Colonna, M. (2000) 2B4: an NK cell activating receptor with unique specificity and signal transduction mechanisms. *Human Immunology* **61**, 39–43.

Nakajima, J., Takamoto, S., Kohno, T., Ohtsuka, T., Matsumot, J. (1999) Expression of CD10 on lymphoid cells associated with thymoma. *Japanese Journal of Cardiovascular Surgery* **47**, 68–72.

Nakamura, T., Kambayashi, J., Okuma, M., Tandon, N.N. (1999) Activation of the GP IIb-IIIa complex induced by platelet adhesion to collagen is mediated by both alpha2beta1 integrin and GP VI. *Journal of Biological Chemistry* **274**, 11897–903.

Nanney, L.B., Skeel, A., Luan, J., Polos, S., Richmond, A., Wang, M.H., Leonard, E.J. (1998) Proteolytic cleavage and activation of pro-macrophage-stimulating protein and upregulation of its receptor in tissue injury. *Journal of Investigative Dermatology* **111**, 573–81.

Nataf, S., Davoust, N., Ames, R.S., Barnum, S.R. (1999) Human T cells express the C5a receptor and are chemoattracted to C3a. *Journal of Immunology* **162**, 4018–23.

Neidhart, M., Wehrli, R., Bruhlmann, P., Michel, B.A., Gay, R.E., Gay, S. (1999) Synovial fluid CD146 (MUC18), a marker for synovial membrane angiogenesis in rheumatoid arthritis. *Arthritis Rheumatism* **42**, 622–30.

Ni, H.T., Deeths, M.J., Li, W., Mueller, D.L., Mescher, M.F. (1999) Signalling pathways activated by leucocyte function-associated Ag-1-dependent costimulation. *Journal of Immunology* **162**, 5183–89.

Nishikomori, R., Ehrhardt, R.O., Strober, W. (2000) T helper

type 2 cell differentiation occurs in the presence of interleukin 12 receptor beta2 chain expression and signaling. *Journal of Experimental Medicine* **191**, 847–58.

Nombedeu, J.F., Mateu, R., Altes, A., Liorente, A., Rio, C., Estivill, C., Lopez, O., Ubeda, J., Rubiol, E. (1999) Enhanced myeloid specificity of CD117 compared with CD13 and CD33. *Leukaemia Research* **23**, 341–7.

Novitzky, N., Thomas, V., Hale, G., Waldman, H. (1999) Ex vivo depletion of T cells from bone marrow grafts with CAMPATH-1 in acute leukaemia: graft-versus-host disease and graft-versus-leukaemia effect. *Transplantation* **67**, 620–6.

Obrink, B. (1997) CEA adhesion molecules: multifunctional proteins with signal-regulatory properties. *Current Opinion in Cell Biology* **9**, 616–26.

Oehler, L., Majdic, O., Pickl, W.F., Stockl, J., Reidl, E., Drach, J., Rappersberger, K., Geissler, K., Knapp, W. (1998) Neutrophil granulocyte-committed cells can be driven to acquire dendritic cell characteristics. *Journal of Experimental Medicine* **187**, 1019–28.

O'Keefe, T.L., Williams, G.T., Batista, F.D., Neuberger, M.S. (1999) Deficiency in CD22, a B cell-specific inhibitory receptor, is sufficient to predispose to development of high affinity autoantibodies. *Journal of Experimental Medicine* **189**, 1307–13.

Papapetropoulos, A., Garcia-Cardena, G., Dengler, T.J., Maisonpierre, P.C., Yancopoulos, G.D., Sessa, W.C. (1999) Direct actions of angiopoietin-1 on human endothelium: evidence for network stabilization, cell survival, and interaction with other angiogenic growth factors. *Laboratory Investigation* **79**, 213–23.

Pass, M.K., Quintini, G., Zarn, J.A., Zimmermann, S.M., Sigrist, J.A., Stahel, R.A. (1998) The 5'-flanking region of human CD24 gene has a cell-type specific promoter activity in small-cell lung cancer. *International Journal of Cancer* **78**, 496–502.

Patel, D.D., Whichard, L.P., Radcliff, G., Denning, S.M., Haynes, B.F. (1995) Characterisation of human thymic epithelial cell surface antigens: phenotypic similarity of thymic epithelial cells to epidermal keratinocytes. *Journal of Clinical Immunology* **15**, 80–92.

Pecora, A.L. (1999) Impact of stem cell dose on hematopoietic recovery in autologous blood stem cell recipients. *Bone marrow Transplant* **23**(suppl 2), 7–12.

Perez-Villar, J.J., Whitney, G.S., Bowen, M.A., Hewgill, D.H., Aruffo, A.A., Kanner, S.B. (1999) CD5 negatively regulates the T-cell antigen receptor signal transduction pathway: involvement of SH2-containin phosphotyrosine phosphatase SHP-1. *Molecular Cell Biology* **19**, 2903–12.

Pfeifer, P.H., Brems, J.J., Branson, M., Heigh, T.E. (2000) Plasma C3a and C4a levels in liver transplant recipients: a longitudinal study. *Immunopharmacology* **46**, 163–74.

Phillips, A.J., Tomasec, P., Wang, E.C., Wilkinson, G.W., Borysiewicz, L.K. (1999) Human cytomegalovirus infection down regulates expression of the cellular immunopeptidases CD10 and CD13. *Virology* **250**, 350–8.

Pickl, W.F., Majdic, O., Kohl, P., Stockl, J., Riedl, E., Scheinecker, C., Bello-Fernandez, C., Knapp, W. (1996) Molecular and functional characteristics of dendritic cells generated from highly purified $CD14^+$ peripheral blood monocytes. *Journal of Immunology* **157**, 3850–9.

Pilarski, L.M., Pruski, E., Wiznaik, J., Paine, D., Seeberger, K., Mant, M.J., Brown, C.B., Belch, A.R. (1999) Potential role for hyaluronan receptor RHAMM in mobilization and trafficking of hematopoietic progenitor cells. *Blood* **93**, 2918–27.

Poggi, A., Zocchi, M.R., Costa, P., Ferrero, E., Borsellino, G., Placido, R., Galgani, S., Salvetti, M., Gasperini, C., Ristori, G., Brosnan, C.F., Battistini, L. (1999) IL-12 mediated NKRP1A up-regulation and consequent enhancement of endothelial transmigration of V delta 2^+ TCR gamma $delta^+$ T lymphocytes from healthy donors and multiple sclerosis patients. *Journal of Immunology* **162**, 4349–54.

Pui, C.H., Rubnitz, J.E., Hancock, M.L., Downing, J.R., Raimondi, S.C., Rivera, G.K., Sandlund, J.T., Ribeiro, R.C., Head, D.R., Relling, M.V., Evans, W.E. (1998) Reappraisal of the clinical and biologic significance of myeloid associated antigen expression in childhood acute lymphoblastic leukaemia. *Journal of Clinical Oncology* **16**, 3768–73.

Rabehi, L.A., Seddiki, N., Benjouad, A., Gluckman, J.C., Gattegno, L. (1999) Interaction of human immunodeficiency virus type 1 envelope glycoprotein V3 loop with CCR5 and CD4 at the membrane of human primary macrophages. [Published erratum appears in *AIDS Research and Human Retroviruses* 1999 **20**, 493]. *AIDS Research and Human Retroviruses* **14**, 1605–15.

Rajaram, S., Baylink, J.D., Mohan, S. (1997) Insulin-like growth factor-binding proteins in serum and other biological fluids. *Regulation and Functions Endocrine Reviews* **10**, 801–31.

Ramachandra, L., Song, R., Harding, C.V. (1999) Phagosomes are fully competent antigen-processing organelles that mediate the formation of peptide:class II MHC complexes. *Journal of Immunology* **162**, 3263–72.

Ranjan, A., Chitnis, C.E. (1999) Mapping regions containing binding regions within functional domains of *Plasmodium vivax* and *Plasmodium knowlesi* erythrocyte-binding proteins. *Proceedings of the National Academy of Sciences of the USA* **96**, 14067–72.

Rawstron, A., Barrans, S., Blythe, D., Davies, F., English, A., Pratt, G., Child, A., Morgan, G., Jack, A. (1999) Distribution of myeloma plasma cells in peripheral blood and bone marrow

correlates with CD56 expression. *British Journal of Haematology* **104**, 138–43.

Rea, I.M., McNerlan, S.E., Alexander, H.D. (1999) CD69, CD25, and HLA-DR activation antigen expression on CD3 + lymphocytes and relationship to serum TNF-alpha, IFN-gamma and sIL-2R levels in aging. *Experimental Gerontology* **34**, 79–93.

Rice, C.M. (1999) Is CD81 the key to hepatitis C virus entry? *Hepatology* **29**, 990–2.

Richardson, D.R. (2000) The role of the membrane-bound tumour antigen, melanotransferrin (p97), in iron uptake by the human malignant melanoma cell. *European Journal of Biochemistry* **267**, 1290–8.

Rieger, R., Lasmezas, C.I., Weiss, S. (1999) Role of the 37 kDa laminin receptor precursor in the life cycle of prions. *Transfusion Clinique et Biologique* **6**, 7–16.

Rittner, H.L., Kalser, M., Brack, A., Szweda, L.I., Goronzy, J.J., Weyland, C.M. (1999) Tissue destructive macrophage in giant cell arteritis. *Circulation Research* **84**, 1050–8.

Root, R.K., Dale, D.C. (1999) Granulocyte colony-stimulating factor and granulocyte-macrophage colony-stimulating factor: comparison and potential for use in the treatment of infections in nonneutropenic patients. *Journal of Infectious Disease* **179**, S342–52.

Rostapshova, E.A., Burns, J.M., Bartlett, S.T., Hadley, G.A. (1998) Integrin-mediated interactions influence the tissue specificity of CD^+ cytotolytic T lymphocytes. *European Journal of Immunology* **28**, 3031–9.

Rudd, P.M., Wormald, M.R., Stanfield, R.L., Huang, M., Mattsson, N., Speir, J.A., DiGennaro, J.A., Fetrow, J.S., Dwek, R.A., Wilson, I.A. (1999) Roles for glycosylation of cell surface receptors involved in cellular immune recognition. *Journal of Molecular Biology* **293**, 351–66.

Rutella, S., Rumu, C., Puggioni, P., Barberi, T., Di Mario, A., Larocca, L.M., Leone, G. (1999) Expression of thrombospondin receptor (CD36) in B cell chronic lymphocytic leukaemia as an indicator of tumor cell dissemination. *Haematologica* **84**, 419–24.

Sainio-Pollanen, S., Erkkila, S., Alanko, S., Hanninen, A., Pollanen, P., Simell, O. (1998) The role of Fas ligand in the development of insulitis in nonobese diabetic mice. *Pancreas* **16**, 154–9.

Salomon, B., Bluestone, J.A. (1998) LFA-1 interaction with ICAM-1 and ICAM-2 regulates Th2 cytokine production. *Journal of Immunology* **161**, 5138–42.

Sandel, P.C., Monroe, JG. (1999) Negative selection of immature B cells by receptor editing or deletion is determined by site of antigen encounter. *Immunity* **10**, 289–99.

Sanders, W.J., Gordon, E.J., Dwir, O., Beck, P.J., Alon, R., Kiessling, L.L. (1999) Inhibition of L-selectin-mediated leucocyte rolling by synthetic glycoprotein mimics. *Journal of Biological Chemistry* **274**, 5271–8.

Sasaki, M., Yamato, T., Nakanuma, Y. (1999) Expression of sialyl-Tn, Tn and T antigens in primary liver cancer. *Pathology International* **49**, 325–31.

Sato, A., Yamamoto, S., Ishihara, K., Hirano, T., Jingami, H. (1999) Novel peptide inhibitor of ecto-ADP-ribosyl cyclase of bone marrow stromal cell antigen-1 (BST-1/CD157). *Biochemical Journal* **337**, 491–6.

Sayos, J., Wu, C., Morra, M., Wang, N., Zhang, X., Allen, D., van Schalk, S., Notarangelo, L., Geha, R., Roncarola, M.G., Oettgen, H., de Vries, J.E., Aversa, G., Terhorst, C. (1998) The X-linked lymphoproliferative-disease gene product SAP regulates signals induced through the co-receptor SLAM. *Nature* **395**, 462–9.

Schwartz, B.R., Karson, A., Bombeli, T., Harlan, J.M. (1999) A novel beta 1 integrin-dependent mechanism of leucocyte adherence to apoptotic cells. *Journal of Immunology* **162**, 4842–48.

Schwartz, H., Arden, K., Lotz, M. (1997) CD137, a member of the tumor necrosis factor receptor family, is located on chromosome 1p36, in a cluster of related genes, the colocalizes with several malignancies. *Biochemical and Biophysical Research Communications* **235**, 699–703.

Schulte, A.M., Esch J. II, Sevigny, J., Kaczmarek, E., Siegel, J.B., Imai, M., Koziak, K., Beaudoin, A.R., Robson, S.C. (1999) Structural elements and limited proteolysis of CD39 influence ATP diphosphohydrolase activity. *Biochemistry* **38**, 2248–58.

Seiffert, M., Cant, C., Chen, Z., Rappold, I., Brugger, W., Kanz, L., Brown, E.J., Ullrich, A., Buhring, H.J. (1999) Human signal-regulatory protein is expressed on normal, but not on subsets of leukaemic myeloid cells and mediates cellular adhesion involving its counter receptor CD47. *Blood* **94**, 3633–43.

Serru, V., Le Naour, F., Billard, M., Azorsa, D.O., Lanza, F., Boucheix, C., Rubinstein, E. (1999) Active tetraspan–integrin complexes (CD81/alpha4beta1, CD151/alpha3beta1, CD151/alpha6beta1) under conditions disrupting tetraspan interactions. *Biochemical Journal* **340**, 103–11.

Shimozato, O., Takeda, K., Yagita, H., Okumura, K. (1999) Expression of CD30 ligand (CD153) on murine activated T cells. *Biochemical and Biophysical Research Communication* **256**, 519–26.

Sieling, P.A., Jullien, D., Dahlem, M., Tedder, T.F, Rea, T.H., Modlin, R.L., Porcelli, S.A. (1999) CD1 expression by dendritic cells in human leprosy lesions: correlation with effective host immunity. *Journal of Immunology* **162**, 1851–8.

Sievers, E.L., Appelbaum, F.R., Speilberger, R.T., Forman, S.J., Flowers, D., Smith, F.O., Shannon-Dorcy, K., Berger, M.S., Bernstein, J. (1999) Selective ablation of acute myeloid leukaemia using antibody targeted chemotherapy: a phase I study of an anti CD33 calicheamicin immunoconjugate. *Blood* **93**, 3678–84.

Sincock, P.M., Fitter, S., Parton, R.G., Bernt, M.C., Gamble, J.R., Ashman, L.K. (1999) PETA-3/CD151, a member of the transmembrane 4 superfamily, is localised to the plasma membrane and endocytic system of endothelial cells, associates with multiple integrins and modulates cell function. *Journal of Cell Science* **112**, 833–44.

Skubitz, K.M., Campbell, K.D., Skubitz, A.P. (1997) CD50 monoclonal antibodies inhibit neutrophil activation. *Journal of Immunology* **159**, 820–8.

Skubitz, K.M., Kuroki, M., Jantscheff, P., Skubitz, A.P., Grunert, F. (1999) CD66F. *Journal of Biological Regulators and Homeostatic Agents* **13**, 250–1.

Slupsky, J.R., Kamiguti, A.S., Rhodes, N.P., Cawley, J.C., Shaw, A.R., Zuzel, M. (1997) The platelet antigens CD9, CD42 and integrin alpha IIb beta IIIa can be topographically associated and transduce functionally similar signals. *European Journal of Biochemistry* **244**, 168–75.

Soares, L.R., Tsavaler, L., Rivas, A., Engleman, E.G. (1998) V7 (CD101) ligation inhibits TCR/CD3-induced IL-2 production by blocking $CD2^{+}$ flux and nuclear factor of activated T cell nuclear translocation. *Journal of Immunology* **161**, 209–17.

Speck, R.F., Esser, U., Penn, M.L., Eckstein, D.A., Pulliam, L., Chan, S.Y., Goldsmith, M.A. (1999) A trans-receptor mechanism for infection of CD4-negative cells by human immunodeficiency virus type 1. *Current Biology* **9**, 547–50.

Stroncek, D.F., Shanker, R., Litz, C., Clement, L. (1998) The expression of the NB1 antigen on myeloid precursors and neutrophils from children and umbilical cords. *Transfusion Medicine* **8**, 119–23.

Sun, X., Funk, C.D., Deng, C., Sahu, A., Lambris, J.D., Song, W.C. (1999) Role of decay-accelerating factor in regulating complement activation on the erythrocyte surface revealed by gene targeting. *Proceedings of the National Academy of Science of the USA* **96**, 628–33.

Syto, R., Murgolo, N.J., Braswell, E.H., Mui, P., Huang, E., Windsor, W.T. (1998) Structural and biological stability of the human interleukin 10 homodimer. *Biochemistry* **37**, 16943–51.

Taylor, V.C., Buckley, C.D., Douglas, M., Cody, A.J., Simmons, D.L., Freeman, S.D. (1999) The myeloid-specific sialic acid-binding receptor, CD33, associates with the protein-tyrosine phosphatases, SHP-1 and SHP-2. *Journal of Biological Chemistry* **274**, 11505–12.

Telen, M.J. (2000) Red blood cell surface adhesion molecules: their possible roles in normal human physiology and disease. *Seminars in Hematology* **37**, 130–42.

Terashi, K., Oka, M., Ohdo, S., Furakubo, T., Ikeda, C., Fukanda, M., Soda, H., Higuchi, S., Kohno, S. (1999) Close association between clearance of recombinant human granulocyte colony-stimulating factor (G-CSF) and G-CSF receptor on neutrophils in cancer patients. *Antimicrobial Agents and Chemotherapy* **43**, 21–4.

Teunis, B., Geijtenbeek, R.T., van Vliet, S.J., van Duijnhoven, G.C.F., Gosse, J.A., Figdor, C.G. (2000) Identification of DC-SIGN, a novel dendritic cell-specific ICAM-3 receptor that supports primary immune responses. *Cell* **100**, 575–85.

Thomas, X., Anglaret, B., Bailly, M., Maritaz, O., Magaud, J.P., Archimbaud, E. (1998) Differential adhesiveness between blood and marrow leukemic cells having similar pattern of VLA adhesion molecule expression. *Leukaemia Research* **22**, 953–60.

Till, K.J., Zurel, M., Cawley, J.C. (1999) The role of hyaluronan and interleukin 8 in the migration of chronic lymphocytic leukaemia cells within lymphoreticular tissues. *Cancer Research* **59**, 4419–26.

Toba, K., Koike, T., Shibata, A., Hashimoto, S., Takahashi, M., Masuko, M., Azegami, T., Takahashi, H., Alzawa, Y. (1999) Novel technique for the direct flow cytofluorometric analysis of human basophils in unseparated blood and bone marrow, and the characterisation of phenotype and peroxidase of human basophils. *Cytometry* **35**, 249–59.

Todd, R.F., Petty, H.R. (1997) Beta 2 (CD11/CD18) integrins can serve as signaling partners for other leukocyte receptors. *Journal of Clinical Laboratory Medicine* **129**, 492–8.

Tomatis, D., Echtermayer, F., Schober, S., Balzac, F., Retta, S.F., Silengo, L., Tarone, G. (1999) The muscle specific laminin receptor alpha7 beta1 integrin negatively regulates alpha5 beta1 fibronectin receptor function. *Experimental Cell Research* **246**, 421–32.

Tsurudome, M., Ito, M., Takabayashi, S., Okumura, K., Nishio, M., Kawano, M., Kusagawa, S., Komada, H., Ito, Y. (1999) Cutting edge: primary structure of the light chain of fusion regulatory protein-1/CD98/4F2 predicts a protein with multiple transmembrane domains that is almost identical to the amino acid transporter E16. *Journal of Immunology* **162**, 2462–6.

Tu, L., Delahunty, M.D., Ding, H., Luscinskas, F.W., Tedder, T.F. (1999) The cutaneous lymphocyte antigen is an essential component of the L-selectin ligand induced on human vascular endothelial cells. *Journal of Experimental Medicine* **189**, 241–52.

Uchida, S., Shimada, Y., Watanabe, G., Li, Z.G., Hong, T.,

Miyake, M., Imamura, M. (1999) Motility-related protein (MRP-1/CD9) and KAI1/CD82 expression inversely correlate with lymph node metastasis in oesophageal squamous cell carcinoma. *Journal of Cancer* **79**, 1168–73.

Valerius, T., Stockmeyer, B., van Spriel, A.B., Graziano, R.F., van Herik-Oudijk, I.E., Repp, R., Deo, Y.M., Lund, J., Kalden, J.R., Gramatzki, M., van der Winkel, J.G. (1997) FcalphaRI as a novel trigger molecule for bispecific antibody therapy. *Blood* **90**, 4485–92.

Valgeirsdottir, S., Claesson-Welsh, L., Bongcam-Rudloff, E., Hellman, U., Westermark, B., Heldin, C.H. (1998) PDGF induces reorganization of vimentin filaments. *Journal of Cell Science* **111**, 1973–80.

Valladeau, J., Ravel, O., Dezutter-Dambuyer, C., Moore, K., Kleijmeer, M., Liu, Y., Duvert-Frances, V., Vincent, C., Schmitt, D., Davoust, J., Caux, C., Lebecque, S., Saeland, S. (2000) Langerin, a novel C-type lectin specific for Langerhans cells, is an endocytic receptor that induces the formation of Birbeck granules. *Immunity* **12**, 71–81.

van den Heuvel-Eibrink, M.M., Sonneveld, P., Pieters, R. (2000) The prognostic significance of membrane transport-associated multidrug resistance (MDR) proteins in leukemia. *International Journal of Clinical Pharmacology and Therapeutics* **38**, 94–110.

van der Velden, V.H., Hulsmann, A.R. (1999) Peptidases: structure, function and modulation of peptide-mediated effects in the human lung. *Clinical and Experimental Allergy* **29**, 445–56.

van Horssen, P.J., van Oosterhout, Y.V., Evers, S., Backus, H.H., van Oijen, M.G., Bongaerts, R., de Witte, T., Preijers, F.W. (1999) Influence of cytotoxicity enhancers in combination with human serum on the activity of CD22-recombinant ricin A against B cell lines, chronic and acute lymphocytic leukaemia cells. *Leukaemia* **13**, 241–9.

van Spriel, A.B., van der Herik-Oudijk, I.E., van Sorge, N.M., Vile, H.A., van Strijp, J.A., van der Winkel, J.G. (1999) Effective phagocytosis and killing of *Candida albicans* via targeting FcgammaRI (CD64) or FcalphaRI (CD89) on neutrophils. *Journal of Infectious Diseases* **179**, 661–9.

Vickers, J., Russwurm, S., Dohrn, B., Portele, T., Spangenberg, P., Reinhart, K., Losche, W. (1998) Monocyte tissue factor (CD142) and Mac-1 (CD11b) are increased in septic patients. *Thrombosis Haemostasis* **79**, 1210–20.

Vogel, W., Gish, G.D., Alves, F., Pawson, T. (1997) The discoidin domain receptor tyrosine kinases are activated by collagen. *Molecular Cell* **1**, 13–23.

Vorchheimer, D.A., Badimon, J.J., Fuster, V. (1999) Platelet glycoprotein IIb/IIIa receptor antagonists in cardiovascular disease. *Journal of American Medical Association* **281**, 1407–14.

Waclavicek, M., Majdic, O., Stulnig, T., Berger, M., Sunder-Plassmann, R., Zlabinger, G.J., Baumruker, T., Stockl, J., Ebher, C., Knapp, W., Pickl, W.F. (1998) CD99 engagement on human peripheral blood T cells results in TCR/CD3-dependent cellular activation and allows Th1-restricted cytokine production. *Journal of Immunology* **161**, 4671–8.

Wada, T., Seki, H., Konno, A., Ohta, K., Nunogami, K., Kaneda, H., Kasahara, Y., Yachie, A., Koizumi, S., Taniguchi, N., Miyawaki, A. (1998) Developmental changes and functional properties of human memory T cell subpopulations defined by CD60 expression. *Cellular Immunology* **187**, 117–23.

Wakeham, A., Karan-Tamir, B., Muller, W.A., Senaldi, G., Zukowski, M.M., Mak, T.W. (1999) Genetic evidence for functional redundancy of platelet/endothelial cell adhesion molecule-1 (PECAM-1): CD31 deficient mice reveal PECAM-1 dependent and PECAM-1 independent functions. *Journal of Immunology* **162**, 3022–30.

Walker, J., Green, J.M. (1999) Structural requirements for CD43 function. *Journal of Immunology* **162**, 4109–14.

Watt, S.M., Buhring, H.J., Rappold, I., Chan, J.Y., Lee-Prudhoe, J., Jones, T., Zannettino, A.C., Simmons, P.J., Doyannas, R., Sheer, D., Butler, L.H. (1998) CD164, a novel sialomucin on CD34 + and erythroid subsets, is located on human chromosome 6q21. *Blood* **92**, 849–66.

Weber, K.S., Klickstein, L.B., Weber, C. (1999) Specific activation of leucocyte beta2 integrins lymphocyte function-associated antigen-1 by chemokines mediated by distinct pathways via the alpha subunit cytoplasmic domains. *Molecular Biology Cell* **10**, 861–73.

Weinberg, A.D., Wegmann, K.W., Funatake, C., Whitham, R.H. (1999) Blocking OX-40/OX-40 ligand interaction in vitro and in vivo leads to decreased T cell function and amelioration of experimental allergic encephalomyelitis. *Journal of Immunology* **162**, 1818–26.

Willett, C.G., Wang, M.H., Emanuel, R.L., Graham, S.A., Smith, D.I., Shridhar, V., Sugarbaker, D.J., Sunday, M.E. (1998) Macrophage stimulating protein and its receptor in non-small-cell lung tumors: induction of receptor tyrosine phosphorylation and cell migration. *American Journal of Respiratory Cell Molecular Biology* **18**, 489–96.

Wright, G.J., Brown, M.H., Barclay, A.N. (2000) The lymphoid/neuronal OX-2 glycoprotein interacts with a novel protein expressed by macrophages. *Tissue Antigens* **55**(suppl. 1), 11.

Wyer, J.R., Willcox, B.E., Gao, G.F., Gerth, U.C., Davis, S.J., Bell, J.I., van der Merwe, P.A., Kakobson, B.K. (1999) T cell recep-

tor and coreceptor CD8 alpha bind peptide-MHC independently and with distinct kinetics. *Immunity* **10**, 219–25.

Xiao, M., Oppenlander, B.K., Plunkett, J.M., Dooley, D.C. (1999) Expression of Flt3 and c-kit during growth and maturation of human $CD34^{+}CD38^{-}$ cells. *Experimental Hematology* **27**, 916–27.

Yamada, K., Yamakawa, M., Imai, Y., Tsukamoto, M. (1997) Expression of cytokine receptors on follicular dendritic cells. *Blood* **90**, 4832–41.

Yamashita, M., Kimura, M., Kubo, M., Shimizu, C., Tada, T., Perimutter, R.M., Nakayama, T. (1999) T cell antigen receptor-mediated activation of the Ras/mitogen activated protein kinase pathway controls interleukin 4 receptor function and type-2 helper T cell differentiation. *Proceedings of the National Academy of Sciences USA* **96**, 1024–9.

Yang, J., Furie, B.C., Furie, B. (1999a) The biology of P-selectin glycoprotein ligand-1: its role as a selectin counterreceptor in leucocyte–endothelial and leucocyte–platelet interactions. *Thrombosis Haemostasis* **81**, 1–7.

Yang, S., Graham, J., Kahn, J.W., Schwartz, E.A. Gerritsen, M.E. (1999b) Functional roles for PECAM-1 (CD31) and VE-cadherin (CD144) in tube assembly and lumen formation in three-dimensional collagen gels. *American Journal of Pathology* **155**, 887–95.

Yoshiyama, H., Higuchi, Y., Kataoka, M., Matsuura, K., Yamamoto, S. (1997) CD156 (human ADAM8): expression, primary amino acid sequence, and gene location. *Genomics* **41**, 56–62.

Yu, X., Abe, R., Hodes, R.J. (1998) The role of B7-CD28 costimulation in tumor rejection. *International Immunology* **10**, 791–7.

Zhang, H.F., Yu, J., Chen, S., Morgan, B.P., Abegyan, R., Tomlinson, S. (1999) Identification of the individual residues that determine human CD59 species selective activity. *Journal of Biological Chemistry* **274**, 10969–74.

Zhang, J.G., Hilton, D.J., Willson, T.A., McFarlane, C., Roberts, B.A., Moritz, R.L., Simpson, R.J., Alexander, W.S., Metcalf, D., Nicola, N.A. (1997) Identification, purification, and characterization of a soluble interleukin(IL)-13-binding protein. Evidence that it is distinct from the cloned IL-13 receptor and IL-4 receptor alpha-chains. *Journal of Biological Chemistry* **272**, 9474–80.

Zimmerman, J.W., Lindermuth, J., Fish, P.A., Palace, G.P., Stevenson, T.T., DeMong, D.E. (1998) A novel carbohydrate–glycosphingolipid interaction between a beta-(1-3)-glycan immunomodulator, PGG-glycan, and lactosylceramide of human leucocytes. *Journal of Biological Chemistry* **273**, 22014–20F.

18

Recent and future developments: conclusions

Desmond A. McCarthy

Queen Mary and Westfield College, London

18.1 Introduction

The second half of the twentieth century witnessed remarkable developments in cytometry, which were made possible by simultaneous advances in a number of different disciplines. It is unlikely, however, that such rapid progress would have been made if the new technologies had not been embraced so enthusiastically by clinical laboratories. That routine cytometric analyses can make such a cost-effective contribution to disease diagnosis and patient management was, and is likely to continue to be, one of the strongest forces influencing innovation in cytometry. In other areas, cytometric techniques that were first established in the biomedical sciences are now being applied increasingly not only to detect and characterise cells but also to quantify soluble analytes.

Conventional clinical flow cytometers measure only the intensity of scattered and fluorescent light but research instruments exist that have the ability to measure other parameters contained in these signals (Roslaniec et al., 1997). If the extra information that can be gained from these measurements proves useful in the clinical context, the facility to measure other parameters could be incorporated in instruments for routine use.

A new generation of radically different cytometers has also just started to emerge. The Compucyte laser scanning cytometer is the first of a number of scanning instruments designed to characterise cells that are held stationary on, or in, a support medium. At present, static cytometers are perhaps not as versatile as their flow-based counterparts but they have some interesting and unique capabilities, which will ensure their wider use in the future. In recent years, laboratory bench-top analytical flow cytometers have been getting steadily smaller and some small 'point of care' and portable instruments are now available. Several research and prototype instruments have been constructed using micrometre scale fluidic channels, but they have not as yet been coupled to miniature optical systems. These developments, together with others in fluorochromes, and applications will be examined and discussed.

18.2 Developments in fluorescent labels

Until a few years ago, most flow cytometers were powered by a single 488 nm laser but increasing numbers of both flow and scanning instruments are being produced with two or three excitation sources and four or more fluorescence detection channels. New and improved luminescent labels are constantly sought but there is a particular need for more dyes that can be excited by the ~633 nm line of the helium–neon laser in order to make full use of these facilities in multiparameter assays. However, as the number of fluorescence parameters to be assayed rises, it inevitably becomes more difficult to set spectral compensation correctly and to correct for the excitation of tandem dyes at multiple wavelengths (laser 'crosstalk'; for which interlaser compensation is needed). It is also necessary to guard against artefacts created by the light-induced breakdown of tandem dyes. An alternative solution to these problems might be to discriminate between fluorochromes on the basis of differences in

their excited state lifetimes (see Section 18.3.4).

Other recent interesting developments in fluorochrome technology include monitoring excimer formation to detect when homologous fluorochrome molecules are in close proximity (see Section 18.2.3) and the use of 'upconverting' phosphors as luminescent labels (below).

18.2.1 Anti-Stokes' or upconverting phosphors

There are some materials that can be excited with infrared irradiation to emit radiation by phosphorescence in the visible wavelengths (materials that continue to emit light for more than 10^{-8} s after irradiation are strictly termed phosphorescent rather than fluorescent). These materials are called anti-Stokes' or upconverting phosphors because they have the unique property of absorbing two or more photons of infrared radiation in order to emit a single photon of higher energy. No natural materials exhibit upconversion over this wavelength range; consequently, there is no background autophosphorescence in assays utilising upconverting phosphors. All upconverting phosphors comprise an absorber and an emitter ion in a crystal lattice; when the absorber is excited by the infrared source it transfers the energy to the emitter, which emits a photon. Many upconverting phosphors commonly employ ytterbium as the absorber ion and erbium, holmium, terbium or thulium as the emitter ion, within alumininosilicates, fluorides, gallates, germanosilicates, plumbosilicates, oxyhalides or oxysulphides as the host crystal material (Zijlmans et al., 1999), although rare-earth-doped chalcogenide glasses (e.g. $70Ga_2S_3 : 30La_2O_3$) have also been used (Amorim et al., 1998). Many different compositions are known that can be excited at wavelengths between 980 and 1540 nm. Emission bandwidths are generally narrow (25–50 nm) and are well separated (> 200 nm) from the exciting wavelengths; moreover the phosphors do not suffer from photobleaching.

Zijlmans et al. (1999) used a green-emitting yttrium/ytterbium/erbium ($(Y.Yb.Er)O_2S$) and a blue-emitting yttrium/ytterbium/thulium ($(Y.Yb.Tm)_2O_2S$) conjugated to NeutrAvidin™ (Pierce Chemical Co.) to detect biotinylated antibodies in an epi-illumination microscope study of prostate structure and $CD4^+$ lymphocytes.

SRI International have developed a flow cytometry-based assay system in which different sized latex beads (e.g. 5, 10 and 15 μm diameter) have been coated with antibodies to capture different analytes. These are then reacted with submicrometre 'upconverting' phosphor particles with antibodies covalently bonded to the surface to act as reporters in a sandwich assay. Many unique phosphor colours (currently 10) can be created for excitation by a 980 nm yttrium aluminium garnet (YAG) laser, thereby allowing multiplexing (see also Section 18.7.3), for example for labelling different pathogens in a single test (Fig. 18.1). This technology was initially developed with a view to detecting biological warfare agents in the field but it could have many more applications in the health sciences.

18.2.2 Lanthanide chelates

Rare earth chelates (or organic lanthanides) have been used in time-resolved fluorescent immunoassays for some time (e.g. DELFIA, Dissociation Enhanced Lanthanide Fluoro-Immuno Assay; Wallac Division of PerkinElmer Life Sciences). However the DELFIA technique itself is not amenable for use in cytometric analysis. The rare earth chelates comprise one of the 14 lanthanide metals attached by double or multiple bonds (chelated) to a large organic ligand. All lanthanides have an unfilled 4fn electronic orbital, which confers a number of useful photochemical properties including a forbidden transition from the ground to the triplet state. However, secondary molecules can donate electrons causing this transition and thus excite lanthanide luminescence. Absorption of ultraviolet light by the organic ligand excites it from the ground to singlet state (~25% of absorbed energy) or triplet state (~75% of absorbed energy) from which energy can then be passed to the lanthanide raising it to a triplet state. As the metal decays from the triplet to

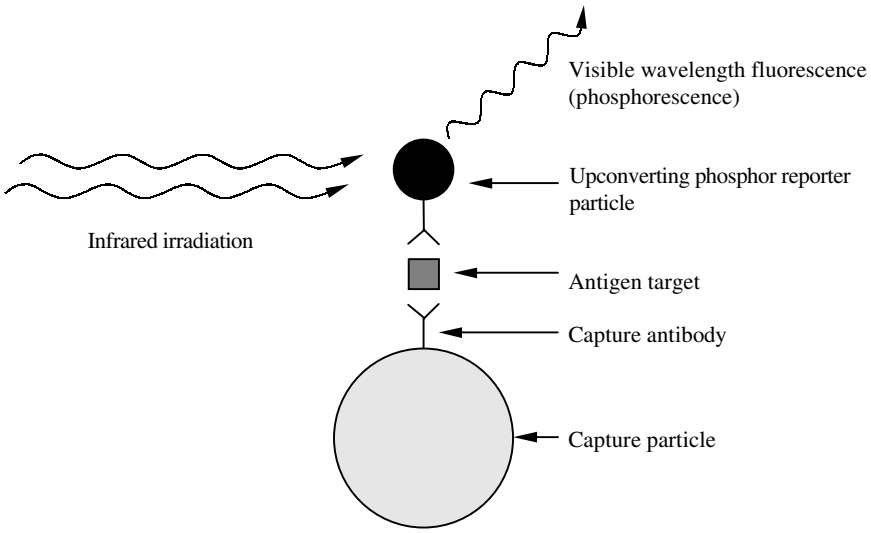

Fig. 18.1 Upconverting submicrometre phosphor particles can be used as reporters in sandwich immunoassays to reveal target antigens bound by an antibody-coated micrometre size capture particle. The capture particle can be colour and size coded and the phosphor particle can be colour coded with respect to the specificity of the antibodies bound to their surfaces. This allows highly multiplexed assays. The size and colour of the capture particles can be discriminated by standard flow cytometry using visible wavelengths and the bound analytes can be detected using an infrared laser to excite the phosphor reporter particles.

the ground state, it loses energy by phosphorescence and by nonradiative means. Important properties of the rare earth chelates are that they have a far greater Stokes' shift (~ 200–300 nm), much narrower emission bandwidths, and far longer fluorescence (actually phosphorescence) lifetimes (see Section 18.3.4) than most conventional fluorochromes. It is the organic ligand that confers characteristics such as light absorption and solubility, whereas the lanthanide determines the emission wavelength, bandwidth and lifetime. Therefore, cerbium chelates emit in the blue, terbium in the green, europium in the red and erbium in the infrared.

Europium cryptates are another class of rare earth-based fluorophores, in which the europium ion is 'caged' by a macropolycyclic compound (Fig. 18.2). The cryptate cage is responsible for trapping light energy and transferring it to the lanthanide ion while at the same time protecting it from solvent (water). Europium cryptates (excitation/emission maxima ~ 337/620 nm) have been used successfully in resonance transfer systems to pass energy to phycobiliproteins (e.g. to XL665, a crosslinked allophycocyanin), resulting in a long-lived fluorescence at 665 nm. The necessary reagents (e.g. antibodies, streptavidin–biotin conjugates and anti-species antibodies) are sold by Packard Instrument Company primarily for use in the HTRF® (Homogeneous Time-Resolved Fluorescence) assays that are used in high-throughput drug screening programmes. (HTRF® is based on the CIS bio International proprietary TRACE™ technology. Packard holds the exclusive licence for this technology in the life science market. HTRF® products are manufactured under one or more of the following patents: EP180492, EP321353, EP539435, EP569496, EP076695. HTRF® is a registered trademark of Packard BioScience Company or its subsidiaries in the USA and/or other countries.) However, they could also have many potential uses where cytometers with the necessary ultraviolet excitation sources are available.

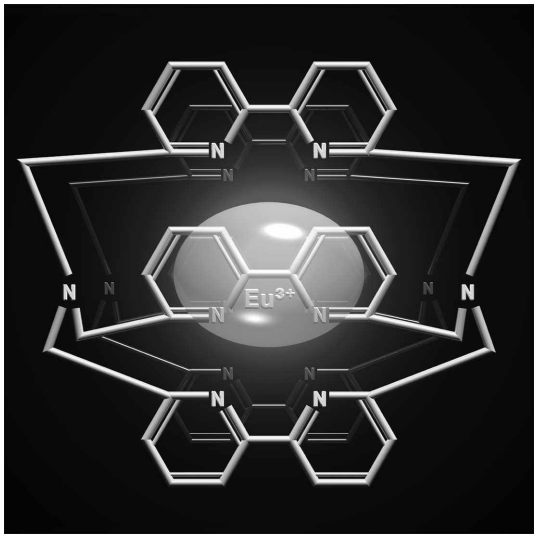

Fig. 18.2 Structure of the europium cryptate used in the Packard HTRF® europium cryptate-crosslinked allophycocyanin fluorescence resonance energy transfer system. (Reprinted with permission of the copyright holder, the Packard BioScience Company.)

18.2.3 Monomer–excimer fluorescence

If two molecules of a fluorochrome are in close (a few angstroms, i.e. less than 1 μm) proximity and have the correct relative orientation, they can form an excimer, which upon excitation has different spectral properties from the corresponding monomer. Excimer fluorescence has been used frequently to probe the structure of biological molecules in solution and recently the principle has been extended to measurements by flow cytometry. Pyrene derivatives are commonly used as the fluorochrome for this purpose because they can be used to label proteins, nucleic acids and lipids. For instance, pyrene decanoic acid (PDA), which can be excited in the ultraviolet (e.g. by the 351 nm line of an argon laser), has monomer and excimer fluorescence at 395 and 478 nm, respectively, and can be used to monitor membrane fluidity (Seidl et al., 1999). Interestingly, the analysis of platelet membrane viscosity as determined with PDA was well correlated with the concentration of serum high density lipoprotein cholesterol in patients (Rothe et al., 1998). Conjugates of pyrene with oligodeoxynucleotides have been used as hybridisation probes, which undergo strong excimer fluorescence when complementary strands are brought into close proximity on duplex formation (Balakin et al., 1998). Adjacent binding of a pair of oligodeoxynucleotide probes with pyrene replacing a DNA base at the 3' and 5' ends can result in up to sevenfold decreases in monomer fluorescence and up to 40-fold increases in excimer fluorescence (Paris et al., 1998). This effect seems to be a powerful sensor suitable for detecting nucleic acid hybridisation in solution, even enabling single base point mutations to be detected; it does not seem to have been used with flow cytometry as yet.

18.3 Gaining additional information from light scatter and fluorescence signals

Several groups have modified commercially available cytometers or have built specialised instruments that are able to retrieve additional information from light scatter or fluorescence signals. In many instances, the extra information gained can be a useful discriminator and the technology employed may eventually find wider application.

18.3.1 Angular light scatter measurements of single cells (the scanning flow cytometer)

Most instruments that are able to measure light scattering over a wide range of angles do so on particles in suspension. Because an 'average' signal is recorded, the technology is only applicable to homogeneous cell populations. In contrast, a scanning flow cytometer allows an entire light scattering trace of individual particles or cells to be made across a wide range of angles (typically 5–100°); the trace, which is characteristic of a given particle, is termed an indicatrix (Soini et al., 1998). Analysis rates at present are slower than usual (600 particles s^{-1}), but given the correct software, the information derived from angular light scatter

measurements could be used as an important additional parameter to discriminate cell or particle populations.

18.3.2 Fluorescence emission spectra measurements of single cells

Microscopes capable of analysing fluorescence spectra have long been available and in recent years this principle has been extended to the flow cytometer. By using a spectrograph and a 512-element linear photodiode array detector, Gauci et al. (1996) demonstrated that it was possible to record emission spectra from single cells. Asbury et al. (1996) took an alternative approach and replaced a photodetector with a monochromator, which scanned continuously over a range of wavelengths. The fluorescence intensity at each wavelength, together with the other fluorescence and scatter signals, for each particle was recorded. Acquiring the complete emission spectrum provides more information, potentially allowing better discrimination between different dyes or cell populations because spectral filters can be set entirely within the software. The technique would be particularly valuable where the study of small spectral shifts is involved.

18.3.3 Measurements of fluorescence polarisation

Fluorescence polarisation (or depolarisation) is a technique that involves exciting a fluorochrome with plane polarised light and then measuring the vertical and horizontal components of the emitted fluorescence. In the time interval between absorbing and emitting light, the fluorochrome will tumble randomly. If it does so only slowly, most of the emitted light remains polarised, whereas if it does so quickly, the light will be depolarised. The rate of depolarisation is, therefore, inversely related to the speed of molecular rotation of the fluorochrome, which is itself related to the fluorochrome's molecular weight. If a small fluorochrome, such as a BODIPY® dye (4,4-difluoro-4-bora-3a,4a-diaza-s-indacene derivatives), is conjugated to a larger molecule such as a peptide or protein, it is the molecular size of the conjugate, not just that of the dye alone, that determines the speed of molecular rotation. Furthermore, the rate of depolarisation of the conjugate will decrease if it associates with other structures that further restrict molecular motion. By combining fluorescence polarisation measurements with flow cytometry, the technique can be used to report on the environment in which a fluorochrome complex is located within a cell. In conjunction with analyses by Western blotting, the technique has been used to demonstrate that changes subsequent to the ingestion of fluorescein-conjugated bovine serum albumin by a macrophage cell line were consistent with transport through the endocytic system and proteolytic degradation (Weaver et al., 1997). The extent of fluorescence polarisation following the staining of lipid membranes with 1,6-diphenyl-1,3,5-hexatriene (DPH) is dependent on rotational movement, which in turn is dependent on membrane fluidity. However, direct comparison of this technique with monitoring PDA excimer formation (see above) showed the latter to be the more sensitive indicator of membrane microviscosity (Rothe et al., 1998).

18.3.4 Time-resolved fluorescence

Time-resolved fluorescence measurements can provide important additional information about fluorochromes. The intrinsic fluorescence lifetimes of some fluorochromes differ sufficiently so that, following a pulse of illumination, emission from one can still be detected long after that from others has ceased. For example, the europium chelates (excitation/emission maxima ~ 350/610 nm) fluoresce for much longer than conventional fluorochromes, enabling their luminescence (decay times 10 μs to 2 ms) to be readily distinguished from autofluorescence and from rapid dye emissions (decay times 1 ns to 10 μs) (Condrau et al., 1994a,b). This technique can, therefore, be used to increase the number of fluorescent labels that can be distinguished in multiparameter studies and also enables rare, labelled events to be separated more easily from autofluorescence in environmental samples. An

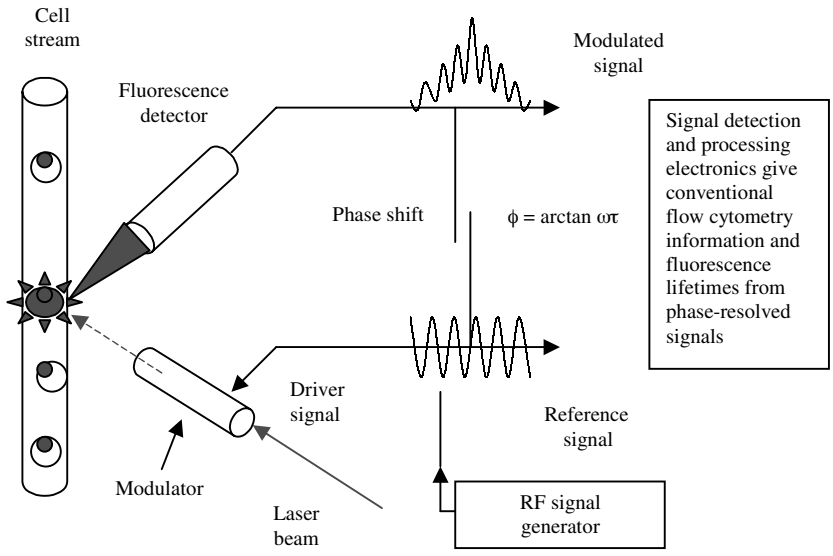

Fig. 18.3 Diagrammatic illustration of the Los Alamos phase-sensitive time-resolved system flow cytometer for the determination of fluorescence lifetimes. Cells are excited by the 488 nm beam from a laser, which is modulated (29 MHz sine wave) by an electro-optic modulator. The emitted fluorescence is processed by phase-shift electronics to yield an intensity signal and the lifetime (deduced from the difference between the phase angles of the reference and fluorescence signals). RF, radiofreqency. (After Roslaniec et al., 1997.)

instrument suitable for discriminating lanthanides, which uses pulsed illumination and counts the number of emitted photons as a function of time, has been described by Condrau et al. (1994b). However, the flow rate in this instrument was an order of magnitude slower than usual, in order to obtain sufficiently accurate data. Time-resolved fluorescence detection has also been applied to resonance energy transfer systems (see Ch. 3), and suitable detection reagents are obtainable from the Wallac Division of PerkinElmer Life Sciences.

Monitoring of much smaller differences in fluorescence lifetimes can provide information on the molecular environment of a bound dye, and even distinguish between two fluorochromes with rapid emissions. An instrument capable of this greatly enhanced time resolution, which uses high-frequency electro-optic modulation (sine wave) of the laser excitation intensity and phase-shift-sensitive detection between the emitted photons and a reference beam, has been described by Steinkamp et al. (1993) (Fig. 18.3). By this means, fluorescence lifetimes of 0.5–350 ns can be measured (Deka et al., 1994). Small changes in fluorescence lifetimes of DNA probes have been observed in different cell types and cell states, and during different stages of the cell cycle (Sailer et al., 1998a,b). For instance, ethidium bromide in apoptotic cells had a fluorescence lifetime of 18 ns in comparison with a lifetime of 22 ns in normal cells, a difference that is probably related to changes in chromatin structure. It has also enabled dyes with overlapping emission spectra to be distinguished on the basis of differences in their fluorescence lifetimes; for example, propidium iodide can be distinguished from phycoerythrin–Texas Red® (Steinkamp et al., 1999). In another study, the fluorescence of Hoechst 33342 (lifetime 15 ns) was distinguished from that of monobromobimane (lifetime 12 ns) allowing changes in glutathione content and DNA content to be monitored simultaneously during the cell cycle (Keij et al., 1999). Although a few flow cytometers in

research institutes have been modified to make time-resolved fluorescence measurements there are none yet available commercially.

18.4 Portable flow cytometers

A few robust portable flow-based instruments that can be used for the analysis of environmental samples in field conditions have been constructed. They are essentially smaller versions of bench-top instruments but suffer from the problem that there is at present no solid-state laser available that can provide excitation at a wavelength close to 488 nm. This is a considerable disadvantage, because it is impossible to use the many fluorochromes that can be excited at this wavelength in conventional instruments.

The Microcyte (Optoflow) is small portable instrument (weight 10 kg) that was originally designed for detecting microorganisms in environmental samples (Fig. 18.4). All of the optics are contained in a solid aluminium block, so no daily alignment is necessary. Excitation is by a single 635 nm laser diode and the light scattering sensitivity allows particles within the size range 0.4–15 μm to be detected. Fluorescence detection is in the range 650–900 nm; consequently its use is limited to dyes that can be excited in the red region of the spectrum.

A mini-flow cytometer for the detection, identification and quantification of pathogens, biological warfare agents in particular, has been developed for use in the field. It incorporates a novel self-alignment technique, designed by the group at the Lawrence Livermore National Laboratory (USA), in which the flow stream itself acts as a waveguide. Analysis takes about 1 min per sample (~160 samples per day), and in field trials an accuracy of 87% correct positives and 0.47% false positives was achieved.

SRI International, a nonprofit organisation, is also developing a compact flow cytometer for detecting biological warfare agents by means of a multiplex antibody capture assay in conjunction with upconverting phosphor microspheres excited by infrared

Fig. 18.4 The Microcyte portable cytometer. The cytometer, which weighs just 12 kg and measures 330 mm × 430 mm × 160 mm, can be powered by rechargeable batteries or an external 12 V d.c. source. (Reprinted with permission of the copyright holder, Optoflow AS.)

irradiation to produce a phosphorescence signal in the visible range.

18.5 Microscale analysis and sorting using miniature fluidic circuits

There have been several interesting developments in microfluidic flow cytometry, in which cells are aligned in very narrow channels, with or without hydrodynamic focusing by a sheath fluid. The technology also has the potential to be cheaper, consume less reagents and to need smaller instrumentation than existing flow cytometry.

The MicroCytometer™ produced by Micronics Inc. uses miniature laser-cut fluid circuits in conjunction with laser (685 nm diode laser) forward (1–2°) and small angle (2–8°) light scattering to count erythrocytes, platelets and leukocytes. The addition of extra data channels could give a fivepart white cell differential count based on characteristic differences in light scattering. The instrument could then constitute a portable 'point of care' hematology analyser (Altendorf et al., 1999a,b). An alternative approach developed by Jacobson and col-

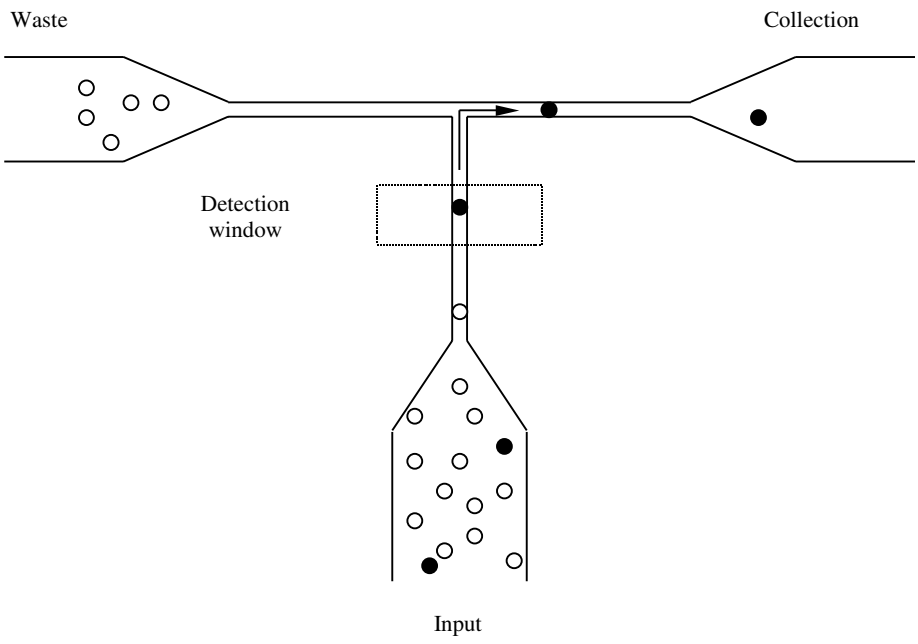

Fig. 18.5 A diagrammatic illustration (not to scale) of the microfabricated T-channel used for DNA and cell sorting by fluorescence flow cytometry. The channels are 100 μm wide at the edges of the illustration and narrow down at the T-junction (to between 5 μm and 20 μm). The channels terminate in cylindrical wells (not shown) that are connected to electrodes. Sample input is in the leg of the 'T' and cells are monitored just before they reach the bifurcation. In the forward sorting mode, cells are then directed to the right (collection) or left (waste) by switching the polarity of the applied voltage. (After Fu et al., 1999.)

leagues (Schrum et al., 1999) uses electrokinetic focusing to confine the flow stream on a microchip, but there do not yet seem to be any reports of its application to biological materials.

Miniaturisation has not been confined only to analysis, as a disposable 'micro-machined chip', comprising a T-shaped arrangement of channels 5–20 μm wide at the junction in a silicone mould under a coverslip, has been used as the flow cell for a miniature cell sorter (Fu et al., 1999) (Fig. 18.5). Cells enter the device through the limb of the 'T' and are monitored before reaching the junction, where they can be directed to right or left by pressure control or electroendo-osmotic flow. The instrument has been used to separate bacteria and DNA fragments according to size (pulse height of fluorescence intensity after staining with YOYO®-1, a DNA dye). Throughput rates (~ 20 cells s^{-1}) are very slow by comparison with conventional sorters but it is thought that they could be substantially increased in future. Currently, the miniature flow cell is used in conjunction with conventional optics, but it is envisaged that the necessary detectors and filters could ultimately be fabricated on the microchip.

18.6 New static cytometers

The greatest recent innovations in cytometry have been in instruments in which cells remain static with respect to their support, which is scanned by an excitation and detection system. Several of these nonflow cytometers are specifically designed for clinical assays and are described in Section 18.8.2; others are discussed here.

Fig. 18.6 The PE Biosystems FMAT® 8100 HTS System macroconfocal analyser intended for monitoring high-throughput homogeneous cell- or bead-based assays. (Reprinted with permission of the copyright holder, PE Biosystems.)

18.6.1 Macroconfocal scanning cytometer

The FMAT® 8100 HTS System from PE Biosystems (developed in conjunction with Biometric Imaging Inc., now incorporated with BD Biosciences) is a macroconfocal scanning instrument that has been produced for use in the high-throughput screening assays that are used in drug discovery programmes (Fig. 18.6). It is powered by a single 18 mW helium–neon laser emitting at 633 nm, scans at 1 $mm^2\ s^{-1}$ with a 100 μm depth of focus and has two detectors at 650–685 and 685–720 nm. It is intended for analysing 'mix and read' assays with live cells or beads in 96-, 384- and 1536-well plates, which can be loaded by means of a robotic 60-plate stacker. Analysis is very fast, with 96- and 384-well plates being read in just 7 and 18.5 min, respectively. Typical assays are cell surface receptor binding, apoptosis, cytotoxicity and bead-based fluorescence-linked immunosorbence assays (FLISAs).

The FMAT® 8100 HTS System (PE Biosystems) has been used successfully by Miraglia et al. (1999a–c) for a number of purposes. These include the detection of intercellular adhesion molecule 1 expression on cultured cells, with or without prior stimulation by cytokines; the identification of apoptotic cells using cyanin 5 (Cy™5)-labelled annexin V in conjunction with a DNA-binding dye (TOTO®-3); and the detection of fluorescent neuropeptide Y binding to cells. Schwartzman et al. (1999) have used the instrument in conjunction with FLISAs to quantify cytokine production from tissue culture supernatants.

18.6.2 Small laser scanning cytometers

A number of small-scale or miniature scanning cytometers have been produced (see also Section 18.8.2) or are in the prototype stage. None are likely to have the resolution of the larger instruments but they may prove adequate for specific tasks such as $CD4^+/CD8^+$ cell counts.

The Cell Track Cytometer (Immunicon; PA, USA) uses technology in which cells that have been labelled both with magnetic nanoparticles and with fluorochrome-conjugated antibodies are placed in micrometre width channels and subjected to a magnetic field gradient (Tibbe, 1999). This causes the required (magnetic nanoparticle labelled) cells to rise to the surface of the channel while the unlabelled cells sediment to the bottom. The tracks in which the cells are now aligned in rows, with the required cells at the surface, can then be scanned using a conventional laser powered optical system and the cell-associated fluorescence recorded.

18.7 New applications of existing technologies

New applications of cytometry and cell sorting in the biomedical and clinical sciences are constantly being reported. Some, for example sperm sorting, can be achieved with unmodified instruments,

whereas others, for example kinetic analysis and multiplex analysis, may require alterations to the hardware and/or software for optimum results.

18.7.1 Kinetic analyses

Flow cytometry can be a useful technique for studying single-cell kinetics, including receptor–ligand interactions, and calcium-mediated signalling. Cunningham et al. (1998) devised an injection system in which a solution containing the stimulus or ligand was added to a thermostated stirred tube containing cells that were already flowing through the cytometer. Using this system, they were able to obtain a time resolution in the range 1–4 s. However, Blankenstein et al. (1996), have devised a coaxial flow mixing device that allows almost instantaneous mixing ($<$60 ms), enabling kinetic measurements to be made over a time range of 100 ms to 3 min. The use of such devices should enable equilibrium binding, association and dissociation constants to be determined for cells under physiological conditions.

18.7.2 Sperm sorting

Spermatozoa bearing X or Y chromosomes can be sorted on the basis of their DNA content; for instance, the human X sperm contains 2.8% more DNA than the Y sperm and will, therefore, stain more intensely with nontoxic fluorescent dyes. Efficiencies of $>$ 90% have been obtained for routine sorting of X and Y animal sperm and of 85–90% for sorting human sperm. Sorting can typically be accomplished at rates of approximately 6×10^6 h^{-1} with rates up to 15×10^6 to 20×10^6 h^{-1} being attainable for special purposes (Johnson and Welch, 1999). An agricultural example of the advantages of sperm sexing is in breeding cattle for dairy or beef production. Flow-sorted human spermatozoa might be used in conjunction with in vitro fertilisation, or intra-oviduct insemination by couples who are at risk for X-linked diseases, preferentially to produce female offspring. Indeed, successful pregnancies and deliveries using this technique have recently been reported by the London Gender Clinic (2000). However, some caution is needed, because dye binding and irradiation in the ultraviolet, during sorting, have the potential to cause DNA damage. More experience is needed before the safety of this procedure can be evaluated.

18.7.3 Bead and multiplex bead assays

Antibody-labelled beads have long been used in immunoassays and are now being used in multiplex assays that are monitored using a cytometer. The principle of multiplex assays is that fluorescent microspheres coated with unlabelled antibody are used to capture an analyte from the sample (e.g. plasma, blood). The beads are washed and reacted with a second fluorochrome-labelled antibody, the fluorescence intensity of which will be proportional to the analyte concentration. More than one analyte can be examined at a time if the capture beads are size or colour coded (e.g. by containing unique mixtures of orange and red dyes in different proportions) with respect to the bound antibody (hence multiplex). A mixture of different specific second antibodies, all of which have been labelled with a common fluorochrome (e.g. green), is added and the sample analysed by flow cytometry. Beads bearing each antibody can be gated by their unique size or colour characteristics and the fluorescence intensity of the second antibody determined (Fig. 18.7). The principle has also been extended to nucleic acid hybridisation for the detection of specific DNA sequences and even single nucleotide polymorphisms. Originally, assays were done with standard flow cytometers but modification kits and dedicated instruments are now available.

The FlowMetrix® system (Luminex Corp., which enables multiplex assays to be done on a single sample as small as 5 μl) uses 64 microspheres with unique proportions of red and orange dyes and a capture sandwich assay with bound antigen revealed by a green labelled antibody. Analysis can be done on a standard BD FACScan™, with some modification to the hardware and software. Assays for widely differing concentrations of analytes are

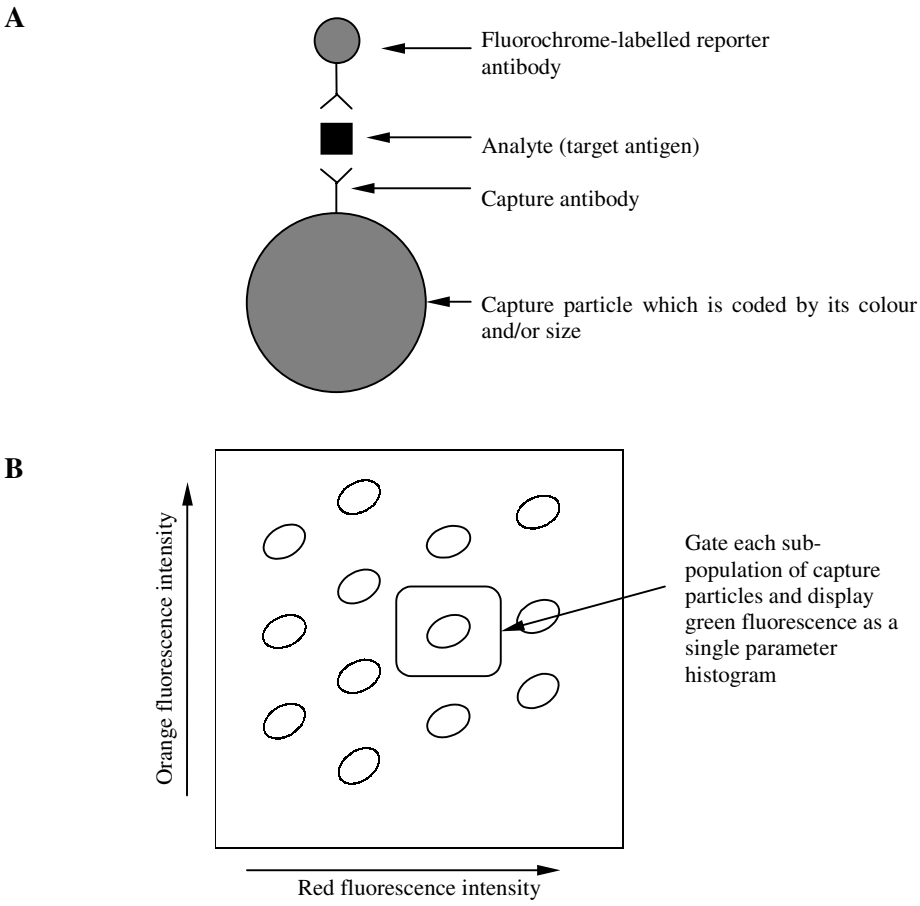

Fig. 18.7 The principle of multiplex immunoassays. Capture microsphere particles are created in a number of different sizes and/or colours, which are unique to the specificity of the antibody that is bound to them. For example, sets of microspheres containing red and orange dyes in different proportions are used in the FlowMetrix system. After capturing their respective analytes from the sample solution, a mixture of secondary antibodies that are all conjugated with the same fluorochrome (e.g. fluorescein isothiocyanate, green) is added (A). Analysis of the mixture by flow cytometry enables the different capture microspheres to be distinguished by their proportion of red-orange dye. (B) gating of each separately allows the fluorescence intensity (green) of the reporter antibody to be determined.

done at different sample dilutions, and calibration curves need to be constructed so that fluorescence results can be converted to analyte concentrations.

The Luminex 100™ system (Luminex Corp.) uses the LabMAP 100 microsphere system containing unique proportions of red and infrared dyes (emission maxima, 660 and 720 nm) and analytes are measured with antibodies labelled with an orange fluorochrome (Fig. 18.8). The flow cytometer designed for use with these assays incorporates a solid-state, frequency-doubled, YAG laser emitting at 580 nm and a red-sensitive photomultiplier giving a sensitivity of ~1000 molecules of phycoerythrin. Pilot studies have shown that the LabMAP system can be used successfully for several immuno- and DNA-based assays, including those for viral

loads in human immunodeficiency virus (HIV)-infected individuals and for cytokines. Coincidentally, Luminex have also produced a new instrument of similar design to the Luminex 100™ that has side and forward light scatter detection and six fluorescence channels and is intended for cell analysis.

A slight variant of the multiplex principle has been introduced by BioErgonomics in which paramagnetic beads of 7 μm diameter are coated with unlabelled capture antibodies specific to particular cytokines. After binding cytokines in serum or blood, the beads are reacted with fluorescent reporter antibodies to create a sandwich, which can then be analysed. An advantage of this system is that assays can be run in whole blood alongside cells because the beads can be separately identified by their different size.

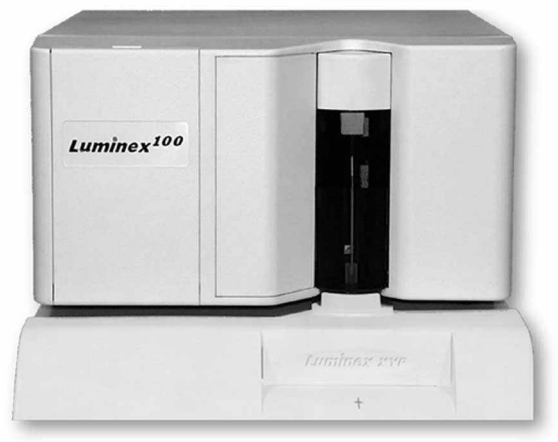

Fig. 18.8 The Luminex 100^{TM} system (Copyright (2000) of the Luminex Corporation TX, USA; all rights reserved); the unit below the cytometer is for the storage and automatic loading of 96-well plates. (Reprinted with permission of the copyright holder, the Luminex Corporation.)

18.8 Current and future clinical needs

At present, flow cytometry is commonly used in the clinical context for:

- immunophenotyping of leukaemias and lymphomas and for monitoring residual disease
- counting $CD34^+$ stem cells for optimising autotransplants
- counting reticulocytes
- counting $CD4^+/CD8^+$ lymphocytes in HIV-infected patients
- the analysis of DNA from solid tumours.

It is used less commonly for the diagnosis of other diseases including: neutrophil malfunction, paroxysmal nocturnal hemoglobulinaemia, autoimmune neutropenia, infectious diseases, and platelet autoantibodies. Costs are in the range $30–100 per test and total costs are estimated to exceed $100 000 000 anually in the USA. The existing uses are likely to continue in the near future but, in addition, flow cytometry could become more widely used for the rapid identification of pathogen-infected cells. For example, infection with human T-cell leukaemia virus, hepatitis B virus, hepatitis C virus and human herpes virus 6 could be detected in blood, and *Mycobacterium tuberculosis* and *Pneumocystis carinii* could be detected in broncheolar lavage fluids using antibody- and/or DNA-based methods. Similar methods could also be used for monitoring numbers of virus-infected cells during chemotherapy and for the rapid detection of viruses in cultured cells after amplification in vitro. This technique would be considerably quicker than the current practice of waiting to observe a cytopathic effect in vitro. There will probably also be an increased demand for monitoring human dendritic cells during therapy and for sperm sorting in both the clinical and agricultural contexts.

With the ever rising level of health care, the number of samples to be analysed by clinical laboratories will continue to increase. Many current test procedures are wasteful of expensive reagents, often employing 100 μl blood and 20 μl of a fluorochrome-labelled antibody(ies) when satisfactory results could be obtained from a fraction of these volumes. Consequently, there is both financial incentive and scope to move towards smaller-scale analyses. At present most of the clinical demands are met using manually operated flow cytometers equipped with a single 488 nm argon

laser and three fluorescence detectors. However, some tasks (e.g. counting $CD4^+/CD8^+$ cells) could be accomplished using simpler, less-expensive instruments. Others (e.g. immunophenotyping leukaemias) might be better undertaken using more sophisticated instruments equipped with multiple wavelength excitation and five/six-colour detection. In the near future, it is likely that a greater diversity of instruments will be employed in the clinical setting. The incentive for their introduction will be that they enable particular tests to be done more quickly, less expensively and more conveniently.

18.8.1 Large versatile high-throughput instruments

In large pathology service departments, there is a need for versatile, high-throughput automated/semiautomated instruments that are as easy to use as the current automated hematology analysers. It is envisaged that these instruments would prepare and analyse blood and bone marrow samples using liquid handling systems and well-established procedures. An ideal instrument would be alignment-free (as is the current BD Biosciences LSR benchtop flow cytometer) and would incorporate software that was capable of setting many of the analysis parameters (as is the current Beckman Coulter EPICS® XL). Calibration, compensation and positioning of cursors could be done on the basis of results obtained from standards comprising different types of fluorescent bead, together with a stable stained (perhaps lyophilised and reconstituted) cell preparation (see Ch. 4). This would enable results to be expressed directly in terms of the equivalent numbers of fluorochrome molecules. For immunophenotyping, automated one-step staining with pre-selected panels of directly labelled antibodies together with LDS-751 or DRAQ5 and/or a fluorochrome-labelled CD45 antibody and beads at a known concentration would allow identification and quantification of leukocytes in live whole blood or bone marrow samples. Alternatively, samples could be processed by a 'stain and lyse' procedure without washing. It can be envisaged that a system could be developed with the ability to programme a different preparation/staining protocol for each sample within a batch, with automatic sample changeover, sample identification by bar-coding or some other means, data recording and information transfer to a laboratory information system and a system for 'flagging' those samples that produce anomalous results. Just recently both Partec (Robby®) and Beckman Coulter (PrepPlus in conjunction with the TQ-Prep™) have introduced automated sample processing work stations that can be linked to their flow cytometers and which incorporate several of these features.

Instead of dispensing fluorochrome-labelled antibodies each time from liquid stocks, it is possible that the appropriate amounts for use in a test could be contained (together with a set number of beads) in sealed tubes to which the samples were added directly during the tests. It might also be possible to prepare the reagents in lyophilised form so that they were reconstituted immediately before, or during, the test. There is also the possibility that the instrument could be linked intelligently to other automated (e.g. hematology, clinical chemistry or immunology) analysers, as part of a suite of instruments connected by a sample management system such as the ADVIA® LabCell™ (Bayer). With appropriate software and predetermined algorithms in the information system, it should be possible to arrange that, dependent on the results of one assay, the same sample could be processed in further assays. Also, a complete set of test results for a single sample (patient) might be evaluated and, where possible, a laboratory diagnosis made. No such instruments are currently available, but they would be a natural step in the development of automated clinical analysers. Although the capital cost of such instruments would be high, there is considerable scope for reducing the sample volumes, with concomitant reductions in reagent usage and hence cost. A manual 'over-ride' option would allow skilled operators to analyse those samples that were outside the capabilities of the installed or locally amended software. Another, although not necessarily mutually exclusive, possibility would be to pro-

duce a new instrument that could function both as a conventional hematology analyser and as a flow cytometer.

18.8.2 Small bench-top or 'point of care' instruments

There is a need for small, bench-top, office or bedside instruments that have only limited capabilities sufficient to accomplish one or a few specific tasks. A few such instruments are already available and have begun to occupy 'niche' markets.

The IMAGN*2000 is a small (620 mm × 520 mm × 610 mm) instrument produced initially by Biometric Imaging (Dietz et al., 1996) but since acquired by BD Biosciences) that can be used near the patient or in the laboratory (Fig. 18.9). It enables the processing and automated counting of fluorochrome-labelled cells in whole blood or other samples. Excitation is by a relatively inexpensive helium–neon laser emitting at 633 nm and cells are labelled with antibodies conjugated to Cy™5 and Cy™5.5 (emission maxima 665 and 695 nm, respectively) or TO-PRO®-3, a DNA stain. The fluorochrome-labelled cells are held stationary in a capillary while a laser beam is swept over them. Fluorescent signals are interpreted by the software and displayed as three-dimensional images reflecting the shape, size and fluorescence intensity of the cells. At present, four tests are marketed for use with the instrument but others are currently under development. Those available at present include: $CD4^+$/$CD8^+$ cells, $CD34^+$ cells (STELLer assay), and two CEQer assays for the enumeration of residual leukocytes in leukoreduced platelet-rich plasma (CEQer PRP Assay) and in red blood cell products (CEQer RBC Assay). Ten samples can be processed in 40 min and the present cost of reagents is approximately $25 per test. The sensitivity for different tests varies between 1 and 5 cells μl^{-1} but the coefficients of variation for rare event analysis are often higher than by flow cytometry because the volume of the microcapillary limits the total number of cells that can be analysed. There is a large potential market in developing countries for instruments used for diagnosing and monitoring the progress of HIV infection, but the price must be affordable. Other tests for use with this instrument that are currently under development include those for fetal hemoglobin (in fetal–maternal hemorrhage) and the detection of bacterial contamination. Given the correct software, the instrument should also be capable of analysing the results of multiplex assays.

Fig. 18.9 The IMAGN*2000 (BD Biosciences) microvolume fluorimeter/cytometer. (Reprinted with permission of the copyright holder, BD Biometric Imaging.)

The DNAnalyzer (RATCOM Inc.) is a commercial instrument stemming from a NASA/American Cancer Society partnership responsible for the design of an 'in-flight' compact flow cytometer (Fig. 18.10). The new instrument is specifically intended for analysis of DNA from solid tumours. It employs a triangular flow cell and is claimed to give twice the resolution and three times more uniformity than conventional flow cytometers for these samples. Other potential uses would be in the detection of leukaemia and pathogenic organisms. The NPE

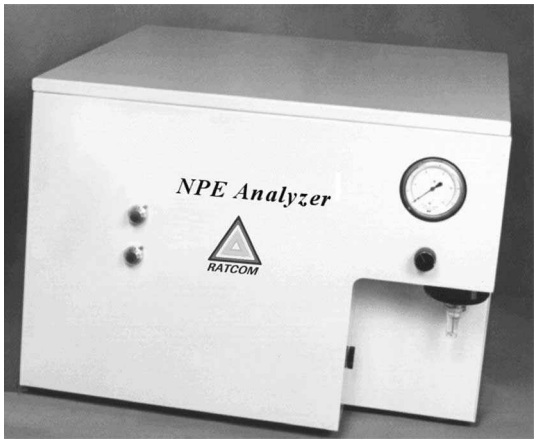

Fig. 18.10 The NPE DNAnalyzer produced by RATCOM Inc. (FL, USA). (Reprinted with permission of the copyright holder, RATCOM, Inc.)

(Nuclear Packing Efficiency) is the second generation of instruments stemming from the NASA In-Flight cytometry programme. It is a multiparameter instrument capable of measuring coulter volume and high-resolution DNA analysis on nuclei. The ratio of the coulter volume to the DNA content of the nucleus is an independent parameter for the identification of abnormal (aneuploid) nuclei. For normal nuclei, the ratio differs between species but is constant for different tissues within a species. However, the ratio clearly separates aneuploid from diploid nuclei, even to the extent of separating tetraploid nuclei from the G_2 and M phase nuclei of the same DNA content.

The Compucyte OnCyte™ Diagnostic System is a small static cytometer, based on the company's LSC® laser scanning cytometer, which functions as an integrated system, performing a new class of solid-phase cell-based diagnostic tests (Fig. 18.11). All of the instrument functions, including quality control and automated sample processing, are computer controlled. The necessary reagents and a cell separation technology are incorporated in single-use disposable test cartridges, for rapid, simple, near patient testing in the emergency room and other clinical settings. The test procedures are being optimised to produce results within 20 min and at

Fig. 18.11 The Compucyte OnCyte^{TM} Diagnostic System. (Reprinted with permission of the copyright holder, the Compucyte Corporation.)

present are directed to the analysis of cellular diagnostic markers in cardiovascular and autoimmune disease, neonatal sepsis and platelet activation. Currently, Compucyte have an initial batch of prototype instruments nearing completion and the test procedures are undergoing evaluation in clinical settings.

The Diagnostic CellScan and Research CellScan instruments produced by Medis-El (Israel) are static cytometers but feature a unique 'cell carrier' comprising a square matrix of 100×100 wells, each of which can hold one cell. Movement of the carrier is computer controlled (as in the Compucyte laser scanning cytometer) allowing the coordinates of each cell to be monitored; individual cells can thus be measured repetitively. Fluorescence excitation is by a 50 mW argon laser but the intensity can be adjusted and monitored to provide measured energy doses. The fluorescence detection system uses

filters and four photomultipliers with optimum responses in the 500–600 nm range, allowing two-colour assays. These instrument configurations clearly have potential for use in the clinical and research settings but few performance details are available as yet.

18.9 Conclusions

When the first cytometer was introduced, few could have anticipated that, within 50 or so years, it would become possible to discriminate not only cells that appeared different microscopically but also functionally different subpopulations amongst cells that otherwise appeared identical, cells that contained integrated viral DNA sequences, or cells with subtle differences in genomic DNA. It would be rash, therefore, to speculate in detail what the future might hold. However, as the provision of high-quality personal health care becomes ever more important throughout the world, there will be increased demands for all types (phenotypic, immunophenotypic, functional and genotypic) of clinical cytometric analysis. Attempts to improve standards of public health will similarly require increased monitoring of pathogens present in both human and animal populations, and in the environment. Potential reservoirs and vectors of infection can be monitored using cytometric techniques that would also be useful in detecting and identifying biological warfare agents if they were ever released. For this expansion to be sustained at a desirable pace, the cost of testing must be reduced. Assays requiring sophisticated instrumentation (e.g. three- or four-colour immunophenotyping) will still need to be done centrally, because of the capital investment in equipment and the need for skilled personnel. Those requiring less-sophisticated instrumentation (e.g. single-colour cell counting and some multiplex assays) will tend to be done locally. In all assays, except perhaps rare event analysis, there will be a drive to use sample volumes that are at least one to two orders of magnitude smaller than at present. This should be readily achieved using the type of microscale components already present in prototype instruments. As soon as miniaturised optical systems, perhaps with a (currently elusive) solid-state laser operating near to 488 nm, become available, it is likely that the first true cytometers on a microchip will be produced. One could then envisage 'point of care' diagnostic instruments, closely related to the present lap-top computers, into which 'analytical cards' could be inserted, each of which was capable of carrying out a particular assay. More versatile forms of such an instrument might also accept 'cards' capable of carrying out those standard hematology, immunological, or clinical chemistry assays that could be monitored optically.

18.10 INTERNET SITES

http://www.ornl.gov/lsm
Oak Ridge National Laboratory Laser Spectroscopy and Micro-instrumentation Group. Micro-chip flow cytometer.
http://www.micronics.net
Micronics Inc., microfluidic cytometer.
http://www.immunicon.com
Cell Track static micro-scale cytometer and magnetic nano-sphere technology.
http://www.bioregio-regensburg.de/eng/instrument.html
Research and development information on fluorescence resonance energy transfer (FRET), excimers, fluorescence polarisation, fluorescence lifetime analysis, etc.
http://www.pcfcij.dbs.aber.ac.uk/aberinst/mycytmain.html
Aber Instruments (UK) Microcyte portable cytometer.
http://lsdiv.lanl.gov/NFCR/newsletter-Oc98/Oct98.html
Los Alamos National Laboratory, Life Sciences Division, National Flow Cytometry Resource. Article by Keij, J.F., Steinkamp, J.A. (1998) Lifetime – a replacement for color? On the phase sensitive time-resolved flow cytometer.
http://www.wallac.fi/catalog/trf.html
Wallac time-resolved fluorimetry, europium chelates and labelling products.
http://www.packardinst.com/cs_catalogs/htrf_reagents.html
Packard Bioscience Company europium chelate-XL665 FRET detection system for time-resolved fluorescence.
http://www.prozyme.com
Time-resolved FRET reagents.
http://www.lgc-uk.com

OnCyte™ fully automated solid-phase cell based test instrument for blood samples.
http://www.diasorin.com
Copalis® and Multiplex™ technology for serum analytes and infectious diseases.
http://www.luminexcorp.com
The Luminex 100™ multiplex analyser for use with LabMAP (Laboratory Multiple Analyte Profiling) multiplex assays.
http://www.medisel.com
The Diagnostic and Research CellScan instruments, static miniature cytometers featuring a cell carrier with 10 000 wells each holding one cell.
http://www.phosphor.demon.co.uk
Phosphor technology; upconverting phosphors.
http://www.sri.com
Upconverting phosphor-based multiplex technology for use with a compact flow cytometer.
http://www.pebio.com/ab/about/hts/fmat.html
The PE Biosystems FMAT™ 8100 HTS macro-confocal static cytometer.
http://www.nctn.hq.nasa.gov/innovation/Innovation_75/shtl.html
The RATCOM DNAnalyzer™.
http://www.biometric.com/html/tech/microscopy.html
The Biometric Imaging IMAGN*2000 microvolume static cytometer.
http://www.kinetics.nsc.ru/llpc/cyto/latex.html
Scanning flow cytometry.
http://thebigone.caltech.edu/quake/research/cellsort.html
Microfabricated fluorescence activated cell sorter.

18.11 REFERENCES

Altendorf, E., Zebert, D., Holl, M., Yager, P. (1999a) Differential blood cell counts obtained using a microchannel based flow cytometer. *Sensors and Actuators* **1**, 531–4.

Altendorf, E., Zebert, D., Holl, M., Vannelli, A., Wu, C., Schulte, T. (1999b) Results obtained using a prototype microfluidics-based hematology analyser. http://www.micronics.net/ericbanffhtml/banff—paperea.html

Amorim, H.T., de Araujo, M.T., Gouveia, E.A., Gouveia-Neto, A.S., Neto, J.A.M., Sombra, A.S.B. (1998) Infra-red to visible up-conversion fluorescence spectroscopy on Er^{3+}-doped chalcogenide glass. *Journal of Luminescence* **74**, 271–7.

Asbury, C.L., Esposito, R., Farmer, C., van den Engh, G. (1996) Fluorescence spectra of DNA dyes measured in a flow cytometer. *Cytometry* **24**, 234–42.

Balakin, K.V., Korshun, V.A., Mikhalev, I.I., Maleev, G.V., Malakhov, D., Prokhorenko, I.A., Berlin, Yu. A. (1998) Conjugates of oligonucleotides with polyaromatic fluorophores as promising DNA probes. *Biosensors and Bioelectronics* **13**, 771–8.

Blankenstein, G., Scampavia, L.D., Ruzicka, J., Christian, G.D. (1996) Coaxial flow mixer for real-time monitoring of cellular responses in flow injection cytometry. *Cytometry* **25**, 200–4.

Condrau, M.A., Schwendener, R.A., Niederer, P., Anliker, M. (1994a) Time-resolved flow cytometry for the measurement of lanthanide chelate fluorescence. I Concept and theoretical evaluation. *Cytometry* **16**, 187–94.

Condrau, M.A., Schwendener, R.A. Zimmerman, M., Muser, M.H., Graf, U., Niederer, P., Anliker, M. (1994b) Time-resolved flow cytometry for the measurement of lanthanide chelate fluorescence. II. Instrument design and experimental results. *Cytometry* **16**, 195–205.

Cunningham, M.E., Gould, R.J., Bednar, B. (1998) An on-line device for temperature control and reagent addition for table-top flow cytometers. http://www.wiley.com/products/subject/life/cytometry/ISAC98/ct129.html

Deka, C., Sklar, L.A., Steinkamp, J.A. (1994) Fluorescence lifetime measurements in a flow cytometer by amplitude demodulation using digital data acquisition technique. *Cytometry* **17**, 94–101.

Dietz, L.J., Dubrow, R.S., Manian, B.S., Sizto, N.L. (1996) Volumetric capillary cytometry: a new method for absolute cell enumeration. *Cytometry* **23**, 177–86.

Fu, A.Y., Spence, C., Scherer, A., Arnold, F.H., Quake, S.R. (1999) A microfabricated fluorescence-activated cell sorter. *Nature Biotechnology* **17**, 1109–11.

Gauci, M.R., Vesy, G., Najari, J., Veal, D., Williams, K.L., Piper, J.A. (1996) Observation of single-cell fluorescence spectra in laser flow cytometry. *Cytometry* **25**, 388–93.

Johnson, L.A., Welch, G.R. (1999) Sex preselection: high-speed flow cytometric sorting of X and Y sperm for maximum efficiency. *Theriogenology* **52**, 1323–41.

Keij, J.F., Bell-Prince, C., Steinkamp, J.A. (1999) Simultaneous analysis of relative DNA and glutathione content in viable cells by phase-resolved flow cytometry. *Cytometry* **35**, 48–54.

London Gender Clinic (2000) human sperm sorting technology. http://www.compucyte.com

Miraglia, S., Schwartzman, E., Evangelista, L., Manian, B., Yuan, P.-M. (1999a) Detecting the binding of fluorescent neuropeptide Y to CHO-K1 cells expressing NPY receptor subtypes. http://www.pebio.com/ab/about/hts/fmat/fmatapps.html

Miraglia, S., Schwartzman, E., Evangelista, L., Manian, B., Yuan, P.-M. (1999b) The use of fluorimetric microvolume assay technology in assessing lead compound cytotoxicity in high throughput screening.

http://www.pebio.com/ab/about/hts/fmat/fmatapps.html

Miraglia, S., Schwartzman, E., Michelotti, J., Evangelista, L., Manian, B., Lohman, K. (1999c) Fluorimetric microvolume assay technology – upregulation of ICAM-1 on the cell surface. http://www.pebio.com/ab/about/hts/fmat/fmatapps.html

Paris, P.L., Langenham, J.M., Kool, E.T. (1998) Probing DNA sequences in solution with a monomer-excimer fluorescence color change. *Nucleic Acids Research* **26**, 3789–93.

Roslaniec, M.C., Bell-Prince, C.S., Crissman, H.A., Fawcett, J.J., Goodwin, P.M., Habbersett, R., Jett, J.H., Keller, R.A., Martin, J.C., Marrone, B.L., Nolan, J.P., Park, M.S., Sailer, B.L., Sklar, L.A., Steinkamp, J.A., Cram, L.S. (1997) New flow cytometric techniques for the 21st century. *Human Cell* **10**, 3–10.

Rothe, G., Schaefer, B., Wimmer, M.S., Schmitz, G. (1998) Excimer fluorescence compared to depolarization in the flow cytometric analysis of lateral membrane mobility in platelets. In: Farkas, D.L., Lief, R.C., Tromberg, B.J. (eds.), *Proceedings of the International Society for Optical Engineering (SPIE)* Vol. 3260, *Optical Investigations of Cells in vitro and in vivo* pp. 255–62. International Society for Optical Engineering, Bellingham, WA.

Sailer, B.L., Steinkamp, J.A., Crisman, H.A. (1998a) Flow cytometric lifetime analysis of DNA-binding probes. *European Journal of Histochemistry* **42** (Special number) 19–27.

Sailer, B.L., Valdez, J.G., Steinkamp, J.A., Crisman, H.A. (1998b) Apoptosis induced with different cycle-perturbing agents produces differential changes in the fluorescence lifetime of DNA–bound ethidium bromide. *Cytometry* **31**, 208–16.

Schrum, D.P., Culbertson, C.T., Jacobson, S.C., Ramsey, J.M. (1999) Microchip flow cytometry using electrokinetic focusing. *Analytical Chemistry* **71**, 4173–7.

Schwartzman, E., Miraglia, S., Michelotti, J., Evangelista, L., Manian, B., Lohman, K. (1999) A homogeneous fluorescent linked immunosorbent assay (FLISA) using fluorimetric microvolume assay technology in a high-throughput screening asssay. http://www.pebio.com/ab/about/hts/fmat/fmatapps.html

Seidl, J., Knuechel, R., Kunz-Schughart, L.A. (1999) Evaluation of membrane physiology following fluorescence activated or magnetic cell separation. *Cytometry* **36**, 102–11.

Soini, J.T., Chernyshev, A.V., Hanninen, P.E., Soini, E., Maltsev, V.P. (1998) A new design of the flow cuvette and optical set-up for the scanning flow cytometer. *Cytometry* **31**, 78–84.

Steinkamp, J.A., Yoshida, T.M., Martin, J.C. (1993) Flow cytometer for resolving signals from heterogenous fluorescence emissions and quantifying lifetime in fluorochrome-labeled cells/particles by phase sensitive detection. *Reviews of Scientific Instruments* **64**, 3440–50.

Steinkamp, J.A., Lehnert, B.E., Lehnert, N.M. (1999) Discrimination of damaged/dead cells by propidium iodide uptake in immunofluorescently labeled populations analyzed by phase-sensitive flow cytometry. *Journal of Immunological Methods* **226**, 59–70.

Tibbe, A.G.J. (1999) Cell analysis system based on compact disk technologies and immuno-magnetic selection and aligning of cells. http://www.tn.utwente.nl/bft/cell/cell.htm

Weaver, D.J. Jr, Durack, G., Voss, E.W. Jr. (1997) Analysis of the intracellular processing of proteins: application of fluorescence polarization and a novel fluorescence probe. *Cytometry* **28**, 25–35.

Zijlmans, H.J.M.A.A., Bonnet, J., Burton, J., Kardos, K., Vail, T., Niedbala, R.S., Tanke, H.J. (1999) Detection of cell and tissue surface antigens using upconverting phosphors: a new reporter technology. *Analytical Biochemistry* **267**, 30–6.

Appendix: Useful internet sites

A.1 Sites of general interest for cytometry

http://www.html
Home page of the International Society for Analytical Cytology. Contains a compendium of Internet sites with direct links to an exhaustive collection of sites that address issues in cytometry.

http://www-ls.lanl.gov/NFCR
Los Alamos National Laboratory National Flow Cytometry Resource.

http://www.bio.umass.edu/mcbfacs/flowcat.html
Catalogue of free flow cytometry software (last updated 24 October 1997).

http://nucleus.immunol.washington.edul/ISAC.html
Compendium of cytometry internet sites.

http://www.biochem.mpg.de/research-groups/vale/cytorel.htl
G. Valet's cytorelay site providing information on recent developments in cytometry and useful links to other sites.

http://www.cytometry.org
The USA Clinical Cytometry Society home page; a directory of suppliers and useful links.

http://www.cyto.purdue.edu
Purdue University cytometry pages; a major site for cytometry information.

http://www.cyto.purdue.edu/hmarchive/Cytometry
Purdue University mailing list archives. Questions and answers in cytometry.

http://pingu.salk.edu/fcm/sitelink.html and http://carmen.salk.edu/fcm/sites.html
Flow cytometry on the Web. Comprehensive links list for cytometry maintained by the Salk Institute, La Jolla, California.

http://www.meds.com/leukemia/leukemia.html
Medicine Online Leukemia Information Library.

http://www.meds.com/leukemia/flow/flow0.html
Medicine Online Leukemia Library: atlas with flow cytometry in acute myeloid leukaemia.

http://www.hss.edu/research/flow/
The Fannie E. Rippel Foundation Flow Cytometry Core Facility at the Hospital for Special Surgery contains very useful links to many cytometry-related sites and resources.

http://www.ncbi.nlm.nih.gov/prow
A useful CD guide.

http://www.bork.emblheidelberg.de/Modules
Useful information on the structure of modules and domains found in leukocyte surface antigens.

http://www.cf.ac.uk/uwcm/hg/hoy/index.html
Royal Microscopical Society (Cytonet UK).

http://www.immune-source.com/html/favorite_links.html
Immune source link site for flow cytometry.

http://bioinformatics.weizmann.ac.il/hotmolecbase/
HotMolecBase: information resource and search engine for 'Hot' research molecules.

http://www.dti.gov.uk/bioguide/hsafety.html
UK Health and Safety Executive page providing access to biosafety information.

http://www.antibody resource.com
The Antibody Resource Page: a multidisciplinary page on antibodies with links to suppliers, databases, immunology and biotechnology sites.

http://www.wiley.com/products/subject/life/cytometry/flo_823710246.html
Wiley: flow cytometry web site

http://www.blackwell-science.com/uk/society/bsh/commit00.htm
The home page of the British Society for Haematology, with links to its subcommittees, including the British Committee for Standards in Haematology.

http://www.cpa-uk.demon.co.uk/

The home page of Clinical Pathology Accreditation (UK) Ltd. http://www.ukneqas.org.uk/

The home page of UK National External Quality Assessment Schemes (UK NEQAS).

http://www.biochem.mpg.de/valet/eurocel1.html

European Working Group on Clinical Cell Analysis (EWGCCA) including the European Group for the Immunological Characterization of leukemias.

A.2 Suppliers of instruments, reagents, antibodies, etc.

Table A.1 gives the internet addresses of some directories of suppliers, which may be searched alphabetically by name or by product; Table A.2 gives the internet addresses of suppliers.

Table A.1 *Directories of suppliers*

Name	Internet address
Abcam (dynamic search for antibodies)	http://www.abcam.com
Anderson's List of Scientific Companies	http://www.actg.com
BioSupplyNet	http://www.biosupplynet.com
Matt's Scientific Suppliers List	http://cmgm.stanford.edu/~footer/companies.html
NetSci's Biotech & Pharmaceutical YellowPages	http://www.netsci.org/Resources/Biotech/Yellowpages/xyz.html
SciQuest™ com	http://www.sciquest.com
The Antibody Resource Page	http://www.antibody resource.com

Table A.2 *Addresses of suppliers*

Name	Internet address	Products and/or services
Aber Instruments Ltd	http://www.aber-instruments.co.uk	Microcyte portable cytometer
Accurate	http://www.accuratechemical.com	Antibodies, cell separation
Actigen	http://www.actigen.com	Affinity proteins, e.g. protein A
Alexis	http://www.alexis-corp.com	Biochemicals for life sciences research
American Type Culture Collection,	http://www.atcc.org	Human hemopoietic cell lines
Amersham Pharmacia Biotech	http://www.apbiotech.com	Molecular biology/biotechnology
Amgen Ltd	http://www.amgen.com	Recombinant cytokines
Amrad (incorporates Silenus Laboratories)	http://www.amrad.com	Antibody-based diagnostic technology
Ancell	http://www.ancell.com	Antibodies, recombinant proteins
Applied Cytometry Systems	http://www.appliedcytometry.com	Flow cytometry software
Bangs Laboratories Inc.	http://www.bagslab.com	Latex microspheres
Bayer Diagnostics	http://www.bayerdiag.com	Clinical analysers
BD Biosciences	http://www.bdms.com/	Flow cytometers, antibodies, assay kits, antigens
Beckman Coulter	http://www.beckmancoulter.com	Flow cytometers, antibodies, assay kits, antigens
Bibby-Sterilin	http://www.bibby-sterilin.com	Cell culture plasticware, glassware and equipment
BioCytex	http://www.biocytex.comhttp://www.alexis.com/	Antibodies, apoptosis and cell enumeration kits

Table A.2 (*cont.*)

Name	Internet address	Products and/or services
Biodesign International	http://www.biodesign.com	Antibodies, antigens and proteins
BioErgonomics	http://www.bioe.com	Preparation and standardisation reagents, assay kits, for flow cytometry
Biogenex	http://www.biogenex.com	Molecular and cellular pathology diagnostics
Biomeda	http://www.biomeda.com	Immunochemicals
Bio-Rad Laboratories Ltd	http://www.biorad.com	Flow cytometers, confocal microscopes, clinical diagnostics, life sciences research products
Biosource	http://www.biosource.com	Antibodies, media, peptides
Bio-Synthesis Inc.	http://www.biosyn.com	DNA, peptides, antibodies
Boehringer-Mannheim (now the Diagnostics Division of Roche)	http://www.roche.com/diagnostics	Molecular biology chemicals, apoptosis and cell proliferation, clinical chemistry
British Biotech plc	http://www.britishbiotech.co.uk	Metalloenzyme inhibitors
Calbiochem	http://www.calbiochem.com	Biochemicals, antibodies, assay kits, immunochemicals and reagents
Caltag Laboratories	http://www.caltag.com	Immunological reagents, particularly multicolour flow cytometry assays
Cambridge Bioscience	http://www.bioscience.co.uk	Molecular and cell biology and immunology research products
Cedarlane	http://www.cedarlane.com	Immunologicals, cell separation media
Chemicon	http://www.chemicon.com	Immunological reagents and kits, antibodies and detection systems
Chroma Technology Corporation	http://www.techexpo.com/firms/chromatc.html	Optical filters, specialising in cytometry and microscopy
Chromaprobe	http://www.chromaprobe.com	Antibodies and fluorochromes for flow cytometry
CLB Reagents	http://www.clb.nl	Blood grouping reagents, antibodies, human cytokines
Coherent Auburn Group	http://www.cohr.com	Lasers and laser-based systems
Compucyte	http://www.compucyte.com	Laser scanning cytometer and OnCyte™ system
CP Pharmaceuticals	http:cppharma.com	Heparin (Monoparin®, Multiparin®), therapeutics
Cymbus Bioscience	http://www.cymbus.com	Monoclonal antibodies and reagents
Cytek Corporation	http://www.cytek.com	Support for electronic product design, software development
Cytimmune Sciences Inc.	http://www.cytimmune.com	Cytokine and angiogenic immunoassay kits
Cytomation, Inc.	http://www.cytomation.com/contactus.htm	Flow cytometers, accessories and upgrades
DAKO Diagnostics Ltd	http://www.dako.com	Immunocytochemistry, flow cytometry, immunological, immunocytochemistry and microbiology reagents

Table A.2 (*cont.*)

Name	Internet address	Products and/or services
DiaSorin	http://www.diasorin.com	Medical diagnostics, immunohistochemistry
Diatek	http://www.diatec.com	Monoclonal antibodies
Dojindo Molecular Technologies, Inc.	http://www.dojindo.com	Antibodies and biochemicals
Dynal	http://www.dynal.no	Dynabeads: magnetic bead separations for cells, DNA, proteins, etc.
Enzyme System Products	http://www.enzymesys.com	Synthetic substrates, inhibitors and enzyme assay kits
European Collection of Cell Cultures	http://www.camr.org.uk/ecacc.htm	Human hemopoietic cell lines
Exalpha	http://www.exalpha.com	Antibodies, flow cytometry reagents, immunophenotyping kits
Exciton Inc.	http://www.exciton.com	Dyes for use with laser excitation
Flow Cytometry Standards Corporation (FCSC)	http://www.fcstd.com	Standardisation, quality control and quantification reagents for flow cytometry
Harlan	http://www.harlan.com	Immunochemicals, laboratory animal models, isolators
Hoechst (now merged with Rhone Poulenc and Aventis	http://hoechst.com	Chemicals and reagents for the life sciences
ICN Biomedicals Ltd	http://www.icnbiomed.com	Biomedical, biochemical, immunological, molecular and cell biology reagents
Immune Source Corporation	http://www.immune-source.com	Antibodies, kits and reagents for flow cytometry
Immunicon Corporation	http://www.immunicon.com	Magnetic nanoparticles for cell selection/depletion
Immuno Quality Products	http://www.iqproducts.nl	Antibodies and assay kits for flow cytometry
Inova Diagnostics Inc.	http://www.inovadx.com	Autoantibody assays/detection
Integrated Genetics		Molecular and cell biology reagents, immunochemicals
Intergen	http://www.intergenco.com	Reagents for biomedical research
IQ Products	http://www.iqproducts.nl	Antibodies, flow cytometry reagents
Jackson ImmunoResearch Laboratories Inc	http://www.jacksonimmuno.com	Secondary antibodies for flow cytometry and other immunodetection systems
KPL, Kirkegaard & Perry Laboratories, Inc.	http://www.kpl.com/open2.html	Antibodies, substrates, DNA, RNA, proteins, in situ detection and analysis
Lab Vision NeoMarkers Corporation	http://www.labvision.com	Antibodies for molecular biology/medicine, apoptosis, cell cycle, etc.
Lampire Biological Laboratories	http://www.lampire.com	Antibodies, antibody production, animal sera and plasma
Leinco Technologies	http://www.leinco.com	Antibodies, recombinant proteins
Life Technologies	http://www.lifetech.com	Cell culture media, sera, primers

Table A.2 (*cont.*)

Name	Internet address	Products and/or services
Linscott's Directory	http://ourworld.compuserve.com/homepages/LINSCOTTSDIRECTORY	Directory of immunological and biological reagents
LOT-Oriel	http://lot-oriel.com	Lasers, optics, filters
Luminex	http://www.luminexcorp.com	Luminex analysers and microspheres
Medarex Inc	http://www.medarex.com	Monoclonal antibodies, including bispecific, humanised and immunotoxins
Medis-El	http://www.medisel.com	Diagnostic and research CellScan instruments
Melles Griot	http://www.mellesgriot.com/OVRVIEW2.HTM	Lasers and optics
Merck	http://www.merck.com	Biomedical and pharmaceutical products. Also online access to the Merck Manual
Micronics	http://www.micronics.net	Miniaturised technologies for the life sciences
Miltenyi Biotec	http://www.miltenyibiotec.com	Magnetic bead cell isolation kits and sorters
Molecular Probes	http://www.probes.com	Fluorescent reagents and techniques for biomedical research
Nalge Nunc International	http://nunc.nalgenunc.com/	Nunc brand products (disposable labware)
National Collections of Type Cultures (NCTC)	http://www.dti.gov.uk/bioguide/culture.html	Cell and microbial culture collections
Novocastra Laboratories Ltd	http://www.novocastra.co.uk	Proteins, antibodies, detection systems
Novus Biologicals, Inc.	http://www.novus-biologicals.com	Antibodies, recombinant proteins, cDNAs
O.E.M. Concepts, Inc.	http://www.oemconcepts.com	Polyclonal and monoclonal antibodies for the production of immunodiagnostics
Omega Optical, Inc.	http://www.omegafilters.com	Optical filters
Oncogene Research Products	http://www.apoptosis.com	Molecular and cell biology research products
One Lambda, Inc.	http://www.onelambda.com	Transplant diagnostics
Optoflow	http://www.optoflow.com/	Manufacturers of the Microcyte portable flow cytometer
Orpegen Pharma	http://www.orpegen.com	Clinical diagnostics, assay kits
Ortho	Have no web address	Flow cytometers, diagnostic reagents
Packard BioScience	http://www.packardbioscience.com	Instruments and consumables for life sciences research
Pall Gelman Laboratory	http://www.pall.com/gelman	Filtration and separation devices
PanVera Corporation	http://www.panvera.com	Fluorescence polarisation, recombinant proteins, molecular and cell biology reagents
Partec	http://www.partec.de	Laser and arc lamp flow cytometers, reagents and standards

Table A.2 (*cont.*)

Name	Internet address	Products and/or services
PE Biosystems	http://www.pebio.com	A division of the PerkinElmer Corporation; life sciences technology and products
PeproTech Inc.	http://www.peprotech.com	Cytokines
PerkinElmer Inc.	http://www.perkinelmer.com	Parent site of the PerkinElmer Corporation
PerSeptive Biosystems, Inc.	http://www.pbio.com	Purification, analysis and synthesis for biomedical research and drug development
Phoenix Flow Systems Inc.	http://www.phnxflow.com	Flow cytometry software and assay kits
Pierce	http://www.piercenet.com	Antibodies, recombinant proteins, derivitisation and crosslinking reagents
Polysciences	http://www.polysciences.com	Microspheres, biochemicals, immunological reagents
Primm Labs, Inc.	http://www.primmlabs.com	DNA reagents
R&D Systems	http://www.rndsystems.com	Cytokines, antibodies, cell separation, immunoassay kits, flow cytometry kits
Research Diagnostics Inc.	http://www.researchd.com	Distributor for immunochemicals
Riese Enterprises	http://www.riese.com	BioSure® standards and controls for flow cytometry, stains and reagents
Rochester MicroSystems Inc.	http://www.rochestermicro.com	Software for flow cytometry and sorting and for automatic colour compensation
Rockland Immunochemicals, Inc.	http://www.rockland-inc.com	Monoclonal and polyclonal antibody, recombinant protein production
Santa Cruz Biotechnology	http://www.scbt.com	Antibodies and proteins for molecular and cell biology research
Sarstedt	http://www.sarstedt.com/	Monovette blood collection tubes, medical equipment, etc.
Serotec	http://www.serotec.co.uk	Immunological and cell culture reagents, recombinant cytokines
Sigma Chemical Company Ltd	http://www.sigma.sial.com	Chemicals, biochemicals, immunological reagents
Signet Laboratories, Inc.	http://www.signetlabs.com	Antibodies, detection kits and associated reagents
Southern Biotechnology Associates	http://www.SouthernBiotech.com	Antibodies, enzyme substrates, apoptosis reagents
Spectra Physics	http://www.spectraphysics.com	Solid state lasers
Spherotech, Inc.	http://www.spherotech.com	Fluorescent, magnetic, coloured microparticles
SRI International	http://www.sri.com	A nonprofit-making research and development organisation
Stratagene	http://www.stratagene.com	Molecular biology products
Sysmex	http://www.sysmex.com	Haematology analysers and products
TCS Microbiology	http://www.tcsmicro.co.uk	Animal blood, plasma and serum, diagnostic kits

Table A.2 (*cont.*)

Name	Internet address	Products and/or services
Terumo	http://www.terumo.co.jp/	Venoject® blood collection tubes, medical equipment, etc.
The Binding Site	http://www.bindingsite.co.uk	Antisera, antibodies and conjugates, immunodiagnostic kits and reagents
Trevigen, Inc.	http://www.trevigen.com	Molecular biology, DNA, apoptosis, flow cytometry reagents
Universal Biologicals Ltd	No web address	Distributor for immunological reagents
Upstate Biotechnology	http://www.upstatebiotech.com	Recombinant enzymes, assay systems, and antibodies for modification states of proteins
Vector Laboratories Ltd	http://www.vectorlabs.com	Antibodies, immunostaining, flow cytometry reagents
VMRD Inc.	http://www.vmrd.com	Monoclonal antibodies, immunoquantification and reagents
Wallac	http://www.wallac.fi/-	Wallac Division of PerkinElmer Inc.: time-resolved fluorescence
Worthington Biochemical Corporation	http://www.worthington-biochem.com	Enzymes, e.g. for tissue dissociation
Zymed Laboratories Inc.	http://www.zymed.com	Cell biology, in situ hybridisation and immunoassay reagents

Index